Document Discussion

Return To Library > Records > ERID-97001 through ERID-97501 > ERID-097431 1) GOLDSIM MODEL DOCUMENTATION AND DATA SELECTION FOR LOS ALAMOS NATIONAL LABORATORY TECHNICAL AREA 54, MATERIAL DISPOSAL AREA G PERFORMANCE ASSESSMENT AND COMPOSITE ANALYSIS

Created By: Aurelia A. Martinez/USERS/LANL
File name: Target-ERID # for Domino.txt
Version: 1.0
Document Type: RPF Record
Description: N/A

Document Details:

Title:	ERID-097431 1) GOLDSIM MODEL DOCUMENTATION AND DATA SELECTION FOR LOS ALAMOS NATIONAL LABORATORY TECHNICAL AREA 54, MATERIAL DISPOSAL AREA G PERFORMANCE ASSESSMENT AND COMPOSITE ANALYSIS
ERID Number.StartPage:	ERID-097431
Office of Record:	ENV-ERSS
Date Received:	07/26/2007
Official Use Only:	N
Page Count:	N/A
Record Type:	Letter
Document Date:	11/01/2007
To:(Addressees - Organization) *(separate multiple values with semicolons)*	N/A
From:(Senders - Organization) *(separate multiple values with semicolons)*	ROB SHUMAN
Other Document Number(s): *(separate multiple values with semicolons)*	N/A
TA: *separate multiple values with semicolons)*	TA-54
PRS Number(s): *(separate multiple values with semicolons)*	
Record Box Number:	

*** Denotes Fields that are mandatory.**

To download this file, right mouse click on the file and select 'Save to Disk' or 'Save Target as'

Target-ERID # for Domino.txt <-- This link points to this version.

To check-out and/or edit this file, select Edit Document or Check Out Document from the Document menu above.

File Cabinet: Records
Binder Category: ERID-90000 through ERID-99999
Binder: ERID-97001 through ERID-97501

31159

LA-UR-06-4391

Approved for public release; distribution is unlimited.

Title: GoldSim Model Documentation and Data Selection for Los Alamos National Laboratory Technical Area 54, Material Disposal Area G Performance Assessment and Composite Analysis

Author(s): Rob Shuman

Submitted to: U.S. Department of Energy

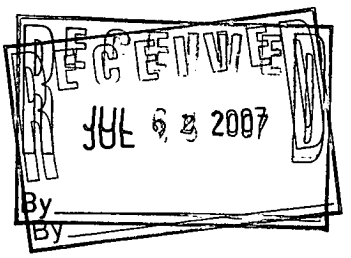

Los Alamos
NATIONAL LABORATORY

Los Alamos National Laboratory, an affirmative action/equal opportunity employer, is operated by the University of California for the U.S. Department of Energy under contract W-7405-ENG-36. By acceptance of this article, the publisher recognizes that the U.S. Government retains a nonexclusive, royalty-free license to publish or reproduce the published form of this contribution, or to allow others to do so, for U.S. Government purposes. Los Alamos National Laboratory requests that the publisher identify this article as work performed under the auspices of the U.S. Department of Energy. Los Alamos National Laboratory strongly supports academic freedom and a researcher's right to publish; as an institution, however, the Laboratory does not endorse the viewpoint of a publication or guarantee its technical correctness.

Form 836 (8/00)

Table of Contents

List of Figures v
List of Tables vi
List of Attachments vii
Acronyms and Abbreviations viii

1.0 Introduction 1
2.0 Model Description and Organization 3
2.1 GoldSim Modeling Basics 3
2.2 Human Exposure Pathways and Exposure Scenarios 5
2.2.1 Operational, Closure, and Active Institutional Control Periods 6
2.2.2 Passive Institutional Control Period 11
2.3 Model Organization 12
2.3.1 MDA G Site Model 12
2.3.1.1 Input Data and Process Models 12
2.3.1.2 Physical Compartments — Site and Exposure Locations 18
2.3.1.3 Physical Compartments — Disposal Facility 19
2.3.2 MDA G Site Diffusion Model 21
2.3.2.1 Input Data and Process Models 21
2.3.2.2 Physical Compartments — Off-Site Media and Exposure Locations 23
2.3.2.3 Physical Compartments — Disposal Units 24
2.3.3 MDA G Intruder Model 24
2.3.3.1 Input Data and Process Models 24
2.3.3.2 Physical Compartments — Off-Site Media 28
2.3.3.3 Physical Compartments — Disposal Facility 28
2.3.4 MDA G Intruder Diffusion Model 29
2.3.4.1 Input Data and Process Models 29
2.3.4.2 Physical Compartments — Off-Site Media 31
2.3.4.3 Physical Compartments — Disposal Facility 32
3.0 Modeling Approach 33
3.1 Biotic Intrusion Model 35
3.1.1 Conceptual Model 35
3.1.2 Mathematical Model 43
3.1.2.1 Plant Intrusion 43
3.1.2.2 Animal Intrusion 50
3.2 Surface Erosion Model 55
3.2.1 Cover Loss 55
3.2.2 Sediment Transport 66
3.3 Human Intrusion Model 68
3.4 Diffusion Model 70
3.5 Dose Model 72
3.5.1 Ingestion Exposure Route 73
3.5.2 Inhalation Exposure Route 76
3.5.3 Direct Radiation Exposure Route 77

Table of Contents (Continued)

3.6 Disposal System Configuration and Contaminant Flows 81
3.6.1 Disposal Facility Configuration and Contaminant Flows 81
3.6.2 Site and Exposure Location Configuration and Contaminant Flows 86
3.6.3 Exposure Concentrations 91
3.6.3.1 Surface Soil, Cap, and Waste 91
3.6.3.2 Air 92
3.6.3.3 Crops 94
3.6.3.4 Animal Products 97
3.6.3.5 Groundwater 100
4.0 Input Parameter Requirements 101
5.0 Model Input Data Selection 242
5.1 Control Parameters 242
5.2 Facility Dimensions and Operations 243
5.2.1 Disposal Areas 243
5.2.2 Erosion Zone Properties 246
5.2.3 Operational Period 248
5.2.4 Cover and Waste Configuration 248
5.2.5 Waste Emplacement Efficiency 270
5.2.6 Shaft Field Efficiency 272
5.3 Material Properties 272
5.3.1 Dry Bulk Density, Porosity, and Moisture Content 274
5.3.2 Partition Coefficients 276
5.3.3 Solubility Limits 279
5.3.4 Mass Attenuation Coefficients 280
5.3.5 Diffusion Coefficients 280
5.3.6 Radon Emanation Coefficient 286
5.3.7 Carbon-14 Gas Generation Rate 286
5.3.8 Carbon Dioxide and Methane Fractions 287
5.3.9 Organic Fraction of Carbon-14 Waste 287
5.4 Radionuclide Inventories 288
5.5 Atmospheric Transport Parameters 334
5.5.1 Dust Loading and Soil Disturbance Factor 334
5.5.2 Vertical Flux 335
5.5.3 Enhancement Factor 338
5.5.4 Dispersion Factor and Deposition Rate 340
5.6 Groundwater Transport Parameters 342
5.6.1 MDA G Infiltration Rate 342
5.6.2 Contaminant Capture Fraction 346
5.6.3 Exposure Location Infiltration Rates 348
5.7 Sediment Transport Parameters 349
5.7.1 Sediment Allocation Fractions 349
5.7.2 Sediment Dispersal Fraction 356
5.7.3 Canyon Sediment Transport Rates 357
5.8 Food-Chain Transport Parameters 358
5.8.1 Crop Uptake Factor 359

Table of Contents (Continued)

5.8.2 Dry-to-Wet-Weight Fraction 363
5.8.3 Translocation Factor 363
5.8.4 Agricultural Productivity 365
5.8.5 Growing Season 366
5.8.6 Plant Mass Loading Factor 368
5.8.7 Rainsplash Enhancement Factor 370
5.8.8 Plant Interception Fraction and Coefficient 371
5.8.9 Weathering Half-Life 373
5.8.10 Animal Product Transfer Factor 373
5.8.11 Animal Food, Water, and Soil Ingestion Rates 380
5.9 Biotic Intrusion Model Parameters 382
5.9.1 Time to Climax 382
5.9.2 Shape Factors 383
5.9.3 Maximum Rooting Depth 383
5.9.4 Aboveground Biomass Density 388
5.9.5 Litter Production Rate 399
5.9.6 Litter Decomposition Half-Life 402
5.9.7 Native Vegetation Plant Uptake Factor 403
5.9.8 Maximum Burrow Depth 404
5.9.9 Burrow Density 408
5.9.10 Harvester Ant Burrow Mass 412
5.9.11 Harvester Ant Colony Life Span 413
5.9.12 Pocket Gopher Soil Removal Rate 413
5.9.13 Mouse, Chipmunk, and Ground Squirrel Burrow Volume 414
5.9.14 Burrow Renewal Fraction 414
5.10 Erosion Model Parameters 415
5.10.1 Shape Factors 415
5.10.2 Erosion Zone Interval Data 415
5.11 Exposure Pathway Parameters 416
5.11.1 Indoor and Outdoor Time Allotments 416
5.11.2 Excavation Occupancy Fraction 416
5.11.3 Soil Mixing Depth 417
5.11.4 Direct Radiation Shielding Factor 417
5.11.5 Inhalation Rate 418
5.11.6 Average Wind Speed 418
5.11.7 Atmospheric Mixing Height 419
5.11.8 Irrigation Rate and Fraction 419
5.11.9 Inadvertent Soil Ingestion Rate 422
5.11.10 Drinking Water Ingestion Rate 423
5.11.11 Indoor Water Usage Rate 423
5.11.12 Types of Animals Raised 423
5.11.13 Fraction of Diet Raised at Receptor Location 423
5.11.14 Crop Ingestion Rates 424
5.11.15 Animal Product Ingestion Rates 425
5.11.16 Animal Numbers 425

Table of Contents (Continued)

5.11.17 Receptor's Lot, House, and Well Dimensions 427
5.11.18 House Ventilation Rate 427
5.12 Miscellaneous Parameters 428
6.0 References 432

List of Figures

Figure 1 General Organization of the MDA G Site Model 13
Figure 2 General Organization of the MDA G Site Diffusion Model 22
Figure 3 General Organization of the MDA G Intruder Model 25
Figure 4 General Organization of MDA G Intruder Diffusion Model 30
Figure 5 Waste Disposal Regions at MDA G 34
Figure 6 Atmospheric Source Areas at MDA G 36
Figure 7 Generalized Vegetative Zones of the Pajarito Plateau 38
Figure 8 Root Depth Distributions for Grasses, Forbs, and Shrubs 46
Figure 9 Root Mass Distributions for Plants with a Maximum Rooting Depth of 1.5 m 49
Figure 10 Burrow Depth Distributions for Animals with a Maximum Burrowing Depth of 3 m 54
Figure 11 Erosion Behavior of Selected Nodes in Erosion Zone 2 60
Figure 12 Erosion Behavior of Selected Nodes in Erosion Zone 5 61
Figure 13 Erosion Behavior of Selected Nodes in Erosion Zone 9 62
Figure 14 Comparison of Cover Loss Functions and Erosion Behavior for Selected Nodes under Moderate Erosion Conditions) 64
Figure 15 MDA G Sediment-Source Areas and Sediment Catchments in Habitable Canyons 67
Figure 16 Histograms of Initial Cover Depth Distribution for Waste Disposal Regions 1 through 6 and 8 251
Figure 17 Calculation of Proposed Shaft Field Area in Zone 4 273
Figure 18 Points of Maximum Exposure for Releases from MDA G 343
Figure 19 Relationship between Canopy Cover and Herbage Yields 395

List of Tables

Table 1 Exposure Scenarios for the Operational, Active Institutional, and Passive Institutional Control Periods 8
Table 2 Elevations of Disposal Units and Depth to Regional Aquifer for the Eight Waste Disposal Regions 35
Table 3 Distribution of Small Mammals in Los Alamos County by Vegetation Overstory Type 40
Table 4 Burrow Depth Distributions for MDA G Animal Species 52
Table 5 Erosion Zones as Defined by Depth of Remaining Cover 56
Table 6 Input Data Requirements for the MDA G Site Model 102
Table 7 Input Data Requirements for the MDA G Site Diffusion Model 136
Table 8 Input Data Requirements for the MDA G Intruder Model 169
Table 9 Input Data Requirements for the MDA G Intruder Diffusion Model 205
Table 10 Pits and Shafts Included in the Eight Waste Disposal Regions of MDA G and the Region-Specific Disposal Areas 244
Table 11 Erosion Zone Allocations Used in 1,000-Year Simulations 247
Table 12 Erosion Zone Depth Intervals and Allocations Used in 50,000-Year Simulation 249
Table 13 Operational Periods for the Eight Waste Disposal Regions at MDA G 250
Table 14 Pathway Parameter Values and Distributions Used in the Performance Assessment and Composite Analysis 252
Table 15 Waste Emplacement Efficiencies for the Eight Waste Disposal Regions 271
Table 16 Distribution Coefficients and Solubility Limits 277
Table 17 Average Photon Energies and Mass Attenuation Coefficients 281
Table 18 Free-Air Diffusion Coefficients for Vapor- and Gas-Phase Radionuclides 284
Table 19 Disposal Region-Specific Inventories Included in the MDA G Performance Assessment and Composite Analysis 289
Table 20 Radionuclide Inventories for the MDA G Performance Assessment by Waste Disposal Region 290
Table 21 Radionuclide Inventories for the MDA G Composite Analysis by Waste Disposal Region 300
Table 22 Inventories Included in the Intruder Dose Assessment 310
Table 23 Radionuclide Inventories for the Intruder Dose Assessment 311
Table 24 Measurement Uncertainty Factors Associated with MDA G Radionuclide-Specific Inventories 319
Table 25 Radionuclide Activity Fractions for 1- to 5-Year-Old Mixed Fission Product Waste Generated by Thermal Fission of U-235 and Pu-239 324
Table 26 Radionuclide Activity Fractions for 6- to 10-Year-Old Mixed Fission Product Waste Generated by Thermal Fission of U-235 and Pu-239 326
Table 27 Material Type Mass Allocation Fractions for the Predominant Material Types Disposed of at MDA G 328
Table 28 Point Estimates of the Mass and Activity Allocation Factors for the Predominant Material Types Disposed of at MDA G 329
Table 29 Spectroscopy Data for Material Type PU52 331
Table 30 Distributions of Radionuclide Mass Allocation Factors for the Predominant Material Types Disposed of at MDA G 333

Table of Contents (Continued)

Table 31	Measured and Projected Flux Rates for MDA G	344
Table 32	Contaminant Capture Fractions for the MDA G Waste Disposal Regions	347
Table 33	Sediment Allocation Factors for the Catchment Areas in Cañada del Buey and Pajarito Canyon	350
Table 34	Sediment Allocation Fractions Averaged over Erosion Scenarios at Various Times after Facility Closure	351
Table 35	Sediment Allocation Fractions Averaged over Time after Facility Closure	354
Table 36	Size of Catchments in Cañada del Buey and Pajarito Canyon	357
Table 37	Parameter Values and Distributional Information for Plant Uptake Factors	360
Table 38	Dry-to-Wet-Weight Fractions for Crops	364
Table 39	Time-to-Maturity Data for Representative Vegetables	367
Table 40	Summary of Plant Mass Loading	369
Table 41	Parameter Values and Distributional Information for Beef and Milk Transfer Factors	375
Table 42	Parameter Values and Distributions for Chicken and Egg Transfer Factors	377
Table 43	Literature-Based Rooting Depths for Grasses, Forbs, Shrubs, and Trees Growing at Los Alamos National Laboratory	385
Table 44	Measured, Estimated, and Literature-Based Plant Rooting Depths for Plants at Los Alamos National Laboratory	387
Table 45	Summary of Cover and Production Studies Used to Estimate Aboveground Biomass (early successional stages at MDA G)	389
Table 46	Aboveground Production of Grasses, Forbs, and Shrubs (early successional stages of piñon-juniper cover types)	391
Table 47	Summary of Cover and Production Studies Used to Estimate Understory Biomass (MDA G climax condition)	394
Table 48	Aboveground Production of Grasses, Forbs, and Shrubs in Mature Piñon-Juniper Woodlands	397
Table 49	Aboveground Biomass and Net Primary Productivity Estimates for Trees in Piñon-Juniper Woodlands	398
Table 50	Litter Decomposition Rate Constants	403
Table 51	Parameter Values and Distributional Information for Native Plant Uptake Factors	405
Table 52	Summary of Harvester Ant (*Pogonomyrmex* spp.) Colony Densities	409
Table 53	Small Mammal Densities at MDA G and Background/Control Areas	410
Table 54	Summary of Harvester Ant Colony Lifetimes	413
Table 55	Water Needs of Crops	420
Table 56	Radionuclide Half-Lives and Dose Conversion Factors	429

List of Attachments

Attachment I Diffusion Model Optimization Analyses

Attachment II Development of Layer-Specific Inventories for the 1988–2004 Disposal Shafts

Acronyms and Abbreviations

ACH	Air exchanges per hour
bgs	Below ground surface
CFR	Code of federal regulations
DOE	Department of Energy
EPA	U.S. Environmental Protection Agency
FEHM	Finite element heat and mass
IAEA	International Atomic Energy Agency
Laboratory	Los Alamos National Laboratory
LANL	Los Alamos National Laboratory
LLW	Low-level (radioactive) waste
MAP	Mixed activation products
MDA	Material Disposal Area
MFP	Mixed fission products
msl	Mean sea level
NCRP	National Council on Radiation Protection and Measurements
NRC	U.S. Nuclear Regulatory Commission
NTS	Nevada Test Site
ORNL	Oak Ridge National Laboratory
TA	Technical Area
TRU	Transuranic waste
USDA	US Department of Agriculture
WAC	Waste acceptance criteria

1.0 Introduction

U.S. Department of Energy (DOE) Order 435.1 (DOE, 2001a), as implemented by the *Radioactive Waste Management Manual*, (DOE, 2001b) requires that site-specific performance assessments and composite analyses be prepared for low-level radioactive waste (LLW) disposal facilities that accept waste after September 26, 1988. These assessments and analyses project the potential impacts of the buried waste on human health and safety, and are used to ensure that potential risks remain within acceptable levels. The performance assessment specifically addresses waste disposed of after September 26, 1988. The composite analysis accounts for all sources of radioactive material that may interact with a LLW disposal facility, and that contribute to any projected impacts on human health and safety.

The Los Alamos National Laboratory (LANL or the Laboratory) generates radioactive waste as a result of various activities. The majority of this is LLW and is disposed of at Technical Area (TA) 54, Material Disposal Area G (MDA G). Disposal operations began at this facility in 1957 and are projected to continue until 2044. The performance assessment and composite analysis for MDA G were first issued in 1997 (Hollis et al., 1997) in compliance with DOE Order 5820.2A (DOE, 1988), the predecessor to DOE Order 435.1 (DOE, 2001a), and have recently been revised (LANL, 2006). These analyses define, quantify, and model the engineering, social, and environmental variables associated with the disposal units located at MDA G.

The MDA G performance assessment and composite analysis use a series of models that simulate radionuclide release, transport, and uptake in the vicinity of the disposal facility. These models have been integrated using the GoldSim™ modeling environment or platform (GoldSim, 2005a and 2005b); the result is four models designed to address different aspects of disposal facility performance:

- The *MDA G Site Model*, which estimates the exposures received by members of the public at locations downgradient and downwind of MDA G for all radionuclides except vapor- and gas-phase isotopes
- The *MDA G Site Diffusion Model*, used to project exposures received by members of the public following releases of vapor- and gas-phase radionuclides
- The *MDA G Intruder Model*, which projects inadvertent intruder doses for all radionuclides except vapor- and gas-phase isotopes
- The *MDA G Intruder Diffusion Model*, which addresses intruder exposures resulting from radionuclides that undergo diffusive release and transport

Both of the site models estimate radionuclide concentrations in various environmental media; these concentrations are used to calculate doses for exposed individuals, or receptors. The two intruder models are used to estimate exposures for persons who inadvertently intrude into the buried waste after active institutional control over the disposal site has ended.

This report documents the GoldSim models that were used to conduct the MDA G performance assessment and composite analysis and the data that were used to implement the models. Section 2 provides a general overview of each model's structure and discusses how the various components of each model fit together. Section 3 describes the conceptual and mathematical models upon which the GoldSim models are based. Section 4 provides a complete tabulated listing of the input parameters required to implement the models. Finally, Section 5 discusses the data adopted for these parameters and how they were selected.

2.0 Model Description and Organization

A general description of the models used to conduct the MDA G performance assessment and composite analysis is provided below. Insight into the GoldSim modeling environment is needed to understand how these models are organized and implemented; Section 2.1 provides information summarized from the user's guides for GoldSim (GoldSim, 2005a) and the GoldSim contaminant transport module (GoldSim, 2005b) to address this need. The primary objective of the performance assessment and composite analysis modeling is to estimate potential exposures to persons, or receptors, exposed to contamination released from MDA G. These receptors determine the transport processes, environmental media, and exposure pathways that must be addressed and thus dictate the overall structure of the models. Section 2.2 discusses the receptors included in the performance assessment and composite analysis. Finally, Section 2.3 describes the general layout of the models used to conduct the performance assessment and composite analysis.

2.1 GoldSim Modeling Basics

GoldSim represents the system being modeled using objects known as elements. These elements are used to input data into the model, perform calculations using defined inputs, and physically represent the system being modeled. To model a facility such as MDA G, the species or radionuclides of interest are defined and their properties are specified. The physical components of the system (e.g., the disposal units, the atmosphere, and the regional aquifer) are represented using transport pathway elements. The system being modeled is reflected by the geometry of these transport pathway elements and the environmental media (e.g., soil, water, and air) that comprise the pathway elements. The transport pathway elements are connected to one another using mass-flux links, which define the rates at which radionuclides move from one physical compartment to another. The result is a dynamic simulation of the movement of radionuclides from the disposal units to locations that are accessible to human receptors. Contaminant concentrations projected for the various environmental media at these locations form the basis for calculating rates of radionuclide intake for the receptors and the consequent doses.

The transport pathway elements used in the MDA G models include cell and external pathways. Cells are mathematically equivalent to mixing cells; contamination introduced into a cell is instantaneously and completely mixed throughout the element. A cell is defined in terms of the environmental media of which it is composed; distribution coefficients and solubility limits are used to partition radionuclides among these media. For example, cells are used in the MDA G models to represent surface soils at the disposal site and at off-site exposure locations. The environmental media used to represent these soils typically include crushed tuff and water (present as soil moisture). These cells may also include the air occupying the pore space in the

soil. Distribution coefficients are used to partition radionuclides present in the surface soil among the crushed tuff and the soil moisture and, in the case of vapor- and gas-phase contaminants, the air in the pore spaces. Solubility limits may be used to place additional limits on the amount of contamination present in the soil moisture.

External pathways are modules that are linked to a GoldSim model as dynamic link libraries at the time the model is run. They are used to integrate specialized contaminant transport models, developed outside of GoldSim, with other GoldSim elements. External pathway elements are used in the MDA G Site Model to simulate the groundwater transport of radionuclides from the disposal units to locations downgradient of the disposal facility. These elements accept as input the masses of radionuclides leached from the waste and transport this contamination vertically through the unsaturated zone until it reaches the regional aquifer. From that point, the contaminants are transported through the aquifer toward a domestic well downgradient of MDA G. The projected quantities of radionuclides reaching the well are passed to GoldSim elements that use the information to project potential groundwater impacts.

Three types of links or transfers are used to represent the transport of contaminants between transport pathway elements. Advective mass-flux links are used to simulate the transport of contamination associated with the movement of environmental media. The media move at rates specified by the user; contaminants that are dissolved in, sorbed to, or otherwise associated with the media are transported in the process. Advective transport is normally associated with the movement of fluid such as water or air. However, it may also be used to simulate the transport of radionuclides associated with solids. For example, the GoldSim models use advective mass-flux links between cells to simulate the transport of soil by burrowing animals to the surface of the disposal facility; advective mass-flux links are also used to pass information to the external pathways and to receive the output from these elements.

Diffusive mass-flux links are used to transport contaminant mass through a stagnant or slowly moving fluid via the process of molecular diffusion. These links are commonly used to simulate transport between pathway elements that are not dominated by advective process. An example relevant to the MDA G models includes the transport of gas- and vapor-phase radionuclides from the waste to the surface of the disposal facility.

Direct-transfer mass-flux links are used to directly move contaminant mass between transport pathway elements in situations where advective or diffusive flows are inappropriate. These links are used in the GoldSim models to simulate the uptake of radionuclides by plants growing in contaminated soils. In this instance, no fluid or solid passes from the source of contamination to the plant, and the diffusion process does not explain the contaminant transfer.

2.2 Human Exposure Pathways and Exposure Scenarios

The performance assessment and composite analysis are conducted to provide assurance that the performance objectives identified in DOE M 435.1-1 (DOE, 2001b) are satisfied. These performance objectives consist primarily of radiation dose limits for humans who are exposed to environmental media contaminated by releases from the waste disposal facility. As a result, MDA G modeling efforts focused on the projection of doses to persons who may come into contact with, or otherwise be exposed to, radionuclides released from the disposal units.

Humans are exposed to radioactive media by means of different exposure pathways. Each exposure pathway includes a source or release from a source, a transport or exposure medium, a location at which the exposure occurs, and an exposure route. The actual exposure pathways that may lead to human exposures will depend upon the patterns of human activity at, and adjacent to, the disposal site. Patterns of human activity are specified using a collection of appropriate exposure pathways generally referred to as an exposure scenario.

The exposure pathways and scenarios through which people may be exposed to the radioactive waste at MDA G are specific to different stages in the lifetime of the facility. Thus, to understand the basis for pathway and scenario development, it is necessary to understand these stages, which can be described as follows:

- *Operational period*, during which waste is placed in disposal pits and shafts, and interim or operational covers are placed over filled units
- *Closure period*, during which any remaining surface structures are removed from the site and all disposal units undergo final closure
- *Active institutional control period*, during which the DOE exercises control over the entire Laboratory
- *Passive institutional control period*, during which the DOE controls access to individual facilities such as MDA G

The operational period is assumed to last through the year 2044. While portions of the disposal facility will undergo final closure prior to 2044, closure of the final units receiving waste is assumed to be completed by the end of 2046. The 100-year active institutional control period starts at the end of final closure and is followed by the passive institutional control period in 2147.

It is assumed that the DOE will retain control over the entire Laboratory throughout the operational, closure, and active institutional control periods. During these periods, members of the public will be prevented from entering the disposal facility, the site will be maintained to

slow the establishment of deep-rooted plants, and actions will be taken as necessary to repair any significant damage to the cover. Although control over the entire Laboratory will cease at the end of the active institutional control period, it is assumed that the DOE will continue to exercise administrative control over individual sites such as MDA G. This level of control will generally prevent people from entering the closed site; no other maintenance activities are assumed to occur during the passive institutional period.

The level of control outlined above limits exposures during the operational, closure, and active institutional control periods to receptors who are located downwind or downgradient of the Laboratory; exposures may occur as radionuclides released from the disposal facility are transported by the prevailing winds, surface water, or groundwater to downwind or downgradient locations. The exposure pathways and scenarios modeled for these periods are discussed in Section 2.2.1. During the passive institutional control period, it is possible that potential receptors may move closer to the disposal area, perhaps as near as the MDA G fence line. The possibility of inadvertent human intrusion into the facility is also considered. The exposure pathways and scenarios modeled for this period are discussed separately, in Section 2.2.2.

2.2.1 Operational, Closure, and Active Institutional Control Periods

The sources of contamination to which members of the public may be exposed will change as the site passes from the operational period to the active institutional control period. Although plants and animals may root or burrow into the buried waste and bring contamination to the surface of the disposal facility, the quantities of contamination deposited on the surface during the operational and closure periods will be small. In part, this is because the establishment of plant and animal communities at the site will be slowed, or even prevented, by ongoing operations and the closure process itself; also, any signs of significant intrusion into the waste will be remedied. The potential does exist, however, for radionuclides to be leached from the buried waste by water infiltrating through the site and for gas or vapor-phase contaminants to diffuse from the waste and enter the atmosphere. Radioactivity leached from the waste may be transported to the regional aquifer and result in exposures to receptors downgradient of the site. Similarly, persons living downwind of MDA G may be exposed to airborne contaminants transported off-site by prevailing winds.

The steps taken to ensure proper facility functioning during the active institutional control period will not prevent plant roots and animal burrows from penetrating into the waste and depositing contamination on the surface. This contamination may be transported by surface runoff into the canyons adjacent to MDA G; it may also be suspended and transported by the prevailing winds to locations downwind of the Laboratory. Contamination transported by surface runoff into Cañada del Buey, the drainage to the north of MDA G, could expose members of the public to contamination during the active institutional control period because a portion of this canyon lies

outside of the Laboratory boundary. Also, members of the public living outside the Laboratory boundary may continue to be exposed to radionuclides discharged to the regional aquifer and to gas- and vapor-phase contaminants carried by the prevailing winds.

The exposure scenarios selected to estimate the exposures received by members of the general public are summarized in Table 1; these scenarios consider the sources of contamination discussed above. Two of these scenarios, the Groundwater Resource Protection Scenario and the All Pathways – Groundwater Scenario, are implemented at the Laboratory boundary near the town of White Rock. Projected exposures for the first are limited to the ingestion of contaminated groundwater and are used to assess compliance with groundwater protection standards. For the All Pathways – Groundwater Scenario, the receptor is assumed to receive exposures from the inhalation and ingestion of radioactivity, and from direct radiation. Radionuclides applied to the surface soil with irrigation water are suspended and inhaled by the individual during the time spent at home. Ingestion doses result from the consumption of crops irrigated with contaminated water, products from animals (e.g., beef and milk or chicken and eggs) raised by the resident, soil, and drinking water. Exposures to direct radiation from airborne contamination at the homestead and radioactivity deposited on the soil add to any internal (inhalation and ingestion) exposures.

The Atmospheric Scenario is implemented at the point of maximum atmospheric exposure outside of the Laboratory's boundaries (Table 1). The receptor inhales radioactive gases (except radon and its progeny) during the operational and closure periods; particulates resuspended from the surface of MDA G and transported with the prevailing winds add to these exposures following closure. The deposition of airborne radionuclides contaminates crops grown by the individual and surface soils at the exposure location. Doses are received through the ingestion of contaminated vegetables, animal products, and soil. External exposures are received from contaminated soil surfaces and airborne radioactivity. Radon fluxes from the disposal site are projected separately.

The All Pathways – Cañada del Buey Scenario addresses exposures to receptors following the transport of contamination from Mesita del Buey to the canyon as a result of surface runoff and erosion. A person residing in the canyon is assumed to be exposed to radiation as a result of inhaling particulates suspended from contaminated soil surfaces and by ingesting contaminated crops, animal products, and soil. Exposures to direct radiation from airborne contamination at the homestead and radioactivity deposited over the resident's lot add to the internal exposures.

Table 1
Exposure Scenarios for the Operational, Active Institutional, and Passive Institutional Control Periods

Period and Exposure Scenario	Exposure Pathways and Routes	Receptor	Point of Exposure
Operational, Closure, and Active Institutional Control Periods			
Groundwater Resource Protection	Ingestion of drinking water	Member of the public	LANL boundary near White Rock
All Pathways — Groundwater	• Ingestion of drinking water • Ingestion of food crops irrigated with well water • Ingestion of animal products from animals raised by the receptor • Ingestion of contaminated soil • Inhalation of airborne radionuclides • Direct radiation from airborne radionuclides • Direct radiation from contaminated soils	Member of the public	LANL boundary near White Rock
Atmospheric	• Ingestion of food crops grown in contaminated soils and contaminated by airborne radionuclides • Ingestion of animal products from animals raised by the receptor • Ingestion of contaminated soil • Inhalation of airborne radionuclides • Direct radiation from airborne radionuclides • Direct radiation from contaminated soils	Member of the public	Point of maximum exposure outside of LANL boundary
All Pathways — Cañada del Buey	• Ingestion of food crops grown in contaminated soils • Ingestion of animal products from animals raised by the receptor • Ingestion of contaminated soil • Inhalation of airborne radionuclides • Direct radiation from airborne radionuclides • Direct radiation from contaminated soils	Member of the public	Cañada del Buey adjacent to MDA G

Table 1 (Continued)
Exposure Scenarios for the Operational, Active Institutional, and Passive Institutional Control Periods

Period and Exposure Scenario	Exposure Pathways and Routes	Receptor	Point of Exposure
Passive Institutional Control Period			
Groundwater Resource Protection	Ingestion of drinking water	Member of the public	100 m downgradient of MDA G
All Pathways — Groundwater	• Ingestion of drinking water • Ingestion of food crops irrigated with well water • Ingestion of animal products from animals raised by the receptor • Ingestion of contaminated soil • Inhalation of airborne radionuclides • Direct radiation from airborne radionuclides • Direct radiation from contaminated soils	Member of the public	100 m downgradient of MDA G
Atmospheric	• Ingestion of food crops grown in contaminated soils and contaminated by airborne radionuclides • Ingestion of animal products from animals raised by the receptor • Ingestion of contaminated soil • Inhalation of airborne radionuclides • Direct radiation from airborne radionuclides • Direct radiation from contaminated soils	Member of the public	Point of maximum exposure outside of MDA G boundary
All Pathways — Cañada del Buey	• Ingestion of food crops grown in contaminated soils • Ingestion of animal products from animals raised by the receptor • Ingestion of contaminated soil • Inhalation of airborne radionuclides • Direct radiation from airborne radionuclides • Direct radiation from contaminated soils	Member of the public	Cañada del Buey adjacent to MDA G

Table 1 (Continued)
Exposure Scenarios for the Operational, Active Institutional, and Passive Institutional Control Periods

Period and Exposure Scenario	Exposure Pathways and Routes	Receptor	Point of Exposure
All Pathways — Pajarito Canyon	• Ingestion of food crops grown in contaminated soils • Ingestion of animal products from animals raised by the receptor • Ingestion of contaminated soil • Inhalation of airborne radionuclides • Direct radiation from airborne radionuclides • Direct radiation from contaminated soils	Member of the public	Pajarito Canyon adjacent to MDA G
Intruder-Construction	• Inhalation of airborne radionuclides • Direct radiation from airborne radionuclides • Direct radiation from contaminated soils	Construction worker	MDA G
Intruder-Agriculture	• Ingestion of food crops grown in contaminated soils • Ingestion of animal products from animals raised by the receptor • Ingestion of contaminated soil • Inhalation of airborne radionuclides • Direct radiation from airborne radionuclides • Direct radiation from contaminated soils	Agricultural intruder	MDA G
Intruder – Post-Drilling	• Ingestion of food crops grown in contaminated soils • Ingestion of animal products from animals raised by the receptor • Ingestion of contaminated soil • Inhalation of airborne radionuclides • Direct radiation from airborne radionuclides • Direct radiation from contaminated soils	Post-drilling intruder	MDA G

2.2.2 Passive Institutional Control Period

Radionuclide releases to groundwater and the atmosphere may continue after active institutional control has ceased and may result in exposures to the members of the public. Also, the change in the scope of DOE control will provide an opportunity for members of the public to locate immediately outside of the MDA G fence line. Exposures to receptors during the passive institutional control period are projected using the exposure scenarios listed in the latter half of Table 1. The two groundwater scenarios and the Atmospheric Scenario are functionally the same as those evaluated for the operational and active institutional control periods. The groundwater scenarios are implemented 100 m (330 ft) downgradient of MDA G. The Atmospheric Scenario is implemented at the point of maximum exposure outside of the MDA G fence line; radon fluxes from the disposal site are projected separately.

The All Pathways – Cañada del Buey Scenario is the same as that evaluated during the active institutional control period. In addition, the loss of control over the entire Laboratory provides an opportunity for persons to reside in Pajarito Canyon, to the south of MDA G. Potential exposures received by a person residing in this canyon are evaluated using the All Pathways – Pajarito Canyon Scenario. Contamination transported into the canyon with surface runoff and erosion is assumed to lead to exposures of the canyon resident via the same pathways described for the scenario in Cañada del Buey.

It is assumed that control over MDA G during both active and passive institutional control periods will prevent members of the public from establishing residences over the closed pits and shafts. Nevertheless, brief lapses in custodial responsibilities after the active institutional control period may provide opportunities for inadvertent intruders to initiate on-site activities that result in exposures to radioactivity. Because these exposures may be substantial, inadvertent intruder analyses are conducted to establish concentration limits for the waste disposed of at MDA G.

The performance assessment models potential exposures for the Intruder-Construction, Intruder-Agriculture, and Intruder – Post-Drilling Scenarios for the purpose of developing waste acceptance criteria (WAC) for MDA G. Descriptions of these scenarios are included in the bottom half of Table 1. Depending upon the scenario under consideration, exposures are received from the inhalation of airborne particulates and gas- and vapor-phase radionuclides (except radon) diffusing from the waste; the ingestion of contaminated crops, animal products, and soil; and external radiation from contaminated soils and airborne radionuclides. The primary source of contamination for the Intruder-Agriculture and Intruder – Post-Drilling Scenarios is waste brought to the surface during basement excavation and well drilling, respectively. Waste brought to the surface during basement excavation and contaminated material in the excavation itself is considered in the estimation of exposures for the Intruder-Construction Scenario. Contamination brought to the surface of the disposal facility as a result of biotic intrusion prior to the arrival of an intruder at the site may add to the intruder's exposures, as may vapor- and gas-phase radionuclides diffusing upward from the waste.

2.3 Model Organization

The MDA G Site Model simulates the release and transport of radionuclides to the surface of the disposal facility and to off-site locations for all natural processes except vapor and gas diffusion, and estimates doses for receptors at these locations. The site diffusion model estimates rates of release of vapor- and gas-phase radionuclides, simulates the diffusion of these species through the buried waste and the overlying cover, and projects exposures for off-site receptors. The two intruder models are used to project doses to persons who inadvertently intrude into the disposed waste after active institutional control has ended. The site and site diffusion models are described in Sections 2.3.1 and 2.3.2, respectively; Sections 2.3.3 and 2.3.4 discuss the intruder and intruder diffusion models.

2.3.1 MDA G Site Model

The general organization of the MDA G Site Model is shown in Figure 1. The model is divided into two major segments, as delineated by the shaded boxes surrounding the model elements. The first segment contains the elements that define the input data required to run model simulations and describe the process models used to estimate rates of radionuclide release and transport, contaminant uptake, and exposure. The second portion of the site model defines the physical compartments that are used to represent MDA G and the surrounding environment. These compartments represent the disposal facility itself and the locations at which receptors are exposed to radioactive contamination.

Each of the major segments of the MDA G Site Model consists of a series of GoldSim elements called containers (shown as open or closed yellow boxes in Figure 1); the segment containing the input data and process models also includes an element called the master clock. The containers are used to group related model input parameters and to organize the process models and physical components. Within each container are the GoldSim elements that define the model; additional containers are used in many instances to further organize the model. The following sections, which describe the general layout of the different segments of the MDA G Site Model, are organized in a manner consistent with Figure 1.

2.3.1.1 Input Data and Process Models

The MasterClock element, input data, and process models used in the MDA G Site Model are found in this segment of the model. The input data characterize the system being modeled; the process models are used to calculate rates of contaminant transport between physical compartments and to project human exposures. The following discussion summarizes the contents of each of the containers shown in Figure 1, including input data and intermediate or calculated parameters. Complete definitions of the input parameters may be found in Section 4. The equations used to calculate intermediate parameters and to implement the process models are discussed in Section 3.

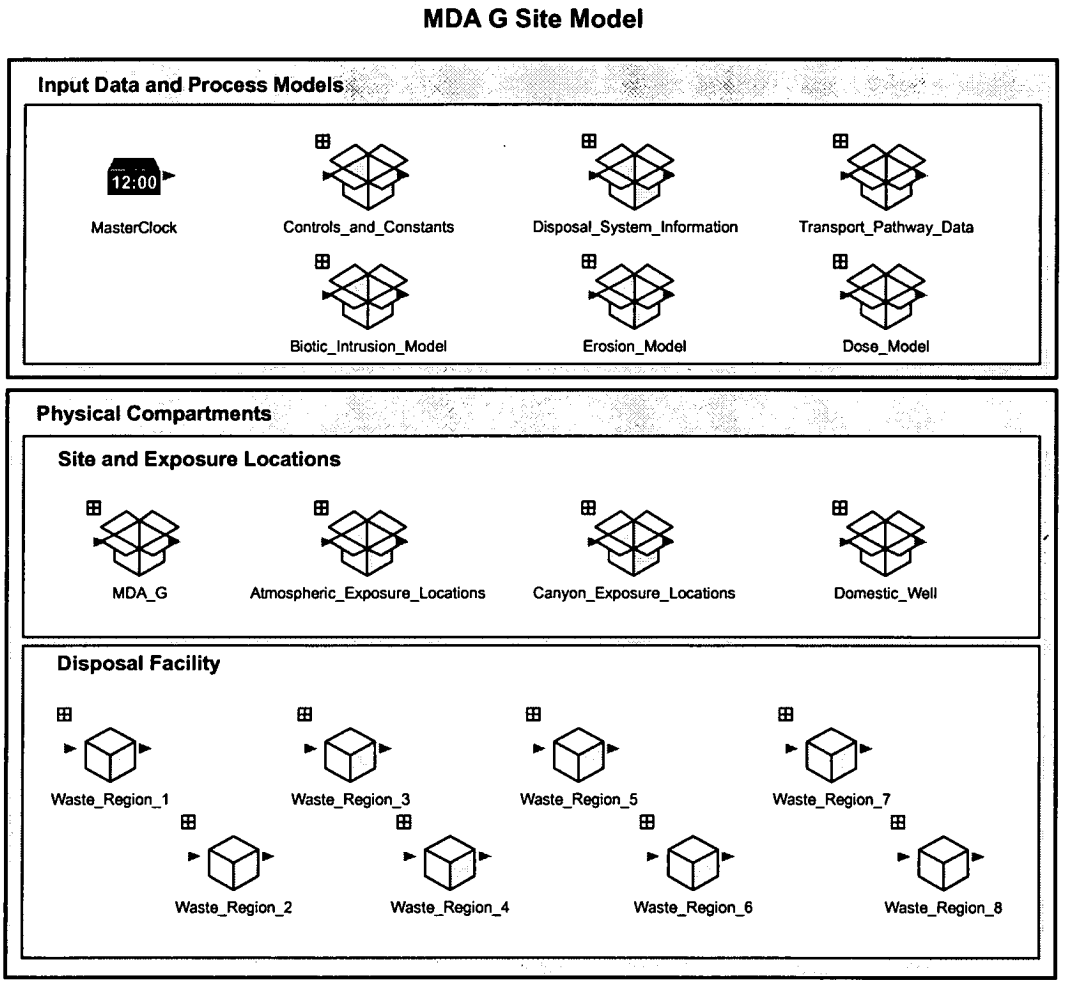

Figure 1
General Organization of the MDA G Site Model

Master clock. The MasterClock element is an inherent part of all models constructed using GoldSim. This element controls how dynamic simulations are implemented, in effect keeping track of time. Parameters tracked by the element include the elapsed time since a specific date or the start of the simulation, the length of the time step(s) used in the simulation, and the realization number within a probabilistic analysis.

Controls and constants. The Controls_and_Constants container includes flag variables used to control the simulation. The Analysis_Flag specifies which analysis is being conducted (i.e., the performance assessment or composite analysis). The primary distinction between the two analyses is the radioactive waste inventory used in the model simulations. The inventory corresponding to the waste disposed of since September 26, 1988 is used if the performance assessment option is selected, while waste disposed of since MDA G opened is included in the composite analysis.

Disposal system information. The Disposal_System_Information container includes data that characterize the radionuclides in the waste, the environmental media comprising the physical compartments, the disposal facility, and the waste inventory. Within this container are found the Species_and_Materials, Site_Geometry_and_Operations, and Inventory containers. The elements found within the Species_and_Materials container include:

- Data elements that specify the half-lives of the radionuclides included in the simulation and calculate the corresponding radioactive decay constants
- A Species element that defines the element, atomic weight, and decay characteristics for each radionuclide included in the modeling
- A Material_Properties container that organizes information about the environmental media that are used in the model. This information includes effective porosities, moisture contents, dry and bulk densities, partition coefficients, the density of water, solubility coefficients, and elements defining carbon and hydrogen contents in soil and water.
- The environmental media (i.e., crushed tuff, waste, water, and air) that are used to define cell pathways

As implied by its name, the Site_Geometry_and_Operations container organizes the parameters that specify key physical dimensions of the disposal units and important operational aspects of MDA G. For reasons discussed in detail in Section 3, the disposal facility is divided into a number of areas. The primary subdivisions are eight waste disposal regions. These regions are defined on the basis of the geohydrologic properties of the underlying unsaturated zone and the depths at which waste has been disposed of in the pits and shafts. Each of these waste disposal regions is divided into 10 erosion zones that represent different rates of surface erosion.

Many of the parameters included in the Site_Geometry_and_Operations container are specific to the waste disposal regions and erosion zones discussed above. One example is the times at which waste disposal start and stop for the eight regions. The times of disposal are used to calculate periods of disposal for the eight regions and are used in conjunction with the closure period to estimate the total operational period for the facility. The Site_Geometry_and_Operations container holds nine additional containers; the Layer_Information container includes information needed to divide the cover and waste into a series of discrete layers. The other eight disposal region-specific containers organize information about the area of each region and the initial thickness of the surface soil, cover, and waste layers; additional elements are used to calculate the areas and fractional areas associated with the 10 erosion zones that comprise each waste region.

The Inventory container includes the elements that are used to estimate the inventories of the radionuclides used in the performance assessment and composite analysis. The majority of the containers and elements shown are used to estimate the uncertainties associated with the inventories. Section 3 provides a full explanation of these elements and the calculations in which they are used.

Transport pathway data. The Transport_Pathway_Data container includes input data and calculated parameters needed to model rates of radionuclide transport. These parameters are organized in four containers labeled Atmospheric_Transport, Groundwater_Transport, Foodchain_Transport, and Sediment_Transport. Input data found in the Atmospheric_Transport container include dust-loading and particulate-resuspension information; the dispersion factors and particulate deposition rates used to estimate radionuclide concentrations for the Atmospheric_Scenario receptor are included in separate containers. These data are organized with respect to the location of the receptor.

The Foodchain_Transport container includes the input data required to estimate the rates of radionuclide uptake for crops raised by the receptors and to estimate radionuclide concentrations in animal products. The crop and animal data are organized in two containers, Plant_Data and Animal_Data. The Plant_Data container is subdivided into the Uptake_Factors and Crop_Characteristics containers. The former includes the plant-to-soil concentration factors for the crops raised by the receptors, including leafy vegetables, produce, grain, and pasture grass. Input data describing the crops are found in the Crop_Characteristics container. These parameters include dry-to-wet-weight conversion factors, translocation factors, agricultural productivities, lengths of growing seasons, and mass-loading factors. The plant interception coefficient, weathering half-life, particle size factor, and plant hydrogen and carbon fractions are also included in the container. Calculated quantities include the plant interception fractions, the weathering constant, and the areas needed to grow crops.

The Animal_Data container, located within the Foodchain_Transport container, includes data that are used to estimate radionuclide concentrations in beef, milk, chicken, and eggs. The Animal_Ingestion_Data container specifies soil, water, and forage ingestion rates for cattle, milk cows, and chickens. The Transfer_Factors container includes the transfer factors needed to estimate radionuclide concentrations in animal products based on contaminant concentrations in the soil, water, and forage consumed by cattle, cows, and chickens.

The Groundwater_Transport container includes the input data and intermediate parameters needed to model groundwater flow in the unsaturated and saturated zones. The input data include natural rates of infiltration on Mesita del Buey, in the adjacent canyons, and at receptor locations east of MDA G. The contaminant capture fraction is also included. The Flowfield element is used to structure the groundwater transport modeling.

The Sediment_Transport container includes information that is used to determine radionuclide concentrations in canyon soils, following the transport of sediments from the mesa top. The data elements specify how sediment transported from the mesa is partitioned among several catchments in Cañada del Buey and Pajarito Canyon, the areas of these catchments, the fraction of each catchment over which sediments spread upon reaching the canyon floor, and the rates of sediment transport between catchments.

Biotic intrusion model. The Biotic_Intrusion_Model container includes the input data and models used to estimate rates of radionuclide transport to the surface of MDA G following penetration of the disposed waste by plant roots and burrowing animals. The impacts of plants and animals change over time as the disposal site undergoes ecological succession from the grassland-dominated landscape shortly after final closure to piñon-juniper woodland. The Eco_Succession_Model container estimates the fraction of the climax condition achieved as a function of time using the user-specified Time_of_Climax parameter. The Shape_Parameters container includes coefficients that are used to estimate plant root and animal burrow distributions with depth.

The data and models used to estimate the impacts of animal intrusion on the buried waste are found in the Animal_Intrusion_Model container. The impacts of four species or categories of burrowing animals are simulated; these categories include harvester ants, pocket gophers, mice, and chipmunks and ground squirrels. The models and data used for each species or group of animals are found in their respective containers. The input data required to model the effects of intrusion are specific to the animal under consideration but include parameters such as maximum burrow depths; burrow densities, volumes, and/or masses; and burrow renewal rates. This information is used with burrow distribution functions to determine rates of soil and soil moisture transport for each animal species or group, within each waste disposal region and erosion zone. This taxa-specific information is used in the Animal_Soil_Transport and

Animal_Water_Transport containers to determine overall soil and soil moisture transport rates for the eight waste disposal regions.

The input data and models used to simulate the intrusion of plants into the buried waste are found in the Plant_Intrusion_Model container. The impacts of plant intrusion are simulated for four plant-growth forms — grasses, forbs, shrubs, and trees. The models and data used for each growth form are found in their respective containers within the Plant_Intrusion_Model container. The data required to model the effects of plants include maximum rooting depths, aboveground biomass densities for early succession and climax conditions, litter production fractions, and plant concentration factors. These data are used in conjunction with functions that describe root distribution with depth to estimate rates of plant litter production within each erosion zone and waste disposal region. Litter production rates across all growth forms are calculated in the Total_Plant_Litter_Production container; they are used in the Plant_Uptake container to estimate the quantities of contamination assimilated by plants for the various erosion zones and waste disposal regions. The Litter_Halflife and Litter_Decay_Constant elements are used to model the incorporation of contaminated plant litter into the surface soil.

Erosion model. The Erosion_Model container includes the data and models used to estimate rates of soil loss across the closed disposal facility. The erosion rate functions are defined using a variety of elements found in the Erosion_Rates container. Included here are the remaining cover depths associated with the 10 erosion zones (found in the Erosion_Zone_Data container), shape factors used to specify the erosion rate functions (located in the Shape_Factors container), the rate functions themselves, and a series of elements that calculate annual erosion rates and cumulative soil loss for the different waste disposal regions and erosion zones. The results of the calculations conducted within the Erosion_Rates container are used to update the cap and waste thicknesses throughout the model simulations. These calculations are organized in a series of waste disposal region-specific containers. Elements inside these containers update cap and waste layer thicknesses and cumulative depths to the bottoms of these layers.

Dose model. The Dose_Model container includes data and functions required to estimate doses for the off-site receptors, using radionuclide masses or concentrations projected for the pertinent physical compartments and environmental media. The input data are organized in two containers. The Dose_Conversion_Factors container includes the ingestion, inhalation, and direct radiation dose conversion factors for exposures to contaminated soils and air immersion. The Exposure_Pathway_Data container includes a variety of parameters required to model exposures. These include indoor and outdoor exposure times for the receptors; the inhalation rate; areas of the receptor's lot and house; and the direct radiation shielding factor for the receptor's house. Crop irrigation data are found in the Irrigation_Rates container; these data are used to calculate well pumping rates and estimate radionuclide concentrations in crops. The ingestion data

container includes consumption rates for crops, animal products, soil, and water, along with expressions that estimate how much of the receptor's diet is raised at the exposure location.

The models that are used to project doses for the performance assessment and composite analysis are found in three exposure scenario containers. These containers organize the calculations that are undertaken to estimate potential doses for the atmospheric, canyon, and groundwater-pathway-based scenarios. The dose calculations for the Atmospheric Scenario are implemented at two locations, corresponding to the points of maximum exposure before and after the end of active institutional control, while the groundwater scenarios are implemented at one location. Exposures to persons residing in the adjacent canyons are evaluated at a total of nine locations, each of which is subject to different rates of sediment transport from the mesa. The exposure concentrations used for each exposure scenario are found in the Media_Concentrations containers; the functions used to estimate receptor doses are organized by exposure route. The calculated doses are summed across exposure routes and radionuclides to provide summary doses for each scenario.

2.3.1.2 Physical Compartments — Site and Exposure Locations

This segment of the MDA G Site Model includes physical representations of site and exposure locations that are used in the modeling. These locations include MDA_G, Atmospheric_Exposure_Locations, Canyon_Exposure_Locations, and the Domestic_Well. The MDA_G location includes the air above the disposal site; estimates of the rates at which resuspension transfers particulates to the air above the site are used to project downwind concentrations of radionuclides for the Atmospheric Scenario. The remaining locations are used to estimate exposures for the atmospheric, all pathways, and groundwater pathway scenarios.

The exposure location containers shown in Figure 1 include the transport pathway elements used by GoldSim to represent environmental media at the points of exposure. Contaminant masses and concentrations are determined for these media based on user-specified rates of inflow and outflow for each transport pathway. These masses and concentrations form the basis of the media concentrations calculated in the Dose_Model container and, therefore, the dose calculations.

In general, cell pathways are used to represent the different environmental media at the site and exposure locations. Three cells are used within the MDA_G container to represent the air above different portions of the disposal site. Advective mass-flux links are used to represent the resuspension of particulates from the surface of the facility to the air above. Two exposure locations are considered for the Atmospheric Scenario including the point of maximum exposure outside of the LANL boundary and the corresponding location immediately downwind of the MDA G fence line; these locations are represented in the Atmospheric_Exposure_Locations container. Two cells are used to represent exposure media at each of these locations. The Exposure_Location_Soils cell represents the surface soils at a given location, an advective mass-

flux link moves soil moisture from this cell to the sink element to represent the transport of contamination with water infiltrating through the receptor's lot.

A total of nine canyon locations are evaluated to estimate doses received by persons residing in Cañada del Buey and Pajarito Canyon. For each location, a cell is used to represent the canyon soils over which the receptor resides and raises crops and animals. Advective mass-flux links join these cells with the surface soils in the eight waste disposal regions on top of Mesita del Buey. These links are used to represent the movement of soils into the canyon due to surface runoff and erosion. Links between the surface soil cells represent the transport of sediment down each canyon; links with a sink term are used to simulate the movement of radionuclides with water percolating through the receptor's lot.

A single receptor location 100 m (330 ft) downgradient of the MDA G fence line is used in the site model for estimating potential groundwater pathway exposures. Four cells found in the Domestic_Well container represent the well, the surface soils at this location, and sink terms for the well water and soils for the All Pathways – Groundwater Scenario. Advective mass-flux links define the inflow of water from the regional aquifer to the well, and the outflow of water to surface soils at locations where receptors irrigate crops. Inflows from the aquifer are ultimately proportional to the total water demands of the receptors, while outflows to the surface soils are proportional to rates of irrigation. Surface soils are subject to the aforementioned inflows of water and outflows to a sink term. The advective flow of soil moisture to the sink term represents the infiltration of water through the receptor's lot while the well sink term is used to represent water within the regional aquifer that flows past the well. Radionuclide concentrations in the water consumed by the Groundwater Resources Protection Scenario receptor are calculated directly from aquifer-to-well advective fluxes projected by the site model; consequently, no physical representation of this receptor's well is included in the model.

While exposures to contaminated groundwater may occur at the boundary of LANL prior to the loss of active institutional control, this exposure location is not included in the site model. This is because the results of the groundwater pathway modeling conducted in support of the performance assessment and composite analysis indicated that no radionuclides reach this location before the end of the 100-year active institutional control period. Groundwater exposures will be greatest immediately downgradient of the disposal facility following the end of active institutional control. Consequently, only a single location needs to be considered.

2.3.1.3 Physical Compartments — Disposal Facility

The eight waste disposal regions used to model the long-term performance of MDA G are represented using a series of cell pathways and other GoldSim elements; these elements are organized in a series of disposal region-specific containers. Within each of these containers are several elements and 10 containers corresponding to the erosion zones within the disposal region.

Cell pathways are used to represent the surface soil, cap material, and waste within each erosion zone. The surface soil cells represent the uppermost portion of the cover placed over the waste; these cells are used to define radionuclide source terms for the Atmospheric, All Pathways – Cañada del Buey, and All Pathways – Pajarito Canyon Scenarios. Advective mass links are used to simulate the transport of contaminants to the surface of the disposal facility by animals that penetrate into the waste; direct transfers are used to simulate the uptake of radionuclides by plants growing over the disposal units and the deposition of these contaminants on the surface through litterfall and decay. The outflows from the surface soil cells account for the settling and collapse of animal burrows, resuspension of particulates, transport of waterborne contaminants downward with infiltrating water, and movement of soils into Cañada del Buey and Pajarito Canyon with surface runoff.

The cap cells represent the cover material placed over the buried waste, less the surface soil layer. The site model uses four cells to represent this portion of the cover; multiple cells more accurately represent the impacts of biotic intrusion on the disposal facility relative to a single layer. These cell pathways may be subject to inflows of infiltrating water and soil from the surface soil or cap layer above, the latter a result of burrow collapse. Outflows from these cells account for the uptake of radionuclides by plants growing in the cover, soil transported by burrowing animals to the surface of MDA G, soil transported downward in response to burrow collapse, and the passage of infiltrating water into the underlying waste. The presence or absence of many of these inflows and outflows depends upon the depth to which plants and animals penetrate into the disposal site.

The waste disposed of in each waste disposal region is also represented using a series of four cell pathways to more accurately model biotic interactions with the waste. Inventories are input directly into the waste cells over the proper period of disposal. These cells may be subject to advective inflows of infiltrating water and soil from above, representing infiltration through the site and burrow collapse. Outflows may include water infiltrating through the site, the uptake of radionuclides by plants, soil transported to the surface by burrowing animals, and soil transported downward in response to burrow collapse. The presence or absence of many of these inflows and outflows depends upon the depth to which plants and animals penetrate into the disposal site.

The Plants cell found in each erosion zone container represents plants growing over the disposal site that extract contamination from the cover and waste and fall to the surface as plant litter. Direct transfers account for the uptake of radionuclides by the plants and the passage of this contamination to the surface soil layer as a result of litterfall and litter decomposition.

Water exiting the bottoms of the disposal units will enter the underlying unsaturated zone; this flow is modeled using advective mass-flux links from the bottommost waste layers to the Unsaturated_Zone cell, which is located just inside the disposal region-specific container. The outflow from this cell enters an external pathway element. This element simulates the transport of

waterborne contaminants vertically to the regional aquifer and horizontally to the receptor's well located downgradient of the disposal site. The final element included in the waste disposal region containers, Disposed_Inventory, accounts for the addition of waste to the disposal units over the appropriate period of disposal.

2.3.2 MDA G Site Diffusion Model

The general organization of the MDA G Site Diffusion Model is shown in Figure 2. Like the site model, the diffusion model is divided into two major segments. The input data, process models, and dose models are contained in the first segment. The second segment includes the physical compartments used to represent MDA G and the various exposure locations. The major elements comprising these two segments are summarized below.

2.3.2.1 Input Data and Process Models

The MasterClock element, input data, and process models used in the diffusion model are found in this segment. The contents of the containers shown in Figure 2 are discussed below. Complete definitions of the input parameters may be found in Section 4. The equations used to calculate intermediate parameters and to implement the process models are discussed in Section 3.

Master clock. The MasterClock element controls how dynamic simulations are implemented, keeping track of time during the simulation. The functions it performs are the same as those discussed for the site model.

Controls and constants. Four flag variables are used to control the diffusion modeling. The model is designed to simulate a single waste disposal region at a time; the Disposal_Region_Flag specifies which of the eight waste disposal regions is being considered in the simulation. The Analysis_Flag determines whether the performance assessment or composite analysis inventory is included for the disposal region of interest. The Diffusion_Flag and Biotic_Intrusion_Flag provide the option of including the effects of diffusion and biotic intrusion in the performance modeling.

Disposal system information. The Disposal_System_Information container includes data that characterize the radionuclides in the waste, the environmental media that are used in the model, the disposal system, and the waste inventory. In general, the contents of this container are similar to those described earlier for the MDA G Site Model. The Species_and_Materials container includes some elements that are unique to the site diffusion model, such as the relative diffusivities of the vapor- and gas-phase radionuclides.

The data characterizing the physical dimensions and operational aspects of the disposal, found in the Site_Geometry_and_Operations container, are largely the same as those discussed for the site model. The manner in which this information is represented in the site diffusion and site models differs because the former considers only one waste disposal region at a time while the site model addresses all regions simultaneously.

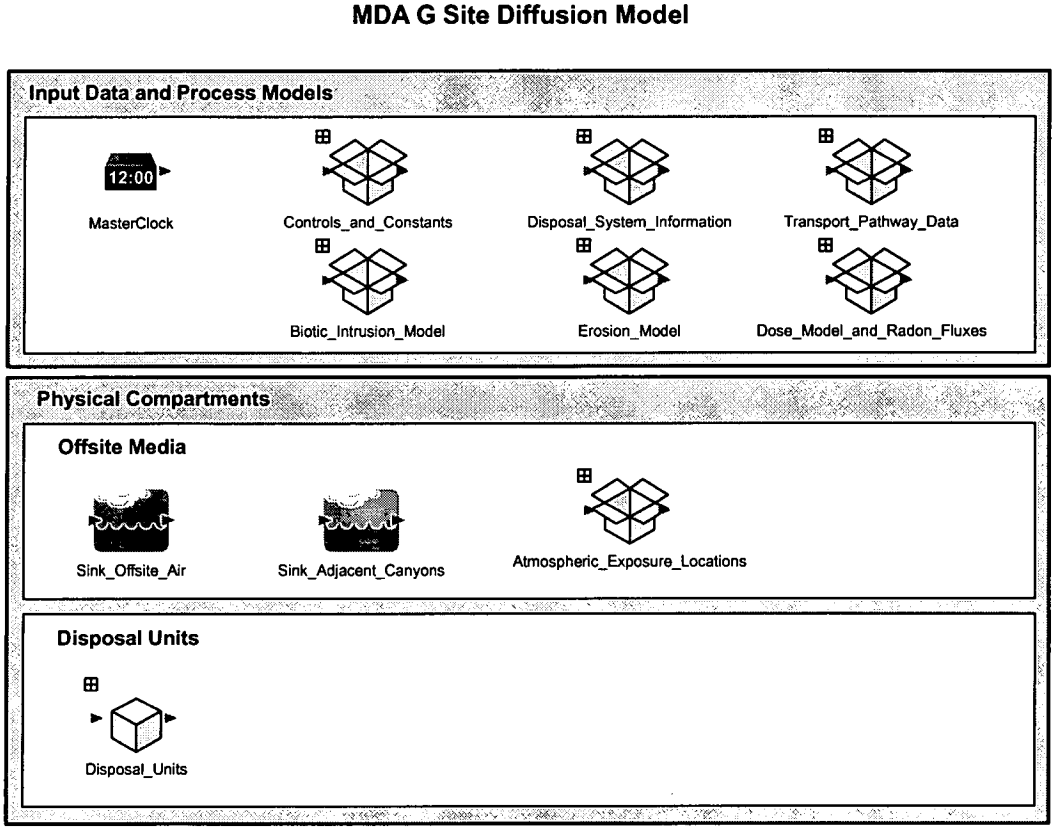

Figure 2
General Organization of the MDA G Site Diffusion Model

The Inventory container organizes the radiological inventories used in the performance assessment and composite analysis. The elements included in this container are generally the same as those discussed for the site model. Some differences in the number and organization of these elements occur because of the limited set of radionuclides addressed by the site diffusion model and because the model considers a single waste disposal region at a time.

Transport pathway data. The Transport_Pathway_Data container includes input data and calculated parameters needed to model rates of radionuclide transport. The contents of this container are similar to those described for the site model.

Biotic intrusion model. The Biotic_Intrusion_Model container includes the input data and models that are used to estimate the impacts of biotic intrusion on disposal facility performance. The layout of this container is similar to that discussed earlier for the site model; the number of elements included is less because the diffusion model considers only a single disposal region at a time.

Erosion model. The surface erosion model used in the site diffusion model is functionally the same as that described for the MDA G Site Model. The configuration of the erosion model is simpler for the site diffusion model, however, because only one waste disposal region is considered at a time.

Dose model and radon fluxes. The Dose_Model_and_Radon_Fluxes container organizes the input data and models used to estimate exposures from radionuclides that are affected by diffusive processes and to estimate the rates at which radon gas diffuses from the disposal facility. Dose calculations are conducted for the Atmospheric, All Pathways – Cañada del Buey, and All Pathways – Pajarito Canyon Scenarios, using the same data and models described earlier for the site model. Elements in the Radon_Flux container calculate fluxes of Rn-220 and Rn-222 exiting the surface of the disposal facility.

2.3.2.2 Physical Compartments — Off-Site Media and Exposure Locations

Cells are used to represent air downwind of MDA G and the atmospheric and canyon exposure locations. The Sink_Offsite_Air cell is used to represent the transport of airborne contaminants to downwind locations. Cells found within the Atmospheric_Exposure_Locations container represent the surface soils at each exposure location. Advective mass-flux links move soil moisture from these cells to sink elements to represent the transport of contamination with water infiltrating through the receptor's lot. Cells are used to represent the surface soils at the nine canyon exposure locations; advective mass-flux links between these cells and the surface soils on top of Mesita del Buey represent the movement of soils into the canyon due to surface runoff and erosion. Links between the nine canyon locations represent the transport of sediment down each canyon while links to a sink term simulate the movement of radionuclides with water percolating through the receptor's lot.

2.3.2.3 Physical Compartments — Disposal Units

The site diffusion model represents the disposal facility using a series of cell pathways. Single cells are used to represent the surface soil layer, the air above the facility, and plants inhabiting the site. A total of 16 cells is used to represent the cap, while 20 more cells represent the waste. The diffusion of gas- and vapor-phase contaminants proceeds from the bottommost waste layer to the surface soil layer; radionuclides reaching the surface layer diffuse into the air above the disposal site. Advective mass-flux links and direct transfer links are used to model the impacts of biotic intrusion, as described for the site model.

2.3.3 MDA G Intruder Model

The general organization of the MDA G Intruder Model is shown in Figure 3. Many aspects of the intruder model are similar to those discussed for the site model in Section 2.3.1. There are, however, differences in structure between these two models, as discussed below.

The MDA G Intruder Model is divided into two major segments. The input data and the process models are contained in the first segment. The second segment includes the physical compartments used to represent the disposal pits and shafts.

2.3.3.1 Input Data and Process Models

The MasterClock element, input data, and process models used in the MDA G Intruder Model are found in this portion of the model. The contents of each of the containers shown in Figure 3 are discussed below. Complete definitions of the input parameters may be found in Section 4. The equations used to calculate intermediate parameters and to implement the process models are discussed in Section 3.

Master clock. The MasterClock element controls how dynamic simulations are implemented, in effect keeping track of time. The functions it performs are the same as those discussed for the site model.

Controls and constants. The Controls_and_Constants container includes four flag variables that are used in the intruder simulations. The Intruder_Flag specifies whether the Intruder – Post-Drilling, Intruder-Agriculture, or Intruder-Construction Scenario is being simulated, while the Disposal_Unit_Flag specifies which disposal units are being considered. The model addresses waste disposed of in pits and shafts from September 27, 1988 through 2004 and the material placed in these units from 2005 through 2044. The Biotic_Intrusion_Flag, in conjunction with the Biota_Presence_Indicator, determines whether the effects of plant and animal intrusion into the waste prior to the arrival of the intruder are taken into account. The Inventory_Flag specifies whether the intruder simulations are being conducted using unit inventories or actual as-disposed inventories.

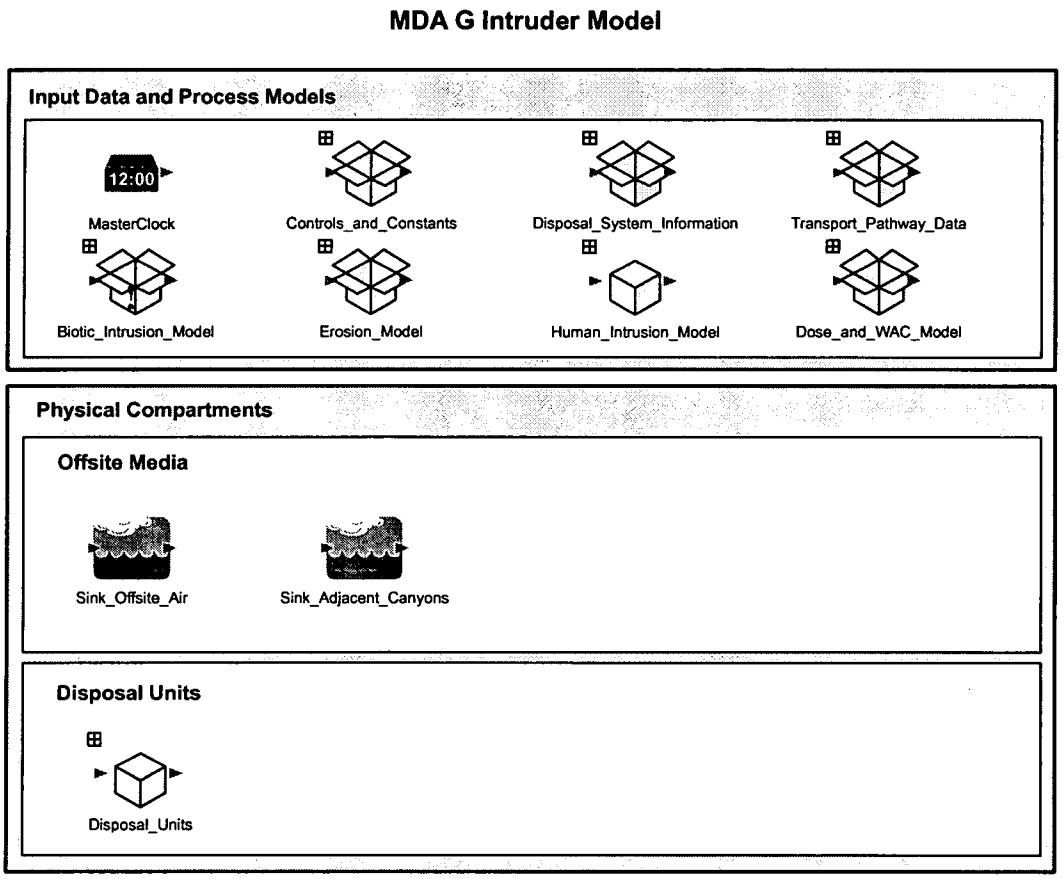

Figure 3
General Organization of the MDA G Intruder Model

Disposal system information. The Disposal_System_Information container includes the data that are used to characterize the radionuclides in the waste, the materials comprising the physical compartments, the disposal system, and the waste inventory. Similar to the MDA G Site Model, the Species_and_Materials container includes radionuclide decay data, a species element, a Material_Properties container, and the environmental media used in the modeling. Unlike the site model, an Attenuation_Coefficients container is found within the Material_Properties container: it contains mass and linear attenuation coefficients needed to estimate external exposures.

The Site_Geometry_and_Operations container includes elements that define the length of the active institutional control period and the disposal area used to estimate intruder doses; several elements known as selectors are used to identify key parameters for the disposal units specified using the Disposal_Unit_Flag. Elements found within the Layer_Information, Disposal_Pits, and Disposal_Shafts containers are used to define the operational period of each set of units and the initial thickness of the surface soil, cap, and waste layers; additional elements in the disposal unit-specific containers are used to calculate the areas and fractional areas associated with the 10 erosion zones that comprise each waste region.

The Inventory container includes elements that specify the radionuclide-specific inventories used in the intruder assessment and others that are used to model the addition of waste to the pits and shafts over time. Elements used to define unit inventories and the as-disposed inventories, with their attendant uncertainties, are found here. Unlike the site model, the as-disposed inventories may be input on a disposal-unit basis or specific to the different waste layers in each set of pits and shafts; an element is included to allow the allocation of the unit inventories to specific waste layers as well. Other elements define the volumes of waste disposed of in each set of disposal units and calculate the rate of addition of the waste to these units.

Transport pathway data. The Transport_Pathway_Data container includes input data and calculated parameters related to atmospheric, food-chain, and groundwater transport. The Atmospheric_Transport container includes dust-loading information needed to estimate airborne radionuclide concentrations for the intruder scenarios and resuspension rate data that are used to model the transport of contamination brought to the surface by plants and animals to off-site locations. The Foodchain_Transport container includes the input data required to estimate rates of radionuclide uptake for the crops raised by the receptors and to estimate radionuclide concentrations in animal products. The types of data found in this container and the manner in which they are organized have been described with respect to the MDA G Site Model. Finally, the Groundwater_Transport container includes the infiltration rate for Mesita del Buey.

Biotic intrusion model. The Biotic_Intrusion_Model container includes the input data and models that are used to estimate the impacts of biotic intrusion into the waste prior to the arrival of the inadvertent intruder. The layout of this container is similar to that discussed earlier for the site

model, although there are fewer elements because the intruder model considers only a single set of disposal units at a time.

Erosion model. The amount of waste that is disturbed by human intrusion activities will be influenced by the patterns and rates of erosion at the disposal site. The erosion model implemented in the intruder model is similar to that described earlier for the site model. Fewer elements are involved, however, because the intruder model considers exposures for one set of disposal units at a time. Projected erosion rates are used to update the thicknesses of the surface soil, cap, and waste layers and to calculate the cumulative depths to the bottom of each layer.

Human intrusion model. The human intrusion model estimates the net volumes of cap material and waste that are brought to the surface of the facility as a result of basement excavation or well drilling, and the thickness of the excavated material after it has been spread across the intruder's lot. Elements needed to conduct these calculations are found here, including the dimensions of the basement and the diameter of the well casing. The model calculations are specific to the type of intrusion under consideration. The Basement_Calculations container addresses basement excavation common to the Intruder-Construction and Intruder-Agriculture Scenarios, while the Drilling_Calculations container includes calculations conducted for the Intruder – Post-Drilling Scenario.

Dose and waste acceptance criteria model. The Dose_and_WAC_Model container includes the data and functions required to estimate doses for the intruder scenarios, using radionuclide masses or concentrations projected for the pertinent physical compartments and environmental media. The projected exposures are subsequently used to calculate waste acceptance criteria for the disposal units. The input data used to conduct these calculations are organized in two containers. The Dose_Conversion_Factors container includes the ingestion, inhalation, and direct radiation dose conversion factors for exposures to contaminated soils and air immersion; external dose conversion factors for contaminated soils are provided for two different depths of contamination. The Exposure_Pathway_Data container includes a variety of parameters required to model exposures. These include indoor and outdoor exposure times for the intruder; crop, animal product, and soil ingestion rates; inhalation rates; the area of the receptor's lot and house; the direct radiation shielding factor for the receptor's house; the soil mixing depth; and the time at which intrusion occurs. Also included are two elements that define the intruder performance objectives used to calculate the WAC.

The models used to project doses for the intruders are found in the Disposal_Unit_Doses_and_WAC container. Inside this container are found Media_Concentrations, Drilling_Intruder, Agricultural_Intruder, and Construction_Intruder containers. Elements found in the Media_Concentrations container estimate radionuclide concentrations in the cover, waste, air, plants, and animal products that are contacted or used by the intruders. The exposure calculations

for the different exposure scenarios are performed using elements in the remaining containers. Calculations of media concentrations and dose are performed separately for the 10 erosion zones; containers within the erosion-zone-specific containers are used to organize dose calculations by exposure route.

Exposure-pathway-specific doses are summed to determine total radionuclide doses; doses for all radionuclides within a given decay chain are summed to determine the parent radionuclide doses. Parent doses are summed appropriately across the 10 erosion zones to yield the total doses for the disposal units under consideration. The peak parent doses are used to calculate the intruder-based WAC for MDA G.

2.3.3.2 Physical Compartments — Off-Site Media

Cell pathways are used to represent the atmosphere downwind of the disposal facility and the canyons adjacent to MDA G. Advective mass-flux links between cells used to represent the disposal facility proper and the Sink_Offsite_Air cell simulate the transport of suspended particulates with the prevailing winds. Links between the disposal facility and the Sink_Adjacent_Canyons cell are used to simulate the movement of contamination off-site with surface runoff.

2.3.3.3 Physical Compartments — Disposal Facility

The intruder model is designed to simulate a single set of disposal units (i.e., different subsets of pits and shafts at MDA G) at a time. The Disposal_Units container includes the elements used to represent these units. The container holds 10 more containers, each of which represents one of the 10 erosion zones. Within each of these containers, a single cell is used to represent the surface soil layer, defined as the top 1 cm (0.4 in.) of the cover. Four cells in each container are used to represent the cap (i.e., the cover less the surface soil layer) and the waste. The degree to which the cover and waste are divided (discretized) is consistent with that seen in the site model and is adopted to simulate the intrusive activities of plants and animals with a reasonable level of accuracy. Additional cells represent the vadose zone beneath the disposal units and native plants that inhabit the closed disposal site prior to the arrival of the intruder.

The quantities of soil, waste, and soil/waste moisture moved to the surface of the disposal facility as a result of human intrusion are calculated using the elements found in the Intrusion_Consequence container. Quantities of cap material are calculated in the Cap_Contaminant_Masses container and the corresponding quantities for the waste are estimated using the elements in the Waste_Contaminant_Masses container. The calculated quantities are assigned to elements known as discrete change elements, found in the Discrete_Change_Elements container. These elements are used to move the appropriate quantities of cap and waste contaminants to the surface of the disposal facility at the time of intrusion.

2.3.4 MDA G Intruder Diffusion Model

The general organization of the MDA G Intruder Diffusion Model is shown in Figure 4. The model is divided into two major segments, the first of which contains input data, process models, and dose models. The second segment includes the physical compartments used to represent MDA G. The major elements comprising these two segments are summarized below.

2.3.4.1 Input Data and Process Models

The MasterClock element, input data, and process models used in the diffusion model are found in this portion of the model. The contents of the containers shown in Figure 4 are discussed below. Complete definitions of the input parameters may be found in Section 4. The equations used to calculate intermediate parameters and to implement the process models are discussed in Section 3.

Master clock. The MasterClock element controls how dynamic simulations are implemented, keeping track of time during the simulation. The functions it performs are the same as those discussed for the site model.

Controls and constants. Five flag variables are used to control the diffusion modeling for the intruder analysis. Like the intruder model, the Intruder_Flag and Disposal_Unit_Flag specify which intruder scenario (i.e., construction, agricultural, or postdrilling) and which set of disposal units (i.e., pits or shafts) is being addressed in the simulation. The Diffusion_Flag provides an option for including the effects of diffusion in the modeling or not; the Biotic_Intrusion_Flag does the same with respect to plant and animal intrusion into the waste. The Biota_Presence_Indicator element uses the value of this flag variable to determine if intrusive plants and animals are present at the site as a function of the time during the simulation. The Inventory_Flag specifies whether the intruder simulations are being conducted using unit inventories or actual as-disposed inventories.

Disposal system information. The Disposal_System_Information container includes information about the radionuclides in the waste, the materials comprising the physical compartments of the model, the disposal units, and the waste inventory. The elements included in the Species_and_Materials container are similar to those found in the site diffusion and intruder models; elements needed to model diffusion within the concrete floor of the foundation of the intruder's house are the notable exception. The elements included in the Site_Geometry_and_Operations container are much the same as those described for the intruder model; differences relate to the manner in which the cap, waste, and concrete foundation were discretized in the two models. The elements found in the Inventory container are also similar to those included in the intruder model. Like the intruder model, the as-disposed inventories may be input on a disposal-unit basis or specific to the different waste layers in each set of pits and shafts. The intruder diffusion model is configured to accept four depth-dependent inventories which are allocated among the waste layers used to represent the disposal units.

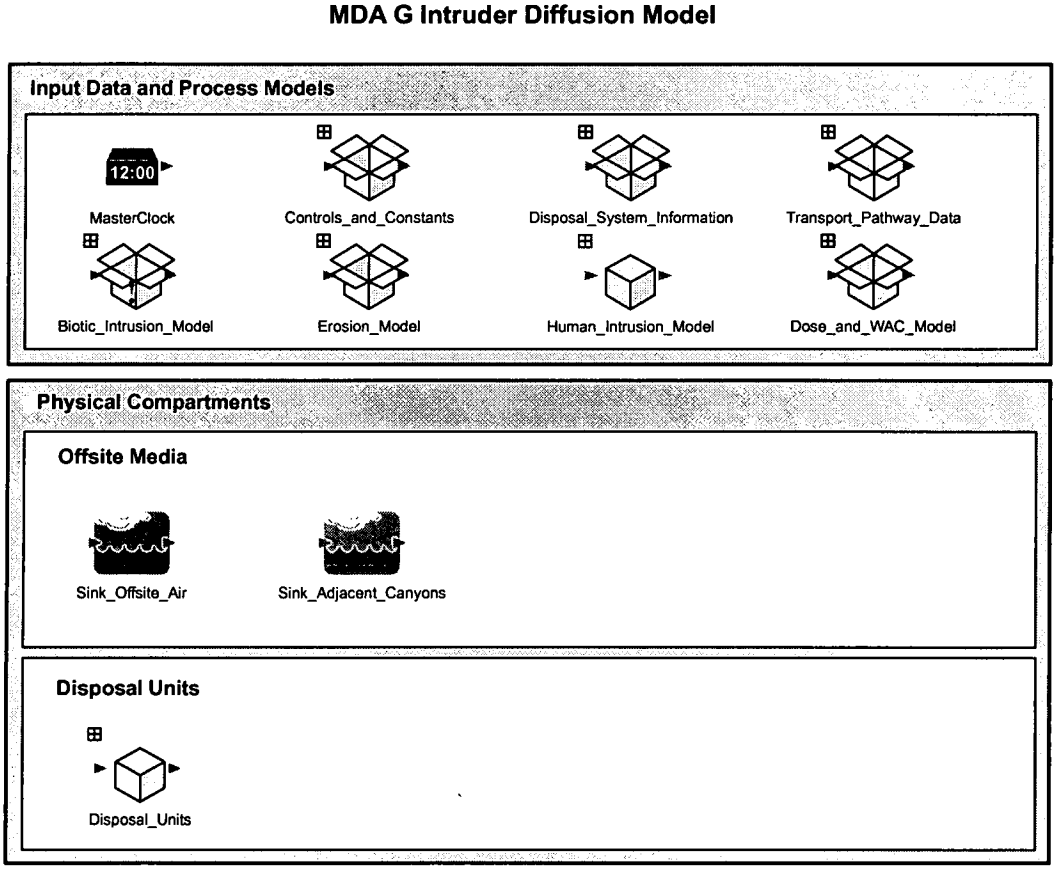

Figure 4
General Organization of the MDA G Intruder Diffusion Model

Transport pathway data. The Transport_Pathway_Data container includes input data and calculated parameters needed to model rates of radionuclide transport. These parameters are organized in three containers labeled Atmospheric_Transport, Foodchain_Transport, and Groundwater_Transport. The input data found in the Atmospheric_Transport container are generally the same as those discussed for the intruder model, with the exception of the wind speed and atmospheric mixing height elements, which are used to estimate exposure concentrations for vapor- and gas-phase radionuclides above the disposal facility. The elements inside the Foodchain_Transport and Groundwater_Transport containers are the same as those found in the intruder model.

Human intrusion model. The Human_Intrusion_Model container includes elements used to calculate the net volumes of waste and cover material brought to the surface and spread over the receptor's lot. The elements included in this container are the same as those seen in the intruder model.

Biotic intrusion model. The Biotic_Intrusion_Model container includes the input data and models that are used to estimate the impacts of biotic intrusion into the waste prior to the arrival of the inadvertent intruder. The layout of this container is similar to that discussed earlier for the site model; fewer elements are included in the container because the intruder diffusion model considers only a single set of disposal units at a time.

Erosion model. The surface erosion model used in the intruder diffusion model is the same as that described for the MDA G Site Model. Rates of erosion are estimated for the 10 erosion zones and used to calculate rates of cover loss for the disposal units specified using the Disposal_Unit_Flag.

Dose model. As in the intruder model, the Dose_and_WAC_Model container includes the data and models used to estimate doses for the intruder scenarios; the results are used in the calculation of WAC for MDA G. The elements used to conduct these calculations are organized in a manner similar to that described for the intruder model.

2.3.4.2 Physical Compartments — Off-Site Media

The intruder diffusion model uses a cell to represent air downwind of MDA G and the canyons adjacent to the disposal facility. An advective mass-flux link is used to transport airborne contaminants from above the intruder's lot to the Sink_Offsite_Air cell; this transfer represents the transport of airborne contaminants with the prevailing winds. Transfers from the intruder's lot to the adjacent canyons represent the transport of sediment from the mesa top with surface runoff.

2.3.4.3 Physical Compartments — Disposal Facility

The cells that are used to represent the disposal facility in the intruder diffusion model are organized in a manner similar to that described earlier for the site diffusion model. Within each of the 10 erosion zone containers, a single cell is used to represent the surface soil layer, while 16 and 20 cells are used to represent the cap and waste, respectively. Additional cells represent the air over the disposal facility and plant litter. Unlike the site diffusion model, however, the intruder diffusion model uses several cells to represent the basement excavation, the concrete floor of the intruder's house, and the house itself. Radionuclides diffusing from the waste may travel through the cap and surface soil layer and enter the air above the site, diffuse through the concrete foundation and enter the intruder's house, or enter the basement excavation prior to construction of the house. As discussed earlier, advective mass-flux links are used to simulate the impacts of animal intrusion into the disposal facility, while direct transfers are used to simulate the uptake of radionuclides by plants growing over the disposal units and the subsequent deposition of these contaminants on the surface through litterfall and decay. Outflows from the surface soil cells account for the settling and collapse of animal burrows, resuspension of particulates, transport of waterborne contaminants downward with infiltrating water, and movement of soils into the canyons bordering Mesita del Buey.

3.0 Modeling Approach

The four GoldSim models described above integrate a series of process models that are used to conduct the MDA G performance assessment and composite analysis. Descriptions of these models are provided below. The first several sections of this discussion present models that are used to estimate rates of radionuclide release, transport, and exposure. The output of many of these models defines the modes and rates of contaminant movement between the physical components that are used to represent the disposal system. The manner in which transfers between the physical components are simulated is addressed in the latter sections of the discussion.

MDA G is a large, complex site. Many aspects of the facility's long-term performance are spatially dependent in response to local variations in topography and geohydrology. To more accurately model the performance of the disposal facility, the disposal site had to be divided, or discretized, into several areas. An understanding of how this was done is critical to the following discussions about models.

The primary subdivisions of the facility are referred to as waste disposal regions; these regions include various subsets of the disposal pits and shafts at MDA G. The active portion of MDA G was divided into seven disposal regions; these regions are shown in Figure 5. Disposal regions 1 and 6 each include some of the shafts in the shaft field west of pits 2 and 4, consequently the boundaries of these regions overlap. Disposal region 7 includes numerous shafts scattered among the units that make up disposal region 3 (i.e., pits 8 through 22), and thus the boundaries of these two regions also overlap. The eighth waste disposal region is used to represent the Zone 4 expansion area and is not shown in Figure 5. The waste disposal regions were defined because the thickness of the Bandelier Tuff, which largely determines groundwater transport times, increases from east to west and because of differences in the depths of the disposal pits and shafts. Table 2 lists the elevation assigned to the bottom of the disposal units within each disposal region and the corresponding depth to the regional aquifer.

Variations in the topography and construction details of the final cover cause patterns and rates of surface erosion to vary across MDA G. To model the impacts of erosion on facility performance, it was necessary to further divide the site into a series of areas referred to as erosion zones. Consequently, each of the eight waste disposal regions was divided into 10 erosion zones, with each zone being characterized by a different erosion rate function.

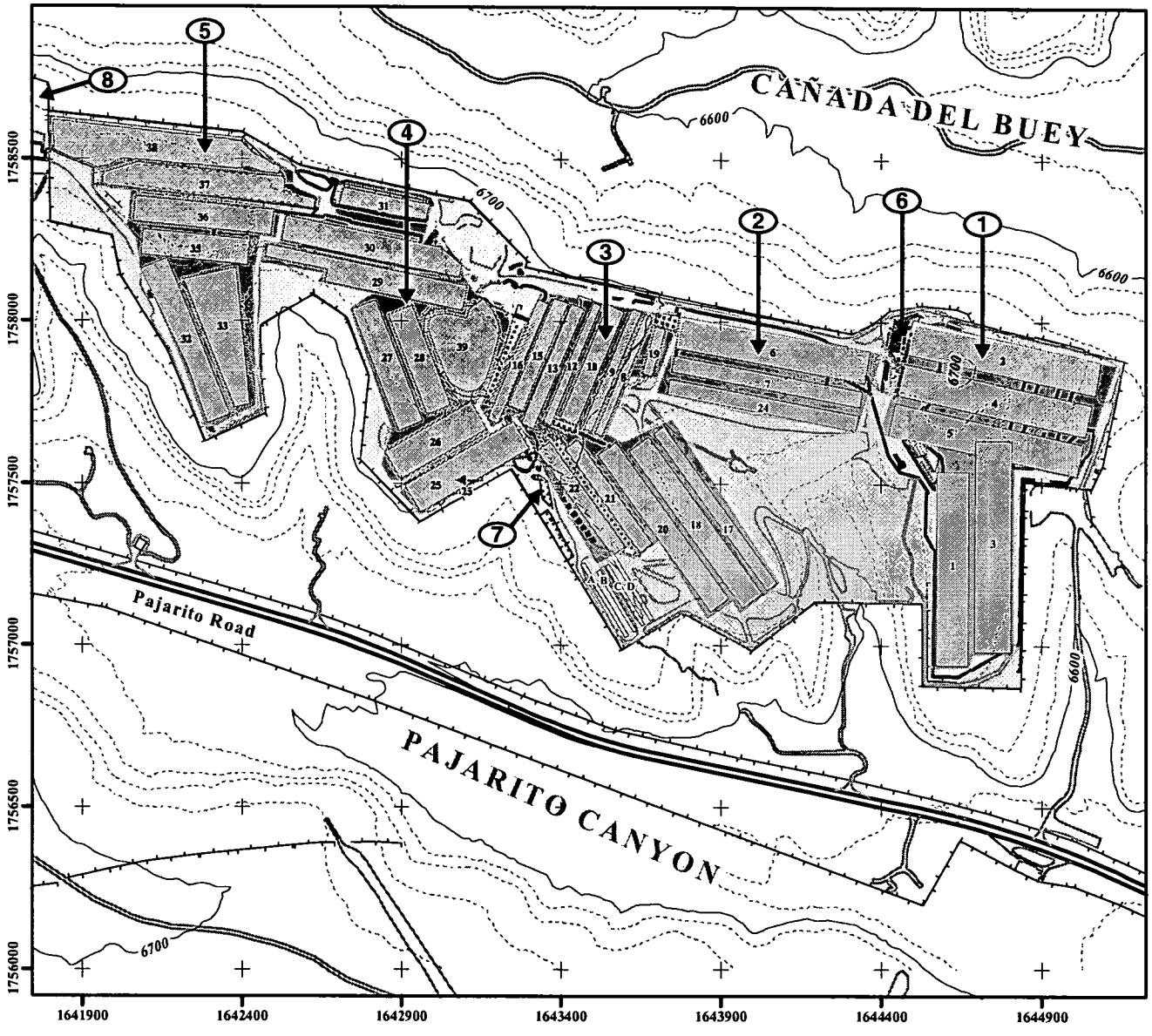

Legend

- Shafts
- Dirt roads
- Paved roads
- Fences
- 20 ft. contours (6 m)
- 100 ft. contours (30 m)
- MDA G (active area)
- Disposal pits
- Waste disposal region (pits or pit/shafts)
- Waste disposal region (shafts)
- Pit number

Notes:
Waste disposal regions 3 and 7 cover the same basic area, but region 3 includes only pits and region 7 only shafts.

Disposal region 8 is in Zone 4 expansion area to the west.

N

0 100 m 200 m

Scale

Projection: NM State Plane
Coordinate System - 3002
Datum: NAD83 (ft)
Scale: 1:5,000

Figure 5
Waste Disposal Regions at MDA G
Source: Apogen Technologies (formerly SEA), LANL RRES Database, Map ID: 4531.021 (1) Rev. 2

Table 2
Elevations of Disposal Units and Depth to Regional Aquifer for the Eight Waste Disposal Regions

Waste Disposal Region	Elevation of Disposal Units (m above msl, from bottom of units)	Depth to Regional Aquifer (m)
1	2024	253
2	2028	257
3	2032	261
4	2036	265
5	2037	266
6	2015	244
7	2020	249
8	2038	267

msl – Mean sea level

Radionuclides released from the disposal facility in the form of suspended particulates, gases, or vapors may be transported by the prevailing winds to locations downwind of the source of the airborne release. The patterns of transport and dispersal depend, in part, upon the portion of the facility from which the airborne releases originate. To better account for these dependencies, the disposal site was divided into three atmospheric source areas, as shown in Figure 6. Each source area consists of one or more of the eight waste disposal regions discussed above.

3.1 Biotic Intrusion Model

The biotic intrusion model is used to estimate rates of radionuclide transport to the surface of MDA G by plants and animals intruding into the disposed waste. This model evaluates the potential for plants and animals to intrude into the disposed waste and transport radioactive contamination to the surface of the disposal facility. The model is an adaptation of the updated biotic intrusion modeling conducted under the MDA G Performance Assessment and Composite Analysis Maintenance Program (Shuman, 1999). It is used in conjunction with all four GoldSim models (i.e., the site, site diffusion, and two intruder models). A discussion of the conceptual and mathematical models upon which the biotic intrusion modeling is based is provided below.

3.1.1 Conceptual Model

The biotic intrusion model addresses the impacts of plant and animal intrusion into the buried waste. The biotic intrusion model for plants is based on the assumption that the roots of plants growing over the site extend into the buried waste. Radionuclides are taken up via these roots and are assimilated by the plants. Litter is formed as plants die and shed their leaves and contamination in the plant material enters the soil as the litter decomposes.

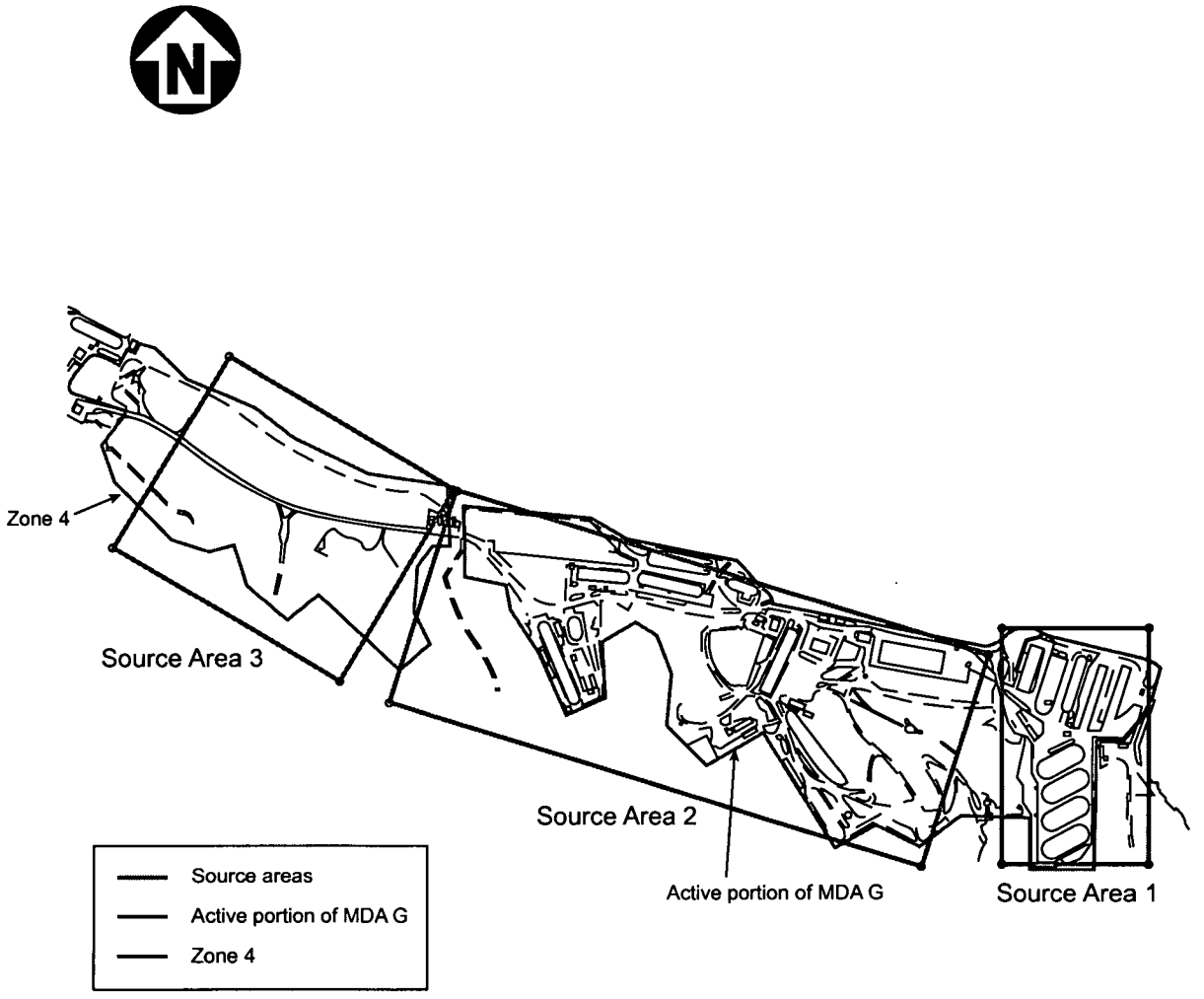

Figure 6
Atmospheric Source Areas at MDA G

The amount of contamination deposited on the surface by plants is a function of the radionuclide concentrations in the litter and the quantity of litter generated by the plants. Radionuclide concentrations in the litter depend upon the distribution of root mass with depth and the efficiency with which radionuclides are extracted from contaminated soils by plant roots. Rates of litter production are estimated on the basis of aboveground plant yields and the fractions of these yields that fall as litter in any given year. Plant yields and litter generation fractions are specific to the plant growth forms under consideration; yields may vary over time as the disposal site undergoes ecological succession.

Animals constructing burrows for cover or as a means of foraging may also penetrate into the buried waste and bring waste contaminants to the surface of the site. This contamination is mixed with clean soil excavated from the portions of the burrows that lie above the waste, and spread over the ground surface. Over time, the burrows excavated by animals will settle or collapse, resulting in the gradual downward movement of contamination brought to the surface by animals and deposited on the ground by plants. Vertical transport of the surface contamination will be enhanced as radionuclides are transported downward with water infiltrating through the site.

The amount of contaminated soil brought to the surface by burrowing animals depends upon the distribution of burrows relative to the waste and the soil removal rates of the various species or taxa of animals. Burrow distributions are used to estimate rates of soil removal with depth; the total quantities of excavated soil are calculated using information about animal densities and life spans, and burrow renewal fractions. Many of these parameters may change over time as the composition of the animal community shifts in response to changes in the plant community.

The potential impact of biotic intrusion on the long-term integrity of MDA G depends, in part, on the ecological characteristics of the site and, hence, on the plant and animal species that can reasonably be expected to inhabit it. A diverse array of plants and animals occurs in the Los Alamos region owing to the 1,500 m (5,900 ft) difference in elevation between the Rio Grande and the top of the Jemez Mountains, and to the canyon and mesa terrain (DOE, 1979). Los Alamos County has six major vegetative community types: juniper-grassland, piñon-juniper, ponderosa pine, mixed conifer, spruce-fir, and subalpine grassland. The juniper-grassland, piñon-juniper, and ponderosa pine communities predominate; each of these communities comprises about one-third of the Laboratory. Juniper-grassland extends from the Rio Grande and eastern part of the Pajarito Plateau up to 1,700 to 1,900 m (5,600 to 6,200 ft) above mean seal level (msl) on south-facing slopes. The piñon-juniper community covers large portions of mesa tops, ranging from about 1,900 to 2,100 m (6,200 to 6,900 ft) above msl. Ponderosa pines occur at elevations from 2,100 to 2,300 m (6,900 to 7,500 ft) above msl on the western plateau (Figure 7).

Undisturbed areas on Mesita del Buey, the mesa where MDA G is located, are dominated by piñon-juniper woodland. Piñon pine (*Pinus edulis*) and one-seed juniper (*Juniperus monosperma*) are the dominant tree species; common shrubs include big sagebrush (*Artemisia tridentata*), four-wing saltbush (*Atriplex canescens*), currant (*Ribes cereum*), and mountain mahogany (*Cercocarpus montanus*). Blue grama (*Bouteloua gracilis*), cryptogamic soil crust, and prickly pear cactus (*Opuntia polyacantha*) are among the most common understory plants on the mesa. Others include snakeweed (*Gutierrezia sarothrae*), pingue (*Hymenoxys richardsonii*), wild chrysanthemum (*Bahia dissecta*), leafy golden aster (*Chrysopsis filiosa*), purple horned-toothed moss (*Ceratadon purpureus*), lichen, three-awn grass (*Aristida* spp.), bottlebrush squirreltail (*Sitanion hystrix*), bluegrass (*Poa* spp.), and false tarragon (*Artemisia dracunculus*).

Waste management operations at MDA G have caused a number of the native understory plants to be replaced by different species. Recently disturbed areas support goosefoot (*Chenopodium fremontii*), Russian thistle (*Salsola kali*), cutleaf evening primrose (*Oenothera caespitosa*), common sunflower (*Helianthus anuus*), and other colonizing species. Vegetation introduced as disposal units are closed consists of native grasses including blue grama, sideoats grama (*Bouteloua curtipendula*), Indian ricegrass (*Oryzopsis hymenoides*), sand dropseed (*Sporobolus cryptandrus*), sheep fescue (*Festuca ovina*), and western wheatgrass (*Agropyron smithii*), and forbs such as blue flax (*Linum perenne lewisii*) and prairie coneflower (*Ratibida columnifera*).

Based on the information provided above, the disposal units at MDA G are expected to undergo ecological succession from their disturbed state shortly after closure to a piñon-juniper woodland climax, characteristic of the undisturbed portions of Mesita del Buey. Annual and perennial grasses and forbs will predominate when the site is in its early successional stages, becoming established as covers over disposal units are seeded and as grasses and forbs invade from surrounding areas on the mesa. Over time, shrubs and trees will take hold and become established at the site. While some species of grasses and forbs will die out, others will continue to thrive. Given enough time, it is assumed that a condition approximating the climax piñon-juniper woodland will result.

The predominant plant communities at MDA G will have a direct influence on the species of burrowing animals that occur at the site following facility closure. Several species of burrowing animals are currently found at MDA G and the area surrounding the site; others may reasonably be expected to inhabit the site after widespread disturbance of the area ceases and as the site undergoes ecological succession to piñon-juniper woodland. The most prevalent of these burrowing species are expected to be harvester ants and several species of small mammals.

There are approximately 20 species of harvester ants (*Pogonomyrmex* spp.) in the southwestern U.S. The combined ranges of *Pogonomyrmex occidentalis* and *Pogonomyrmex rugosa* cover the state of New Mexico; the ants are commonly found in high grasslands and piñon-juniper

woodland (Allen, 1996). Carlson and Whitford (1991) observed harvester ants (*Pogonomyrmex occidentalis*) in piñon-juniper and ponderosa pine communities near the LANL. It is not surprising, then, that harvester ants have been observed in undisturbed piñon-juniper woodland on Mesita del Buey. They were also seen at MDA J, 2 km (1.2 mi) west of MDA G, shortly after closure of that disposal site.

A variety of species of small mammals inhabit the Laboratory and surrounding lands. Many of these species, and the habitats within which they occur, were discussed in the Los Alamos final environmental impact statement issued in 1979 (DOE, 1979). Table 3 summarizes this information, which includes the species of small mammals found in the vegetation overstory types that occur most often at the Laboratory. MDA G is expected to most closely resemble the juniper-grassland shortly after closure, and the piñon-juniper woodland as it undergoes ecological succession. Deer mice (*Peromyscus maniculatus*), piñon mice (*Peromyscus truei*), woodrats (*Neotoma* spp.), and mountain cottontails (*Sylvilagus nuttalli*) are common to both of these plant communities; chipmunks (*Eutamias* spp.) are anticipated as the site passes into piñon-juniper woodland.

Table 3
Distribution of Small Mammals in Los Alamos County by Vegetation Overstory Type

Vegetation Overstory Type	Approximate Elevation (m above msl)	Small Mammal Species	
Spruce-Fir	2,900 – 3,200	Deer mouse Northern pocket gopher Least chipmunk Montane vole	Boreal red-backed vole Tassel-eared squirrel Woodrat Shrew
Mixed Conifer	2,300 – 2,900	Deer mouse Northern pocket gopher Least chipmunk Montane vole	Gapper's red-backed vole Tassel-eared squirrel Woodrat Shrew
Ponderosa Pine	2,100 – 2,300	Deer mouse Valley pocket gopher Least chipmunk Colorado chipmunk	Pine squirrel Tassel-eared squirrel Woodrat
Piñon-Juniper	1,900 – 2,100	Deer mouse Piñon mouse Colorado chipmunk	Woodrat Mountain cottontail
Juniper-Grassland	1,700 – 1,900	Deer mouse Piñon mouse	Woodrat Mountain cottontail
Canyons		Western harvest mouse Valley pocket gopher Least chipmunk	Meadow vole Rock squirrel Mountain cottontail

Source: DOE, 1979

Trapping studies conducted at the Laboratory over the past several years have generally confirmed the small mammal distributions shown in Table 3 for the grassland and piñon-juniper woodland communities. The most commonly trapped species in disturbed areas at MDA G has been the deer mouse; western harvest mice (*Reithrodontomys megalotis*), pocket gophers (*Thomomys* spp.), piñon mice, and brush mice (*Peromyscus boylei*) have also been caught (Biggs et al., 1995, 1997; Bennett et al., 1997, 1998, and 2002). The piñon mouse has been the most commonly trapped species in piñon-juniper woodland areas, although deer mice, harvest mice, brush mice, and silky pocket mice (*Perognathus flavus*) have also been caught.

Additional insight into the small mammals that may inhabit MDA G following its succession to piñon-juniper woodland may be gained from a literature review. Zarn (1977) summarized the work of several investigators who characterized the species of small mammals found in piñon-juniper woodlands in Utah, western Colorado, and Arizona. Species found in those woodlands include deer mice, western harvest mice, brush mice, Great Basin pocket mice (*Perognathus parvus*), piñon mice, northern grasshopper mice (*Onychomys leucogaster*), longtail voles (*Microtus longicaudus*), Mexican voles (*Microtus mexicanus*), sagebrush voles (*Lagurus curtatus*), Great Basin kangaroo rats (*Dipodomys microps*), least chipmunks (*Eutamias minimus*), rock squirrels (*Citellus variegatus*), and several species of woodrats and lagomorphs (*Lepus* spp., *Sylvilagus* spp.).

In a food habits study conducted in western Colorado, Haufler and Nagy (1984) found deer mice, plains pocket mice (*Perognathus flavescens*), golden-mantled ground squirrels (*Citellus lateralis*), bushytail woodrats (*Neotoma cinerea*), least chipmunks, and mountain cottontails associated with disturbed and undisturbed piñon-juniper woodlands. Smith and Urness (1984) conducted a trapping study in several habitats in southern Utah, including one piñon-juniper community. Deer mice, Great Basin pocket mice, and piñon mice were the predominant species caught; deer mice accounted for 79 percent of all trapped animals. Severson (1986) examined the effects of piñon-juniper woodland treatments on rodent abundance in southern New Mexico. White-throated woodrats (*Neotoma albigula*); brush, piñon, and southern grasshopper mice (*Onychomys torridus*); and Ord's kangaroo rat (*Dipodomys ordi*) were the most abundant species on untreated woodland.

The background information provided above was used to identify the plants and animals included in the biotic intrusion modeling. Although the general nature of the vegetative cover at MDA G can be predicted for the site in its early successional stages and climax condition, predicting the species-specific plant composition with any degree of accuracy is essentially impossible. Given this, the plant communities present at the site were identified in terms of the general growth forms present under each set of conditions, rather than on a species-specific basis. Four growth forms were identified for the modeling: annual and perennial grasses, annual and perennial forbs, shrubs (including subshrubs), and trees. The impacts of grasses, forbs, and

shrubs are simulated during the early stages of site succession. Grasses and forbs are expected to be early colonizers at the site. Shrubs are expected to begin colonization of MDA G within a few years after closure. Consequently, this growth form is included in the simulation of the site. Simulation of the disposal site as it passes to piñon-juniper woodland considers the impacts of trees in addition to grasses, forbs, and shrubs.

Four species or taxa of burrowing animals were selected to simulate the impacts of animal intrusion upon MDA G. These include harvester ants, mice, pocket gophers, and chipmunks and ground squirrels. As mentioned earlier, harvester ants, which are found throughout much of New Mexico, have been observed at a recently closed disposal site and in piñon-juniper woodland adjacent to the disposal units at MDA G. The deer mouse and a host of other mouse species have been trapped at MDA G and in piñon-juniper woodland communities. Although the trapping efforts of Biggs et al. (1995 and 1997) and Bennett et al. (1997, 1998, and 2002) have indicated relatively little in the way of pocket gopher activity, these animals have been observed at MDA G. Gopher mounds have been found near several disposal shafts in the past, and have been encountered in the course of conducting vegetation transects at the Laboratory (Tierney and Foxx, 1987).

Chipmunks and ground squirrels are currently uncommon at MDA G, but are expected to become more common as the site passes from grassland to piñon-juniper woodland. The DOE (1979) does not include ground squirrels as potential inhabitants of the site; however, other published literature suggests species such as the rock squirrel and golden-mantled ground squirrel could take up residence at the site. The rock squirrel occurs in canyons at the Laboratory (DOE, 1979), and both of these species have been found in piñon-juniper woodland in Arizona, Colorado, and Utah. The spotted ground squirrel (*Spermophilus spilosoma*) has also been observed in the vicinity of the Laboratory; this species occurs throughout much of New Mexico but tends to inhabit grasslands on sandy soils (Streubel and Fitzgerald, 1978).

The animal species selected for the biotic intrusion modeling are expected to reasonably capture the range of species that will be present at MDA G after closure, which will enable reasonably accurate projections of the potential impacts of animal intrusion. While other burrowing animals may be present at the site at various points in time, the potential of these species to cause significant disruption of the waste is expected to be small. For example, one or more species of voles may inhabit the site, but these animals generally restrict burrowing activities to depths of 0.5 m (1.6 ft) below ground surface (bgs) or less. Although Hall (1928 and 1946, cited in CDFG, 2003) found the tunnels of the sagebrush vole as deep as 56 cm (1.8 ft), Reynolds and Laundre (1988) found that only one of 48 burrows of the montane vole (*Microtus montanus*) extended to a depth greater than 50 cm (1.6 ft). Both of these species of voles are found in northern New Mexico. Maser et al. (1974, cited in Carroll and Genoways, 1980) found nest chambers of the sage vole that were 8 to 25 cm (0.3 to 0.8 ft) bgs, while James and Booth (1952, also cited in

Carroll and Genoways, 1980) reported burrow depths of 10 to 46 cm (0.3 to 1.5 ft) bgs. Woodrats are common to New Mexico but generally live among rocks, cliffs, and vegetation, and do not establish extensive burrows for cover or foraging. While cottontail rabbits may establish burrows for cover or to give birth, these excavations are not expected to extend to great depths. For example, Ingles (1941) found desert cottontail (*Sylvilagus audubonii*) breeding burrows were 15 to 25 cm (0.5 to 0.8 ft) deep, while Orr (1940, cited in Chapman, 1975) found a maximum burrow depth of 0.6 m (2 ft) bgs for the mountain cottontail.

3.1.2 Mathematical Model

The mathematical expressions used to implement the biotic intrusion model are presented and discussed in the following sections. Section 3.1.2.1 describes the plant intrusion model and the equations used to simulate the impacts of animal intrusion are discussed in Section 3.1.2.2.

As discussed earlier, MDA G is divided into eight waste disposal regions, each of which is divided into 10 erosion zones. The conditions under which biotic intrusion occurs are unique to each combination of waste disposal region and erosion zone. Consequently, the biotic intrusion model is implemented for each of these discrete locations. However, to reduce the complexity of the equations shown below, most references to specific waste disposal regions and erosion zones have been excluded.

3.1.2.1 Plant Intrusion

The rate at which contamination is deposited on the surface of MDA G by plants is equal to the product of the litter production rate and the radionuclide concentrations in the litter. Litter production rates are calculated for the four plant growth forms included in the biotic intrusion model (i.e., grasses, forbs, shrubs, and trees) using the following:

$$l_{p,g,t} = (b_{a,g,e} \times (1. - f_{c,t}) + b_{a,g,c} \times f_{c,t}) \times l_{f,g} \qquad 1$$

Where

$l_{p,g,t}$ = litter production rate for plant growth form g at time t (kg/m^2/yr)
$b_{a,g,e}$ = aboveground biomass density of plant growth form g during early succession (kg/m^2)
$f_{c,t}$ = fraction of climax condition achieved at time t
$b_{a,g,c}$ = aboveground biomass density of plant growth form g under climax conditions (kg/m^2)
$l_{f,g}$ = litter production fraction for plant growth form g (yr^{-1})

The litter production fraction, $l_{f,g}$, represents the fraction of the aboveground biomass density that falls as litter during each year of the simulation.

The fraction of climax condition achieved at time t, $f_{c,t}$, is a measure of how far the site has progressed from the grassland conditions present at the time of facility closure to the piñon-juniper woodland characteristic of the expected climax condition. This fraction is estimated, based on the assumption that there is a linear transition between the condition of the disposal site at the time of final closure and the climax condition represented by piñon-juniper woodland, as follows:

$$f_{c,t} = 0.0 \qquad \text{for } t \le t_i \qquad (2)$$

$$f_{c,t} = \frac{(t - t_i)}{t_c} \qquad \text{for } ti < t < t_i + t_c \qquad (3)$$

$$f_{c,t} = 1.0 \qquad \text{for } t \ge t_i + t_c \qquad (4)$$

Where

- t = elapsed time since final closure of the disposal facility (yr)
- t_i = length of institutional control period, measured from final closure of the disposal facility (yr)
- t_c = length of time required to reach climax conditions under natural conditions

Maintenance activities are assumed to prevent succession toward piñon-juniper woodland throughout the active institutional control period. Site succession is assumed to start at the end of this period and to continue for a period equal to t_c, at which point the climax woodland is assumed to exist for the remainder of the simulation.

The radionuclide concentrations in the litter deposited on the surface of MDA G will be proportional to the radionuclide concentrations in the soil in which the plant that produced the litter grew. The plant intrusion model assumes that litter is generated in proportion to the root mass found in each layer of the disposal system (i.e., the surface soil, cap, and waste layers). For example, if 50 percent of the root mass for a given growth form occurred in a given layer of the cap, 50 percent of the total litter production is assumed to have radionuclide concentrations proportional to the contaminant concentrations within that layer. Total radionuclide concentrations in the litter, then, represent the contaminant concentrations calculated for each layer of the disposal system, weighted by the root mass in each layer.

The product of the litter production rate given in Equation 1 and the fractions of the total plant root mass in the cap and waste layers yields the layer-specific litter production rates needed to estimate the average contaminant concentrations in the litter deposited on the surface of MDA G. For each growth form, root distribution functions are used to calculate the fraction of the root mass that lies between the ground surface and the bottom of each layer. The difference between

the estimated fractions for a given layer and the overlying layer yields the fraction of the root mass found in the bottommost of the two layers. For instance, the fraction of the root mass that lies between the ground surface and the bottom of the first cap layer minus the corresponding fraction for the surface soil layer yields the fraction of the total root mass found in the uppermost cap layer for the growth form under consideration.

Foxx et al. (1984) conducted a comprehensive review of rooting data for species of plants that grow at LANL disposal sites and used the compiled data to develop rooting depth distributions for individual plant species. A distribution was developed for any species with at least six data points. If species-specific data were insufficient, distributions were developed on the basis of plant genera. All told, rooting depth distributions were developed for 12 species or genera of grasses, 10 species or genera of forbs, 2 species or genera of shrubs, and a single species of tree.

Least-squares regression analyses of the data developed by Foxx et al. (1984) for grasses and forbs were used to estimate composite rooting depth distributions for these two growth forms. The data used to conduct these analyses and the predicted composite distributions for grasses and forbs are shown in Figures 8a and 8b, respectively. Foxx et al. developed rooting distributions for only two species of shrubs, a number considered inadequate for estimating a composite rooting depth distribution for the growth form. Data from this study were supplemented with information from Tierney and Foxx (1987) to estimate rooting distributions for two additional shrub species, four-wing saltbush and rabbitbrush (*Chrysothamnus* spp.), which were then used in the development of the composite distribution shown in Figure 8c. Foxx et al. did not provide rooting distributions for tree species, reflecting a general lack of root distribution data for these plants. An average rooting depth of 6.4 m is cited by Foxx et al. for piñon pine; Tierney and Foxx cite estimated maximum root lengths of 1.1 to 1.3 m (3.6 to 4.3 ft) for this species. Foxx et al. cite average rooting depths ranging from 5.8 to 61 m (19 to 200 ft) for one-seed juniper, while Tierney and Foxx list a maximum root length of 1.7 m (5.6 ft).

The rooting depth distributions discussed above represent the frequencies with which plant roots penetrate to specified depths below the ground surface. As discussed earlier, plant uptake of radionuclides is assumed to be proportional to the root mass in a given layer or segment of the waste and cover. While rooting depth frequencies and root mass distributions may be highly correlated, information in the literature suggests otherwise. For example, Jackson et al. (1996) conducted a literature review on root biomass distributions with depth. Based on that review, Jackson et al. estimated that 53, 83, and 52 percent of the total root biomass in deserts, temperate grasslands, and temperate coniferous forests, respectively, occurs within 30 cm (1 ft) of the soil surface. Looking at plant growth forms across all biomes except tundra, it was estimated that 75 percent of the root mass of grasses occurs in the top 30 cm (1 ft) of soil; the corresponding figures for shrubs and trees are 47 and 60 percent. If the regression curves shown in Figure 8 were used to represent root mass with depth it would be concluded that less than 20 percent of the root mass of grasses, forbs, and shrubs lie within 30 cm (1 ft) of the ground surface.

Figure 8a
Root depth distributions for grasses

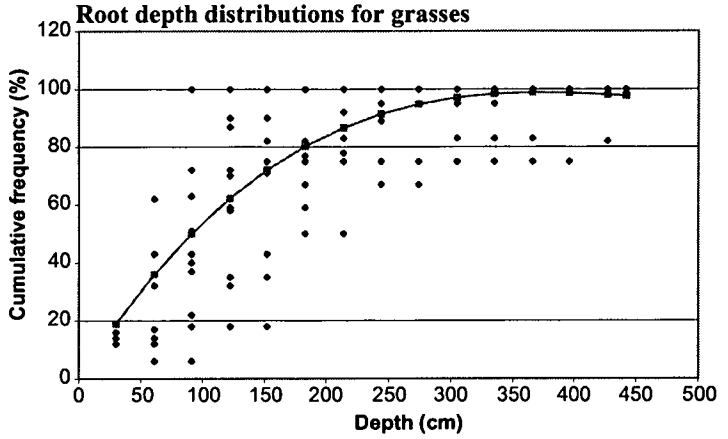

Figure 8b
Root depth distribution for forbs

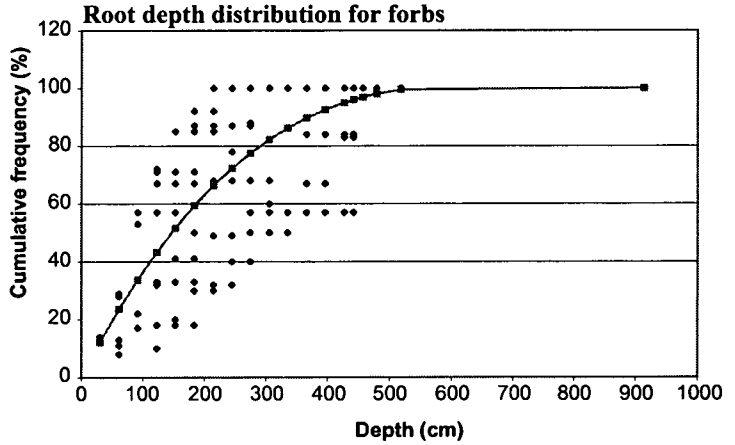

Figure 8c
Root depth distribution for shrubs

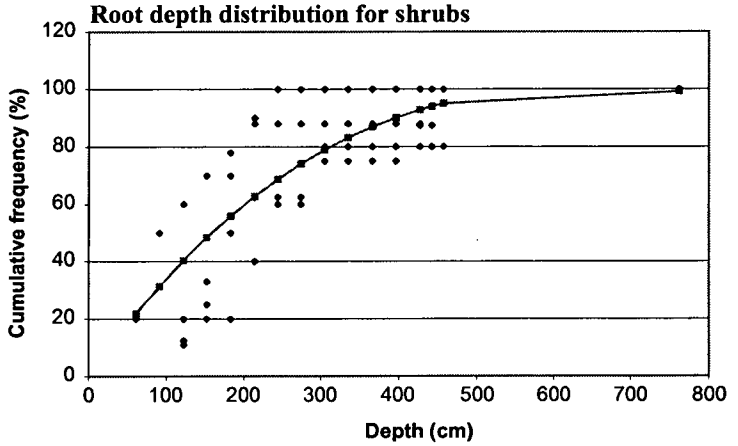

◆ Observed —■— Regression

Figure 8
Root Depth Distribution for Grasses, Forbs, and Shrubs

The information needed to accurately characterize the distribution of root mass with depth for the grasses, forbs, shrubs, and trees that inhabit MDA G is unavailable. Consequently, a series of functions was adopted to represent the distribution of root mass between the ground surface and the maximum rooting depth. This modeling was conducted using beta functions, the parameters for which were selected to evaluate a range of distribution patterns. The general form of the functions used to estimate root mass distribution with depth is:

$$R_{g,d} = B \times d^{\alpha} \times (d_{r,g,max} - d)^{\beta} \quad 5$$

Where

$R_{g,d}$ = fraction of root mass between ground surface and depth d for plant growth form g
B = beta function
d = depth (m)
α = shape factor
$d_{r,g,max}$ = maximum rooting depth of plant growth form g (m)
β = shape factor

The beta function is given by:

$$B = \frac{\Gamma(\alpha + \beta)}{\Gamma(\alpha) \times \Gamma(\beta) \times d_{r,g,max}^{\alpha+\beta}} \quad 6$$

Where

Γ = factorial of the quantities within the parentheses

The beta function can be simplified if α, one of the two shape factors, is set equal to zero, as shown in Equation 7:

$$B = \frac{1}{d_{r,g,\max}^{\alpha+\beta}} \quad 7$$

Using this formulation, the cumulative root mass distribution for a given depth, d, is given by the following:

$$R_{g,d} = 1 - \left(B \times d^{\alpha} \times (d_{r,g,\max} - d)^{\beta}\right) \quad 8$$

This is the form of the function that is implemented in the model. This quantity is set equal to 1.0 if the depth of interest exceeds the maximum rooting depth of the plant.

An example of the series of root mass distributions generated using the beta functions is shown in Figure 9. This figure shows the distribution curves for a plant growth form that has a maximum rooting depth of 1.5 m (4.9 ft). Similar curves are generated for alternate values of maximum rooting depth. In general, the root mass distributions estimated using this approach span the range of distributions suggested by the rooting depth frequencies discussed above and the findings of Jackson et al. (1996).

The radionuclide concentrations in the layer-specific litter fractions are determined by the rate at which plants extract contamination from the soil or waste via their roots. The uptake of radionuclides by plants is modeled in GoldSim using direct-transfer mass-flux links. These links specify the fractional rate at which radionuclides move from the soil or waste to the plant. They differ from advective mass-flux links in that only the contaminants in the soil or waste are transferred to the plants; advective mass-flux links transfer a quantity of an environmental medium (e.g., soil or water), along with whatever radionuclides it contains.

The transfer rate that is used to simulate the uptake of radionuclides by the fraction of the plant biomass that undergoes litterfall is given by the following equation:

$$p_{t,i,g,l,t} = \frac{l_{p,g,l,t} \times A_{ez} \times B_{i,c}}{A_{ez} \times t_l \times \rho} \qquad 9$$

Where

$p_{t,i,g,l,t}$ = plant transfer rate for radionuclide i in plant growth form g growing in layer l at time t (yr^{-1})
$l_{p,g,l,t}$ = litter production rate for plant growth form g growing in layer l at time t ($kg/m^2/yr$)
A_{ez} = area of disposal units over which the plants of interest are growing (m^2)
$B_{i,c}$ = soil-to-plant concentration factor for radionuclide i in crop c (Ci/kg dry weight vegetation per Ci/kg dry weight soil)
t_l = thickness of layer l (m)
ρ = bulk density of the soil or waste comprising layer l (kg/m^3)

Unlike the litter production rate included in Equation 1, the litter production rate in Equation 9 pertains only to the cover or waste layer for which the plant transfer rate is being calculated.

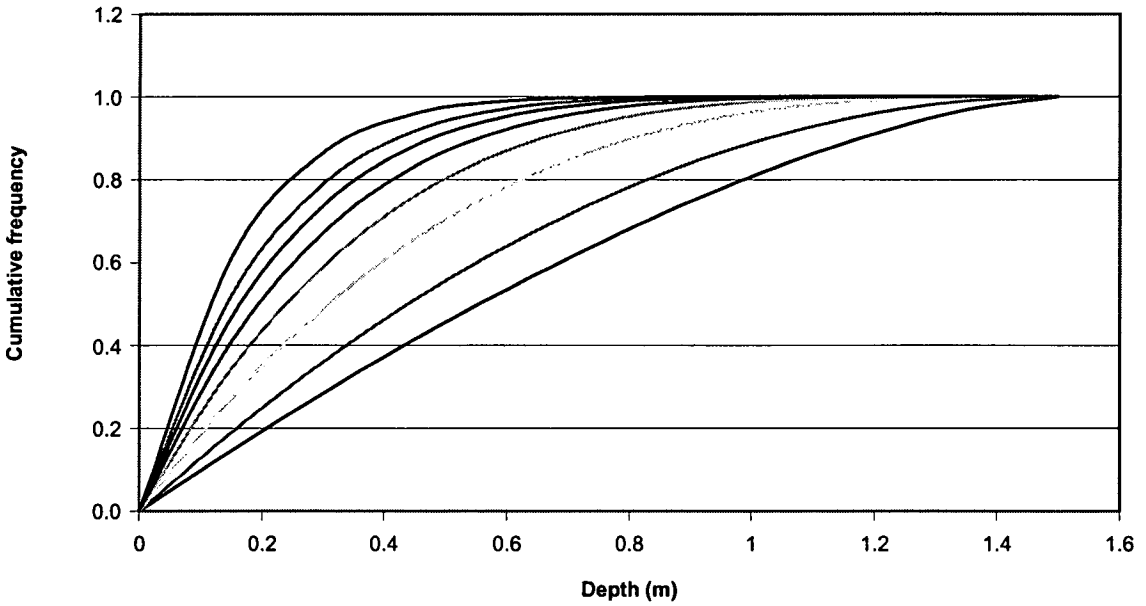

Figure 9
Root Mass Distributions for Plants with Maximum Rooting Depth of 1.5 m

The radionuclides in the litter that falls to the ground will enter the surface soil at a rate proportional to the plant matter decomposition rate. A direct transfer mass-flux link is used to model the passage of contamination from the litter to the soil. The transfer factor used to describe this process is given by Equation 10:

$$l_t = \frac{\ln(2)}{\lambda_l} \qquad 10$$

Where

l_t = litter decomposition transfer factor (yr^{-1})
λ_l = litter decomposition half-life (yr)

The same transfer factor is used to model the decomposition of litter for all four plant growth forms included in the plant intrusion modeling.

3.1.2.2 Animal Intrusion

The animal intrusion model simulates the transport of contamination to the surface of MDA G by harvester ants, pocket gophers, mice, and chipmunks and ground squirrels. The amount of contamination transported by these species is proportional to the amount of material excavated from the surface soil, cap, and waste layers and the radionuclide concentrations in each layer. The quantity of material excavated is estimated differently for each animal species. For harvester ants, the volume of material excavated in any given year is calculated using the following:

$$m_{s,ha,t} = (b_{d,ha,e} \times (1 - f_{c,t}) + b_{d,ha,c} \times f_{c,t}) \times b_{m,ha} \times r_{b,ha} \qquad 11$$

Where

$m_{s,ha,t}$ = rate of soil or waste excavation by harvester ants at time t (kg/ha/yr)
$b_{d,ha,e}$ = burrow density for harvester ants during early succession (ha^{-1})
$b_{d,ha,c}$ = burrow density for harvester ants under climax conditions (ha^{-1})
$b_{m,ha}$ = mass of harvester ant burrow (kg)
$r_{b,ha}$ = burrow renewal rate for harvester ants (yr^{-1})

The fraction of climax condition achieved at time t, $f_{c,t}$, is given by Equations 2 through 4. The burrow renewal rate is set equal to 1.0/yr for the first year following final closure of the disposal facility; thereafter, it is estimated as the inverse of the harvester ant colony life span.

Soil and waste excavation rates for pocket gophers are given by the following:

$$m_{s,pg,t} = (r_{r,pg,e} \times (1 - f_{c,t}) + r_{r,pg,c} \times f_{c,t}) \times r_{b,pg} \times \rho \qquad 12$$

Where

$m_{s,pg,t}$ = rate of soil or waste excavation by pocket gophers at time t (kg/ha/yr)
$r_{r,pg,e}$ = soil or waste removal rate during early succession (m^3/ha)
$r_{r,pg,c}$ = soil or waste removal rate under climax conditions (m^3/ha)
$r_{b,pg}$ = burrow renewal fraction for pocket gophers (yr^{-1})

Soil and waste excavation rates for mice, chipmunks, and ground squirrels are calculated as follows:

$$m_{s,a,t} = (b_{d,a,e} \times (1 - f_{c,t}) + b_{d,a,c} \times f_{c,t}) \times b_{m,a} \times r_{b,a} \times \rho \qquad 13$$

Where

$m_{s,a,t}$ = rate of soil or waste excavation by animal species a at time t (kg/ha/yr)
$b_{d,a,e}$ = burrow density for animal species a during early succession (ha^{-1})
$b_{d,a,c}$ = burrow density for animal species a under climax conditions (ha^{-1})
$b_{m,a}$ = volume of animal species' burrows (kg)
$r_{b,a}$ = burrow renewal fraction for animal species (yr^{-1})

The burrow renewal fractions in Equations 12 and 13 are set equal to 1.0/yr for the first year of the simulation following facility closure, and to the user-specified fraction thereafter.

The soil removal rates calculated for the animals are allocated among the cover and waste layers that comprise the disposal facility using burrow depth distribution functions. These functions, like the plant root-mass distributions discussed earlier, calculate the fraction of the burrow system that lies between the ground surface and the bottom of each layer. Taking the difference between the estimated fraction for a given layer and the one above it yields the fraction of the total burrow volume found in the bottommost of the two layers. For instance, if the fraction of the burrow between the ground surface and the bottom of the first waste layer is 0.9, and the corresponding fraction for the surface soil layer and entire cap is 0.8, then the fraction of the total burrow volume found in the first waste layer is 0.1.

Relatively little information is available to describe the distribution of animal burrows with depth. McKenzie et al. (1982) conducted a review of the burrowing habits of several species of harvester ants and small mammals, many of which are expected to occur at MDA G. As part of that work, they estimated burrow distributions with depth; these estimates are provided in Table 4. Reynolds and Laundre (1988) examined the distribution of burrows with depth for Townsend's ground squirrel (*Spermophilus townsendii*), Ord's kangaroo rat (*Dipodomys ordii*), the deer mouse, and the montane vole. The data collected for the ground squirrel and kangaroo rat indicate that the burrows of these species are shallower than indicated by McKenzie et al. (see Table 4). However, the decrease in the fraction of the burrow system with depth was less pronounced than that suggested by the data given in McKenzie et al.

Table 4
Burrow Depth Distributions for MDA G Animal Species

Animal Species	Fraction of Burrow Systems within Indicated Depth Interval				
	0 – 0.5 m	0.5 – 1.0 m	1.0 – 1.5 m	1.5 – 2.0 m	> 2.0 m
Harvester Ants	7.0E-01	1.0E-01	1.0E-01	5.0E-02	5.0E-02
Pocket Mice and Kangaroo Rats	5.0E-01	4.0E-01	5.0E-02	5.0E-02	0.0E+00
Pocket Gophers	8.5E-01	1.5E-01	0.0E+00	0.0E+00	0.0E+00
Ground Squirrels	5.0E-01	3.0E-01	1.5E-01	5.0E-02	0.0E+00

Source: McKenzie et al., 1982

The paucity of burrow depth distribution data makes it difficult to develop accurate depth distributions for the GoldSim model. Lacking the required information, a series of burrow depth distributions was developed using beta functions. The parameters for these functions were selected to evaluate a range of burrow distribution patterns. The general form of the functions used to estimate burrow distributions with depth is as follows:

$$B_{a,d} = B \times d^{\alpha} \times (d_{b,a,\max} - d)^{\beta} \qquad 14$$

Where

$B_{a,d}$ = fraction of burrow between ground surface and depth d for animal species a
B = beta function
d = depth (m)
α = shape factor
$d_{b,a,max}$ = maximum burrowing depth of animal species a (m)
β = shape factor

The beta function is given by:

$$B = \frac{\Gamma(\alpha + \beta)}{\Gamma(\alpha) \times \Gamma(\beta) \times d_{b,a,\max}^{\alpha+\beta}} \qquad 15$$

Where

Γ = factorial of the quantities within the parentheses

Consistent with the earlier discussion about plant root-mass distributions, the beta function can be simplified to the following if α, one of the two shape factors, is set equal to zero:

$$B = \frac{1}{d_{b,a,\max}^{\alpha+\beta}} \quad 16$$

Using this formulation, the cumulative burrow distribution for a given depth, d, is as follows:

$$B_{a,d} = 1 - \left(B \times d^{\alpha} \times (d_{b,a,\max} - d)^{\beta}\right) \quad 17$$

This is the form of the function that is implemented in the model. This quantity is set to 1.0 if the depth of interest exceeds the maximum burrowing depth of the animal.

An example of the series of burrow depth distributions generated using the beta functions is shown in Figure 10. This figure shows the distribution curves for an animal species that has a maximum burrowing depth of 3.0 m (10 ft). Similar curves are generated for alternate values of maximum burrowing depth.

Multiplying the soil or waste removal rate for a given animal species by the fractions of the burrow system within the cap and waste layers yields layer-specific bulk removal rates for that material. Any radionuclides contained in the soil (or waste) will be distributed between the soil (or waste) and the moisture occupying the pores of the material. The radionuclides in the solid and liquid phases are transported separately by the model, requiring that the bulk removal rates be allocated to the corresponding soil (or waste) and water removal rates. The equations used to calculate the soil (or waste) and water removal rates for the cap and waste layers are shown below for the harvester ant:

$$m_{ss,ha,l,t} = \frac{m_{s,ha,t} \times f_{ha,l,t} \times \rho_d}{\rho} \quad 18$$

$$m_{sm,ha,l,t} = \frac{m_{s,ha,t} \times f_{ha,l,t} \times m_s}{\rho} \quad 19$$

Where

$m_{ss,ha,l,t}$	=	dry soil or waste excavation rate by harvester ants for layer l at time t (kg/ha/yr)
$f_{ha,l,t}$	=	fraction of harvester ant burrow in layer l at time t
ρ_d	=	dry density of soil or waste (kg/m^3)
$m_{sm,ha,l,t}$	=	soil or waste moisture excavation rate by harvester ants for layer l at time t (kg/ha/yr)
m_s	=	moisture content of soil or waste

The soil and water removal rates are summed across animal species to yield layer-specific soil and water transport rates for each erosion zone in the eight waste disposal regions.

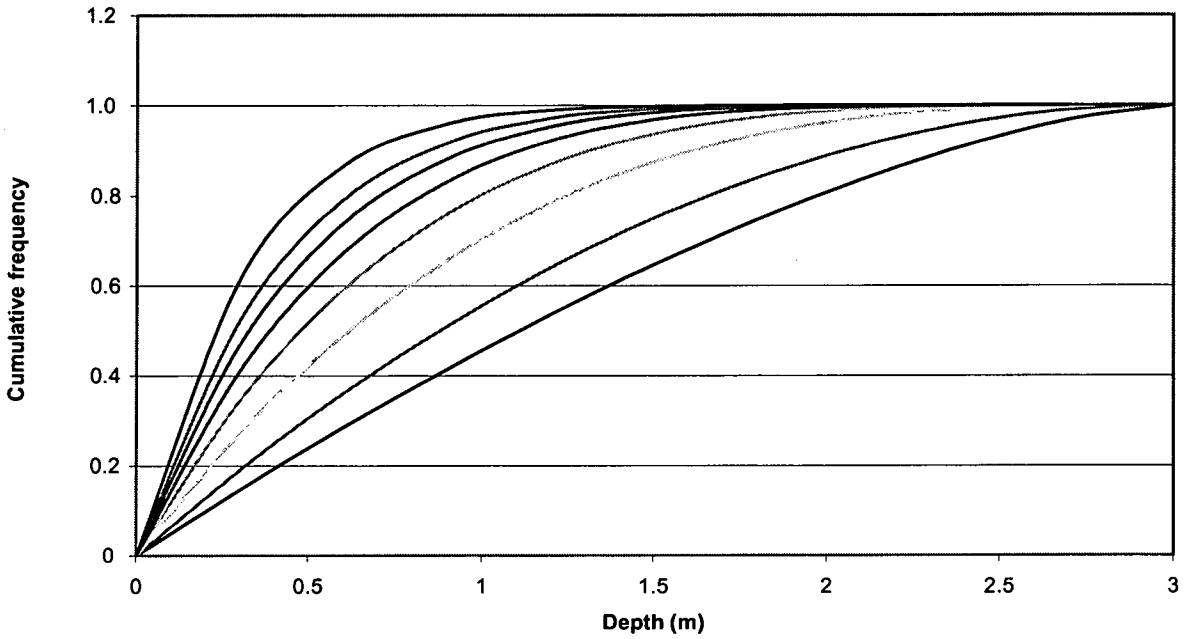

Figure 10
Burrow Depth Distributions for Animals with Maximum Burrowing Depth of 3 m

The impacts of biotic intrusion are modeled in the site and site diffusion models throughout the simulation period. The intruder models assume native plants and animals inhabit the site and intrude into the waste until the intruder arrives at the disposal facility.

3.2 Surface Erosion Model

The surface erosion model is used to evaluate the impacts of surface erosion on the long-term performance of the closed disposal facility. Erosion of the disposal site will reduce the thickness of the cover overlying the disposed waste, thereby permitting greater penetration into the waste by plants and animals and by inadvertent human intruders. The rate at which erosion occurs determines how quickly surface contamination is transported into Cañada del Buey and Pajarito Canyons and, hence, has a direct bearing on the doses projected for the canyon-resident scenarios. Finally, thinning of the cover may increase the release rates of vapor- and gas-phase contaminants. The erosion model is incorporated into the site, intruder, and diffusion models.

Surface erosion modeling is conducted to project rates of cover loss at MDA G and to estimate rates of sediment transport into the adjacent canyons. These aspects of the modeling are discussed in the following sections.

3.2.1 Cover Loss

In general, patterns and rates of surface erosion at MDA G are complex, due to the characteristic mesa and canyon topography of the Laboratory and the construction details of the final cover. Rates of soil loss are spatially dependent, affected by local variations in slope and drainage area, the presence of engineered features placed during cover construction, and changes in relationships between the disposal units and the underlying bedrock. Given the potential importance of surface erosion on long-term facility performance, the surface of the site was represented in three dimensions to capture this spatial dependence.

As stated earlier, MDA G is represented using waste disposal regions and erosion zones. The erosion model estimates the cumulative soil loss within each erosion zone throughout the model simulations; these losses are used to update the thickness of the surface soil, cap, and waste layers for each zone. The erosion model calculations yield the cumulative depths from the ground surface to the bottoms of the different layers, and the thickness of each layer.

Patterns and rates of erosion projected by the GoldSim models are based on long-term surface erosion modeling conducted using the SIBERIA computer code (Willgoose and Riley, 1998). A series of 10,000-year simulations was conducted using SIBERIA to estimate changes in cover depth over the disposal pits and/or shafts comprising each region. Separate simulations were conducted for conditions that are expected to yield low-, moderate-, and high-erosion impacts. A detailed description of this modeling effort may be found in Wilson et al. (2005).

The SIBERIA modeling results demonstrate a wide range of erosive pressures across the site. Large portions of the site are characterized by relatively little soil loss over the 10,000-year simulation period. In other areas, however, significant reductions in the cover thickness are observed, especially under high-erosion conditions. It became evident from these results that the definition of the erosion zones needed to be capable of addressing areas where little or no cover loss occurred as well as areas where all the cover was lost.

The erosion zones are defined in terms of the amount of cover remaining at the end of a specified interval, as shown in Table 5. Portions of the site with 0 to 2 m (0 to 6.6 ft) of cover remaining were divided into eight erosion zones, each with a depth interval of 25 cm (0.8 ft). For example, erosion zone 1 is used to represent portions of the site with 0 to 25 cm (0 to 0.8 ft) of cover remaining at the end of a given simulation period, while erosion zone 6 is used to represent portions of the site with 1.25 to 1.5 m (4.1 to 4.9 ft) of remaining cover. The final two erosion zones were defined as regions where 2.0 to 2.5 m (6.6 ft to 8.2 ft) and more than 2.5 m (8.2 ft) of cover remain.

Table 5
Erosion Zones as Defined by Depth of Remaining Cover

Erosion Zone	Amount of Remaining Cover (cm)
1	0 –25
2	25 –50
3	50 – 75
4	75 – 100
5	100 –125
6	125 – 150
7	150 – 175
8	175 – 200
9	200 – 250
10	>250

To model the spatial variation in erosion at the disposal site, the proportion of the site that falls within each zone at the end of the simulation period of interest must be known. Consequently, SIBERIA was used to project remaining cover depths for each waste disposal region over a 10,000-year period. Using these results, the proportion of a region that falls within a given erosion zone can be determined for simulation times up to 10,000 years. For example, assume 12 percent of a disposal region is projected to have 2.0 to 2.5 m (6.6 to 8.2 ft) of cover remaining

after 1,000 years, while the remainder of the region has a minimum of 2.5 m (8.2 ft) of cover remaining. In this example, the fractional area of the region that is assigned to erosion zone 9 is 0.12 while the fraction of the region assigned to erosion 10 is 0.88. The fraction of the disposal region that is assigned to each of the other eight erosion zones is 0.0.

SIBERIA was used to estimate cover loss for three erosion scenarios marked by low, moderate, and high erosion (Wilson et al., 2005). Based on these results, the cells used to physically represent the disposal units were allocated among the 10 erosion zones for the simulation period of interest; separate assignments were made for the three erosion scenarios. These cell assignments are used to estimate continuous distributions of erosion zone areas and fractional areas for each waste disposal region, which allows consideration of erosion pressures intermediate to these scenarios. To do this, a triangular distribution of the fraction of cells that were assigned to erosion zone 10 (> 2.5 m [8.2 ft] of cover remaining) was defined using the SIBERIA model results for the low-, moderate-, and high-erosion scenarios. In this distribution, the fractional area projected for the moderate-erosion scenario is used to represent the most likely value of the distribution, while the minimum and maximum values of the distribution are defined using model results for the high- and low-erosion scenarios, respectively. The values sampled from the distribution during the GoldSim simulations are compared to the most likely value, and the differences are used to estimate the distribution of nodes among the other 9 erosion zones using a linear scaling process.

To illustrate, if the fractional area selected from the erosion zone 10 distribution is greater than that observed for the moderate-erosion scenario, a scaling factor is calculated using the following:

$$f_s = \frac{a_{f,d,10} - a_{f,m,10}}{a_{f,m,10} - a_{f,h,10}} \qquad 20$$

Where

f_s = fractional area scaling factor
$a_{f,d,10}$ = fractional area sampled from the erosion zone 10 distribution
$a_{f,m,10}$ = fractional area for erosion zone 10 under moderate-erosion conditions
$a_{f,h,10}$ = fractional area for erosion zone 10 under high-erosion conditions

Conversely, if the sampled fractional area is less than that observed under moderate-erosion conditions the scaling factor is calculated as follows:

$$f_s = \frac{a_{f,d,10} - a_{f,m,10}}{a_{f,m,10} - a_{f,l,10}} \qquad 21$$

Where

$a_{f,l,10}$ = fractional area for erosion zone 10 under low-erosion conditions

The scaling factors calculated using Equations 20 and 21 are used to modify the fractional areas for the other nine erosion zones. If the scaling factor was calculated using Equation 20, then the fractional areas for the other erosion zones are estimated as follows:

$$a_{f,d,i} = a_{f,m,i} + f_s \times (a_{f,m,i} - a_{f,h,i}) \quad 22$$

Where

$a_{f,d,i}$ = sampled fractional area for erosion zone i
$a_{f,m,i}$ = fractional area for erosion zone i under moderate-erosion conditions
$a_{f,h,i}$ = fractional area for erosion zone i under high-erosion conditions

If the scaling factor was calculated using Equation 21, the fractional areas for the other erosion zones are calculated as follows:

$$a_{f,d,i} = a_{f,m,i} + f_s \times (a_{f,m,i} - a_{f,l,i}) \quad 23$$

Where

$a_{f,l,i}$= fractional area for erosion zone i under low-erosion conditions

The area associated with the cells within an erosion zone is the product of the number of cells in the zone and the area of each cell. The SIBERIA modeling used almost 7×10^4 cells to represent the disposal units at MDA G; the area of each cell is 6.25 m^2 (67 ft^2).

Each of the 10 erosion zones is characterized by unique surface erosion characteristics that are reflected in the erosion or cover loss function assigned to the zone. The process of defining the cover loss functions began with an examination of the SIBERIA modeling results (Wilson et al., 2005). Because the modeling projects rates of soil loss for each grid location or node within a given erosion zone, it was clear that only a portion of these results could be examined. Consequently, up to 15 nodes were randomly selected from the 10 erosion zones for each of the three erosion scenarios; data for erosion zones were combined across all waste disposal regions. Plots were constructed of the remaining cover thickness as a function of time for these cells and used to guide the development of the cover loss functions used in the four GoldSim models.

The projected cover loss data for some of the randomly selected nodes are shown in Figures 11 through 13; these functions represent the remaining cover depth as a function of time over a 10,000-year period. Figure 11 shows the remaining cover depth for up to 15 randomly selected cells in erosion zone 2 under moderate- and high-erosion conditions, respectively. Erosion zone 2 is marked by relatively high cover loss; all cells within it have only 0.25 to 0.5 m (0.82 to 1.6 ft) of cover remaining at the end of the simulation period. Results for the low-erosion scenario are not shown because all cells used to represent the disposal units have a cover thickness greater than 0.5 m (1.6 ft) after 10,000 years.

Rates of soil loss within erosion zone 2 are greatest within the first 2,000 years under moderate-erosion conditions, tending to slow thereafter (Figure 11a). In general, the selected nodes exhibit the same erosion behavior. In contrast, a range of behaviors is observed under high-erosion conditions (Figure 11b). Although most cells shown tend to lose cover throughout the 10,000-year period, patterns of cover loss change at some locations. Some cells exhibit the gradually tapering behavior noted under moderate-erosion conditions, others exhibit relatively linear rates of erosion throughout the simulation period, and one cell even shows deposition occurring for a period of about 3,000 years. The rapid loss of cover observed for some cells under high-erosion conditions is probably the result of gully formation.

Figure 12 shows cover depth as a function of time for erosion zone 5 under low-, moderate-, and high-erosion conditions; Figure 13 summarizes the corresponding information for erosion zone 9. Erosion zone 5 is characterized by 1.0 to 1.25 m (3.3 to 4.1 ft) of cover remaining at the end of 10,000 years, while 2.0 to 2.5 m (6.6 to 8.2 ft) of cover material remains over the waste in zone 9. Under low- and moderate-erosion conditions, rates of cover loss appear greatest within 2,000 to 3,000 years of closure in erosion zone 5, decreasing slightly thereafter (Figures 12a and 12b). A wide range of behaviors is found in this zone under high-erosion conditions (Figure 12c). Deposition occurs at some cells; in general, however, rates of cover loss are greatest in the earlier part of the simulation. Rates of cover loss appear relatively linear within erosion zone 9 (Figure 13) for the majority of the sampled cells. Cells that exhibit abrupt changes in remaining cover depth most likely lie in areas marked by gully formation.

The data summarized in Figures 11 through 13 indicate that rates of surface erosion will vary temporally and spatially within and between the 10 erosion zones. While it is not reasonable to model soil loss on a node-by-node basis, it is clear that a single function will not adequately describe the range of cover loss behavior demonstrated by the disposal facility. Consequently, a family of normalized cover loss functions was used to describe the variability inherent in the rates and patterns of cover loss over the disposal units.

Figure 11a
Moderate erosion conditions

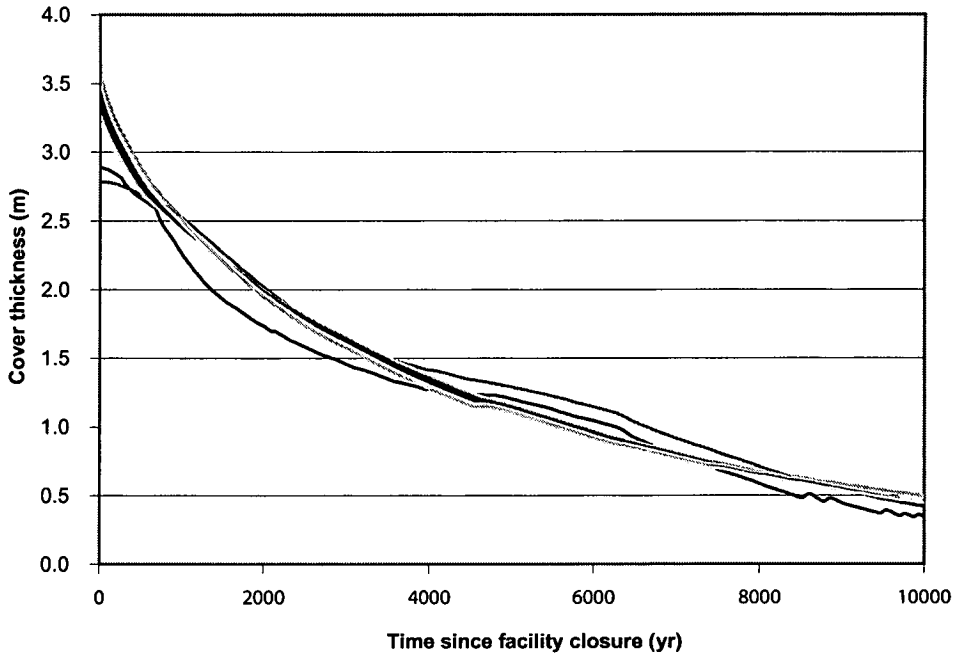

Figure 11b
High erosion conditions

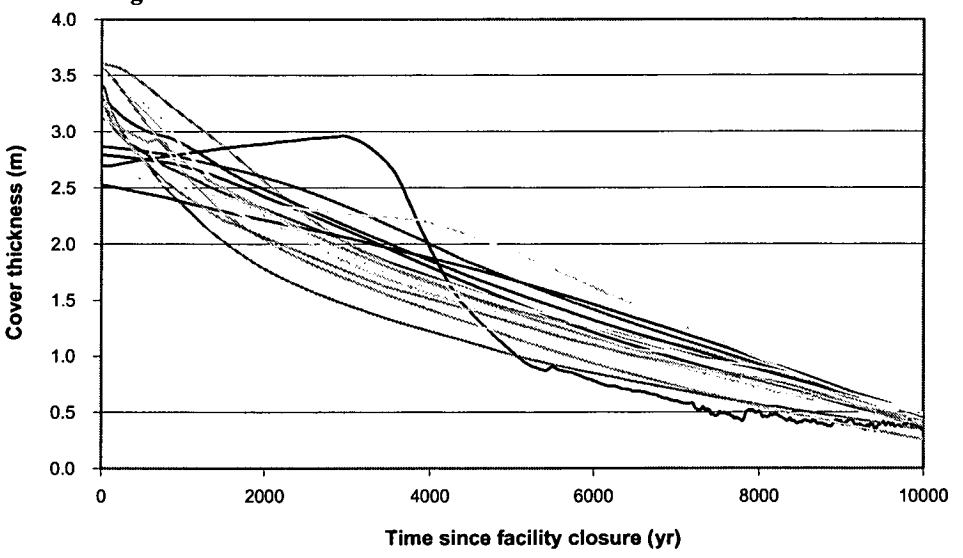

Figure 11
Erosion Behavior of Selected Nodes in Erosion Zone 2

Figure 12a
Low erosion conditions

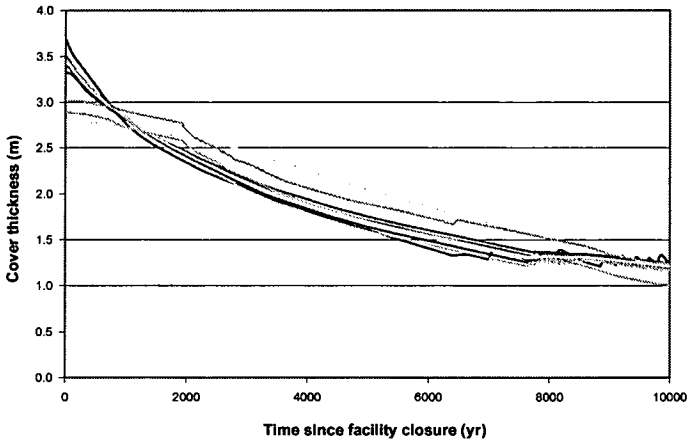

Figure 12b
Moderate erosion conditions

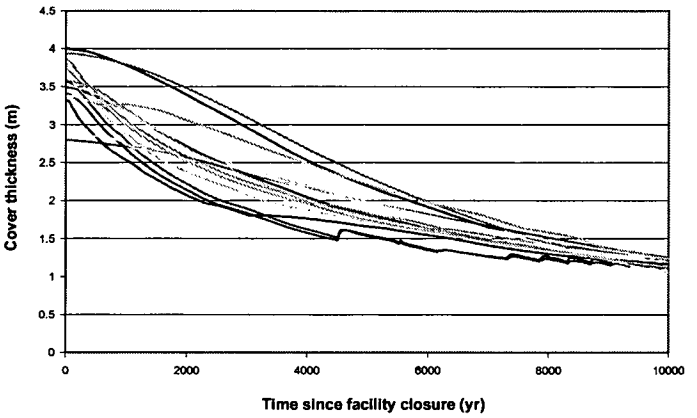

Figure 12c
High erosion conditions

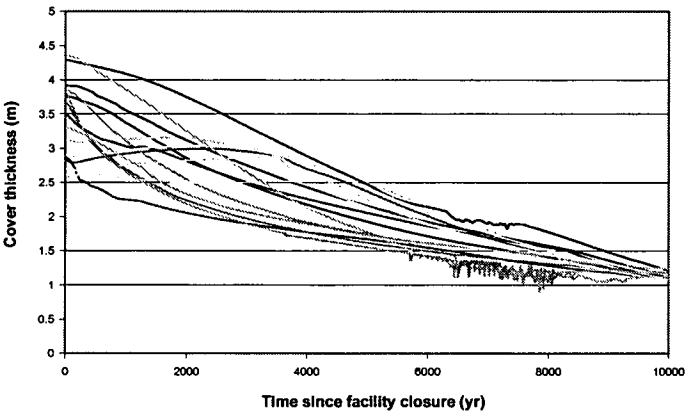

Figure 12
Erosion Behavior of Selected Nodes in Erosion Zone 5

Figure 13a
Low erosion conditions

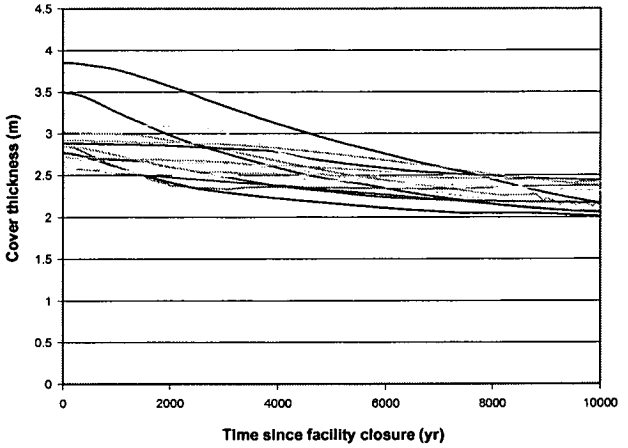

Figure 13b
Moderate erosion conditions

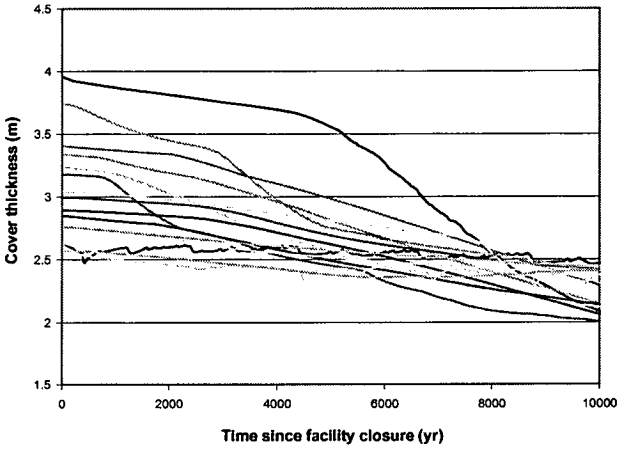

Figure 13c
High erosion conditions

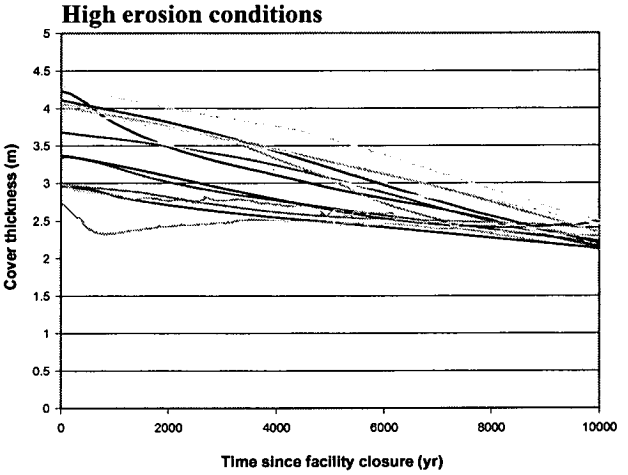

Figure 13
Erosion Behavior of Selected Nodes in Erosion Zone 9

The general form of the cover loss functions is given by the following equation:

$$d_{c,t} = B \times t^{\alpha} \times (t_{\max} - t)^{\beta} \quad 24$$

Where

$d_{c,t}$ = fraction of initial cover remaining at time t
B = beta function
t = time (yr)
α = shape factor
t_{max} = simulation period (yr)
β = shape factor

The beta function was discussed earlier with respect to plant root and animal burrow distributions. As applied here, the beta function is determined as follows:

$$B = \frac{\Gamma(\alpha+\beta)}{\Gamma(\alpha) \times \Gamma(\beta) \times t_{max}^{\alpha+\beta}} \quad 25$$

Where

Γ = factorial of the quantities within the parentheses

Equation 25 simplifies to the following if α, one of the shape factors, is set equal to zero:

$$B = \frac{1}{t_{\max}^{\alpha+\beta}} \quad 26$$

Using this formulation, the fraction of the initial cover that remains at time t, is as follows:

$$B_{a,d} = \left(B \times t^{\alpha} \times (t_{max} - t)^{\beta}\right) \quad 27$$

This is the form of the cover loss function that is implemented in the erosion modeling.

The shape factor, β, determines the form of the normalized cover loss functions. This parameter is assigned values to generate functions that generally encompass the soil loss behavior displayed by the cells shown in Figures 11 through 13. Figure 14 illustrates this by superimposing the cover loss functions implemented in the GoldSim models over the erosion data for erosion zones 2, 5, and 9 under moderate-erosion conditions. The erosion data were modified so they could be compared to the normalized cover loss functions. Specifically, the remaining cover was normalized to the total amount of cover lost during the 10,000-year simulation. The comparisons show that the derived cover loss functions generally capture the erosion behavior noted for the cells in erosion zones 2 and 5 (Figures 14a and 14b); the derived functions overestimate rates of erosion for some cells in the latter zone. The cover loss functions tend to overestimate rates of erosion when overall rates of soil loss are small, as seen in Figure 14c for erosion zone 9.

Figure 14a
Erosion Zone 2

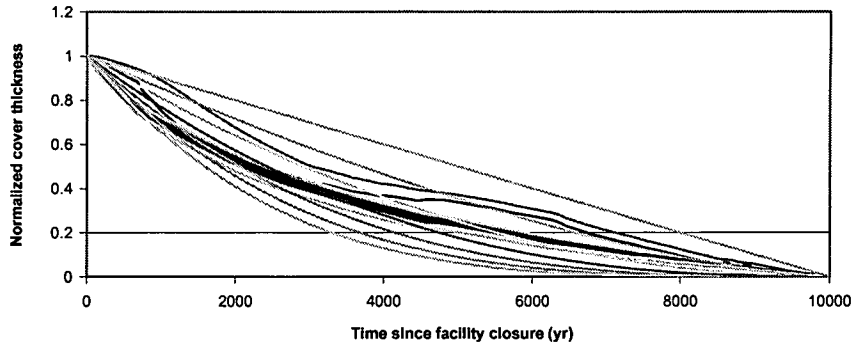

Figure 14b
Erosion Zone 5

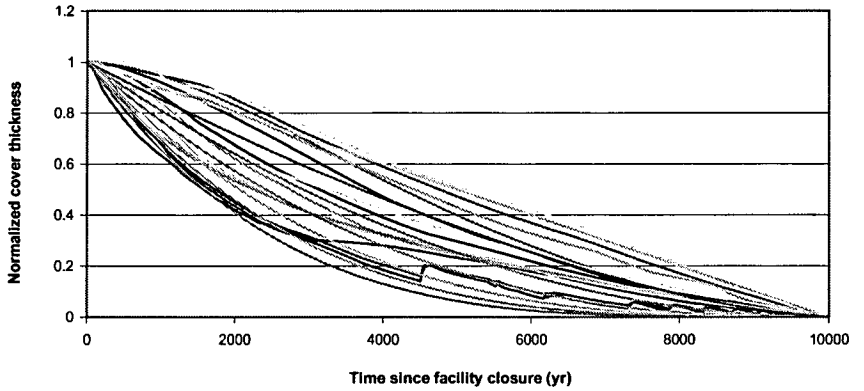

Figure 14c
Erosion Zone 9

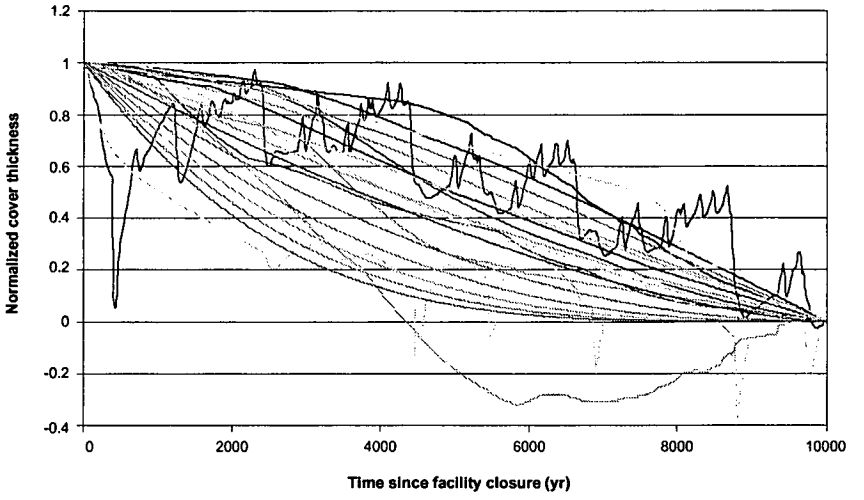

Figure 14
Comparison of Cover Loss Functions and Erosion Behavior for Selected Nodes under Moderate Erosion Conditions

The cover loss functions described above are used to estimate normalized rates of soil loss over time in the 10 erosion zones. To calculate actual soil losses, these normalized losses are multiplied by the total depth of material that is initially available for erosion. This depth is equal to the initial cap thickness minus the thickness of material remaining at the end of the simulation. For example, if the initial cap depth is 3.5 m (11.5 ft) and the erosion zone under consideration is defined to have 1.5 m (4.9 ft) of cover remaining at the end of the simulation, the depth of material available for erosion is 2.0 m (6.6 ft).

Projected rates of soil loss are used to reduce the thickness of the waste repository cover over time. Although actual soil loss progresses downward from the surface of the disposal facility, a different approach was adopted for the GoldSim models. Integral to this approach is the division of the cover into two components, the surface soil layer and the cap. The surface soil layer is defined as the top 1 cm (0.4 in.) of cover material, while the cap represents the entire cover less this top 1 cm (0.4 in.). This division allows a more accurate estimation of the radionuclide concentrations in the material subject to resuspension and transport by surface runoff.

For modeling purposes, the surface soil layer is maintained at a constant 1 cm (0.4 in.) depth. However, this thin layer is subject to rapid erosion. To avoid the need to constantly redefine the surface layer, the GoldSim models account for the effects of erosion by replenishing it with material from the underlying cap or, if the cap has been eroded away, the waste. This is done by transporting the quantity of soil lost annually due to erosion from the surface soil layer to the adjacent canyons and then transporting a like quantity from the cap or waste to the surface soil layer to maintain the material balance in the surface layer.

The material transferred from the cap or waste to the surface soil layer is drawn from the uppermost layer of cap (or waste) material. For example, shortly after site closure, bulk crushed tuff is transferred from cap layer 1 to the surface soil layer to simulate the loss of soil due to erosion; the thickness of the cap layer is reduced accordingly. Later, if the uppermost cap layer has been lost due to erosion, material used to replenish the surface soil layer is taken from cap layer 2 and the thickness of that layer is reduced accordingly. This process is repeated until the end of the simulation.

The origin of the cover or waste material used to replenish the surface soil layer is tracked using a series of cap-and-waste-loss fractions. The elements used for this process are found in the Erosion_Impacts container, which, in turn, is found in the Erosion_Model container. These elements determine if the soil loss for the current year of the simulation is less than the remaining cap or waste material in the uppermost layer of material. If so, the loss fraction for the cap or waste layer is set equal to 1.0, which indicates that all material used to replenish the surface soil layer originates from the uppermost cap or waste layer. This layer is then reduced in thickness and the process is repeated in the next time step of the simulation. If, however, the

projected soil loss exceeds the remaining thickness of the uppermost cap or waste layer, the model transfers material from the next cap or waste layer to make up the difference and the thickness of each layer is adjusted.

Over a long enough time period, surface erosion of the disposal facility may result in the complete removal of part or all of the waste repository cover. However, because the GoldSim models become less stable when one or more of the layers used to represent the disposal system profile is completely lost, a simplification incorporated into the erosion model prevents this occurrence. Soil loss from the cap layers is assumed to continue until the total thickness of the cap reaches 1 cm (0.4 in.), after which erosion is assumed to cease for the remainder of the simulation. As a result, the minimum thickness for each cap layer is 1 cm (0.4 in.) divided by the number of cap layers. This minimum cap thickness combined with the 1 cm (0.4 in.) surface soil layer (which is held constant) results in a minimum total cover thickness of 2 cm (0.8 in.), even after complete cover loss is projected to occur. A similar approach is applied to the erosion of the waste layers; erosion is assumed to continue until 1 cm (0.4 in.) of waste remains, at which time the thickness of each waste layer is 1 cm (0.4 in.) divided by the number of waste layers.

3.2.2 Sediment Transport

In general, surface contamination transported from MDA G by runoff will enter either Cañada del Buey or Pajarito Canyon, both of which are adjacent to the disposal facility. The portion of contamination allocated to each canyon will depend upon several factors including the location of the disposal units relative to the axis of the mesa, local slope characteristics of the cover, and engineered features of the cover. Although surface erosion modeling was conducted primarily to estimate rates of cover removal, the results of this work also provide insight into spatial aspects of contaminant transport at the disposal facility.

The SIBERIA modeling results (Wilson et al., 2005) were used to estimate sediment flows into Cañada del Buey and Pajarito Canyon for the three erosion scenarios. Each canyon was divided into two or more catchments based on expected sediment transport patterns, as depicted in Figure 15. In terms of Cañada del Buey, catchment CdB1 includes the majority of the canyon that may receive contaminated sediments from MDA G; catchment CdB2 lies at the east end of the disposal facility and is projected to capture sediment transported from a portion of waste disposal region 1. Pajarito Canyon was divided into seven catchments, primarily on the basis of the small drainages that transport the majority of the sediment generated on top of Mesita del Buey.

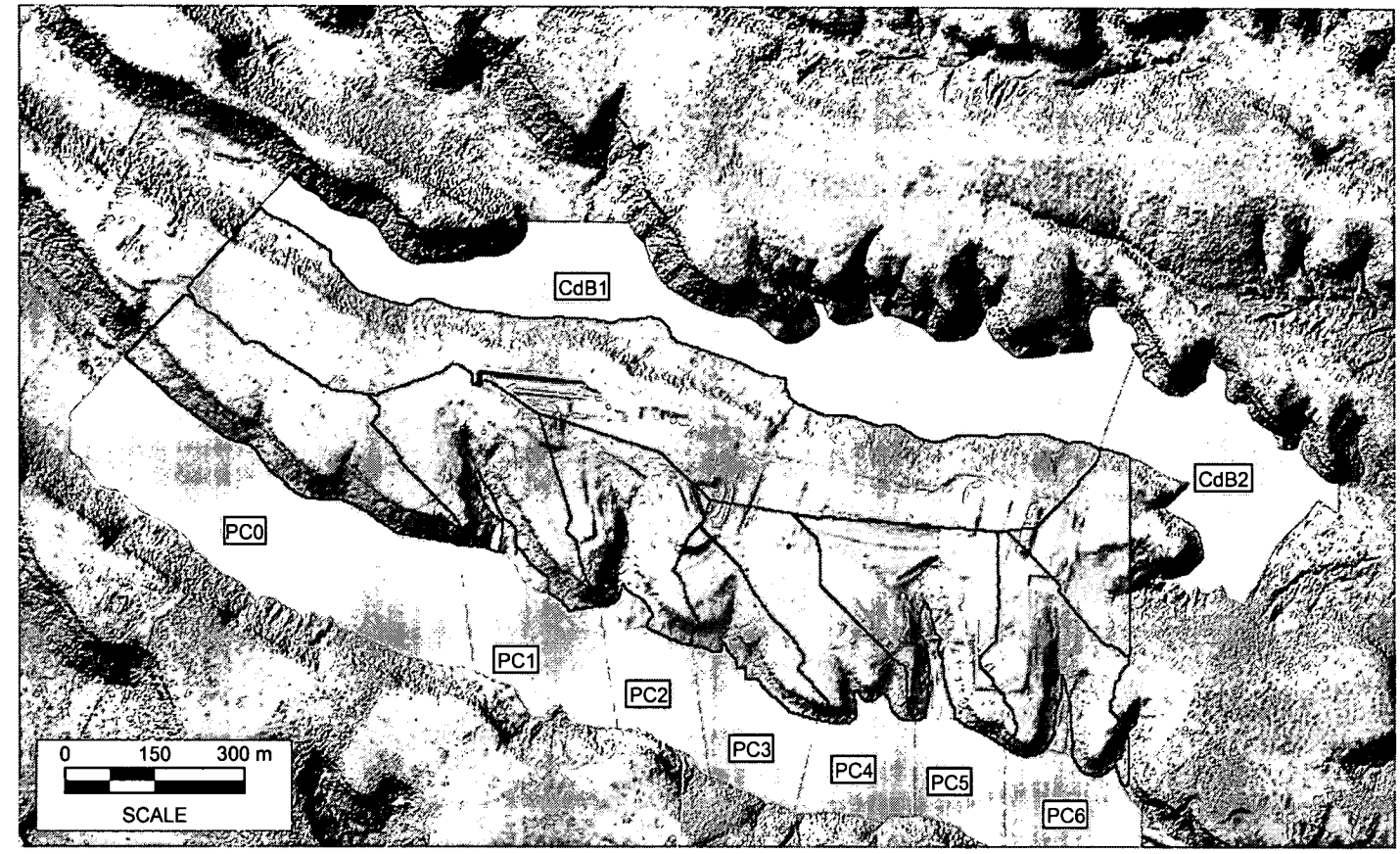

Figure 15
MDA G Sediment-Source Areas and Sediment Catchments in Habitable Canyon Bottoms

The SIBERIA model was used to estimate the quantities of sediment transported from the eight waste disposal regions to the canyon catchments. Sediment was tracked from its source on the mesa to the point at which it was transported over the edge of the mesa. The sediment was then assigned to the catchment below this point. Estimates were made of the total sediment transported from each disposal region and the sediment yield from the surface of the pits and shafts within each disposal region. Sediment transported from disposal region 7, which consists mainly of shafts scattered among the region 3 pits, was assumed to follow the paths estimated for region 3. The allocation of sediment among the nine catchments was evaluated at periods of 100, 200, 500, 1,000, 5,000, and 10,000 years after facility closure.

The results of the sediment mapping indicate that 20 to almost 100 percent of the sediment within a waste disposal region is transported to Cañada del Buey. Sediments transported from each of the waste disposal regions to Pajarito Canyon enter one to three of the catchments, depending upon the region under consideration. The small drainages along the south side of the mesa tend to focus sediment flows into this canyon. Detailed results of the sediment mapping analysis are included in Section 5.7.1 of this report.

3.3 Human Intrusion Model

The human intrusion model is used to calculate the amount of cover material and waste that is excavated and spread across the receptor's lot for the Intruder-Construction, Intruder-Agriculture and Intruder – Post-Drilling Scenarios. The total volume of material brought to the surface of the disposal site as a result of basement excavation is calculated using the following equation:

$$V_b = \frac{b_d \times (b_w \times b_l + e_{w,s} \times e_{l,s} + 4 \times e_{w,0.5b} \times e_{l,0.5b})}{6} \qquad 28$$

Where

V_b = volume of material excavated during basement construction (m^3)
b_d = depth of basement (m)
b_w = width of basement (m)
b_l = length of basement (m)
$e_{w,s}$ = width of basement excavation at ground surface (m)
$e_{l,s}$ = length of basement excavation at ground surface (m)
$e_{w,0.5b}$ = width of basement excavation at one-half of the basement depth (m)
$e_{l,0.5b}$ = length of basement excavation at one-half of the basement depth (m)

The material brought to the surface during basement excavation will include cover material and waste. Assuming the waste is a single layer of material, the volume of waste brought to the surface is calculated as follows:

$$V_{w,b} = \frac{t_w \times (b_w \times b_l + e_{w,w} \times e_{l,w} + 4 \times e_{w,0.5w} \times e_{l,0.5w})}{6} \quad 29$$

Where

$V_{w,b}$ = volume of waste excavated during basement construction (m^3)
t_w = thickness of waste (m)
$e_{w,w}$ = width of basement excavation at cover-waste interface (m)
$e_{l,w}$ = length of basement excavation at cover-waste interface (m)
$e_{w,0.5w}$ = width of basement excavation at one-half of the waste thickness (m)
$e_{l,0.5w}$ = length of basement excavation at one-half of the waste thickness (m)

The difference between the total amount of excavated material and the amount of excavated waste is the volume of cover material excavated during basement construction.

Equation 29 is applicable only if the waste is represented by a single layer of material. In fact, the cap and waste are represented using 4 cells each in the intruder model, while the intruder model with diffusion represents the cap and waste using 16 and 20 cells, respectively. In these models, then, the volumes of material removed during basement excavation are explicitly calculated for each of the affected cap and waste layers. Although the same general equation is used to conduct these calculations, the parameters are defined in terms of the lengths and widths of the excavation at the top, midpoint, and bottom of the cap or waste layer under consideration, and the thickness of that layer.

The cover material and waste excavated during basement construction is assumed to be thoroughly mixed. A portion of the mixed material is used for backfill around the foundation of the house. The volume of this backfill is the difference between the total volume of excavated material and the product of the dimensions of the basement. The remaining material is spread over the intruder's lot. The thickness of the material over the lot is calculated as the excavation volume less the volume of material used for backfilling, divided by the net lot area. The net lot area is the total lot size less the area of the receptor's house.

The Intruder – Post-Drilling Scenario assumes that the well that is established to supply water for domestic needs will pass through the cover, waste, and strata underlying the disposal units. The volume of waste brought to the surface during drilling is given by the following equation:

$$V_{w,d} = \pi \times r_{wc}^2 \times t_w \quad 30$$

Where

$V_{w,d}$ = volume of waste excavated during well drilling (m^3)
r_{wc} = radius of the well casing (m)
π = the constant *pi* (3.1416)

Equation 30 is used to calculate the volume of cover material brought to the surface during drilling by substituting the cover thickness for the waste thickness. The thickness of the cover is modified over time to account for the effects of surface erosion at MDA G. The well will also pass through the strata that lie between the bottom of the disposal units and the regional aquifer. While this material will also be brought to the surface, it is ignored in terms of determining radionuclide concentrations in the surface soils to which the intruder is exposed.

3.4 Diffusion Model

The MDA G Site Diffusion Model and the intruder diffusion model estimate the rates of generation of gas- and vapor-phase radionuclides, and simulate the upward movement of the radionuclides from the disposed waste. Contamination is transported from the cover to the air above the disposal facility in the site diffusion model. The intruder diffusion model transports radionuclides to the surface of the facility, into the basement excavation, or through the floor of the concrete foundation of the intruder's house, depending upon the exposure scenario under consideration.

The diffusion of radionuclides between cells is invoked by linking the transport pathway elements with diffusive mass-flux links. The mathematical model used by GoldSim to model transport under these conditions is discussed in the user's manual for the contaminant transport module (GoldSim, 2005b).

The site and intruder diffusion models divide the cap into 16 layers and the waste into 20 layers. Dividing the cap and waste into several layers is necessary to ensure accurate estimates of the diffusion rates through these materials. Using too few layers to represent the cover and waste will artificially increase rates of transport through the disposal system, while using an excessive number of layers complicates the model and slows model execution. The level of discretization adopted for the diffusion models was determined on the basis of the analyses described in *Attachment I.*

The thickness of all but the uppermost cap layer is set equal to the total cover thickness divided by 16; the thickness of cap layer 1 is reduced by 1 cm (0.4 in.) to account for the presence of the surface soil layer. The thickness of the waste layers varies with depth. The individual thickness of the top 10 waste layers is set to either one-twentieth of the total waste thickness or 0.25 m (0.8 ft), whichever is less. The thickness of each of the bottommost 10 layers is set to one-tenth of the total waste thickness less the combined thickness of the top 10 layers. The intruder

diffusion model divides the floor of the receptor's concrete foundation into 4 layers of equal thickness.

The two diffusion models simulate the movement of tritiated water vapor, C-14 gas, krypton, and radon through the disposal system. The gas-to-water partition coefficients are calculated within the models to describe how these species are allocated between their vapor or gas phase and the water occupying the pores of the cover and waste. The partition coefficient for tritium is given by the following:

$$KD_{H3,air} = \frac{VP \times M}{R \times T \times \rho_{H2O}} \qquad 31$$

Where

$KD_{H3,air}$ = air-to-water partition coefficient for H-3
VP = vapor pressure of H-3 (atm)
M = molecular weight of water (g/mol)
R = ideal gas constant (atm-m^3/mol-°K)
T = temperature (°K)
ρ_{H_2O} = density of water (g/m^3)

C-14 (as CO_2 or CH_4), krypton, and radon will partition between air and water in the pore spaces of the cap and waste in proportion to their Henry's Law constant. The partition coefficients for these species are given by Equation 32:

$$KD_{j,air} = \frac{1}{H_j \times R \times T} \qquad 32$$

Where

$KD_{j,air}$ = air-to-water partition coefficient for gas j
H_j = Henry's Law constant for gas j (mol/m^3-atm)
R = ideal gas constant (atm-m^3/mol-°K)
T = temperature (°K)

The diffusion coefficients used in the diffusion modeling are calculated using the empirical relationship developed by Millington (1959):

$$D_e = D_o \times \frac{p_a^{10/3}}{p^2} \qquad 33$$

Where

D_e = pore diffusion coefficient (m^2/s)

D_o = gas diffusion coefficient in free air (m^2/s)
p_a = air-filled porosity
p = effective porosity

Separate diffusion coefficients are calculated for the waste in the disposal units, the cap, and the concrete used to construct the foundation of the intruder's house. The cap and waste diffusion coefficients calculated for tritium are multiplied by a thermal gradient factor to account for the effect of thermal gradients in these materials upon the apparent rate of diffusion (Philip and DeVries, 1957); thermal gradient effects are not considered for the concrete foundation.

The diffusion coefficients estimated using Equation 33 are modified to conform to the manner in which GoldSim parameterizes the diffusion process. GoldSim requires input of unitless quantities called relative diffusivities, which it multiplies by the reference diffusivity and the available porosity, effective porosity, and tortuosity of the porous medium to yield the final effective diffusion coefficients used in the model simulations. Given this approach, the diffusion coefficients calculated above are divided by the reference diffusivity and effective porosity of the porous medium under consideration to calculate the desired relative diffusivities. The available porosity and tortuosity of the medium are both set to 1 under this modeling approach.

The amount of C-14 available for diffusion as C-14 gas is given by the product of the C-14 inventory and the organic fraction of the waste. The organic waste inventory is multiplied by a gas generation rate constant that describes the rate at which the waste biodegrades. The gas generated as a result of biodegradation is allocated to CO_2 and CH_4.

Only a portion of the radon gas generated by the decay of its long-lived parents will be available for diffusion; the rest will remain trapped within the solid waste until it decays to negligible levels. Radon gas generation rates are represented by modifying the decay characteristics of the parents of Rn-220 and Rn-222. Specifically, the fraction of time the parents of the radon isotopes decay to form radon gas is set equal to the radon emanation coefficient; during the remainder of the time, the decay of the parents forms daughters of Rn-220 and Rn-222.

3.5 Dose Model

The MDA G performance assessment and composite analysis project potential human exposures for the exposure scenarios described in Section 2.1 (Table 1). In these scenarios, the receptor is postulated to come in contact with contamination and receive doses via ingestion, inhalation, and direct radiation. The models used to estimate the exposures received through these routes are discussed in the following sections.

3.5.1 Ingestion Exposure Route

The performance assessment and composite analysis receptors are postulated to ingest contaminated soil, food crops, animal products, and water. In general, the ingested activity of a given radionuclide is the product of the consumption rate of the ingested item, the proportion of the total material ingested that is contaminated, and the radionuclide concentration in the soil, food, or water:

$$I_{g,m,i,t} = U_m \times f_m \times C_{m,i,t} \qquad 34$$

Where

$I_{g,m,i,t}$ = intake, through material *m*, of radionuclide *i* through time *t* (Ci/yr)
U_m = consumption rate of material *m* (kg/yr)
f_m = fraction of consumed material that is contaminated
$C_{m,i,t}$ = concentration, in material *m*, of radionuclide *i* at time *t* (Ci/kg)

The quantities of substances ingested by a receptor are given by the ingestion rates for vegetables, animal products, soil, and water. The receptors for the All Pathways – Groundwater, Atmospheric, All Pathways – Canyon, Intruder-Agriculture, and Intruder – Post-Drilling Scenarios are assumed to consume homegrown vegetables, animal products from animals raised on location, and soil. The receptor for the Groundwater Resource Protection Scenario is assumed to ingest contamination only through drinking water, while the construction intruder scenario assumes that the receptor receives contamination only from ingested soil.

The fraction of a receptor's intake of vegetables that is grown at the exposure location is defined initially from a user-specified input value. The ratio of the area available for growing crops and the area needed to raise the specified quantities of leafy vegetables, produce, and grain is then calculated using the following equation:

$$f_{cc} = \frac{A_l - A_h}{\frac{U_{lv}}{Y_{lv}} + \frac{U_p}{Y_p} + \frac{U_g}{Y_g}} \times f_{uc} \times 1 \qquad 35$$

Where

f_{cc} = crop capacity factor, or the proportion of the specified crops that can be grown on the receptor's lot
A_l = area of receptor's lot (m^2)
A_h = area of receptor's house (m^2)
U_{lv} = human consumption rate of leafy vegetables (kg/yr)
Y_{lv} = annual agricultural yield of leafy vegetables (kg/m^2 wet weight)
U_p = human consumption rate of produce (kg/yr)
Y_{lv} = annual agricultural yield of produce (kg/m^2 wet weight)

U_g = human consumption rate of grain (kg/yr)
Y_g = annual agricultural yield of grain (kg/m^2 wet weight)
f_{uc} = user-specified fraction of crops that is grown on-site
1 = constant (yr)

The crop capacity factor is set equal to the lesser of the calculated fraction or 1.0. The result is multiplied by the user-specified fraction of crops grown on-site to yield the fraction used in the dose assessment. A factor of 1.0 indicates that the area required to raise the crops exists and the user-specified homegrown fraction is used in the dose calculations. Factors less than 1.0 indicate that the specified space requirements cannot be satisfied and the fraction of the receptor's intake that is contaminated is reduced.

After the area required to raise the vegetables at the receptor location is defined, the remaining portion of the receptor's lot area may be allocated for raising animals (to be consumed by the receptor). Human consumption rates of animal products are used in conjunction with crop productivities to determine the amount of land needed to raise forage for the animals. This calculation accounts for both the number of animals needed to supply the receptor's food requirements and the forage requirements of these animals. The equation used to estimate the animal forage capacity factor for cattle and cows is as follows:

$$f_{pg} = \frac{A_l - A_h - \left(\frac{U_{lv}}{Y_{lv}} + \frac{U_p}{Y_p} + \frac{U_g}{Y_g}\right) \times f_{uc} \times f_{cc} \times 1}{\frac{\left(N_{ct} \times Q_{f,ct} + N_{cw} \times Q_{f,cw}\right)}{Y_{pg}} \times 1} \qquad 36$$

Where

f_{pg} = forage capacity factor for cattle and cows, or the proportion of animals' forage requirements that can be grown on the receptor's lot
N_{ct} = number of full-time cattle equivalents required to supply the specified quantity of beef
$Q_{f,ct}$ = forage consumption rate of cattle (kg/yr dry weight)
N_{cw} = number of full-time cow equivalents required to supply the specified quantity of milk
$Q_{f,cw}$ = forage consumption rate of cows (kg/yr dry weight)
Y_{pg} = annual agricultural yield of pasture grass (kg/m^2 dry weight)
1 = constant (yr)

The numerator of Equation 36 is set to the greater of the calculated quantity or 0 m^2 (0 ft^2), and the animal forage capacity factor is set to the lesser of the calculated fraction or 1. Factors less than 1.0 indicate that the forage needed by the animals to supply the specified amounts of beef

and milk cannot be grown on the land available on-site. Under these conditions, portions of the animals' diet requirements are assumed to come from uncontaminated lands.

The numbers of cattle and cows required to supply the beef and milk are calculated as follows:

$$N_{ct} = \frac{U_{bf} \times f_{bf} \times 1}{w_{ct} \times r_{cl} \times f_{cb}} \quad 37$$

$$N_{cw} = \frac{U_{mk} \times f_{mk}}{y_{mk}} \quad 38$$

Where

U_{bf} = human consumption rate of beef (kg/yr)
f_{bf} = fraction of receptor-consumed beef supplied by animals raised on-site
1 = constant (yr)
w_{ct} = weight of cattle at slaughter (kg)
r_d = carcass-to-live-weight ratio
f_{cb} = fraction of carcass that is edible meat
U_{mk} = human consumption rate of milk (kg/yr)
f_{mk} = fraction of receptor-consumed milk supplied by animals raised on-site
y_{mk} = milk production rate (kg/yr)

An equation similar to Equation 36 is used to calculate the forage capacity factor for chickens:

$$f_g = \frac{A_l - A_h - \left(\frac{U_{lv}}{Y_{lv}} + \frac{U_p}{Y_p} + \frac{U_g}{Y_g}\right) \times f_{uc} \times f_{cc} \times 1}{\frac{\left(N_{ch} \times Q_{g,ch} + N_{cl} \times Q_{g,ch}\right)}{Y_g \times dw_g} \times 1} \quad 39$$

Where

f_g = forage capacity factor for chickens, or the proportion of the birds' forage requirements that can be grown on the receptor's lot
N_{ch} = number of full-time equivalent chickens required to supply the specified quantity of chicken
$Q_{g,ch}$ = grain consumption rate of chickens (kg/yr dry weight)
N_{cl} = number of full-time equivalent layers required to supply the specified quantity of eggs
$d_{w,g}$ = dry-to-wet-weight fraction for grain

The numbers of chickens required to supply the chicken and eggs are calculated as follows:

$$N_{ch} = \frac{U_{ch} \times f_{ch} \times 1}{w_{ch} \times r_{cl} \times f_{cm}} \quad 40$$

$$N_{cl} = \frac{U_{eg} \times f_{eg}}{y_{eg} \times m_{eg} \times (1 - f_{sl})} \quad 41$$

Where

U_{ch} = human consumption rate of chicken (kg/yr)
f_{ch} = fraction of receptor-consumed chicken supplied by animals raised on-site
1 = constant (yr)
w_{ch} = weight of chickens at slaughter (kg)
r_{cl} = ratio of ready-to-cook and live weights of chickens
f_{cm} = fraction of ready-to-cook weight of chicken that is edible meat
U_{eg} = human consumption rate of eggs (kg/yr)
f_{eg} = fraction of receptor-consumed eggs supplied by animals raised on-site
y_{eg} = egg production rate of layers (kg/yr)
m_{eg} = mass of egg (kg)
f_{sl} = fraction of egg mass contributed by the shell

The doses received from the ingestion of contaminated materials are given by the following:

$$D_{g,i,m,t} = I_{g,m,i,t} \times D_{g,i} \quad 42$$

Where

$D_{g,i,m,t}$ = whole-body effective dose equivalent from the ingestion of radionuclide i in material m at time t (mrem/yr)
$D_{g,i}$ = ingestion dose conversion factor for radionuclide i (mrem/Ci).

The total dose from the ingestion of the contaminated material is the sum of the radionuclide doses. Total ingestion doses are determined by summing over all media ingested by the receptor.

3.5.2 Inhalation Exposure Route

The dose assessment includes the projection of doses due to the inhalation of radioactivity suspended in the form of particulates and released as vapors or gases. The radionuclide intake via inhalation is calculated using the following equation:

$$I_{h,i,t} = U_{air} \times t_{exp} \times C_{at,i,t} \quad 43$$

Where

$I_{h,i,t}$ = intake, through inhalation, of radionuclide i at time t (Ci/yr)

U_{air} = inhalation rate (m^3/d)
t_{exp} = time of exposure (d/yr)
$C_{at,i,t}$ = concentration, in air, of radionuclide i at time t (Ci/m^3)

The time of exposure is the sum of the time spent indoors and outdoors at the receptor location. The sum of the sampled indoor and outdoor exposure times may exceed 365 d/yr when the models are run in a probabilistic fashion; the outdoor exposure time is adjusted downward if this occurs.

The product of the inhalation intakes calculated using Equation 43 and the inhalation dose conversion factors yields the radionuclide doses due to the inhalation of contaminated air:

$$D_{h,i,t} = I_{h,i,t} \times D_{h,i} \qquad 44$$

Where

$D_{h,i,t}$ = whole body effective dose equivalent from the inhalation of radionuclide i at time t (mrem/yr)
$D_{h,i}$ = inhalation dose conversion factor for radionuclide i (mrem/Ci)

The total dose from the inhalation of airborne contamination is the sum of the radionuclide doses.

3.5.3 Direct Radiation Exposure Route

All receptors included in the performance assessment and composite analysis may be exposed to direct radiation from contaminated ground surfaces. These exposures are calculated using the following:

$$D_{es,i,t} = \frac{C_{s,i,t}(f_i \times f_s + f_o) \times D_{es,i}}{\rho_s} \qquad 45$$

Where

$D_{es,i,t}$ = whole-body effective dose equivalent for direct radiation from surface soil, for radionuclide i at time t (mrem/yr)
$C_{s,i,t}$ = concentration, in soil, of radionuclide i at time t (Ci/kg)
f_i = fraction of year individual spends indoors at the receptor location
f_s = shielding factor for the time spent indoors
f_o = fraction of year individual spends outdoors at the receptor location
$D_{es,i}$ = external radiation dose conversion factor for radionuclide i (mrem/yr/Ci/m^3)
ρ_s = bulk density of the surface soil (kg/m^3)

The dose conversion factors used to estimate direct exposures to surface soil differ depending upon the depth to which the contamination in those soils is mixed. External dose conversion

factors for soil contaminated to a depth of 15 cm (6 in.) are used if the contamination is mixed to a depth of 15 cm (6 in.) or less. If the contaminant mixing depth is greater than 15 cm (6 in.), as it is for some inadvertent intruder scenarios, external dose conversion factors for soil contaminated to an infinite depth are applied.

Several other modes of external exposure exist for the inadvertent intruders. All three receptors may be exposed to direct radiation, emitted from contaminated cap material and undisturbed waste, after it travels upward through the surface soil layer. The construction intruder is subject to direct radiation from the bottom and sides of the basement excavation during the time spent in the excavation; the agricultural intruder is exposed to these same sources of radiation during the time spent inside the house, although the radiation will be attenuated by the concrete foundation.

Direct exposures received from buried waste during the time intruders spend outside are estimated as follows:

$$D_{ew,i,t} = \frac{C_{w,i,t} \times D_{es,i} \times e^{-\mu_{ls,i} * d_m}}{\rho_w} \qquad 46$$

Where

$D_{ew,i,t}$ = whole-body effective dose equivalent for direct radiation from buried waste, for radionuclide i at time t (mrem/yr)
$C_{w,i,t}$ = concentration, in waste, of radionuclide i at time t (Ci/kg)
$\mu_{ls,i}$ = linear attenuation coefficient of radionuclide i in soil (m^{-1})
d_m = thickness of material overlying the waste (m)
ρ_w = bulk density of waste (kg/m^3)

The linear attenuation coefficient for radionuclide i is given by

$$\mu_{ls,i} = \mu_{ms,i} \times \rho_s \qquad 47$$

Where

$\mu_{ms,i}$ = mass attenuation coefficient of radionuclide i in soil (kg/m^3)

The dose conversion factors used in Equation 46 are those for soil contaminated to an infinite depth.

Equation 46 is applied to all waste layers included in the intruder and intruder diffusion models, using layer-specific radionuclide concentrations and adjusting d_m to account for the thickness of surface soil, cap, and waste material present over each waste layer. The estimated exposures do not account for the attenuation of radiation within the waste itself.

The cap may become contaminated prior to the arrival of the intruder as a result of biotic intrusion into the waste or vapor- and gas-phase radionuclides diffusing upward from the waste. External radiation emitted from contaminants in a given layer of the cap will be attenuated by any other cap layers that lie above it as well as by the surface soil layer. The doses received from the contaminated cap layers are calculated using Equation 46, substituting the cap layer radionuclide concentrations, the appropriate d_m for each cap layer, and the bulk density of the cap material for the waste properties.

Resident intruders also may be exposed to radiation from the buried waste and contaminated cap material during the time spent indoors. For indoor exposures to occur, radiation originating in any contaminated cap or waste layer must pass through any material separating the foundation of the intruder's house from that layer and the concrete foundation itself. For example, exposure calculations for a single layer of waste account for the attenuation of the radiation as it passes through any cap material and waste that lies between the layer and the foundation and the concrete basement or slab itself. These exposures are expressed as follows:

$$D_{ew,i,t} = \frac{C_{w,i,t} \times f_i \times D_{es,i} \times e^{-\mu_{ls,i} * d_m} \times e^{-\mu_{lc,i} * d_c}}{\rho_w} \qquad 48$$

Where

$\mu_{lc,i}$ = linear attenuation coefficient of radionuclide i in concrete (m^{-1})
d_c = thickness of the floor of the concrete foundation (m)

The linear attenuation coefficient for radionuclide i in concrete is given by the following:

$$\mu_{lc,i} = \mu_{mc,i} \times \rho_c \qquad 49$$

Where

$\mu_{mc,i}$ = mass attenuation coefficient of radionuclide i in concrete (m^{-1})
ρ_c = bulk density of concrete (kg/m^3)

The dose conversion factors used in Equation 48 are those for soil contaminated to an infinite depth. Exposure calculations for the contaminated cap layers consider attenuation from the cap and concrete only, and substitute cap contaminant concentrations and bulk density for the waste properties.

The material thickness used in Equations 46 and 48 will depend upon the intruder scenario under consideration, the location of the receptor, and the cap or waste source layer. For the time spent outdoors, radiation will be attenuated by any excavated material and the cap and waste layers separating the source layer from the receptor. The amount of material separating the construction

and agricultural intruders from a given layer during the time spent in the excavation or inside the house will depend upon the depth of the basement excavation relative to the cap and waste layer thicknesses. For example, if the basement depth is greater than the thickness of the cover, no cap material separates the intruder from the waste. The material thickness used to estimate indoor exposures for the post-drilling intruder is the total amount of material overlying the source layer at the time of intrusion.

The construction and agricultural intruders may also be exposed to contamination in the walls of the basement excavation; such an exposure will occur while the receptor is in the excavation or the house, respectively. Potential doses for the construction intruder are calculated using the following:

$$D_{esw,i,t} = \frac{C_{sw,i,t} \times f_e \times D_{es,i}}{\rho} \qquad 50$$

Where

$D_{esw,i,t}$ = whole-body effective dose equivalent for direct radiation from the sidewall of the basement excavation, radionuclide i at time t (mrem/yr)
$C_{sw,i,t}$ = average concentration, in the exposed cap and waste layers within the basement excavation, of radionuclide i at time t (Ci/kg)
f_e = fraction of year individual spends in the basement excavation

The exposures for the agricultural intruder are calculated using the fraction of the year spent inside, rather than within the excavation, and account for the attenuation of the radiation from the walls of the excavation by the concrete foundation. The dose conversion factors used in Equation 50 are those for soil contaminated to an infinite depth.

The use of external dose conversion factors for an infinite soil medium will overstate actual exposures from the relatively thin cap and waste layers. Consequently, the dose conversion factors used in Equations 46 and 48 are adjusted before they are applied in the external exposure calculations (RAE, 1998); no such adjustment is made for the factors used in Equation 50. This adjustment is given by the following expression:

$$D_{es,i,inf} = D_{es,i,inf}(1. - e^{-\mu_{lc,i} * d_l}) \qquad 51$$

Where

$D_{es,i,inf}$ = external radiation dose conversion factor for radionuclide i in an infinite medium (mrem/yr/Ci/m^3)
d_l = thickness of the cap or waste layer for which exposures are being estimated (m)

Direct exposures received from immersion in airborne radioactivity are calculated using the following equation:

$$D_{ea,i,t} = C_{at,i,t} \times (f_i \times f_s + f_o) \times D_{ea,i} \qquad 52$$

Where

$D_{ea,i,t}$ = whole-body effective dose equivalent from direct radiation in air for radionuclide i at time t (mrem/yr)
$D_{ea,i}$ = air immersion dose conversion factor for radionuclide i (mrem/yr/Ci/m^3)

3.6 Disposal System Configuration and Contaminant Flows

As discussed earlier, transport pathway elements are used to represent the physical compartments through which radionuclides are projected to migrate in the vicinity of MDA G. The elements are defined and linked with one another in a manner consistent with the conceptual model of the site. Rates of contaminant transport along the established links ultimately determine the timing and magnitude of the doses received by the various receptors.

The following sections discuss the interactions among the transport pathway elements used to conduct the performance assessment and composite analysis. Many of these interactions are characterized using the models described above. Additional submodels that are used to link the physical components of the MDA G models are introduced where appropriate.

3.6.1 Disposal Facility Configuration and Contaminant Flows

The disposal facility is represented differently across the four GoldSim models. The facility configuration seen in the site model includes the pits and shafts in which waste is placed, the cover material overlying these units, and the underlying unsaturated zone; the intruder model is similar but does not include the unsaturated zone. The diffusion models expand the facility definition to include the air above the disposal facility; the intruder diffusion model also includes the intruder's house.

The manner in which the disposal units are represented in GoldSim also depends upon the model under consideration. The site and intruder models divide the disposal facility into surface soil, cap material, and the waste within the pits and shafts. A single cell is used to represent the surface soil, while four cells are used to represent the cap and waste. The cap and waste are represented using multiple layers to more accurately simulate the dynamics of contaminant transport by plants and animals while maintaining model complexity at a reasonable level. Both models include a Plants cell that represents plants growing on the surface of the disposal site.

The two diffusion models use 16 cells to represent the cap and 20 cells to model the waste. The intruder diffusion model uses 4 cells to represent the concrete foundation of the intruder's house,

while single cells are used to represent the house itself, the air above the disposal units, and air within the basement excavation. As discussed in Section 3.4, dividing the cover and waste into several layers is necessary to ensure accurate estimates of the rates of diffusion through these materials; the analyses that were conducted to determine the level of discretization for the diffusion modeling are discussed in *Attachment I.* Both diffusion models include a cell representing plants growing at the site.

The surface soil, cap, concrete, and waste cells are defined in terms of the environmental media they consist of or that are transported into or out of them. These media are specified in the cell pathway properties dialog box under the definitions tab. The media used to define the disposal facility layers depend upon the model under consideration, but include crushed tuff, waste, concrete, water, and air. "Crushed tuff" is used to define the solids in the surface soil and cap, while "waste" is used to represent the solids in the waste layers. "Concrete" is used to represent the solid fraction of the foundation of the inadvertent intruder's house in the intruder diffusion model. "Water" represents the moisture present in the pore space of the surface soil, cap, waste, and concrete. "Air" is used to represent the air-filled pore spaces in porous media and the atmosphere above the site. To account for differences in diffusion behavior, the diffusion models distinguish between the air that exists in the pore spaces of the cover, waste, and concrete. All media that undergo advective transport into or out of a cell must be present in that cell. Consequently, the models include crushed tuff in the waste layers and waste in the surface soil and cap layers, albeit in very small amounts.

The transport pathway elements are defined in a manner that is consistent with the geometry of the disposal site. In terms of the site and site diffusion models, each cell within a given waste disposal region is sized to correspond to the area of the erosion zone that it represents. The areas of the cells used in the intruder models are set to the area of the intruder's lot. The thickness of each layer or cell is defined to account for the effects of surface erosion while remaining within the boundary conditions imposed by GoldSim. As discussed earlier, the effects of surface erosion are represented in all of the models by maintaining a constant surface-layer thickness that is replenished with material from the cap or waste.

The quantities of environmental media in each cell are a function of the cell volumes and the properties of the materials being represented. Thus, the mass of crushed tuff in the surface soil and cap cells, waste in the waste cells, or concrete in the foundation of the intruder's house is the product of the cell volumes and the dry density of the respective medium. Very small quantities of waste occur in the surface soil and cap layers, while very small quantities of crushed tuff occur in the waste layers. These media are included for reasons discussed above; their magnitude is arbitrary. The volume of water present in the pore space of the surface soil, cap, and waste layers is equal to the volume of each cell times the moisture content of the environmental medium. In general, the volume of air in porous media is estimated as the cell volume times the

air-filled porosity. The volume of air above the disposal units in the intruder diffusion model is given by the product of the average annual wind speed, the square root of the area of the disposal area, and the atmospheric mixing height.

The two diffusion models place lower bounds on the volume of air in the cells that represent the surface soil layer and the layers of the cap. Modeling diffusion through very thin soil layers may lead to very high rates of diffusive transport; these rates are flagged by GoldSim as "excessive" and possibly in error. Conditions such as this occur, for instance, when cap layers erode to the minimum thickness. Increasing the amount of air in the cell increases the contaminant storage term and all but prevents the generation of "excessive transport" warnings while having no effect on the accuracy of the projected contaminant fluxes.

The source of contamination for the site, intruder, and diffusion models is the waste disposed of in the waste disposal regions. The waste disposal region inventories used in the site and site diffusion models represent estimates of the actual quantities of material disposed of, or expected to be disposed of, in the pits and shafts at MDA G; a detailed description of this waste may be found in Shuman (2005). The user has the option of using actual inventories or unit inventories (i.e., an assumed inventory assigned to all radionuclides) when running the intruder and intruder diffusion models. The intruder models also provide the option of specifying total disposal unit inventories or inventories that are specific to the layers of waste in the pits and shafts. The actual inventories are used to estimate doses from the disposal units under consideration; however, the calculation of WAC for a wide range of radionuclides is more easily conducted using unit inventories because many of the contaminants encountered at MDA G may not be found in a given set of disposal units. In all cases, the inventories included in the models are added to the appropriate disposal units at a uniform rate over the period of time that the units were active. In terms of the site and site diffusion models, waste added to the disposal units is apportioned among each waste layer in accordance with the layer volume. This is also the case for the intruder and intruder diffusion models unless waste-layer-specific inventories are to be applied.

The site, intruder, and diffusion models use a series of inflows and outflows to represent contaminant movement within the disposal facility and to simulate radionuclide transport beyond the pits and shafts. For the site model, the surface soil is subject to inflows from the four cap and waste layers due to biotic intrusion into the waste. Specifically, advective mass-flux links are used to move soil from the cap and waste layers in proportion to the rates at which soil is excavated by burrowing animals. Two links are defined for each layer-to-layer transfer, representing the movement of solid media such as crushed tuff and waste as well as the transport of water, which is present in the pores of the cap material and waste. Direct-transfer mass links to and from the Plants cell account for the uptake of radionuclides by plants growing over the disposal units and the incorporation of this contamination into the surface soils following litter

deposition and decay. The equations governing the transfers associated with plant and animal intrusion are provided in Sections 3.1.2.1 and 3.1.2.2, respectively.

Within the site model, the surface soil layer is subject to outflows to the cap, the air over MDA G, and the cells representing Cañada del Buey and Pajarito Canyon soils (found in the Canyon_Exposure_Locations container). The transfer of contamination to the cap is defined using advective flows of solids and water. Bulk soil, including solids and soil moisture, is simulated to move downward in response to the collapse and settlement of burrows constructed by animals. The rate of burrow collapse and settlement is assumed to be equal to the rate at which material is brought to the surface by the animals, resulting in no net change in the thickness of the surface soil layer. Additional water is transported from the surface soil layer to the cap to represent water percolating through the disposal site. The rate of passage between these layers is specified by the parameter MdB_Infiltration_Rate, which refers to the infiltration rate through Mesita del Buey. This rate is equal to the natural infiltration rate estimated for the disposal site.

The outflows of crushed tuff and water from the surface soil to the air over the disposal site represent the resuspension of particulates. These particulates are subsequently transported by the prevailing winds to receptor locations downwind of MDA G. Outflows of bulk soil into Cañada del Buey and Pajarito Canyon account for the effects of surface erosion and runoff. As discussed earlier, the thickness of the cap is reduced over time to account for soil loss due to erosion. Advective mass-flux links are used to transfer bulk soil from the cap to the surface soil at rates that are consistent with the amount of soil lost due to erosion.

Advective flows into the cap and waste layers account for the movement of bulk soil downward due to burrow collapse and settlement, and the infiltration of water through the disposal site. Outflows from these cells to the surface soil layer represent the excavation of soils by burrowing animals. The flow of water through the cover and disposal units is assumed to occur under steady-state conditions, such that rates of flow are simply equal to the mesa-top infiltration rate. Direct-transfer mass links from the cap and waste cells account for the uptake of radionuclides by plants; these contaminants are deposited on the surface of the disposal facility in conjunction with litterfall and decay.

Within each waste disposal region, advective flows from the bottommost waste layers of the 10 erosion zones account for movement of water from the bottom of the disposal units into the unsaturated zone underlying the pits and shafts. The Unsaturated_Zone cell is used to collect the output from the erosion zones. Water entering the cell immediately flows into the Finite Element Heat and Mass (FEHM) external element found in each waste disposal region. As discussed in detail in Stauffer et al. (2005), FEHM is a transfer code used to estimate rates of contaminant transport vertically through the unsaturated zone and horizontally within the regional aquifer.

The FEHM elements are external one-dimensional abstractions of three-dimensional FEHM model simulations that accept infiltration rates, distribution coefficients, and radionuclide release rates from GoldSim and pass the contaminant masses crossing the groundwater compliance boundary back to GoldSim at the end of each time step. These results are subsequently used to estimate exposures for the groundwater scenarios.

Although many of the contaminant flows in the MDA G Site Diffusion Model are similar to those described for the site model, differences also exist. The site diffusion model includes inflows and outflows between surface soil, cap, and waste layers that simulate the movement of material due to biotic intrusion and the infiltration of water through the disposal facility. However, diffusive fluxes are included that simulate the movement of gas- and vapor-phase radionuclides from the waste upward through the cap and surface soil layers to the air above the disposal site. The diffusion path lengths for the source and destination media, the porous media through which contaminants diffuse, and the area over which diffusion is taking place must be defined for each diffusive link. The diffusion length for a given mass link is set equal to one-half of the appropriate cap, waste, or concrete layer thickness. With the exception of the bottommost waste layer, each cell in the site diffusion model is subject to the influx of contamination from the layer below. The diffusive area is set equal to the surface area of the layer, adjusted downward by the ratio of the air-filled porosity and the effective porosity. GoldSim assumes the effective porosity is saturated with the medium within which diffusion is taking place which, in this case, is air. In fact, water occupies some of the pore space; making the adjustment described above accounts for the presence of this moisture.

The MDA G Intruder Model is similar to the site model in terms of the flow of contamination among the cells representing the surface soil, cap, and waste. Although the inflows and outflows found in the intruder diffusion model generally resemble those seen in the site diffusion model, there are a few differences. The intruder diffusion model accounts for the transport of cap material and waste to the surface following human intrusion (basement excavation of well drilling). The amounts of material moved between the surface soil, cap, and waste cells depend upon the intruder scenario under consideration. Elements in the Intrusion_Consequences container calculate the radionuclide masses that are transferred between the cells. These calculations use the contaminant concentrations in the affected layers and the excavated quantities of cap material and waste calculated by the Human_Intrusion_Model. Material transfers are implemented using discrete change elements.

Differences also arise between the diffusion models because the intruder diffusion model also considers the transport of vapor- and gas-phase contaminants through the foundation of the intruder's house. Prior to the arrival of the intruder, vapor- and gas-phase contaminants diffuse from the waste and exit from the surface of the closed disposal facility. Once the intruder arrives, however, the pathways followed by these radionuclides change; the nature of these changes

depends upon the intruder scenario under consideration. For the postdrilling scenario, a portion of the gases and vapors in the surface soil layer pass through the concrete slab of the receptor's house; the remainder diffuses into the air above the site. The contaminants passing into the house and the air are apportioned on the basis of the area of the house and the portion of the intruder's lot that is not occupied by the dwelling.

Following basement excavation and prior to pouring the foundation, a portion of the contamination diffuses into the excavation while the remainder continues upward through the cover. After the foundation has been constructed, vapor- and gas-phase radionuclides either diffuse through the concrete floor of the house or travel through the cover to the surface of the site. In either case, the relative areas of the house and the intruder's lot are used to apportion the radionuclides between the two paths.

The layer from which radionuclides diffuse into the basement excavation or the floor of the intruder's basement depends upon the depth of the cover at the time of intrusion and the depth of the basement. The intruder diffusion model calculates the cumulative depth to the bottom of each cap and waste layer at the time of intrusion, and compares this to the depth of the basement. If the bottom of the basement lies within a given cap or waste layer the diffusive species within that layer are assumed to enter the excavation or concrete.

The MDA G Intruder Diffusion Model uses the House and Air_in_Excavation cells found in each erosion zone container to estimate doses for the intruder scenarios. Air and water are used to define both cells; water is included only because of requirements imposed by GoldSim. The volume of air inside the house is the product of the house area and room height; the excavation air volume is the product of the area and depth of the basement. Contaminants enter the house as vapor or gas and diffuse upward from the floor of the concrete foundation. A single advective outflow is used to simulate the passage of fresh air through the house due to ventilation; the flow rate is the product of the volume of the house and the ventilation rate. Similarly, an advective flow equal to the volume of the basement times the ventilation rate is used to simulate the renewal of air in the excavation. The air flows from the House and Air_in_Excavation cells and enters the Onsite_Air cell, which is linked to the Sink_Offsite_Air cell.

3.6.2 Site and Exposure Location Configuration and Contaminant Flows

The MDA G Site Model projects doses for off-site receptors at several exposure locations including (1) the point of maximum atmospheric exposure outside the LANL boundary and the MDA G fence line, (2) several locations in Cañada del Buey and Pajarito Canyon, and (3) a domestic well 100 m (330 ft) east of the MDA G fence line. Cells are used to represent relevant environmental media at these exposure locations. The site diffusion model projects atmospheric exposures along the LANL boundary and MDA G fence line and also uses cells to represent the

environmental media at these locations. The disposal facility is the only exposure location evaluated by the intruder and intruder diffusion models.

The three cells found inside the MDA_G container in the site model represent the air over the three atmospheric source areas (Figure 6). These cells are used to simulate the resuspension of particulates from the surface of the disposal facility and are defined in terms of three environmental media: air, water, and crushed tuff. Air is the primary medium; the small quantities of water and crushed tuff are included to enable the simulation of soil resuspension from the disposal site. The volumes of the materials comprising the cell are arbitrary; only the rate of particulate transfer to the cell is used in the performance modeling, and this rate is unaffected by the volumes of the materials in the cell.

Radionuclides in the surface soils at MDA G are partitioned between the solids and the soil moisture. As discussed earlier, GoldSim models the transport of these media separately. Consequently, the Onsite_Air cell for each atmospheric source area has pairs of inflows to account for the "resuspension" of water and solids from the disposal units within the source area under consideration. This modeling approach is conceptually equivalent to assuming that radionuclides in the soil moisture precipitate out when the liquid is exposed to surface conditions and evaporates. When the solids are resuspended, they carry with them all sorbed and previously soluble contaminants.

The Sink_Offsite_Air cell serves as a sink term in the site and intruder diffusion models. In the former, the cell receives contaminants diffusing from the undisturbed site; it is placed outside of the waste zone containers because, under these circumstances, GoldSim assumes the concentrations of contaminants in the air are zero. Assuming little or no airborne contamination above the undisturbed site is consistent with the assumption that prevailing winds refresh the site air in relatively short order, and tends to maximize the projected site fluxes. In the intruder diffusion model, the Sink_Offsite_Air cell receives air from above each erosion zone; these transfers represent the transport of airborne contamination by the prevailing winds to locations downwind of the intruder exposure locations.

The on-site and off-site air cells are defined using three materials: air, water, and crushed tuff. Air is the primary medium; very small quantities of water and crushed tuff are included because of requirements imposed by GoldSim. A single diffusive mass-flux link is used to transfer diffusing contaminants from the surface soil layer to the air over the disposal facility in the diffusion models. Advective mass-flux links are used in the intruder diffusion model to transport air from above the 10 erosion zones to the sink term.

The cells found inside the Atmospheric_Exposure_Locations container are used in the estimation of Atmospheric Scenario doses for the receptor at the point of maximum exposure prior to and

following the end of active institutional control. The cells inside the LANL_Boundary container are used to represent the location of the receptor prior to the end of institutional control; these two cells represent soils at the exposure location and a sink term. The cell representing the soils is defined using water and crushed tuff; these materials represent the soil moisture and solids, respectively. The volume of water and mass of solid specified are consistent with the area of the receptor's lot, the depth to which contamination is mixed, the moisture content of the soil, and the dry density of the solids. Similarly configured cells inside the MDA_G_Fenceline container represent the point of maximum exposure after active institutional control has ceased.

The atmospheric transport modeling conducted within the site and site diffusion models is a representation of the detailed modeling conducted by Jacobson (2005). The results of complex terrain modeling are used to estimate radionuclide concentrations in air and rates of particulate deposition at the Atmospheric Scenario exposure locations. Projections of particulate deposition are used to estimate contaminant additions to the surface soils. Using discrete change elements, the appropriate radionuclide activities are added to the Exposure_Location_Soils cell. The rate of addition is given by the following equation:

$$Q_{d,i,t,j} = C_{s,i,t} \times d_{f,j} \times (A_l - A_h) \times r_{fr} \times s_{ar} \qquad 53$$

Where

$Q_{d,i,t,j}$ = quantity of radionuclide i deposited on surface soils at the point of maximum atmospheric exposure at time t for contamination originating in atmospheric source area j (Ci/yr)
d_{fj} = particulate deposition rate for contamination originating in atmospheric source area j (kg/m^2/yr)
A_l = area of receptor's lot (m^2)
A_h = area of receptor's house (m^2)
r_{fr} = resuspension flux ratio
s_{ar} = source area ratio

The soil concentration term in this equation ($C_{s,i,t}$) refers to radionuclide concentrations in MDA G soils. Radionuclide fluxes at the exposure location are calculated for contamination originating at the three atmospheric source areas at the facility (Figure 6); these rates are summed to determine the total rate of radionuclide deposition.

The atmospheric transport modeling conducted in support of the performance assessment and composite analysis used a generic value for the particulate resuspension rate. The radionuclide deposition rates at downwind locations scale directly with the resuspension factor. Consequently, it is a simple matter to adjust the modeling results to take the actual site resuspension characteristics into account. This is done in Equation 53 using the resuspension flux ratio, which

is the ratio of the actual site resuspension flux and the default resuspension flux used in the atmospheric transport modeling.

In general, particulates less than 10 μm (3.9×10^{-4} in.) in diameter will be resuspended from the surface of the disposal site; radionuclide concentrations in this resuspendable fraction will tend to be greater than those estimated by the GoldSim models for the total soil (i.e., including all size fractions). As a result, the resuspension flux input by the user is multiplied by an enhancement factor to account for differences in radionuclide concentrations among the different soil size fractions.

The modeled rates of particulate resuspension from MDA G assume that all resuspended material originates from the surfaces of the disposal pits and shafts; this ignores the resuspension of uncontaminated material from portions of the site that lie between pits or near the edges of the mesa. As a result, the deposition rates projected by Jacobson (2005) were adjusted to account for the fact that the source area for modeling resuspension was smaller than the source area as shown in Figure 6. This adjustment is provided in Equation 53 by the source area ratio, which represents the surface area of the disposal units divided by the source area used in the atmospheric transport modeling.

Advective outflows of water from the soils at the Atmospheric Scenario exposure locations to the soil sink terms are used to simulate the depletion of soil contamination due to groundwater transport. Water passes out of the soil at a rate determined by the water infiltration rate at the exposure locations, carrying the soluble component of the soil contamination with it.

The canyon exposure locations are found in the MDA G Site and MDA G Site Diffusion Models, while the well exposure location occurs only in the site model. The canyon locations are used to project exposures for the All Pathways – Cañada del Buey and All Pathways – Pajarito Canyon Scenarios. Cells representing the canyon soils and a sink term are used to model radionuclide concentrations at these locations. The canyon soils are defined in terms of water and crushed tuff. The volume of water is given by the product of the area over which the sediment transported from the mesa spreads within each catchment, the contaminant mixing depth, and the moisture content of the bulk soil. The product of the area of sediment dispersal, the contaminant mixing depth, and the dry density of the crushed tuff yields the mass of solids in this compartment. The area over which the sediment spreads is specific to the catchment under consideration.

The soils in Cañada del Buey and Pajarito Canyon receive advective flows of soil moisture and solids from all 10 erosion zones within the eight waste disposal regions. These inflows represent the transport with surface runoff of contamination deposited on the surface of MDA G by plants and animals intruding into the waste. As has been discussed, separate flows are used to transport radionuclides that are soluble in the soil moisture and that are sorbed to the crushed tuff. Rates of

flow are proportional to the erosion rate at the disposal site and the disposal area associated with each erosion zone. Direct transfer links between the canyon exposure locations are used to transport sediment down Cañada del Buey and Pajarito Canyon; the flows from catchments CdB2 and PC6 (Figure 15) go to a sink term. An additional flow from each canyon soil cell accounts for the depletion of contamination by water infiltrating through the exposure location.

A single well location is used to project groundwater pathway impacts for the performance assessment and composite analysis. This well is located 100 m (330 ft) downgradient of the disposal facility boundary, and represents the exposure location for the groundwater pathway-based scenarios after the end of the active institutional control period. As discussed earlier, persons living downgradient of MDA G may receive groundwater exposures along the LANL boundary prior to the end of active institutional control. However, groundwater contaminant travel times from MDA G to this boundary are such that no exposures are projected to occur within 100 years of facility closure (Stauffer et al., 2005). Therefore, an exposure location along the LANL boundary is not included in the site model.

Four cells are used to represent the groundwater pathway exposure location. The first of these, the AP_Well cell, represents the receptor's well for the All Pathways – Groundwater Scenario. A second cell represents surface soils at the exposure location; the remaining two cells act as sinks for surface soil and groundwater contamination. The cell used to represent the well includes a single material, water, and is sized to correspond to the water usage rate of the receptor. The water usage rates for the receptor include the water needed for irrigating crops, watering animals, indoor consumption, and drinking.

Advective flows between the FEHM external elements (found in the eight waste disposal region containers that comprise the disposal facility) and the AP_Well cell account for the withdrawal of water from the regional aquifer. An advective flow from the AP_Well cell to the Surface_Soil_at_100m_Well cell accounts for the application of water during irrigation of vegetable and animal forage crops. A second advective flow to the Sink_for_Well_Water cell accounts for the withdrawal of the remaining water for indoor use and personal consumption.

The FEHM external elements simulate the transport of radionuclides from the bottoms of the disposal units to the well located 100 m (330 ft) downgradient of the MDA G fence line, represented by the AP_Well cell. Although these elements account for the decay and sorption characteristics of the radionuclides during transit, they are not designed to account for the effects of dilution and dispersion that occur between the point of discharge and the regional aquifer or well. Thus, using the output of these elements directly will overestimate contaminant concentrations in the water drawn from the well.

Direct exposures received from immersion in airborne radioactivity are calculated using the following equation:

$$D_{ea,i,t} = C_{at,i,t} \times (f_i \times f_s + f_o) \times D_{ea,i} \qquad 52$$

Where

$D_{ea,i,t}$ = whole-body effective dose equivalent from direct radiation in air for radionuclide i at time t (mrem/yr)

$D_{ea,i}$ = air immersion dose conversion factor for radionuclide i (mrem/yr/Ci/m^3)

3.6 Disposal System Configuration and Contaminant Flows

As discussed earlier, transport pathway elements are used to represent the physical compartments through which radionuclides are projected to migrate in the vicinity of MDA G. The elements are defined and linked with one another in a manner consistent with the conceptual model of the site. Rates of contaminant transport along the established links ultimately determine the timing and magnitude of the doses received by the various receptors.

The following sections discuss the interactions among the transport pathway elements used to conduct the performance assessment and composite analysis. Many of these interactions are characterized using the models described above. Additional submodels that are used to link the physical components of the MDA G models are introduced where appropriate.

3.6.1 Disposal Facility Configuration and Contaminant Flows

The disposal facility is represented differently across the four GoldSim models. The facility configuration seen in the site model includes the pits and shafts in which waste is placed, the cover material overlying these units, and the underlying unsaturated zone; the intruder model is similar but does not include the unsaturated zone. The diffusion models expand the facility definition to include the air above the disposal facility; the intruder diffusion model also includes the intruder's house.

The manner in which the disposal units are represented in GoldSim also depends upon the model under consideration. The site and intruder models divide the disposal facility into surface soil, cap material, and the waste within the pits and shafts. A single cell is used to represent the surface soil, while four cells are used to represent the cap and waste. The cap and waste are represented using multiple layers to more accurately simulate the dynamics of contaminant transport by plants and animals while maintaining model complexity at a reasonable level. Both models include a Plants cell that represents plants growing on the surface of the disposal site.

The two diffusion models use 16 cells to represent the cap and 20 cells to model the waste. The intruder diffusion model uses 4 cells to represent the concrete foundation of the intruder's house,

while single cells are used to represent the house itself, the air above the disposal units, and air within the basement excavation. As discussed in Section 3.4, dividing the cover and waste into several layers is necessary to ensure accurate estimates of the rates of diffusion through these materials; the analyses that were conducted to determine the level of discretization for the diffusion modeling are discussed in *Attachment I.* Both diffusion models include a cell representing plants growing at the site.

The surface soil, cap, concrete, and waste cells are defined in terms of the environmental media they consist of or that are transported into or out of them. These media are specified in the cell pathway properties dialog box under the definitions tab. The media used to define the disposal facility layers depend upon the model under consideration, but include crushed tuff, waste, concrete, water, and air. "Crushed tuff" is used to define the solids in the surface soil and cap, while "waste" is used to represent the solids in the waste layers. "Concrete" is used to represent the solid fraction of the foundation of the inadvertent intruder's house in the intruder diffusion model. "Water" represents the moisture present in the pore space of the surface soil, cap, waste, and concrete. "Air" is used to represent the air-filled pore spaces in porous media and the atmosphere above the site. To account for differences in diffusion behavior, the diffusion models distinguish between the air that exists in the pore spaces of the cover, waste, and concrete. All media that undergo advective transport into or out of a cell must be present in that cell. Consequently, the models include crushed tuff in the waste layers and waste in the surface soil and cap layers, albeit in very small amounts.

The transport pathway elements are defined in a manner that is consistent with the geometry of the disposal site. In terms of the site and site diffusion models, each cell within a given waste disposal region is sized to correspond to the area of the erosion zone that it represents. The areas of the cells used in the intruder models are set to the area of the intruder's lot. The thickness of each layer or cell is defined to account for the effects of surface erosion while remaining within the boundary conditions imposed by GoldSim. As discussed earlier, the effects of surface erosion are represented in all of the models by maintaining a constant surface-layer thickness that is replenished with material from the cap or waste.

The quantities of environmental media in each cell are a function of the cell volumes and the properties of the materials being represented. Thus, the mass of crushed tuff in the surface soil and cap cells, waste in the waste cells, or concrete in the foundation of the intruder's house is the product of the cell volumes and the dry density of the respective medium. Very small quantities of waste occur in the surface soil and cap layers, while very small quantities of crushed tuff occur in the waste layers. These media are included for reasons discussed above; their magnitude is arbitrary. The volume of water present in the pore space of the surface soil, cap, and waste layers is equal to the volume of each cell times the moisture content of the environmental medium. In general, the volume of air in porous media is estimated as the cell volume times the

air-filled porosity. The volume of air above the disposal units in the intruder diffusion model is given by the product of the average annual wind speed, the square root of the area of the disposal area, and the atmospheric mixing height.

The two diffusion models place lower bounds on the volume of air in the cells that represent the surface soil layer and the layers of the cap. Modeling diffusion through very thin soil layers may lead to very high rates of diffusive transport; these rates are flagged by GoldSim as "excessive" and possibly in error. Conditions such as this occur, for instance, when cap layers erode to the minimum thickness. Increasing the amount of air in the cell increases the contaminant storage term and all but prevents the generation of "excessive transport" warnings while having no effect on the accuracy of the projected contaminant fluxes.

The source of contamination for the site, intruder, and diffusion models is the waste disposed of in the waste disposal regions. The waste disposal region inventories used in the site and site diffusion models represent estimates of the actual quantities of material disposed of, or expected to be disposed of, in the pits and shafts at MDA G; a detailed description of this waste may be found in Shuman (2005). The user has the option of using actual inventories or unit inventories (i.e., an assumed inventory assigned to all radionuclides) when running the intruder and intruder diffusion models. The intruder models also provide the option of specifying total disposal unit inventories or inventories that are specific to the layers of waste in the pits and shafts. The actual inventories are used to estimate doses from the disposal units under consideration; however, the calculation of WAC for a wide range of radionuclides is more easily conducted using unit inventories because many of the contaminants encountered at MDA G may not be found in a given set of disposal units. In all cases, the inventories included in the models are added to the appropriate disposal units at a uniform rate over the period of time that the units were active. In terms of the site and site diffusion models, waste added to the disposal units is apportioned among each waste layer in accordance with the layer volume. This is also the case for the intruder and intruder diffusion models unless waste-layer-specific inventories are to be applied.

The site, intruder, and diffusion models use a series of inflows and outflows to represent contaminant movement within the disposal facility and to simulate radionuclide transport beyond the pits and shafts. For the site model, the surface soil is subject to inflows from the four cap and waste layers due to biotic intrusion into the waste. Specifically, advective mass-flux links are used to move soil from the cap and waste layers in proportion to the rates at which soil is excavated by burrowing animals. Two links are defined for each layer-to-layer transfer, representing the movement of solid media such as crushed tuff and waste as well as the transport of water, which is present in the pores of the cap material and waste. Direct-transfer mass links to and from the Plants cell account for the uptake of radionuclides by plants growing over the disposal units and the incorporation of this contamination into the surface soils following litter

deposition and decay. The equations governing the transfers associated with plant and animal intrusion are provided in Sections 3.1.2.1 and 3.1.2.2, respectively.

Within the site model, the surface soil layer is subject to outflows to the cap, the air over MDA G, and the cells representing Cañada del Buey and Pajarito Canyon soils (found in the Canyon_Exposure_Locations container). The transfer of contamination to the cap is defined using advective flows of solids and water. Bulk soil, including solids and soil moisture, is simulated to move downward in response to the collapse and settlement of burrows constructed by animals. The rate of burrow collapse and settlement is assumed to be equal to the rate at which material is brought to the surface by the animals, resulting in no net change in the thickness of the surface soil layer. Additional water is transported from the surface soil layer to the cap to represent water percolating through the disposal site. The rate of passage between these layers is specified by the parameter MdB_Infiltration_Rate, which refers to the infiltration rate through Mesita del Buey. This rate is equal to the natural infiltration rate estimated for the disposal site.

The outflows of crushed tuff and water from the surface soil to the air over the disposal site represent the resuspension of particulates. These particulates are subsequently transported by the prevailing winds to receptor locations downwind of MDA G. Outflows of bulk soil into Cañada del Buey and Pajarito Canyon account for the effects of surface erosion and runoff. As discussed earlier, the thickness of the cap is reduced over time to account for soil loss due to erosion. Advective mass-flux links are used to transfer bulk soil from the cap to the surface soil at rates that are consistent with the amount of soil lost due to erosion.

Advective flows into the cap and waste layers account for the movement of bulk soil downward due to burrow collapse and settlement, and the infiltration of water through the disposal site. Outflows from these cells to the surface soil layer represent the excavation of soils by burrowing animals. The flow of water through the cover and disposal units is assumed to occur under steady-state conditions, such that rates of flow are simply equal to the mesa-top infiltration rate. Direct-transfer mass links from the cap and waste cells account for the uptake of radionuclides by plants; these contaminants are deposited on the surface of the disposal facility in conjunction with litterfall and decay.

Within each waste disposal region, advective flows from the bottommost waste layers of the 10 erosion zones account for movement of water from the bottom of the disposal units into the unsaturated zone underlying the pits and shafts. The Unsaturated_Zone cell is used to collect the output from the erosion zones. Water entering the cell immediately flows into the Finite Element Heat and Mass (FEHM) external element found in each waste disposal region. As discussed in detail in Stauffer et al. (2005), FEHM is a transfer code used to estimate rates of contaminant transport vertically through the unsaturated zone and horizontally within the regional aquifer.

The FEHM elements are external one-dimensional abstractions of three-dimensional FEHM model simulations that accept infiltration rates, distribution coefficients, and radionuclide release rates from GoldSim and pass the contaminant masses crossing the groundwater compliance boundary back to GoldSim at the end of each time step. These results are subsequently used to estimate exposures for the groundwater scenarios.

Although many of the contaminant flows in the MDA G Site Diffusion Model are similar to those described for the site model, differences also exist. The site diffusion model includes inflows and outflows between surface soil, cap, and waste layers that simulate the movement of material due to biotic intrusion and the infiltration of water through the disposal facility. However, diffusive fluxes are included that simulate the movement of gas- and vapor-phase radionuclides from the waste upward through the cap and surface soil layers to the air above the disposal site. The diffusion path lengths for the source and destination media, the porous media through which contaminants diffuse, and the area over which diffusion is taking place must be defined for each diffusive link. The diffusion length for a given mass link is set equal to one-half of the appropriate cap, waste, or concrete layer thickness. With the exception of the bottommost waste layer, each cell in the site diffusion model is subject to the influx of contamination from the layer below. The diffusive area is set equal to the surface area of the layer, adjusted downward by the ratio of the air-filled porosity and the effective porosity. GoldSim assumes the effective porosity is saturated with the medium within which diffusion is taking place which, in this case, is air. In fact, water occupies some of the pore space; making the adjustment described above accounts for the presence of this moisture.

The MDA G Intruder Model is similar to the site model in terms of the flow of contamination among the cells representing the surface soil, cap, and waste. Although the inflows and outflows found in the intruder diffusion model generally resemble those seen in the site diffusion model, there are a few differences. The intruder diffusion model accounts for the transport of cap material and waste to the surface following human intrusion (basement excavation of well drilling). The amounts of material moved between the surface soil, cap, and waste cells depend upon the intruder scenario under consideration. Elements in the Intrusion_Consequences container calculate the radionuclide masses that are transferred between the cells. These calculations use the contaminant concentrations in the affected layers and the excavated quantities of cap material and waste calculated by the Human_Intrusion_Model. Material transfers are implemented using discrete change elements.

Differences also arise between the diffusion models because the intruder diffusion model also considers the transport of vapor- and gas-phase contaminants through the foundation of the intruder's house. Prior to the arrival of the intruder, vapor- and gas-phase contaminants diffuse from the waste and exit from the surface of the closed disposal facility. Once the intruder arrives, however, the pathways followed by these radionuclides change; the nature of these changes

depends upon the intruder scenario under consideration. For the postdrilling scenario, a portion of the gases and vapors in the surface soil layer pass through the concrete slab of the receptor's house; the remainder diffuses into the air above the site. The contaminants passing into the house and the air are apportioned on the basis of the area of the house and the portion of the intruder's lot that is not occupied by the dwelling.

Following basement excavation and prior to pouring the foundation, a portion of the contamination diffuses into the excavation while the remainder continues upward through the cover. After the foundation has been constructed, vapor- and gas-phase radionuclides either diffuse through the concrete floor of the house or travel through the cover to the surface of the site. In either case, the relative areas of the house and the intruder's lot are used to apportion the radionuclides between the two paths.

The layer from which radionuclides diffuse into the basement excavation or the floor of the intruder's basement depends upon the depth of the cover at the time of intrusion and the depth of the basement. The intruder diffusion model calculates the cumulative depth to the bottom of each cap and waste layer at the time of intrusion, and compares this to the depth of the basement. If the bottom of the basement lies within a given cap or waste layer the diffusive species within that layer are assumed to enter the excavation or concrete.

The MDA G Intruder Diffusion Model uses the House and Air_in_Excavation cells found in each erosion zone container to estimate doses for the intruder scenarios. Air and water are used to define both cells; water is included only because of requirements imposed by GoldSim. The volume of air inside the house is the product of the house area and room height; the excavation air volume is the product of the area and depth of the basement. Contaminants enter the house as vapor or gas and diffuse upward from the floor of the concrete foundation. A single advective outflow is used to simulate the passage of fresh air through the house due to ventilation; the flow rate is the product of the volume of the house and the ventilation rate. Similarly, an advective flow equal to the volume of the basement times the ventilation rate is used to simulate the renewal of air in the excavation. The air flows from the House and Air_in_Excavation cells and enters the Onsite_Air cell, which is linked to the Sink_Offsite_Air cell.

3.6.2 Site and Exposure Location Configuration and Contaminant Flows

The MDA G Site Model projects doses for off-site receptors at several exposure locations including (1) the point of maximum atmospheric exposure outside the LANL boundary and the MDA G fence line, (2) several locations in Cañada del Buey and Pajarito Canyon, and (3) a domestic well 100 m (330 ft) east of the MDA G fence line. Cells are used to represent relevant environmental media at these exposure locations. The site diffusion model projects atmospheric exposures along the LANL boundary and MDA G fence line and also uses cells to represent the

environmental media at these locations. The disposal facility is the only exposure location evaluated by the intruder and intruder diffusion models.

The three cells found inside the MDA_G container in the site model represent the air over the three atmospheric source areas (Figure 6). These cells are used to simulate the resuspension of particulates from the surface of the disposal facility and are defined in terms of three environmental media: air, water, and crushed tuff. Air is the primary medium; the small quantities of water and crushed tuff are included to enable the simulation of soil resuspension from the disposal site. The volumes of the materials comprising the cell are arbitrary; only the rate of particulate transfer to the cell is used in the performance modeling, and this rate is unaffected by the volumes of the materials in the cell.

Radionuclides in the surface soils at MDA G are partitioned between the solids and the soil moisture. As discussed earlier, GoldSim models the transport of these media separately. Consequently, the Onsite_Air cell for each atmospheric source area has pairs of inflows to account for the "resuspension" of water and solids from the disposal units within the source area under consideration. This modeling approach is conceptually equivalent to assuming that radionuclides in the soil moisture precipitate out when the liquid is exposed to surface conditions and evaporates. When the solids are resuspended, they carry with them all sorbed and previously soluble contaminants.

The Sink_Offsite_Air cell serves as a sink term in the site and intruder diffusion models. In the former, the cell receives contaminants diffusing from the undisturbed site; it is placed outside of the waste zone containers because, under these circumstances, GoldSim assumes the concentrations of contaminants in the air are zero. Assuming little or no airborne contamination above the undisturbed site is consistent with the assumption that prevailing winds refresh the site air in relatively short order, and tends to maximize the projected site fluxes. In the intruder diffusion model, the Sink_Offsite_Air cell receives air from above each erosion zone; these transfers represent the transport of airborne contamination by the prevailing winds to locations downwind of the intruder exposure locations.

The on-site and off-site air cells are defined using three materials: air, water, and crushed tuff. Air is the primary medium; very small quantities of water and crushed tuff are included because of requirements imposed by GoldSim. A single diffusive mass-flux link is used to transfer diffusing contaminants from the surface soil layer to the air over the disposal facility in the diffusion models. Advective mass-flux links are used in the intruder diffusion model to transport air from above the 10 erosion zones to the sink term.

The cells found inside the Atmospheric_Exposure_Locations container are used in the estimation of Atmospheric Scenario doses for the receptor at the point of maximum exposure prior to and

following the end of active institutional control. The cells inside the LANL_Boundary container are used to represent the location of the receptor prior to the end of institutional control; these two cells represent soils at the exposure location and a sink term. The cell representing the soils is defined using water and crushed tuff; these materials represent the soil moisture and solids, respectively. The volume of water and mass of solid specified are consistent with the area of the receptor's lot, the depth to which contamination is mixed, the moisture content of the soil, and the dry density of the solids. Similarly configured cells inside the MDA_G_Fenceline container represent the point of maximum exposure after active institutional control has ceased.

The atmospheric transport modeling conducted within the site and site diffusion models is a representation of the detailed modeling conducted by Jacobson (2005). The results of complex terrain modeling are used to estimate radionuclide concentrations in air and rates of particulate deposition at the Atmospheric Scenario exposure locations. Projections of particulate deposition are used to estimate contaminant additions to the surface soils. Using discrete change elements, the appropriate radionuclide activities are added to the Exposure_Location_Soils cell. The rate of addition is given by the following equation:

$$Q_{d,i,t,j} = C_{s,i,t} \times d_{f,j} \times (A_l - A_h) \times r_{fr} \times s_{ar} \qquad 53$$

Where

$Q_{d,i,t,j}$ = quantity of radionuclide i deposited on surface soils at the point of maximum atmospheric exposure at time t for contamination originating in atmospheric source area j (Ci/yr)
d_{fj} = particulate deposition rate for contamination originating in atmospheric source area j (kg/m^2/yr)
A_l = area of receptor's lot (m^2)
A_h = area of receptor's house (m^2)
r_{fr} = resuspension flux ratio
s_{ar} = source area ratio

The soil concentration term in this equation ($C_{s,i,t}$) refers to radionuclide concentrations in MDA G soils. Radionuclide fluxes at the exposure location are calculated for contamination originating at the three atmospheric source areas at the facility (Figure 6); these rates are summed to determine the total rate of radionuclide deposition.

The atmospheric transport modeling conducted in support of the performance assessment and composite analysis used a generic value for the particulate resuspension rate. The radionuclide deposition rates at downwind locations scale directly with the resuspension factor. Consequently, it is a simple matter to adjust the modeling results to take the actual site resuspension characteristics into account. This is done in Equation 53 using the resuspension flux ratio, which

is the ratio of the actual site resuspension flux and the default resuspension flux used in the atmospheric transport modeling.

In general, particulates less than 10 μm (3.9×10^{-4} in.) in diameter will be resuspended from the surface of the disposal site; radionuclide concentrations in this resuspendable fraction will tend to be greater than those estimated by the GoldSim models for the total soil (i.e., including all size fractions). As a result, the resuspension flux input by the user is multiplied by an enhancement factor to account for differences in radionuclide concentrations among the different soil size fractions.

The modeled rates of particulate resuspension from MDA G assume that all resuspended material originates from the surfaces of the disposal pits and shafts; this ignores the resuspension of uncontaminated material from portions of the site that lie between pits or near the edges of the mesa. As a result, the deposition rates projected by Jacobson (2005) were adjusted to account for the fact that the source area for modeling resuspension was smaller than the source area as shown in Figure 6. This adjustment is provided in Equation 53 by the source area ratio, which represents the surface area of the disposal units divided by the source area used in the atmospheric transport modeling.

Advective outflows of water from the soils at the Atmospheric Scenario exposure locations to the soil sink terms are used to simulate the depletion of soil contamination due to groundwater transport. Water passes out of the soil at a rate determined by the water infiltration rate at the exposure locations, carrying the soluble component of the soil contamination with it.

The canyon exposure locations are found in the MDA G Site and MDA G Site Diffusion Models, while the well exposure location occurs only in the site model. The canyon locations are used to project exposures for the All Pathways – Cañada del Buey and All Pathways – Pajarito Canyon Scenarios. Cells representing the canyon soils and a sink term are used to model radionuclide concentrations at these locations. The canyon soils are defined in terms of water and crushed tuff. The volume of water is given by the product of the area over which the sediment transported from the mesa spreads within each catchment, the contaminant mixing depth, and the moisture content of the bulk soil. The product of the area of sediment dispersal, the contaminant mixing depth, and the dry density of the crushed tuff yields the mass of solids in this compartment. The area over which the sediment spreads is specific to the catchment under consideration.

The soils in Cañada del Buey and Pajarito Canyon receive advective flows of soil moisture and solids from all 10 erosion zones within the eight waste disposal regions. These inflows represent the transport with surface runoff of contamination deposited on the surface of MDA G by plants and animals intruding into the waste. As has been discussed, separate flows are used to transport radionuclides that are soluble in the soil moisture and that are sorbed to the crushed tuff. Rates of

flow are proportional to the erosion rate at the disposal site and the disposal area associated with each erosion zone. Direct transfer links between the canyon exposure locations are used to transport sediment down Cañada del Buey and Pajarito Canyon; the flows from catchments CdB2 and PC6 (Figure 15) go to a sink term. An additional flow from each canyon soil cell accounts for the depletion of contamination by water infiltrating through the exposure location.

A single well location is used to project groundwater pathway impacts for the performance assessment and composite analysis. This well is located 100 m (330 ft) downgradient of the disposal facility boundary, and represents the exposure location for the groundwater pathway-based scenarios after the end of the active institutional control period. As discussed earlier, persons living downgradient of MDA G may receive groundwater exposures along the LANL boundary prior to the end of active institutional control. However, groundwater contaminant travel times from MDA G to this boundary are such that no exposures are projected to occur within 100 years of facility closure (Stauffer et al., 2005). Therefore, an exposure location along the LANL boundary is not included in the site model.

Four cells are used to represent the groundwater pathway exposure location. The first of these, the AP_Well cell, represents the receptor's well for the All Pathways – Groundwater Scenario. A second cell represents surface soils at the exposure location; the remaining two cells act as sinks for surface soil and groundwater contamination. The cell used to represent the well includes a single material, water, and is sized to correspond to the water usage rate of the receptor. The water usage rates for the receptor include the water needed for irrigating crops, watering animals, indoor consumption, and drinking.

Advective flows between the FEHM external elements (found in the eight waste disposal region containers that comprise the disposal facility) and the AP_Well cell account for the withdrawal of water from the regional aquifer. An advective flow from the AP_Well cell to the Surface_Soil_at_100m_Well cell accounts for the application of water during irrigation of vegetable and animal forage crops. A second advective flow to the Sink_for_Well_Water cell accounts for the withdrawal of the remaining water for indoor use and personal consumption.

The FEHM external elements simulate the transport of radionuclides from the bottoms of the disposal units to the well located 100 m (330 ft) downgradient of the MDA G fence line, represented by the AP_Well cell. Although these elements account for the decay and sorption characteristics of the radionuclides during transit, they are not designed to account for the effects of dilution and dispersion that occur between the point of discharge and the regional aquifer or well. Thus, using the output of these elements directly will overestimate contaminant concentrations in the water drawn from the well.

The magnitudes of the flows between the FEHM elements and the AP_Well cell are modified to account for contaminant dispersion in the regional aquifer. The flow from the FEHM element within a given waste disposal region is equal to the infiltration rate through that disposal region times the contaminant capture fraction. The contaminant capture fraction specifies the portion of the contaminant plume that reaches and is withdrawn from the well. It is largely a function of the dispersion characteristics of the aquifer between the point of contaminant discharge and the well, and the well pump rate. The approach used to define the contaminant capture fractions is described in Stauffer et al. (2005).

The cell used to represent the surface soils at the well location includes water and crushed tuff. The volume of water and mass of tuff in these cells are based on the net area of the receptor's lot (i.e., the lot area less the house area), the contaminant mixing depth, and the moisture content and dry density of the soil. The rate of water flow into the cell is the sum of the crop irrigation rates. Outflows of water to the Sink_for_Soil_Moisture cell account for the transport of radionuclides downward with water percolating through the receptor's lot.

Although several cells are used to represent the physical location of the receptor for the All Pathways – Groundwater Scenario, no physical representation of the exposure location is necessary for the Groundwater Resource Protection Scenario. Physical modeling of the exposure location is needed for the all pathways scenario to estimate contaminant concentrations in the surface soils at the receptor's residence. In contrast, the resource protection scenario addresses the use of contaminated water only as a source of drinking water. Radionuclide concentrations in the water are calculated directly from the amount of contamination withdrawn at the well and water usage rates.

3.6.3 Exposure Concentrations

The doses projected for the performance assessment and composite analysis are proportional to the radionuclide concentrations in the environmental media to which the receptor is exposed. In some cases the contaminant concentrations are taken directly from the cells used to represent the exposure media; in other cases, they are calculated using contaminant masses. This section discusses how the exposure concentrations used in the dose model are defined using the GoldSim models.

3.6.3.1 Surface Soil, Cap, and Waste

A combination of approaches is used to define the radionuclide concentrations in the surface soil, cap material, and waste to which members of the public and inadvertent intruders are exposed. For the site and site diffusion models, surface soil concentrations are calculated similarly for exposure locations downwind and downgradient of MDA G and those in the adjacent canyons. In all cases, radionuclide concentrations are calculated as the quotient of the contaminant activities and the total soil mass in the cells used to represent soils at the exposure locations. The

total soil mass for the atmospheric and groundwater scenarios is given by the product of the receptor's lot size less the area occupied by the house (i.e., the net lot area), the soil mixing depth, and the soil density. Soil concentrations for the exposure locations in the canyon take into account the area within each catchment over which sediments are dispersed.

The intruder model simulates the release and transport of radionuclides resulting from biotic intrusion prior to the arrival of the intruder, but does not explicitly model the movement of contamination resulting from human intrusion. In this approach, radionuclide concentrations in surface soil are calculated by summing the contaminant activities present in the surface soil layer at the time of intrusion and the activities brought to the surface as a result of basement excavation or well drilling. These activities are divided by the product of the net lot area, the mixing depth, and soil-density-to-yield concentrations. The mixing thickness is set equal to the greater of the thickness of the excavated material after it has been spread over the intruder's lot or a user-specified minimum mixing depth. If the minimum mixing depth is used, the calculated radionuclide concentrations take into account any contamination present in the layers within which the excavated material is mixed.

The intruder model tracks contaminant concentrations in each layer of the cap and waste. Concentrations in the layers of the cap and waste that are disturbed by the basement excavation are used to estimate average radionuclide concentrations in the side walls of the excavation. Radionuclide concentrations in the material at the bottom of the basement are set equal to those estimated for the cap or waste layer that lies at the bottom of the excavation.

In contrast to the intruder model, the intruder diffusion model explicitly models the movement of contaminants resulting from human intrusion; radionuclides are physically moved to the surface soil layer to reflect the impacts of well drilling and basement excavation. Radionuclide concentrations are calculated as the quotient of the contaminant activities in the surface soil layer and total soil mass. The total soil mass is given by the product of the net lot area, mixing depth, and soil density; as with the intruder model, the mixing depth may vary with the intruder scenario under consideration.

3.6.3.2 Air

The Atmospheric Scenario receptor is assumed to breathe airborne radioactivity transported from MDA G with the prevailing winds. The general equation used to calculate contaminant concentrations in air resulting from particulate resuspension is as follows:

$$C_{at,i,t,j} = \left(\frac{\chi}{Q}\right)_j \times Q_{r,i,t,j} \qquad 54$$

Where

$C_{at,i,t,j}$ = concentration, in air, of radionuclide i at time t for contamination originating in atmospheric source area j (Ci/m^3)

$\left(\frac{\chi}{Q}\right)_j$ = atmospheric dispersion factor for contamination originating in atmospheric source area j (yr/m^3)

$Q_{r,i,t,j}$ = quantity of radionuclide i resuspended at time t from atmospheric source area j (Ci/yr).

Equation 54 is implemented for each of the three source areas used in the atmospheric transport modeling; the concentrations for these areas are summed to determine the exposure location concentrations due to particulate resuspension from the entire site. The dispersion factor used in the equation is one of the results from the atmospheric transport modeling that is calculated outside of the GoldSim models. The quantities of radionuclides resuspended from the surface of the disposal facility are taken directly from the fluxes projected by the site model for the mass-flux links between the Surface_Soil and the Onsite_Air sink terms for the three atmospheric source areas.

The airborne concentrations calculated above account only for the radionuclides present in the plume as it passes over the exposure location. Particulates deposited on the receptor's lot may also become suspended and add to these air concentrations. Similarly, contamination deposited on the lot of the inadvertent intruder, the receptor residing at the downgradient well location, or the receptors in Cañada del Buey and Pajarito Canyon may be resuspended, leading to inhalation exposures. Airborne radionuclide concentrations resulting from the resuspension of particulates at these receptor locations are calculated as the product of the effective dust-loading factor and the soil-contaminant concentrations. The effective dust loading for the off-site receptor is calculated using the following:

$$d_e = d \times f_d \qquad 55$$

Where

d_e = effective dust loading (kg/m^3)
d = dust loading under undisturbed conditions (kg/m^3)
f_d = human disturbance factor

The human disturbance factor, f_d, is greater than or equal to 1.0 and accounts for increases in rates of resuspension due to disturbance of the soil by humans walking over the site.

Vapor- and gas-phase radionuclides that diffuse from the site will be transported to downwind locations by the prevailing winds. Airborne concentrations of these contaminants are estimated

for the Atmospheric Scenario by replacing the resuspension-based release rate in Equation 54 with the diffusive flux from the surface of each atmospheric source area. The exposure location concentrations estimated for the three atmospheric source areas are summed to estimate the air concentration due to releases from the entire site. The concentrations of vapor- and gas-phase radionuclides in the inadvertent intruder's house and in the air over the intruder's lot are taken directly from the House and Onsite_Air cells included in the intruder diffusion model.

3.6.3.3 Crops

Crops grown by the receptor may become contaminated with radionuclides due to the deposition of airborne and waterborne contaminants and as a result of root uptake of contaminants in the soil. These processes are represented using the following equation:

$$C_{c,i,t} = \left[\frac{C_{at,i,t} \times v_d \times T_c \times R_{w,c}(1.-e^{-\lambda_w * t_{g,c}})}{Y_{v,c}\lambda_w} + \frac{C_{w,i,t} \times I_r \times I_f \times T_c \times R_{w,c}(1.-e^{-\lambda_w * t_{g,c}})}{Y_{v,c}\lambda_w} + \right. \quad 56$$

$$\left. C_{s,i,t} \times M_c \times T_c \times D_c \times p_f + C_{s,i,t} \times B_{c,i} \times D_c \right] \times e^{-\lambda * t_{h,c}}$$

Where

$C_{c,i,t}$ = concentration, in crop *c*, of radionuclide *i* at time *t* (Ci/kg (wet weight))
$C_{at,i,t}$ = concentration, in air, of radionuclide *i* at time *t* (Ci/m^3)
v_d = particulate deposition velocity (m/hr)
T_c = translocation factor for crop *c*
$R_{w,c}$ = plant interception fraction of crop *c*
λ_w = weathering removal coefficient (hr^{-1})
$t_{g,c}$ = growing season for crop *c* (hr)
$Y_{v,c}$ = agricultural yield of crop *c* (kg wet weight crop/m^2)
$C_{w,i,t}$ = concentration, in irrigation water, of radionuclide *i* at time *t* (Ci/m^3)
I_r = irrigation rate (m/yr)
I_f = fraction of year crops are irrigated
$C_{s,i,t}$ = concentration, in soil, of radionuclide *i* at time *t* (Ci/kg dry weight soil)
M_c = plant mass-loading factor (Ci/kg dry weight plant per Ci/kg dry weight soil)
D_c = dry-to-wet-weight ratio for crop *c*
p_f = particle size factor
$B_{c,i}$ = soil-to-plant-concentration factor, in crop c, for radionuclide *i* (Ci/kg dry weight vegetation per Ci/kg dry weight soil)
λ = radioactive decay constant (hr^{-1})
$t_{h,c}$ = delay time between crop harvest and consumption (hr)

Radionuclide concentrations in crops due to depositional processes are estimated using the first three terms in Equation 56. The first term accounts for the deposition of airborne particulates on plant surfaces as contamination is transported over the receptor's lot by prevailing winds. The second and third terms account for contamination of the plants from irrigation with contaminated

water and from rainsplash, respectively. The final term in the equation accounts for root uptake of radionuclides in soil.

The plant interception fraction, $R_{w,c}$, specifies the fraction of particulates deposited on plant surfaces that is initially retained by the crops. A number of investigators have related the plant interception fraction to the agricultural productivity of the crop under consideration. This approach is implemented in the GoldSim models using the following equation (Ng et al., 1978):

$$R_{w,c} = 1.0 - e^{-\mu Y_{v,c}} \qquad 57$$

Where

μ = interception coefficient (m^2/kg)

The agricultural productivity, $Y_{v,c}$, is converted to a dry-weight basis before it is used in Equation 57; this is accomplished by multiplying the productivity by the dry-to-wet-weight ratio for the crop under consideration.

The level of contamination in crops resulting from the use of contaminated irrigation water will depend, in part, on the mode of irrigation employed. Information provided in Peterson (1983) indicates rates of contaminant uptake when water is applied in furrows may be approximately half of those observed for spray irrigation due to the effects of soil sorption. The expression used to estimate plant assimilation of radionuclides in irrigation water is based on the assumption that spray irrigation techniques are used.

The expression used to estimate plant concentrations due to rainsplash represents a departure from the model used in the 1997 MDA G performance assessment and composite analysis (Hollis et al., 1997). Those analyses used a resuspension factor approach to estimate the rates at which soil contamination was deposited on plant surfaces following the impact of raindrops on the ground surface. As discussed by Hinton (1992), this approach was not originally developed for the purposes of estimating plant concentrations. Furthermore, it is susceptible to a high level of uncertainty. Resuspension factor data are limited, and the data that do exist range over 5 to 10 orders of magnitude. Uncertainty associated with the deposition velocity, which is used to estimate the rate at which suspended particulates are deposited on plant surfaces, adds to the overall uncertainty in the projected plant concentrations.

Hinton (1992) proposed the mass-loading factor approach as a more effective means of estimating the impacts of processes such as rainsplash. The mass-loading factor is the ratio of the radionuclide concentration on the plant to the concentration in the soil (i.e., Ci/kg dry weight plant per Ci/kg dry weight soil). Multiplying the mass-loading factor by the soil radionuclide concentrations yields an estimate of contaminant concentrations on the plant. Multiplying these

surficial concentrations by the translocation factor yields internal plant concentrations. The mass-loading approach is discussed in greater detail in Hinton (1992) and Pinder and McLeod (1989).

Mass-loading factors reported in the literature have been calculated using two distinct approaches. In one approach, the factor is calculated using the contaminant concentrations in the resuspendable fraction of the soil, while in the other approach concentrations in the total soil are used. The four GoldSim models are designed to accept as input the mass-loading factors for the resuspendable fraction of the soil. Given that the GoldSim-estimated soil concentrations are total soil concentrations, these factors are multiplied by the ratio of radionuclide concentrations in the resuspendable fraction to the concentrations in the total soil. This ratio is referred to here as the particle size factor.

The soil-to-plant-uptake factors used in Equation 57 are input by the user for all radionuclides except for tritium; a specific activity model is used to estimate the concentrations of tritium in crops. Using this model, tritium concentrations in plant tissues are given by the following equation (Wood et al., 1994):

$$C_{H-3,c,t} = C_{H-3,sm,t} \times F_v^w \qquad 58$$

Where

$C_{H\text{-}3,c,t}$ = tritium concentration in crop c at time t (Ci/kg)
$C_{H\text{-}3,sm,t}$ = tritium concentration in soil moisture at time t (Ci/kg)
F_v^w = fraction of water in vegetation

The fraction of water in the vegetation was modified to take into account the tritium that is organically bound in the produce. This adjustment is made using the following equation (Wood et al., 1994):

$$F_v^{w2} = F_v^w + (1. - F_v^w) \times F_v^H \times 9 \qquad 59$$

Where

F_v^{w2} = effective water fraction in vegetation
F_v^H = fraction of hydrogen in vegetation
9 = coefficient to convert tritium concentration to hydrogen concentration

The quantities calculated using Equations 58 and 59 are used to estimate the plant uptake factor for tritium in a manner that is consistent with the plant uptake factors for the other radionuclides. This is accomplished using the following:

$$B_{H-3,c} = \frac{F_v^{w2}}{\theta_s \times \rho_{H2O} / \rho_{ds} \times D_c} \quad 60$$

Where

$B_{H-3,c}$ = plant uptake factor for tritium in crop c (Ci/kg dry weight vegetation per Ci/kg dry weight soil)
θ_s = moisture content of soil (volume basis)
ρ_{ds} = density of dry soil (kg/m^3)

The actual mechanisms of plant uptake used to model receptor exposures depend upon the exposure scenario under consideration. Contamination of crops as a result of rainsplash and root uptake is considered for all receptors included in the performance assessment and composite analysis. Plant uptake due to atmospheric deposition is considered for the Atmospheric Scenario, while contamination on plants resulting from the application of contaminated irrigation water is considered for the All Pathways – Groundwater Scenario.

3.6.3.4 Animal Products

Animals raised by the receptors may ingest contaminated forage, water, and soil/grit, resulting in the contamination of animal products consumed by the individuals. For all scenarios except the Groundwater Resource Protection and Intruder-Construction Scenarios, the four GoldSim models assume the receptor raises cattle and cows to supply a portion of household beef and milk, or raises chickens as a source of meat and eggs. Radionuclide concentrations in animal products are calculated using the following general expression:

$$C_{ap,i,t} = f_{i,ap}(C_{c,i,t} \times Q_c \times f_c + C_{w,i,t} \times Q_w \times f_w \times C_{s,i,t} \times Q_s \times f_s \quad 61$$

Where

$C_{ap,i,t}$ = concentration, in animal product *ap,* of radionuclide i at time t (Ci/kg)
$f_{i,ap}$ = forage-to-animal-product transfer factor for radionuclide i and animal product *ap* (d/kg wet weight animal product)
$C_{c,i,t}$ = concentration, in forage crop *c,* of radionuclide i at time t (Ci/kg dry weight crop)
Q_c = animal consumption rate of forage crop c (kg dry weight crop/d)
f_c = fraction of consumed forage crop c that is contaminated
$C_{w,i,t}$ = concentration, in water, of radionuclide i at time t (Ci/kg)
Q_w = animal consumption rate of water (kg/d)
f_w = fraction of consumed water that is contaminated
Q_s = animal consumption rate of soil/grit (kg dry weight soil/d)
f_s = fraction of ingested soil/grit that is contaminated

The forage-to-animal transfer factor relates the radionuclide concentration in the animal product to the intake of contaminated media ingested by the animal. Separate transfer factors are used to project contaminant concentrations in beef, milk, chicken, and eggs. These transfer factors are assumed to apply to all ingested substances including the pasture grass consumed by cattle and cows, the grain eaten by chickens, and the water and soil/grit ingested by all classes of livestock.

The user is responsible for the entry of transfer factors for all radionuclides except tritium and C-14; specific activity models are used to estimate the concentrations of these contaminants in beef, milk, chicken, and eggs. Tritium concentrations in animal products are calculated by correlation with the transfer of stable hydrogen to beef, milk, chicken, and eggs (ANL, 2001). In this approach, the transfer factor for tritium is given by the following equation:

$$f_{H-3,ap} = \frac{F_{H,ap}}{F_{H,c} \times Q_c + F_{H,s} \times Q_s + F_{H,w} \times Q_w} \quad 62$$

Where

$f_{H\text{-}3,ap}$ = effective tritium transfer factor for animal product p (d/kg)
$F_{H,ap}$ = mass fraction of stable hydrogen in animal product ap
$F_{H,c}$ = mass fraction of stable hydrogen in forage crop c
$F_{H,s}$ = mass fraction of stable hydrogen in soil
$F_{H,w}$ = mass fraction of stable hydrogen in water

The mass fraction of stable hydrogen in animal products is calculated as follows:

$$F_{H,ap} = F_{H,w} \times F_{w,ap} \quad 63$$

Where

$F_{w,ap}$ = mass water fraction in animal product ap

The fraction of the soil that consists of stable hydrogen is given by the following expression (ANL, 2001):

$$F_{H,s} = \frac{[\rho_b \times K_d + P \times R_s] \times F_{H,w} \times \rho_w}{\rho_b} \quad 64$$

Where

ρ_b = bulk density of soil (kg/m3)
K_d = hydrogen distribution coefficient in soil (m3/kg)
P = soil porosity
R_s = volumetric water content of soil
ρ_w = density of water (kg/m^3)

The first term of the expression in the brackets ($\rho_b \times K_d$) drops out when the distribution coefficient for hydrogen is zero.

The concentration of C-14 in animal products is given by the following (Napier et al., 2004):

$$C_{ap,C-14,t} = F_{ap}^{c} \times \left(\frac{C_{c,C-14,t} \times Q_c + C_{s,C-14,t} \times Q_s + C_{w,C-14,t} \times Q_w}{F_c^c \times Q_c + F_s^c \times Q_s + F_w^c \times Q_w} \right) \quad 65$$

Where

$C_{ap,C-14,t}$ = concentration, in animal product *ap*, of C-14 at time *t* (Ci/kg)

F_{ap}^{c} = fraction of animal product *ap* that is carbon (dry-weight basis)

$C_{c,\,C-14,t}$ = concentration, in forage crop *c*, of C-14 at time *t* (Ci/kg dry weight)

$C_{s,\,C-14,t}$ = concentration, in soil, of C-14 at time *t* (Ci/kg dry weight)

$C_{w,C-14,t}$ = concentration, in water, of C-14 at time *t* (Ci/kg)

F_c^c = fraction of forage crop *c* that is carbon (dry-weight basis)

F_s^c = fraction of soil that is carbon (dry-weight basis)

F_w^c = fraction of water that is carbon

The quotient of the concentration calculated using Equation 65 and the daily animal intake of C-14 yields the effective transfer factors needed for the performance assessment and composite analysis. Given that the numerator of Equation 65 includes the animal intake, this expression simplifies to the following:

$$f_{C-14,ap} = \frac{F_{ap}^{c}}{F_c^c \times Q_c + F_s^c \times Q_s + F_w^c \times Q_w} \quad 66$$

Where

$f_{C-14,ap}$ = C-14 transfer factor for animal product *ap* (d/kg)

The radionuclide concentrations in animal products will depend upon the fraction of the animals' diets that consist of contaminated media. The fraction of forage crop *c* that is contaminated is calculated as follows:

$$f_c = \frac{(A_l - A_h - A_c) \times Y_{v,c}}{Q_c / D_c \times 365.} \quad 67$$

Where

A_c = area of receptor's lot used to raise leafy vegetables, produce, and grain (m^2)
365. = 365 d

The fraction calculated using Equation 67 is also used to represent the fraction of the soil ingested by the animals that is contaminated; all water consumed by the animals is assumed to come from contaminated sources.

The sources of contamination that contribute to contaminant concentrations in animal products depend upon the exposure scenario under consideration. Animals are assumed to ingest contaminated soil and forage for all scenarios in which the receptor raises animals. The ingestion of contaminated drinking water by the animals is assumed only for the All Pathways – Groundwater Scenario.

3.6.3.5 Groundwater

The groundwater pathway receptors are assumed to use contaminated water drawn from the regional aquifer for irrigation, watering animals, and personal consumption. For a given scenario, the radionuclide concentrations in the water are calculated by dividing the annual flow from the FEHM elements to the well by the water usage rates of the receptor. Usage rates for the Groundwater Resources Protection Scenario take into account the water consumed by the individual and water needed for domestic uses (e.g., washing, food preparation, and bathing); the usage rates for the all pathways receptor are higher because they include irrigation needs.

4.0 Input Parameter Requirements

A variety of input data is required to implement the MDA G Site, Site Diffusion, Intruder, and Intruder Diffusion Models. This section provides a listing of the input parameters required to run these models. Included are the variable names used in the models, the units associated with each variable, and descriptions of the parameters. Input requirements for the MDA G Site Model are provided in Table 6, while data requirements for the site diffusion model are found in Table 7; the data requirements for the intruder and intruder diffusion models are listed in Tables 8 and 9, respectively.

The majority of the data used in the MDA G models are input using objects referred to in the GoldSim documentation (GoldSim, 2005a) as data and stochastic elements. Data elements accept single input values, or vectors and matrices of such. Stochastic elements allow the user to represent the uncertainty inherent in a variable by designating a distribution for the parameter. These elements also allow the user to specify deterministic values for parameters that can be used when the models are run in deterministic mode.

The type of element used by the MDA G models will determine the type of information required of the user. The summaries of the input data requirements provided below specify the type of element used for each parameter.

Table 6
Input Data Requirements for the MDA G Site Model

Model Container/Parameter Name	Units	Parameter Description	Parameter Type	Input Element Type
Controls_and_Constants				
Analysis_Flag		Flag used to indicate whether the performance assessment or composite analysis is being considered. A value of 1 indicates the composite analysis inventory is included in the simulation; a value of 2 indicates the performance assessment inventory is being used.	Scalar	Data
Disposal_System_Information				
Species_and_Materials				
Halflives	yr	Radionuclide half-lives	Vector (radionuclide)	Data
Material_Properties				
Density_of_Water	kg/m^3	Density of water	Scalar	Data
Soil_Carbon_Fraction		Fraction of surface soil that is carbon	Scalar	Data
Water_Carbon_Fraction		Fraction of water that is carbon	Scalar	Data
Water_Hydrogen_Fraction		Fraction of water that is hydrogen	Scalar	Data
Solubility_Limits	mg/L	Elemental solubility limits for crushed tuff and waste	Vector (element)	Data
Organic_Waste_Fraction		Fraction of C-14 waste that is organic and susceptible to biodegradation	Scalar	Stochastic
C14_Gas_Generation_Rate	yr^{-1}	Rate constant describing the rate of C-14 gas generation due to biodegradation of organic waste	Scalar	Stochastic
CO2_Fraction		Fraction of C-14 gas generated by the biodegradation of organic waste that is carbon dioxide	Scalar	Stochastic
Radon_Emanation_Fraction		Emanation coefficient for Rn-220 and Rn-222	Scalar	Stochastic

Table 6 (Continued)
Input Data Requirements for the MDA G Site Model

Model Container/Parameter Name	Units	Parameter Description	Parameter Type	Input Element Type
Dry_Densities				
DD_Crushed_Tuff	kg/m³	Dry density of crushed tuff	Scalar	Stochastic
DD_Waste	kg/m³	Dry density of waste	Scalar	Stochastic
Moisture_Contents				
MC_Crushed_Tuff	volume basis	Moisture content of crushed tuff	Scalar	Stochastic
MC_Waste	volume basis	Moisture content of waste	Scalar	Stochastic
Effective_Porosities				
EP_Crushed_Tuff		Effective porosity of crushed tuff	Scalar	Stochastic
EP_Waste		Effective porosity of waste	Scalar	Stochastic
Partition_Coefficients				
Soil_and_Waste_Kds				
Elemental_Kds	m³/kg	Elemental distribution coefficients for crushed tuff and waste	Vector (element)	Data
Kd_Distributions			Scalar	Data
Ag	m³/kg	Distribution coefficient for silver in crushed tuff and waste	Scalar	Stochastic
Am	m³/kg	Distribution coefficient for americium in crushed tuff and waste	Scalar	Stochastic
Ba	m³/kg	Distribution coefficient for barium in crushed tuff and waste	Scalar	Stochastic
Cs	m³/kg	Distribution coefficient for cesium in crushed tuff and waste	Scalar	Stochastic
Np	m³/kg	Distribution coefficient for neptunium in crushed tuff and waste	Scalar	Stochastic
Pa	m³/kg	Distribution coefficient for protactinium in crushed tuff and waste	Scalar	Stochastic
Pu	m³/kg	Distribution coefficient for plutonium in crushed tuff and waste	Scalar	Stochastic
Ra	m³/kg	Distribution coefficient for radium in crushed tuff and waste	Scalar	Stochastic

Table 6 (Continued)
Input Data Requirements for the MDA G Site Model

Model Container/Parameter Name	Units	Parameter Description	Parameter Type	Input Element Type
Sr	m^3/kg	Distribution coefficient for strontium in crushed tuff and waste	Scalar	Stochastic
Th	m^3/kg	Distribution coefficient for thorium in crushed tuff and waste	Scalar	Stochastic
U	m^3/kg	Distribution coefficient for uranium in crushed tuff and waste	Scalar	Stochastic
Intact_Tuff_KDs				
Elemental_Kds	m^3/kg	Elemental distribution coefficients for intact tuff	Vector (element)	Data
Kd_Distributions			Scalar	Data
Ag	m^3/kg	Distribution coefficient for silver in intact tuff	Scalar	Stochastic
Am	m^3/kg	Distribution coefficient for americium in intact tuff	Scalar	Stochastic
Ba	m^3/kg	Distribution coefficient for barium in intact tuff	Scalar	Stochastic
Cs	m^3/kg	Distribution coefficient for cesium in intact tuff	Scalar	Stochastic
Np	m^3/kg	Distribution coefficient for neptunium in intact tuff	Scalar	Stochastic
Pa	m^3/kg	Distribution coefficient for protactinium in intact tuff	Scalar	Stochastic
Pu	m^3/kg	Distribution coefficient for plutonium in intact tuff	Scalar	Stochastic
Ra	m^3/kg	Distribution coefficient for radium in intact tuff	Scalar	Stochastic
Sr	m^3/kg	Distribution coefficient for strontium in intact tuff	Scalar	Stochastic
Th	m^3/kg	Distribution coefficient for thorium in intact tuff	Scalar	Stochastic
U	m^3/kg	Distribution coefficient for uranium in intact tuff	Scalar	Stochastic
Air_to_Water_Coefficients				
H2O_Vapor_Pressure	atm	Vapor pressure of water	Scalar	Data
H2O_Molecular_Weight	g/mol	Molecular weight of water	Scalar	Data

Table 6 (Continued)
Input Data Requirements for the MDA G Site Model

Model Container/Parameter Name	Units	Parameter Description	Parameter Type	Input Element Type
CO2_Coefficient				
CO2_Henry's_Law_Constant	mol/L-atm	Henry's Law constant for carbon dioxide	Scalar	Data
CH_4_Coefficient				
CH4_Henrys_Law_Constant	mol/L-atm	Henry's Law constant for methane	Scalar	Data
Kr_Coefficient				
Kr_Henry's_Law_Constant	mol/L-atm	Henry's Law constant for krypton	Scalar	Data
Rn_Coefficient				
Rn_Henrys_Law_Constant	mol/L-atm	Henry's Law constant for radon	Scalar	Data
Relative_Diffusivities				
Free_Air_Diff_Coefficients	cm^2/s	Free-air diffusion coefficients	Vector (radionuclide)	Data
Thermal_Gradient_Factor		Factor used to account for the effects of thermal gradients on the rate of diffusion of tritiated water vapor	Scalar	Stochastic
Reference_Diff_Coefficient	cm^2/s	Reference diffusion coefficient	Scalar	Data
Attenuation_Coefficients				
Soil_Mass_Atten_Coeff	cm^2/g	Mass attenuation coefficient for soil	Vector (radionuclide)	Data
Concrete_Mass_Atten_Coeff	cm^2/g	Mass attenuation coefficient for concrete	Vector (radionuclide)	Data
Site_Geometry_and_Operations				
Institutional_Control_Period	yr	The length of the active institutional control period, measured from the time of facility closure	Scalar	Data
Atmospheric_Source_Areas	m^2	Areas associated wit h the atmospheric transport modeling source areas	Vector (atmospheric source area)	Data

Table 6 (Continued)
Input Data Requirements for the MDA G Site Model

Model Container/Parameter Name	Units	Parameter Description	Parameter Type	Input Element Type
Start_of_Region_Disposal	yr	The year of the simulation in which waste is first placed in the disposal units of the waste disposal region under consideration	Vector (waste disposal region)	Data
End_of_Region_Disposal	yr	The last year of the simulation that waste is placed in the disposal units of the waste disposal region under consideration	Vector (waste disposal region)	Data
Closure_Period	yr	The length of time required to achieve final closure of the disposal facility following the end of disposal operations	Scalar	Data
Layer_Information				
Number_of_Cap_Layers		The number of discrete layers used to represent the cap	Scalar	Data
Number_of_Waste_Layers		The number of discrete layers used to represent the buried waste	Scalar	Data
Waste_Region_1 – Waste_Region_8				
Initial_Cover_Thickness	m	Initial thickness of the cover over the disposal units	Scalar	Stochastic
Surface_Soil_Thickness	m	Thickness of the surface soil layer	Vector (disposal region)	Data
Waste_Thickness	m	Thickness of the disposed waste	Vector (disposal region)	Data
Upper_Waste_Layer_Thickness	m	Thickness of the uppermost three layers of waste	Scalar	Data
Disposal_Unit_Area	m^2	Surface area of the disposal units	Scalar	Data
Fractional_Area_Calculations				
Low_Erosion_Fraction		Fractional area of the erosion zones for the low erosion scenario at the end of the simulation	Vector (erosion zone)	Data
Moderate_Erosion_Fraction		Fractional area of the erosion zones for the moderate erosion scenario at the end of the simulation	Vector (erosion zone)	Data
High_Erosion_Fraction		Fractional area of the erosion zones for the high erosion scenario at the end of the simulation	Vector (erosion zone)	Data

Table 6 (Continued)
Input Data Requirements for the MDA G Site Model

Model Container/Parameter Name	Units	Parameter Description	Parameter Type	Input Element Type
Inventory				
Measurement_Errors				
Rad_Specific_Errors				
Pre_1990_Lower_Bounds		Factor used to estimate the lower bound of pre-1990 radionuclide inventories, taking into account errors introduced by measurement uncertainty	Vector (radionuclide)	Data
Pre_1990_Upper_Bounds		Factor used to estimate the upper bound of pre-1990 radionuclide inventories, taking into account errors introduced by measurement uncertainty	Vector (radionuclide)	Data
Post_1989_Lower_Bounds		Factor used to estimate the lower bound of post-1989 radionuclide inventories, taking into account errors introduced by measurement uncertainty	Vector (radionuclide)	Data
Post_1989_Upper_Bounds		Factor used to estimate the upper bound of post-1989 radionuclide inventories, taking into account errors introduced by measurement uncertainty	Vector (radionuclide)	Data
Material_Type_Errors				
Pre_1990_Lower_Bounds		Factor used to estimate the lower bound of pre-1990 material type inventories, taking into account errors introduced by measurement uncertainty	Vector (material type)	Data
Pre_1990_Upper_Bounds		Factor used to estimate the upper bound of pre-1990 material type inventories, taking into account errors introduced by measurement uncertainty	Vector (material type)	Data
Post_1989_Lower_Bounds		Factor used to estimate the lower bound of post-1989 material type inventories, taking into account errors introduced by measurement uncertainty	Vector (material type)	Data

Table 6 (Continued)
Input Data Requirements for the MDA G Site Model

Model Container/Parameter Name	Units	Parameter Description	Parameter Type	Input Element Type
Post_1989_Upper_Bounds		Factor used to estimate the upper bound of post-1989 material type inventories, taking into account errors introduced by measurement uncertainty	Vector (material type)	Data
Rad_Specific_Inventories				
Waste_Region_1				
Pre_1990_CA_Point_Estimates	Ci	Point estimates of radionuclide-specific inventories in the pre-1990 composite analysis waste disposed of in waste disposal region 1	Vector (radionuclide)	Data
Pre_1990_PA_Point_Estimates	Ci	Point estimates of radionuclide-specific inventories in the pre-1990 performance assessment waste disposed of in waste disposal region 1	Vector (radionuclide)	Data
Waste_Region_2				
Pre_1990_CA_Point_Estimates	Ci	Point estimates of radionuclide-specific inventories in the pre-1990 composite analysis waste disposed of in waste disposal region 2	Vector (radionuclide)	Data
Pre_1990_PA_Point_Estimates	Ci	Point estimates of radionuclide-specific inventories in the pre-1990 performance assessment waste disposed of in waste disposal region 2	Vector (radionuclide)	Data
Waste_Region_3				
Pre_1990_CA_Point_Estimates	Ci	Point estimates of radionuclide-specific inventories in the pre-1990 composite analysis waste disposed of in waste disposal region 3	Vector (radionuclide)	Data
Pre_1990_PA_Point_Estimates	Ci	Point estimates of radionuclide-specific inventories in the pre-1990 performance assessment waste disposed of in waste disposal region 3	Vector (radionuclide)	Data

Table 6 (Continued)
Input Data Requirements for the MDA G Site Model

Model Container/Parameter Name	Units	Parameter Description	Parameter Type	Input Element Type
Post_1989_CA_Point_Estimates	Ci	Point estimates of radionuclide-specific inventories in the post-1989 composite analysis waste disposed of in waste disposal region 3	Vector (radionuclide)	Data
Post_1989_PA_Point_Estimates	Ci	Point estimates of radionuclide-specific inventories in the post-1989 performance assessment waste disposed of in waste disposal region 3	Vector (radionuclide)	Data
Waste_Region_4				
Pre_1990_CA_Point_Estimates	Ci	Point estimates of radionuclide-specific inventories in the pre-1990 composite analysis waste disposed of in waste disposal region 4	Vector (radionuclide)	Data
Pre_1990_PA_Point_Estimates	Ci	Point estimates of radionuclide-specific inventories in the pre-1990 performance assessment waste disposed of in waste disposal region 4	Vector (radionuclide)	Data
Post_1989_CA_Point_Estimates	Ci	Point estimates of radionuclide-specific inventories in the post-1989 composite analysis waste disposed of in waste disposal region 4	Vector (radionuclide)	Data
Post_1989_PA_Point_Estimates	Ci	Point estimates of radionuclide-specific inventories in the post-1989 performance assessment waste disposed of in waste disposal region 4	Vector (radionuclide)	Data
Waste_Region_5				
Pre_1990_CA_Point_Estimates	Ci	Point estimates of radionuclide-specific inventories in the pre-1990 composite analysis waste disposed of in waste disposal region 5	Vector (radionuclide)	Data
Pre_1990_PA_Point_Estimates	Ci	Point estimates of radionuclide-specific inventories in the pre-1990 performance assessment waste disposed of in waste disposal region 5	Vector (radionuclide)	Data

Table 6 (Continued)
Input Data Requirements for the MDA G Site Model

Model Container/Parameter Name	Units	Parameter Description	Parameter Type	Input Element Type
Post_1989_CA_Point_Estimates	Ci	Point estimates of radionuclide-specific inventories in the post-1989 composite analysis waste disposed of in waste disposal region 5	Vector (radionuclide)	Data
Post_1989_PA_Point_Estimates	Ci	Point estimates of radionuclide-specific inventories in the post-1989 performance assessment waste disposed of in waste disposal region 5	Vector (radionuclide)	Data
Waste_Region_6				
Pre_1990_CA_Point_Estimates	Ci	Point estimates of radionuclide-specific inventories in the pre-1990 composite analysis waste disposed of in waste disposal region 6	Vector (radionuclide)	Data
Pre_1990_PA_Point_Estimates	Ci	Point estimates of radionuclide-specific inventories in the pre-1990 performance assessment waste disposed of in waste disposal region 6	Vector (radionuclide)	Data
Waste_Region_7				
Pre_1990_CA_Point_Estimates	Ci	Point estimates of radionuclide-specific inventories in the pre-1990 composite analysis waste disposed of in waste disposal region 7	Vector (radionuclide)	Data
Pre_1990_PA_Point_Estimates	Ci	Point estimates of radionuclide-specific inventories in the pre-1990 performance assessment waste disposed of in waste disposal region 7	Vector (radionuclide)	Data
Post_1989_CA_Point_Estimates	Ci	Point estimates of radionuclide-specific inventories in the post-1989 composite analysis waste disposed of in waste disposal region 7	Vector (radionuclide)	Data
Post_1989_PA_Point_Estimates	Ci	Point estimates of radionuclide-specific inventories in the post-1989 performance assessment waste disposed of in waste disposal region 7	Vector (radionuclide)	Data

Table 6 (Continued)
Input Data Requirements for the MDA G Site Model

Model Container/Parameter Name	Units	Parameter Description	Parameter Type	Input Element Type
Waste_Region_8				
Post_1989_CA_Point_Estimates	Ci	Point estimates of radionuclide-specific inventories in the post-1989 composite analysis waste disposed of in waste disposal region 8	Vector (radionuclide)	Data
Post_1989_PA_Point_Estimates	Ci	Point estimates of radionuclide-specific inventories in the post-1989 performance assessment waste disposed of in waste disposal region 8	Vector (radionuclide)	Data
Material_Type_Inventories				
Waste_Region_1				
Pre_1990_CA_Point_Estimates	Ci	Point estimates of material type inventories in the pre-1990 composite analysis waste disposed of in waste disposal region 1	Vector (material type)	Data
Pre_1990_PA_Point_Estimates	Ci	Point estimates of material type inventories in the pre-1990 performance assessment waste disposed of in waste disposal region 1	Vector (material type)	Data
Waste_Region_2				
Pre_1990_CA_Point_Estimates	Ci	Point estimates of material type inventories in the pre-1990 composite analysis waste disposed of in waste disposal region 2	Vector (material type)	Data
Pre_1990_PA_Point_Estimates	Ci	Point estimates of material type inventories in the pre-1990 performance assessment waste disposed of in waste disposal region 2	Vector (material type)	Data
Waste_Region_3				
Pre_1990_CA_Point_Estimates	Ci	Point estimates of material type inventories in the pre-1990 composite analysis waste disposed of in waste disposal region 3	Vector (material type)	Data
Pre_1990_PA_Point_Estimates	Ci	Point estimates of material type inventories in the pre-1990 performance assessment waste disposed of in waste disposal region 3	Vector (material type)	Data

Table 6 (Continued)
Input Data Requirements for the MDA G Site Model

Model Container/Parameter Name	Units	Parameter Description	Parameter Type	Input Element Type
Post_1989_CA_Point_Estimates	Ci	Point estimates of material type inventories in the post-1989 composite analysis waste disposed of in waste disposal region 3	Vector (material type)	Data
Post_1989_PA_Point_Estimates	Ci	Point estimates of material type inventories in the post-1989 performance assessment waste disposed of in waste disposal region 3	Vector (material type)	Data
Waste_Region_4				
Pre_1990_CA_Point_Estimates	Ci	Point estimates of material type inventories in the pre-1990 composite analysis waste disposed of in waste disposal region 4	Vector (material type)	Data
Pre_1990_PA_Point_Estimates	Ci	Point estimates of material type inventories in the pre-1990 performance assessment waste disposed of in waste disposal region 4	Vector (material type)	Data
Post_1989_CA_Point_Estimates	Ci	Point estimates of material type inventories in the post-1989 composite analysis waste disposed of in waste disposal region 4	Vector (material type)	Data
Post_1989_PA_Point_Estimates	Ci	Point estimates of material type inventories in the post-1989 performance assessment waste disposed of in waste disposal region 4	Vector (material type)	Data
Waste_Region_5				
Pre_1990_CA_Point_Estimates	Ci	Point estimates of material type inventories in the pre-1990 composite analysis waste disposed of in waste disposal region 5	Vector (material type)	Data
Pre_1990_PA_Point_Estimates	Ci	Point estimates of material type inventories in the pre-1990 performance assessment waste disposed of in waste disposal region 5	Vector (material type)	Data
Post_1989_CA_Point_Estimates	Ci	Point estimates of material type inventories in the post-1989 composite analysis waste disposed of in waste disposal region 5	Vector (material type)	Data
Post_1989_PA_Point_Estimates	Ci	Point estimates of material type inventories in the post-1989 performance assessment waste disposed of in waste disposal region 5	Vector (material type)	Data

Table 6 (Continued)
Input Data Requirements for the MDA G Site Model

Model Container/Parameter Name	Units	Parameter Description	Parameter Type	Input Element Type
Waste_Region_6				
Pre_1990_CA_Point_Estimates	Ci	Point estimates of material type inventories in the pre-1990 composite analysis waste disposed of in waste disposal region 6	Vector (material type)	Data
Pre_1990_PA_Point_Estimates	Ci	Point estimates of material type inventories in the pre-1990 performance assessment waste disposed of in waste disposal region 6	Vector (material type)	Data
Waste_Region_7				
Pre_1990_CA_Point_Estimates	Ci	Point estimates of material type inventories in the pre-1990 composite analysis waste disposed of in waste disposal region 7	Vector (material type)	Data
Pre_1990_PA_Point_Estimates	Ci	Point estimates of material type inventories in the pre-1990 performance assessment waste disposed of in waste disposal region 7	Vector (material type)	Data
Post_1989_CA_Point_Estimates	Ci	Point estimates of material type inventories in the post-1989 composite analysis waste disposed of in waste disposal region 7	Vector (material type)	Data
Post_1989_PA_Point_Estimates	Ci	Point estimates of material type inventories in the post-1989 performance assessment waste disposed of in waste disposal region 7	Vector (material type)	Data
Waste_Region_8				
Post_1989_CA_Point_Estimates	Ci	Point estimates of material type inventories in the post-1989 composite analysis waste disposed of in waste disposal region 8	Vector (material type)	Data
Post_1989_PA_Point_Estimates	Ci	Point estimates of material type inventories in the post-1989 performance assessment waste disposed of in waste disposal region 8	Vector (material type)	Data
Fission_Yields				
Fraction_of_Pu239		Fraction of fission events that originate with Pu-239	Scalar	Stochastic

Table 6 (Continued)
Input Data Requirements for the MDA G Site Model

Model Container/Parameter Name	Units	Parameter Description	Parameter Type	Input Element Type
Age_of_MFP_Waste	yr	Age of mixed fission product waste at the time of disposal	Scalar	Stochastic
U235_Fission_Yields				
U235_1yr_Thermal		U-235 thermal fission yields for 1-year-old waste	Scalar	Data
U235_2yr_Thermal		U-235 thermal fission yields for 2-year-old waste	Scalar	Data
U235_3yr_Thermal		U-235 thermal fission yields for 3-year-old waste	Scalar	Data
U235_4yr_Thermal		U-235 thermal fission yields for 4-year-old waste	Scalar	Data
U235_5yr_Thermal		U-235 thermal fission yields for 5-year-old waste	Scalar	Data
U235_6yr_Thermal		U-235 thermal fission yields for 6-year-old waste	Scalar	Data
U235_7yr_Thermal		U-235 thermal fission yields for 7-year-old waste	Scalar	Data
U235_8yr_Thermal		U-235 thermal fission yields for 8-year-old waste	Scalar	Data
U235_9yr_Thermal		U-235 thermal fission yields for 9-year-old waste	Scalar	Data
U235_10yr_Thermal		U-235 thermal fission yields for 10-year-old waste	Scalar	Data
Pu239_Fission_Yields				
Pu239_1yr_Thermal		Pu-239 thermal fission yields for 1-year-old waste	Scalar	Data
Pu239_2yr_Thermal		Pu-239 thermal fission yields for 2-year-old waste	Scalar	Data
Pu239_3yr_Thermal		Pu-239 thermal fission yields for 3-year-old waste	Scalar	Data
Pu239_4yr_Thermal		Pu-239 thermal fission yields for 4-year-old waste	Scalar	Data
Pu239_5yr_Thermal		Pu-239 thermal fission yields for 5-year-old waste	Scalar	Data
Pu239_6yr_Thermal		Pu-239 thermal fission yields for 6-year-old waste	Scalar	Data
Pu239_7yr_Thermal		Pu-239 thermal fission yields for 7-year-old waste	Scalar	Data
Pu239_8yr_Thermal		Pu-239 thermal fission yields for 8-year-old waste	Scalar	Data

Table 6 (Continued)
Input Data Requirements for the MDA G Site Model

Model Container/Parameter Name	Units	Parameter Description	Parameter Type	Input Element Type
Pu239_9yr_Thermal		Pu-239 thermal fission yields for 9-year-old waste	Scalar	Data
Pu239_10yr_Thermal		Pu-239 thermal fission yields for 10-year-old waste	Scalar	Data
Activation_Yields				
MAP_Allocation_Fractions		Radionuclide-specific activity fractions for mixed activation product waste	Vector (radionuclide)	Data
Material_Type_Act_Fractions				
Nominal_Masses	g	Material type waste radionuclide masses	Matrix (radionuclide, material type)	Data
PU51				
Activity_Fractions		Radionuclide activity fractions in material type PU51 waste	Vector (radionuclide)	Data
PU52				
Pu238_Mass_Fraction		Mass fraction of Pu-238 in material type PU52 waste	Scalar	Stochastic
Pu240_Mass_Fraction		Mass fraction of Pu-240 in material type PU52 waste	Scalar	Stochastic
Pu241_Mass_Fraction		Mass fraction of Pu-241 in material type PU52 waste	Scalar	Stochastic
Pu242_Mass_Fraction		Mass fraction of Pu-242 in material type PU52 waste	Scalar	Stochastic
PU53				
Pu238_Mass_Fraction		Mass fraction of Pu-238 in material type PU53 waste	Scalar	Stochastic
Pu240_Mass_Fraction		Mass fraction of Pu-240 in material type PU53 waste	Scalar	Stochastic
Pu241_Mass_Fraction		Mass fraction of Pu-241 in material type PU53 waste	Scalar	Stochastic
Pu242_Mass_Fraction		Mass fraction of Pu-242 in material type PU53 waste	Scalar	Stochastic
PU54				
Pu238_Mass_Fraction		Mass fraction of Pu-238 in material type PU54 waste	Scalar	Stochastic

Table 6 (Continued)
Input Data Requirements for the MDA G Site Model

Model Container/Parameter Name	Units	Parameter Description	Parameter Type	Input Element Type
Pu240_Mass_Fraction		Mass fraction of Pu-240 in material type PU54 waste	Scalar	Stochastic
Pu241_Mass_Fraction		Mass fraction of Pu-241 in material type PU54 waste	Scalar	Stochastic
Pu242_Mass_Fraction		Mass fraction of Pu-242 in material type PU54 waste	Scalar	Stochastic
PU55				
Activity_Fractions		Radionuclide activity fractions in material type PU55 waste	Vector (radionuclide)	Data
PU56				
Pu238_Mass_Fraction		Mass fraction of Pu-238 in material type PU56 waste	Scalar	Stochastic
Pu240_Mass_Fraction		Mass fraction of Pu-240 in material type PU56 waste	Scalar	Stochastic
Pu241_Mass_Fraction		Mass fraction of Pu-241 in material type PU56 waste	Scalar	Stochastic
Pu242_Mass_Fraction		Mass fraction of Pu-242 in material type PU56 waste	Scalar	Stochastic
PU57				
Activity_Fractions		Radionuclide activity fractions in material type PU57 waste	Vector (radionuclide)	Data
PU83				
Pu238_Mass_Fraction		Mass fraction of Pu-238 in material type PU83 waste	Scalar	Stochastic
Pu240_Mass_Fraction		Mass fraction of Pu-240 in material type PU83 waste	Scalar	Stochastic
Pu241_Mass_Fraction		Mass fraction of Pu-241 in material type PU83 waste	Scalar	Stochastic
Pu242_Mass_Fraction		Mass fraction of Pu-242 in material type PU83 waste	Scalar	Stochastic
U10				
Activity_Fractions		Radionuclide activity fractions in material type U10 waste	Vector (radionuclide)	Data
U11				
Activity_Fractions		Radionuclide activity fractions in material type U11 waste	Vector (radionuclide)	Data

Table 6 (Continued)
Input Data Requirements for the MDA G Site Model

Model Container/Parameter Name	Units	Parameter Description	Parameter Type	Input Element Type
U12				
U234_Mass_Fraction		Mass fraction of U-234 in material type U12 waste	Scalar	Stochastic
U245_Mass_Fraction		Mass fraction of U-235 in material type U12 waste	Scalar	Stochastic
U35				
Activity_Fractions		Radionuclide activity fractions in material type U35 waste	Vector (radionuclide)	Data
U36				
Activity_Fractions		Radionuclide activity fractions in material type U36 waste	Vector (radionuclide)	Data
U38				
Activity_Fractions		Radionuclide activity fractions in material type U38 waste	Vector (radionuclide)	Data
U39				
Activity_Fractions		Radionuclide activity fractions in material type U39 waste	Vector (radionuclide)	Data
U81				
Activity_Fractions		Radionuclide activity fractions in material type U81 waste	Vector (radionuclide)	Data
UNAT				
Activity_Fractions		Radionuclide activity fractions in material type UNAT waste	Vector (radionuclide)	Data
D38				
U234_Mass_Fraction		Mass fraction of U-234 in material type D38 waste	Scalar	Stochastic
U245_Mass_Fraction		Mass fraction of U-235 in material type D38 waste	Scalar	Stochastic
TH88				
Activity_Fractions		Radionuclide activity fractions in material type TH88 waste	Vector (radionuclide)	Data

Table 6 (Continued)
Input Data Requirements for the MDA G Site Model

Model Container/Parameter Name	Units	Parameter Description	Parameter Type	Input Element Type
Transport_Pathway_Data				
Atmospheric_Transport				
Dust_Loading	kg/m^3	Dust loading	Scalar	Stochastic
Soil_Disturbance_Factor		Factor by which the dust loading is increased due to human disturbance of the surface soil	Scalar	Stochastic
Default_Resuspension_Flux	g/m^2-s	Resuspension flux used to conduct the complex terrain atmospheric transport modeling	Scalar	Data
Resuspension_Flux	g/m^2/yr	Resuspension for particulates at MDA G	Scalar	Stochastic
Enhancement_Factor		Ratio of radionuclide concentrations in the resuspendable fraction of the soil to those in the total soil	Scalar	Stochastic
Dispersion_Factors				
LANL_Boundary				
Grassland_Land_Use				
CA_Factors				
X_Q_SA1_Grassland	s/m^3	Air dispersion factor for atmospheric source area 1 and the grassland land use — composite analysis	Scalar	Stochastic
X_Q_SA2_Grassland	s/m^3	Air dispersion factor for atmospheric source area 2 and the grassland land use — composite analysis	Scalar	Stochastic
X_Q_SA3_Grassland	s/m^3	Air dispersion factor for atmospheric source area 3 and the grassland land use — composite analysis	Scalar	Stochastic
PA_Factors				
X_Q_SA1_Grassland	s/m^3	Air dispersion factor for atmospheric source area 1 and the grassland land use — performance assessment	Scalar	Stochastic

Table 6 (Continued)
Input Data Requirements for the MDA G Site Model

Model Container/Parameter Name	Units	Parameter Description	Parameter Type	Input Element Type
X_Q_SA2_Grassland	s/m³	Air dispersion factor for atmospheric source area 2 and the grassland land use – performance assessment	Scalar	Stochastic
X_Q_SA3_Grassland	s/m³	Air dispersion factor for atmospheric source area 3 and the grassland land use — performance assessment	Scalar	Stochastic
Woodland_Land_Use				
CA_Factors				
X_Q_SA1_Woodland	s/m³	Air dispersion factor for atmospheric source area 1 and the woodland land use — composite analysis	Scalar	Stochastic
X_Q_SA2_Woodland	s/m³	Air dispersion factor for atmospheric source area 2 and the woodland land use — composite analysis	Scalar	Stochastic
X_Q_SA3_Woodland	s/m³	Air dispersion factor for atmospheric source area 3 and the woodland land use — composite analysis	Scalar	Stochastic
PA_Factors				
X_Q_SA1_Woodland	s/m³	Air dispersion factor for atmospheric source area 1 and the woodland land use — performance assessment	Scalar	Stochastic
X_Q_SA2_Woodland	s/m³	Air dispersion factor for atmospheric source area 2 and the woodland land use — performance assessment	Scalar	Stochastic
X_Q_SA3_Woodland	s/m³	Air dispersion factor for atmospheric source area 3 and the woodland land use — performance assessment	Scalar	Stochastic
MDA_G_Fenceline				
Grassland_Land_Use				
CA_Factors				
X_Q_SA1_Grassland	s/m³	Air dispersion factor for atmospheric source area 1 and the grassland land use — composite analysis	Scalar	Stochastic

Table 6 (Continued)
Input Data Requirements for the MDA G Site Model

Model Container/Parameter Name	Units	Parameter Description	Parameter Type	Input Element Type
X_Q_SA2_Grassland	s/m³	Air dispersion factor for atmospheric source area 2 and the grassland land use — composite analysis	Scalar	Stochastic
X_Q_SA3_Grassland	s/m³	Air dispersion factor for atmospheric source area 3 and the grassland land use — composite analysis	Scalar	Stochastic
PA_Factors				
X_Q_SA1_Grassland	s/m³	Air dispersion factor for atmospheric source area 1 and the grassland land use — performance assessment	Scalar	Stochastic
X_Q_SA2_Grassland	s/m³	Air dispersion factor for atmospheric source area 2 and the grassland land use — performance assessment	Scalar	Stochastic
X_Q_SA3_Grassland	s/m³	Air dispersion factor for atmospheric source area 3 and the grassland land use — performance assessment	Scalar	Stochastic
Woodland_Land_Use				
CA_Factors				
X_Q_SA1_Woodland	s/m³	Air dispersion factor for atmospheric source area 1 and the woodland land use — composite analysis	Scalar	Stochastic
X_Q_SA2_Woodland	s/m³	Air dispersion factor for atmospheric source area 2 and the woodland land use — composite analysis	Scalar	Stochastic
X_Q_SA3_Woodland	s/m³	Air dispersion factor for atmospheric source area 3 and the woodland land use — composite analysis	Scalar	Stochastic
PA_Factors				
X_Q_SA1_Woodland	s/m³	Air dispersion factor for atmospheric source area 1 and the woodland land use — performance assessment	Scalar	Stochastic
X_Q_SA2_Woodland	s/m³	Air dispersion factor for atmospheric source area 2 and the woodland land use — performance assessment	Scalar	Stochastic

Table 6 (Continued)
Input Data Requirements for the MDA G Site Model

Model Container/Parameter Name	Units	Parameter Description	Parameter Type	Input Element Type
X_Q_SA3_Woodland	s/m^3	Air dispersion factor for atmospheric source area 3 and the woodland land use — performance assessment	Scalar	Stochastic
Deposition_Rates				
LANL_Boundary				
Grassland_Land_Use				
CA_Factors				
DepRate_SA1_Grassland	$g/m^2/s$	Particulate deposition rate for atmospheric source area 1 and the grassland land use — composite analysis	Scalar	Stochastic
DepRate_SA2_Grassland	$g/m^2/s$	Particulate deposition rate for atmospheric source area 2 and the grassland land use — composite analysis	Scalar	Stochastic
DepRate_SA3_Grassland	$g/m^2/s$	Particulate deposition rate for atmospheric source area 3 and the grassland land use — composite analysis	Scalar	Stochastic
PA_Factors				
DepRate_SA1_Grassland	$g/m^2/s$	Particulate deposition rate for atmospheric source area 1 and the grassland land use — performance assessment	Scalar	Stochastic
DepRate_SA2_Grassland	$g/m^2/s$	Particulate deposition rate for atmospheric source area 2 and the grassland land use — performance assessment	Scalar	Stochastic
DepRate_SA3_Grassland	$g/m^2/s$	Particulate deposition rate for atmospheric source area 3 and the grassland land use — performance assessment	Scalar	Stochastic
Woodland_Land_Use				
CA_Factors				
DepRate_SA1_Woodland	$g/m^2/s$	Particulate deposition rate for atmospheric source area 1 and the woodland land use — composite analysis	Scalar	Stochastic

Table 6 (Continued)
Input Data Requirements for the MDA G Site Model

Model Container/Parameter Name	Units	Parameter Description	Parameter Type	Input Element Type
DepRate_SA2_Woodland	g/m²/s	Particulate deposition rate for atmospheric source area 2 and the woodland land use — composite analysis	Scalar	Stochastic
DepRate_SA3_Woodland	g/m²/s	Particulate deposition rate for atmospheric source area 3 and the woodland land use — composite analysis	Scalar	Stochastic
PA_Factors				
DepRate_SA1_Woodland	g/m²/s	Particulate deposition rate for atmospheric source area 1 and the woodland land use — performance assessment	Scalar	Stochastic
DepRate_SA2_Woodland	g/m²/s	Particulate deposition rate for atmospheric source area 2 and the woodland land use — performance assessment	Scalar	Stochastic
DepRate_SA3_Woodland	g/m²/s	Particulate deposition rate for atmospheric source area 3 and the woodland land use — performance assessment	Scalar	Stochastic
MDA_G_Fenceline				
Grassland_Land_Use				
CA_Factors				
DepRate_SA1_Grassland	g/m²/s	Particulate deposition rate for atmospheric source area 1 and the grassland land use — composite analysis	Scalar	Stochastic
DepRate_SA2_Grassland	g/m²/s	Particulate deposition rate for atmospheric source area 2 and the grassland land use — composite analysis	Scalar	Stochastic
DepRate_SA3_Grassland	g/m²/s	Particulate deposition rate for atmospheric source area 3 and the grassland land use — composite analysis	Scalar	Stochastic
PA_Factors				
DepRate_SA1_Grassland	g/m²/s	Particulate deposition rate for atmospheric source area 1 and the grassland land use — performance assessment	Scalar	Stochastic
DepRate_SA2_Grassland	g/m²/s	Particulate deposition rate for atmospheric source area 2 and the grassland land use — performance assessment	Scalar	Stochastic

Table 6 (Continued)
Input Data Requirements for the MDA G Site Model

Model Container/Parameter Name	Units	Parameter Description	Parameter Type	Input Element Type
DepRate_SA3_Grassland	g/m²/s	Particulate deposition rate for atmospheric source area 3 and the grassland land use — performance assessment	Scalar	Stochastic
Woodland_Land_Use				
CA_Factors				
DepRate_SA1_Woodland	g/m²/s	Particulate deposition rate for atmospheric source area 1 and the woodland land use — composite analysis	Scalar	Stochastic
DepRate_SA2_Woodland	g/m²/s	Particulate deposition rate for atmospheric source area 2 and the woodland land use — composite analysis	Scalar	Stochastic
DepRate_SA3_Woodland	g/m²/s	Particulate deposition rate for atmospheric source area 3 and the woodland land use — composite analysis	Scalar	Stochastic
PA_Factors				
DepRate_SA1_Woodland	g/m²/s	Particulate deposition rate for atmospheric source area 1 and the woodland land use — performance assessment	Scalar	Stochastic
DepRate_SA2_Woodland	g/m²/s	Particulate deposition rate for atmospheric source area 2 and the woodland land use — performance assessment	Scalar	Stochastic
DepRate_SA3_Woodland	g/m²/s	Particulate deposition rate for atmospheric source area 3 and the woodland land use — performance assessment	Scalar	Stochastic
Foodchain_Transport				
Plant_Data				
Uptake_Factors				
Leafy_Vegetable_GM	Ci/kg plant per Ci/kg soil (dry weight)	Geometric means of the plant uptake factors for leafy vegetables	Vector (element)	Data

Table 6 (Continued)
Input Data Requirements for the MDA G Site Model

Model Container/Parameter Name	Units	Parameter Description	Parameter Type	Input Element Type
Produce_GM	Ci/kg plant per Ci/kg soil (dry weight)	Geometric means of the plant uptake factors for produce	Vector (element)	Data
Grain_GM	Ci/kg plant per Ci/kg soil (dry weight)	Geometric means of the plant uptake factors for grain	Vector (element)	Data
PGrass_and_Native_GM	Ci/kg plant per Ci/kg soil (dry weight)	Geometric means of the plant uptake factors for pasture grass and native vegetation	Vector (element)	Data
Crop_GSD		Geometric standard deviation of the plant uptake factors for all crops		
Crop_Characteristics				
Particle_Size_Factor		Ratio of radionuclide concentrations in the fraction of the soil resuspended due to rainsplash to those in the total soil	Scalar	Stochastic
Plant_Carbon_Fraction		Fraction of plant that is carbon (dry-weight basis)	Vector (crop)	Data
Plant_Hydrogen_Fraction		Fraction of plant that is hydrogen (dry-weight basis)	Vector (crop)	Data
Plant_Interception_Coefficient	m^2/kg	Coefficient used to estimate the fraction of contamination deposited on plants that is initially retained	Scalar	Stochastic
Weathering_Halflife	d	Time required for 50 percent of the surface contamination on plants to be removed due to weathering processes	Scalar	Stochastic
Dry_to_Wet_Weight_Fractions				
DW_Leafy_Vegetables		Dry-to-wet-weight fraction for leafy vegetables	Scalar	Stochastic
DW_Produce		Dry-to-wet-weight fraction for produce	Scalar	Stochastic
DW_Grain		Dry-to-wet-weight fraction for grain	Scalar	Stochastic
DW_Pasture_Grass		Dry-to-wet-weight fraction for pasture grass	Scalar	Stochastic

Table 6 (Continued)
Input Data Requirements for the MDA G Site Model

Model Container/Parameter Name	Units	Parameter Description	Parameter Type	Input Element Type
Translocation_Factors				
TF_Leafy_Vegetables		Translocation factor for leafy vegetables	Scalar	Stochastic
TF_Produce		Translocation factor for produce	Scalar	Stochastic
TF_Grain		Translocation factor for grain	Scalar	Stochastic
TF_Pasture_Grass		Translocation factor for pasture grass	Scalar	Stochastic
Agricultural_Productivities				
AP_Leafy_Vegetables	kg (wet weight) /m^2	Agricultural productivity for leafy vegetables	Scalar	Stochastic
AP_Produce	kg (wet weight) /m^2	Agricultural productivity for produce	Scalar	Stochastic
AP_Grain	kg (wet weight) /m^2	Agricultural productivity for grain	Scalar	Stochastic
AP_Pasture_Grass	kg (dry weight) /m^2	Agricultural productivity for pasture grass	Scalar	Stochastic
Growing_Season				
GS_Leafy_Vegetables	d	Growing season for leafy vegetables	Scalar	Stochastic
GS_Produce	d	Growing season for produce	Scalar	Stochastic
GS_Grain	d	Growing season for grain	Scalar	Stochastic
GS_Pasture_Grass	d	Growing season for pasture grass	Scalar	Stochastic
Mass_Loading_Factors				
MLF_Leafy_Vegetables	g soil/g plant (dry weight)	Mass-loading factor for leafy vegetables	Scalar	Stochastic

Table 6 (Continued)
Input Data Requirements for the MDA G Site Model

Model Container/Parameter Name	Units	Parameter Description	Parameter Type	Input Element Type
MLF_Produce	g soil/g plant (dry weight)	Mass-loading factor for produce	Scalar	Stochastic
MLF_Grain	g soil/g plant (dry weight)	Mass-loading factor for grain	Scalar	Stochastic
MLF_Pasture_Grass	g soil/g plant (dry weight)	Mass-loading factor for pasture grass	Scalar	Stochastic
Animal_Data				
Animal_Ingestion_Data				
Cattle_and_Cows				
Cattle_Food	kg/d (dry weight)	Food consumption rate of cattle	Scalar	Stochastic
Cow_Food	kg/d (dry weight)	Food consumption rate of cows	Scalar	Stochastic
Cattle_Soil	kg/d (dry weight)	Soil consumption rate of cattle	Scalar	Stochastic
Cow_Soil	kg/d (dry weight)	Soil consumption rate of cows	Scalar	Stochastic
Cattle_Water	kg/d	Water consumption rate of cattle	Scalar	Stochastic
Cow_Water	kg/d	Water consumption rate of cows	Scalar	Stochastic
Chickens				
Chicken_Feed	kg/d (dry weight)	Food consumption rate of chickens	Scalar	Stochastic
Chicken_Water	kg/d	Water consumption rate of chickens	Scalar	Stochastic
Grit_to_Food_Ratio		Ratio of grit or soil intake to food intake for chickens	Scalar	Data

Table 6 (Continued)
Input Data Requirements for the MDA G Site Model

Model Container/Parameter Name	Units	Parameter Description	Parameter Type	Input Element Type
Transfer_Factors				
Beef_GM	d/kg	Geometric means of the forage-to-beef transfer factors	Vector (element)	Stochastic
Beef_GSD		Geometric standard deviation of the forage-to-beef transfer factors	Vector (element)	Data
Milk_GM	d/kg	Geometric means of the forage-to-milk transfer factors	Vector (element)	Stochastic
Milk_GSD		Geometric standard deviation of the forage-to-milk transfer factors	Vector (element)	Data
Chicken_GM	d/kg	Geometric means of the forage-to-chicken transfer factors	Vector (element)	Stochastic
Chicken_GSD		Geometric standard deviation of the forage-to-chicken transfer factors	Vector (element)	Data
Eggs_GM	d/kg	Geometric means of the forage-to-eggs transfer factors	Vector (element)	Stochastic
Eggs_GSD		Geometric standard deviation of the forage-to-eggs transfer factors	Vector (element)	Data
H3_and_C14_Transfer_Factors				
H3_Factors				
Water_Fraction_Animal_Products		Mass water fractions of animal products	Vector (animal product)	Data
C14_Factors				
Animal_Prod_Carbon_Fraction		Carbon fractions of animal products	Vector (animal product)	Data
Groundwater_Transport				
MdB_Infiltration_Rate	m/yr	Water infiltration rate on Mesita del Buey	Scalar	Stochastic

Table 6 (Continued)
Input Data Requirements for the MDA G Site Model

Model Container/Parameter Name	Units	Parameter Description	Parameter Type	Input Element Type
CdB_Infiltration_Rate	m/yr	Water infiltration rate at the receptor location for the All Pathways – Cañada del Buey Scenario	Scalar	Stochastic
PC_Infiltration_Rate	m/yr	Water infiltration rate at the receptor location for the All Pathways – Pajarito Canyon Scenario	Scalar	Stochastic
Well_Infiltration_Rate	m/yr	Water infiltration rate at the receptor location for the groundwater pathway-based scenarios	Scalar	Stochastic
PME_Infiltration_Rate	m/yr	Water infiltration rate at the receptor location for the Atmospheric Scenario	Scalar	Stochastic
Contaminant_Capture_Fraction		Fraction of contaminant plume in the regional aquifer that is captured by the groundwater pathway receptors	Vector (waste disposal region)	Data
Sediment_Transport				
Sediment_Allocation_Factors		Fraction of contaminated sediment that is transported to each canyon catchment	Matrix (waste disposal region, canyon catchment)	Data
Catchment_Area	m^2	Area of each canyon catchment	Vector (canyon catchment)	Data
Sediment_Dispersal_Fraction		Fraction of canyon catchment over which sediments disperse	Scalar	Stochastic
Sediment_Transport_Rate	yr^{-1}	Rate constant describing the rate at which canyon sediments are flushed	Scalar	Stochastic
Biotic_Intrusion_Model				
Eco_Succession_Model				
Time_of_Climax	yr	Period required for disposal site to reach a piñon-juniper climax condition, measured from the time of facility closure	Scalar	Stochastic

Table 6 (Continued)
Input Data Requirements for the MDA G Site Model

Model Container/Parameter Name	Units	Parameter Description	Parameter Type	Input Element Type
Intrusion_Shape_Parameters				
Alpha_Shape_Factor		Shape factor used to model animal burrow and plant root distributions with depth	Scalar	Data
Beta_Shape_Factor		Shape factor used to model animal burrow and plant root distributions with depth	Scalar	Data
Animal_Intrusion_Model				
Harvester_Ants				
Maximum_Burrow_Depth	m	Maximum burrowing depth for harvester ants	Scalar	Stochastic
Burrow_Density_Grassland	ha^{-1}	Density of harvester ant burrows during early succession	Scalar	Stochastic
Burrow_Density_Woodland	ha^{-1}	Density of harvester ant burrows in the piñon-juniper climax condition	Scalar	Stochastic
Burrow_Mass	kg	Mass of soil excavated per harvester ant burrow	Scalar	Stochastic
Colony_Life_Span	yr	Life span of harvester ant colonies	Scalar	Stochastic
Pocket_Gophers				
Maximum_Burrow_Depth	m	Maximum burrowing depth for pocket gophers	Scalar	Stochastic
Soil_Removal_Rate_Grassland	m^3/ha	Rate of soil removal by pocket gophers during early succession	Scalar	Stochastic
Soil_Removal_Rate_Woodland	m^3/ha	Rate of soil removal by pocket gophers in the piñon-juniper climax condition	Scalar	Stochastic
Burrow_Renewal_Rate	yr^{-1}	Rate at which existing pocket gopher burrows are replaced with new ones	Scalar	Stochastic
Mice				
Maximum_Burrow_Depth	m	Maximum burrowing depth for mice	Scalar	Stochastic
Burrow_Density_Grassland	ha^{-1}	Density of mouse burrows during early succession	Scalar	Stochastic

Table 6 (Continued)
Input Data Requirements for the MDA G Site Model

Model Container/Parameter Name	Units	Parameter Description	Parameter Type	Input Element Type
Burrow_Density_Woodland	ha^{-1}	Density of mouse burrows in the piñon-juniper climax condition	Scalar	Stochastic
Burrow_Volume	kg	Volume of soil excavated per mouse burrow	Scalar	Stochastic
Burrow_Renewal_Rate	yr^{-1}	Rate at which existing mouse burrows are replaced with new ones	Scalar	Stochastic
Chipmunks_and_Squirrels				
Maximum_Burrow_Depth	m	Maximum burrowing depth for chipmunks and ground squirrels	Scalar	Stochastic
Burrow_Density_Grassland	ha^{-1}	Density of chipmunk and ground squirrel burrows during early succession	Scalar	Stochastic
Burrow_Density_Woodland	ha^{-1}	Density of chipmunk and ground squirrel burrows in the piñon-juniper climax condition	Scalar	Stochastic
Burrow_Volume	kg	Volume of soil excavated per chipmunk and ground squirrel burrow	Scalar	Stochastic
Burrow_Renewal_Rate	yr^{-1}	Rate at which existing chipmunk and ground squirrel burrows are replaced with new ones	Scalar	Stochastic
Plant_Intrusion_Model				
Litter_Halflife	yr	Decomposition half-life of plant litter	Scalar	Stochastic
Grasses				
Maximum_Root_Depth	m	Maximum rooting depth of grasses	Scalar	Stochastic
Biomass_Density_Grassland	kg/m^2	Aboveground biomass density of grasses during early succession	Scalar	Stochastic
Biomass_Density_Woodland	kg/m^2	Aboveground biomass density of grasses in the piñon-juniper climax condition	Scalar	Stochastic
Litter_Prod_Rate	yr^{-1}	Fraction of the aboveground biomass that falls as litter	Scalar	Stochastic

Table 6 (Continued)
Input Data Requirements for the MDA G Site Model

Model Container/Parameter Name	Units	Parameter Description	Parameter Type	Input Element Type
Forbs				
Maximum_Root_Depth	m	Maximum rooting depth of forbs	Scalar	Stochastic
Biomass_Density_Grassland	kg/m^2	Aboveground biomass density of forbs during early succession	Scalar	Stochastic
Biomass_Density_Woodland	kg/m^2	Aboveground biomass density of forbs in the piñon-juniper climax condition	Scalar	Stochastic
Litter_Prod_Rate	yr^{-1}	Fraction of the aboveground biomass that falls as litter	Scalar	Stochastic
Shrubs				
Maximum_Root_Depth	m	Maximum rooting depth of shrubs	Scalar	Stochastic
Biomass_Density_Grassland	kg/m^2	Aboveground biomass density of shrubs during early succession	Scalar	Stochastic
Biomass_Density_Woodland	kg/m^2	Aboveground biomass density of shrubs in the piñon-juniper climax condition	Scalar	Stochastic
Litter_Prod_Rate	yr^{-1}	Fraction of the aboveground biomass that falls as litter	Scalar	Stochastic
Trees				
Maximum_Root_Depth	m	Maximum rooting depth of trees	Scalar	Stochastic
Biomass_Density_Grassland	kg/m^2	Aboveground biomass density of trees during early succession	Scalar	Stochastic
Biomass_Density_Woodland	kg/m^2	Aboveground biomass density of trees in the piñon-juniper climax condition	Scalar	Stochastic
Litter_Prod_Rate	yr^{-1}	Fraction of the aboveground biomass that falls as litter	Scalar	Stochastic
Erosion_Model				
Erosion_Rates				
Erosion_Rate_Functions	yr^{-1}	Cover loss rate as a function of time	Scalar	Lookup Table

Table 6 (Continued)
Input Data Requirements for the MDA G Site Model

Model Container/Parameter Name	Units	Parameter Description	Parameter Type	Input Element Type
Erosion_Zone_Data				
Remaining_Cover_EZ1	m	Minimum cover remaining in erosion zone 1	Scalar	Stochastic
Remaining_Cover_EZ2	m	Minimum cover remaining in erosion zone 2	Scalar	Stochastic
Remaining_Cover_EZ3	m	Minimum cover remaining in erosion zone 3	Scalar	Stochastic
Remaining_Cover_EZ4	m	Minimum cover remaining in erosion zone 4	Scalar	Stochastic
Remaining_Cover_EZ5	m	Minimum cover remaining in erosion zone 5	Scalar	Stochastic
Remaining_Cover_EZ6	m	Minimum cover remaining in erosion zone 6	Scalar	Stochastic
Remaining_Cover_EZ7	m	Minimum cover remaining in erosion zone 7	Scalar	Stochastic
Remaining_Cover_EZ8	m	Minimum cover remaining in erosion zone 8	Scalar	Stochastic
Remaining_Cover_EZ9	m	Minimum cover remaining in erosion zone 9	Scalar	Stochastic
Remaining_Cover_EZ10	m	Minimum cover remaining in erosion zone 10	Scalar	Stochastic
Erosion_Shape_Parameters				
Alpha_Shape_Factor		Shape factor used to model surface erosion	Scalar	Data
Beta_Shape_Factor		Shape factor used to model surface erosion	Scalar	Data
Dose_and_WAC_Model				
Dose_Conversion_Factors				
Ingestion_DCFs	mrem/pCi	Dose conversion factors for the ingestion exposure route	Vector (radionuclide)	Data
Inhalation_DCFs	mrem/pCi	Dose conversion factors for the inhalation exposure route	Vector (radionuclide)	Data
Soil_External_DCFs_15_cm	mrem/yr per pCi/m^3	Dose conversion factors for direct radiation from soils contaminated to a depth of 15 cm	Vector (radionuclide)	Data
Air_External_DCFs	mrem/yr per pCi/m^3	Dose conversion factors for direct radiation from air immersion	Vector (radionuclide)	Data

Table 6 (Continued)
Input Data Requirements for the MDA G Site Model

Model Container/Parameter Name	Units	Parameter Description	Parameter Type	Input Element Type
Exposure_Pathway_Data				
Indoor_Exposure_Time	hr/d	Time spent inside by the receptor	Scalar	Stochastic
Outdoor_Exposure_Time	hr/d	Time spent outside by the receptor	Scalar	Stochastic
Soil_Mixing_Depth	m	Contaminant mixing depth	Scalar	Data
Shielding_Factor		Direct radiation shielding factor for the time spent indoors	Scalar	Stochastic
Inhalation_Rate	m^3/d	Inhalation rate of the receptor	Scalar	Stochastic
Area_of_Lot	m^2	Area of the receptor's lot	Scalar	Stochastic
Area_of_House	m^2	Area of the receptor's house	Scalar	Data
Indoor_Water_Usage	m^3/d	Receptor's daily indoor water usage	Scalar	Stochastic
Ingestion_Data				
Soil_Ingestion_Rate	kg (dry weight)/yr	Rate of soil ingestion for the receptor	Scalar	Stochastic
AP_DW_Ingestion_Rate	L/d	Rate of water ingestion for the All Pathways – Groundwater Scenario	Scalar	Stochastic
GP_DW_Ingestion_Rate	L/d	Rate of water ingestion for the Groundwater Resource Protection Scenario	Scalar	Data
Input_Vegetable_Fraction		User-specified fraction of the receptor's diet of leafy vegetables, produce, and grain that is grown at the receptor's location	Scalar	Stochastic
Animals_Raised		The types of animals raised by the receptor to supply a portion of their diet	Scalar	Stochastic
Crop_Ingestion_Rates				
Cl_Leafy_Vegetables	kg (wet weight)/yr	Rate of ingestion of leafy vegetables for the receptor	Scalar	Stochastic

Table 6 (Continued)
Input Data Requirements for the MDA G Site Model

Model Container/Parameter Name	Units	Parameter Description	Parameter Type	Input Element Type
Cl_Produce	kg (wet weight)/yr	Rate of ingestion of produce for the receptor	Scalar	Stochastic
Cl_Grain	kg (wet weight)/yr	Rate of ingestion of grain for the receptor	Scalar	Stochastic
Animal_Product_Ingestion_Rates				
API_Beef	kg/yr	Rate of ingestion of beef for the receptor	Scalar	Stochastic
API_Milk	kg/yr	Rate of ingestion of milk for the receptor	Scalar	Stochastic
API_Chicken	kg/yr	Rate of ingestion of chicken for the receptor	Scalar	Stochastic
API_Eggs	kg/yr	Rate of ingestion of eggs for the receptor	Scalar	Stochastic
Animal_Numbers				
Cattle_Weight_at_Slaughter	kg	Weight of cattle at the time of slaughter	Scalar	Stochastic
Dressing_Percentage		Ratio of the carcass weight to live weight of the animal	Scalar	Stochastic
Cutability		Fraction of the carcass that is sold as meat	Scalar	Stochastic
Milk_Production_Rate	kg/yr	Production rate of milk by cows	Scalar	Stochastic
Chicken_Weight_at_Slaughter	kg	Weight of chicken at the time of slaughter	Scalar	Stochastic
Cooked_to_Live_Ratio		Ratio of cooked weight of chicken to the live weight of the bird	Scalar	Stochastic
Meat_Fraction		Fraction of the cooked chicken that is meat	Scalar	Stochastic
Egg_Production_Rate	d^{-1}	Production rate of eggs by layers	Scalar	Stochastic
Egg_Mass	kg	Mass of egg	Scalar	Stochastic
Shell_Fraction		Fraction of the egg mass that is contributed by the shell	Scalar	Data

Table 6 (Continued)
Input Data Requirements for the MDA G Site Model

Model Container/Parameter Name	Units	Parameter Description	Parameter Type	Input Element Type
Animal_Product_Fractions				
Beef		User-specified fraction of the receptor's diet of beef that is taken from animals living at the exposure location	Scalar	Stochastic
Milk		User-specified fraction of the receptor's diet of milk that is produced by animals living at the exposure location	Scalar	Stochastic
Chicken		User-specified fraction of the receptor's diet of chicken that is taken from animals living at the exposure location	Scalar	Stochastic
Eggs		User-specified fraction of the receptor's diet of eggs that is produced by animals living at the exposure location	Scalar	Stochastic
Irrigation_Rates				
IR_Leafy_Vegetables	cm/yr	Irrigation rate for leafy vegetables	Scalar	Stochastic
IR_Produce	cm/yr	Irrigation rate for produce	Scalar	Stochastic
IR_Grain	cm/yr	Irrigation rate for grain	Scalar	Stochastic
IR_Pasture_Grass	cm/yr	Irrigation rate for pasture grass	Scalar	Stochastic

Table 7
Input Data Requirements for the MDA G Site Diffusion Model

Model Container/Parameter Name	Units	Parameter Description	Parameter Type	Input Element Type
Controls_and_Constants				
Disposal_Region_Flag		Flag used to indicate the number of the waste disposal region that is being considered in the simulation	Scalar	Data
Analysis_Flag		Flag used to indicate whether the performance assessment or composite analysis is being considered. A value of 1 indicates the composite analysis inventory is included in the simulation; a value of 2 indicates the performance assessment inventory is being used.	Scalar	Data
Diffusion_Flag		Flag used to indicate whether the effects of vapor- and gas-phase diffusion are taken into account in the intruder modeling. A value of 0 indicates that the effects of diffusion are not taken into account; a value of 1 indicates diffusive transport is modeled.	Scalar	Data
Biotic_Intrusion_Flag		Flag used to specify if the effects of biotic intrusion will be taken into account in the intruder modeling. A value of 0 indicates that biotic intrusion will not be considered; a value of 1 specifies allows plant and animal intrusion into the disposal site prior to the time of human intrusion.	Scalar	Data
Disposal_System_Information				
Species_and_Materials				
Halflives	yr	Radionuclide half-lives	Vector (radionuclide)	Data
Material_Properties				
Density_of_Water	kg/m^3	Density of water	Scalar	Data
Soil_Carbon_Fraction		Fraction of surface soil that is carbon	Scalar	Data
Water_Carbon_Fraction		Fraction of water that is carbon	Scalar	Data

Table 7 (Continued)
Input Data Requirements for the MDA G Site Diffusion Model

Model Container/Parameter Name	Units	Parameter Description	Parameter Type	Input Element Type
Water_Hydrogen_Fraction		Fraction of water that is hydrogen	Scalar	Data
Solubility_Limits	mg/L	Elemental solubility limits for crushed tuff and waste	Vector (element)	Data
Organic_Waste_Fraction		Fraction of C-14 waste that is organic and susceptible to biodegradation	Scalar	Stochastic
C14_Gas_Generation_Rate	yr^{-1}	Rate constant describing the rate of C-14 gas generation due to biodegradation of organic waste	Scalar	Stochastic
CO2_Fraction		Fraction of C-14 gas generated by the biodegradation of organic waste that is carbon dioxide	Scalar	Stochastic
Radon_Emanation_Fraction		Emanation coefficient for Rn-220 and Rn-222	Scalar	Stochastic
Air_Diffusion_Length	m	Diffusion length in air	Scalar	Data
Dry_Densities				
DD_Crushed_Tuff	kg/m^3	Dry density of crushed tuff	Scalar	Stochastic
DD_Waste	kg/m^3	Dry density of waste	Scalar	Stochastic
Moisture_Contents				
MC_Crushed_Tuff	(volume basis)	Moisture content of crushed tuff	Scalar	Stochastic
MC_Waste	(volume basis)	Moisture content of waste	Scalar	Stochastic
Effective_Porosities				
EP_Crushed_Tuff		Effective porosity of crushed tuff	Scalar	Stochastic
EP_Waste		Effective porosity of waste	Scalar	Stochastic

Table 7 (Continued)
Input Data Requirements for the MDA G Site Diffusion Model

Model Container/Parameter Name	Units	Parameter Description	Parameter Type	Input Element Type
Distribution_Coefficients				
Crushed_Tuff_and_Waste_KDs				
KD_CTW_GM	m^3/kg	Geometric means of the distribution coefficients for crushed tuff and waste	Vector (element)	Data
KD_GSD		Geometric standard deviation of the distribution coefficients for crushed tuff and waste	Scalar	Data
Solubility_Constants				
SL_GM	m^3/kg	Geometric means of the water solubility limits	Vector (element)	Data
SL_GSD		Geometric standard deviations of the water solubility limits	Vector (element)	Data
Relative_Diffusivities				
Free_Air_Diff_Coefficients	cm^2/s	Free-air diffusion coefficients	Vector (radionuclide)	Data
Thermal_Gradient_Factor		Factor used to account for the effects of thermal gradients on the rate of diffusion of tritiated water vapor	Scalar	Stochastic
Reference_Diff_Coefficient	cm^2/s	Reference diffusion coefficient	Scalar	Data
Site_Geometry_and_Operations				
Institutional_Control_Period	yr	The length of the institutional control period, measured from the time of facility closure	Scalar	Data
Closure_Period	yr	The length of time required to achieve final closure of the disposal facility following the end of disposal operations	Scalar	Data
Minimum_Air_Thickness	m	Minimum air thickness in surface soil and cap cells	Scalar	Data
Atmospheric_Source_Areas	m^2	Areas associated wit h the atmospheric transport modeling source areas	Vector (atmospheric source area)	Data

Table 7 (Continued)
Input Data Requirements for the MDA G Site Diffusion Model

Model Container/Parameter Name	Units	Parameter Description	Parameter Type	Input Element Type
Waste_Region_1 – Waste_Region_8				
Initial_Cover_Thickness	m	Initial thickness of the cover over the disposal units	Scalar	Stochastic
Surface_Soil_Thickness	m	Thickness of the surface soil layer	Vector (waste disposal region)	Data
Waste_Thickness	m	Thickness of the disposed waste	Vector (waste disposal region)	Data
Disposal_Unit_Area	m^2	Surface area of the disposal units	Scalar	Data
Inventory				
Measurement_Errors				
Rad_Specific_Errors				
Pre_1990_Lower_Bounds		Factor used to estimate the lower bound of pre-1990 radionuclide inventories, taking into account errors introduced by measurement uncertainty	Vector (radionuclide)	Data
Pre_1990_Upper_Bounds		Factor used to estimate the upper bound of pre-1990 radionuclide inventories, taking into account errors introduced by measurement uncertainty	Vector (radionuclide)	Data
Post_1989_Lower_Bounds		Factor used to estimate the lower bound of post-1989 radionuclide inventories, taking into account errors introduced by measurement uncertainty	Vector (radionuclide)	Data
Post_1989_Upper_Bounds		Factor used to estimate the upper bound of post-1989 radionuclide inventories, taking into account errors introduced by measurement uncertainty	Vector (radionuclide)	Data
Material_Type_Errors				
Pre_1990_Lower_Bounds		Factor used to estimate the lower bound of pre-1990 material type inventories, taking into account errors introduced by measurement uncertainty	Vector (material type)	Data

Table 7 (Continued)
Input Data Requirements for the MDA G Site Diffusion Model

Model Container/Parameter Name	Units	Parameter Description	Parameter Type	Input Element Type
Pre_1990_Upper_Bounds		Factor used to estimate the upper bound of pre-1990 material type inventories, taking into account errors introduced by measurement uncertainty	Vector (material type)	Data
Post_1989_Lower_Bounds		Factor used to estimate the lower bound of post-1989 material type inventories, taking into account errors introduced by measurement uncertainty	Vector (material type)	Data
Post_1989_Upper_Bounds		Factor used to estimate the upper bound of post-1989 material type inventories, taking into account errors introduced by measurement uncertainty	Vector (material type)	Data
Rad_Specific_Inventories				
Waste_Region_1				
Pre_1990_CA_Point_Estimates	Ci	Point estimates of radionuclide-specific inventories in the pre-1990 composite analysis waste disposed of in waste disposal region 1	Vector (radionuclide)	Data
Pre_1990_PA_Point_Estimates	Ci	Point estimates of radionuclide-specific inventories in the pre-1990 performance assessment waste disposed of in waste disposal region 1	Vector (radionuclide)	Data
Waste_Region_2				
Pre_1990_CA_Point_Estimates	Ci	Point estimates of radionuclide-specific inventories in the pre-1990 composite analysis waste disposed of in waste disposal region 2	Vector (radionuclide)	Data
Pre_1990_PA_Point_Estimates	Ci	Point estimates of radionuclide-specific inventories in the pre-1990 performance assessment waste disposed of in waste disposal region 2	Vector (radionuclide)	Data

Table 7 (Continued)
Input Data Requirements for the MDA G Site Diffusion Model

Model Container/Parameter Name	Units	Parameter Description	Parameter Type	Input Element Type
Waste_Region_3				
Pre_1990_CA_Point_Estimates	Ci	Point estimates of radionuclide-specific inventories in the pre-1990 composite analysis waste disposed of in waste disposal region 3	Vector (radionuclide)	Data
Pre_1990_PA_Point_Estimates	Ci	Point estimates of radionuclide-specific inventories in the pre-1990 performance assessment waste disposed of in waste disposal region 3	Vector (radionuclide)	Data
Post_1989_CA_Point_Estimates	Ci	Point estimates of radionuclide-specific inventories in the post-1989 composite analysis waste disposed of in waste disposal region 3	Vector (radionuclide)	Data
Post_1989_PA_Point_Estimates	Ci	Point estimates of radionuclide-specific inventories in the post-1989 performance assessment waste disposed of in waste disposal region 3	Vector (radionuclide)	Data
Waste_Region_4				
Pre_1990_CA_Point_Estimates	Ci	Point estimates of radionuclide-specific inventories in the pre-1990 composite analysis waste disposed of in waste disposal region 4	Vector (radionuclide)	Data
Pre_1990_PA_Point_Estimates	Ci	Point estimates of radionuclide-specific inventories in the pre-1990 performance assessment waste disposed of in waste disposal region 4	Vector (radionuclide)	Data
Post_1989_CA_Point_Estimates	Ci	Point estimates of radionuclide-specific inventories in the post-1989 composite analysis waste disposed of in waste disposal region 4	Vector (radionuclide)	Data
Post_1989_PA_Point_Estimates	Ci	Point estimates of radionuclide-specific inventories in the post-1989 performance assessment waste disposed of in waste disposal region 4	Vector (radionuclide)	Data

Table 7 (Continued)
Input Data Requirements for the MDA G Site Diffusion Model

Model Container/Parameter Name	Units	Parameter Description	Parameter Type	Input Element Type
Waste_Region_5				
Pre_1990_CA_Point_Estimates	Ci	Point estimates of radionuclide-specific inventories in the pre-1990 composite analysis waste disposed of in waste disposal region 5	Vector (radionuclide)	Data
Pre_1990_PA_Point_Estimates	Ci	Point estimates of radionuclide-specific inventories in the pre-1990 performance assessment waste disposed of in waste disposal region 5	Vector (radionuclide)	Data
Post_1989_CA_Point_Estimates	Ci	Point estimates of radionuclide-specific inventories in the post-1989 composite analysis waste disposed of in waste disposal region 5	Vector (radionuclide)	Data
Post_1989_PA_Point_Estimates	Ci	Point estimates of radionuclide-specific inventories in the post-1989 performance assessment waste disposed of in waste disposal region 5	Vector (radionuclide)	Data
Waste_Region_6				
Pre_1990_CA_Point_Estimates	Ci	Point estimates of radionuclide-specific inventories in the pre-1990 composite analysis waste disposed of in waste disposal region 6	Vector (radionuclide)	Data
Pre_1990_PA_Point_Estimates	Ci	Point estimates of radionuclide-specific inventories in the pre-1990 performance assessment waste disposed of in waste disposal region 6	Vector (radionuclide)	Data
Waste_Region_7				
Pre_1990_CA_Point_Estimates	Ci	Point estimates of radionuclide-specific inventories in the pre-1990 composite analysis waste disposed of in waste disposal region 7	Vector (radionuclide)	Data
Pre_1990_PA_Point_Estimates	Ci	Point estimates of radionuclide-specific inventories in the pre-1990 performance assessment waste disposed of in waste disposal region 7	Vector (radionuclide)	Data

Table 7 (Continued)
Input Data Requirements for the MDA G Site Diffusion Model

Model Container/Parameter Name	Units	Parameter Description	Parameter Type	Input Element Type
Post_1989_CA_Point_Estimates	Ci	Point estimates of radionuclide-specific inventories in the post-1989 composite analysis waste disposed of in waste disposal region 7	Vector (radionuclide)	Data
Post_1989_PA_Point_Estimates	Ci	Point estimates of radionuclide-specific inventories in the post-1989 performance assessment waste disposed of in waste disposal region 7	Vector (radionuclide)	Data
Waste_Region_8				
Post_1989_CA_Point_Estimates	Ci	Point estimates of radionuclide-specific inventories in the post-1989 composite analysis waste disposed of in waste disposal region 8	Vector (radionuclide)	Data
Post_1989_PA_Point_Estimates	Ci	Point estimates of radionuclide-specific inventories in the post-1989 performance assessment waste disposed of in waste disposal region 8	Vector (radionuclide)	Data
Material_Type_Inventories				
Waste_Region_1				
Pre_1990_CA_Point_Estimates	Ci	Point estimates of material type inventories in the pre-1990 composite analysis waste disposed of in waste disposal region 1	Vector (material type)	Data
Pre_1990_PA_Point_Estimates	Ci	Point estimates of material type inventories in the pre-1990 performance assessment waste disposed of in waste disposal region 1	Vector (material type)	Data
Waste_Region_2				
Pre_1990_CA_Point_Estimates	Ci	Point estimates of material type inventories in the pre-1990 composite analysis waste disposed of in waste disposal region 2	Vector (material type)	Data
Pre_1990_PA_Point_Estimates	Ci	Point estimates of material type inventories in the pre-1990 performance assessment waste disposed of in waste disposal region 2	Vector (material type)	Data

Table 7 (Continued)
Input Data Requirements for the MDA G Site Diffusion Model

Model Container/Parameter Name	Units	Parameter Description	Parameter Type	Input Element Type
Waste_Region_3				
Pre_1990_CA_Point_Estimates	Ci	Point estimates of material type inventories in the pre-1990 composite analysis waste disposed of in waste disposal region 3	Vector (material type)	Data
Pre_1990_PA_Point_Estimates	Ci	Point estimates of material type inventories in the pre-1990 performance assessment waste disposed of in waste disposal region 3	Vector (material type)	Data
Post_1989_CA_Point_Estimates	Ci	Point estimates of material type inventories in the post-1989 composite analysis waste disposed of in waste disposal region 3	Vector (material type)	Data
Post_1989_PA_Point_Estimates	Ci	Point estimates of material type inventories in the post-1989 performance assessment waste disposed of in waste disposal region 3	Vector (material type)	Data
Waste_Region_4				
Pre_1990_CA_Point_Estimates	Ci	Point estimates of material type inventories in the pre-1990 composite analysis waste disposed of in waste disposal region 4	Vector (material type)	Data
Pre_1990_PA_Point_Estimates	Ci	Point estimates of material type inventories in the pre-1990 performance assessment waste disposed of in waste disposal region 4	Vector (material type)	Data
Post_1989_CA_Point_Estimates	Ci	Point estimates of material type inventories in the post-1989 composite analysis waste disposed of in waste disposal region 4	Vector (material type)	Data
Post_1989_PA_Point_Estimates	Ci	Point estimates of material type inventories in the post-1989 performance assessment waste disposed of in waste disposal region 4	Vector (material type)	Data
Waste_Region_5				
Pre_1990_CA_Point_Estimates	Ci	Point estimates of material type inventories in the pre-1990 composite analysis waste disposed of in waste disposal region 5	Vector (material type)	Data

Table 7 (Continued)
Input Data Requirements for the MDA G Site Diffusion Model

Model Container/Parameter Name	Units	Parameter Description	Parameter Type	Input Element Type
Pre_1990_PA_Point_Estimates	Ci	Point estimates of material type inventories in the pre-1990 performance assessment waste disposed of in waste disposal region 5	Vector (material type)	Data
Post_1989_CA_Point_Estimates	Ci	Point estimates of material type inventories in the post-1989 composite analysis waste disposed of in waste disposal region 5	Vector (material type)	Data
Post_1989_PA_Point_Estimates	Ci	Point estimates of material type inventories in the post-1989 performance assessment waste disposed of in waste disposal region 5	Vector (material type)	Data
Waste_Region_6				
Pre_1990_CA_Point_Estimates	Ci	Point estimates of material type inventories in the pre-1990 composite analysis waste disposed of in waste disposal region 6	Vector (material type)	Data
Pre_1990_PA_Point_Estimates	Ci	Point estimates of material type inventories in the pre-1990 performance assessment waste disposed of in waste disposal region 6	Vector (material type)	Data
Waste_Region_7				
Pre_1990_CA_Point_Estimates	Ci	Point estimates of material type inventories in the pre-1990 composite analysis waste disposed of in waste disposal region 7	Vector (material type)	Data
Pre_1990_PA_Point_Estimates	Ci	Point estimates of material type inventories in the pre-1990 performance assessment waste disposed of in waste disposal region 7	Vector (material type)	Data
Post_1989_CA_Point_Estimates	Ci	Point estimates of material type inventories in the post-1989 composite analysis waste disposed of in waste disposal region 7	Vector (material type)	Data
Post_1989_PA_Point_Estimates	Ci	Point estimates of material type inventories in the post-1989 performance assessment waste disposed of in waste disposal region 7	Vector (material type)	Data

Table 7 (Continued)
Input Data Requirements for the MDA G Site Diffusion Model

Model Container/Parameter Name	Units	Parameter Description	Parameter Type	Input Element Type
Waste_Region_8				
Post_1989_CA_Point_Estimates	Ci	Point estimates of material type inventories in the post-1989 composite analysis waste disposed of in waste disposal region 8	Vector (material type)	Data
Post_1989_PA_Point_Estimates	Ci	Point estimates of material type inventories in the post-1989 performance assessment waste disposed of in waste disposal region 8	Vector (material type)	Data
Fission_Yields				
Fraction_of_Pu239		Fraction of fission events that originate with Pu-239	Scalar	Stochastic
Age_of_MFP_Waste	yr	Age of mixed fission product waste at the time of disposal	Scalar	Stochastic
U235_Fission_Yields				
U235_1yr_Thermal		U-235 thermal fission yields for 1-year-old waste	Scalar	Data
U235_2yr_Thermal		U-235 thermal fission yields for 2-year-old waste	Scalar	Data
U235_3yr_Thermal		U-235 thermal fission yields for 3-year-old waste	Scalar	Data
U235_4yr_Thermal		U-235 thermal fission yields for 4-year-old waste	Scalar	Data
U235_5yr_Thermal		U-235 thermal fission yields for 5-year-old waste	Scalar	Data
U235_6yr_Thermal		U-235 thermal fission yields for 6-year-old waste	Scalar	Data
U235_7yr_Thermal		U-235 thermal fission yields for 7-year-old waste	Scalar	Data
U235_8yr_Thermal		U-235 thermal fission yields for 8-year-old waste	Scalar	Data
U235_9yr_Thermal		U-235 thermal fission yields for 9-year-old waste	Scalar	Data
U235_10yr_Thermal		U-235 thermal fission yields for 10-year-old waste	Scalar	Data
Pu239_Fission_Yields				
Pu239_1yr_Thermal		Pu-239 thermal fission yields for 1-year-old waste	Scalar	Data

Table 7 (Continued)
Input Data Requirements for the MDA G Site Diffusion Model

Model Container/Parameter Name	Units	Parameter Description	Parameter Type	Input Element Type
Pu239_2yr_Thermal		Pu-239 thermal fission yields for 2-year-old waste	Scalar	Data
Pu239_3yr_Thermal		Pu-239 thermal fission yields for 3-year-old waste	Scalar	Data
Pu239_4yr_Thermal		Pu-239 thermal fission yields for 4-year-old waste	Scalar	Data
Pu239_5yr_Thermal		Pu-239 thermal fission yields for 5-year-old waste	Scalar	Data
Pu239_6yr_Thermal		Pu-239 thermal fission yields for 6-year-old waste	Scalar	Data
Pu239_7yr_Thermal		Pu-239 thermal fission yields for 7-year-old waste	Scalar	Data
Pu239_8yr_Thermal		Pu-239 thermal fission yields for 8-year-old waste	Scalar	Data
Pu239_9yr_Thermal		Pu-239 thermal fission yields for 9-year-old waste	Scalar	Data
Pu239_10yr_Thermal		Pu-239 thermal fission yields for 10-year-old waste	Scalar	Data
Activation_Yields				
MAP_Allocation_Fractions		Radionuclide-specific activity fractions for mixed activation product waste	Vector (radionuclide)	Data
Material_Type_Act_Fractions				
Nominal_Masses	g	Material type waste radionuclide masses	Matrix (radionuclide, material type)	Data
PU51				
Activity_Fractions		Radionuclide activity fractions in material type PU51 waste	Vector (radionuclide)	Data
PU52				
Pu238_Mass_Fraction		Mass fraction of Pu-238 in material type PU52 waste	Scalar	Stochastic
Pu240_Mass_Fraction		Mass fraction of Pu-240 in material type PU52 waste	Scalar	Stochastic
Pu241_Mass_Fraction		Mass fraction of Pu-241 in material type PU52 waste	Scalar	Stochastic
Pu242_Mass_Fraction		Mass fraction of Pu-242 in material type PU52 waste	Scalar	Stochastic

Table 7 (Continued)
Input Data Requirements for the MDA G Site Diffusion Model

Model Container/Parameter Name	Units	Parameter Description	Parameter Type	Input Element Type
PU53				
Pu238_Mass_Fraction		Mass fraction of Pu-238 in material type PU53 waste	Scalar	Stochastic
Pu240_Mass_Fraction		Mass fraction of Pu-240 in material type PU53 waste	Scalar	Stochastic
Pu241_Mass_Fraction		Mass fraction of Pu-241 in material type PU53 waste	Scalar	Stochastic
Pu242_Mass_Fraction		Mass fraction of Pu-242 in material type PU53 waste	Scalar	Stochastic
PU54				
Pu238_Mass_Fraction		Mass fraction of Pu-238 in material type PU54 waste	Scalar	Stochastic
Pu240_Mass_Fraction		Mass fraction of Pu-240 in material type PU54 waste	Scalar	Stochastic
Pu241_Mass_Fraction		Mass fraction of Pu-241 in material type PU54 waste	Scalar	Stochastic
Pu242_Mass_Fraction		Mass fraction of Pu-242 in material type PU54 waste	Scalar	Stochastic
PU55				
Activity_Fractions		Radionuclide activity fractions in material type PU55 waste	Vector (radionuclide)	Data
PU56				
Pu238_Mass_Fraction		Mass fraction of Pu-238 in material type PU56 waste	Scalar	Stochastic
Pu240_Mass_Fraction		Mass fraction of Pu-240 in material type PU56 waste	Scalar	Stochastic
Pu241_Mass_Fraction		Mass fraction of Pu-241 in material type PU56 waste	Scalar	Stochastic
Pu242_Mass_Fraction		Mass fraction of Pu-242 in material type PU56 waste	Scalar	Stochastic
PU57				
Activity_Fractions		Radionuclide activity fractions in material type PU57 waste	Vector (radionuclide)	Data
PU83				
Pu238_Mass_Fraction		Mass fraction of Pu-238 in material type PU83 waste	Scalar	Stochastic

Table 7 (Continued)
Input Data Requirements for the MDA G Site Diffusion Model

Model Container/Parameter Name	Units	Parameter Description	Parameter Type	Input Element Type
Pu240_Mass_Fraction		Mass fraction of Pu-240 in material type PU83 waste	Scalar	Stochastic
Pu241_Mass_Fraction		Mass fraction of Pu-241 in material type PU83 waste	Scalar	Stochastic
Pu242_Mass_Fraction		Mass fraction of Pu-242 in material type PU83 waste	Scalar	Stochastic
U10				
Activity_Fractions		Radionuclide activity fractions in material type U10 waste	Vector (radionuclide)	Data
U11				
Activity_Fractions		Radionuclide activity fractions in material type U11 waste	Vector (radionuclide)	Data
U12				
U234_Mass_Fraction		Mass fraction of U-234 in material type U12 waste	Scalar	Stochastic
U245_Mass_Fraction		Mass fraction of U-235 in material type U12 waste	Scalar	Stochastic
U35				
Activity_Fractions		Radionuclide activity fractions in material type U35 waste	Vector (radionuclide)	Data
U36				
Activity_Fractions		Radionuclide activity fractions in material type U36 waste	Vector (radionuclide)	Data
U38				
Activity_Fractions		Radionuclide activity fractions in material type U38 waste	Vector (radionuclide)	Data
U39				
Activity_Fractions		Radionuclide activity fractions in material type U39 waste	Vector (radionuclide)	Data
U81				
Activity_Fractions		Radionuclide activity fractions in material type U81 waste	Vector (radionuclide)	Data

Table 7 (Continued)
Input Data Requirements for the MDA G Site Diffusion Model

Model Container/Parameter Name	Units	Parameter Description	Parameter Type	Input Element Type
UNAT				
Activity_Fractions		Radionuclide activity fractions in material type UNAT waste	Vector (radionuclide)	Data
D38				
U234_Mass_Fraction		Mass fraction of U-234 in material type D38 waste	Scalar	Stochastic
U245_Mass_Fraction		Mass fraction of U-235 in material type D38 waste	Scalar	Stochastic
TH88				
Activity_Fractions		Radionuclide activity fractions in material type TH88 waste	Vector (radionuclide)	Data
Transport_Pathway_Data				
Atmospheric_Transport				
Dust_Loading	kg/m^3	Dust loading	Scalar	Stochastic
Soil_Disturbance_Factor		Factor by which the dust loading is increased due to human disturbance of the surface soil	Scalar	Stochastic
Default_Resuspension_Flux	$g/m^2/s$	Resuspension flux used to conduct the complex terrain atmospheric transport modeling	Scalar	Data
Resuspension_Flux	$g/m^2/yr$	Resuspension for particulates at MDA G	Scalar	Stochastic
Enhancement_Factor		Ratio of radionuclide concentrations in the resuspendable fraction of the soil to those in the total soil	Scalar	Stochastic
Average_Wind_Speed	m/s	Average wind speed at MDA G	Scalar	Stochastic
Atmospheric_Mixing_Height	m	Height to which radionuclides diffusing from the disposal site are mixed	Scalar	Data

Table 7 (Continued)
Input Data Requirements for the MDA G Site Diffusion Model

Model Container/Parameter Name	Units	Parameter Description	Parameter Type	Input Element Type
Particulate Dispersion_Factors				
LANL_Boundary				
Grassland_Land_Use				
CA_Factors				
X_Q_SA1_Grassland	s/m³	Air dispersion factor for atmospheric source area 1 and the grassland land use — composite analysis	Scalar	Stochastic
X_Q_SA2_Grassland	s/m³	Air dispersion factor for atmospheric source area 2 and the grassland land use — composite analysis	Scalar	Stochastic
X_Q_SA3_Grassland	s/m³	Air dispersion factor for atmospheric source area 3 and the grassland land use — composite analysis	Scalar	Stochastic
PA_Factors				
X_Q_SA1_Grassland	s/m³	Air dispersion factor for atmospheric source area 1 and the grassland land use — performance assessment	Scalar	Stochastic
X_Q_SA2_Grassland	s/m³	Air dispersion factor for atmospheric source area 2 and the grassland land use — performance assessment	Scalar	Stochastic
X_Q_SA3_Grassland	s/m³	Air dispersion factor for atmospheric source area 3 and the grassland land use — performance assessment	Scalar	Stochastic
Woodland_Land_Use				
CA_Factors				
X_Q_SA1_Woodland	s/m³	Air dispersion factor for atmospheric source area 1 and the woodland land use — composite analysis	Scalar	Stochastic
X_Q_SA2_Woodland	s/m³	Air dispersion factor for atmospheric source area 2 and the woodland land use — composite analysis	Scalar	Stochastic

Table 7 (Continued)
Input Data Requirements for the MDA G Site Diffusion Model

Model Container/Parameter Name	Units	Parameter Description	Parameter Type	Input Element Type
X_Q_SA3_Woodland	s/m³	Air dispersion factor for atmospheric source area 3 and the woodland land use — composite analysis	Scalar	Stochastic
PA_Factors				
X_Q_SA1_Woodland	s/m³	Air dispersion factor for atmospheric source area 1 and the woodland land use — performance assessment	Scalar	Stochastic
X_Q_SA2_Woodland	s/m³	Air dispersion factor for atmospheric source area 2 and the woodland land use — performance assessment	Scalar	Stochastic
X_Q_SA3_Woodland	s/m³	Air dispersion factor for atmospheric source area 3 and the woodland land use — performance assessment	Scalar	Stochastic
MDA_G_Fenceline				
Grassland_Land_Use				
CA_Factors				
X_Q_SA1_Grassland	s/m³	Air dispersion factor for atmospheric source area 1 and the grassland land use — composite analysis	Scalar	Stochastic
X_Q_SA2_Grassland	s/m³	Air dispersion factor for atmospheric source area 2 and the grassland land use — composite analysis	Scalar	Stochastic
X_Q_SA3_Grassland	s/m³	Air dispersion factor for atmospheric source area 3 and the grassland land use — composite analysis	Scalar	Stochastic
PA_Factors				
X_Q_SA1_Grassland	s/m³	Air dispersion factor for atmospheric source area 1 and the grassland land use — performance assessment	Scalar	Stochastic
X_Q_SA2_Grassland	s/m³	Air dispersion factor for atmospheric source area 2 and the grassland land use — performance assessment	Scalar	Stochastic
X_Q_SA3_Grassland	s/m³	Air dispersion factor for atmospheric source area 3 and the grassland land use — performance assessment	Scalar	Stochastic

Table 7 (Continued)
Input Data Requirements for the MDA G Site Diffusion Model

Model Container/Parameter Name	Units	Parameter Description	Parameter Type	Input Element Type
Woodland_Land_Use				
CA_Factors				
X_Q_SA1_Woodland	s/m³	Air dispersion factor for atmospheric source area 1 and the woodland land use — composite analysis	Scalar	Stochastic
X_Q_SA2_Woodland	s/m³	Air dispersion factor for atmospheric source area 2 and the woodland land use — composite analysis	Scalar	Stochastic
X_Q_SA3_Woodland	s/m³	Air dispersion factor for atmospheric source area 3 and the woodland land use — composite analysis	Scalar	Stochastic
PA_Factors				
X_Q_SA1_Woodland	s/m³	Air dispersion factor for atmospheric source area 1 and the woodland land use — performance assessment	Scalar	Stochastic
X_Q_SA2_Woodland	s/m³	Air dispersion factor for atmospheric source area 2 and the woodland land use — performance assessment	Scalar	Stochastic
X_Q_SA3_Woodland	s/m³	Air dispersion factor for atmospheric source area 3 and the woodland land use — performance assessment	Scalar	Stochastic
Gas_Dispersion_Factors				
LANL_Boundary				
Grassland_Land_Use				
X_Q_SA1_Grassland	s/m³	Air dispersion factor for atmospheric source area 1 and the grassland land use	Scalar	Stochastic
X_Q_SA2_Grassland	s/m³	Air dispersion factor for atmospheric source area 2 and the grassland land use	Scalar	Stochastic
X_Q_SA3_Grassland	s/m³	Air dispersion factor for atmospheric source area 3 and the grassland land use	Scalar	Stochastic

Table 7 (Continued)
Input Data Requirements for the MDA G Site Diffusion Model

Model Container/Parameter Name	Units	Parameter Description	Parameter Type	Input Element Type
Deposition_Rates				
LANL_Boundary				
Grassland_Land_Use				
CA_Factors				
DepRate_SA1_Grassland	g/m²/s	Particulate deposition rate for atmospheric source area 1 and the grassland land use — composite analysis	Scalar	Stochastic
DepRate_SA2_Grassland	g/m²/s	Particulate deposition rate for atmospheric source area 2 and the grassland land use — composite analysis	Scalar	Stochastic
DepRate_SA3_Grassland	g/m²/s	Particulate deposition rate for atmospheric source area 3 and the grassland land use — composite analysis	Scalar	Stochastic
PA_Factors				
DepRate_SA1_Grassland	g/m²/s	Particulate deposition rate for atmospheric source area 1 and the grassland land use — performance assessment	Scalar	Stochastic
DepRate_SA2_Grassland	g/m²/s	Particulate deposition rate for atmospheric source area 2 and the grassland land use — performance assessment	Scalar	Stochastic
DepRate_SA3_Grassland	g/m²/s	Particulate deposition rate for atmospheric source area 3 and the grassland land use — performance assessment	Scalar	Stochastic
Woodland_Land_Use				
CA_Factors				
DepRate_SA1_Woodland	g/m²/s	Particulate deposition rate for atmospheric source area 1 and the woodland land use — composite analysis	Scalar	Stochastic
DepRate_SA2_Woodland	g/m²/s	Particulate deposition rate for atmospheric source area 2 and the woodland land use — composite analysis	Scalar	Stochastic

Table 7 (Continued)
Input Data Requirements for the MDA G Site Diffusion Model

Model Container/Parameter Name	Units	Parameter Description	Parameter Type	Input Element Type
DepRate_SA3_Woodland	g/m²/s	Particulate deposition rate for atmospheric source area 3 and the woodland land use — composite analysis	Scalar	Stochastic
PA_Factors				
DepRate_SA1_Woodland	g/m²/s	Particulate deposition rate for atmospheric source area 1 and the woodland land use — performance assessment	Scalar	Stochastic
DepRate_SA2_Woodland	g/m²/s	Particulate deposition rate for atmospheric source area 2 and the woodland land use — performance assessment	Scalar	Stochastic
DepRate_SA3_Woodland	g/m²/s	Particulate deposition rate for atmospheric source area 3 and the woodland land use — performance assessment	Scalar	Stochastic
MDA_G_Fenceline				
Grassland_Land_Use				
CA_Factors				
DepRate_SA1_Grassland	g/m²/s	Particulate deposition rate for atmospheric source area 1 and the grassland land use — composite analysis	Scalar	Stochastic
DepRate_SA2_Grassland	g/m²/s	Particulate deposition rate for atmospheric source area 2 and the grassland land use — composite analysis	Scalar	Stochastic
DepRate_SA3_Grassland	g/m²/s	Particulate deposition rate for atmospheric source area 3 and the grassland land use — composite analysis	Scalar	Stochastic
PA_Factors				
DepRate_SA1_Grassland	g/m²/s	Particulate deposition rate for atmospheric source area 1 and the grassland land use — performance assessment	Scalar	Stochastic
DepRate_SA2_Grassland	g/m²/s	Particulate deposition rate for atmospheric source area 2 and the grassland land use — performance assessment	Scalar	Stochastic
DepRate_SA3_Grassland	g/m²/s	Particulate deposition rate for atmospheric source area 3 and the grassland land use — performance assessment	Scalar	Stochastic

Table 7 (Continued)
Input Data Requirements for the MDA G Site Diffusion Model

Model Container/Parameter Name	Units	Parameter Description	Parameter Type	Input Element Type
Woodland_Land_Use				
CA_Factors				
DepRate_SA1_Woodland	g/m²/s	Particulate deposition rate for atmospheric source area 1 and the woodland land use — composite analysis	Scalar	Stochastic
DepRate_SA2_Woodland	g/m²/s	Particulate deposition rate for atmospheric source area 2 and the woodland land use — composite analysis	Scalar	Stochastic
DepRate_SA3_Woodland	g/m²/s	Particulate deposition rate for atmospheric source area 3 and the woodland land use — composite analysis	Scalar	Stochastic
PA_Factors				
DepRate_SA1_Woodland	g/m²/s	Particulate deposition rate for atmospheric source area 1 and the woodland land use — performance assessment	Scalar	Stochastic
DepRate_SA2_Woodland	g/m²/s	Particulate deposition rate for atmospheric source area 2 and the woodland land use — performance assessment	Scalar	Stochastic
DepRate_SA3_Woodland	g/m²/s	Particulate deposition rate for atmospheric source area 3 and the woodland land use — performance assessment	Scalar	Stochastic
Foodchain_Transport				
Plant_Data				
Uptake_Factors				
Leafy_Vegetable_GM	Ci/kg plant per Ci/kg soil (dry weight)	Geometric means of the plant uptake factors for leafy vegetables	Vector (element)	Data
Produce_GM	Ci/kg plant per Ci/kg soil (dry weight)	Geometric means of the plant uptake factors for produce	Vector (element)	Data

Table 7 (Continued)
Input Data Requirements for the MDA G Site Diffusion Model

Model Container/Parameter Name	Units	Parameter Description	Parameter Type	Input Element Type
Grain_GM	Ci/kg plant per Ci/kg soil (dry weight)	Geometric means of the plant uptake factors for grain	Vector (element)	Data
PGrass_and_Native_GM	Ci/kg plant per Ci/kg soil (dry weight)	Geometric means of the plant uptake factors for pasture grass and native vegetation	Vector (element)	Data
Crop_GSD		Geometric standard deviation of the plant uptake factors for all crops		
Crop_Characteristics				
Particle_Size_Factor		Ratio of radionuclide concentrations in the fraction of the soil resuspended due to rainsplash to those in the total soil	Scalar	Stochastic
Plant_Carbon_Fraction		Fraction of plant that is carbon (dry-weight basis)	Vector (crop)	Data
Plant_Hydrogen_Fraction		Fraction of plant that is hydrogen (dry-weight basis)	Vector (crop)	Data
Plant_Interception_Coefficient	m^2/kg	Coefficient used to estimate the fraction of contamination deposited on plants that is initially retained	Scalar	Stochastic
Weathering_Halflife	d	Time required for 50 percent of the surface contamination on plants to be removed due to weathering processes	Scalar	Stochastic
Dry_to_Wet_Weight_Fractions				
DW_Leafy_Vegetables		Dry-to-wet-weight fraction for leafy vegetables	Scalar	Stochastic
DW_Produce		Dry-to-wet-weight fraction for produce	Scalar	Stochastic
DW_Grain		Dry-to-wet-weight fraction for grain	Scalar	Stochastic
DW_Pasture_Grass		Dry-to-wet-weight fraction for pasture grass	Scalar	Stochastic
Translocation_Factors				
TF_Leafy_Vegetables		Translocation factor for leafy vegetables	Scalar	Stochastic

Table 7 (Continued)
Input Data Requirements for the MDA G Site Diffusion Model

Model Container/Parameter Name	Units	Parameter Description	Parameter Type	Input Element Type
TF_Produce		Translocation factor for produce	Scalar	Stochastic
TF_Grain		Translocation factor for grain	Scalar	Stochastic
TF_Pasture_Grass		Translocation factor for pasture grass	Scalar	Stochastic
Agricultural_Productivities				
AP_Leafy_Vegetables	kg (wet weight) /m^2	Agricultural productivity for leafy vegetables	Scalar	Stochastic
AP_Produce	kg (wet weight) /m^2	Agricultural productivity for produce	Scalar	Stochastic
AP_Grain	kg (wet weight) /m^2	Agricultural productivity for grain	Scalar	Stochastic
AP_Pasture_Grass	kg (dry weight) /m^2	Agricultural productivity for pasture grass	Scalar	Stochastic
Growing_Season				
GS_Leafy_Vegetables	d	Growing season for leafy vegetables	Scalar	Stochastic
GS_Produce	d	Growing season for produce	Scalar	Stochastic
GS_Grain	d	Growing season for grain	Scalar	Stochastic
GS_Pasture_Grass	d	Growing season for pasture grass	Scalar	Stochastic
Mass_Loading_Factors				
MLF_Leafy_Vegetables	g soil/g plant (dry weight)	Mass-loading factor for leafy vegetables	Scalar	Stochastic
MLF_Produce	g soil/g plant (dry weight)	Mass-loading factor for produce	Scalar	Stochastic
MLF_Grain	g soil/g plant (dry weight)	Mass-loading factor for grain	Scalar	Stochastic

Table 7 (Continued)
Input Data Requirements for the MDA G Site Diffusion Model

Model Container/Parameter Name	Units	Parameter Description	Parameter Type	Input Element Type
MLF_Pasture_Grass	g soil/g plant (dry weight)	Mass-loading factor for pasture grass	Scalar	Stochastic
Animal_Data				
Animal_Ingestion_Data				
Cattle_and_Cows				
Cattle_Food	kg/d (dry weight)	Food consumption rate of cattle	Scalar	Stochastic
Cow_Food	kg/d (dry weight)	Food consumption rate of cows	Scalar	Stochastic
Cattle_Soil	kg/d (dry weight)	Soil consumption rate of cattle	Scalar	Stochastic
Cow_Soil	kg/d (dry weight)	Soil consumption rate of cows	Scalar	Stochastic
Cattle_Water	kg/d	Water consumption rate of cattle	Scalar	Stochastic
Cow_Water	kg/d	Water consumption rate of cows	Scalar	Stochastic
Chickens				
Chicken_Feed	kg/d (dry weight)	Food consumption rate of chickens	Scalar	Stochastic
Chicken_Water	kg/d	Water consumption rate of chickens	Scalar	Stochastic
Grit_to_Food_Ratio		Ratio of grit or soil intake to food intake for chickens	Scalar	Data
Transfer_Factors				
Beef_GM	d/kg	Geometric means of the forage-to-beef transfer factors	Vector (element)	Stochastic
Beef_GSD		Geometric standard deviation of the forage-to-beef transfer factors	Vector (element)	Data

Table 7 (Continued)
Input Data Requirements for the MDA G Site Diffusion Model

Model Container/Parameter Name	Units	Parameter Description	Parameter Type	Input Element Type
Milk_GM	d/kg	Geometric means of the forage-to-milk transfer factors	Vector (element)	Stochastic
Milk_GSD		Geometric standard deviation of the forage-to-milk transfer factors	Vector (element)	Data
Chicken_GM	d/kg	Geometric means of the forage-to-chicken transfer factors	Vector (element)	Stochastic
Chicken_GSD		Geometric standard deviation of the forage-to-chicken transfer factors	Vector (element)	Data
Eggs_GM	d/kg	Geometric means of the forage-to-eggs transfer factors	Vector (element)	Stochastic
Eggs_GSD		Geometric standard deviation of the forage-to-eggs transfer factors	Vector (element)	Data
H3_and_C14_Transfer_Factors				
H3_Factors				
Water_Fraction_Animal_Products		Mass water fractions of animal products	Vector (animal product)	Data
C14_Factors				
Animal_Prod_Carbon_Fraction		Carbon fractions of animal products	Vector (animal product)	Data
Groundwater_Transport				
MdB_Infiltration_Rate	m/yr	Water infiltration rate on Mesita del Buey	Scalar	Stochastic
CdB_Infiltration_Rate	m/yr	Water infiltration rate at the receptor location for the All Pathways – Cañada del Buey Scenario	Scalar	Stochastic
PC_Infiltration_Rate	m/yr	Water infiltration rate at the receptor location for the All Pathways – Pajarito Canyon Scenario	Scalar	Stochastic
PME_Infiltration_Rate	m/yr	Water infiltration rate at the receptor location for the Atmospheric Scenario	Scalar	Stochastic

Table 7 (Continued)
Input Data Requirements for the MDA G Site Diffusion Model

Model Container/Parameter Name	Units	Parameter Description	Parameter Type	Input Element Type
Sediment_Transport				
Catchment_Area	m^2	Area of each canyon catchment	Vector (canyon catchment)	Data
Sediment_Dispersal_Fraction		Fraction of canyon catchment over which sediments disperse	Scalar	Stochastic
Sediment_Transport_Rate	yr^{-1}	Rate constant describing the rate at which canyon sediments are flushed	Scalar	Stochastic
Sediment_Allocations				
Waste_Region_1		Fraction of contaminated sediment that is transported to each canyon catchment from waste disposal region 1	Vector (canyon catchment)	Data
Waste_Region_2		Fraction of contaminated sediment that is transported to each canyon catchment from waste disposal region 2	Vector (canyon catchment)	Data
Waste_Region_3		Fraction of contaminated sediment that is transported to each canyon catchment from waste disposal region 3	Vector (canyon catchment)	Data
Waste_Region_4		Fraction of contaminated sediment that is transported to each canyon catchment from waste disposal region 4	Vector (canyon catchment)	Data
Waste_Region_5		Fraction of contaminated sediment that is transported to each canyon catchment from waste disposal region 5	Vector (canyon catchment)	Data
Waste_Region_6		Fraction of contaminated sediment that is transported to each canyon catchment from waste disposal region 6	Vector (canyon catchment)	Data
Waste_Region_7		Fraction of contaminated sediment that is transported to each canyon catchment from waste disposal region 7	Vector (canyon catchment)	Data
Waste_Region_8		Fraction of contaminated sediment that is transported to each canyon catchment from waste disposal region 8	Vector (canyon catchment)	Data

Table 7 (Continued)
Input Data Requirements for the MDA G Site Diffusion Model

Model Container/Parameter Name	Units	Parameter Description	Parameter Type	Input Element Type
Biotic_Intrusion_Model				
Eco_Succession_Model				
Time_of_Climax	yr	Period required for disposal site to reach a piñon-juniper climax condition, measured from the time of facility closure	Scalar	Stochastic
Intrusion_Shape_Parameters				
Alpha_Shape_Factor		Shape factor used to model animal burrow and plant root distributions with depth	Scalar	Data
Beta_Shape_Factor		Shape factor used to model animal burrow and plant root distributions with depth	Scalar	Data
Animal_Intrusion_Model				
Harvester_Ants				
Maximum_Burrow_Depth	m	Maximum burrowing depth for harvester ants	Scalar	Stochastic
Burrow_Density_Grassland	ha^{-1}	Density of harvester ant burrows during early succession	Scalar	Stochastic
Burrow_Density_Woodland	ha^{-1}	Density of harvester ant burrows in the piñon-juniper climax condition	Scalar	Stochastic
Burrow_Mass	kg	Mass of soil excavated per harvester ant burrow	Scalar	Stochastic
Colony_Life_Span	yr	Life span of harvester ant colonies	Scalar	Stochastic
Pocket_Gophers				
Maximum_Burrow_Depth	m	Maximum burrowing depth for pocket gophers	Scalar	Stochastic
Soil_Removal_Rate_Grassland	m^3/ha	Rate of soil removal by pocket gophers during early succession	Scalar	Stochastic
Soil_Removal_Rate_Woodland	m^3/ha	Rate of soil removal by pocket gophers in the piñon-juniper climax condition	Scalar	Stochastic

Table 7 (Continued)
Input Data Requirements for the MDA G Site Diffusion Model

Model Container/Parameter Name	Units	Parameter Description	Parameter Type	Input Element Type
Burrow_Renewal_Rate	yr^{-1}	Rate at which existing pocket gopher burrows are replaced with new ones	Scalar	Stochastic
Mice				
Maximum_Burrow_Depth	m	Maximum burrowing depth for mice	Scalar	Stochastic
Burrow_Density_Grassland	ha^{-1}	Density of mouse burrows during early succession	Scalar	Stochastic
Burrow_Density_Woodland	ha^{-1}	Density of mouse burrows in the piñon-juniper climax condition	Scalar	Stochastic
Burrow_Volume	kg	Volume of soil excavated per mouse burrow	Scalar	Stochastic
Burrow_Renewal_Rate	yr^{-1}	Rate at which existing mouse burrows are replaced with new ones	Scalar	Stochastic
Chipmunks_and_Squirrels				
Maximum_Burrow_Depth	m	Maximum burrowing depth for chipmunks and ground squirrels	Scalar	Stochastic
Burrow_Density_Grassland	ha^{-1}	Density of chipmunk and ground squirrel burrows during early succession	Scalar	Stochastic
Burrow_Density_Woodland	ha^{-1}	Density of chipmunk and ground squirrel burrows in the piñon-juniper climax condition	Scalar	Stochastic
Burrow_Volume	kg	Volume of soil excavated per chipmunk and ground squirrel burrow	Scalar	Stochastic
Burrow_Renewal_Rate	yr^{-1}	Rate at which existing chipmunk and ground squirrel burrows are replaced with new ones	Scalar	Stochastic
Plant_Intrusion_Model				
Litter_Halflife	yr	Decomposition half-life of plant litter	Scalar	Stochastic
Grasses				
Maximum_Root_Depth	m	Maximum rooting depth of grasses	Scalar	Stochastic

Table 7 (Continued)
Input Data Requirements for the MDA G Site Diffusion Model

Model Container/Parameter Name	Units	Parameter Description	Parameter Type	Input Element Type
Biomass_Density_Grassland	kg/m^2	Aboveground biomass density of grasses during early succession	Scalar	Stochastic
Biomass_Density_Woodland	kg/m^2	Aboveground biomass density of grasses in the piñon-juniper climax condition	Scalar	Stochastic
Litter_Prod_Rate	yr^{-1}	Fraction of the aboveground biomass that falls as litter	Scalar	Stochastic
Forbs				
Maximum_Root_Depth	m	Maximum rooting depth of forbs	Scalar	Stochastic
Biomass_Density_Grassland	kg/m^2	Aboveground biomass density of forbs during early succession	Scalar	Stochastic
Biomass_Density_Woodland	kg/m^2	Aboveground biomass density of forbs in the piñon-juniper climax condition	Scalar	Stochastic
Litter_Prod_Rate	yr^{-1}	Fraction of the aboveground biomass that falls as litter	Scalar	Stochastic
Shrubs				
Maximum_Root_Depth	m	Maximum rooting depth of shrubs	Scalar	Stochastic
Biomass_Density_Grassland	kg/m^2	Aboveground biomass density of shrubs during early succession	Scalar	Stochastic
Biomass_Density_Woodland	kg/m^2	Aboveground biomass density of shrubs in the piñon-juniper climax condition	Scalar	Stochastic
Litter_Prod_Rate	yr^{-1}	Fraction of the aboveground biomass that falls as litter	Scalar	Stochastic
Trees				
Maximum_Root_Depth	m	Maximum rooting depth of trees	Scalar	Stochastic
Biomass_Density_Grassland	kg/m^2	Aboveground biomass density of trees during early succession	Scalar	Stochastic
Biomass_Density_Woodland	kg/m^2	Aboveground biomass density of trees in the piñon-juniper climax condition	Scalar	Stochastic
Litter_Prod_Rate	yr^{-1}	Fraction of the aboveground biomass that falls as litter	Scalar	Stochastic

Table 7 (Continued)
Input Data Requirements for the MDA G Site Diffusion Model

Model Container/Parameter Name	Units	Parameter Description	Parameter Type	Input Element Type
Erosion_Model				
Erosion_Rates				
Erosion_Rate_Functions	yr^{-1}	Cover loss rate as a function of time	Scalar	Lookup Table
Erosion_Zone_Data				
Remaining_Cover_EZ1	m	Minimum cover remaining in erosion zone 1	Scalar	Stochastic
Remaining_Cover_EZ2	m	Minimum cover remaining in erosion zone 2	Scalar	Stochastic
Remaining_Cover_EZ3	m	Minimum cover remaining in erosion zone 3	Scalar	Stochastic
Remaining_Cover_EZ4	m	Minimum cover remaining in erosion zone 4	Scalar	Stochastic
Remaining_Cover_EZ5	m	Minimum cover remaining in erosion zone 5	Scalar	Stochastic
Remaining_Cover_EZ6	m	Minimum cover remaining in erosion zone 6	Scalar	Stochastic
Remaining_Cover_EZ7	m	Minimum cover remaining in erosion zone 7	Scalar	Stochastic
Remaining_Cover_EZ8	m	Minimum cover remaining in erosion zone 8	Scalar	Stochastic
Remaining_Cover_EZ9	m	Minimum cover remaining in erosion zone 9	Scalar	Stochastic
Remaining_Cover_EZ10	m	Minimum cover remaining in erosion zone 10	Scalar	Stochastic
Erosion_Shape_Parameters				
Alpha_Shape_Factor		Shape factor used to model surface erosion	Scalar	Data
Beta_Shape_Factor		Shape factor used to model surface erosion	Scalar	Data
Dose_Model_and_Radon_Fluxes				
Dose_Conversion_Factors				
Ingestion_DCFs	mrem/pCi	Dose conversion factors for the ingestion exposure route	Vector (radionuclide)	Data
Inhalation_DCFs	mrem/pCi	Dose conversion factors for the inhalation exposure route	Vector (radionuclide)	Data

Table 7 (Continued)
Input Data Requirements for the MDA G Site Diffusion Model

Model Container/Parameter Name	Units	Parameter Description	Parameter Type	Input Element Type
Soil_External_DCFs_15_cm	mrem/yr per pCi/m^3	Dose conversion factors for direct radiation from soils contaminated to a depth of 15 cm	Vector (radionuclide)	Data
Air_External_DCFs	mrem/yr per pCi/m^3	Dose conversion factors for direct radiation from air immersion	Vector (radionuclide)	Data
Exposure_Pathway_Data				
Indoor_Exposure_Time	hr/d	Time spent indoors at the receptor location	Scalar	Stochastic
Outdoor_Exposure_Time	hr/d	Time spent outdoors at the receptor location	Scalar	Stochastic
Soil_Mixing_Depth	m	Contaminant mixing depth	Scalar	Data
Shielding_Factor		Direct radiation shielding factor for the time spent indoors	Scalar	Stochastic
Inhalation_Rate	m^3/d	Inhalation rate of the receptor	Scalar	Stochastic
Area_of_Lot	m^2	Area of the receptor's lot	Scalar	Stochastic
Area_of_House	m^2	Area of the receptor's house	Scalar	Data
Ingestion_Data				
Soil_Ingestion_Rate	kg (dry weight)/yr	Rate of soil ingestion for the receptor	Scalar	Stochastic
Worker_Soil_Ingestion_Rate	kg (dry weight)/yr	Rate of soil ingestion for the receptor	Scalar	Stochastic
Food_Ingestion_Data				
Input_Vegetable_Fraction		User-specified fraction of the receptor's diet of leafy vegetables, produce, and grain that is grown at the receptor's location	Scalar	Stochastic
Animals_Raised		The types of animals raised by the receptor to supply a portion of their diet	Scalar	Stochastic

Table 7 (Continued)
Input Data Requirements for the MDA G Site Diffusion Model

Model Container/Parameter Name	Units	Parameter Description	Parameter Type	Input Element Type
Crop_Ingestion_Rates				
CI_Leafy_Vegetables	kg (wet weight)/yr	Rate of ingestion of leafy vegetables for the receptor	Scalar	Stochastic
CI_Produce	kg (wet weight)/yr	Rate of ingestion of produce for the receptor	Scalar	Stochastic
CI_Grain	kg (wet weight)/yr	Rate of ingestion of grain for the receptor	Scalar	Stochastic
Animal_Product_Ingestion_Rates				
API_Beef	kg/yr	Rate of ingestion of beef for the receptor	Scalar	Stochastic
API_Milk	kg/yr	Rate of ingestion of milk for the receptor	Scalar	Stochastic
API_Chicken	kg/yr	Rate of ingestion of chicken for the receptor	Scalar	Stochastic
API_Eggs	kg/yr	Rate of ingestion of eggs for the receptor	Scalar	Stochastic
Animal_Numbers				
Cattle_Weight_at_Slaughter	kg	Weight of cattle at the time of slaughter	Scalar	Stochastic
Dressing_percentage		Ratio of the carcass weight to live weight of the animal	Scalar	Stochastic
Cutability		Fraction of the carcass that is sold as meat	Scalar	Stochastic
Milk_Production_Rate	kg/yr	Production rate of milk by cows	Scalar	Stochastic
Chicken_Weight_at_Slaughter	kg	Weight of chicken at the time of slaughter	Scalar	Stochastic
Cooked_to_Live_Ratio		Ratio of cooked weight of chicken to the live weight of the bird	Scalar	Stochastic
Meat_Fraction		Fraction of the cooked chicken that is meat	Scalar	Stochastic
Egg_Production_Rate	d^{-1}	Production rate of eggs by layers	Scalar	Stochastic
Egg_Mass	kg	Mass of egg	Scalar	Stochastic

Table 7 (Continued)
Input Data Requirements for the MDA G Site Diffusion Model

Model Container/Parameter Name	Units	Parameter Description	Parameter Type	Input Element Type
Shell_Fraction		Fraction of the egg mass that is contributed by the shell	Scalar	Data
Animal_Product_Fractions				
Beef		User-specified fraction of the receptor's diet of beef that is taken from animals living at the exposure location	Scalar	Stochastic
Milk		User-specified fraction of the receptor's diet of milk that is produced by animals living at the exposure location	Scalar	Stochastic
Chicken		User-specified fraction of the receptor's diet of chicken that is taken from animals living at the exposure location	Scalar	Stochastic
Eggs		User-specified fraction of the receptor's diet of eggs that is produced by animals living at the exposure location	Scalar	Stochastic
Irrigation_Rates				
IR_Leafy_Vegetables	cm/yr	Irrigation rate for leafy vegetables	Scalar	Stochastic
IR_Produce	cm/yr	Irrigation rate for produce	Scalar	Stochastic
IR_Grain	cm/yr	Irrigation rate for grain	Scalar	Stochastic
IR_Pasture_Grass	cm/yr	Irrigation rate for pasture grass	Scalar	Stochastic

Table 8
Input Data Requirements for the MDA G Intruder Model

Model Container/Parameter Name	Units	Parameter Description	Parameter Type	Input Element Type
Controls_and_Constants				
Intruder_Flag		Flag used to indicate which intruder scenario is being evaluated. A value of 1 indicates the Intruder – Post-Drilling Scenario is under consideration; a value of 2 indicates the Intruder-Agriculture Scenario is being modeled; a value of 3 indicates the Intruder-Construction Scenario is being assessed.	Scalar	Data
Disposal_Unit_Flag		Flag used to indicate which disposal units are being simulated. A value of 1 is input to consider the disposal pits in the expansion area; a value of 2 causes the model to consider the disposal shafts.	Scalar	Data
Biotic_Intrusion_Flag		Flag used to specify if the effects of biotic intrusion will be taken into account in the intruder modeling. A value of 0 indicates that biotic intrusion will not be considered; a value of 1 specifies allows plant and animal intrusion into the disposal site prior to the time of human intrusion.	Scalar	Data
Inventory_Flag		Flag used to indicate whether unit inventories or actual pit and shaft inventories are used in the modeling. A value of 1 is input to use unit inventories; a value of 2 specifies that actual disposal unit inventories will be used.	Scalar	Data
Depth_of_Disposal_Flag		Flag used to indicate whether the input inventory will be distributed homogeneously throughout the disposal units or if waste-layer-specific inventories will be used. A value of 1 is input to use a homogeneously distributed inventory; a value of 2 specifies that waste-layer-specific inventories will be applied.	Scalar	Data

Table 8 (Continued)
Input Data Requirements for the MDA G Intruder Model

Model Container/Parameter Name	Units	Parameter Description	Parameter Type	Input Element Type
Disposal_System_Information				
Species_and_Materials				
Halflives	yr	Radionuclide half-lives	Vector (radionuclide)	Data
Material_Properties				
Density_of_Water	kg/m^3	Density of water	Scalar	Data
Soil_Carbon_Fraction		Fraction of surface soil that is carbon	Scalar	Data
Water_Carbon_Fraction		Fraction of water that is carbon	Scalar	Data
Water_Hydrogen_Fraction		Fraction of water that is hydrogen	Scalar	Data
Dry_Densities				
DD_Crushed_Tuff	kg/m^3	Dry density of crushed tuff	Scalar	Stochastic
DD_Waste	kg/m^3	Dry density of waste	Scalar	Stochastic
DD_Concrete	kg/m^3	Dry density of concrete	Scalar	Stochastic
Moisture_Contents				
MC_Crushed_Tuff	(volume basis)	Moisture content of crushed tuff	Scalar	Stochastic
MC_Waste	(volume basis)	Moisture content of waste	Scalar	Stochastic
Concrete_Saturation		Saturation level of concrete	Scalar	Stochastic
Effective_Porosities				
EP_Crushed_Tuff		Effective porosity of crushed tuff	Scalar	Stochastic

Table 8 (Continued)
Input Data Requirements for the MDA G Intruder Model

Model Container/Parameter Name	Units	Parameter Description	Parameter Type	Input Element Type
EP_Waste		Effective porosity of waste	Scalar	Stochastic
EP_Concrete		Effective porosity of concrete	Scalar	Stochastic
Partition_Coefficients				
Soil_and_Waste_Kds				
Elemental_Kds	m^3/kg	Elemental distribution coefficients for crushed tuff and waste	Vector (element)	Data
Kd_Distributions				
Ag	m^3/kg	Distribution coefficient for silver in crushed tuff and waste	Scalar	Stochastic
Am	m^3/kg	Distribution coefficient for americium in crushed tuff and waste	Scalar	Stochastic
Ba	m^3/kg	Distribution coefficient for barium in crushed tuff and waste	Scalar	Stochastic
Cs	m^3/kg	Distribution coefficient for cesium in crushed tuff and waste	Scalar	Stochastic
Np	m^3/kg	Distribution coefficient for neptunium in crushed tuff and waste	Scalar	Stochastic
Pa	m^3/kg	Distribution coefficient for protactinium in crushed tuff and waste	Scalar	Stochastic
Pu	m^3/kg	Distribution coefficient for plutonium in crushed tuff and waste	Scalar	Stochastic
Ra	m^3/kg	Distribution coefficient for radium in crushed tuff and waste	Scalar	Stochastic
Sr	m^3/kg	Distribution coefficient for strontium in crushed tuff and waste	Scalar	Stochastic
Th	m^3/kg	Distribution coefficient for thorium in crushed tuff and waste	Scalar	Stochastic

Table 8 (Continued)
Input Data Requirements for the MDA G Intruder Model

Model Container/Parameter Name	Units	Parameter Description	Parameter Type	Input Element Type
U	m^3/kg	Distribution coefficient for uranium in crushed tuff and waste	Scalar	Stochastic
Attenuation_Coefficients				
Soil_Mass_Atten_Coeff	cm^2/g	Mass attenuation coefficient for soil	Vector (radionuclide)	Data
Concrete_Mass_Atten_Coeff	cm^2/g	Mass attenuation coefficient for concrete	Vector (radionuclide)	Data
Site_Geometry_and_Operations				
Institutional_Control_Period	yr	The length of the active institutional control period, measured from the time of facility closure	Scalar	Data
Start_of_Disposal	yr	The year of the simulation in which waste is first placed in the disposal units	Scalar	Data
End_of_Disposal	yr	The last year of the simulation that waste is placed in the disposal units	Scalar	Data
Closure_Period	yr	The length of time required to achieve final closure of the disposal facility following the end of disposal operations	Scalar	Data
Disposal_Unit_Area	m^2	Surface area of the disposal units	Scalar	Data
Concrete_Floor_Thickness	m	The thickness of the floor of the concrete foundation of the intruder's house	Scalar	Data
Layer_Information				
Number_of_Cap_Layers		The number of discrete layers used to represent the cap	Scalar	Data
Number_of_Waste_Layers		The number of discrete layers used to represent the disposed waste	Scalar	Data

Table 8 (Continued)
Input Data Requirements for the MDA G Intruder Model

Model Container/Parameter Name	Units	Parameter Description	Parameter Type	Input Element Type
Disposal_Pits				
Pits_1988_2004				
Initial_Cover_Thickness	m	Initial thickness of the cover over the disposal units	Scalar	Stochastic
Surface_Soil_Thickness	m	Thickness of the surface soil layer	Vector (waste disposal region)	Data
Waste_Thickness	m	Thickness of the disposed waste	Vector (waste disposal region)	Data
Upper_Waste_Layer_Thickness	m	Thickness of the uppermost three layers of waste	Scalar	Data
Waste_Emplacement_Efficiency		The fraction of the disposal capacity of the pits filled with waste	Scalar	Data
Start_of_Disposal	yr	The first year of the simulation that waste is placed in the disposal units	Scalar	Data
End_of_Disposal	yr	The last year of the simulation that waste is placed in the disposal units	Scalar	Data
Fractional_Area_Calculations				
Low_Erosion_Fraction		Fractional area of the erosion zones for the low-erosion scenario at the end of the simulation	Vector (erosion zone)	Data
Moderate_Erosion_Fraction		Fractional area of the erosion zones for the moderate-erosion scenario at the end of the simulation	Vector (erosion zone)	Data
High_Erosion_Fraction		Fractional area of the erosion zones for the high-erosion scenario at the end of the simulation	Vector (erosion zone)	Data

Table 8 (Continued)
Input Data Requirements for the MDA G Intruder Model

Model Container/Parameter Name	Units	Parameter Description	Parameter Type	Input Element Type
Pits_2005_2044				
Initial_Cover_Thickness	m	Initial thickness of the cover over the disposal units	Scalar	Stochastic
Surface_Soil_Thickness	m	Thickness of the surface soil layer	Vector (waste disposal region)	Data
Waste_Thickness	m	Thickness of the disposed waste	Vector (waste disposal region)	Data
Upper_Waste_Layer_Thickness	m	Thickness of the uppermost three layers of waste	Scalar	Data
Waste_Emplacement_Efficiency		The fraction of the disposal capacity of the pits filled with waste	Scalar	Data
Start_of_Disposal	yr	The first year of the simulation that waste is placed in the disposal units	Scalar	Data
End_of_Disposal	yr	The last year of the simulation that waste is placed in the disposal units	Scalar	Data
Fractional_Area_Calculations				
Low_Erosion_Fraction		Fractional area of the erosion zones for the low-erosion scenario at the end of the simulation	Vector (erosion zone)	Data
Moderate_Erosion_Fraction		Fractional area of the erosion zones for the moderate-erosion scenario at the end of the simulation	Vector (erosion zone)	Data
High_Erosion_Fraction		Fractional area of the erosion zones for the high-erosion scenario at the end of the simulation	Vector (erosion zone)	Data

Table 8 (Continued)
Input Data Requirements for the MDA G Intruder Model

Model Container/Parameter Name	Units	Parameter Description	Parameter Type	Input Element Type
Disposal_Shafts				
Shafts_1988_2004				
Initial_Cover_Thickness	m	Initial thickness of the cover over the disposal units	Scalar	Stochastic
Surface_Soil_Thickness	m	Thickness of the surface soil layer	Vector (waste disposal region)	Data
Waste_Thickness	m	Thickness of the disposed waste	Vector (waste disposal region)	Data
Upper_Waste_Layer_Thickness	m	Thickness of the uppermost three layers of waste	Scalar	Data
Shaft_Field_Efficiency		The fraction of the surface area of the shaft field that is occupied by disposal shafts	Scalar	Data
Waste_Emplacement_Efficiency		The fraction of the disposal capacity of the shafts filled with waste	Scalar	Data
Start_of_Disposal	yr	The first year of the simulation that waste is placed in the disposal units	Scalar	Data
End_of_Disposal	yr	The last year of the simulation that waste is placed in the disposal units	Scalar	Data
Fractional_Area_Calculations				
Low_Erosion_Fraction		Fractional area of the erosion zones for the low-erosion scenario at the end of the simulation	Vector (erosion zone)	Data
Moderate_Erosion_Fraction		Fractional area of the erosion zones for the moderate-erosion scenario at the end of the simulation	Vector (erosion zone)	Data

Table 8 (Continued)
Input Data Requirements for the MDA G Intruder Model

Model Container/Parameter Name	Units	Parameter Description	Parameter Type	Input Element Type
High_Erosion_Fraction		Fractional area of the erosion zones for the high-erosion scenario at the end of the simulation	Vector (erosion zone)	Data
Shafts_2005_2044				
Initial_Cover_Thickness	m	Initial thickness of the cover over the disposal units	Scalar	Stochastic
Surface_Soil_Thickness	m	Thickness of the surface soil layer	Vector (waste disposal region)	Data
Waste_Thickness	m	Thickness of the disposed waste	Vector (waste disposal region)	Data
Upper_Waste_Layer_Thickness	m	Thickness of the uppermost three layers of waste	Scalar	Data
Shaft_Field_Efficiency		The fraction of the surface area of the shaft field that is occupied by disposal shafts	Scalar	Data
Waste_Emplacement_Efficiency		The fraction of the disposal capacity of the shafts filled with waste	Scalar	Data
Start_of_Disposal	yr	The first year of the simulation that waste is placed in the disposal units	Scalar	Data
End_of_Disposal	yr	The last year of the simulation that waste is placed in the disposal units	Scalar	Data
Fractional_Area_Calculations				
Low_Erosion_Fraction		Fractional area of the erosion zones for the low-erosion scenario at the end of the simulation	Vector (erosion zone)	Data
Moderate_Erosion_Fraction		Fractional area of the erosion zones for the moderate-erosion scenario at the end of the simulation	Vector (erosion zone)	Data

Table 8 (Continued)
Input Data Requirements for the MDA G Intruder Model

Model Container/Parameter Name	Units	Parameter Description	Parameter Type	Input Element Type
High_Erosion_Fraction		Fractional area of the erosion zones for the high-erosion scenario at the end of the simulation	Vector (erosion zone)	Data
Inventory				
Unit_Inventory				
Assumed Inventory	Ci	The as-disposed inventory for all parent radionuclides included in the intruder modeling	Scalar	Data
Inventory_Distribution_Factor		Fraction of assumed inventory in each layer of waste in the disposal units.	Vector (waste layers)	Data
As-Disposed_Inventory				
Measurement_Errors				
Rad_Specific_Errors				
Pre_1990_Lower_Bounds		Factor used to estimate the lower bound of pre-1990 radionuclide inventories, taking into account errors introduced by measurement uncertainty	Vector (radionuclide)	Data
Pre_1990_Upper_Bounds		Factor used to estimate the upper bound of pre-1990 radionuclide inventories, taking into account errors introduced by measurement uncertainty	Vector (radionuclide)	Data
Post_1989_Lower_Bounds		Factor used to estimate the lower bound of post-1989 radionuclide inventories, taking into account errors introduced by measurement uncertainty	Vector (radionuclide)	Data
Post_1989_Upper_Bounds		Factor used to estimate the upper bound of post-1989 radionuclide inventories, taking into account errors introduced by measurement uncertainty	Vector (radionuclide)	Data

Table 8 (Continued)
Input Data Requirements for the MDA G Intruder Model

Model Container/Parameter Name	Units	Parameter Description	Parameter Type	Input Element Type
Material_Type_Errors				
Pre_1990_Lower_Bounds		Factor used to estimate the lower bound of pre-1990 material type inventories, taking into account errors introduced by measurement uncertainty	Vector (material type)	Data
Pre_1990_Upper_Bounds		Factor used to estimate the upper bound of pre-1990 material type inventories, taking into account errors introduced by measurement uncertainty	Vector (material type)	Data
Post_1989_Lower_Bounds		Factor used to estimate the lower bound of post-1989 material type inventories, taking into account errors introduced by measurement uncertainty	Vector (material type)	Data
Post_1989_Upper_Bounds		Factor used to estimate the upper bound of post-1989 material type inventories, taking into account errors introduced by measurement uncertainty	Vector (material type)	Data
Rad_Specific_Inventories				
Pit_Waste_1988_2004				
Depth_Indept_Inventory				
Pre_1990_PA_Point_Estimate	Ci	Point estimates of radionuclide-specific inventories in the pre-1990 performance assessment waste disposed of in 1988–2004 pits	Vector (radionuclide)	Data
Post_1989_PA_Point_Estimate	Ci	Point estimates of radionuclide-specific inventories in the post-1989 performance assessment waste disposed of in 1988–2004 pits	Vector (radionuclide)	Data

Table 8 (Continued)
Input Data Requirements for the MDA G Intruder Model

Model Container/Parameter Name	Units	Parameter Description	Parameter Type	Input Element Type
Depth_Dept_Inventory				
Pre_1990_PA_PtEst_Layer1	Ci	Point estimates of radionuclide-specific inventories in waste inventory layer 1 of the pre-1990 performance assessment waste disposed of in 1988–2004 pits	Vector (radionuclide)	Data
Pre_1990_PA_PtEst_Layer2	Ci	Point estimates of radionuclide-specific inventories in waste inventory layer 2 of the pre-1990 performance assessment waste disposed of in 1988–2004 pits	Vector (radionuclide)	Data
Pre_1990_PA_PtEst_Layer3	Ci	Point estimates of radionuclide-specific inventories in waste inventory layer 3 of the pre-1990 performance assessment waste disposed of in 1988–2004 pits	Vector (radionuclide)	Data
Pre_1990_PA_PtEst_Layer4	Ci	Point estimates of radionuclide-specific inventories in waste inventory layer 4 of the pre-1990 performance assessment waste disposed of in 1988–2004 pits	Vector (radionuclide)	Data
Post_1989_PA_PtEst_Layer1	Ci	Point estimates of radionuclide-specific inventories in waste inventory layer 1 of the post-1989 performance assessment waste disposed of in 1988–2004 pits	Vector (radionuclide)	Data
Post_1989_PA_PtEst_Layer2	Ci	Point estimates of radionuclide-specific inventories in waste inventory layer 2 of the post-1989 performance assessment waste disposed of in 1988–2004 pits	Vector (radionuclide)	Data
Post_1989_PA_PtEst_Layer3	Ci	Point estimates of radionuclide-specific inventories in waste inventory layer 3 of the post-1989 performance assessment waste disposed of in 1988–2004 pits	Vector (radionuclide)	Data
Post_1989_PA_PtEst_Layer4	Ci	Point estimates of radionuclide-specific inventories in waste inventory layer 4 of the post-1989 performance assessment waste disposed of in 1988–2004 pits	Vector (radionuclide)	Data

Table 8 (Continued)
Input Data Requirements for the MDA G Intruder Model

Model Container/Parameter Name	Units	Parameter Description	Parameter Type	Input Element Type
Pit_Waste_2005_2044				
Depth_Indept_Inventory				
Post_1989_PA_Point_Estimate	Ci	Point estimates of radionuclide-specific inventories in the post-1989 performance assessment waste disposed of in 2005–2044 pits	Vector (radionuclide)	Data
Depth_Dept_Inventory				
Post_1989_PA_PtEst_Layer1	Ci	Point estimates of radionuclide-specific inventories in waste inventory layer 1 of the post-1989 performance assessment waste disposed of in 2005-2044 pits	Vector (radionuclide)	Data
Post_1989_PA_PtEst_Layer2	Ci	Point estimates of radionuclide-specific inventories in waste inventory layer 2 of the post-1989 performance assessment waste disposed of in 2005-2044 pits	Vector (radionuclide)	Data
Post_1989_PA_PtEst_Layer3	Ci	Point estimates of radionuclide-specific inventories in waste inventory layer 3 of the post-1989 performance assessment waste disposed of in 2005-2044 pits	Vector (radionuclide)	Data
Post_1989_PA_PtEst_Layer4	Ci	Point estimates of radionuclide-specific inventories in waste inventory layer 4 of the post-1989 performance assessment waste disposed of in 2005-2044 pits	Vector (radionuclide)	Data
Shaft_Waste_1988_2004				
Depth_Indept_Inventory				
Pre_1990_PA_Point_Estimate	Ci	Point estimates of radionuclide-specific inventories in the pre-1990 performance assessment waste disposed of in 1988–2004 shafts	Vector (radionuclide)	Data

Table 8 (Continued)
Input Data Requirements for the MDA G Intruder Model

Model Container/Parameter Name	Units	Parameter Description	Parameter Type	Input Element Type
Post_1989_PA_Point_Estimate	Ci	Point estimates of radionuclide-specific inventories in the post-1989 performance assessment waste disposed of in 2005–2044 shafts	Vector (radionuclide)	Data
Depth_Dept_Inventory				
Pre_1990_PA_PtEst_Layer1	Ci	Point estimates of radionuclide-specific inventories in waste inventory layer 1 of the pre-1990 performance assessment waste disposed of in 1988–2004 shafts	Vector (radionuclide)	Data
Pre_1990_PA_PtEst_Layer2	Ci	Point estimates of radionuclide-specific inventories in waste inventory layer 2 of the pre-1990 performance assessment waste disposed of in 1988–2004 shafts	Vector (radionuclide)	Data
Pre_1990_PA_PtEst_Layer3	Ci	Point estimates of radionuclide-specific inventories in waste inventory layer 3 of the pre-1990 performance assessment waste disposed of in 1988–2004 shafts	Vector (radionuclide)	Data
Pre_1990_PA_PtEst_Layer4	Ci	Point estimates of radionuclide-specific inventories in waste inventory layer 4 of the pre-1990 performance assessment waste disposed of in 1988–2004 shafts	Vector (radionuclide)	Data
Post_1989_PA_PtEst_Layer1	Ci	Point estimates of radionuclide-specific inventories in waste inventory layer 1 of the post-1989 performance assessment waste disposed of in 1988–2004 shafts	Vector (radionuclide)	Data
Post_1989_PA_PtEst_Layer2	Ci	Point estimates of radionuclide-specific inventories in waste inventory layer 2 of the post-1989 performance assessment waste disposed of in 1988–2004 shafts	Vector (radionuclide)	Data
Post_1989_PA_PtEst_Layer3	Ci	Point estimates of radionuclide-specific inventories in waste inventory layer 3 of the post-1989 performance assessment waste disposed of in 1988–2004 shafts	Vector (radionuclide)	Data

Table 8 (Continued)
Input Data Requirements for the MDA G Intruder Model

Model Container/Parameter Name	Units	Parameter Description	Parameter Type	Input Element Type
Post_1989_PA_PtEst_Layer4	Ci	Point estimates of radionuclide-specific inventories in waste inventory layer 4 of the post-1989 performance assessment waste disposed of in 1988–2004 shafts	Vector (radionuclide)	Data
Shaft_Waste_2005_2044				
Depth_Indept_Inventory				
Post_1989_PA_Point_Estimate	Ci	Point estimates of radionuclide-specific inventories in the post-1989 performance assessment waste disposed of in 2005–2044 shafts	Vector (radionuclide)	Data
Depth_Dept_Inventory				
Post_1989_PA_PtEst_Layer1	Ci	Point estimates of radionuclide-specific inventories in waste inventory layer 1 of the post-1989 performance assessment waste disposed of in 2005-2044 shafts	Vector (radionuclide)	Data
Post_1989_PA_PtEst_Layer2	Ci	Point estimates of radionuclide-specific inventories in waste I inventory ayer 2 of the post-1989 performance assessment waste disposed of in 2005-2044 shafts	Vector (radionuclide)	Data
Post_1989_PA_PtEst_Layer3	Ci	Point estimates of radionuclide-specific inventories in waste inventory layer 3 of the post-1989 performance assessment waste disposed of in 2005-2044 shafts	Vector (radionuclide)	Data
Post_1989_PA_PtEst_Layer4	Ci	Point estimates of radionuclide-specific inventories in waste inventory layer 4 of the post-1989 performance assessment waste disposed of in 2005-2044 shafts	Vector (radionuclide)	Data

Table 8 (Continued)
Input Data Requirements for the MDA G Intruder Model

Model Container/Parameter Name	Units	Parameter Description	Parameter Type	Input Element Type
Material_Type_Inventories				
Pit_Waste_1988_2004				
Depth_Indept_Inventory				
Pre_1990_PA_Point_Estimate	Ci	Point estimates of material type inventories in the pre-1990 performance assessment waste disposed of in 1988–2004 pits	Vector (material type)	Data
Post_1989_PA_Point_Estimate	Ci	Point estimates of material type inventories in the post-1989 performance assessment waste disposed of in 1988–2004 pits	Vector (material type)	Data
Depth_Dept_Inventory				
Pre_1990_PA_PtEst_Layer1	Ci	Point estimates of material type inventories in waste inventory layer 1 of the pre-1990 performance assessment waste disposed of in 1988–2004 pits	Vector (material type)	Data
Pre_1990_PA_PtEst_Layer2	Ci	Point estimates of material type inventories in waste inventory layer 2 of the pre-1990 performance assessment waste disposed of in 1988–2004 pits	Vector (material type)	Data
Pre_1990_PA_PtEst_Layer3	Ci	Point estimates of material type inventories in waste inventory layer 3 of the pre-1990 performance assessment waste disposed of in 1988–2004 pits	Vector (material type)	Data
Pre_1990_PA_PtEst_Layer4	Ci	Point estimates of material type inventories in waste inventory layer 4 of the pre-1990 performance assessment waste disposed of in 1988–2004 pits	Vector (material type)	Data
Post_1989_PA_PtEst_Layer1	Ci	Point estimates of material type inventories in waste inventory layer 1 of the post-1989 performance assessment waste disposed of in 1988–2004 pits	Vector (material type)	Data

Table 8 (Continued)
Input Data Requirements for the MDA G Intruder Model

Model Container/Parameter Name	Units	Parameter Description	Parameter Type	Input Element Type
Post_1989_PA_PtEst_Layer2	Ci	Point estimates of material type inventories in waste inventory layer 2 of the post-1989 performance assessment waste disposed of in 1988–2004 pits	Vector (material type)	Data
Post_1989_PA_PtEst_Layer3	Ci	Point estimates of material type inventories in waste inventory layer 3 of the post-1989 performance assessment waste disposed of in 1988–2004 pits	Vector (material type)	Data
Post_1989_PA_PtEst_Layer4	Ci	Point estimates of material type inventories in waste inventory layer 4 of the post-1989 performance assessment waste disposed of in 1988–2004 pits	Vector (material type)	Data
Pit_Waste_2005_2044				
Depth_Indept_Inventory				
Post_1989_PA_Point_Estimate	Ci	Point estimates of material type inventories in the post-1989 performance assessment waste disposed of in 2005–2044 pits	Vector (material type)	Data
Depth_Dept_Inventory				
Post_1989_PA_PtEst_Layer1	Ci	Point estimates of material type inventories in waste inventory layer 1 of the post-1989 performance assessment waste disposed of in 2005-2044 pits	Vector (material type)	Data
Post_1989_PA_PtEst_Layer2	Ci	Point estimates of material type inventories in waste inventory layer 2 of the post-1989 performance assessment waste disposed of in 2005-2044 pits	Vector (material type)	Data
Post_1989_PA_PtEst_Layer3	Ci	Point estimates of material type inventories in waste inventory layer 3 of the post-1989 performance assessment waste disposed of in 2005-2044 pits	Vector (material type)	Data

Table 8 (Continued)
Input Data Requirements for the MDA G Intruder Model

Model Container/Parameter Name	Units	Parameter Description	Parameter Type	Input Element Type
Post_1989_PA_PtEst_Layer4	Ci	Point estimates of material type inventories in waste inventory layer 4 of the post-1989 performance assessment waste disposed of in 2005-2044 pits	Vector (material type)	Data
Shaft_Waste_1988_2004				
Depth_Indept_Inventory				
Pre_1990_PA_Point_Estimate	Ci	Point estimates of material type inventories in the pre-1990 performance assessment waste disposed of in 1988–2004 shafts	Vector (material type)	Data
Post_1989_PA_Point_Estimate	Ci	Point estimates of material type inventories in the post-1989 performance assessment waste disposed of in 1988–2004 shafts	Vector (material type)	Data
Depth_Dept_Inventory				
Pre_1990_PA_PtEst_Layer1	Ci	Point estimates of material type inventories in waste inventory layer 1 of the pre-1990 performance assessment waste disposed of in 1988–2004 shafts	Vector (material type)	Data
Pre_1990_PA_PtEst_Layer2	Ci	Point estimates of material type inventories in waste inventory layer 2 of the pre-1990 performance assessment waste disposed of in 1988–2004 shafts	Vector (material type)	Data
Pre_1990_PA_PtEst_Layer3	Ci	Point estimates of material type inventories in waste inventory layer 3 of the pre-1990 performance assessment waste disposed of in 1988–2004 shafts	Vector (material type)	Data
Pre_1990_PA_PtEst_Layer4	Ci	Point estimates of material type inventories in waste inventory layer 4 of the pre-1990 performance assessment waste disposed of in 1988–2004 shafts	Vector (material type)	Data

Table 8 (Continued)
Input Data Requirements for the MDA G Intruder Model

Model Container/Parameter Name	Units	Parameter Description	Parameter Type	Input Element Type
Post_1989_PA_PtEst_Layer1	Ci	Point estimates of material type inventories in waste inventory layer 1 of the post-1989 performance assessment waste disposed of in 1988–2004 shafts	Vector (material type)	Data
Post_1989_PA_PtEst_Layer2	Ci	Point estimates of material type inventories in waste inventory layer 2 of the post-1989 performance assessment waste disposed of in 1988–2004 shafts	Vector (material type)	Data
Post_1989_PA_PtEst_Layer3	Ci	Point estimates of material type inventories in waste inventory layer 3 of the post-1989 performance assessment waste disposed of in 1988–2004 shafts	Vector (material type)	Data
Post_1989_PA_PtEst_Layer4	Ci	Point estimates of material type inventories in waste inventory layer 4 of the post-1989 performance assessment waste disposed of in 1988–2004 shafts	Vector (material type)	Data
Shaft_Waste_2005_2044				
Depth_Indept_Inventory				
Post_1989_PA_Point_Estimate	Ci	Point estimates of material type inventories in the post-1989 performance assessment waste disposed of in 2005–2044 shafts	Vector (material type)	Data
Depth_Dept_Inventory				
Post_1989_PA_PtEst_Layer1	Ci	Point estimates of material type inventories in waste inventory layer 1 of the post-1989 performance assessment waste disposed of in 2005-2044 shafts	Vector (material type)	Data
Post_1989_PA_PtEst_Layer2	Ci	Point estimates of material type inventories in waste inventory layer 2 of the post-1989 performance assessment waste disposed of in 2005-2044 shafts	Vector (material type)	Data

Table 8 (Continued)
Input Data Requirements for the MDA G Intruder Model

Model Container/Parameter Name	Units	Parameter Description	Parameter Type	Input Element Type
Post_1989_PA_PtEst_Layer3	Ci	Point estimates of material type inventories in waste inventory layer 3 of the post-1989 performance assessment waste disposed of in 2005-2044 shafts	Vector (material type)	Data
Post_1989_PA_PtEst_Layer4	Ci	Point estimates of material type inventories in waste inventory layer 4 of the post-1989 performance assessment waste disposed of in 2005-2044 shafts	Vector (material type)	Data
Fission_Yields				
Fraction_of_Pu239		Fraction of fission events that originate with Pu-239	Scalar	Stochastic
Age_of_MFP_Waste	yr	Age of mixed fission product waste at the time of disposal	Scalar	Stochastic
U235_Fission_Yields				
U235_1yr_Thermal		U-235 thermal fission yields for 1-year-old waste	Scalar	Data
U235_2yr_Thermal		U-235 thermal fission yields for 2-year-old waste	Scalar	Data
U235_3yr_Thermal		U-235 thermal fission yields for 3-year-old waste	Scalar	Data
U235_4yr_Thermal		U-235 thermal fission yields for 4-year-old waste	Scalar	Data
U235_5yr_Thermal		U-235 thermal fission yields for 5-year-old waste	Scalar	Data
U235_6yr_Thermal		U-235 thermal fission yields for 6-year-old waste	Scalar	Data
U235_7yr_Thermal		U-235 thermal fission yields for 7-year-old waste	Scalar	Data
U235_8yr_Thermal		U-235 thermal fission yields for 8-year-old waste	Scalar	Data
U235_9yr_Thermal		U-235 thermal fission yields for 9-year-old waste	Scalar	Data
U235_10yr_Thermal		U-235 thermal fission yields for 10-year-old waste	Scalar	Data
Pu239_Fission_Yields				
Pu239_1yr_Thermal		Pu-239 thermal fission yields for 1-year-old waste	Scalar	Data

Table 8 (Continued)
Input Data Requirements for the MDA G Intruder Model

Model Container/Parameter Name	Units	Parameter Description	Parameter Type	Input Element Type
Pu239_2yr_Thermal		Pu-239 thermal fission yields for 2-year-old waste	Scalar	Data
Pu239_3yr_Thermal		Pu-239 thermal fission yields for 3-year-old waste	Scalar	Data
Pu239_4yr_Thermal		Pu-239 thermal fission yields for 4-year-old waste	Scalar	Data
Pu239_5yr_Thermal		Pu-239 thermal fission yields for 5-year-old waste	Scalar	Data
Pu239_6yr_Thermal		Pu-239 thermal fission yields for 6-year-old waste	Scalar	Data
Pu239_7yr_Thermal		Pu-239 thermal fission yields for 7-year-old waste	Scalar	Data
Pu239_8yr_Thermal		Pu-239 thermal fission yields for 8-year-old waste	Scalar	Data
Pu239_9yr_Thermal		Pu-239 thermal fission yields for 9-year-old waste	Scalar	Data
Pu239_10yr_Thermal		Pu-239 thermal fission yields for 10-year-old waste	Scalar	Data
Activation_Yields				
MAP_Allocation_Fractions		Radionuclide-specific activity fractions for mixed activation product waste	Vector (radionuclide)	Data
Material_Type_Act_Fractions				
Nominal_Masses	g	Material type waste radionuclide masses	Matrix (radionuclide, material type)	Data
PU51				
Activity_Fractions		Radionuclide activity fractions in material type PU51 waste	Vector (radionuclide)	Data
PU52				
Pu238_Mass_Fraction		Mass fraction of Pu-238 in material type PU52 waste	Scalar	Stochastic
Pu240_Mass_Fraction		Mass fraction of Pu-240 in material type PU52 waste	Scalar	Stochastic

Table 8 (Continued)
Input Data Requirements for the MDA G Intruder Model

Model Container/Parameter Name	Units	Parameter Description	Parameter Type	Input Element Type
Pu241_Mass_Fraction		Mass fraction of Pu-241 in material type PU52 waste	Scalar	Stochastic
Pu242_Mass_Fraction		Mass fraction of Pu-242 in material type PU52 waste	Scalar	Stochastic
PU53				
Pu238_Mass_Fraction		Mass fraction of Pu-238 in material type PU53 waste	Scalar	Stochastic
Pu240_Mass_Fraction		Mass fraction of Pu-240 in material type PU53 waste	Scalar	Stochastic
Pu241_Mass_Fraction		Mass fraction of Pu-241 in material type PU53 waste	Scalar	Stochastic
Pu242_Mass_Fraction		Mass fraction of Pu-242 in material type PU53 waste	Scalar	Stochastic
PU54				
Pu238_Mass_Fraction		Mass fraction of Pu-238 in material type PU54 waste	Scalar	Stochastic
Pu240_Mass_Fraction		Mass fraction of Pu-240 in material type PU54 waste	Scalar	Stochastic
Pu241_Mass_Fraction		Mass fraction of Pu-241 in material type PU54 waste	Scalar	Stochastic
Pu242_Mass_Fraction		Mass fraction of Pu-242 in material type PU54 waste	Scalar	Stochastic
PU55				
Activity_Fractions		Radionuclide activity fractions in material type PU55 waste	Vector (radionuclide)	Data
PU56				
Pu238_Mass_Fraction		Mass fraction of Pu-238 in material type PU56 waste	Scalar	Stochastic
Pu240_Mass_Fraction		Mass fraction of Pu-240 in material type PU56 waste	Scalar	Stochastic
Pu241_Mass_Fraction		Mass fraction of Pu-241 in material type PU56 waste	Scalar	Stochastic
Pu242_Mass_Fraction		Mass fraction of Pu-242 in material type PU56 waste	Scalar	Stochastic

Table 8 (Continued)
Input Data Requirements for the MDA G Intruder Model

Model Container/Parameter Name	Units	Parameter Description	Parameter Type	Input Element Type
PU57				
Activity_Fractions		Radionuclide activity fractions in material type PU57 waste	Vector (radionuclide)	Data
PU83				
Pu238_Mass_Fraction		Mass fraction of Pu-238 in material type PU83 waste	Scalar	Stochastic
Pu240_Mass_Fraction		Mass fraction of Pu-240 in material type PU83 waste	Scalar	Stochastic
Pu241_Mass_Fraction		Mass fraction of Pu-241 in material type PU83 waste	Scalar	Stochastic
Pu242_Mass_Fraction		Mass fraction of Pu-242 in material type PU83 waste	Scalar	Stochastic
U10				
Activity_Fractions		Radionuclide activity fractions in material type U10 waste	Vector (radionuclide)	Data
U11				
Activity_Fractions		Radionuclide activity fractions in material type U11 waste	Vector (radionuclide)	Data
U12				
U234_Mass_Fraction		Mass fraction of U-234 in material type U12 waste	Scalar	Stochastic
U245_Mass_Fraction		Mass fraction of U-235 in material type U12 waste	Scalar	Stochastic
U35				
Activity_Fractions		Radionuclide activity fractions in material type U35 waste	Vector (radionuclide)	Data

Table 8 (Continued)
Input Data Requirements for the MDA G Intruder Model

Model Container/Parameter Name	Units	Parameter Description	Parameter Type	Input Element Type
U36				
Activity_Fractions		Radionuclide activity fractions in material type U36 waste	Vector (radionuclide)	Data
U38				
Activity_Fractions		Radionuclide activity fractions in material type U38 waste	Vector (radionuclide)	Data
U39				
Activity_Fractions		Radionuclide activity fractions in material type U39 waste	Vector (radionuclide)	Data
U81				
Activity_Fractions		Radionuclide activity fractions in material type U81 waste	Vector (radionuclide)	Data
UNAT				
Activity_Fractions		Radionuclide activity fractions in material type UNAT waste	Vector (radionuclide)	Data
D38				
U234_Mass_Fraction		Mass fraction of U-234 in material type D38 waste	Scalar	Stochastic
U245_Mass_Fraction		Mass fraction of U-235 in material type D38 waste	Scalar	Stochastic
TH88				
Activity_Fractions		Radionuclide activity fractions in material type TH88 waste	Vector (radionuclide)	Data

Table 8 (Continued)
Input Data Requirements for the MDA G Intruder Model

Model Container/Parameter Name	Units	Parameter Description	Parameter Type	Input Element Type
Waste_Disposal_Volumes				
Pit_Waste_1988_2004	m^3	Volume of waste disposed of in pits from September 27, 1988 through 2004	Scalar	Data
Pit_Waste_2005_2044	m^3	Volume of waste disposed of in pits from 2005 through 2044	Scalar	Data
Shaft_Waste_1988_2004	m^3	Volume of waste disposed of in shafts from September 27, 1988 through 2004	Scalar	Data
Shaft_Waste_2005_2044	m^3	Volume of waste disposed of in shafts from 2005 through 2044	Scalar	Data
Inventory_Multiplier		Element used to set selected radionuclide inventories to zero	Vector (radionuclide)	Data
Transport_Pathway_Data				
Atmospheric_Transport				
Resident_Dust_Loading	kg/m^3	Dust loading for the Intruder – Post-Drilling and Intruder-Agriculture Scenarios	Scalar	Stochastic
Soil_Disturbance_Factor		Factor by which the dust loading is increased due to human disturbance of the surface soil	Scalar	Stochastic
Worker_Dust_Loading	kg/m^3	Dust loading for the Intruder-Construction Scenario	Scalar	Stochastic
Resuspension_Flux	$g/m^2/yr$	Resuspension for particulates at MDA G	Scalar	Stochastic
Enhancement_Factor		Ratio of radionuclide concentrations in the resuspendable fraction of the soil to those in the total soil	Scalar	Stochastic

Table 8 (Continued)
Input Data Requirements for the MDA G Intruder Model

Model Container/Parameter Name	Units	Parameter Description	Parameter Type	Input Element Type
Foodchain_Transport				
Plant_Data				
Uptake_Factors				
Leafy_Vegetable_GM	Ci/kg plant per Ci/kg soil (dry weight)	Geometric means of the plant uptake factors for leafy vegetables	Vector (element)	Data
Produce_GM	Ci/kg plant per Ci/kg soil (dry weight)	Geometric means of the plant uptake factors for produce	Vector (element)	Data
Grain_GM	Ci/kg plant per Ci/kg soil (dry weight)	Geometric means of the plant uptake factors for grain	Vector (element)	Data
PGrass_and_Native_GM	Ci/kg plant per Ci/kg soil (dry weight)	Geometric means of the plant uptake factors for pasture grass and native vegetation	Vector (element)	Data
Crop_GSD		Geometric standard deviation of the plant uptake factors for all crops	Scalar	Data
Crop_Characteristics				
Particle_Size_Factor		Ratio of radionuclide concentrations in the fraction of the soil resuspended due to rainsplash to those in the total soil	Scalar	Stochastic
Plant_Carbon_Fraction		Fraction of plant that is carbon (dry-weight basis)	Vector (crop)	Data
Plant_Hydrogen_Fraction		Fraction of plant that is hydrogen (dry-weight basis)	Vector (crop)	Data
Dry_to_Wet_Weight_Fractions				
DWW_Leafy_Vegetables		Dry-to-wet-weight fraction for leafy vegetables	Scalar	Stochastic

Table 8 (Continued)
Input Data Requirements for the MDA G Intruder Model

Model Container/Parameter Name	Units	Parameter Description	Parameter Type	Input Element Type
DWW_Produce		Dry-to-wet-weight fraction for produce	Scalar	Stochastic
DWW_Grain		Dry-to-wet-weight fraction for grain	Scalar	Stochastic
DWW_Pasture_Grass		Dry-to-wet-weight fraction for pasture grass	Scalar	Stochastic
Translocation_Factors				
TF_Leafy_Vegetables		Translocation factor for leafy vegetables	Scalar	Stochastic
TF_Produce		Translocation factor for produce	Scalar	Stochastic
TF_Grain		Translocation factor for grain	Scalar	Stochastic
TF_Pasture_Grass		Translocation factor for pasture grass	Scalar	Stochastic
Agricultural_Productivities				
AP_Leafy_Vegetables	kg (wet weight)/m^2	Agricultural productivity for leafy vegetables	Scalar	Stochastic
AP_Produce	kg (wet weight)/m^2	Agricultural productivity for produce	Scalar	Stochastic
AP_Grain	kg (wet weight)/m^2	Agricultural productivity for grain	Scalar	Stochastic
AP_Pasture_Grass	kg (dry weight)/m^2	Agricultural productivity for pasture grass	Scalar	Stochastic
Mass_Loading_Factors				
MLF_Leafy_Vegetables	g soil/g plant (dry weight)	Mass-loading factor for leafy vegetables	Scalar	Stochastic
MLF_Produce	g soil/g plant (dry weight)	Mass-loading factor for produce	Scalar	Stochastic

Table 8 (Continued)
Input Data Requirements for the MDA G Intruder Model

Model Container/Parameter Name	Units	Parameter Description	Parameter Type	Input Element Type
MLF_Grain	g soil/g plant (dry weight)	Mass-loading factor for grain	Scalar	Stochastic
MLF_Pasture_Grass	g soil/g plant (dry weight)	Mass-loading factor for pasture grass	Scalar	Stochastic
Animal_Data				
Animal_Ingestion_Data				
Cattle_and_Cows				
Cattle_Food_Ingestion	kg/d (dry weight)	Food consumption rate of cattle	Scalar	Stochastic
Cow_Food_Ingestion	kg/d (dry weight)	Food consumption rate of cows	Scalar	Stochastic
Cattle_Soil_Ingestion	kg/d (dry weight)	Soil consumption rate of cattle	Scalar	Stochastic
Cow_Soil_Ingestion	kg/d (dry weight)	Soil consumption rate of cows	Scalar	Stochastic
Cattle_Water_Ingestion	kg/d	Water consumption rate of cattle	Scalar	Stochastic
Cow_Water_Ingestion	kg/d	Water consumption rate of cows	Scalar	Stochastic
Chickens				
Chicken_Feed_Ingestion	kg/d (dry weight)	Food consumption rate of chickens	Scalar	Stochastic
Chicken_Water_Ingestion	kg/d	Water consumption rate of chickens	Scalar	Stochastic
Grit_to_Food_Ratio		Ratio of grit or soil intake to food intake for chickens	Scalar	Data

Table 8 (Continued)
Input Data Requirements for the MDA G Intruder Model

Model Container/Parameter Name	Units	Parameter Description	Parameter Type	Input Element Type
Transfer_Factors				
Beef_GM	d/kg	Geometric means of the forage-to-beef transfer factors	Vector (element)	Stochastic
Beef_GSD		Geometric standard deviation of the forage-to-beef transfer factors	Vector (element)	Data
Milk_GM	d/kg	Geometric means of the forage-to-milk transfer factors	Vector (element)	Stochastic
Milk_GSD		Geometric standard deviation of the forage-to-milk transfer factors	Vector (element)	Data
Chicken_GM	d/kg	Geometric means of the forage-to-chicken transfer factors	Vector (element)	Stochastic
Chicken_GSD		Geometric standard deviation of the forage-to-chicken transfer factors	Vector (element)	Data
Eggs_GM	d/kg	Geometric means of the forage-to-eggs transfer factors	Vector (element)	Stochastic
Eggs_GSD		Geometric standard deviation of the forage-to-eggs transfer factors	Vector (element)	Data
H3_and_C14_Transfer_Factors				
H3_Factors				
Water_Fraction_Animal_Products		Mass water fractions of animal products	Vector (animal product)	Data
C14_Factors				
Animal_Prod_Carbon_Fraction		Carbon fractions of animal products	Vector (animal product)	Data

Table 8 (Continued)
Input Data Requirements for the MDA G Intruder Model

Model Container/Parameter Name	Units	Parameter Description	Parameter Type	Input Element Type
Groundwater_Transport				
MdB_Infiltration_Rate	m/yr	Water infiltration rate on Mesita del Buey	Scalar	Stochastic
Biotic_Intrusion_Model				
Eco_Succession_Model				
Time_of_Climax	yr	Period required for disposal site to reach a piñon-juniper climax condition, measured from the time of facility closure	Scalar	Stochastic
Intrusion_Shape_Parameters				
Alpha_Shape_Factor		Shape factor used to model animal burrow and plant root distributions with depth	Scalar	Data
Beta_Shape_Factor		Shape factor used to model animal burrow and plant root distributions with depth	Scalar	Stochastic
Animal_Intrusion_Model				
Harvester_Ants				
Maximum_Burrow_Depth	m	Maximum burrowing depth for harvester ants	Scalar	Stochastic
Burrow_Density_Grassland	ha^{-1}	Density of harvester ant burrows during early succession	Scalar	Stochastic
Burrow_Density_Woodland	ha^{-1}	Density of harvester ant burrows in the piñon-juniper climax condition	Scalar	Stochastic
Burrow_Mass	kg	Mass of soil excavated per harvester ant burrow	Scalar	Stochastic
Colony_Life_Span	yr	Life span of harvester ant colonies	Scalar	Stochastic
Pocket_Gophers				
Maximum_Burrow_Depth	m	Maximum burrowing depth for pocket gophers	Scalar	Stochastic

Table 8 (Continued)
Input Data Requirements for the MDA G Intruder Model

Model Container/Parameter Name	Units	Parameter Description	Parameter Type	Input Element Type
Soil_Removal_Rate_Grassland	m^3/ha	Rate of soil removal by pocket gophers during early succession	Scalar	Stochastic
Soil_Removal_Rate_Woodland	m^3/ha	Rate of soil removal by pocket gophers in the piñon-juniper climax condition	Scalar	Stochastic
Burrow_Renewal_Rate	yr^{-1}	Rate at which existing pocket gopher burrows are replaced with new ones	Scalar	Stochastic
Mice				
Maximum_Burrow_Depth	m	Maximum burrowing depth for mice	Scalar	Stochastic
Burrow_Density_Grassland	ha^{-1}	Density of mouse burrows during early succession	Scalar	Stochastic
Burrow_Density_Woodland	ha^{-1}	Density of mouse burrows in the piñon-juniper climax condition	Scalar	Stochastic
Burrow_Volume	kg	Volume of soil excavated per mouse burrow	Scalar	Stochastic
Burrow_Renewal_Rate	yr^{-1}	Rate at which existing mouse burrows are replaced with new ones	Scalar	Stochastic
Chipmunks_and_Squirrels				
Maximum_Burrow_Depth	m	Maximum burrowing depth for chipmunks and ground squirrels	Scalar	Stochastic
Burrow_Density_Grassland	ha^{-1}	Density of chipmunk and ground squirrel burrows during early succession	Scalar	Stochastic
Burrow_Density_Woodland	ha^{-1}	Density of chipmunk and ground squirrel burrows in the piñon-juniper climax condition	Scalar	Stochastic
Burrow_Volume	kg	Volume of soil excavated per chipmunk and ground squirrel burrow	Scalar	Stochastic

Table 8 (Continued)
Input Data Requirements for the MDA G Intruder Model

Model Container/Parameter Name	Units	Parameter Description	Parameter Type	Input Element Type
Burrow_Renewal_Rate	yr^{-1}	Rate at which existing chipmunk and ground squirrel burrows are replaced with new ones	Scalar	Stochastic
Plant_Intrusion_Model				
Litter_Halflife	yr	Decomposition half-life of plant litter	Scalar	Stochastic
Grasses				
Maximum_Root_Depth	m	Maximum rooting depth of grasses	Scalar	Stochastic
Biomass_Density_Grassland	kg/m^2	Aboveground biomass density of grasses during early succession	Scalar	Stochastic
Biomass_Density_Woodland	kg/m^2	Aboveground biomass density of grasses in the piñon-juniper climax condition	Scalar	Stochastic
Litter_Prod_Rate	yr^{-1}	Fraction of the aboveground biomass that falls as litter	Scalar	Stochastic
Forbs				
Maximum_Root_Depth	m	Maximum rooting depth of forbs	Scalar	Stochastic
Biomass_Density_Grassland	kg/m^2	Aboveground biomass density of forbs during early succession	Scalar	Stochastic
Biomass_Density_Woodland	kg/m^2	Aboveground biomass density of forbs in the piñon-juniper climax condition	Scalar	Stochastic
Litter_Prod_Rate	yr^{-1}	Fraction of the aboveground biomass that falls as litter	Scalar	Stochastic
Shrubs				
Maximum_Root_Depth	m	Maximum rooting depth of shrubs	Scalar	Stochastic
Biomass_Density_Grassland	kg/m^2	Aboveground biomass density of shrubs during early succession	Scalar	Stochastic

Table 8 (Continued)
Input Data Requirements for the MDA G Intruder Model

Model Container/Parameter Name	Units	Parameter Description	Parameter Type	Input Element Type
Biomass_Density_Woodland	kg/m^2	Aboveground biomass density of shrubs in the piñon-juniper climax condition	Scalar	Stochastic
Litter_Prod_Rate	yr^{-1}	Fraction of the aboveground biomass that falls as litter	Scalar	Stochastic
Trees				
Maximum_Root_Depth	m	Maximum rooting depth of trees	Scalar	Stochastic
Biomass_Density_Grassland	kg/m^2	Aboveground biomass density of trees during early succession	Scalar	Stochastic
Biomass_Density_Woodland	kg/m^2	Aboveground biomass density of trees in the piñon-juniper climax condition	Scalar	Stochastic
Litter_Prod_Rate	yr^{-1}	Fraction of the aboveground biomass that falls as litter	Scalar	Stochastic
Erosion_Model				
Erosion_Rates				
Erosion_Rate_Functions	yr^{-1}	Cover loss rate as a function of time	Scalar	Lookup Table
Erosion_Zone_Data				
Remaining_Cover_EZ1	m	Minimum cover remaining in erosion zone 1	Scalar	Stochastic
Remaining_Cover_EZ2	m	Minimum cover remaining in erosion zone 2	Scalar	Stochastic
Remaining_Cover_EZ3	m	Minimum cover remaining in erosion zone 3	Scalar	Stochastic
Remaining_Cover_EZ4	m	Minimum cover remaining in erosion zone 4	Scalar	Stochastic
Remaining_Cover_EZ5	m	Minimum cover remaining in erosion zone 5	Scalar	Stochastic
Remaining_Cover_EZ6	m	Minimum cover remaining in erosion zone 6	Scalar	Stochastic
Remaining_Cover_EZ7	m	Minimum cover remaining in erosion zone 7	Scalar	Stochastic

Table 8 (Continued)
Input Data Requirements for the MDA G Intruder Model

Model Container/Parameter Name	Units	Parameter Description	Parameter Type	Input Element Type
Remaining_Cover_EZ8	m	Minimum cover remaining in erosion zone 8	Scalar	Stochastic
Remaining_Cover_EZ9	m	Minimum cover remaining in erosion zone 9	Scalar	Stochastic
Remaining_Cover_EZ10	m	Minimum cover remaining in erosion zone 10	Scalar	Stochastic
Erosion_Shape_Parameters				
Alpha_Shape_Factor		Shape factor used to model surface erosion	Scalar	Data
Beta_Shape_Factor		Shape factor used to model surface erosion	Scalar	Stochastic
Human_Intrusion_Model				
Basement_Length	m	Length of the intruder's basement	Scalar	Data
Basement_Width	m	Width of the intruder's basement	Scalar	Data
Basement_Depth	m	Depth of the intruder's basement	Scalar	Data
Well_Casing_Diameter	m	Diameter of the well casing	Scalar	Data
Dose_and_WAC_Model				
Dose_Conversion_Factors				
Ingestion_DCFs	mrem/pCi	Dose conversion factors for the ingestion exposure route	Vector (radionuclide)	Data
Inhalation_DCFs	mrem/pCi	Dose conversion factors for the inhalation exposure route	Vector (radionuclide)	Data
Soil_External_DCFs_15_cm	mrem/yr per pCi/m^3	Dose conversion factors for direct radiation from soils contaminated to a depth of 15 cm	Vector (radionuclide)	Data
Soil_External_DCFs_Infinite	mrem/yr per pCi/m^3	Dose conversion factors for direct radiation from soils contaminated to an infinite depth	Vector (radionuclide)	Data

Table 8 (Continued)
Input Data Requirements for the MDA G Intruder Model

Model Container/Parameter Name	Units	Parameter Description	Parameter Type	Input Element Type
Air_External_DCFs	mrem/yr per pCi/m^3	Dose conversion factors for direct radiation from air immersion	Vector (radionuclide)	Data
Exposure_Pathway_Data				
Minimum_Soil_Mixing_Depth	m	Contaminant mixing depth	Scalar	Data
Shielding_Factor		Direct radiation shielding factor for the time spent indoors	Scalar	Stochastic
Resident_Inhalation_Rate	m^3/d	Inhalation rate of the resident intruder	Scalar	Stochastic
Worker_Inhalation_Rate	m^3/d	Inhalation rate of the construction intruder	Scalar	Stochastic
Area_of_Lot	m^2	Area of the receptor's lot	Scalar	Stochastic
Area_of_House	m^2	Area of the receptor's house	Scalar	Data
Resident_Intruder_PO	mrem/yr	Performance objective for the postdrilling and agricultural intruders	Scalar	Data
Construction_Intruder_PO	mrem/yr	Performance objective for the construction worker	Scalar	Data
Exposure_Times				
Resident_Indoor_Exposure_Time	hr/d	Time spent inside by the resident intruder	Scalar	Stochastic
Resident_Outdoor_Exposure_Time	hr/d	Time spent outside by the resident intruder	Scalar	Stochastic
Worker_Exposure_Time	hr/d	Time spent building the house by the construction worker	Scalar	Data
Excavation_Occupancy_Factor		Fraction of time spent building the house that is spent in the bottom of the basement excavation	Scalar	Stochastic
Ingestion_Data				
Resident_Soil_Ingestion_Rate	kg (dry weight)/yr	Rate of soil ingestion for the resident intruder	Scalar	Stochastic

Table 8 (Continued)
Input Data Requirements for the MDA G Intruder Model

Model Container/Parameter Name	Units	Parameter Description	Parameter Type	Input Element Type
Worker_Soil_Ingestion_Rate	kg (dry weight)/yr	Rate of soil ingestion for the construction worker	Scalar	Stochastic
Food_Ingestion_Data				
Input_Vegetable_Fraction		User-specified fraction of the receptor's diet of leafy vegetables, produce, and grain that is grown at the receptor's location	Scalar	Stochastic
Animals_Raised		The types of animals raised by the receptor to supply a portion of their diet	Scalar	Stochastic
Crop_Ingestion_Rates				
CI_Leafy_Vegetables	kg (wet weight)/yr	Rate of ingestion of leafy vegetables for the resident intruders	Scalar	Stochastic
CI_Produce	kg (wet weight)/yr	Rate of ingestion of produce for the resident intruders	Scalar	Stochastic
CI_Grain	kg (wet weight)/yr	Rate of ingestion of grain for the resident intruders	Scalar	Stochastic
Animal_Product_Ingestion_Rates				
API_Beef	kg/yr	Rate of ingestion of beef for the resident intruders	Scalar	Stochastic
API_Milk	kg/yr	Rate of ingestion of milk for the resident intruders	Scalar	Stochastic
API_Chicken	kg/yr	Rate of ingestion of chicken for the resident intruders	Scalar	Stochastic
API_Eggs	kg/yr	Rate of ingestion of eggs for the resident intruders	Scalar	Stochastic
Animal_Numbers				
Cattle_Weight_at_Slaughter	kg	Weight of cattle at the time of slaughter	Scalar	Stochastic
Dressing_Percentage		Ratio of the carcass weight to live weight of the animal	Scalar	Stochastic

Table 8 (Continued)
Input Data Requirements for the MDA G Intruder Model

Model Container/Parameter Name	Units	Parameter Description	Parameter Type	Input Element Type
Cutability		Fraction of the carcass that is sold as meat	Scalar	Stochastic
Milk_Production_Rate	kg/yr	Production rate of milk by cows	Scalar	Stochastic
Chicken_Weight_at_Slaughter	kg	Weight of chicken at the time of slaughter	Scalar	Stochastic
Cook_to_Live_Ratio		Ratio of ready to cook weight of chicken to the live weight of the bird	Scalar	Stochastic
Meat_Fraction		Fraction of the cooked chicken that is meat	Scalar	Stochastic
Egg_Production_Rate	d^{-1}	Production rate of eggs by layers	Scalar	Stochastic
Egg_Mass	kg	Mass of egg	Scalar	Stochastic
Shell_Fraction		Fraction of the egg mass that is contributed by the shell	Scalar	Data
Animal_Product_Fractions				
Beef		User-specified fraction of the receptor's diet of beef that is taken from animals living at the exposure location	Scalar	Stochastic
Milk		User-specified fraction of the receptor's diet of milk that is produced by animals living at the exposure location	Scalar	Stochastic
Chicken		User-specified fraction of the receptor's diet of chicken that is taken from animals living at the exposure location	Scalar	Stochastic
Eggs		User-specified fraction of the receptor's diet of eggs that is produced by animals living at the exposure location	Scalar	Stochastic

Table 9
Input Data Requirements for the MDA G Intruder Diffusion Model

Model Container/Parameter Name	Units	Parameter Description	Parameter Type	Input Element Type
Controls_and_Constants				
Intruder_Flag		Flag used to indicate which intruder scenario is being evaluated. A value of 1 indicates the Intruder – Post-Drilling Scenario is under consideration; a value of 2 indicates the Intruder-Agriculture Scenario is being modeled; a value of 3 indicates the Intruder-Construction Scenario is being assessed.	Scalar	Data
Disposal_Unit_Flag		Flag used to indicate which disposal units are being simulated. Values of 1 and 2 are used to consider the 1988–2004 and 2005–2044 disposal pits, respectively; values of 3 and 4 specify the 1988–2004 and 2005–2044 disposal shafts.	Scalar	Data
Diffusion_Flag		Flag used to indicate whether the effects of vapor- and gas-phase diffusion are taken into account in the intruder modeling. A value of 0 indicates that the effects of diffusion are not taken into account; a value of 1 indicates diffusive transport is modeled.	Scalar	Data
Biotic_Intrusion_Flag		Flag used to specify if the effects of biotic intrusion will be taken into account in the intruder modeling. A value of 0 indicates that biotic intrusion will not be considered; a value of 1 specifies allows plant and animal intrusion into the disposal site prior to the time of human intrusion.	Scalar	Data
Inventory_Flag		Flag used to indicate whether unit inventories or actual pit and shaft inventories are used in the modeling. A value of 1 is input to use unit inventories; a value of 2 specifies that actual disposal unit inventories will be used.	Scalar	Data

Table 9 (Continued)
Input Data Requirements for the MDA G Intruder Diffusion Model

Model Container/Parameter Name	Units	Parameter Description	Parameter Type	Input Element Type
Depth_of_Disposal_Flag		Flag used to indicate whether the input inventory will be distributed homogeneously throughout the disposal units or the waste-layer-specific inventories will be used. A value of 1 is input to use a homogeneously distributed inventory; a value of 2 specifies that waste layer specific inventories will be applied.	Scalar	Data
Disposal_System_Information				
Species_and_Materials				
Halflives	yr	Radionuclide half-lives	Vector (radionuclide)	Data
Material_Properties				
Density_of_Water	kg/m^3	Density of water	Scalar	Data
Soil_Carbon_Fraction		Fraction of surface soil that is carbon	Scalar	Data
Water_Carbon_Fraction		Fraction of water that is carbon	Scalar	Data
Water_Hydrogen_Fraction		Fraction of water that is hydrogen	Scalar	Data
Air_Diffusion_Length	m	Diffusion length in air	Scalar	Data
Radon_Emanation_Coefficient		Emanation coefficient for Rn-220 and Rn-222	Scalar	Stochastic
C-14_Gas_Generation_Rate	yr^{-1}	Rate constant describing the rate of C-14 gas generation due to biodegradation of organic waste	Scalar	Stochastic
CO2_Fraction		Fraction of C-14 gas generated by the biodegradation of organic waste that is carbon dioxide	Scalar	Stochastic
Organic_Waste_Fraction		Fraction of C-14 waste that is organic and susceptible to biodegradation	Scalar	Stochastic

Table 9 (Continued)
Input Data Requirements for the MDA G Intruder Diffusion Model

Model Container/Parameter Name	Units	Parameter Description	Parameter Type	Input Element Type
Dry_Densities				
DD_Crushed_Tuff	kg/m³	Dry density of crushed tuff	Scalar	Stochastic
DD_Waste	kg/m³	Dry density of waste	Scalar	Stochastic
DD_Concrete	kg/m³	Dry density of concrete	Scalar	Stochastic
Moisture_Contents				
MC_Crushed_Tuff	(volume basis)	Moisture content of crushed tuff	Scalar	Stochastic
MC_Waste	(volume basis)	Moisture content of waste	Scalar	Stochastic
Concrete_Saturation		Saturation level of concrete	Scalar	Stochastic
Effective_Porosities				
EP_Crushed_Tuff		Effective porosity of crushed tuff	Scalar	Stochastic
EP_Waste		Effective porosity of waste	Scalar	Stochastic
EP_Concrete		Effective porosity of concrete	Scalar	Stochastic
Partition_Coefficients				
Soil_and_Waste_KDs				
Elemental_Kds	m³/kg	Elemental distribution coefficients for crushed tuff, waste, and concrete	Vector (element)	Data
Kd_Distributions				
Pu	m³/kg	Distribution coefficient for plutonium in crushed tuff, waste, and concrete	Scalar	Stochastic
Ra	m³/kg	Distribution coefficient for radium in crushed tuff, waste, and concrete	Scalar	Stochastic

Table 9 (Continued)
Input Data Requirements for the MDA G Intruder Diffusion Model

Model Container/Parameter Name	Units	Parameter Description	Parameter Type	Input Element Type
Th	m^3/kg	Distribution coefficient for thorium in crushed tuff, waste, and concrete	Scalar	Stochastic
U	m^3/kg	Distribution coefficient for uranium in crushed tuff, waste, and concrete	Scalar	Stochastic
Air_to_Water_Coefficients				
Soil_Temperature	°K	Temperature of the cap and waste	Scalar	Stochastic
Tritium_Coefficient				
H2O_Vapor_Pressure	atm	Vapor pressure of water	Scalar	Data
H2O_Molecular_Weight	g/mol	Molecular weight of water	Scalar	Data
CO2_Coefficient				
CO2_Henry's_Law_Constant	mol/L-atm	Henry's Law constant for carbon dioxide	Scalar	Data
CH4_Coefficient				
CH4_Henrys_Law_Constant	mol/L-atm	Henry's Law constant for methane	Scalar	Data
Kr_Coefficient				
Kr_Henry's_Law_Constant	mol/L-atm	Henry's Law constant for krypton	Scalar	Data
Rn_Coefficient				
Rn_Henrys_Law_Constant	mol/L-atm	Henry's Law constant for radon	Scalar	Data
Relative_Diffusivities				
Free_Air_Diff_Coefficients	cm^2/s	Free-air diffusion coefficients	Vector (radionuclide)	Data

Table 9 (Continued)
Input Data Requirements for the MDA G Intruder Diffusion Model

Model Container/Parameter Name	Units	Parameter Description	Parameter Type	Input Element Type
Thermal_Gradient_Factor		Factor used to account for the effects of thermal gradients on the rate of diffusion of tritiated water vapor	Scalar	Stochastic
Reference_Diff_Coefficient	cm^2/s	Reference diffusion coefficient	Scalar	Data
Attenuation_Coefficients				
Soil_Mass_Atten_Coeff	cm^2/g	Mass attenuation coefficient for soil	Vector (radionuclide)	Data
Concrete_Mass_Atten_Coeff	cm^2/g	Mass attenuation coefficient for concrete	Vector (radionuclide)	Data
Site_Geometry_and_Operations				
Institutional_Control_Period	yr	The length of the institutional control period, measured from the time of facility closure	Scalar	Data
Closure_Period	yr	The length of time required to achieve final closure of the disposal facility following the end of disposal operations	Scalar	Data
Disposal_Unit_Area	m^2	Surface area of the disposal units	Scalar	Data
Minimum_Air_Thickness	cm	Minimum thickness used to calculate the amount of air in the cap cells	Scalar	Data
Concrete_Floor_Thickness	m	The thickness of the floor of the concrete foundation of the intruder's house	Scalar	Data
Number_of_Basement_Layers		The number of discrete layers used to represent the floor of the intruder's foundation	Scalar	Data
Layer_Information				
Number_of_Waste_Layers		The number of discrete layers used to represent the disposed waste	Scalar	Data

Table 9 (Continued)
Input Data Requirements for the MDA G Intruder Diffusion Model

Model Container/Parameter Name	Units	Parameter Description	Parameter Type	Input Element Type
Number_of_Cap_Layers		The number of discrete layers used to represent the cap	Scalar	Data
Disposal_Pits				
Pits_1988_2004				
Initial_Cover_Thickness	m	Initial thickness of the cover over the disposal units	Scalar	Stochastic
Surface_Soil_Thickness	m	Thickness of the surface soil layer	Vector (disposal region)	Data
Waste_Thickness	m	Thickness of the disposed waste	Vector (disposal region)	Data
Waste_Emplacement_Efficiency		The fraction of the disposal capacity of the pits filled with waste	Scalar	Data
Start_of_Disposal	yr	The first year of the simulation that waste is placed in the disposal units	Scalar	Data
End_of_Disposal	yr	The last year of the simulation that waste is placed in the disposal units	Scalar	Data
Fractional_Area_Calculations				
Low_Erosion_Fraction		Fractional area of the erosion zones for the low-erosion scenario at the end of the simulation	Vector (erosion zone)	Data
Moderate_Erosion_Fraction		Fractional area of the erosion zones for the moderate-erosion scenario at the end of the simulation	Vector (erosion zone)	Data
High_Erosion_Fraction		Fractional area of the erosion zones for the high-erosion scenario at the end of the simulation	Vector (erosion zone)	Data
Pits_2005_2044				
Initial_Cover_Thickness	m	Initial thickness of the cover over the disposal units	Scalar	Stochastic

Table 9 (Continued)
Input Data Requirements for the MDA G Intruder Diffusion Model

Model Container/Parameter Name	Units	Parameter Description	Parameter Type	Input Element Type
Surface_Soil_Thickness	m	Thickness of the surface soil layer	Vector (disposal region)	Data
Waste_Thickness	m	Thickness of the disposed waste	Vector (disposal region)	Data
Waste_Emplacement_Efficiency		The fraction of the disposal capacity of the pits filled with waste	Scalar	Data
Start_of_Disposal	yr	The first year of the simulation that waste is placed in the disposal units	Scalar	Data
End_of_Disposal	yr	The last year of the simulation that waste is placed in the disposal units	Scalar	Data
Fractional_Area_Calculations				
Low_Erosion_Fraction		Fractional area of the erosion zones for the low-erosion scenario at the end of the simulation	Vector (erosion zone)	Data
Moderate_Erosion_Fraction		Fractional area of the erosion zones for the moderate-erosion scenario at the end of the simulation	Vector (erosion zone)	Data
High_Erosion_Fraction		Fractional area of the erosion zones for the high-erosion scenario at the end of the simulation	Vector (erosion zone)	Data
Disposal_Shafts				
Shafts_1988_2004				
Initial_Cover_Thickness	m	Initial thickness of the cover over the disposal units	Scalar	Stochastic
Surface_Soil_Thickness	m	Thickness of the surface soil layer	Vector (disposal region)	Data
Waste_Thickness	m	Thickness of the disposed waste	Vector (disposal region)	Data

Table 9 (Continued)
Input Data Requirements for the MDA G Intruder Diffusion Model

Model Container/Parameter Name	Units	Parameter Description	Parameter Type	Input Element Type
Shaft_Field_Efficiency		The fraction of the surface area of the shaft field that is occupied by disposal shafts	Scalar	Data
Waste_Emplacement_Efficiency		The fraction of the disposal capacity of the shafts filled with waste	Scalar	Data
Start_of_Disposal	yr	The first year of the simulation that waste is placed in the disposal units	Scalar	Data
End_of_Disposal	yr	The last year of the simulation that waste is placed in the disposal units	Scalar	Data
Fractional_Area_Calculations				
Low_Erosion_Fraction		Fractional area of the erosion zones for the low-erosion scenario at the end of the simulation	Vector (erosion zone)	Data
Moderate_Erosion_Fraction		Fractional area of the erosion zones for the moderate-erosion scenario at the end of the simulation	Vector (erosion zone)	Data
High_Erosion_Fraction		Fractional area of the erosion zones for the high-erosion scenario at the end of the simulation	Vector (erosion zone)	Data
Shafts_2005_2044				
Initial_Cover_Thickness	m	Initial thickness of the cover over the disposal units	Scalar	Stochastic
Surface_Soil_Thickness	m	Thickness of the surface soil layer	Vector (disposal region)	Data
Waste_Thickness	m	Thickness of the disposed waste	Vector (disposal region)	Data
Shaft_Field_Efficiency		The fraction of the surface area of the shaft field that is occupied by disposal shafts	Scalar	Data

Table 9 (Continued)
Input Data Requirements for the MDA G Intruder Diffusion Model

Model Container/Parameter Name	Units	Parameter Description	Parameter Type	Input Element Type
Waste_Emplacement_Efficiency		The fraction of the disposal capacity of the shafts filled with waste	Scalar	Data
Start_of_Disposal	yr	The first year of the simulation that waste is placed in the disposal units	Scalar	Data
End_of_Disposal	yr	The last year of the simulation that waste is placed in the disposal units	Scalar	Data
Fractional_Area_Calculations				
Low_Erosion_Fraction		Fractional area of the erosion zones for the low-erosion scenario at the end of the simulation	Vector (erosion zone)	Data
Moderate_Erosion_Fraction		Fractional area of the erosion zones for the moderate-erosion scenario at the end of the simulation	Vector (erosion zone)	Data
High_Erosion_Fraction		Fractional area of the erosion zones for the high-erosion scenario at the end of the simulation	Vector (erosion zone)	Data
Inventory				
Unit_Inventory				
Assumed_Inventory	Ci	The as-disposed inventory for all parent radionuclides included in the intruder modeling	Scalar	Data
Inventory_Distribution_Factor		Fraction of assumed inventory in each layer of waste in the disposal units.	Vector (waste inventory layers)	Data

Table 9 (Continued)
Input Data Requirements for the MDA G Intruder Diffusion Model

Model Container/Parameter Name	Units	Parameter Description	Parameter Type	Input Element Type
As_Disposed_Inventory				
Measurement_Errors				
Rad_Specific_Errors				
Pre_1990_Lower_Bounds		Factor used to estimate the lower bound of pre-1990 radionuclide inventories, taking into account errors introduced by measurement uncertainty	Vector (radionuclide)	Data
Pre_1990_Upper_Bounds		Factor used to estimate the upper bound of pre-1990 radionuclide inventories, taking into account errors introduced by measurement uncertainty	Vector (radionuclide)	Data
Post_1989_Lower_Bounds		Factor used to estimate the lower bound of post-1989 radionuclide inventories, taking into account errors introduced by measurement uncertainty	Vector (radionuclide)	Data
Post_1989_Upper_Bounds		Factor used to estimate the upper bound of post-1989 radionuclide inventories, taking into account errors introduced by measurement uncertainty	Vector (radionuclide)	Data
Material_Type_Errors				
Pre_1990_Lower_Bounds		Factor used to estimate the lower bound of pre-1990 material type inventories, taking into account errors introduced by measurement uncertainty	Vector (material type)	Data
Pre_1990_Upper_Bounds		Factor used to estimate the upper bound of pre-1990 material type inventories, taking into account errors introduced by measurement uncertainty	Vector (material type)	Data
Post_1989_Lower_Bounds		Factor used to estimate the lower bound of post-1989 material type inventories, taking into account errors introduced by measurement uncertainty	Vector (material type)	Data

Table 9 (Continued)
Input Data Requirements for the MDA G Intruder Diffusion Model

Model Container/Parameter Name	Units	Parameter Description	Parameter Type	Input Element Type
Post_1989_Upper_Bounds		Factor used to estimate the upper bound of post-1989 material type inventories, taking into account errors introduced by measurement uncertainty	Vector (material type)	Data
Rad_Specific_Inventories				
Pit_Waste_1988_2004				
Depth_Indept_Inventory				
Pre_1990_PA_Point_Estimate	Ci	Point estimates of radionuclide-specific inventories in the pre-1990 performance assessment waste disposed of in 1988–2004 pits	Vector (radionuclide)	Data
Post_1989_PA_Point_Estimate	Ci	Point estimates of radionuclide-specific inventories in the post-1989 performance assessment waste disposed of in 1988–2004 pits	Vector (radionuclide)	Data
Depth_Dept_Inventory				
Pre_1990_PA_PtEst_Layer1	Ci	Point estimates of radionuclide-specific inventories in waste inventory layer 1 of the pre-1990 performance assessment waste disposed of in 1988–2004 pits	Vector (radionuclide)	Data
Pre_1990_PA_PtEst_Layer2	Ci	Point estimates of radionuclide-specific inventories in waste inventory layer 2 of the pre-1990 performance assessment waste disposed of in 1988–2004 pits	Vector (radionuclide)	Data
Pre_1990_PA_PtEst_Layer3	Ci	Point estimates of radionuclide-specific inventories in waste inventory layer 3 of the pre-1990 performance assessment waste disposed of in 1988–2004 pits	Vector (radionuclide)	Data
Pre_1990_PA_PtEst_Layer4	Ci	Point estimates of radionuclide-specific inventories in waste inventory layer 4 of the pre-1990 performance assessment waste disposed of in 1988–2004 pits	Vector (radionuclide)	Data

Table 9 (Continued)
Input Data Requirements for the MDA G Intruder Diffusion Model

Model Container/Parameter Name	Units	Parameter Description	Parameter Type	Input Element Type
Post_1989_PA_PtEst_Layer1	Ci	Point estimates of radionuclide-specific inventories in waste inventory layer 1 of the post-1989 performance assessment waste disposed of in 1988–2004 pits	Vector (radionuclide)	Data
Post_1989_PA_PtEst_Layer2	Ci	Point estimates of radionuclide-specific inventories in waste inventory layer 2 of the post-1989 performance assessment waste disposed of in 1988–2004 pits	Vector (radionuclide)	Data
Post_1989_PA_PtEst_Layer3	Ci	Point estimates of radionuclide-specific inventories in waste inventory layer 3 of the post-1989 performance assessment waste disposed of in 1988–2004 pits	Vector (radionuclide)	Data
Post_1989_PA_PtEst_Layer4	Ci	Point estimates of radionuclide-specific inventories in waste inventory layer 4 of the post-1989 performance assessment waste disposed of in 1988–2004 pits	Vector (radionuclide)	Data
Pit_Waste_2005_2044				
Depth_Indept_Inventory				
Post_1989_PA_Point_Estimate	Ci	Point estimates of radionuclide-specific inventories in the post-1989 performance assessment waste disposed of in 2005–2044 pits	Vector (radionuclide)	Data
Depth_Dept_Inventory				
Post_1989_PA_PtEst_Layer1	Ci	Point estimates of radionuclide-specific inventories in waste inventory layer 1 of the post-1989 performance assessment waste disposed of in 2005-2044 pits	Vector (radionuclide)	Data
Post_1989_PA_PtEst_Layer2	Ci	Point estimates of radionuclide-specific inventories in waste inventory layer 2 of the post-1989 performance assessment waste disposed of in 2005-2044 pits	Vector (radionuclide)	Data

Table 9 (Continued)
Input Data Requirements for the MDA G Intruder Diffusion Model

Model Container/Parameter Name	Units	Parameter Description	Parameter Type	Input Element Type
Post_1989_PA_PtEst_Layer3	Ci	Point estimates of radionuclide-specific inventories in waste inventory layer 3 of the post-1989 performance assessment waste disposed of in 2005-2044 pits	Vector (radionuclide)	Data
Post_1989_PA_PtEst_Layer4	Ci	Point estimates of radionuclide-specific inventories in waste inventory layer 4 of the post-1989 performance assessment waste disposed of in 2005-2044 pits	Vector (radionuclide)	Data
Post_1989_PA_PtEst_Layer1	Ci	Point estimates of radionuclide-specific inventories in waste inventory layer 1 of the post-1989 performance assessment waste disposed of in 2005-2044 pits	Vector (radionuclide)	Data
Shaft_Waste_1988_2004				
Depth_Indept_Inventory				
Pre_1990_PA_Point_Estimate	Ci	Point estimates of radionuclide-specific inventories in the pre-1990 performance assessment waste disposed of in 1988–2004 shafts	Vector (radionuclide)	Data
Post_1989_PA_Point_Estimate	Ci	Point estimates of radionuclide-specific inventories in the post-1989 performance assessment waste disposed of in 2005–2044 shafts	Vector (radionuclide)	
Depth_Dept_Inventory				
Pre_1990_PA_PtEst_Layer1	Ci	Point estimates of radionuclide-specific inventories in waste inventory layer 1 of the pre-1990 performance assessment waste disposed of in 1988–2004 shafts	Vector (radionuclide)	Data
Pre_1990_PA_PtEst_Layer2	Ci	Point estimates of radionuclide-specific inventories in waste inventory layer 2 of the pre-1990 performance assessment waste disposed of in 1988–2004 shafts	Vector (radionuclide)	Data

Table 9 (Continued)
Input Data Requirements for the MDA G Intruder Diffusion Model

Model Container/Parameter Name	Units	Parameter Description	Parameter Type	Input Element Type
Pre_1990_PA_PtEst_Layer3	Ci	Point estimates of radionuclide-specific inventories in waste inventory layer 3 of the pre-1990 performance assessment waste disposed of in 1988–2004 shafts	Vector (radionuclide)	Data
Pre_1990_PA_PtEst_Layer4	Ci	Point estimates of radionuclide-specific inventories in waste inventory layer 4 of the pre-1990 performance assessment waste disposed of in 1988–2004 shafts	Vector (radionuclide)	Data
Post_1989_PA_PtEst_Layer1	Ci	Point estimates of radionuclide-specific inventories in waste inventory layer 1 of the post-1989 performance assessment waste disposed of in 1988–2004 shafts	Vector (radionuclide)	Data
Post_1989_PA_PtEst_Layer2	Ci	Point estimates of radionuclide-specific inventories in waste inventory layer 2 of the post-1989 performance assessment waste disposed of in 1988–2004 shafts	Vector (radionuclide)	Data
Post_1989_PA_PtEst_Layer3	Ci	Point estimates of radionuclide-specific inventories in waste inventory layer 3 of the post-1989 performance assessment waste disposed of in 1988–2004 shafts	Vector (radionuclide)	Data
Post_1989_PA_PtEst_Layer4	Ci	Point estimates of radionuclide-specific inventories in waste inventory layer 4 of the post-1989 performance assessment waste disposed of in 1988–2004 shafts	Vector (radionuclide)	Data
Shaft_Waste_2005_2044				
Depth_Indept_Inventory				
Post_1989_PA_Point_Estimate	Ci	Point estimates of radionuclide-specific inventories in the post-1989 performance assessment waste disposed of in 2005–2044 shafts	Vector (radionuclide)	Data

Table 9 (Continued)
Input Data Requirements for the MDA G Intruder Diffusion Model

Model Container/Parameter Name	Units	Parameter Description	Parameter Type	Input Element Type
Depth_Dept_Inventory				
Post_1989_PA_PtEst_Layer1	Ci	Point estimates of radionuclide-specific inventories in waste inventory layer 1 of the post-1989 performance assessment waste disposed of in 2005-2044 shafts	Vector (radionuclide)	Data
Post_1989_PA_PtEst_Layer2	Ci	Point estimates of radionuclide-specific inventories in waste inventory layer 2 of the post-1989 performance assessment waste disposed of in 2005-2044 shafts	Vector (radionuclide)	Data
Post_1989_PA_PtEst_Layer3	Ci	Point estimates of radionuclide-specific inventories in waste inventory layer 3 of the post-1989 performance assessment waste disposed of in 2005-2044 shafts	Vector (radionuclide)	Data
Post_1989_PA_PtEst_Layer4	Ci	Point estimates of radionuclide-specific inventories in waste inventory layer 4 of the post-1989 performance assessment waste disposed of in 2005-2044 shafts	Vector (radionuclide)	Data
Material_Type_Inventories				
Pit_Waste_1988_2004				
Depth_Indept_Inventory				
Pre_1990_PA_Point_Estimate	Ci	Point estimates of material type inventories in the pre-1990 performance assessment waste disposed of in 1988–2004 pits	Vector (material type)	Data
Post_1989_PA_Point_Estimate	Ci	Point estimates of material type inventories in the post-1989 performance assessment waste disposed of in 1988–2004 pits	Vector (material type)	Data
Depth_Dept_Inventory				
Pre_1990_PA_PtEst_Layer1	Ci	Point estimates of material type inventories in waste inventory layer 1 of the pre-1990 performance assessment waste disposed of in 1988–2004 pits	Vector (material type)	Data

Table 9 (Continued)
Input Data Requirements for the MDA G Intruder Diffusion Model

Model Container/Parameter Name	Units	Parameter Description	Parameter Type	Input Element Type
Pre_1990_PA_PtEst_Layer2	Ci	Point estimates of material type inventories in waste inventory layer 2 of the pre-1990 performance assessment waste disposed of in 1988–2004 pits	Vector (material type)	Data
Pre_1990_PA_PtEst_Layer3	Ci	Point estimates of material type inventories in waste inventory layer 3 of the pre-1990 performance assessment waste disposed of in 1988–2004 pits	Vector (material type)	Data
Pre_1990_PA_PtEst_Layer4	Ci	Point estimates of material type inventories in waste inventory layer 4 of the pre-1990 performance assessment waste disposed of in 1988–2004 pits	Vector (material type)	Data
Post_1989_PA_PtEst_Layer1	Ci	Point estimates of material type inventories in waste inventory layer 1 of the post-1989 performance assessment waste disposed of in 1988–2004 pits	Vector (material type)	Data
Post_1989_PA_PtEst_Layer2	Ci	Point estimates of material type inventories in waste inventory layer 2 of the post-1989 performance assessment waste disposed of in 1988–2004 pits	Vector (material type)	Data
Post_1989_PA_PtEst_Layer3	Ci	Point estimates of material type inventories in waste inventory layer 3 of the post-1989 performance assessment waste disposed of in 1988–2004 pits	Vector (material type)	Data
Post_1989_PA_PtEst_Layer4	Ci	Point estimates of material type inventories in waste inventory layer 4 of the post-1989 performance assessment waste disposed of in 1988–2004 pits	Vector (material type)	Data
Pit_Waste_2005_2044				
Depth_Indept_Inventory				
Post_1989_PA_Point_Estimate	Ci	Point estimates of material type inventories in the post-1989 performance assessment waste disposed of in 2005–2044 pits	Vector (material type)	Data

Table 9 (Continued)
Input Data Requirements for the MDA G Intruder Diffusion Model

Model Container/Parameter Name	Units	Parameter Description	Parameter Type	Input Element Type
Depth_Dept_Inventory				
Post_1989_PA_PtEst_Layer1	Ci	Point estimates of material type inventories in waste inventory layer 1 of the post-1989 performance assessment waste disposed of in 2005-2044 pits	Vector (material type)	Data
Post_1989_PA_PtEst_Layer2	Ci	Point estimates of material type inventories in waste inventory layer 2 of the post-1989 performance assessment waste disposed of in 2005-2044 pits	Vector (material type)	Data
Post_1989_PA_PtEst_Layer3	Ci	Point estimates of material type inventories in waste inventory layer 3 of the post-1989 performance assessment waste disposed of in 2005-2044 pits	Vector (material type)	Data
Post_1989_PA_PtEst_Layer4	Ci	Point estimates of material type inventories in waste inventory layer 4 of the post-1989 performance assessment waste disposed of in 2005-2044 pits	Vector (material type)	Data
Shaft_Waste_1988_2004				
Depth_Indept_Inventory				
Pre_1990_PA_Point_Estimate	Ci	Point estimates of material type inventories in the pre-1990 performance assessment waste disposed of in 1988–2004 shafts	Vector (material type)	Data
Post_1989_PA_Point_Estimate	Ci	Point estimates of material type inventories in the post-1989 performance assessment waste disposed of in 1988–2004 shafts	Vector (material type)	Data
Depth_Dept_Inventory				
Pre_1990_PA_PtEst_Layer1	Ci	Point estimates of material type inventories in waste inventory layer 1 of the pre-1990 performance assessment waste disposed of in 1988–2004 shafts	Vector (material type)	Data

Table 9 (Continued)
Input Data Requirements for the MDA G Intruder Diffusion Model

Model Container/Parameter Name	Units	Parameter Description	Parameter Type	Input Element Type
Pre_1990_PA_PtEst_Layer2	Ci	Point estimates of material type inventories in waste inventory layer 2 of the pre-1990 performance assessment waste disposed of in 1988–2004 shafts	Vector (material type)	Data
Pre_1990_PA_PtEst_Layer3	Ci	Point estimates of material type inventories in waste inventory layer 3 of the pre-1990 performance assessment waste disposed of in 1988–2004 shafts	Vector (material type)	Data
Pre_1990_PA_PtEst_Layer4	Ci	Point estimates of material type inventories in waste inventory layer 4 of the pre-1990 performance assessment waste disposed of in 1988–2004 shafts	Vector (material type)	Data
Post_1989_PA_PtEst_Layer1	Ci	Point estimates of material type inventories in waste inventory layer 1 of the post-1989 performance assessment waste disposed of in 1988–2004 shafts	Vector (material type)	Data
Post_1989_PA_PtEst_Layer2	Ci	Point estimates of material type inventories in waste inventory layer 2 of the post-1989 performance assessment waste disposed of in 1988–2004 shafts	Vector (material type)	Data
Post_1989_PA_PtEst_Layer3	Ci	Point estimates of material type inventories in waste inventory layer 3 of the post-1989 performance assessment waste disposed of in 1988–2004 shafts	Vector (material type)	Data
Post_1989_PA_PtEst_Layer4	Ci	Point estimates of material type inventories in waste inventory layer 4 of the post-1989 performance assessment waste disposed of in 1988–2004 shafts	Vector (material type)	Data
Shaft_Waste_2005_2044				
Depth_Indept_Inventory				
Post_1989_PA_Point_Estimate	Ci	Point estimates of material type inventories in the post-1989 performance assessment waste disposed of in 2005–2044 shafts	Vector (material type)	Data

Table 9 (Continued)
Input Data Requirements for the MDA G Intruder Diffusion Model

Model Container/Parameter Name	Units	Parameter Description	Parameter Type	Input Element Type
Depth_Dept_Inventory				
Post_1989_PA_PtEst_Layer1	Ci	Point estimates of material type inventories in waste inventory layer 1 of the post-1989 performance assessment waste disposed of in 2005-2044 shafts	Vector (material type)	Data
Post_1989_PA_PtEst_Layer2	Ci	Point estimates of material type inventories in waste inventory layer 2 of the post-1989 performance assessment waste disposed of in 2005-2044 shafts	Vector (material type)	Data
Post_1989_PA_PtEst_Layer3	Ci	Point estimates of material type inventories in waste inventory layer 3 of the post-1989 performance assessment waste disposed of in 2005-2044 shafts	Vector (material type)	Data
Post_1989_PA_PtEst_Layer4	Ci	Point estimates of material type inventories in waste inventory layer 4 of the post-1989 performance assessment waste disposed of in 2005-2044 shafts	Vector (material type)	Data
Fission_Yields				
Fraction_of_Pu239		Fraction of fission events that originate with Pu-239	Scalar	Stochastic
Age_of_MFP_Waste	yr	Age of mixed fission product waste at the time of disposal	Scalar	Stochastic
U235_Fission_Yields				
U235_1yr_Thermal		U-235 thermal fission yields for 1-year-old waste	Scalar	Data
U235_2yr_Thermal		U-235 thermal fission yields for 2-year-old waste	Scalar	Data
U235_3yr_Thermal		U-235 thermal fission yields for 3-year-old waste	Scalar	Data
U235_4yr_Thermal		U-235 thermal fission yields for 4-year-old waste	Scalar	Data
U235_5yr_Thermal		U-235 thermal fission yields for 5-year-old waste	Scalar	Data
U235_6yr_Thermal		U-235 thermal fission yields for 6-year-old waste	Scalar	Data

Table 9 (Continued)
Input Data Requirements for the MDA G Intruder Diffusion Model

Model Container/Parameter Name	Units	Parameter Description	Parameter Type	Input Element Type
U235_7yr_Thermal		U-235 thermal fission yields for 7-year-old waste	Scalar	Data
U235_8yr_Thermal		U-235 thermal fission yields for 8-year-old waste	Scalar	Data
U235_9yr_Thermal		U-235 thermal fission yields for 9-year-old waste	Scalar	Data
U235_10yr_Thermal		U-235 thermal fission yields for 10-year-old waste	Scalar	Data
Pu239_Fission_Yields				
Pu239_1yr_Thermal		Pu-239 thermal fission yields for 1-year-old waste	Scalar	Data
Pu239_2yr_Thermal		Pu-239 thermal fission yields for 2-year-old waste	Scalar	Data
Pu239_3yr_Thermal		Pu-239 thermal fission yields for 3-year-old waste	Scalar	Data
Pu239_4yr_Thermal		Pu-239 thermal fission yields for 4-year-old waste	Scalar	Data
Pu239_5yr_Thermal		Pu-239 thermal fission yields for 5-year-old waste	Scalar	Data
Pu239_6yr_Thermal		Pu-239 thermal fission yields for 6-year-old waste	Scalar	Data
Pu239_7yr_Thermal		Pu-239 thermal fission yields for 7-year-old waste	Scalar	Data
Pu239_8yr_Thermal		Pu-239 thermal fission yields for 8-year-old waste	Scalar	Data
Pu239_9yr_Thermal		Pu-239 thermal fission yields for 9-year-old waste	Scalar	Data
Pu239_10yr_Thermal		Pu-239 thermal fission yields for 10-year-old waste	Scalar	Data
Activation_Yields				
MAP_Allocation_Fractions		Radionuclide-specific activity fractions for mixed activation product waste	Vector (radionuclide)	Data

Table 9 (Continued)
Input Data Requirements for the MDA G Intruder Diffusion Model

Model Container/Parameter Name	Units	Parameter Description	Parameter Type	Input Element Type
Material_Type_Act_Fractions				
Nominal_Masses	g	Material type waste radionuclide masses	Matrix (radionuclide, material type)	Data
PU51				
Activity_Fractions		Radionuclide activity fractions in material type PU51 waste	Vector (radionuclide)	Data
PU52				
Pu238_Mass_Fraction		Mass fraction of Pu-238 in material type PU52 waste	Scalar	Stochastic
Pu240_Mass_Fraction		Mass fraction of Pu-240 in material type PU52 waste	Scalar	Stochastic
Pu241_Mass_Fraction		Mass fraction of Pu-241 in material type PU52 waste	Scalar	Stochastic
Pu242_Mass_Fraction		Mass fraction of Pu-242 in material type PU52 waste	Scalar	Stochastic
PU53				
Pu238_Mass_Fraction		Mass fraction of Pu-238 in material type PU53 waste	Scalar	Stochastic
Pu240_Mass_Fraction		Mass fraction of Pu-240 in material type PU53 waste	Scalar	Stochastic
Pu241_Mass_Fraction		Mass fraction of Pu-241 in material type PU53 waste	Scalar	Stochastic
Pu242_Mass_Fraction		Mass fraction of Pu-242 in material type PU53 waste	Scalar	Stochastic
PU54				
Pu238_Mass_Fraction		Mass fraction of Pu-238 in material type PU54 waste	Scalar	Stochastic
Pu240_Mass_Fraction		Mass fraction of Pu-240 in material type PU54 waste	Scalar	Stochastic
Pu241_Mass_Fraction		Mass fraction of Pu-241 in material type PU54 waste	Scalar	Stochastic

Table 9 (Continued)
Input Data Requirements for the MDA G Intruder Diffusion Model

Model Container/Parameter Name	Units	Parameter Description	Parameter Type	Input Element Type
Pu242_Mass_Fraction		Mass fraction of Pu-242 in material type PU54 waste	Scalar	Stochastic
PU55				
Activity_Fractions		Radionuclide activity fractions in material type PU55 waste	Vector (radionuclide)	Data
PU56				
Pu238_Mass_Fraction		Mass fraction of Pu-238 in material type PU56 waste	Scalar	Stochastic
Pu240_Mass_Fraction		Mass fraction of Pu-240 in material type PU56 waste	Scalar	Stochastic
Pu241_Mass_Fraction		Mass fraction of Pu-241 in material type PU56 waste	Scalar	Stochastic
Pu242_Mass_Fraction		Mass fraction of Pu-242 in material type PU56 waste	Scalar	Stochastic
PU57				
Activity_Fractions		Radionuclide activity fractions in material type PU57 waste	Vector (radionuclide)	Data
PU83				
Pu238_Mass_Fraction		Mass fraction of Pu-238 in material type PU83 waste	Scalar	Stochastic
Pu240_Mass_Fraction		Mass fraction of Pu-240 in material type PU83 waste	Scalar	Stochastic
Pu241_Mass_Fraction		Mass fraction of Pu-241 in material type PU83 waste	Scalar	Stochastic
Pu242_Mass_Fraction		Mass fraction of Pu-242 in material type PU83 waste	Scalar	Stochastic
U10				
Activity_Fractions		Radionuclide activity fractions in material type U10 waste	Vector (radionuclide)	Data

Table 9 (Continued)
Input Data Requirements for the MDA G Intruder Diffusion Model

Model Container/Parameter Name	Units	Parameter Description	Parameter Type	Input Element Type
U11				
Activity_Fractions		Radionuclide activity fractions in material type U11 waste	Vector (radionuclide)	Data
U12				
U234_Mass_Fraction		Mass fraction of U-234 in material type U12 waste	Scalar	Stochastic
U245_Mass_Fraction		Mass fraction of U-235 in material type U12 waste	Scalar	Stochastic
U35				
Activity_Fractions		Radionuclide activity fractions in material type U35 waste	Vector (radionuclide)	Data
U36				
Activity_Fractions		Radionuclide activity fractions in material type U36 waste	Vector (radionuclide)	Data
U38				
Activity_Fractions		Radionuclide activity fractions in material type U38 waste	Vector (radionuclide)	Data
U39				
Activity_Fractions		Radionuclide activity fractions in material type U39 waste	Vector (radionuclide)	Data
U81				
Activity_Fractions		Radionuclide activity fractions in material type U81 waste	Vector (radionuclide)	Data

Table 9 (Continued)
Input Data Requirements for the MDA G Intruder Diffusion Model

Model Container/Parameter Name	Units	Parameter Description	Parameter Type	Input Element Type
UNAT				
Activity_Fractions		Radionuclide activity fractions in material type UNAT waste	Vector (radionuclide)	Data
D38				
U234_Mass_Fraction		Mass fraction of U-234 in material type D38 waste	Scalar	Stochastic
U245_Mass_Fraction		Mass fraction of U-235 in material type D38 waste	Scalar	Stochastic
TH88				
Activity_Fractions		Radionuclide activity fractions in material type TH88 waste	Vector (radionuclide)	Data
Waste_Disposal_Volumes				
Pit_Waste_1988_2004	m^3	Volume of waste disposed of in pits from September 27, 1988 through 2004	Scalar	Data
Pit_Waste_2005_2044	m^3	Volume of waste disposed of in pits from 2005 through 2044	Scalar	Data
Shaft_Waste_1988_2004	m^3	Volume of waste disposed of in shafts from September 27, 1988 through 2004	Scalar	Data
Shaft_Waste_2005_2044	m^3	Volume of waste disposed of in shafts from 2005 through 2044	Scalar	Data
Inventory_Multiplier		Element used to set selected radionuclide inventories to zero	Vector (radionuclide)	Data
Transport_Pathway_Data				
Atmospheric_Transport				
Resident_Dust_Loading	kg/m^3	Dust loading for the Intruder – Post-Drilling and Intruder-Agriculture Scenarios	Scalar	Stochastic

Table 9 (Continued)
Input Data Requirements for the MDA G Intruder Diffusion Model

Model Container/Parameter Name	Units	Parameter Description	Parameter Type	Input Element Type
Soil_Disturbance_Factor		Factor by which the dust loading is increased due to human disturbance of the surface soil	Scalar	Stochastic
Worker_Dust_Loading	kg/m^3	Dust loading for the Intruder-Construction Scenario	Scalar	Stochastic
Resuspension_Flux	$g/m^2/yr$	Resuspension for particulates at MDA G	Scalar	Stochastic
Enhancement_Factor		Ratio of radionuclide concentrations in the resuspendable fraction of the soil to those in the total soil	Scalar	Stochastic
Average_Wind_Speed	m/s	Average wind speed at MDA G	Scalar	Stochastic
Atmospheric_Mixing_Height	m	Height to which radionuclides diffusing from the disposal site are mixed	Scalar	Data
Transport_Pathway_Data				
Atmospheric_Transport				
Resident_Dust_Loading	kg/m^3	Dust loading for the Intruder – Post-Drilling and Intruder-Agriculture Scenarios	Scalar	Stochastic
Soil_Disturbance_Factor		Factor by which the dust loading is increased due to human disturbance of the surface soil	Scalar	Stochastic
Worker_Dust_Loading	kg/m^3	Dust loading for the Intruder-Construction Scenario	Scalar	Stochastic
Resuspension_Flux	$g/m^2/yr$	Resuspension for particulates at MDA G	Scalar	Stochastic
Enhancement_Factor		Ratio of radionuclide concentrations in the resuspendable fraction of the soil to those in the total soil	Scalar	Stochastic

Table 9 (Continued)
Input Data Requirements for the MDA G Intruder Diffusion Model

Model Container/Parameter Name	Units	Parameter Description	Parameter Type	Input Element Type
Foodchain_Transport				
Plant_Data				
Uptake_Factors				
Leafy_Vegetable_GM	Ci/kg plant per Ci/kg soil (dry weight)	Geometric means of the plant uptake factors for leafy vegetables	Vector (element)	Data
Produce_GM	Ci/kg plant per Ci/kg soil (dry weight)	Geometric means of the plant uptake factors for produce	Vector (element)	Data
Grain_GM	Ci/kg plant per Ci/kg soil (dry weight)	Geometric means of the plant uptake factors for grain	Vector (element)	Data
PGrass_and_Native_GM	Ci/kg plant per Ci/kg soil (dry weight)	Geometric means of the plant uptake factors for pasture grass and native vegetation	Vector (element)	Data
Crop_GSD		Geometric standard deviation of the plant uptake factors for all crops		
Crop_Characteristics				
Particle_Size_Factor		Ratio of radionuclide concentrations in the fraction of the soil resuspended due to rainsplash to those in the total soil	Scalar	Stochastic
Plant_Carbon_Fraction		Fraction of plant that is carbon (dry-weight basis)	Vector (crop)	Data
Plant_Hydrogen_Fraction		Fraction of plant that is hydrogen (dry-weight basis)	Vector (crop)	Data

Table 9 (Continued)
Input Data Requirements for the MDA G Intruder Diffusion Model

Model Container/Parameter Name	Units	Parameter Description	Parameter Type	Input Element Type
Dry_to_Wet_Weight_Fractions				
DWW_Leafy_Vegetables		Dry-to-wet-weight fraction for leafy vegetables	Scalar	Stochastic
DWW_Produce		Dry-to-wet-weight fraction for produce	Scalar	Stochastic
DWW_Grain		Dry-to-wet-weight fraction for grain	Scalar	Stochastic
DWW_Pasture_Grass		Dry-to-wet-weight fraction for pasture grass	Scalar	Stochastic
Translocation_Factors				
TF_Leafy_Vegetables		Translocation factor for leafy vegetables	Scalar	Stochastic
TF_Produce		Translocation factor for produce	Scalar	Stochastic
TF_Grain		Translocation factor for grain	Scalar	Stochastic
TF_Pasture_Grass		Translocation factor for pasture grass	Scalar	Stochastic
Agricultural_Productivities				
AP_Leafy_Vegetables	kg (wet weight) /m^2	Agricultural productivity for leafy vegetables	Scalar	Stochastic
AP_Produce	kg (wet weight) /m^2	Agricultural productivity for produce	Scalar	Stochastic
AP_Grain	kg (wet weight) /m^2	Agricultural productivity for grain	Scalar	Stochastic
AP_Pasture_Grass	kg (dry weight) /m^2	Agricultural productivity for pasture grass	Scalar	Stochastic
Mass_Loading_Factors				
MLF_Leafy_Vegetables	g soil/g plant (dry weight)	Mass-loading factor for leafy vegetables	Scalar	Stochastic

Table 9 (Continued)
Input Data Requirements for the MDA G Intruder Diffusion Model

Model Container/Parameter Name	Units	Parameter Description	Parameter Type	Input Element Type
MLF_Produce	g soil/g plant (dry weight)	Mass-loading factor for produce	Scalar	Stochastic
MLF_Grain	g soil/g plant (dry weight)	Mass-loading factor for grain	Scalar	Stochastic
MLF_PGrass_and_Native	g soil/g plant (dry weight)	Mass-loading factor for pasture grass	Scalar	Stochastic
Animal_Data				
Animal_Ingestion_Data				
Cattle_and_Cows				
Cattle_Food_Ingestion	kg/d (dry weight)	Food consumption rate of cattle	Scalar	Stochastic
Cow_Food_Ingestion	kg/d (dry weight)	Food consumption rate of cows	Scalar	Stochastic
Cattle_Soil_Ingestion	kg/d (dry weight)	Soil consumption rate of cattle	Scalar	Stochastic
Cow_Soil_Ingestion	kg/d (dry weight)	Soil consumption rate of cows	Scalar	Stochastic
Cattle_Water_Ingestion	kg/d	Water consumption rate of cattle	Scalar	Stochastic
Cow_Water_Ingestion	kg/d	Water consumption rate of cows	Scalar	Stochastic
Chickens				
Chicken_Feed_Ingestion	kg/d (dry weight)	Food consumption rate of chickens	Scalar	Stochastic
Chicken_Water_Ingestion	kg/d	Water consumption rate of chickens	Scalar	Stochastic

Table 9 (Continued)
Input Data Requirements for the MDA G Intruder Diffusion Model

Model Container/Parameter Name	Units	Parameter Description	Parameter Type	Input Element Type
Grit_to_Food_Ratio		Ratio of grit or soil intake to food intake for chickens	Scalar	Data
Transfer				
Beef_GM	d/kg	Geometric means of the forage-to-beef transfer factors	Vector (element)	Stochastic
Beef_GSD		Geometric standard deviation of the forage-to-beef transfer factors	Vector (element)	Data
Milk_GM	d/kg	Geometric means of the forage-to-milk transfer factors	Vector (element)	Stochastic
Milk_GSD		Geometric standard deviation of the forage-to-milk transfer factors	Vector (element)	Data
Chicken_GM	d/kg	Geometric means of the forage-to-chicken transfer factors	Vector (element)	Stochastic
Chicken_GSD		Geometric standard deviation of the forage-to-chicken transfer factors	Vector (element)	Data
Eggs_GM	d/kg	Geometric means of the forage-to-eggs transfer factors	Vector (element)	Stochastic
Eggs_GSD		Geometric standard deviation of the forage-to-eggs transfer factors	Vector (element)	Data
H-3_and_C-14_Transfer_Factors				
H3_Factors				
Water_Fraction_Animal_Products		Mass water fractions of animal products	Vector (animal product)	Data
C14_Factors				
Animal_Prod_Carbon_Fraction		Carbon fractions of animal products	Vector (animal product)	Data

Table 9 (Continued)
Input Data Requirements for the MDA G Intruder Diffusion Model

Model Container/Parameter Name	Units	Parameter Description	Parameter Type	Input Element Type
Groundwater_Transport				
MdB_Infiltration_Rate	m/yr	Water infiltration rate on Mesita del Buey	Scalar	Stochastic
Biotic_Intrusion_Model				
Eco_Succession_Model				
Time_of_Climax	yr	Period required for disposal site to reach a piñon-juniper climax condition, measured from the time of facility closure	Scalar	Stochastic
Intrusion_Shape_Parameters				
Alpha_Shape		Shape factor used to model animal burrow and plant root distributions with depth	Scalar	Data
Beta_Shape		Shape factor used to model animal burrow and plant root distributions with depth	Scalar	Stochastic
Animal_Intrusion_Model				
Harvester_Ants				
Maximum_Burrow_Depth	m	Maximum burrowing depth for harvester ants	Scalar	Stochastic
Burrow_Density_Grassland	ha^{-1}	Density of harvester ant burrows during early succession	Scalar	Stochastic
Burrow_Density_Woodland	ha^{-1}	Density of harvester ant burrows in the piñon-juniper climax condition	Scalar	Stochastic
Burrow_Mass	kg	Mass of soil excavated per harvester ant burrow	Scalar	Stochastic
Colony_Life_Span	yr	Life span of harvester ant colonies	Scalar	Stochastic
Pocket_Gophers				
Maximum_Burrow_Depth	m	Maximum burrowing depth for pocket gophers	Scalar	Stochastic

Table 9 (Continued)
Input Data Requirements for the MDA G Intruder Diffusion Model

Model Container/Parameter Name	Units	Parameter Description	Parameter Type	Input Element Type
Soil_Removal_Rate_Grassland	m^3/ha	Rate of soil removal by pocket gophers during early succession	Scalar	Stochastic
Soil_Removal_Rate_Woodland	m^3/ha	Rate of soil removal by pocket gophers in the piñon-juniper climax condition	Scalar	Stochastic
Burrow_Renewal_Rate	yr^{-1}	Rate at which existing pocket gopher burrows are replaced with new ones	Scalar	Stochastic
Mice				
Maximum_Burrow_Depth	m	Maximum burrowing depth for mice	Scalar	Stochastic
Burrow_Density_Grassland	ha^{-1}	Density of mouse burrows during early succession	Scalar	Stochastic
Burrow_Density_Woodland	ha^{-1}	Density of mouse burrows in the piñon-juniper climax condition	Scalar	Stochastic
Burrow_Volume	kg	Volume of soil excavated per mouse burrow	Scalar	Stochastic
Burrow_Renewal_Rate	yr^{-1}	Rate at which existing mouse burrows are replaced with new ones	Scalar	Stochastic
Chipmunks_and_Squirrels				
Maximum_Burrow_Depth	m	Maximum burrowing depth for chipmunks and ground squirrels	Scalar	Stochastic
Burrow_Density_Grassland	ha^{-1}	Density of chipmunk and ground squirrel burrows during early succession	Scalar	Stochastic
Burrow_Density_Woodland	ha^{-1}	Density of chipmunk and ground squirrel burrows in the piñon-juniper climax condition	Scalar	Stochastic
Burrow_Volume	kg	Volume of soil excavated per chipmunk and ground squirrel burrow	Scalar	Stochastic
Burrow_Renewal_Rate	yr^{-1}	Rate at which existing chipmunk and ground squirrel burrows are replaced with new ones	Scalar	Stochastic

Table 9 (Continued)
Input Data Requirements for the MDA G Intruder Diffusion Model

Model Container/Parameter Name	Units	Parameter Description	Parameter Type	Input Element Type
Plant_Intrusion_Model				
Litter_Halflife	yr	Litter decomposition half-life	Scalar	Stochastic
Grasses				
Maximum_Root_Depth	m	Maximum rooting depth of grasses	Scalar	Stochastic
Biomass_Density_Grassland	kg/m^2	Aboveground biomass density of grasses during early succession	Scalar	Stochastic
Biomass_Density_Woodland	kg/m^2	Aboveground biomass density of grasses in the piñon-juniper climax condition	Scalar	Stochastic
Litter_Prod_Rate	yr^{-1}	Fraction of the aboveground biomass that falls as litter	Scalar	Stochastic
Forbs				
Maximum_Root_Depth	m	Maximum rooting depth of forbs	Scalar	Stochastic
Biomass_Density_Grassland	kg/m^2	Aboveground biomass density of forbs during early succession	Scalar	Stochastic
Biomass_Density_Woodland	kg/m^2	Aboveground biomass density of forbs in the piñon-juniper climax condition	Scalar	Stochastic
Litter_Prod_Rate	yr^{-1}	Fraction of the aboveground biomass that falls as litter	Scalar	Stochastic
Shrubs				
Maximum_Root_Depth	m	Maximum rooting depth of shrubs	Scalar	Stochastic
Biomass_Density_Grassland	kg/m^2	Aboveground biomass density of shrubs during early succession	Scalar	Stochastic
Biomass_Density_Woodland	kg/m^2	Aboveground biomass density of shrubs in the piñon-juniper climax condition	Scalar	Stochastic
Litter_Prod_Rate	yr^{-1}	Fraction of the aboveground biomass that falls as litter	Scalar	Stochastic

Table 9 (Continued)
Input Data Requirements for the MDA G Intruder Diffusion Model

Model Container/Parameter Name	Units	Parameter Description	Parameter Type	Input Element Type
Trees				
Maximum_Root_Depth	m	Maximum rooting depth of trees	Scalar	Stochastic
Biomass_Density_Grassland	kg/m^2	Aboveground biomass density of trees during early succession	Scalar	Stochastic
Biomass_Density_Woodland	kg/m^2	Aboveground biomass density of trees in the piñon-juniper climax condition	Scalar	Stochastic
Litter_Prod_Rate	yr^{-1}	Fraction of the aboveground biomass that falls as litter	Scalar	Stochastic
Erosion_Model				
Erosion_Rates				
Erosion_Rate_Functions	yr^{-1}	Cover loss rate as a function of time	Scalar	Lookup Table
Erosion_Zone_Data				
Remaining_Cover_EZ1	m	Minimum cover remaining in erosion zone 1	Scalar	Stochastic
Remaining_Cover_EZ2	m	Minimum cover remaining in erosion zone 2	Scalar	Stochastic
Remaining_Cover_EZ3	m	Minimum cover remaining in erosion zone 3	Scalar	Stochastic
Remaining_Cover_EZ4	m	Minimum cover remaining in erosion zone 4	Scalar	Stochastic
Remaining_Cover_EZ5	m	Minimum cover remaining in erosion zone 5	Scalar	Stochastic
Remaining_Cover_EZ6	m	Minimum cover remaining in erosion zone 6	Scalar	Stochastic
Remaining_Cover_EZ7	m	Minimum cover remaining in erosion zone 7	Scalar	Stochastic
Remaining_Cover_EZ8	m	Minimum cover remaining in erosion zone 8	Scalar	Stochastic
Remaining_Cover_EZ9	m	Minimum cover remaining in erosion zone 9	Scalar	Stochastic
Remaining_Cover_EZ10	m	Minimum cover remaining in erosion zone 10	Scalar	Stochastic

Table 9 (Continued)
Input Data Requirements for the MDA G Intruder Diffusion Model

Model Container/Parameter Name	Units	Parameter Description	Parameter Type	Input Element Type
Erosion_Shape_Parameters				
Alpha_Shape_Factor		Shape factor used to model surface erosion	Scalar	Data
Beta_Shape_Factor		Shape factor used to model surface erosion	Scalar	Stochastic
Human_Intrusion_Model				
Basement_Length	m	Length of the intruder's basement	Scalar	Data
Basement_Width	m	Width of the intruder's basement	Scalar	Data
Basement_Depth	m	Depth of the intruder's basement	Scalar	Data
Well_Casing_Diameter	m	Diameter of the well casing	Scalar	Data
Dose_and_WAC_Model				
Dose_Conversion_Factors				
Ingestion_DCFs	mrem/pCi	Dose conversion factors for the ingestion exposure route	Vector (radionuclide)	Data
Inhalation_DCFs	mrem/pCi	Dose conversion factors for the inhalation exposure route	Vector (radionuclide)	Data
Soil_External_DCFs_15_cm	mrem/yr per pCi/m^3	Dose conversion factors for direct radiation from soils contaminated to a depth of 15 cm	Vector (radionuclide)	Data
Soil_External_DCFs_Infinite	mrem/yr per pCi/m^3	Dose conversion factors for direct radiation from soils contaminated to an infinite depth	Vector (radionuclide)	Data
Air_External_DCFs	mrem/yr per pCi/m^3	Dose conversion factors for direct radiation from air immersion	Vector (radionuclide)	Data
Exposure_Pathway_Data				
Minimum_Soil_Mixing_Depth	m	Contaminant mixing depth	Scalar	Data

Table 9 (Continued)
Input Data Requirements for the MDA G Intruder Diffusion Model

Model Container/Parameter Name	Units	Parameter Description	Parameter Type	Input Element Type
Shielding_Factor		Direct radiation shielding factor for the time spent indoors	Scalar	Stochastic
Resident_Inhalation_Rate	m^3/d	Inhalation rate of the resident intruder	Scalar	Stochastic
Worker_Inhalation_Rate	m^3/d	Inhalation rate of the construction intruder	Scalar	Stochastic
Ventilation_Rate	hr^{-1}	Ventilation rate of the intruder's house	Scalar	Stochastic
Room_Height	m	Height of rooms inside the intruder's house	Scalar	Data
Area_of_Lot	m^2	Area of the receptor's lot	Scalar	Stochastic
Area_of_House	m^2	Area of the receptor's house	Scalar	Data
Time_of_Intrusion	yr	Length of time before intrusion into the waste occurs, measured from the time of facility closure	Scalar	Data
Resident_Intruder_PO	mrem/yr	Performance objective for the post-drilling and agricultural intruders	Scalar	Data
Construction_Intruder_PO	mrem/yr	Performance objective for the construction worker	Scalar	Data
Exposure_Times				
Resident_Indoor_Exposure_Time	hr/d	Time spent inside by the resident intruder	Scalar	Stochastic
Resident_Outdoor_Exposure_Time	hr/d	Time spent outside by the resident intruder	Scalar	Stochastic
Worker_Exposure_Time	hr/d	Time spent building the house by the construction worker	Scalar	Data
Excavation_Occupancy_Factor		Fraction of worker exposure period spent in the bottom of the basement excavation	Scalar	Stochastic
Ingestion_Data				
Resident_Soil_Ingestion_Rate	kg (dry weight)/yr	Rate of soil ingestion for the resident intruder	Scalar	Stochastic

Table 9 (Continued)
Input Data Requirements for the MDA G Intruder Diffusion Model

Model Container/Parameter Name	Units	Parameter Description	Parameter Type	Input Element Type
Worker_Soil_Ingestion_Rate	kg (dry weight)/yr	Rate of soil ingestion for the construction worker	Scalar	Stochastic
Food_Ingestion_Data				
Input_Vegetable_Fraction		User-specified fraction of the receptor's diet of leafy vegetables, produce, and grain that is grown at the receptor's location	Scalar	Stochastic
Animals_Raised		The types of animals raised by the receptor as a food source	Scalar	Stochastic
Crop_Ingestion_Rates				
CI_Leafy_Vegetables	kg (wet weight)/yr	Rate of ingestion of leafy vegetables for the resident intruders	Scalar	Stochastic
CI_Produce	kg (wet weight)/yr	Rate of ingestion of produce for the resident intruders	Scalar	Stochastic
CI_Grain	kg (wet weight)/yr	Rate of ingestion of grain for the resident intruders	Scalar	Stochastic
Animal_Product_Ingestion_Rates				
API_Beef	kg/yr	Rate of ingestion of beef for the resident intruders	Scalar	Stochastic
API_Milk	kg/yr	Rate of ingestion of milk for the resident intruders	Scalar	Stochastic
API_Chicken	kg/yr	Rate of ingestion of chicken for the resident intruders	Scalar	Stochastic
API_Eggs	kg/yr	Rate of ingestion of eggs for the resident intruders	Scalar	Stochastic
Animal_Numbers				
Cattle_Weight_at_Slaughter	kg	Weight of cattle at the time of slaughter	Scalar	Stochastic
Dressing_Percentage		Ratio of the carcass weight to live weight of the animal	Scalar	Stochastic
Cutability		Fraction of the carcass that is sold as meat	Scalar	Stochastic

Table 9 (Continued)
Input Data Requirements for the MDA G Intruder Diffusion Model

Model Container/Parameter Name	Units	Parameter Description	Parameter Type	Input Element Type
Milk_Production_Rate	kg/yr	Production rate of milk by cows	Scalar	Stochastic
Chicken_Weight_at_Slaughter	kg	Weight of chicken at the time of slaughter	Scalar	Stochastic
Cook_to_Live_Ratio		Ratio of cooked weight of chicken to the live weight of the bird	Scalar	Stochastic
Meat_Fraction		Fraction of the cooked chicken that is meat	Scalar	Stochastic
Egg_Production_Rate	d^{-1}	Production rate of eggs by layers	Scalar	Stochastic
Egg_Mass	kg	Mass of egg	Scalar	Stochastic
Shell_Fraction		Fraction of the egg mass that is contributed by the shell	Scalar	Data
Animal_Product_Fractions				
Beef		User-specified fraction of the receptor's diet of beef that is taken from animals living at the exposure location	Scalar	Stochastic
Milk		User-specified fraction of the receptor's diet of milk that is produced by animals living at the exposure location	Scalar	Stochastic
Chicken		User-specified fraction of the receptor's diet of chicken that is taken from animals living at the exposure location	Scalar	Stochastic
Eggs		User-specified fraction of the receptor's diet of eggs that is produced by animals living at the exposure location	Scalar	Stochastic

5.0 Model Input Data Selection

The parameters required to implement the GoldSim performance assessment and composite analysis models are described in Section 4. This section presents the input data selected to implement the models and provides the bases for the adopted values. Section 5.1 addresses the parameters used to control or define the simulations conducted in support of the performance assessment and composite analysis. Section 5.2 discusses the data used to characterize the disposal facility and describe disposal operations. The parameters used to characterize the environmental media included in the GoldSim modeling are considered in Section 5.3, while radionuclide inventories are addressed in Section 5.4. Sections 5.5 through 5.10 discuss parameters needed to conduct atmospheric transport, groundwater transport, sediment transport, food-chain transport, biotic intrusion, and surface erosion modeling, respectively. Parameters used to characterize the exposures received by members of the public and inadvertent intruders are discussed in Section 5.11, and Section 5.12 provides information about miscellaneous parameters.

The majority of the input parameters discussed below are characterized using distributions to describe the variability associated with the value; these distributions are also used to model uncertainty and sensitivity. Also listed are point estimates or deterministic values that were used to conduct evaluations of facility performance well beyond the 1,000-year compliance period and benchmarking analyses. Some of the parameters are not defined using distributions, either because it was inappropriate to do so or because the information needed to define the distributions was unavailable.

5.1 Control Parameters

The Analysis_Flag, found only in the MDA G Site and Site Diffusion Models, designates whether the performance assessment or composite analysis inventory is used in the model simulation. The flag was set appropriately to consider each inventory.

The Biotic_Intrusion_Flag is found in all four GoldSim models and indicates whether the effects of biotic intrusion are taken into account when estimating exposures for members of the public and inadvertent intruders. This flag was set to 1 for all modeling, indicating the impacts of plants and animals intruding into the disposed waste were considered.

The Diffusion_Flag controls whether the effects of vapor- and gas-phase diffusion are taken into account in the site and intruder diffusion models. This variable was generally set to 1 for all simulations conducted using these models, indicating that diffusive transport was taken into account. Some simulations were conducted with this variable set to 0 (no diffusion) to investigate the effects of diffusive transport on projected exposures.

The Intruder_Flag and Disposal_Unit_Flag are unique to the MDA G Intruder and Intruder Diffusion Models; the former specifies the intruder scenario under consideration while the latter determines the set of pits or shafts to be evaluated. These flag variables were set appropriately to estimate exposures for the Intruder – Post-Drilling, Intruder-Agriculture, and Intruder-Construction Scenarios following intrusion into the pits and shafts.

The Depth_of_Disposal_Flag, also unique to the intruder and intruder diffusion models, was set equal to 1 for the disposal pits, causing the input inventories to be homogeneously distributed throughout the units. For the two sets of shafts, values of 1 and 2 were used to examine exposures based on homogeneously distributed inventories and layer-specific inventories. respectively.

5.2 Facility Dimensions and Operations

Several parameters that are used in the GoldSim modeling address the layout and key operational aspects of the disposal facility. Dimensional parameters describe the physical layout of the disposal units and characterize the final covers placed over the pits and shafts. Operational parameters identify the periods over which the disposal units are active and define periods of administrative control over the facility.

5.2.1 Disposal Areas

MDA G was divided into eight waste disposal regions for the modeling conducted using the site and site diffusion models; these disposal regions are shown in Figure 5 and information pertaining to them is summarized in Table 10. Table 10 lists the pits and shafts included in each region and shows the associated disposal area, which represents the surface area of the pits and shafts in each region. The disposal areas associated with the pits in disposal regions 1 through 5 were estimated using two approaches. In the first, the dimensions of the pits in a given region were used to calculate the pit area and the pit areas were summed to yield the region's disposal area. The second approach relied on maps of the pit locations. Coordinates along the edges of the pits were taken from these maps and used to conduct the surface erosion modeling (Wilson et al., 2005). Each pit was represented in this modeling using 6.25 m^2 (67 ft^2) cells. Multiplying the number of cells used to represent the surfaces of the pits within a region by 6.25 m^2 (67 ft^2) yields a second estimate of the pit disposal area for that region.

The two sets of estimates of the pit disposal areas differed by 7 to 21 percent; the estimates based on pit dimensions were consistently higher than those based on the map coordinates. The areas calculated on the basis of the map coordinates were, however, adopted for the performance assessment and composite analysis for two reasons. First, the maps are generally expected to more accurately represent the extent of each disposal unit. Second, use of the map-based disposal areas is consistent with the information used to conduct the surface erosion modeling.

Table 10
Pits and Shafts Included in the Eight Waste Disposal Regions of MDA G and the Region-Specific Disposal Areas

Disposal Region	Disposal Units Included in Disposal Region		Disposal Area (m^2)		
	Pits	Shafts	Pits	Shafts	All Disposal Units
1	1-5	1-33, 35-38, 40-49, 51-58, 60-69, 71-90	2.8E+04	2.8E+02	2.8E+04
2	6, 7, 24	—	1.1E+04	—	1.1E+04
3	8-10, 12, 13, 15-22	—	2.3E+04	—	2.3E+04
4	25-31, 39	—	2.5E+04	—	2.5E+04
5	32, 33, 35-38	—	2.4E+04	—	2.4E+04
6	—	34, 39, 50, 59, 70, 91-97, 99-112, 114, 115, 118-135	—	7.0E+02	7.0E+02
7	—	136-144, 147-177, 189-192, 196, 197, 206, 301, 307, 308, 327, 329, 331, 333, 335, 339, 341, 343, 345, 347, 349, 351, 355, 357, 360-367, 370, C01-C14	—	2.4E+03	2.4E+03
8	All future pits	All future shafts	2.8E+04	1.4E+03	2.9E+04

— = None

The pits in waste disposal region 8 have not been constructed yet, so the surface area associated with these pits was estimated using drawings developed in conjunction with the conceptual design of Zone 4 (Day et al., 2005). A second estimate of the surface area of the pits was developed using the following equation:

$$A_{d,p} = \frac{V_p}{d_p \times E_p} \qquad 68$$

Where

$A_{d,p}$= pit disposal area (m^2)
V_p = volume of waste requiring disposal in the pits (m^3)
d_p = thickness of waste in the pits (m)
E_p = waste emplacement efficiency factor for the pits

The volume of waste requiring disposal is considered in Section 5.4. The disposal pits were assumed to be 18 m (60 ft) deep and the top 3 m (10 ft) of each unit was assumed to contain clean fill, consistent with the conceptual design for the expansion area. A waste emplacement efficiency of 50 percent was assumed; this factor is discussed below.

The disposal area estimate for the region 8 pits that was based on the conceptual drawings was almost two times greater than that calculated using Equation 68. This discrepancy occurs because the area calculated using Equation 68 does not account for that portion of the disposal units occupied by access ramps. If the ramp-occupied areas are taken into account, the two estimates of disposal area fall within 10 percent of one another. The area developed on the basis of the drawings was adopted for the performance assessment, composite analysis, and surface erosion modeling.

The process of defining the disposal areas associated with the shafts is complicated by the fact that these units have a small surface expression and are clustered in groups across the disposal facility. Consequently, a different approach was adopted for defining the shaft disposal areas. The shafts in waste disposal regions 1 and 6 are concentrated in groups referred to as shaft fields. The disposal areas for these units were estimated on the basis of the size of the shaft fields. The areas of the shafts in each disposal region were summed and these sums were divided by the shaft field efficiency factor described in Section 5.2.6 to yield the corresponding disposal area.

The shafts in disposal region 7 are widely scattered among the disposal region 3 pits. The disposal area for these units was calculated as if the shafts were located in a single shaft field, as was done for the shafts in waste disposal regions 1 and 6.

The disposal area for the shafts in disposal region 8 could not be estimated using the procedure used for the shafts in regions 1 and 6 because the region 8 shafts have not been constructed. The cross-sectional area of the shafts needed to dispose of future waste was estimated as follows:

$$A_{d,s} = \frac{V_s}{d_s \times E_s \times E_f} \qquad 69$$

Where

$A_{d,s}$ = shaft disposal area (m^2)
V_s = volume of waste requiring disposal in the shafts (m^3)
d_s = thickness of waste in the shafts (m)
E_s = waste emplacement efficiency factor for the shafts
E_f = shaft field efficiency factor

It was assumed that the shafts will be 18 m (60 ft) deep and that the top 3 m (10 ft) of each unit will contain clean fill. The waste emplacement efficiency and shaft field efficiency were set equal to 50 and 11 percent, respectively; these factors are discussed in Sections 5.2.5 and 5.2.6.

The inadvertent intruder analysis estimates doses received from subsets of the performance assessment inventory and calculates waste acceptance criteria for waste disposed of in Zone 4. The disposal area for this modeling is equal to 2,300 m^2 (0.6 ac), which is the assumed area of the lot upon which the intruder's house is built.

5.2.2 *Erosion Zone Properties*

The erosion zones comprising each waste disposal region represent portions of the site that are characterized by erosion conditions that are more or less severe relative to the other erosion zones. Each erosion zone is associated with a specific range of "remaining cover depth" as listed in Table 5; these depth intervals were selected to address the range of conditions projected by a series of 10,000-year SIBERIA model simulations. Complete details of this modeling may be found in Wilson et al. (2005).

Once the cover-depth intervals corresponding to each erosion zone were defined, SIBERIA modeling results were used to assign the cells overlying the disposal units to the 10 erosion zones; these assignments were based on the cover depths projected to remain at the end of 1,000-year simulations. For instance, all cells within a waste disposal region with projected cover depths ranging from 1.75 to 2 m (5.7 to 6.6 ft) at 1,000 years postclosure were assigned to erosion zone 8. For all four GoldSim models, the assignment of cells to an erosion zone was performed separately for each of the low-, moderate-, and high-erosion scenarios considered in the SIBERIA modeling. The allocation of the waste disposal regions among erosion zones is summarized in Table 11; note that none of the regions had cells allocated to erosion zones 1 through 6, indicating that cover depths remained greater than 1.5 m (4.9 ft) throughout the 1,000-year simulation period. Separate allocations are shown for the disposal pits and shafts within disposal region 8; this information was needed to calculate unit-specific intruder doses and intruder-based WAC.

Table 11
Erosion Zone Allocations Used in 1,000-Year Simulations

Disposal Region by Erosion Scenario	Fraction of Waste Disposal Region Area by Erosion Zone				
	Zones 1 – 6	Zone 7	Zone 8	Zone 9	Zone 10
Low Erosion					
1	---	---	---	1.4E-02	9.9E-01
2	---	---	---	---	1.0E+00
3	---	---	---	4.4E-03	9.9E-01
4	---	---	---	1.3E-03	9.9E-01
5	---	---	---	9.5E-03	9.9E-01
6	---	---	---	---	1.0E+00
7	---	---	---	4.4E-03	9.9E-01
8	---	---	---	2.2E-03	1.0E+00
8 (pits only)	---	---	---	6.8E-04	1.0E+00
8 (shafts only)	---	---	---	3.7E-02	9.6E-01
Moderate Erosion					
1	---	---	---	3.1E-02	9.7E-01
2	---	---	---	---	1.0E+00
3	---	2.7E-04	1.1E-03	2.2E-02	9.8E-01
4	---	---	2.5E-04	1.7E-02	9.8E-01
5	---	---	---	2.3E-02	9.8E-01
6	---	---	---	---	1.0E+00
7		2.7E-04	1.1E-03	2.2E-02	9.8E-01
8	---	---	---	3.9E-03	1.0E+00
8 (pits only)	---	---	---	2.3E-03	1.0E+00
8 (shafts only)	---	---	---	4.2E-02	9.6E-01
High Erosion					
1	---	---	---	3.3E-02	9.7E-01
2	---	---	---	---	1.0E+00
3	---	---	2.7E-04	3.1E-02	9.7E-01
4	---	---	1.2E-03	3.3E-02	9.7E-01
5	---	---	---	4.7E-02	9.5E-01
6	---	---	---	7.6E-03	9.9E-01
7	---	---	2.7E-04	3.1E-02	9.7E-01
8	---	---	---	6.5E-03	9.9E-01
8 (pits only)	---	---	---	2.5E-03	1.0E+00
8 (shafts only)	---	---	---	1.0E-01	9.0E-01

--- = Indicates that none of the waste disposal region lies within the erosion zone.

The process outlined above was easily applied to the disposal pits within each region because these units have substantial surface areas. It was more difficult to apply it to the disposal shafts, which are small and scattered over the disposal facility. As discussed in Section 5.2.1, the shafts included in waste disposal regions 1 and 6 are concentrated in a single shaft field located at the west end of pits 2 and 4; the shafts included in disposal region 8 are also arranged in a single shaft field in Zone 4. For these shafts, the assignment of cells to erosion zones was conducted on the basis of the shaft field, rather than on the basis of individual shafts. The cells representing the shafts in disposal regions 1 and 6 were assigned to the erosion zones in the same proportions.

The shafts in waste disposal region 7 are not confined to a single shaft field, but instead are scattered among the disposal region 3 pits. The cells representing these units were not explicitly assigned to the different erosion zones. Instead, the cell-to-erosion-zone distribution developed for the pits comprising disposal region 3 was assumed to apply to the shafts in region 7.

A 50,000-year simulation of moderate erosion conditions was conducted using SIBERIA to investigate the performance of the disposal facility long after the 1,000-year compliance period. The results of the modeling were used in a deterministic GoldSim simulation to estimate downwind and canyon exposures over this same period. To conduct this modeling, the erosion zones were redefined in terms of the depth intervals they represented, and the results of the SIBERIA modeling were used to assign cells to each zone. The erosion zone depth intervals and the cell assignments are shown in Table 12.

5.2.3 Operational Period

The operational period covers the time during which MDA G was used for the disposal of radioactive waste and, more specifically, the periods during which waste was placed in pits and shafts in each of the eight disposal regions. The operational period for MDA G as a whole is 88 years; this figure is based on the fact that routine waste disposal operations began in 1959 and the assumption that final closure of the site will occur in 2046 following the end of disposal operations in Zone 4 (disposal region 8) in 2044. Table 13 summarizes the operational periods for the eight disposal regions. These periods are based on data provided in Shuman (2005). All waste disposed of after 2004 was assumed to be placed in waste disposal region 8.

5.2.4 Cover and Waste Configuration

The cover and waste configuration parameters define the thickness of the cover placed over the disposal units and the thickness of the waste in these units. Current plans call for the application of a minimum of 2.5 m (8.2 ft) of cover material over all pits and shafts at MDA G; a complete description of the final cover may be found in Day et al. (2005). In fact, the thickness of the final cover will be greater than 2.5 m (8.2 ft) over large portions of the disposal site because of the extensive contouring and shaping that is required to achieve the desired configuration.

Table 12
Erosion Zone Depth Intervals and Allocations Used in 50,000-Year Simulation

Waste Disposal Region	Fraction of Waste Disposal Region by Erosion Zone [a]									
	1	2	3	4	5	6	7	8	9	10
	-2.25 – -2.00 m	-1.75 – -1.50 m	-1.25 – -1.00 m	-0.75 – -0.50 m	-0.25 – 0.00 m	0.25 – 0.50 m	0.75 – 1.00 m	1.25 – 1.50 m	2.25 – 2.50 m	>2.50 m
1	---	---	---	---	6.0E-03	3.0E-02	5.3E-02	8.1E-02	3.0E-01	5.3E-01
2	---	---	---	---	---	2.3E-03	1.5E-02	5.8E-02	2.1E-01	7.1E-01
3	5.5E-02	3.8E-02	4.8E-02	7.2E-02	9.3E-02	7.4E-02	6.3E-02	6.3E-02	1.1E-01	3.8E-01
4	9.9E-04	4.0E-03	3.2E-02	5.0E-02	4.6E-02	8.5E-02	1.2E-01	1.5E-01	3.2E-01	1.9E-01
5	---	---	---	---	1.3E-03	3.5E-02	8.6E-02	1.4E-01	4.0E-01	3.4E-01
6	---	---	---	7.6E-03	4.5E-02	9.1E-02	6.1E-02	2.1E-01	3.2E-01	2.7E-01
8	---	---	4.3E-04	2.3E-02	3.3E-02	2.4E-02	1.2E-02	7.4E-02	2.8E-01	5.5E-01

--- = Indicates that none of the waste disposal region lies within the erosion zone.

[a] Depth intervals specify the amount of cover remaining at the end of the 50,000-year simulation; negative values signify the removal of the indicated thickness of waste.

Table 13
Operational Periods for the Eight Waste Disposal Regions at MDA G

Disposal Region	Operational Period	
	First Year of Disposal	Last Year of Disposal
1	1959	1979
2	1971[a]	1976
3	1971	2001
4	1980	2004
5	1982	2004
6	1970	1995
7	1976	2004
8	2005	2044

[a] *Waste was disposed of in pit 6, one of the units included in this disposal region, starting in 1970. However, the waste that was placed prior to 1971 was included in the waste disposal region 1 inventory.*

Distributions of initial cover thickness were developed for the pit and shafts in each waste disposal region. Initial depth data were estimated using the cover depths assigned to the cells representing the disposal units in the SIBERIA surface erosion modeling; these depths are based on the conceptual cover design effort (Day et al., 2005). The distributions of these depths are shown in Figure 16 for waste disposal regions 1 through 6 and 8. These data were used to create triangular distributions of initial depths, with the ranges defining the end points and the medians defining the most likely values; the resulting distributions are included in Table 14. The shafts that comprise waste disposal region 7 are scattered among the pits assigned to disposal region 3; the distribution of initial cover was assumed to be the same for these two disposal regions. Disposal region 1 includes 5 pits and more than 80 shafts arranged in a shaft field near the west end of pits 2 and 4; the initial cover depths for the cells overlying the pits and the shaft field were combined to develop the initial depth distribution. The distribution of cover depths shown for disposal region 6 is based on information for the shaft field located at the west end of pits 2 and 4; this shaft field actually includes disposal units belonging to disposal regions 1 and 6. The initial pit and shaft cover depths were combined to develop the distribution for waste disposal region 8 for the site model, but the initial depths over these units were considered separately for the intruder modeling. The distribution shown in Figure 16 for this region includes the pits and shafts.

Figure 16a
Waste diposal region 1

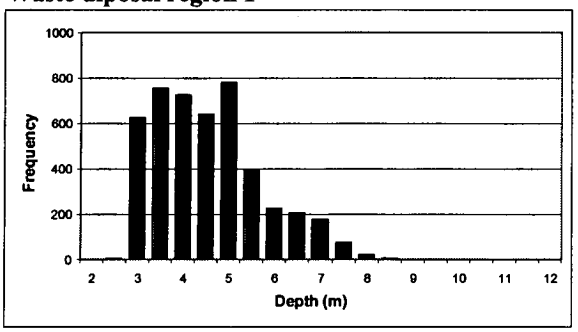

Figure 16b
Waste diposal region 2

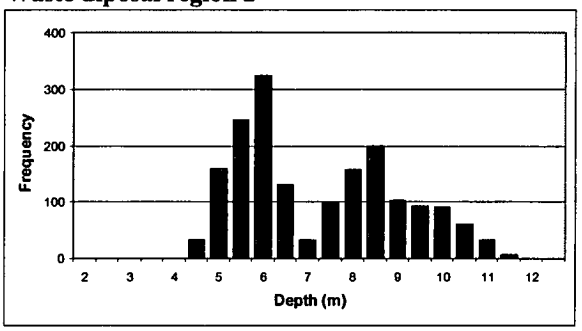

Figure 16c
Waste diposal region 3

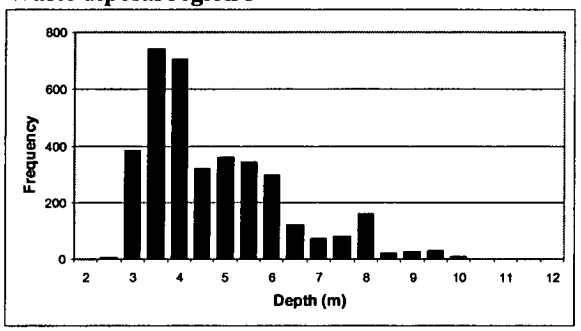

Figure 16d
Waste diposal region 4

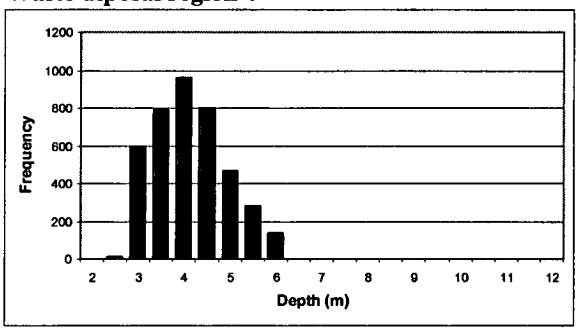

Figure 16e
Waste diposal region 5

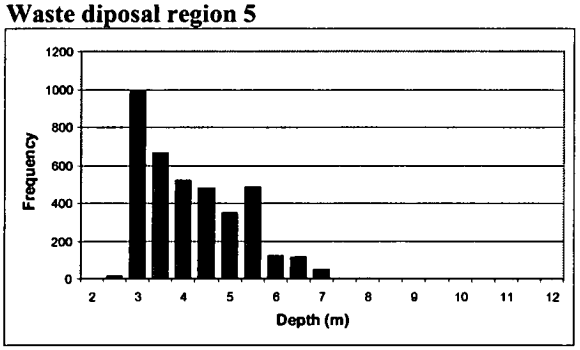

Figure 16f
Waste diposal region 6

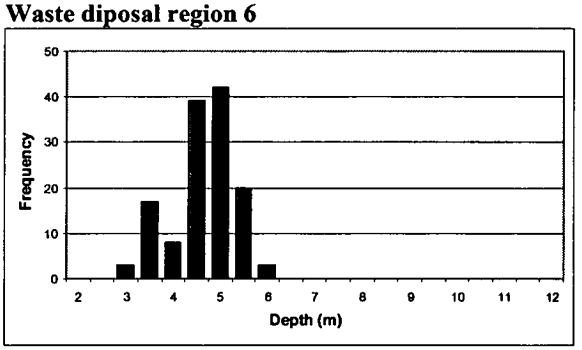

Figure 16g
Waste diposal region 8

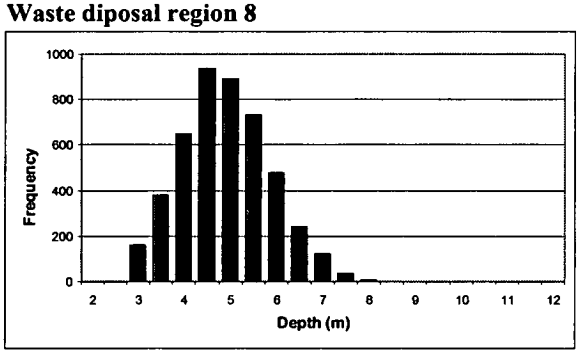

Note: Graphs shown with different ranges on vertical scales.

Figure 16
Histograms of Initial Cover Depth Distribution for Waste Disposal Regions 1 through 6 and 8

Table 14
Pathway Parameter Values and Distributions Used in the Performance Assessment and Composite Analysis

Parameter	Units [a]	Deterministic Value	Distribution [b]
Site Geometry and Operations			
Initial Cover Depth			
Waste Disposal Region 1	m	4.1E+00	T(2.5E+00, 4.1E+00, 8.3E+00)
Waste Disposal Region 2	m	5.8E+00	T(3.7E+00, 5.8E+00, 1.1E+01)
Waste Disposal Region 3	m	4.0E+00	T(2.5E+00, 4.0E+00, 9.6E+00)
Waste Disposal Region 4	m	3.8E+00	T(2.5E+00, 3.8E+00, 6.0E+00)
Waste Disposal Region 5	m	3.6E+00	T(2.5E+00, 3.6E+00, 6.8E+00)
Waste Disposal Region 6	m	4.5E+00	T(2.9E+00, 4.5E+00, 5.6E+00)
Waste Disposal Region 7	m	4.0E+00	T(2.5E+00, 4.0E+00, 9.6E+00)
Waste Disposal Region 8			
Disposal Pits	m	4.7E+00	T(2.5E+00, 4.7E+00, 7.8E+00)
Disposal Shafts	m	3.0E+00	T(2.5E+00, 3.0E+00, 4.0E+00)
All Disposal Units	m	4.6E+00	T(2.5E+00, 4.6E+00, 7.8E+00)
Waste Thickness			
Waste Disposal Region 1	m	7.7E+00	---
Waste Disposal Region 2	m	7.7E+00	---

--- = No distribution was defined for this parameter. *[a] Blank cells indicate value is unitless.*

[b] Distribution designations refer to the following distribution types: CD = cumulative distribution (cumulative probability, value), D = discrete (probability, value), LN = lognormal (geometric mean, geometric standard deviation), T = triangular (minimum, most likely, maximum), TLN = truncated lognormal distribution (geometric mean, geometric standard deviation, minimum, maximum), TN = truncated normal distribution (mean, standard deviation, minimum, maximum), U = uniform (minimum, maximum).

[c] The first value was used for the Intruder – Post-Drilling and Intruder-Agriculture Scenarios; the second value was used for the Intruder-Construction Scenario

[d] The first value represents the performance assessment; the second value the composite analysis.

[e] The distribution of the soil intake rate of chickens is a function of the bird's food intake rate.

[f] The listed mixing depth was used for the off-site exposure scenarios and the Intruder – Post-Drilling Scenario; for the Intruder-Construction and Intruder-Agriculture Scenarios the mixing depth was set equal to the thickness of the soil excavated during house construction after it was spread across the intruder's lot.

Table 14 (Continued)
Pathway Parameter Values and Distributions Used in the Performance Assessment and Composite Analysis

Parameter	Units [a]	Deterministic Value	Distribution [b]
Waste Disposal Region 3	m	7.3E+00	---
Waste Disposal Region 4	m	1.1E+01	---
Waste Disposal Region 5	m	1.4E+01	---
Waste Disposal Region 6	m	1.7E+01	---
Waste Disposal Region 7	m	1.7E+01	---
Waste Disposal Region 8	m	1.5E+01	---
Waste Emplacement Efficiency			
1988–2004 Pits		3.5E-01	T(1.8E-01, 3.5E-01, 4.2E-01)
2005–2044 Pits		5.0E-01	---
1988–2004 Shafts		2.6E-01	T(7.5E-02, 2.6E-01, 8.2E-01)
2005–2044 Shafts		5.0E-01	---
Shaft Field Efficiency		1.1E-01	---
Material Properties			
Bulk Density			
Crushed Tuff	kg/m^3 (dry weight)	1.4E+03	N(1.4E+03, 6.9E+01)
Waste	kg/m^3 (dry weight)	1.4E+03	N(1.4E+03, 6.9E+01)

--- = No distribution was defined for this parameter *[a] Blank cells indicate value is unitless*

[b] Distribution designations refer to the following distribution types: CD = cumulative distribution (cumulative probability, value), D = discrete (probability, value), LN = lognormal (geometric mean, geometric standard deviation), T = triangular (minimum, most likely, maximum), TLN = truncated lognormal distribution (geometric mean, geometric standard deviation, minimum, maximum), TN = truncated normal distribution (mean, standard deviation, minimum, maximum), U = uniform (minimum, maximum).

[c] The first value was used for the Intruder – Post-Drilling and Intruder-Agriculture Scenarios; the second value was used for the Intruder-Construction Scenario

[d] The first value represents the performance assessment; the second value the composite analysis.

[e] The distribution of the soil intake rate of chickens is a function of the bird's food intake rate.

[f] The listed mixing depth was used for the off-site exposure scenarios and the Intruder – Post-Drilling Scenario; for the Intruder-Construction and Intruder-Agriculture Scenarios the mixing depth was set equal to the thickness of the soil excavated during house construction after it was spread across the intruder's lot.

Table 14 (Continued)
Pathway Parameter Values and Distributions Used in the Performance Assessment and Composite Analysis

Parameter	Units [a]	Deterministic Value	Distribution [b]
Concrete	kg/m^3 (dry weight)	2.0E+03	N(2.0E+03, 8.1E+01)
Porosity			
Crushed Tuff		4.1E-01	N(4.1E-01, 3.3E-02)
Waste		4.1E-01	N(4.1E-01, 3.3E-02)
Concrete		2.0E-01	N(2.0E-01, 3.2E-02)
Moisture Content			
Crushed Tuff	(volume basis)	7.5E-02	T(5.0E-02, 7.5E-02, 1.2E-01)
Waste	(volume basis)	7.5E-02	T(5.0E-02, 7.5E-02, 1.2E-01)
Saturation Content			
Concrete	(volume basis)	1.0E-01	U(5.0E-02, 1.5E-01)
Radon Emanation Coefficient		2.5E-01	U(1.0E-01, 4.0E-01)
Carbon Gas Generation Rate	yr^{-1}	1.2E-02	U(3.0E-03, 2.0E-02)
Carbon Dioxide Fraction		5.0E-01	U(4.0E-01, 6.0E-01)
Organic Fraction of C-14 Waste		5.0E-02	T(1.0E-02, 5.0E-02, 1.0E-01)

— = No distribution was defined for this parameter

[a] Blank cells indicate value is unitless

[b] Distribution designations refer to the following distribution types: CD = cumulative distribution (cumulative probability, value), D = discrete (probability, value), LN = lognormal (geometric mean, geometric standard deviation), T = triangular (minimum, most likely, maximum), TLN = truncated lognormal distribution (geometric mean, geometric standard deviation, minimum, maximum), TN = truncated normal distribution (mean, standard deviation, minimum, maximum), U = uniform (minimum, maximum).

[c] The first value was used for the Intruder – Post-Drilling and Intruder-Agriculture Scenarios; the second value was used for the Intruder-Construction Scenario

[d] The first value represents the performance assessment; the second value the composite analysis.

[e] The distribution of the soil intake rate of chickens is a function of the bird's food intake rate.

[f] The listed mixing depth was used for the off-site exposure scenarios and the Intruder – Post-Drilling Scenario; for the Intruder-Construction and Intruder-Agriculture Scenarios the mixing depth was set equal to the thickness of the soil excavated during house construction after it was spread across the intruder's lot.

Table 14 (Continued)
Pathway Parameter Values and Distributions Used in the Performance Assessment and Composite Analysis

Parameter	Units [a]	Deterministic Value	Distribution [b]
Atmospheric Transport Parameters			
Dust Loading			
Inadvertent Intruder	µg/m³	1.0E-07, 1.5E-07 [c]	LN(3.0E-08, 1.6), LN(4.5E-08, 1.6) [c]
Members of Public	µg/m³	3.0E-08	LN(3.0E-08, 1.6)
Vertical Flux	g/m²/yr	1.3E+01	TN(1.3E+01, 8.4E+00, 0.0E+00, 1.0E+10)
Soil Disturbance Factor		2.0E+00	T(1.1E+00, 2.0E+00, 3.0E+00)
Enhancement Factor		3.0E+00	T(1.0E+00, 3.0E+00, 6.0E+00)
Particulate Dispersion Factor			
Grassland Land Use			
LANL Boundary			
Atmospheric Source Area 1 Releases	s/m³	1.1E-06; 9.7E-06 [d]	N(1.1E-06, 1.1E-07); N(9.7E-06, 6.2E-07) [d]
Atmospheric Source Area 2 Releases	s/m³	1.7E-05; 4.5E-06 [d]	N(1.7E-05, 8.9E-07); N(4.5E-06, 8.5E-07) [d]
Atmospheric Source Area 3 Releases	s/m³	6.3E-06; 3.1E-06 [d]	N(6.3E-06, 1.5E-06); N(3.1E-06, 1.2E-06) [d]
MDA G Fence Line			
Atmospheric Source Area 1 Releases	s/m³	3.0E-04; 4.3E-04 [d]	N(3.0E-04, 7.3E-05); N(4.3E-04, 1.2E-05) [d]
Atmospheric Source Area 2 Releases	s/m³	1.1E-06; 9.0E-06 [d]	N(1.1E-06, 1.4E-07); N(9.0E-06, 1.6E-06) [d]

— = No distribution was defined for this parameter

[a] Blank cells indicate value is unitless

[b] Distribution designations refer to the following distribution types: CD = cumulative distribution (cumulative probability, value), D = discrete (probability, value), LN = lognormal (geometric mean, geometric standard deviation), T = triangular (minimum, most likely, maximum), TLN = truncated lognormal distribution (geometric mean, geometric standard deviation, minimum, maximum), TN = truncated normal distribution (mean, standard deviation, minimum, maximum), U = uniform (minimum, maximum).

[c] The first value was used for the Intruder – Post-Drilling and Intruder-Agriculture Scenarios; the second value was used for the Intruder-Construction Scenario

[d] The first value represents the performance assessment; the second value the composite analysis.

[e] The distribution of the soil intake rate of chickens is a function of the bird's food intake rate.

[f] The listed mixing depth was used for the off-site exposure scenarios and the Intruder – Post-Drilling Scenario; for the Intruder-Construction and Intruder-Agriculture Scenarios the mixing depth was set equal to the thickness of the soil excavated during house construction after it was spread across the intruder's lot.

Table 14 (Continued)
Pathway Parameter Values and Distributions Used in the Performance Assessment and Composite Analysis

Parameter	Units [a]	Deterministic Value	Distribution [b]
Atmospheric Source Area 3 Releases	s/m³	1.8E-04; 3.5E-06 [d]	N(1.8E-04, 4.3E-05); N(3.5E-06, 1.4E-06) [d]
Woodland Land Use			
LANL Boundary			
Atmospheric Source Area 1 Releases	s/m³	6.0E-07; 3.4E-06 [d]	N(6.0E-07, 6.8E-08); N(3.4E-06, 2.8E-07) [d]
Atmospheric Source Area 2 Releases	s/m³	1.2E-05, 1.6E-06 [d]	N(1.2E-05, 8.6E-07); N(1.6E-06, 1.3E-07) [d]
Atmospheric Source Area 3 Releases	s/m³	8.0E-06, 1.2E-06 [d]	N(8.0E-06, 5.9E-07); 1.2E-06, 1.2E-07) [d]
MDA G Fence Line			
Atmospheric Source Area 1 Releases	s/m³	1.8E-07; 2.9E-04 [d]	N(1.8E-07, 3.4E-08); N(2.9E-04, 1.1E-05) [d]
Atmospheric Source Area 2 Releases	s/m³	6.2E-07; 3.7E-06 [d]	N(6.2E-07, 8.4E-08); N(3.7E-06, 2.4E-07) [d]
Atmospheric Source Area 3 Releases	s/m³	1.1E-04; 1.6E-06 [d]	N(1.1E-04, 3.8E-06); N(1.6E-06, 1.7E-07) [d]
Vapor and Gas Dispersion Factors			
LANL Boundary			
Atmospheric Source Area 1 Releases	s/m³	1.3E-06; 1.3E-06 [d]	N(1.3E-06, 1.4E-07); N(1.3E-06, 1.4E-07) [d]
Atmospheric Source Area 2 Releases	s/m³	1.8E-05; 1.8E-05 [d]	N(1.8E-06, 3.7E-06); N(1.8E-06, 3.7E-06) [d]
Atmospheric Source Area 3 Releases	s/m³	1.6E-05; 1.6E-05 [d]	N(1.6E-05, 1.3E-06); N(1.6E-05, 1.3E-06) [d]
MDA G Fence Line			

--- = No distribution was defined for this parameter *[a] Blank cells indicate value is unitless*

[b] Distribution designations refer to the following distribution types: CD = cumulative distribution (cumulative probability, value), D = discrete (probability, value), LN = lognormal (geometric mean, geometric standard deviation), T = triangular (minimum, most likely, maximum), TLN = truncated lognormal distribution (geometric mean, geometric standard deviation, minimum, maximum), TN = truncated normal distribution (mean, standard deviation, minimum, maximum), U = uniform (minimum, maximum).

[c] The first value was used for the Intruder – Post-Drilling and Intruder-Agriculture Scenarios; the second value was used for the Intruder-Construction Scenario

[d] The first value represents the performance assessment; the second value the composite analysis.

[e] The distribution of the soil intake rate of chickens is a function of the bird's food intake rate.

[f] The listed mixing depth was used for the off-site exposure scenarios and the Intruder – Post-Drilling Scenario; for the Intruder-Construction and Intruder-Agriculture Scenarios the mixing depth was set equal to the thickness of the soil excavated during house construction after it was spread across the intruder's lot.

Table 14 (Continued)
Pathway Parameter Values and Distributions Used in the Performance Assessment and Composite Analysis

Parameter	Units [a]	Deterministic Value	Distribution [b]
Atmospheric Source Area 1 Releases	s/m³	1.4E-06; 1.4E-06 [d]	N(1.4E-06, 1.7E-07); N(1.4E-06, 1.7E-07) [d]
Atmospheric Source Area 2 Releases	s/m³	2.0E-04; 2.0E-04 [d]	N(2.0E-04, 1.9E-05); N(2.0E-04, 1.9E-05) [d]
Atmospheric Source Area 3 Releases	s/m³	2.8E-05; 2.8E-05 [d]	N(2.8E-05, 1.9E-06); N(2.8E-05, 1.9E-06) [d]
Deposition Rate			
Grassland Land Use			
LANL Boundary			
Atmospheric Source Area 1 Releases	g/m²/s	2.6E-04; 2.7E-03 [d]	N(2.6E-04, 3.1E-05); N(2.7E-03, 2.5E-04) [d]
Atmospheric Source Area 2 Releases	g/m²/s	1.3E-02; 3.1E-03 [d]	N(1.3E-02; 7.3E-04); N(3.1E-03, 1.4E-04) [d]
Atmospheric Source Area 3 Releases	g/m²/s	1.8E-03; 8.9E-04 [d]	N(1.8E-03, 7.6E-04); N(8.9E-04, 3.6E-04) [d]
MDA G Fence Line			
Atmospheric Source Area 1 Releases	g/m²/s	6.9E-05; 1.1E-01 [d]	N(6.9E-05, 8.6E-06); N(1.1E-01, 1.8E-02) [d]
Atmospheric Source Area 2 Releases	g/m²/s	9.7E-04; 5.8E-03 [d]	N(9.7E-04, 1.1E-04); N(5.8E-03, 2.5E-04) [d]
Atmospheric Source Area 3 Releases	g/m²/s	5.6E-02; 9.6E-04 [d]	N(5.6E-02, 2.4E-02); N(9.6E-04, 3.9E-04) [d]
Woodland Land Use			
LANL Boundary			
Atmospheric Source Area 1 Releases	g/m²/s	3.2E-04; 3.3E-03 [d]	N(3.2E-04, 3.9E-05); N(3.3E-03, 2.8E-04) [d]

--- = No distribution was defined for this parameter

[a] Blank cells indicate value is unitless

[b] Distribution designations refer to the following distribution types: CD = cumulative distribution (cumulative probability, value), D = discrete (probability, value), LN = lognormal (geometric mean, geometric standard deviation), T = triangular (minimum, most likely, maximum), TLN = truncated lognormal distribution (geometric mean, geometric standard deviation, minimum, maximum), TN = truncated normal distribution (mean, standard deviation, minimum, maximum), U = uniform (minimum, maximum).

[c] The first value was used for the Intruder – Post-Drilling and Intruder-Agriculture Scenarios; the second value was used for the Intruder-Construction Scenario

[d] The first value represents the performance assessment; the second value the composite analysis.

[e] The distribution of the soil intake rate of chickens is a function of the bird's food intake rate.

[f] The listed mixing depth was used for the off-site exposure scenarios and the Intruder – Post-Drilling Scenario; for the Intruder-Construction and Intruder-Agriculture Scenarios the mixing depth was set equal to the thickness of the soil excavated during house construction after it was spread across the intruder's lot.

Table 14 (Continued)
Pathway Parameter Values and Distributions Used in the Performance Assessment and Composite Analysis

Parameter	Units [a]	Deterministic Value	Distribution [b]
Atmospheric Source Area 2 Releases	g/m²/s	3.8E-02; 2.8E-03 [d]	N(3.8E-02, 3.3E-03); N(2.8E-03, 1.2E-04) [d]
Atmospheric Source Area 3 Releases	g/m²/s	1.0E-02; 8.1E-04 [d]	N(1.0E-02, 8.8E-04); N(8.1E-04, 4.8E-05) [d]
MDA G Fence Line			
Atmospheric Source Area 1 Releases	g/m²/s	9.4E-05; 2.9E-01 [d]	N(9.4E-05, 1.4E-05); N(2.9E-01, 6.6E-02) [d]
Atmospheric Source Area 2 Releases	g/m²/s	1.7E-03; 4.8E-03 [d]	N(1.7E-03, 1.3E-04); N(4.8E-03, 1.8E-04) [d]
Atmospheric Source Area 3 Releases	g/m²/s	1.3E-01; 9.0E-04 [d]	N(1.3E-01, 8.0E-03); N(9.0E-04, 6.2E-05) [d]
Groundwater Transport Parameters			
Infiltration Rate			
Mesita del Buey	cm/yr	6.9E-02	TN(6.9E-02, 5.3E-05, 0.0E+00, 1.0E+10))
Pajarito Canyon	cm/yr	4.0E+01	TN(4.0E+01, 2.6E-01, 0.0E+00, 1.0E+10)
Cañada del Buey	cm/yr	2.2E-01	TN(2.2E-01, 2.7E-03, 0.0E+00, 1.0E+10)
East of MDA G Fence Line	cm/yr	5.0E-01	TN(5.0E-01, 6.4E-03, 0.0E+00, 1.0E+10)
Contaminant Capture Fraction			
Waste Disposal Region 1		4.1E-02	—
Waste Disposal Region 2		1.1E-01	—
Waste Disposal Region 3		3.6E-02	—

— = No distribution was defined for this parameter

[a] Blank cells indicate value is unitless

[b] Distribution designations refer to the following distribution types: CD = cumulative distribution (cumulative probability, value), D = discrete (probability, value), LN = lognormal (geometric mean, geometric standard deviation), T = triangular (minimum, most likely, maximum), TLN = truncated lognormal distribution (geometric mean, geometric standard deviation, minimum, maximum), TN = truncated normal distribution (mean, standard deviation, minimum, maximum), U = uniform (minimum, maximum).

[c] The first value was used for the Intruder – Post-Drilling and Intruder-Agriculture Scenarios; the second value was used for the Intruder-Construction Scenario

[d] The first value represents the performance assessment; the second value the composite analysis.

[e] The distribution of the soil intake rate of chickens is a function of the bird's food intake rate.

[f] The listed mixing depth was used for the off-site exposure scenarios and the Intruder – Post-Drilling Scenario; for the Intruder-Construction and Intruder-Agriculture Scenarios the mixing depth was set equal to the thickness of the soil excavated during house construction after it was spread across the intruder's lot.

Table 14 (Continued)
Pathway Parameter Values and Distributions Used in the Performance Assessment and Composite Analysis

Parameter	Units [a]	Deterministic Value	Distribution [b]
Waste Disposal Region 4		3.6E-02	---
Waste Disposal Region 5		5.8E-02	---
Waste Disposal Region 6		1.1E-01	---
Waste Disposal Region 7		3.6E-02	---
Waste Disposal Region 8		8.1E-02	---
Sediment Transport Parameters			
Fraction of Catchment over which Sediments Disperse		3.0E-01	T(1.0E-01, 3.0E-01, 5.0E-01)
Canyon Sediment Transport Rate	yr^{-1}	5.0E-03	N(5.0E-03, 1.0E-03)
Food-Chain Transport Parameters			
Dry-to-Wet Weight Fraction			
Leafy Vegetables		9.8E-02	TN(9.8E-02, 3.4E-02, 4.8E-02, 1.7E-01)
Produce		1.3E-01	TLN(1.3E-01, 1.1E-01, 4.1E-01)
Grain		9.1E-01	TN(9.1E-01, 1.3E-02, 8.9E-01, 9.3E-01)
Pasture Grass		2.0E-01	T(1.5E-01, 2.0E-01, 2.5E-01)
Translocation Factor			
Leafy Vegetables and Pasture Grass		1.0E+00	T(8.0E-01, 9.0E-01, 1.0E+00)

--- = No distribution was defined for this parameter

[a] Blank cells indicate value is unitless

[b] Distribution designations refer to the following distribution types: CD = cumulative distribution (cumulative probability, value), D = discrete (probability, value), LN = lognormal (geometric mean, geometric standard deviation), T = triangular (minimum, most likely, maximum), TLN = truncated lognormal distribution (geometric mean, geometric standard deviation, minimum, maximum), TN = truncated normal distribution (mean, standard deviation, minimum, maximum), U = uniform (minimum, maximum).

[c] The first value was used for the Intruder – Post-Drilling and Intruder-Agriculture Scenarios; the second value was used for the Intruder-Construction Scenario

[d] The first value represents the performance assessment; the second value the composite analysis.

[e] The distribution of the soil intake rate of chickens is a function of the bird's food intake rate.

[f] The listed mixing depth was used for the off-site exposure scenarios and the Intruder – Post-Drilling Scenario; for the Intruder-Construction and Intruder-Agriculture Scenarios the mixing depth was set equal to the thickness of the soil excavated during house construction after it was spread across the intruder's lot.

Table 14 (Continued)
Pathway Parameter Values and Distributions Used in the Performance Assessment and Composite Analysis

Parameter	Units [a]	Deterministic Value	Distribution [b]
Produce and Grain		1.0E-01	T(1.0E-02, 1.0E-01, 4.0E-01)
Agricultural Productivity			
Leafy Vegetables	kg/m² (wet weight)	1.5E+00	T(1.0E+00, 1.5E+00, 2.0E+00)
Produce	kg/m² (wet weight)	1.0E+00	T(5.0E-01, 1.0E+00, 1.5E+00)
Grain	kg/m² (wet weight)	5.0E-01	T(2.0E-01, 5.0E-01, 7.5E-01)
Pasture Grass	kg/m² (dry weight)	5.0E-01	T(1.0E-01, 5.0E-01, 7.0E-01)
Growing Season			
Leafy Vegetables	d	6.0E+01	T(4.0E+01, 6.0E+01, 1.0E+02)
Produce	d	8.0E+01	T(4.5E+01, 8.0E+01, 1.2E+02)
Grain	d	1.1E+02	T(7.0E+01, 1.1E+02, 1.2E+02)
Pasture Grass	d	4.5E+01	T(3.0E+01, 4.5E+01, 6.0E+01)
Mass Loading Factors			
Leafy Vegetables	mg soil per g plant (dry weight)	2.6E+02	TN(2.6E+02, 1.0E+02, 0.0E+00, 1.0E+04)
Produce, Grain, and Pasture Grass	mg soil per g plant (dry weight)	3.0E+01	T(1.0E+00, 3.0E+01, 1.0E+02)
Enhancement Factor		1.5E+00	T(1.0E+00, 1.5E+00, 2.0E+00)

--- = No distribution was defined for this parameter [a] *Blank cells indicate value is unitless*

[b] *Distribution designations refer to the following distribution types: CD = cumulative distribution (cumulative probability, value), D = discrete (probability, value), LN = lognormal (geometric mean, geometric standard deviation), T = triangular (minimum, most likely, maximum), TLN = truncated lognormal distribution (geometric mean, geometric standard deviation, minimum, maximum), TN = truncated normal distribution (mean, standard deviation, minimum, maximum), U = uniform (minimum, maximum).*

[c] *The first value was used for the Intruder – Post-Drilling and Intruder-Agriculture Scenarios; the second value was used for the Intruder-Construction Scenario*

[d] *The first value represents the performance assessment; the second value the composite analysis.*

[e] *The distribution of the soil intake rate of chickens is a function of the bird's food intake rate.*

[f] *The listed mixing depth was used for the off-site exposure scenarios and the Intruder – Post-Drilling Scenario; for the Intruder-Construction and Intruder-Agriculture Scenarios the mixing depth was set equal to the thickness of the soil excavated during house construction after it was spread across the intruder's lot.*

Table 14 (Continued)
Pathway Parameter Values and Distributions Used in the Performance Assessment and Composite Analysis

Parameter	Units [a]	Deterministic Value	Distribution [b]
Plant Interception Coefficient	m^2/kg	3.0E+00	T(2.0E+00, 3.0E+00, 4.0E+00)
Weathering Half-Life	d	1.7E+01	LN(1.7E+01, 1.6E+00)
Dry Matter Fraction			
Beef		3.3E-01	---
Milk		1.0E-01	---
Chicken		3.3E-01	---
Eggs		2.6E-01	---
Water Equivalent Fraction			
Beef		8.0E-01	---
Milk		6.7E-01	---
Chicken		8.0E-01	---
Eggs		8.4E-01	---
Carbon Fraction			
All Crops	(dry-weight basis)	4.5E-01	---
Soil	(dry-weight basis)	3.0E-02	---
Beef	(wet-weight basis)	2.4E-01	---

--- = No distribution was defined for this parameter

[a] Blank cells indicate value is unitless

[b] Distribution designations refer to the following distribution types: CD = cumulative distribution (cumulative probability, value), D = discrete (probability, value), LN = lognormal (geometric mean, geometric standard deviation), T = triangular (minimum, most likely, maximum), TLN = truncated lognormal distribution (geometric mean, geometric standard deviation, minimum, maximum), TN = truncated normal distribution (mean, standard deviation, minimum, maximum), U = uniform (minimum, maximum).

[c] The first value was used for the Intruder – Post-Drilling and Intruder-Agriculture Scenarios; the second value was used for the Intruder-Construction Scenario

[d] The first value represents the performance assessment; the second value the composite analysis.

[e] The distribution of the soil intake rate of chickens is a function of the bird's food intake rate.

[f] The listed mixing depth was used for the off-site exposure scenarios and the Intruder – Post-Drilling Scenario; for the Intruder-Construction and Intruder-Agriculture Scenarios the mixing depth was set equal to the thickness of the soil excavated during house construction after it was spread across the intruder's lot.

Table 14 (Continued)
Pathway Parameter Values and Distributions Used in the Performance Assessment and Composite Analysis

Parameter	Units [a]	Deterministic Value	Distribution [b]
Milk	(wet-weight basis)	7.0E-02	---
Chicken	(wet-weight basis)	2.0E-01	---
Eggs	(wet-weight basis)	1.5E-01	---
Animal Food Ingestion Rates			
Cows	kg/d (dry weight)	1.6E+01	T(1.0E+01, 1.6E+01, 2.5E+01)
Cattle	kg/d (dry weight)	1.2E+01	T(7.5E+00, 1.2E+01, 1.8E+01)
Chickens	kg/d (dry weight)	7.0E-02	T(5.0E-02, 7.0E-02, 1.5E-01)
Animal Water Ingestion Rates			
Cows	L/d	7.5E+01	T(5.0E+01, 7.5E+01, 1.0E+02)
Cattle	L/d	4.0E+01	T(2.0E+01, 4.0E+01, 6.0E+01)
Chickens	L/d	2.0E-01	T(1.0E-01, 2.0E-01, 3.0E-01)
Animal Soil/Grit Ingestion Rate			
Cows and Cattle	kg/d	1.0E+00	T(4.0E-01, 1.0E+00, 2.2E+00)
Chickens [e]	% of dry forage intake	2.0E-01	D(1.0E+00, 2.0E-02)
Biotic Intrusion Model Parameters			
Time of Climax	yr	2.0E+02	T(1.0E+02, 2.0E+02, 3.0E+02)

--- = No distribution was defined for this parameter

[a] Blank cells indicate value is unitless

[b] Distribution designations refer to the following distribution types: CD = cumulative distribution (cumulative probability, value), D = discrete (probability, value), LN = lognormal (geometric mean, geometric standard deviation), T = triangular (minimum, most likely, maximum), TLN = truncated lognormal distribution (geometric mean, geometric standard deviation, minimum, maximum), TN = truncated normal distribution (mean, standard deviation, minimum, maximum), U = uniform (minimum, maximum).

[c] The first value was used for the Intruder – Post-Drilling and Intruder-Agriculture Scenarios; the second value was used for the Intruder-Construction Scenario

[d] The first value represents the performance assessment; the second value the composite analysis.

[e] The distribution of the soil intake rate of chickens is a function of the bird's food intake rate.

[f] The listed mixing depth was used for the off-site exposure scenarios and the Intruder – Post-Drilling Scenario; for the Intruder-Construction and Intruder-Agriculture Scenarios the mixing depth was set equal to the thickness of the soil excavated during house construction after it was spread across the intruder's lot.

Table 14 (Continued)
Pathway Parameter Values and Distributions Used in the Performance Assessment and Composite Analysis

Parameter	Units [a]	Deterministic Value	Distribution [b]
Maximum Rooting Depth			
Grasses	m	1.7E+00	T(7.6E-01, 1.7E+00, 4.0E+00)
Forbs	m	2.4E+00	T(3.0E-01, 2.4E+00, 9.1E+00)
Shrubs	m	2.9E+00	T(1.4E+00, 2.9E+00, 9.1E+00)
Trees	m	6.0E+00	T(2.0E+00, 6.0E+00, 1.0E+01)
Biomass Density			
Grasses – Early Succession	kg/m^2	5.6E-02	T(2.8E-03, 5.6E-02, 1.5E-01)
Grasses – Climax Condition	kg/m^2	1.0E-02	T(2.0E-03, 1.0E-02, 6.2E-02)
Forbs – Early Succession	kg/m^2	4.3E-03	T(0.0E+00, 4.3E-03, 4.8E-02)
Forbs – Climax Condition	kg/m^2	3.5E-03	T(1.0E-03, 3.5E-03, 7.7E-03)
Shrubs – Early Succession	kg/m^2	8.3E-03	T(7.9E-04, 8.3E-03, 3.8E-02)
Shrubs – Climax Condition	kg/m^2	7.1E-03	T(3.0E-03, 7.1E-03, 1.3E-02)
Trees	kg/m^2	5.3E+00	T(2.3E+00, 5.3E+00, 1.2E+01)
Litter Production Fraction			
Grasses	yr^{-1}	6.0E-01	T(3.0E-01, 6.0E-01, 1.0E+00)
Forbs	yr^{-1}	6.0E-01	T(3.0E-01, 6.0E-01, 1.0E+00)

--- = No distribution was defined for this parameter

[a] Blank cells indicate value is unitless

[b] Distribution designations refer to the following distribution types: CD = cumulative distribution (cumulative probability, value), D = discrete (probability, value), LN = lognormal (geometric mean, geometric standard deviation), T = triangular (minimum, most likely, maximum), TLN = truncated lognormal distribution (geometric mean, geometric standard deviation, minimum, maximum), TN = truncated normal distribution (mean, standard deviation, minimum, maximum), U = uniform (minimum, maximum).

[c] The first value was used for the Intruder – Post-Drilling and Intruder-Agriculture Scenarios; the second value was used for the Intruder-Construction Scenario

[d] The first value represents the performance assessment; the second value the composite analysis.

[e] The distribution of the soil intake rate of chickens is a function of the bird's food intake rate.

[f] The listed mixing depth was used for the off-site exposure scenarios and the Intruder – Post-Drilling Scenario; for the Intruder-Construction and Intruder-Agriculture Scenarios the mixing depth was set equal to the thickness of the soil excavated during house construction after it was spread across the intruder's lot.

Table 14 (Continued)
Pathway Parameter Values and Distributions Used in the Performance Assessment and Composite Analysis

Parameter	Units [a]	Deterministic Value	Distribution [b]
Shrubs	yr^{-1}	1.3E-01	T(6.0E-02, 1.3E-01, 6.0E-01)
Trees	yr^{-1}	7.5E-02	T(1.0E-02, 7.5E-02, 1.4E-01)
Litter Decomposition Half-Life	yr	2.0E+00	T(1.0E+00, 20E+00, 6.0E+00)
Maximum Burrow Depth			
Harvester Ants	m	3.0E+00	T(2.0E+00, 3.0E+00, 4.0E+00)
Mice	m	1.0E+00	T(5.0E-01, 1.0E+00, 2.0E+00)
Pocket Gophers	m	1.3E+00	T(5.0E-01, 1.3E+00, 2.0E+00)
Chipmunks and Ground Squirrels	m	1.0E+00	T(5.0E-01, 1.0E+00, 2.0E+00)
Burrow Density			
Harvester Ants	ha^{-1}	2.8E+01	TN(2.8E+01, 2.0E+01, 0.0E+00, 1.0E+03)
Mice – Early Succession	ha^{-1}	2.0E+01	T(1.0E+01, 2.0E+01, 3.2E+01)
Mice – Climax Condition	ha^{-1}	7.7E+00	T(1.5E+00, 7.7E+00, 8.5E+01)
Chipmunks and Ground Squirrels	ha^{-1}	1.5E+01	T(5.0E+00, 1.5E+01, 2.5E+01)
Burrow Mass or Volume			
Harvester Ants	kg	3.8E+01	T(2.3E+01, 3.8E+01, 6.5E+01)
Mice	m^3	1.4E-02	T(3.0E-03, 1.4E-02, 1.0E-01)

— = No distribution was defined for this parameter [a] *Blank cells indicate value is unitless*

[b] *Distribution designations refer to the following distribution types: CD = cumulative distribution (cumulative probability, value), D = discrete (probability, value), LN = lognormal (geometric mean, geometric standard deviation), T = triangular (minimum, most likely, maximum), TLN = truncated lognormal distribution (geometric mean, geometric standard deviation, minimum, maximum), TN = truncated normal distribution (mean, standard deviation, minimum, maximum), U = uniform (minimum, maximum).*

[c] *The first value was used for the Intruder – Post-Drilling and Intruder-Agriculture Scenarios; the second value was used for the Intruder-Construction Scenario*

[d] *The first value represents the performance assessment; the second value the composite analysis.*

[e] *The distribution of the soil intake rate of chickens is a function of the bird's food intake rate.*

[f] *The listed mixing depth was used for the off-site exposure scenarios and the Intruder – Post-Drilling Scenario; for the Intruder-Construction and Intruder-Agriculture Scenarios the mixing depth was set equal to the thickness of the soil excavated during house construction after it was spread across the intruder's lot.*

Table 14 (Continued)
Pathway Parameter Values and Distributions Used in the Performance Assessment and Composite Analysis

Parameter	Units [a]	Deterministic Value	Distribution [b]
Chipmunks and Ground Squirrels	m^3	2.0E-02	T(8.0E-03, 2.0E-02, 7.7E-02)
Harvester Ant Colony Lifespan	yr	2.1E+01	T(5.0E+00, 2.1E+01, 5.8E+01)
Pocket Gopher Soil Removal Rate	m^3/ha/yr	8.3E+00	T(5.1E-01, 8.3E+00, 8.2E+01)
Burrow Renewal Fraction			
Pocket Gophers	yr^{-1}	8.8E-01	T(7.5E-01, 8.8E-01, 1.0E+00)
Mice	yr^{-1}	8.8E-01	T(7.5E-01, 8.8E-01, 1.0E+00)
Chipmunks and Ground Squirrels	yr^{-1}	7.5E-01	T(5.0E-01, 7.5E-01, 1.0E+00)
Exposure Pathway Parameters			
Indoor Time Allotment	hr/d	1.6E+01	CD(0.0E+00, 9.6E+00; 5.0E-02, 9.6E+00; 2.5E-01, 1.3E+01; 5.0E-01, 1.6E+01; 7.5E-01, 2.1E+01; 9.0E-01, 2.3E+01; 9.5E-01, 2.4E+01; 1.0E+00, 2.4E+01)
Outdoor Time Allotment	hr/d	1.8E+00	CD(0.0E+00, 0.0E+00; 5.0E-02, 8.3E-02; 2.5E-01, 6.7E-01; 5.0E-01, 1.8E+00; 7.5E-01, 3.5E+00; 9.0E-01, 6.0E+00; 9.5E-01, 8.0E+00; 9.8E-01, 1.0E+01; 9.9E-01, 1.2E+01; 1.0E+01,2.2E+01)
Construction Worker Exposure Time	hr	5.0E+02	---
Excavation Occupancy Factor		1.0E-01	T(0.0E+00, 1.0E-01, 2.0E-01)
Soil Mixing Depth	cm	1.5E+01 [f]	---
Direct Radiation Shielding Factor	---	4.0E-01	U(2.0E-01, 6.0E-01)

--- = No distribution was defined for this parameter

[a] Blank cells indicate value is unitless

[b] Distribution designations refer to the following distribution types: CD = cumulative distribution (cumulative probability, value), D = discrete (probability, value), LN = lognormal (geometric mean, geometric standard deviation), T = triangular (minimum, most likely, maximum), TLN = truncated lognormal distribution (geometric mean, geometric standard deviation, minimum, maximum), TN = truncated normal distribution (mean, standard deviation, minimum, maximum), U = uniform (minimum, maximum).

[c] The first value was used for the Intruder – Post-Drilling and Intruder-Agriculture Scenarios; the second value was used for the Intruder-Construction Scenario

[d] The first value represents the performance assessment; the second value the composite analysis.

[e] The distribution of the soil intake rate of chickens is a function of the bird's food intake rate.

[f] The listed mixing depth was used for the off-site exposure scenarios and the Intruder – Post-Drilling Scenario; for the Intruder-Construction and Intruder-Agriculture Scenarios the mixing depth was set equal to the thickness of the soil excavated during house construction after it was spread across the intruder's lot.

Table 14 (Continued)
Pathway Parameter Values and Distributions Used in the Performance Assessment and Composite Analysis

Parameter	Units [a]	Deterministic Value	Distribution [b]
Inhalation Rate			
Resident Receptors	m^3/d	1.5E+01	T(1.3E+01, 1.5E+01, 1.7E+01)
Intruder-Construction Scenario	m^3/hr	1.5E+00	TN(1.5E+00, 6.0E-01, 5.0E-01, 1.0E+10)
Average Wind Speed	m/s	2.6E+00	LN(2.6E+00, 1.4E+00)
Atmospheric Mixing Height	m	2.0E+00	---
House Ventilation Rate	hr^{-1}	4.7E-01	LN(4.7E-01, 2.1E+00)
Irrigation Rate			
Leafy Vegetables	cm/yr	4.8E+01	T(1.2E+01, 4.8E+01, 8.3E+01)
Produce	cm/yr	7.4E+01	T(2.3E+01, 7.4E+01, 1.2E+02)
Grain	cm/yr	6.5E+01	T(3.5E+01, 6.5E+01. 8.8E+01)
Pasture Grass	cm/yr	8.4E+01	T(4.6E+01, 8.4E+01, 1.2E+02)
Inadvertent Soil Ingestion Rate	kg/yr	3.6E-02	LN(3.6E-02, 3.2E+00)
Drinking Water Ingestion Rate	L/d	2.0E+00	CD(0.0E+00, 1.5E-01; 5.0E-02, 4.2E-01; 1.0E-01, 5.6E-01; 2.5E-01, 8.7E-01; 5.0E-01, 1.3E+00; 7.5E-01, 1.7E+00; 9.0E-01, 2.3E+00; 9.5E-01, 2.7E+00; 1.0E+00, 3.8E+00)
Fraction of Vegetables from Site		3.1E-01	T(1.7E-01, 3.1E-01, 4.2E-01)

— = No distribution was defined for this parameter

[a] Blank cells indicate value is unitless

[b] Distribution designations refer to the following distribution types: CD = cumulative distribution (cumulative probability, value), D = discrete (probability, value), LN = lognormal (geometric mean, geometric standard deviation), T = triangular (minimum, most likely, maximum), TLN = truncated lognormal distribution (geometric mean, geometric standard deviation, minimum, maximum), TN = truncated normal distribution (mean, standard deviation, minimum, maximum), U = uniform (minimum, maximum).

[c] The first value was used for the Intruder – Post-Drilling and Intruder-Agriculture Scenarios; the second value was used for the Intruder-Construction Scenario

[d] The first value represents the performance assessment; the second value the composite analysis.

[e] The distribution of the soil intake rate of chickens is a function of the bird's food intake rate.

[f] The listed mixing depth was used for the off-site exposure scenarios and the Intruder – Post-Drilling Scenario; for the Intruder-Construction and Intruder-Agriculture Scenarios the mixing depth was set equal to the thickness of the soil excavated during house construction after it was spread across the intruder's lot.

Table 14 (Continued)
Pathway Parameter Values and Distributions Used in the Performance Assessment and Composite Analysis

Parameter	Units [a]	Deterministic Value	Distribution [b]
Fraction of Animal Products from Site			
Beef		5.0E-01	T(4.0E-01, 5.0E-01, 6.0E-01)
Milk		1.5E-01	T(1.2E-01, 1.5E-01, 1.8E-01)
Chicken		2.5E-01	T(1.2E-01, 1.5E-01, 1.8E-01)
Eggs		2.0E-01	T(1.6E-01, 2.0E-01, 2.4E-01)
Crop Ingestion Rates			
Leafy Vegetables	kg/yr	1.5E+01	CD(0.0E+00, 0.0E+00; 5.0E-02, 3.2E+00; 1.0E-01, 5.2E+00; 2.5E-01, 8.6E+00; 5.0E-01, 1.3E+01; 7.5E-01, 1.9E+01; 9.0E-01, 2.6E+01; 9.5E-01, 3.1E+01; 9.9E-01, 4.3E+01; 1.0E+00, 8.4E+01)
Produce	kg/yr	8.5E+01	CD(0.0E+00, 0.0E+00; 5.0E-02, 1.8E+01; 1.0E-01, 2.9E+01; 2.5E-01, 4.8E+01; 5.0E-01, 7.5E+01; 7.5E-01, 1.1E+02; 9.0E-01, 1.5E+02; 9.5E-01, 1.7E+02; 9.9E-01, 2.4E+02; 1.0E+00, 4.7E+02)
Grain	kg/yr	7.9E+01	CD(0.0E+00, 0.0E+00; 1.0E-02, 1.1E+00; 5.0E-02, 1.9E+01; 1.0E-01, 2.7E+01; 2.5E-01, 4.4E+01; 5.0E-01, 6.8E+01; 7.5E-01, 9.9E+01; 9.0E-01, 1.4E+02; 9.5E-010, 1.7E+02; 9.9E-01, 2.4E+02; 1.0E+00, 5.9E+02)

— = No distribution was defined for this parameter

[a] Blank cells indicate value is unitless

[b] Distribution designations refer to the following distribution types: CD = cumulative distribution (cumulative probability, value), D = discrete (probability, value), LN = lognormal (geometric mean, geometric standard deviation), T = triangular (minimum, most likely, maximum), TLN = truncated lognormal distribution (geometric mean, geometric standard deviation, minimum, maximum), TN = truncated normal distribution (mean, standard deviation, minimum, maximum), U = uniform (minimum, maximum).

[c] The first value was used for the Intruder – Post-Drilling and Intruder-Agriculture Scenarios; the second value was used for the Intruder-Construction Scenario

[d] The first value represents the performance assessment; the second value the composite analysis.

[e] The distribution of the soil intake rate of chickens is a function of the bird's food intake rate.

[f] The listed mixing depth was used for the off-site exposure scenarios and the Intruder – Post-Drilling Scenario; for the Intruder-Construction and Intruder-Agriculture Scenarios the mixing depth was set equal to the thickness of the soil excavated during house construction after it was spread across the intruder's lot.

Table 14 (Continued)
Pathway Parameter Values and Distributions Used in the Performance Assessment and Composite Analysis

Parameter	Units [a]	Deterministic Value	Distribution [b]
Animal Product Ingestion Rates			
Beef	kg/yr	1.9E+01	CD(0.0E+00, 0.0E+00; 1.0E-01, 1.3E+00; 2.5E-01, 6.3E+00; 5.0E-01, 1.5E+01; 7.5E-01, 2.6E+01; 9.0E-01, 4.0E+01; 9.5E-01, 5.0E+01; 9.9E-01, 7.1E+01; 1.0E+00, 1.4E+02)
Milk	L/yr	7.4E+01	CD(0.0E+00, 0.0E+00; 5.0E-02, 2.4E+00; 1.0E-01, 6.2E+00; 2.5E-01, 2.1E+01; 5.0E-01, 5.2E+01; 7.5E-01, 9.8E+01; 9.0E-01, 1.6E+02; 9.5E-01, 2.0E+02; 9.9E-01, 3.1E+02; 1.0E+00, 7.7E+02)
Chicken	kg/yr	1.4E+01	CD(0.0E+00, 0.0E+00; 5.0E-01, 4.7E-02; 1.0E-01, 3.5E-01; 2.5E-01, 2.3E+00; 5.0E-01, 8.0E+00; 7.5E-01, 1.9E+01; 9.0E-01, 3.3E+01; 9.5E-01, 4.2E+01; 9.9E-01, 6.4E+01; 1.0E+00, 1.3E+02)
Eggs	kg/yr	9.5E+00	CD(0.0E+00, 0.0E+00; 7.5E-01, 1.0E+01; 9.0E-01, 2.0E+01; 9.5E-01, 2.8E+01; 9.9E-01, 4.2E+01; 1.0E+00, 1.0E+02)
Weight of Cattle at Slaughter	kg	5.0E+02	N(5.0E+02, 2.5E+01)
Carcass-to-Live Weight Ratio for Cattle		6.4E-01	N(6.4E-01, 2.0E-02)
Fraction of Beef Carcass Sold as Meat		5.0E-01	N(5.0E-01, 2.4E-02)
Milk Prodction Rate of Cows	kg/yr	8.6E+03	N(8.6E+03, 1.5E+02)
Weight of Chicken at Slaughter	kg	2.3E+00	N(2.3E+00, 4.5E-01)
Ratio of Ready-to-Cook Chicken and Live Weight		7.4E-01	N(7.4E-01, 4.5E-03)

--- = No distribution was defined for this parameter

[a] Blank cells indicate value is unitless

[b] Distribution designations refer to the following distribution types: CD = cumulative distribution (cumulative probability, value), D = discrete (probability, value), LN = lognormal (geometric mean, geometric standard deviation), T = triangular (minimum, most likely, maximum), TLN = truncated lognormal distribution (geometric mean, geometric standard deviation, minimum, maximum), TN = truncated normal distribution (mean, standard deviation, minimum, maximum), U = uniform (minimum, maximum).

[c] The first value was used for the Intruder – Post-Drilling and Intruder-Agriculture Scenarios; the second value was used for the Intruder-Construction Scenario

[d] The first value represents the performance assessment; the second value the composite analysis.

[e] The distribution of the soil intake rate of chickens is a function of the bird's food intake rate.

[f] The listed mixing depth was used for the off-site exposure scenarios and the Intruder – Post-Drilling Scenario; for the Intruder-Construction and Intruder-Agriculture Scenarios the mixing depth was set equal to the thickness of the soil excavated during house construction after it was spread across the intruder's lot.

Table 14 (Continued)
Pathway Parameter Values and Distributions Used in the Performance Assessment and Composite Analysis

Parameter	Units [a]	Deterministic Value	Distribution [b]
Fraction of Ready-to-Cook Weight of Chicken that is Meat	5.0E-01	---	
Egg Production Rate	yr^{-1}	2.6E+02	N(2.6E+02, 1.3E+01)
Mass of Egg	kg	6.0E-02	N(6.0E-02, 3.5E-03)
Fraction of Egg Mass that is Shell		5.0E-01	---
Area of Receptor's House	m^2	2.0E+02	---
Room Height	m	2.4E+00	---
Well Diameter	cm	2.5E+01	---

--- = No distribution was defined for this parameter

[a] Blank cells indicate value is unitless

[b] Distribution designations refer to the following distribution types: CD = cumulative distribution (cumulative probability, value), D = discrete (probability, value), LN = lognormal (geometric mean, geometric standard deviation), T = triangular (minimum, most likely, maximum), TLN = truncated lognormal distribution (geometric mean, geometric standard deviation, minimum, maximum), TN = truncated normal distribution (mean, standard deviation, minimum, maximum), U = uniform (minimum, maximum).

[c] The first value was used for the Intruder – Post-Drilling and Intruder-Agriculture Scenarios; the second value was used for the Intruder-Construction Scenario

[d] The first value represents the performance assessment; the second value the composite analysis.

[e] The distribution of the soil intake rate of chickens is a function of the bird's food intake rate.

[f] The listed mixing depth was used for the off-site exposure scenarios and the Intruder – Post-Drilling Scenario; for the Intruder-Construction and Intruder-Agriculture Scenarios the mixing depth was set equal to the thickness of the soil excavated during house construction after it was spread across the intruder's lot.

The thickness of the waste in the disposal pits and shafts varies among the eight disposal regions. To determine these thicknesses it is necessary to know the distance from the surface of the ground to the top of the waste, or the head space. The minimum distance to waste depends upon the operational period of the disposal unit. While no explicit guidelines were in place when pits 1 through 4 were active, guidelines issued in subsequent years have specified minimum distances to waste ranging from 0.6 to 3 m (2 to 3.3 ft) (Koopman, 1965; LANL, 1975; LANL, 1998). Because specific knowledge of the distance to waste for the closed disposal units was not available, the waste thickness for each disposal region was estimated by subtracting 1 m (3.3 ft) from the average depth of the disposal units comprising that region; the average depth was calculated using the unit-specific depths summarized in Shuman (2005). The thickness of the waste that will be disposed of in Zone 4 units was calculated based on the assumption that all units will be 18 m (60 ft) deep with a head space of 3 m (10 ft), as specified by Day et al. (2005). Estimates of waste thickness are included in Table 14.

Waste disposal region 1 includes both pits and shafts; the average thickness of the waste in the pits is about 0.8 m (2.7 ft) greater than that in the shafts. A single waste thickness was estimated for this region by weighting the average pit and shaft waste thicknesses by the volumes of waste placed in the two types of units. Given that 99 percent of the volume of waste disposed in this region was placed in pits, the waste thickness adopted for this region was essentially the average thickness of the waste in the pits.

5.2.5 Waste Emplacement Efficiency

The waste emplacement efficiency is the fraction of the pit or shaft disposal capacity occupied by waste, with the remainder consisting of uncontaminated backfill. Radionuclide concentrations in the disposal units depend, in part, upon the emplacement efficiency. Consequently, it directly or indirectly enters into all estimates of potential impacts to human health and safety.

The waste emplacement efficiency is specified directly in the intruder and intruder diffusion models, where is it used to estimate radionuclide concentrations in the disposed waste. The emplacement efficiencies used in these models pertain to the disposal pits and shafts used from 1988 through 2004 and those destined to receive waste from 2005 through 2044. The efficiencies for the pits and shafts used from 1988 through 2004 were estimated on basis of the units that were active during this period and that have undergone interim closure. The distributions of those emplacement efficiencies are included in Table 14. A waste emplacement efficiency of 0.5 was assumed for all pits and shafts in the Zone 4 expansion area, which is the efficiency upon which the Zone 4 design is based (Day et al., 2005).

The waste emplacement efficiency is not directly input into the site and site diffusion models but is reflected by the selection of the dimensions of the disposal pits and shafts relative to the disposed waste volumes. The implied efficiencies for the eight waste disposal regions are

summarized in Table 15. The efficiencies for disposal regions 1 through 7 were estimated using two approaches. In the first, disposal volumes were divided by the volumes of the pits and shafts, which were calculated using the listed dimensions of the disposal units and an assumed 1 m (3.3 ft) head space. The second approach uses the disposal areas listed in Table 9 and the waste thicknesses included in Table 15. Together, these estimates suggest that waste composes approximately 10 to 35 percent of the material that has been placed in pits and shafts in waste disposal regions 1 through 7. The use of waste containers combined with more efficiently designed disposal units is expected to yield higher future waste emplacement efficiencies for disposal region 8. The emplacement efficiency listed in Table 15 for disposal region 8 is the assumed efficiency upon which the Zone 4 design is based (Day et al., 2005).

Table 15
Waste Emplacement Efficiencies for the Eight Waste Disposal Regions

Waste Disposal Region	Waste Emplacement Efficiency	
	Based on Disposal Unit Dimensions	Based on Disposal Unit Coordinates and Average Waste Thickness
1	2.1E-01	2.3E-01
2	1.8E-01	1.1E-01
3	2.2E-01	2.4E-01
4	1.8E-01	1.0E-01
5	1.3E-01	1.1E-01
6	3.3E-01	3.4E-01
7	1.8E-01	1.2E-01
8	5.0E-01	5.0E-01

The two sets of emplacement efficiencies listed in Table 15 differ because of differences in the disposal unit areas used in their calculation and because the coordinate-based approach shown in the last column uses an average depth for all waste within a disposal region. Nevertheless, the two sets of estimates are in general agreement. The coordinate-based estimates were adopted for the performance assessment and composite analysis because they are self-consistent with the surface erosion modeling and other aspects of the performance modeling.

The emplacement efficiencies listed in Table 15 do not accurately represent the efficiency with which the pit disposal capacity at MDA G has been used over the years. In actuality, the disposal capacity of a pit is much less than the volume estimated from the unit's surface dimensions, which indicates that usage efficiencies are much higher than those listed in the table. One reason for the discrepancy is that a significant portion of the pit is occupied by the access ramp used to

transport waste into the unit; another reason is that the inward slope of the pit walls reduces the volume available for waste placement.

5.2.6 Shaft Field Efficiency

The disposal shafts at MDA G are typically distributed in groups of 5 to more than 20 units; these groups are referred to as shaft fields. The shafts within the shaft fields are placed subject to minimum spacing requirements. Historically, shafts with diameters of 0.9 m (3 ft) or less had a minimum center-to-center spacing of 2.3 m (7.5 ft); larger shafts were arranged to maintain at least 5.5 m (18 ft) between centers (Kopp, 1991). The conceptual design for Zone 4 was developed based on the assumption that the sides of adjacent shafts will be separated by 3 m (10 ft).

The shaft field efficiency refers to the fractional area within a shaft field that consists of actual disposal units. It is used to define the disposal areas for the regions with shafts, and in the development of intruder dose projections and intruder-based WAC. The 1997 performance assessment (Hollis et al., 1997) estimated a shaft field efficiency factor of 0.107; this estimate is based on data representing the majority of the shafts present at MDA G today. A shaft field efficiency was estimated for Zone 4 using the conceptual design developed for this area by Day et al. (2005). The design was for a single shaft field with 158 disposal shafts. These shafts included eight 6.1 m (20 ft) diameter shafts and three groups of 50 shafts with diameters of 1.2 m (4 ft), 1.8 m (6 ft), and 2.4 m (8 ft).

The shaft field efficiency for Zone 4 was estimated by dividing the combined surface area of the 158 shafts by the area of the entire shaft field. The area of the shaft field was estimated by drawing polygons around the disposal units and estimating the total area of those polygons. Figure 17 illustrates this process, depicting the expansion area shaft field and the two polygons drawn to encompass the disposal units (A and B). The total area of these polygons is approximately 5,900 m^2 (1.5 ac). Dividing this total shaft field area into the total summed area of the individual shafts yields a shaft field efficiency of 0.11.

The shaft field efficiency estimated in 1997 (Hollis et al., 1997) and that calculated for the Zone 4 expansion area are virtually identical. Given this, a single efficiency of 0.11 was adopted for this revision of the performance assessment and composite analysis. This efficiency was assumed to be constant across all disposal shafts.

5.3 Material Properties

The GoldSim models simulate the release and transport of radionuclides from the disposal pits and shafts to locations accessible to the off-site receptors and inadvertent intruders. Cells are used to represent the physical media within which release and transport take place, as discussed in Section 3.6.1. Each of these cells is defined in terms of its physical dimensions and the

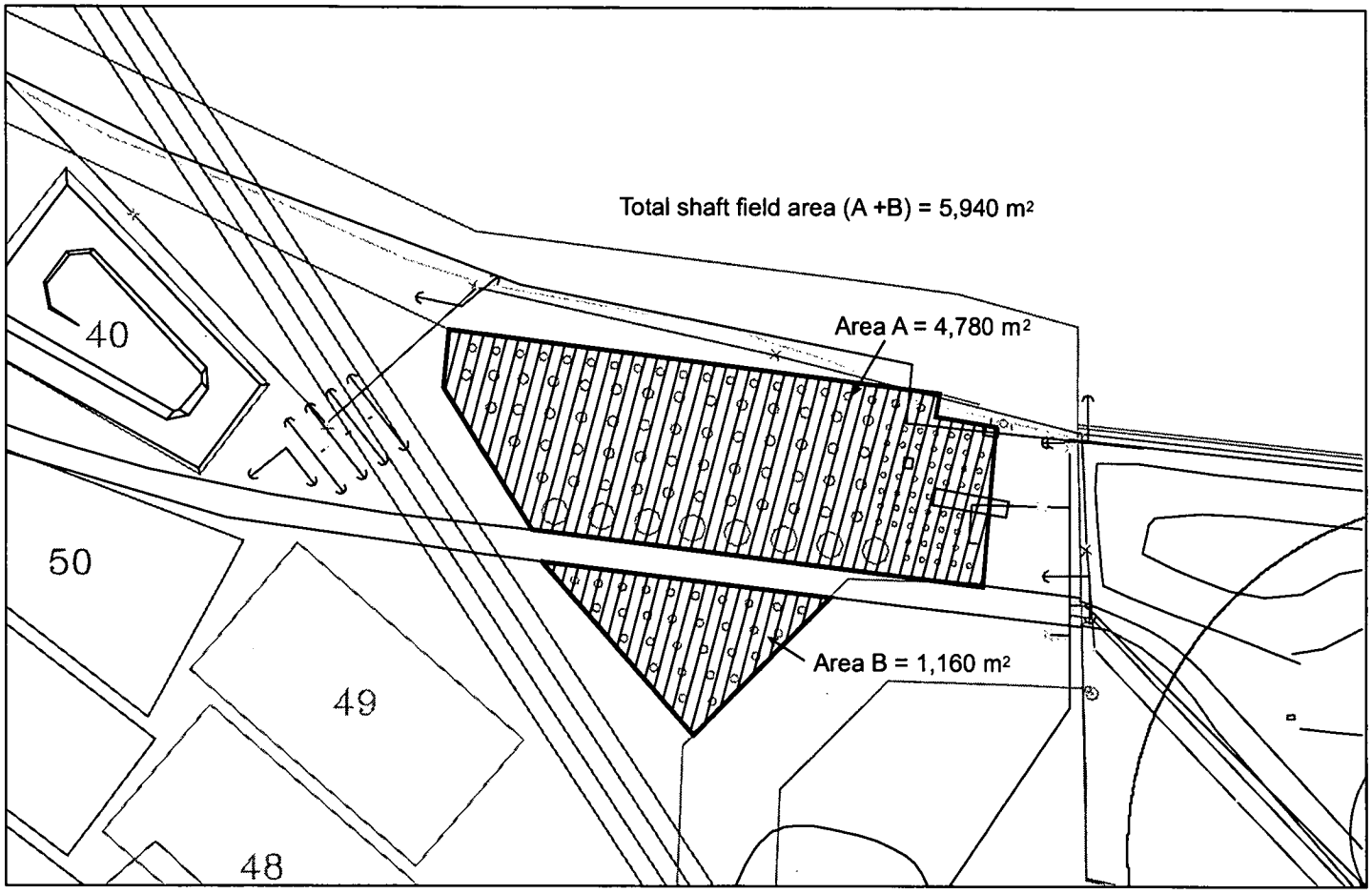

Figure 17
Calculation of Proposed Shaft Field Area in Zone 4

environmental media of which it is comprised. Cells representing the buried waste, for instance, have dimensions consistent with the disposal units in which the material is disposed. Each waste cell consists of the waste itself, the water that occupies pore space in the waste, and the air that occupies the air-filled fraction of the pores. The various physical properties and parameters used to describe these media are described below.

5.3.1 Dry Bulk Density, Porosity, and Moisture Content

Limited information is available regarding the dry bulk density of crushed tuff. In their summary of unsaturated hydraulic properties of the Bandelier Tuff, Rogers and Gallaher (1995) cite a bulk density of 1,400 kg/m^3 (87 lb/ft^3) for crushed tuff; the bulk density of Tshirege unit 2b, which forms the surface at MDA G, ranged from 1,280 to 1,460 kg/m^3 (80 to 91 lb/ft^3) with a mean and median of 1,370 kg/m^3 (85 lb/ft^3). Springer (2004) reviewed matrix hydrologic properties for the Bandelier Tuff and developed distributions of unsaturated zone properties at various technical areas at the Laboratory. The density data summarized by Springer for Tshirege unit 2 at TA-54 yield mean and median densities of 1,400 kg/m^3 (87 lb/ft^3); a portion of the data evaluated for this area was common to the data evaluated by Rogers and Gallaher (1995). Finally, Abeele (1984) reported a bulk density of 1,400 kg/m^3 (87 lb/ft^3) for crushed tuff.

Information about the porosity of crushed tuff is also limited. Rogers and Gallaher (1995) cite a porosity of 0.38 for crushed tuff. A median porosity of 0.45 was found for Tshirege unit 2b; the measured values range from 0.4 to 0.74, with all but one of the measurements falling below 0.55. Springer (2004) summarized data collected from Tshirege unit 2 at TA-54 and reported porosities ranging from 0.37 to 0.46 with mean and median values of 0.41. Abeele (1984) reported a crushed tuff porosity of 0.45.

Moisture content has been measured for crushed tuff and the waste disposed of at MDA G. Rogers and Gallaher (1995) cite a moisture content of 7.5 percent (volume basis) for crushed tuff. Loaiza and Vold (1995) reported measurements collected from a series of vertical boreholes located across the facility; some of these boreholes are located within disposal units or in otherwise disturbed tuff, while others occur in areas undisturbed by disposal operations. Data for the undisturbed boreholes indicate surface moisture contents ranging from 5 to 7 percent; water contents typically decreased to 1 to 2 percent at depths of 3.5 m (12 ft) or more. Moisture contents measured at disturbed locations generally ranged from 7.5 to 14 percent near the surface. The authors cite moisture content data from other studies; Abeele and Wheeler (1981) found tuff moisture contents of 5 to 10 percent at the surface, while Abeele (1986) reported tuff moisture contents ranging from 5 to 15 percent in the upper 3 to 4.5 m (10 to 15 ft). Haagenstad (2002) reviewed moisture content data collected from pits 15, 37, and 39 and concluded the moisture content averaged 6.8 percent within 1.2 m (4 ft) of the surface, 9.5 percent at depths of 1.5 to 6.4 m (5 to 21 ft), and 10.2 percent at depths of 6.7 and 11 m (22 and 35 ft).

The bulk densities, porosities, and moisture contents adopted for the performance assessment and composite analysis are included in Table 14. The data cited by Springer (2004) for Tshirege unit 2 were used to estimate the bulk density of crushed tuff. A normal distribution with a mean and standard deviation of 1,400 and 69 kg/m^3 (87 and 4.3 lb/ft^3), respectively, was adopted for the analyses; the mean was used for the deterministic modeling. While the data used to define this distribution represent tuff from Tshirege unit 2 and not crushed material used for cover construction, the densities of the two materials do not appear to diverge significantly. The porosity measurements summarized by Springer (2004) for Tshirege unit 2 at TA-54 were used to estimate a distribution of porosities for the crushed tuff. A normal distribution was defined with a mean and standard deviation of 0.41 and 0.03, respectively.

The bulk density and porosity of the waste placed in the pits and shafts are unknown and are expected to be highly variable within and among units. However, 50 percent or more of the material placed in the disposal units is expected to consist of crushed tuff that has been used as backfill. Given this, along with the inability to accurately determine the properties of the waste itself, the dry bulk densities and porosities assigned to crushed tuff were also assumed to apply to the waste.

The moisture content data discussed above suggest that higher water contents exist near the surface of the disposal units than in relatively undisturbed areas. Given that the modeling focuses on the transport of radionuclides from the pits and shafts, the data for disturbed areas were relied upon to define the moisture content distribution. A triangular distribution was assumed, with minimum, most likely, and maximum values of 5, 7.5, and 12 percent (volume basis); these data were used for both crushed tuff and waste.

The material properties of the concrete used to represent the foundation of the inadvertent intruder's house could vary widely. Lacking specific concrete-mix design specifications, it was assumed that the dry bulk density of concrete was normally distributed with a mean and standard deviation of 2,000 and 81 kg/m^3 (130 and 5.0 lb/ft^3), based on information reported by Rogers et al. (1994) for 25 samples of residential concrete. Using information for these same samples, the porosity of the material was assigned a normal distribution with mean and standard deviation of 0.2 and 0.032, respectively.

The equilibrium moisture content of the concrete used to construct the foundation of the intruder's house is expected to vary along the cross section of the member, being greatest where the foundation contacts the underlying waste or cover. Lacking specific information regarding this parameter, it was assumed that the saturation level of the concrete was uniformly distributed between 5 and 15 percent. Values sampled from this distribution were multiplied by the porosity of the concrete to estimate the moisture content (volume basis) of the material.

5.3.2 Partition Coefficients

Partition coefficients are used to describe the manner in which radionuclides are distributed between the liquid, solid, and gas phases of the soils and geologic materials found at MDA G. Solid-to-liquid partition coefficients, or distribution coefficients, were developed for the cover material, the buried waste, and the unsaturated zone. A single set of coefficients was adopted for the cover placed over the pits and shafts and the waste placed in these units. These coefficients are based on partitioning data for tuff. Crushed tuff is the primary component of the interim and final covers and has been used historically to backfill the pits and shafts. All elements were assumed to have a partition coefficient of zero in the saturated zone. The regional aquifer lies within the poorly constrained and highly fractured Cerros del Rio basalts, conditions under which sorption is expected to be low.

The element-specific soil-to-water distribution coefficients adopted for the performance assessment and composite analysis are listed in Table 16. The sources of the coefficients are provided in the table; when available, coefficients were taken first from Longmire et al. (1996) and second from Bechtel/SAIC (2004). Longmire et al. provided coefficients for Am, Np, Pu, and U for crushed and intact tuff. These data were used to define triangular distributions for all four radionuclides. Distributions for the intact tuff were defined using the ranges as end points and the medians as the most likely values. Distribution coefficients for Am, Np, Pu, and U in crushed tuff were estimated on the basis of only two samples (Longmire et al., 1996). Given the small amount of data, triangular distributions were assumed using the reported ranges to define the end points of the distributions and the means as the most likely values. The distributions reported in Bechtel/SAIC (2004) for devitrified tuff in the unsaturated zone were used directly.

Krier et al. (1997) listed several sources of distribution coefficients for volcanic tuff; coefficients from these sources were used for elements not addressed by Longmire et al. (1996) or Bechtel/SAIC (2004). Some of the listed distribution coefficients from these sources are based on chemical similarities between elements. Baes et al. (1984) was consulted for any remaining elements that were not addressed by the sources listed above. Point estimates of the distribution coefficients were adopted for elements for which distributions could not be developed. The mean and most likely values of normal and triangular distributions, respectively, were used in the deterministic modeling; the point estimates for the uniform distributions are included in Table 16. When data specific to the material in the disposal units were unavailable, distribution coefficients for intact tuff were used for the crushed tuff.

Table 16
Distribution Coefficients and Solubility Limits

Element	Distribution Coefficient (mL/g) [a]		Solubility Limits [b] (mg/L)
	Crushed Tuff and Waste	Intact Tuff	
Ac	1.3E+02 [c]	1.3E+02 [c]	2.7E-04
Ag	T(2.7E+00, 9.0E+01, 1.0E+03) [d]	T(2.7E+00, 9.0E+01, 1.0E+03) [d]	6.0E-05
Al	1.3E+02 [c]	1.3E+02 [c]	9.4E-07
Am	T(1.6E+03, 2.1E+03, 2.6E+03) [e]	T(2.0E+02, 2.4E+03, 2.7E+04) [e]	2.9E-04
Ba	T(4.3E+02, 9.5E+02, 1.5E+03) [f]	T(4.3E+02, 9.5E+02, 1.5E+03) [f]	6.2E+00
Be	2.5E+02 [d]	2.5E+02 [d]	Not considered [g]
Bi	1.0E+02 [d]	1.0E+02 [d]	Not considered [g]
Bk	1.3E+02 [h]	1.3E+02 [h]	Not considered [g]
C	0.0E+00 [i]	0.0E+00 [i]	4.1E+00
Ca	5.0E+00 [d]	5.0E+00 [d]	Not considered [g]
Cf	1.3E+02 [c]	1.3E+02 [c]	3.0E-04
Cl	0.0E+00 [j]	0.0E+00 [j]	Very large [k]
Cm	5.0E+01 [i]	5.0E+01 [i]	3.0E-04
Co	4.5E-01 [l]	4.5E-01 [l]	1.0E-02
Cs	U(1.0E+00, 1.5E+01; 7.5E+00) [m]	U(1.0E+00, 1.5E+01; 7.5E+00) [m]	Large [k]
Eu	5.0E+01 [i]	5.0E+01 [i]	1.8E-04
Gd	5.0E+01 [n]	5.0E+01 [n]	1.9E-04
H	0.0E+00 [j]	0.0E+00 [j]	Very large [k]
Ho	2.5E+02 [d]	2.5E+02 [d]	Not considered [g]
I	0.0E+00 [i]	0.0E+00 [i]	Very large [k]
K	1.5E+01 [d]	1.5E+01 [d]	Not considered [g]
Kr	NC [o]	NC [o]	Not considered [o]
Lu	5.0E+01 [n]	5.0E+01 [n]	Not considered [g]
Mo	4.0E+00 [i]	4.0E+00 [i]	Large [k]
Nb	1.0E+02 [i]	1.0E+02 [i]	1.9E-49
Nd	6.5E+02 [p]	6.5E+02 [p]	Not considered [g]
Ni	5.0E+01 [i]	5.0E+01 [i]	5.9E-01
Np	T(7.0E+01, 7.5E+00, 8.0E+00) [e]	T(1.7E-01, 2.2E+00, 3.1E+00) [e]	3.1E+01
Os	4.5E+02 [p]	4.5E+02 [p]	Not considered [g]
Pa	TN(5.50E+03, 1.50E+03, 1.00E+03, 1.00E+04) [m]	TN(5.50E+03, 1.50E+03, 1.00E+03, 1.00E+04) [m]	3.0E+01
Pb	2.5E+01 [i]	2.5E+01 [i]	3.3E-01

See footnotes on next page

Table 16 (Continued)
Distribution Coefficients and Solubility Limits

Element	Distribution Coefficient (mL/g) [a]		Solubility Limits [b] (mg/L)
	Crushed Tuff and Waste	Intact Tuff	
Pm	5.0E+01 [n]	5.0E+01 [n]	1.9E+01
Pu	T(6.5E+02, 7.1E+02, 7.7E+02) [e]	T(1.2E+00, 4.1E+00, 1.9E+01) [e]	5.6E-02
Ra	U(1.0E+02, 1.0E+03; 5.0E+02) [m]	U(1.0E+02, 1.0E+03; 5.0E+02) [m]	1.2E-05
Si	3.5E+01 [d]	3.5E+01 [d]	7.9E+00
Sm	5.0E+01 [i]	5.0E+01 [i]	1.8E-04
Sn	5.0E+01 [i]	5.0E+01 [i]	5.1E-32
Sr	U(1.0E+00, 7.0E+01; 4.0E+01) [m]	U(1.0E+00, 7.0E+01; 4.0E+01) [m]	1.2E+02
Tb	5.0E+01 [n]	5.0E+01 [n]	Not considered [g]
Tc	0.0E+00 [e]	0.0E+00 [e]	Large [k]
Th	U(1.0E+03, 1.0E+04; 5.0E+03) [m]	U(1.0E+03, 1.0E+04; 5.0E+03) [m]	4.4E-05
Ti	1.0E+03 [p]	1.0E+03 [p]	Not considered [g]
U	T(1.4E+00, 2.6E+00, 3.8E+00) [e]	T(1.4E+00, 2.4E+00, 3.5E+00) [e]	2.6E+01
Zr	5.0E+02 [i]	5.0E+02 [i]	9.1E-11

[a] *Single values indicate no distribution was identified for the element and/or parameter. Where present, the distribution designations refer to the following distribution types: T = triangular (minimum, most likely, maximum), TN = truncated normal distribution (mean, standard deviation, minimum, maximum), U = uniform (minimum, maximum; deterministic value)*

[b] *Source: Krier et al., 1997, unless noted otherwise*

[c] *Distribution coefficients were estimated based on chemical similarities between americium (III) and actinium (III), americium (III) and aluminum (III), and americium (III) and californium (III) (Krier et al., 1997); the listed values were taken from Wolfsberg (1980)*

[d] *Source: Thibault et al., 1990*

[e] *Source: Longmire et al., 1996*

[f] *Source: Wolfsberg, 1980*

[g] *No solubility limit was provided in Krier et al. (1997); no solubility effects were considered.*

[h] *Distribution coefficients were estimated based on assumed similarities between americium and berkelium; the listed values were taken from Wolfsberg (1980).*

[i] *Source: Brookins, 1984*

[j] *Distribution coefficients were assumed to equal zero.*

[k] *Solubility effects were not considered for elements that have solubility limits listed as large or very large.*

[l] *Source: Polzer et al., 1985*

[m] *Source: Bechtel/SAIC, 2004*

[n] *Distribution coefficients were estimated based on assumed similarities between europium, dysprosium, gadolinium, lanthanum, lutetium, promethium, and terbium, as suggested by Baes et al. (1984).*

[o] *Krypton exists as a noble gas, sorption and solubility effects were not considered.*

[p] *Source: Baes et al., 1984*

Air-to-water partition coefficients are used by the site and intruder diffusion models to simulate the diffusion of vapor- or gas-phase radionuclides including tritium, C-14, and Kr-85 and isotopes of radon. These coefficients describe how such species are allocated between their vapor or gas phase and the water occupying the pores of the cover and waste. The ratio of the vapor-to-water concentration of tritium is given by the following expression:

$$\frac{C_{H-3,v}}{C_{H-3,w}} = \frac{VP_w \times M}{R \times T \times \rho_w} \qquad 70$$

Where

$C_{H-3,v}$ = tritium concentration in water vapor (Ci/m^3)
$C_{H-3,w}$ = tritium concentration in pore water (Ci/m^3)
VP_w = vapor pressure of water (atm)
M = molecular weight of water (g/mol)
R = ideal gas constant (atm-m^3/mol-°K)
T = temperature (°K)
ρ_w = density of water (g/m^3)

Equation 70 was implemented using a water vapor pressure of 0.017 atm at 15°C (250 psi at 59°F) (CRC, 1999), a molecular weight of water of 18 g/mol, an ideal gas constant of 8.2×10^{-5} atm-m^3/mol-°K, and a temperature of 288°K (15°C).

The air-to-water partition coefficients for C-14 gas (as CO_2 or CH_4), Kr-85, and isotopes of radon were calculated as follows:

$$K_{p,i} = \frac{1}{k_{H,i} \times R \times T} \qquad 71$$

Where

$K_{p,i}$ = air-to-water partition coefficient for radionuclide i
$k_{H,i}$ = Henry's Law constant for radionuclide i (mol/L-atm)

The Henry's Law constants for CO_2, CH_4, krypton, and radon at 288°K (15°C) and 1 atm are 0.026, 0.0011, 0.002, and 0.0068 mol/L-atm, respectively (Sander, 1999).

5.3.3 Solubility Limits

Solubility limits represent the maximum concentrations at which elements may occur in pore water within the intact or crushed tuff. The solubility limits adopted for the performance assessment and the composite analysis are included in Table 16. The data included in the table were taken from Krier et al. (1997); solubility effects were not considered for elements that were not addressed by this reference or for elements that have solubility limit values of "large" or

"very large." Lacking the information needed to describe the variability of these limits, no distributions were developed. Solubility effects were not considered in the intruder modeling.

5.3.4 Mass Attenuation Coefficients

Mass attenuation coefficients are used to estimate the direct radiation exposures received by the inadvertent intruder. These coefficients are a function of the energy of the radiation emitted by the radionuclide. Average photon energies were estimated using the MICROSHIELD computer code (Grove Engineering, 1996); mass attenuation coefficients for soil and concrete were calculated using the linear attenuation coefficients provided by MICROSHIELD and soil and concrete densities of 1,400 and 2,050 kg/m^3 (87 and 128 lb/ft^3) respectively. Radionuclides that were not included in MICROSHIELD or for which no photon energies were provided were assigned mass attenuation coefficients for 0.015 MeV photons. The average photon energies and the corresponding mass attenuation coefficients are listed in Table 17.

5.3.5 Diffusion Coefficients

Diffusion coefficients are used to model the vertical movement of gas- and vapor-phase radionuclides from the waste to the surface of the disposal facility. Tritiated water vapor, C-14 gas, and isotopes of krypton and radon may diffuse from the surface of the disposal site and be transported by the prevailing winds, resulting in exposures of receptors living downwind of the disposal facility. The diffusion of gas- and vapor-phase radionuclides from the waste may also expose inadvertent intruders to contamination when they are outside and in their homes.

A diffusion coefficient is specific to the radionuclide under consideration and the material through which it is moving. The diffusion modeling conducted to estimate exposures to off-site members of the public and to demonstrate compliance with radon flux performance objectives required diffusion coefficients for water vapor, C-14 as CO_2 and CH_4, Kr-85, and radon in the waste and cover. The diffusion modeling for the intruder analysis required coefficients for these same constituents in the waste, cover, and concrete floor of the receptor's house.

The gas-diffusion coefficient is typically estimated using empirical relationships; one of the more commonly used formulations is that developed by Millington (1959):

$$D_e = D_o \times \frac{p_a^{10/3}}{p^2} \qquad 72$$

Where

D_e = pore diffusion coefficient (m^2/s)
D_o = gas diffusion coefficient in free air (m^2/s)
p_a = air-filled porosity
p = effective porosity

Table 17
Average Photon Energies and Mass Attenuation Coefficients

Radionuclide	Average Photon Energy (MeV)	Mass Attenuation Coefficient (cm^2/g)	
		Soil	Concrete
Ac-227	3.2E-01	1.0E-01	1.0E-01
Ag-108m	6.4E-01	7.8E-02	7.9E-02
Al-26	1.6E+00	5.1E-02	5.1E-02
Am-241	5.9E-02	2.8E-01	2.8E-01
Am-243	1.6E-01	1.4E-01	1.4E-01
Ba-133	3.3E-01	1.0E-01	1.0E-01
Be-10	---	8.1E+00	8.1E+00
Bi207	9.0E-01	6.5E-02	6.7E-02
Bk-247	---	8.1E+00	8.1E+00
C-14	---	8.1E+00	8.1E+00
Ca-41	---	8.1E+00	8.1E+00
Cd-113m	---	8.1E+00	8.1E+00
Cf-249	3.7E-01	9.9E-02	9.9E-02
Cf-251	1.6E-01	1.4E-01	1.4E-01
Cf-252	6.0E-02	2.7E-01	2.7E-01
Cl-36	---	8.1E+00	8.1E+00
Cm-243	2.0E-01	1.3E-01	1.3E-01
Cm-244	6.0E-02	2.7E-01	2.7E-01
Cm-245	1.1E-01	1.6E-01	1.6E-01
Cm-247	3.7E-01	9.9E-02	9.9E-02
Cm-248	6.0E-02	2.7E-01	2.7E-01
Co-60	1.3E+00	5.7E-02	5.7E-02
Cs-135	---	8.1E+00	8.1E+00
Cs-137	6.0E-01	8.1E-02	8.1E-02
Dy-154	---	8.1E+00	8.1E+00
Eu-152	1.0E+00	6.4E-02	6.4E-02
Eu-154	1.1E+00	6.1E-02	6.1E-02
Gd-148	---	8.1E+00	8.1E+00
Gd-150	---	8.1E+00	8.1E+00

--- = No average energy is provided because the radionuclide was not considered by MICROSHIELD or because photon energies were provided by the code. The mass attenuation coefficient for these radionuclides was set to the value for 0.015 MeV photons.

Table 17 (Continued)
Maximum Photon Energies and Mass Attenuation Coefficients

Radionuclide	Average Photon Energy (MeV)	Mass Attenuation Coefficient (cm^2/g)	
		Soil	Concrete
H-3	---	8.1E+00	8.1E+00
Hf-182	9.3E-01	6.4E-02	6.6E-02
Ho-163	---	8.1E+00	8.1E+00
Ho-166m	6.8E-01	7.5E-02	7.7E-02
I-129	3.1E-02	1.1E+00	1.1E+00
K-40	1.5E+00	5.2E-02	5.2E-02
Kr-81	3.0E-01	1.1E-01	1.1E-01
Kr-85	5.0E-01	8.7E-02	8.7E-02
La-137	---	8.1E+00	8.1E+00
Lu-176	---	8.1E+00	8.1E+00
Mo-93	1.6E-02	7.2E+00	7.2E+00
Nb-91	8.4E-02	1.9E-01	1.9E-01
Nb-92	8.5E-01	6.5E-02	6.9E-02
Nb-93m	1.6E-02	7.2E+00	7.2E+00
Nb-94	8.0E-01	6.6E-02	7.1E-02
Nd-144	---	8.1E+00	8.1E+00
Ni-59	---	8.1E+00	8.1E+00
Ni-63	---	8.1E+00	8.1E+00
Np-237	2.5E-01	1.2E-01	1.2E-01
Os-194	5.7E-01	8.3E-02	8.3E-02
Pa-231	2.5E-01	1.2E-01	1.2E-01
Pb-210	5.0E-02	3.6E-01	3.6E-01
Pd-107	---	8.1E+00	8.1E+00
Pm-145	4.3E-02	5.2E-01	5.2E-01
Pu-236	6.0E-02	2.7E-01	2.7E-01
Pu-238	6.0E-02	2.7E-01	2.7E-01
Pu-239	1.0E-01	1.7E-01	1.7E-01
Pu-240	5.0E-02	3.6E-01	3.6E-01
Pu-241	---	8.1E+00	8.1E+00

--- = No average energy is provided because the radionuclide was not considered by MICROSHIELD or because photon energies were provided by the code. The mass attenuation coefficient for these radionuclides was set to the value for 0.015 MeV photons.

Table 17 (Continued)
Maximum Photon Energies and Mass Attenuation Coefficients

Radionuclide	Average Photon Energy (MeV)	Mass Attenuation Coefficient (cm^2/g)	
		Soil	Concrete
Pu-242	6.0E-02	2.7E-01	2.7E-01
Pu-244	7.6E-01	6.8E-02	7.3E-02
Ra-226	1.2E+00	5.9E-02	5.9E-02
Ra-228	9.7E-01	6.4E-02	6.5E-02
Se79	—	8.1E+00	8.1E+00
Si-32	—	8.1E+00	8.1E+00
Sm-146	—	8.1E+00	8.1E+00
Sm-147	—	8.1E+00	8.1E+00
Sm-151	2.0E-02	3.5E+00	3.5E+00
Sn-121m	—	8.1E+00	8.1E+00
Sn-126	6.8E-02	2.5E-01	2.5E-01
Sr-90	—	8.1E+00	8.1E+00
Tb-157	4.2E-02	5.2E-01	5.2E-01
Tb-158	—	8.1E+00	8.1E+00
Tc-97	1.6E-02	7.1E+00	7.1E+00
Tc-99	8.0E-02	2.0E-01	2.0E-01
Th-228	1.0E+00	6.3E-02	6.3E-02
Th-229	4.1E-01	9.5E-02	9.5E-02
Th-230	7.5E-02	2.2E-01	2.2E-01
Th-232	9.2E-02	1.8E-01	1.8E-01
Ti-44	7.2E-01	7.2E-02	7.5E-02
U-232	1.0E-01	1.7E-01	1.7E-01
U-233	1.0E-01	1.7E-01	1.7E-01
U-234	7.0E-02	2.4E-01	2.4E-01
U-235	1.8E-01	1.2E-01	1.2E-01
U-236	6.0E-02	2.7E-01	2.7E-01
U-238	6.3E-01	7.8E-02	7.9E-02
Zr-93	1.6E-02	7.2E+00	7.2E+00

— = No average energy is provided because the radionuclide was not considered by MICROSHIELD or because photon energies were provided by the code. The mass attenuation coefficient for these radionuclides was set to the value for 0.015 MeV photons.

Using an effective porosity of 0.41, a moisture content of 0.075, and the free-air diffusion coefficients listed in Table 18, the diffusion coefficients calculated for tritiated water vapor, CO_2, CH_4, Kr-85, and radon are 3.7×10^{-6}, 2.2×10^{-6}, 3.0×10^{-6}, 2.7×10^{-6}, and 1.7×10^{-6} m^2/s (4.0×10^{-5}, 2.4×10^{-5}, 3.3×10^{-5}, 2.9×10^{-5}, and 1.8×10^{-5} ft^2/s), respectively.

Table 18
Free-Air Diffusion Coefficients for Vapor- and Gas-Phase Radionuclides

Radionuclide	Diffusion Coefficient (cm^2/s)	Source
Tritium (as water vapor)	2.4E-01[a]	CRC, 1999
CO_2	1.6E-01[a]	CRC, 1999
CH_4	2.0E-01[b]	Marrero and Mason, 1972
Krypton	1.8E-01[c]	Estimated
Radon	1.1E-01[d]	Rogers and Nielson, 1991

[a] *At a temperature of 293° K (20° C) and 1 atm*

[b] *At a temperature of 282° K (9° C) and a pressure of 1 atm*

[c] *The free-air diffusion coefficient for Kr-85 was estimated using the following empirical relationship:*

$D_2 = D_1 \sqrt{m_2/m_1}$ where D_2 and m_2 are the free-air diffusion coefficient and molecular mass of Kr-85 and D_1 and m_1 are the corresponding quantities for Rn-222. The calculated diffusion coefficient is consistent with the coefficient of 1.5×10^{-1} cm^2/s cited in Schack-Kirchner et al., (2001) for Kr-N_2 when differences between the mass of Kr-N_2 and Kr are taken into account.

[d] *At a temperature of 298° K (25° C) and a pressure of 1 atm*

The quantity calculated using Equation 72 represents diffusion in a porous medium. The diffusion coefficient in the air-filled pore spaces only is given by Shan and Stephens (1995):

$$D_e = D_o \times \frac{p_a^{7/3}}{p^2} \qquad 73$$

This is the diffusion coefficient applied in the GoldSim modeling. Using the porosity, moisture content, and free-air diffusion coefficients discussed above, this equation yields diffusion coefficients that are about three times the values for the porous medium.

Rogers and Nielson (1991) reported a correlation between the diffusion coefficient of radon in soils and the saturation fraction of the soil. That correlation, which is based on 1,073 soil-diffusion coefficient measurements, is given by the following equation:

$$D_e = D_{o,Rn} \times p \times \exp(-6Sp - 6S^{14p}) \qquad 74$$

Where

$D_{o,Rn}$ = radon diffusion coefficient in air
S = volume fraction of water saturation

Using a porosity of 0.41 and a moisture content of 0.075 (volume basis) to represent the cover and waste, this equation yields a radon diffusion coefficient of 3.8×10^{-6} m^2/s (4.1×10^{-5} ft^2/s). This diffusion coefficient, which accounts for pore air-water interactions and the transfer of radon between the two phases, lies between the values calculated using Equations 72 and 73.

Philip and DeVries (1957) concluded that thermal gradients may significantly increase the apparent diffusion coefficient of water vapor in soil. Based on an "admittedly approximate" analysis, the authors concluded that the observed transfer rate of vapor may be 3.6 to 9.8 times greater than that predicted when gradients were not taken into account.

Rates of diffusion in the air-filled pore spaces of concrete can also be estimated using Equation 73. Using a concrete porosity of 0.2, a saturation level of 10 percent, and the free-air diffusion coefficients listed in Table 18, diffusion coefficients of 1.1×10^{-5}, 7.3×10^{-6}, 9.2×10^{-6}, 8.2×10^{-6}, and 5.0×10^{-6} m^2/s (2.2×10^{-5}, 1.2×10^{-5}, 1.7×10^{-5}, 1.5×10^{-5}, and 9.8×10^{-6} ft^2/s) are calculated for water vapor, CO_2, CH_4, Kr-85, and radon, respectively. These values are comparable to the coefficients estimated for diffusion in the air-filled pores in the cover and waste. Concrete diffusion coefficients for the porous media are five to six times smaller than the coefficients for the air-filled pore spaces (Equation 72).

Several studies provide additional insight into the diffusion of radon in bulk concrete. Rogers et al. (1994) summarized pore diffusion coefficients measured in six separate studies, finding coefficients that ranged from 7.0×10^{-9} to 1.7×10^{-7} m^2/s (7.5×10^{-8} to 1.8×10^{-6} ft^2/s). These investigators also conducted diffusion coefficient measurements using 25 samples of residential concretes and test cylinders of the same; diffusion coefficients for these samples ranged from 3.7×10^{-8} to 5.2×10^{-7} m^2/s (4.0×10^{-7} to 5.6×10^{-6} ft^2/s). Rogers et al. (1995) measured radon diffusion coefficients in aged residential concretes that ranged from 1.5×10^{-7} to 5.5×10^{-7} m^2/s (1.6×10^{-6} to 5.9×10^{-6} ft^2/s). Nielson et al. (1997) characterized diffusion coefficients in 12 samples of residential concrete with different configurations of cracks, pipe penetrations, cold joints, and other defects. The coefficients averaged 6.5×10^{-8} m^2/s (7.0×10^{-7} ft^2/s) over the 1,000-day study, or approximately four times greater than the pore diffusion coefficients measured in three core samples. All of these radon diffusion coefficients are similar to those estimated for porous media using the relationship developed by Millington (1959) (Equation 72).

The diffusion coefficients used to estimate radon fluxes from the site and to estimate the potential exposures received by inadvertent intruders and members of the public were calculated using Equation 73 and the free-air diffusion coefficients listed in Table 18. The calculated diffusion coefficients for tritiated water vapor in the cover and waste were multiplied by a factor to account for possible increases in the diffusion coefficient because of thermal gradients. This multiplier was assumed to have a uniform distribution and range from 3.6 to 9.8, consistent with

the data reported by Philip and DeVries (1957). The effect of thermal gradients on the diffusion of tritium were not taken into account for the 0.1 m (0.3 ft) thick concrete floor of the intruder's house.

5.3.6 Radon Emanation Coefficient

The radon emanation coefficient represents the fraction of the radon gas generated by the decay of radium precursors that enters into the pores of the waste and is available for diffusion. This coefficient is a function of many factors including the recoil energy of the radon isotope under consideration, and the pore structure and moisture content of the medium in which the gas is generated. Rogers et al. (1984) summarize emanation coefficients for several samples of uranium mill tailings; coefficients range from about 0.03 to 0.35 for very dry samples and from 0.1 to 0.4 for samples with moisture contents of about 5 percent (dry weight) or more. Yu et al. (1993) summarize emanation coefficients for several porous media of varying moisture content. The coefficients provided in the report range from 0.02 to 0.7. Values for unconsolidated soils of unknown moisture content ranged from 0.06 to 0.4; mean values for these materials ranged from 0.14 to 0.28. The U.S. Nuclear Regulatory Commission (NRC) adopted a radon emanation coefficient of 0.35 for all materials (1989). Based on these data, the emanation coefficient was assumed to be uniformly distributed, ranging from 0.1 to 0.4.

5.3.7 Carbon-14 Gas Generation Rate

The C-14 gas generation rate describes the rate at which C-14 gas is generated as a result of biodegradation of the organic fraction of the buried waste. The parameter is used to project generation rates of C-14 gas in the form of $^{14}CO_2$ and $^{14}CH_4$. Relatively little information is available to quantify organic waste biodegradation rates and, hence, gas generation rates.

The Agency for Toxic Substances and Disease Registry (ATSDR) (2001) reports that recently buried waste will generate more gas than older waste. Appreciable amounts of gas are generated within landfills 1 to 3 years after disposal, with peak generation typically occurring within 5 to 7 years of disposal. While all gas is typically generated within 20 years of disposal, gas production may continue for 50 years or more as the waste slowly degrades under anaerobic conditions. Rates of generation are generally found or assumed to be lower in arid climates, where waste moisture contents are lower. Recognizing the limitations of existing information, the U.S. Environmental Protection Agency (EPA) (2005) simulated the production of gas in a landfill gas generation model using a first-order decomposition rate equation. For generic applications, the EPA recommends generation rate constants of 0.02/yr and 0.04/yr for conventional landfills in arid and nonarid settings, respectively, and cites rate constants ranging from 0.003/yr to 0.21/yr. Environment Canada (2003) cites generation rate constants ranging from 0.006/yr to 0.024/yr as recommended values for calculating landfill emissions in Canada.

The information needed to estimate the rate at which C-14 gas will be generated in conjunction with the degradation of organic waste disposed of at MDA G is unavailable. Although the EPA (2005) suggests a rate constant of 0.02/yr for arid climates, values recommended for modeling gas generation in Canadian provinces tend to be lower. Opseth (1998) concluded that the default value cited by the EPA more nearly approximated field results for a semiarid location in Canada. The arid nature of the Laboratory and low moisture contents of the crushed tuff and waste in the disposal units at MDA G suggest low rates of gas generation would prevail. Given this and the limited information summarized above, the rate constant was assumed to have a uniform distribution ranging from 0.003/yr to 0.02/yr. The midpoint of the distribution was used for deterministic modeling.

5.3.8 Carbon Dioxide and Methane Fractions

The CO_2 and CH_4 fractions are used in the site and intruder diffusion models to specify the fractionation of the C-14 gas generated during biodegradation of organic waste. In general, CO_2 will be the predominant species while an adequate oxygen supply exists, and methane-producing anaerobic bacteria will dominate after the oxygen is exhausted. Typically, CO_2 accounts for 40 to 60 percent of the total gas generation on a volume basis, while 45 to 60 percent of the total gas production consists of CH_4 (ATSDR, 2001). Based on this information, the CO_2 fraction was assigned a uniform distribution ranging from 0.4 to 0.6; the CH_4 fraction was calculated as the complement of the CO_2 fraction.

5.3.9 Organic Fraction of Carbon-14 Waste

The organic fraction of the C-14 waste represents the fraction of the waste that is available for biodegradation. The organic fraction of the C-14 waste disposed of at MDA G was estimated on the basis of the waste-form characteristics of the material upon which the C-14 inventory projection is based. The composite analysis inventory projection for C-14 is approximately 120 Ci (Shuman, 2005); this includes all waste that has been or is expected to be disposed of at MDA G by the time the facility closes in 2044. Approximately 80 percent of the total activity of the waste was estimated on the basis of a shipment of waste generated during the decommissioning of the Omega Reactor. The waste profile for this material indicates it is combined combustible/noncombustible lab trash (waste code 19) consisting of 45 to 55 percent metal, 20 to 30 percent graphite, 15 to 25 percent concrete, and 3 to 8 percent glass /rubber/plastic/wood/herculite. Almost all of the remainder of the projected C-14 inventory consists of material classified as other combustibles (waste code 60), scrap metal (waste code 52), and combined combustible/noncombustible lab trash (waste code 19). On an activity basis, these three waste streams account for approximately 93, 5, and 2 percent of this portion of the inventory.

The 1997 performance assessment and composite analysis (Hollis et al., 1997) assumed that all of the C-14 waste identified as combustible lab trash waste (waste code 18) and 50 percent of the material identified as combined combustible/noncombustible lab trash (waste code 19) was organic. Based on the information provided above, however, it appears that less than 10 percent of waste code 19 will consist of organic material that might undergo biodegradation and generate C-14 gas. Waste from other combustibles (waste code 60) may include organic material, but this waste accounts for only 13 percent of the total C-14 inventory.

The organic fraction of the C-14 inventory was estimated on the basis of the information provided above. The parameter was assigned a triangular distribution with minimum, most likely, and maximum values of 0, 0.05, and 0.1, respectively. The range of this distribution is consistent with the profile for the reactor waste and the contribution made by material classified as waste code 19 to the remainder of the projected inventory. This distribution was assumed to apply to all C-14 waste disposed of at MDA G.

5.4 Radionuclide Inventories

The radionuclide inventories in the buried waste ultimately determine the magnitude of the projected exposures. Deterministic estimates of these inventories were developed for the performance assessment and composite analysis, based largely on information found in the LLW and transuranic (TRU) waste databases. Shuman (2005) provides a complete description of the analysis used to estimate these inventories.

The radiological inventories reported in Shuman (2005) were reformulated prior to their use in the performance assessment and composite analysis; this reformulation was undertaken for two primary reasons. First, the inventories presented in Shuman were provided on a waste-form-specific basis. Given that no distinctions were made between these waste forms in terms of release characteristics, this level of detail was not required for the modeling. Combining the waste-form-specific inventories significantly reduced the complexity of the GoldSim models. Second, while the reported inventories were provided for subsets of the disposal units at MDA G, inventories had not been developed for the eight waste disposal regions into which the facility was divided.

The region-specific inventories are summarized in Tables 19 through 21. Table 19 provides the total volumes and activities for the waste associated with each region, as used in the performance assessment and composite analysis. The radionuclide-specific inventories included in the performance assessment are listed in Table 20, and the inventories for the composite analysis are provided in Table 21. The volumes provided in Tables 20 and 21 are the quantities of waste contaminated with each radionuclide. Because several radionuclides may occur in a single waste package, the sum of these volumes is greater than the total volume of waste disposed of in the disposal units.

Table 19
Disposal Region-Specific Inventories Included in the MDA G Performance Assessment and Composite Analysis

Disposal Region	Performance Assessment Inventory		Composite Analysis Inventory	
	Volume (m^3)	Activity (Ci)	Volume (m^3)	Activity (Ci)
1	1.3E-01	1.5E+00	5.0E+04	8.8E+04
2	—	—	1.4E+04	2.2E+02
3	3.6E+03	2.1E+02	4.4E+04	3.8E+04
4	3.8E+04	6.0E+01	6.4E+04	4.4E+03
5	1.8E+04	3.3E+02	1.8E+04	3.3E+02
6	2.5E+01	2.1E+03	4.5E+02	5.9E+04
7	4.4E+02	1.8E+06	8.4E+02	2.5E+06
8	1.1E+05	1.0E+06	1.1E+05	1.0E+06

— = No waste was disposed of in this disposal region after September 26, 1988.

Table 20
Radionuclide Inventories for the MDA G Performance Assessment by Waste Disposal Region

Radionuclide	Measurement Units [a]	Waste Disposal Region							
		1	2	3	4	5	6	7	8
Ac-227	m^3	—	—	—	—	5.8E-02	—	6.0E-04	1.5E-01
	Ci	—	—	—	—	4.0E-06	—	5.9E-07	1.2E-05
Ag-108m	m^3	—	—	1.0E+01	9.4E+00	1.8E+01	—	1.7E+00	1.7E+02
	Ci	—	—	1.1E-04	4.9E-05	2.0E-05	—	5.0E+00	2.2E+01
Al-26	m^3	—	—	—	—	3.9E-02	—	—	4.7E-02
	Ci	—	—	—	—	2.9E-04	—	—	1.3E-03
Am-241	m^3	1.9E-02	—	2.9E+03	1.8E+04	9.4E+03	—	4.0E+01	4.2E+04
	Ci	5.0E-07	—	1.7E-01	8.9E-01	6.6E+00	—	7.3E-02	3.0E+01
Am-243	m^3	—	—	2.5E+01	5.0E+01	2.1E+02	—	6.6E-02	8.9E+02
	Ci	—	—	1.3E-05	1.3E-06	8.9E-03	—	1.1E-09	3.9E-02
Ba-133	m^3	2.6E-02	—	1.3E+01	6.7E+00	6.9E+01	—	4.4E-03	3.9E+02
	Ci	2.5E-04	—	6.2E-06	1.6E-06	9.0E-03	—	1.4E-03	4.1E-02
Be-10	m^3	—	—	—	—	1.8E+01	—	—	8.0E+01
	Ci	—	—	—	—	5.1E-03	—	—	2.3E-02
Bi-207	m^3	—	—	—	3.8E-03	4.1E+00	—	1.3E-01	1.6E+01
	Ci	—	—	—	7.4E-05	7.1E-03	—	6.0E-05	3.2E-02
Bk-247	m^3	—	—	—	—	3.3E+01	—	—	6.7E+01
	Ci	—	—	—	—	3.1E-07	—	—	1.1E-06
C-14	m^3	7.6E-03	—	6.6E+00	4.8E+01	1.8E+02	—	2.0E+01	7.4E+02
	Ci	2.7E-09	—	5.2E-07	4.8E-05	3.7E+00	—	1.8E+01	9.6E+01

— = None reported for this waste disposal region.

[a] Inventories given by volume (m^3) and activity (Ci).

Table 17
Average Photon Energies and Mass Attenuation Coefficients

Radionuclide	Average Photon Energy (MeV)	Mass Attenuation Coefficient (cm^2/g)	
		Soil	Concrete
Ac-227	3.2E-01	1.0E-01	1.0E-01
Ag-108m	6.4E-01	7.8E-02	7.9E-02
Al-26	1.6E+00	5.1E-02	5.1E-02
Am-241	5.9E-02	2.8E-01	2.8E-01
Am-243	1.6E-01	1.4E-01	1.4E-01
Ba-133	3.3E-01	1.0E-01	1.0E-01
Be-10	---	8.1E+00	8.1E+00
Bi207	9.0E-01	6.5E-02	6.7E-02
Bk-247	---	8.1E+00	8.1E+00
C-14	---	8.1E+00	8.1E+00
Ca-41	---	8.1E+00	8.1E+00
Cd-113m	---	8.1E+00	8.1E+00
Cf-249	3.7E-01	9.9E-02	9.9E-02
Cf-251	1.6E-01	1.4E-01	1.4E-01
Cf-252	6.0E-02	2.7E-01	2.7E-01
Cl-36	---	8.1E+00	8.1E+00
Cm-243	2.0E-01	1.3E-01	1.3E-01
Cm-244	6.0E-02	2.7E-01	2.7E-01
Cm-245	1.1E-01	1.6E-01	1.6E-01
Cm-247	3.7E-01	9.9E-02	9.9E-02
Cm-248	6.0E-02	2.7E-01	2.7E-01
Co-60	1.3E+00	5.7E-02	5.7E-02
Cs-135	---	8.1E+00	8.1E+00
Cs-137	6.0E-01	8.1E-02	8.1E-02
Dy-154	---	8.1E+00	8.1E+00
Eu-152	1.0E+00	6.4E-02	6.4E-02
Eu-154	1.1E+00	6.1E-02	6.1E-02
Gd-148	---	8.1E+00	8.1E+00
Gd-150	---	8.1E+00	8.1E+00

--- = No average energy is provided because the radionuclide was not considered by MICROSHIELD or because photon energies were provided by the code. The mass attenuation coefficient for these radionuclides was set to the value for 0.015 MeV photons.

Table 17 (Continued)
Maximum Photon Energies and Mass Attenuation Coefficients

Radionuclide	Average Photon Energy (MeV)	Mass Attenuation Coefficient (cm^2/g)	
		Soil	Concrete
H-3	---	8.1E+00	8.1E+00
Hf-182	9.3E-01	6.4E-02	6.6E-02
Ho-163	---	8.1E+00	8.1E+00
Ho-166m	6.8E-01	7.5E-02	7.7E-02
I-129	3.1E-02	1.1E+00	1.1E+00
K-40	1.5E+00	5.2E-02	5.2E-02
Kr-81	3.0E-01	1.1E-01	1.1E-01
Kr-85	5.0E-01	8.7E-02	8.7E-02
La-137	---	8.1E+00	8.1E+00
Lu-176	---	8.1E+00	8.1E+00
Mo-93	1.6E-02	7.2E+00	7.2E+00
Nb-91	8.4E-02	1.9E-01	1.9E-01
Nb-92	8.5E-01	6.5E-02	6.9E-02
Nb-93m	1.6E-02	7.2E+00	7.2E+00
Nb-94	8.0E-01	6.6E-02	7.1E-02
Nd-144	---	8.1E+00	8.1E+00
Ni-59	---	8.1E+00	8.1E+00
Ni-63	---	8.1E+00	8.1E+00
Np-237	2.5E-01	1.2E-01	1.2E-01
Os-194	5.7E-01	8.3E-02	8.3E-02
Pa-231	2.5E-01	1.2E-01	1.2E-01
Pb-210	5.0E-02	3.6E-01	3.6E-01
Pd-107	---	8.1E+00	8.1E+00
Pm-145	4.3E-02	5.2E-01	5.2E-01
Pu-236	6.0E-02	2.7E-01	2.7E-01
Pu-238	6.0E-02	2.7E-01	2.7E-01
Pu-239	1.0E-01	1.7E-01	1.7E-01
Pu-240	5.0E-02	3.6E-01	3.6E-01
Pu-241	---	8.1E+00	8.1E+00

--- = No average energy is provided because the radionuclide was not considered by MICROSHIELD or because photon energies were provided by the code. The mass attenuation coefficient for these radionuclides was set to the value for 0.015 MeV photons.

Table 17 (Continued)
Maximum Photon Energies and Mass Attenuation Coefficients

Radionuclide	Average Photon Energy (MeV)	Mass Attenuation Coefficient (cm^2/g)	
		Soil	Concrete
Pu-242	6.0E-02	2.7E-01	2.7E-01
Pu-244	7.6E-01	6.8E-02	7.3E-02
Ra-226	1.2E+00	5.9E-02	5.9E-02
Ra-228	9.7E-01	6.4E-02	6.5E-02
Se79	---	8.1E+00	8.1E+00
Si-32	---	8.1E+00	8.1E+00
Sm-146	---	8.1E+00	8.1E+00
Sm-147	---	8.1E+00	8.1E+00
Sm-151	2.0E-02	3.5E+00	3.5E+00
Sn-121m	---	8.1E+00	8.1E+00
Sn-126	6.8E-02	2.5E-01	2.5E-01
Sr-90	---	8.1E+00	8.1E+00
Tb-157	4.2E-02	5.2E-01	5.2E-01
Tb-158	---	8.1E+00	8.1E+00
Tc-97	1.6E-02	7.1E+00	7.1E+00
Tc-99	8.0E-02	2.0E-01	2.0E-01
Th-228	1.0E+00	6.3E-02	6.3E-02
Th-229	4.1E-01	9.5E-02	9.5E-02
Th-230	7.5E-02	2.2E-01	2.2E-01
Th-232	9.2E-02	1.8E-01	1.8E-01
Ti-44	7.2E-01	7.2E-02	7.5E-02
U-232	1.0E-01	1.7E-01	1.7E-01
U-233	1.0E-01	1.7E-01	1.7E-01
U-234	7.0E-02	2.4E-01	2.4E-01
U-235	1.8E-01	1.2E-01	1.2E-01
U-236	6.0E-02	2.7E-01	2.7E-01
U-238	6.3E-01	7.8E-02	7.9E-02
Zr-93	1.6E-02	7.2E+00	7.2E+00

--- = No average energy is provided because the radionuclide was not considered by MICROSHIELD or because photon energies were provided by the code. The mass attenuation coefficient for these radionuclides was set to the value for 0.015 MeV photons.

Using an effective porosity of 0.41, a moisture content of 0.075, and the free-air diffusion coefficients listed in Table 18, the diffusion coefficients calculated for tritiated water vapor, CO_2, CH_4, Kr-85, and radon are 3.7×10^{-6}, 2.2×10^{-6}, 3.0×10^{-6}, 2.7×10^{-6}, and 1.7×10^{-6} m^2/s (4.0×10^{-5}, 2.4×10^{-5}, 3.3×10^{-5}, 2.9×10^{-5}, and 1.8×10^{-5} ft^2/s), respectively.

Table 18
Free-Air Diffusion Coefficients for Vapor- and Gas-Phase Radionuclides

Radionuclide	Diffusion Coefficient (cm^2/s)	Source
Tritium (as water vapor)	2.4E-01[a]	CRC, 1999
CO_2	1.6E-01[a]	CRC, 1999
CH_4	2.0E-01[b]	Marrero and Mason, 1972
Krypton	1.8E-01[c]	Estimated
Radon	1.1E-01[d]	Rogers and Nielson, 1991

[a] *At a temperature of 293° K (20° C) and 1 atm*

[b] *At a temperature of 282° K (9° C) and a pressure of 1 atm*

[c] *The free-air diffusion coefficient for Kr-85 was estimated using the following empirical relationship:*

$D_2 = D_1 \sqrt{m_2/m_1}$ *where* D_2 *and* m_2 *are the free-air diffusion coefficient and molecular mass of Kr-85 and* D_1 *and* m_1 *are the corresponding quantities for Rn-222. The calculated diffusion coefficient is consistent with the coefficient of* 1.5×10^{-1} cm^2/s *cited in Schack-Kirchner et al., (2001) for* $Kr\text{-}N_2$ *when differences between the mass of* $Kr\text{-}N_2$ *and Kr are taken into account.*

[d] *At a temperature of 298° K (25° C) and a pressure of 1 atm*

The quantity calculated using Equation 72 represents diffusion in a porous medium. The diffusion coefficient in the air-filled pore spaces only is given by Shan and Stephens (1995):

$$D_e = D_o \times \frac{p_a^{7/3}}{p^2} \qquad 73$$

This is the diffusion coefficient applied in the GoldSim modeling. Using the porosity, moisture content, and free-air diffusion coefficients discussed above, this equation yields diffusion coefficients that are about three times the values for the porous medium.

Rogers and Nielson (1991) reported a correlation between the diffusion coefficient of radon in soils and the saturation fraction of the soil. That correlation, which is based on 1,073 soil-diffusion coefficient measurements, is given by the following equation:

$$D_e = D_{o,Rn} \times p \times \exp(-6Sp - 6S^{14p}) \qquad 74$$

Where

$D_{o,Rn}$ = radon diffusion coefficient in air
S = volume fraction of water saturation

Using a porosity of 0.41 and a moisture content of 0.075 (volume basis) to represent the cover and waste, this equation yields a radon diffusion coefficient of 3.8×10^{-6} m^2/s (4.1×10^{-5} ft^2/s). This diffusion coefficient, which accounts for pore air-water interactions and the transfer of radon between the two phases, lies between the values calculated using Equations 72 and 73.

Philip and DeVries (1957) concluded that thermal gradients may significantly increase the apparent diffusion coefficient of water vapor in soil. Based on an "admittedly approximate" analysis, the authors concluded that the observed transfer rate of vapor may be 3.6 to 9.8 times greater than that predicted when gradients were not taken into account.

Rates of diffusion in the air-filled pore spaces of concrete can also be estimated using Equation 73. Using a concrete porosity of 0.2, a saturation level of 10 percent, and the free-air diffusion coefficients listed in Table 18, diffusion coefficients of 1.1×10^{-5}, 7.3×10^{-6}, 9.2×10^{-6}, 8.2×10^{-6}, and 5.0×10^{-6} m^2/s (2.2×10^{-5}, 1.2×10^{-5}, 1.7×10^{-5}, 1.5×10^{-5}, and 9.8×10^{-6} ft^2/s) are calculated for water vapor, CO_2, CH_4, Kr-85, and radon, respectively. These values are comparable to the coefficients estimated for diffusion in the air-filled pores in the cover and waste. Concrete diffusion coefficients for the porous media are five to six times smaller than the coefficients for the air-filled pore spaces (Equation 72).

Several studies provide additional insight into the diffusion of radon in bulk concrete. Rogers et al. (1994) summarized pore diffusion coefficients measured in six separate studies, finding coefficients that ranged from 7.0×10^{-9} to 1.7×10^{-7} m^2/s (7.5×10^{-8} to 1.8×10^{-6} ft^2/s). These investigators also conducted diffusion coefficient measurements using 25 samples of residential concretes and test cylinders of the same; diffusion coefficients for these samples ranged from 3.7×10^{-8} to 5.2×10^{-7} m^2/s (4.0×10^{-7} to 5.6×10^{-6} ft^2/s). Rogers et al. (1995) measured radon diffusion coefficients in aged residential concretes that ranged from 1.5×10^{-7} to 5.5×10^{-7} m^2/s (1.6×10^{-6} to 5.9×10^{-6} ft^2/s). Nielson et al. (1997) characterized diffusion coefficients in 12 samples of residential concrete with different configurations of cracks, pipe penetrations, cold joints, and other defects. The coefficients averaged 6.5×10^{-8} m^2/s (7.0×10^{-7} ft^2/s) over the 1,000-day study, or approximately four times greater than the pore diffusion coefficients measured in three core samples. All of these radon diffusion coefficients are similar to those estimated for porous media using the relationship developed by Millington (1959) (Equation 72).

The diffusion coefficients used to estimate radon fluxes from the site and to estimate the potential exposures received by inadvertent intruders and members of the public were calculated using Equation 73 and the free-air diffusion coefficients listed in Table 18. The calculated diffusion coefficients for tritiated water vapor in the cover and waste were multiplied by a factor to account for possible increases in the diffusion coefficient because of thermal gradients. This multiplier was assumed to have a uniform distribution and range from 3.6 to 9.8, consistent with

the data reported by Philip and DeVries (1957). The effect of thermal gradients on the diffusion of tritium were not taken into account for the 0.1 m (0.3 ft) thick concrete floor of the intruder's house.

5.3.6 Radon Emanation Coefficient

The radon emanation coefficient represents the fraction of the radon gas generated by the decay of radium precursors that enters into the pores of the waste and is available for diffusion. This coefficient is a function of many factors including the recoil energy of the radon isotope under consideration, and the pore structure and moisture content of the medium in which the gas is generated. Rogers et al. (1984) summarize emanation coefficients for several samples of uranium mill tailings; coefficients range from about 0.03 to 0.35 for very dry samples and from 0.1 to 0.4 for samples with moisture contents of about 5 percent (dry weight) or more. Yu et al. (1993) summarize emanation coefficients for several porous media of varying moisture content. The coefficients provided in the report range from 0.02 to 0.7. Values for unconsolidated soils of unknown moisture content ranged from 0.06 to 0.4; mean values for these materials ranged from 0.14 to 0.28. The U.S. Nuclear Regulatory Commission (NRC) adopted a radon emanation coefficient of 0.35 for all materials (1989). Based on these data, the emanation coefficient was assumed to be uniformly distributed, ranging from 0.1 to 0.4.

5.3.7 Carbon-14 Gas Generation Rate

The C-14 gas generation rate describes the rate at which C-14 gas is generated as a result of biodegradation of the organic fraction of the buried waste. The parameter is used to project generation rates of C-14 gas in the form of $^{14}CO_2$ and $^{14}CH_4$. Relatively little information is available to quantify organic waste biodegradation rates and, hence, gas generation rates.

The Agency for Toxic Substances and Disease Registry (ATSDR) (2001) reports that recently buried waste will generate more gas than older waste. Appreciable amounts of gas are generated within landfills 1 to 3 years after disposal, with peak generation typically occurring within 5 to 7 years of disposal. While all gas is typically generated within 20 years of disposal, gas production may continue for 50 years or more as the waste slowly degrades under anaerobic conditions. Rates of generation are generally found or assumed to be lower in arid climates, where waste moisture contents are lower. Recognizing the limitations of existing information, the U.S. Environmental Protection Agency (EPA) (2005) simulated the production of gas in a landfill gas generation model using a first-order decomposition rate equation. For generic applications, the EPA recommends generation rate constants of 0.02/yr and 0.04/yr for conventional landfills in arid and nonarid settings, respectively, and cites rate constants ranging from 0.003/yr to 0.21/yr. Environment Canada (2003) cites generation rate constants ranging from 0.006/yr to 0.024/yr as recommended values for calculating landfill emissions in Canada.

The information needed to estimate the rate at which C-14 gas will be generated in conjunction with the degradation of organic waste disposed of at MDA G is unavailable. Although the EPA (2005) suggests a rate constant of 0.02/yr for arid climates, values recommended for modeling gas generation in Canadian provinces tend to be lower. Opseth (1998) concluded that the default value cited by the EPA more nearly approximated field results for a semiarid location in Canada. The arid nature of the Laboratory and low moisture contents of the crushed tuff and waste in the disposal units at MDA G suggest low rates of gas generation would prevail. Given this and the limited information summarized above, the rate constant was assumed to have a uniform distribution ranging from 0.003/yr to 0.02/yr. The midpoint of the distribution was used for deterministic modeling.

5.3.8 Carbon Dioxide and Methane Fractions

The CO_2 and CH_4 fractions are used in the site and intruder diffusion models to specify the fractionation of the C-14 gas generated during biodegradation of organic waste. In general, CO_2 will be the predominant species while an adequate oxygen supply exists, and methane-producing anaerobic bacteria will dominate after the oxygen is exhausted. Typically, CO_2 accounts for 40 to 60 percent of the total gas generation on a volume basis, while 45 to 60 percent of the total gas production consists of CH_4 (ATSDR, 2001). Based on this information, the CO_2 fraction was assigned a uniform distribution ranging from 0.4 to 0.6; the CH_4 fraction was calculated as the complement of the CO_2 fraction.

5.3.9 Organic Fraction of Carbon-14 Waste

The organic fraction of the C-14 waste represents the fraction of the waste that is available for biodegradation. The organic fraction of the C-14 waste disposed of at MDA G was estimated on the basis of the waste-form characteristics of the material upon which the C-14 inventory projection is based. The composite analysis inventory projection for C-14 is approximately 120 Ci (Shuman, 2005); this includes all waste that has been or is expected to be disposed of at MDA G by the time the facility closes in 2044. Approximately 80 percent of the total activity of the waste was estimated on the basis of a shipment of waste generated during the decommissioning of the Omega Reactor. The waste profile for this material indicates it is combined combustible/noncombustible lab trash (waste code 19) consisting of 45 to 55 percent metal, 20 to 30 percent graphite, 15 to 25 percent concrete, and 3 to 8 percent glass /rubber/plastic/wood/herculite. Almost all of the remainder of the projected C-14 inventory consists of material classified as other combustibles (waste code 60), scrap metal (waste code 52), and combined combustible/noncombustible lab trash (waste code 19). On an activity basis, these three waste streams account for approximately 93, 5, and 2 percent of this portion of the inventory.

The 1997 performance assessment and composite analysis (Hollis et al., 1997) assumed that all of the C-14 waste identified as combustible lab trash waste (waste code 18) and 50 percent of the material identified as combined combustible/noncombustible lab trash (waste code 19) was organic. Based on the information provided above, however, it appears that less than 10 percent of waste code 19 will consist of organic material that might undergo biodegradation and generate C-14 gas. Waste from other combustibles (waste code 60) may include organic material, but this waste accounts for only 13 percent of the total C-14 inventory.

The organic fraction of the C-14 inventory was estimated on the basis of the information provided above. The parameter was assigned a triangular distribution with minimum, most likely, and maximum values of 0, 0.05, and 0.1, respectively. The range of this distribution is consistent with the profile for the reactor waste and the contribution made by material classified as waste code 19 to the remainder of the projected inventory. This distribution was assumed to apply to all C-14 waste disposed of at MDA G.

5.4 Radionuclide Inventories

The radionuclide inventories in the buried waste ultimately determine the magnitude of the projected exposures. Deterministic estimates of these inventories were developed for the performance assessment and composite analysis, based largely on information found in the LLW and transuranic (TRU) waste databases. Shuman (2005) provides a complete description of the analysis used to estimate these inventories.

The radiological inventories reported in Shuman (2005) were reformulated prior to their use in the performance assessment and composite analysis; this reformulation was undertaken for two primary reasons. First, the inventories presented in Shuman were provided on a waste-form-specific basis. Given that no distinctions were made between these waste forms in terms of release characteristics, this level of detail was not required for the modeling. Combining the waste-form-specific inventories significantly reduced the complexity of the GoldSim models. Second, while the reported inventories were provided for subsets of the disposal units at MDA G, inventories had not been developed for the eight waste disposal regions into which the facility was divided.

The region-specific inventories are summarized in Tables 19 through 21. Table 19 provides the total volumes and activities for the waste associated with each region, as used in the performance assessment and composite analysis. The radionuclide-specific inventories included in the performance assessment are listed in Table 20, and the inventories for the composite analysis are provided in Table 21. The volumes provided in Tables 20 and 21 are the quantities of waste contaminated with each radionuclide. Because several radionuclides may occur in a single waste package, the sum of these volumes is greater than the total volume of waste disposed of in the disposal units.

Table 19
Disposal Region-Specific Inventories Included in the MDA G Performance Assessment and Composite Analysis

Disposal Region	Performance Assessment Inventory		Composite Analysis Inventory	
	Volume (m^3)	Activity (Ci)	Volume (m^3)	Activity (Ci)
1	1.3E-01	1.5E+00	5.0E+04	8.8E+04
2	—	—	1.4E+04	2.2E+02
3	3.6E+03	2.1E+02	4.4E+04	3.8E+04
4	3.8E+04	6.0E+01	6.4E+04	4.4E+03
5	1.8E+04	3.3E+02	1.8E+04	3.3E+02
6	2.5E+01	2.1E+03	4.5E+02	5.9E+04
7	4.4E+02	1.8E+06	8.4E+02	2.5E+06
8	1.1E+05	1.0E+06	1.1E+05	1.0E+06

— = No waste was disposed of in this disposal region after September 26, 1988.

Table 20
Radionuclide Inventories for the MDA G Performance Assessment by Waste Disposal Region

Radionuclide	Measurement Units [a]	Waste Disposal Region							
		1	2	3	4	5	6	7	8
Ac-227	m^3	---	---	---	---	5.8E-02	---	6.0E-04	1.5E-01
	Ci	---	---	---	---	4.0E-06	---	5.9E-07	1.2E-05
Ag-108m	m^3	---	---	1.0E+01	9.4E+00	1.8E+01	---	1.7E+00	1.7E+02
	Ci	---	---	1.1E-04	4.9E-05	2.0E-05	---	5.0E+00	2.2E+01
Al-26	m^3	---	---	---	---	3.9E-02	---	---	4.7E-02
	Ci	---	---	---	---	2.9E-04	---	---	1.3E-03
Am-241	m^3	1.9E-02	---	2.9E+03	1.8E+04	9.4E+03	---	4.0E+01	4.2E+04
	Ci	5.0E-07	---	1.7E-01	8.9E-01	6.6E+00	---	7.3E-02	3.0E+01
Am-243	m^3	---	---	2.5E+01	5.0E+01	2.1E+02	---	6.6E-02	8.9E+02
	Ci	---	---	1.3E-05	1.3E-06	8.9E-03	---	1.1E-09	3.9E-02
Ba-133	m^3	2.6E-02	---	1.3E+01	6.7E+00	6.9E+01	---	4.4E-03	3.9E+02
	Ci	2.5E-04	---	6.2E-06	1.6E-06	9.0E-03	---	1.4E-03	4.1E-02
Be-10	m^3	---	---	---	---	1.8E+01	---	---	8.0E+01
	Ci	---	---	---	---	5.1E-03	---	---	2.3E-02
Bi-207	m^3	---	---	---	3.8E-03	4.1E+00	---	1.3E-01	1.6E+01
	Ci	---	---	---	7.4E-05	7.1E-03	---	6.0E-05	3.2E-02
Bk-247	m^3	---	---	---	---	3.3E+01	---	---	6.7E+01
	Ci	---	---	---	---	3.1E-07	---	---	1.1E-06
C-14	m^3	7.6E-03	---	6.6E+00	4.8E+01	1.8E+02	---	2.0E+01	7.4E+02
	Ci	2.7E-09	---	5.2E-07	4.8E-05	3.7E+00	---	1.8E+01	9.6E+01

--- = None reported for this waste disposal region.

[a] Inventories given by volume (m^3) and activity (Ci).

Table 20 (Continued)
Radionuclide Inventories for the MDA G Performance Assessment by Waste Disposal Region

Radionuclide	Measurement Units [a]	Waste Disposal Region							
		1	2	3	4	5	6	7	8
Ca-41	m^3	---	---	---	---	1.8E+01	---	---	8.1E+01
	Ci	---	---	---	---	3.1E-01	---	---	1.4E+00
Cf-249	m^3	---	---	2.7E+00	---	3.2E+00	---	---	2.6E+01
	Ci	---	---	4.3E-07	---	3.8E-07	---	---	3.6E-06
Cf-251	m^3	---	---	---	---	0.0E+00	---	---	---
	Ci	---	---	---	---	0.0E+00	---	---	---
Cf-252	m^3	---	---	---	---	1.4E-01	---	4.8E-03	4.7E-03
	Ci	---	---	---	---	1.4E-05	---	7.6E-08	1.4E-07
Cl-36	m^3	---	---	---	---	1.8E+01	---	6.0E-04	8.1E+01
	Ci	---	---	---	---	2.0E-02	---	1.1E-08	8.8E-02
Cm-243	m^3	---	---	5.4E+00	---	2.0E+01	---	---	1.0E+02
	Ci	---	---	7.2E-07	---	4.6E-05	---	---	2.1E-04
Cm-244	m^3	---	---	---	---	3.4E-01	---	2.1E-02	1.6E+00
	Ci	---	---	---	---	1.1E-04	---	4.5E-09	5.0E-04
Cm-245	m^3	---	---	---	---	2.5E+01	---	---	1.1E+02
	Ci	---	---	---	---	5.2E-05	---	---	2.3E-04
Co-60	m^3	2.2E-02	---	1.8E+03	1.8E+04	4.0E+03	2.3E+00	1.0E+02	2.2E+04
	Ci	1.5E+00	---	2.4E+00	6.7E+00	3.8E+01	7.6E+01	3.2E+03	1.2E+04
Cs-135	m^3	---	---	1.8E+00	3.8E+01	9.0E+01	---	2.7E+00	2.1E+02
	Ci	---	---	5.9E-07	1.0E-04	3.7E-01	---	4.5E-06	5.6E-04

--- = None reported for this waste disposal region.

[a] Inventories given by volume (m^3) and activity (Ci).

Table 20 (Continued)
Radionuclide Inventories for the MDA G Performance Assessment by Waste Disposal Region

Radionuclide	Measurement Units [a]	Waste Disposal Region							
		1	2	3	4	5	6	7	8
Cs-137	m^3	3.4E-02	—	2.0E+03	1.8E+04	5.8E+03	4.0E-01	6.1E+00	2.7E+04
	Ci	9.0E-04	—	1.0E+00	2.2E+00	1.9E+00	1.5E+01	6.8E+01	1.4E+01
D38	m^3	—	—	1.1E+02	3.5E+02	5.8E+02	—	6.7E+00	—
	Ci	—	—	4.1E-01	2.0E-01	2.5E+00	—	2.4E+00	—
Eu-152	m^3	7.6E-03	—	1.1E+01	5.3E+03	7.7E+02	1.1E-01	1.4E+00	1.5E+04
	Ci	7.5E-09	—	2.7E-03	1.2E-02	3.5E-01	1.9E-03	4.1E-04	6.3E-01
Eu-154	m^3	—	—	2.8E+00	3.9E+01	2.1E+02	3.4E-01	4.4E-03	6.5E+02
	Ci	—	—	2.1E-06	1.2E-04	4.6E-02	9.7E-02	1.4E-06	8.6E-02
Gd-148	m^3	—	—	—	5.7E-02	7.1E-03	—	6.0E-04	2.9E-01
	Ci	—	—	—	1.0E-05	1.2E-06	—	8.6E-09	5.0E-05
H-3	m^3	—	—	1.8E+02	6.2E+03	3.2E+03	—	1.1E+02	2.3E+04
	Ci	—	—	1.5E+02	4.9E+00	5.2E+02	—	1.7E+06	9.8E+05
Ho-163	m^3	—	—	—	—	2.6E+01	—	2.0E+00	6.9E+01
	Ci	—	—	—	—	1.0E+00	—	7.8E-02	4.9E+00
Ho-166m	m^3	—	—	2.5E+00	—	3.2E+00	—	—	2.5E+01
	Ci	—	—	6.2E-06	—	1.4E-06	—	—	3.4E-05
I-129	m^3	—	—	2.3E-01	3.6E+01	3.2E+01	—	—	3.0E+02
	Ci	—	—	1.0E-06	1.1E-06	2.9E-05	—	—	1.4E-04
K-40	m^3	—	—	9.3E+01	2.1E+02	2.4E+02	—	1.2E+00	1.4E+03
	Ci	—	—	3.3E-04	1.8E-03	3.0E-03	—	4.8E-07	1.1E-02

— = None reported for this waste disposal region.

[a] Inventories given by volume (m^3) and activity (Ci).

Table 20 (Continued)
Radionuclide Inventories for the MDA G Performance Assessment by Waste Disposal Region

Radionuclide	Measurement Units [a]	Waste Disposal Region							
		1	2	3	4	5	6	7	8
Kr-85	m^3	1.1E-03	---	2.1E-01	1.5E+00	1.4E+01	---	---	1.4E+02
	Ci	1.0E-03	---	2.2E-06	4.3E-02	5.0E-03	---	---	5.9E-02
Lu-176	m^3	---	---	---	---	2.3E-01	---	---	1.0E+00
	Ci	---	---	---	---	1.9E-06	---	---	8.5E-06
MAP	m^3	---	---	---	1.9E+03	1.2E+03	2.3E-01	5.6E+01	---
	Ci	---	---	---	7.9E+00	5.0E+00	1.0E+00	5.6E+03	---
MFP	m^3	---	---	---	5.1E+02	1.0E+03	---	8.2E-01	---
	Ci	---	---	---	1.7E+01	6.2E-01	---	6.0E+01	---
Mo-93	m^3	---	---	---	---	1.9E-01	---	3.0E+01	1.3E+02
	Ci	---	---	---	---	2.3E-05	---	1.5E-02	6.5E-02
Nb-91	m^3	---	---	---	---	6.4E-02	---	---	2.8E-01
	Ci	---	---	---	---	5.6E-07	---	---	2.5E-06
Nb-92	m^3	---	---	---	---	6.4E-02	1.1E-01	---	2.8E-01
	Ci	---	---	---	---	3.4E-06	4.0E-03	---	1.5E-05
Nb-93m	m^3	---	---	---	---	3.1E+00	---	---	3.9E+00
	Ci	---	---	---	---	2.5E-05	---	---	1.1E-04
Nb-94	m^3	---	---	8.5E-01	1.1E-01	9.1E+00	---	---	2.2E+01
	Ci	---	---	1.7E-05	1.0E-05	4.2E-02	---	---	7.5E-02
Nd-144	m^3	---	---	---	5.7E-02	7.1E-03	---	---	2.8E-01
	Ci	---	---	---	1.0E-08	1.2E-09	---	---	5.0E-08

--- = None reported for this waste disposal region.

[a] Inventories given by volume (m^3) and activity (Ci).

Table 20 (Continued)
Radionuclide Inventories for the MDA G Performance Assessment by Waste Disposal Region

Radionuclide	Measurement Units [a]	Waste Disposal Region							
		1	2	3	4	5	6	7	8
Ni-59	m^3	---	---	2.3E-01	5.3E+01	5.1E+01	---	3.7E+00	3.8E+02
	Ci	---	---	6.1E-06	2.4E-03	4.0E-03	---	2.8E+00	1.3E+01
Ni-63	m^3	3.8E-03	---	3.1E+00	3.7E+01	2.4E+02	---	4.8E+01	9.1E+02
	Ci	3.0E-05	---	5.5E-04	5.2E-04	2.1E+00	---	1.3E+03	5.7E+03
Np-237	m^3	---	---	1.1E+02	8.7E+01	2.0E+02	---	1.2E+00	1.6E+03
	Ci	---	---	1.1E-04	6.3E-04	2.7E-03	---	3.4E-08	1.2E-02
Os-194	m^3	---	---	---	---	4.5E-01	---	---	2.0E+00
	Ci	---	---	---	---	1.5E-07	---	---	6.5E-07
Pa-231	m^3	---	---	2.3E-01	8.3E+00	6.4E+00	---	1.2E+00	4.1E+01
	Ci	---	---	1.0E-09	1.8E-05	6.2E-05	---	5.7E-08	3.1E-04
Pb-210	m^3	1.9E-02	---	1.4E+03	1.2E+04	1.2E+03	---	1.2E+00	4.5E+02
	Ci	2.3E-09	---	1.6E-01	9.3E-02	3.7E-02	---	2.9E-08	9.5E-01
Pm-145	m^3	---	---	---	---	3.1E+01	---	---	6.0E+01
	Ci	---	---	---	---	1.2E-01	---	---	5.5E-01
Pu-236	m^3	---	---	---	---	6.4E-02	---	---	2.8E-01
	Ci	---	---	---	---	1.1E-09	---	---	5.0E-09
Pu-238	m^3	---	---	2.5E+03	2.1E+04	7.9E+03	3.1E+00	3.3E+01	4.9E+04
	Ci	---	---	1.2E+00	3.5E+00	8.9E+00	1.0E-05	2.6E-01	4.3E+01
Pu-239	m^3	7.6E-02	---	3.7E+03	2.5E+04	1.1E+04	1.1E-01	3.9E+01	6.4E+04
	Ci	4.1E-05	---	9.6E-01	1.8E+00	1.2E+01	2.0E-09	7.1E-02	4.9E+01

--- = None reported for this waste disposal region.

[a] Inventories given by volume (m^3) and activity (Ci).

Table 20 (Continued)
Radionuclide Inventories for the MDA G Performance Assessment by Waste Disposal Region

Radionuclide	Measurement Units [a]	Waste Disposal Region							
		1	2	3	4	5	6	7	8
Pu-240	m^3	---	---	1.8E+03	1.3E+04	3.1E+03	---	1.8E+00	1.0E+04
	Ci	---	---	6.9E-02	2.7E-01	1.6E-01	---	1.3E-03	1.5E+00
Pu-241	m^3	---	---	4.5E+02	3.8E+02	9.9E+02	---	1.3E+00	6.8E+03
	Ci	---	---	1.2E+00	6.7E-01	9.8E-01	---	4.2E-02	1.1E+01
Pu-242	m^3	---	---	3.6E+02	3.7E+02	8.2E+02	---	2.1E-03	6.1E+03
	Ci	---	---	5.1E-04	7.5E-06	2.0E-03	---	1.1E-09	1.0E-02
Pu-244	m^3	---	---	---	---	7.0E+00	---	---	3.1E+01
	Ci	---	---	---	---	3.9E-06	---	---	1.8E-05
PU51	m^3	---	---	---	---	---	---	---	---
	Ci	---	---	---	---	---	---	---	---
PU52	m^3	---	---	---	5.3E+02	9.0E+02	---	4.2E-01	---
	Ci	---	---	---	7.4E-01	4.4E+00	---	5.7E-02	---
PU53	m^3	---	---	---	---	---	---	---	---
	Ci	---	---	---	---	---	---	---	---
PU54	m^3	---	---	---	---	---	---	---	---
	Ci	---	---	---	---	---	---	---	---
PU55	m^3	---	---	---	---	---	---	---	---
	Ci	---	---	---	---	---	---	---	---
PU56	m^3	---	---	---	---	---	---	---	---
	Ci	---	---	---	---	---	---	---	---

--- = None reported for this waste disposal region.

[a] Inventories given by volume (m^3) and activity (Ci).

Table 20 (Continued)
Radionuclide Inventories for the MDA G Performance Assessment by Waste Disposal Region

Radionuclide	Measurement Units [a]	Waste Disposal Region							
		1	2	3	4	5	6	7	8
PU57	m^3	---	---	---	---	---	---	---	---
	Ci	---	---	---	---	---	---	---	---
PU83	m^3	---	---	---	---	---	---	---	---
	Ci	---	---	---	---	---	---	---	---
Ra-226	m^3	---	---	8.9E+01	1.7E+02	1.6E+02	---	1.7E+00	1.1E+03
	Ci	---	---	2.1E-03	2.8E-03	3.5E-02	---	8.6E-01	3.9E+00
Ra-228	m^3	---	---	1.3E+03	1.2E+04	1.2E+03	---	---	1.1E+02
	Ci	---	---	2.4E-03	1.9E-02	2.0E-03	---	---	3.8E-04
Si-32	m^3	---	---	4.0E-01	1.1E-01	2.3E-01	---	---	3.0E+00
	Ci	---	---	1.2E-05	1.1E-07	2.0E-06	---	---	6.1E-05
Sm-151	m^3	---	---	---	7.4E-01	2.2E+01	---	---	1.7E+02
	Ci	---	---	---	9.0E-10	6.1E-09	---	---	1.8E-07
Sn-121m	m^3	---	---	---	---	2.0E+00	---	---	8.0E+01
	Ci	---	---	---	---	4.5E-07	---	---	1.8E-05
Sn-126	m^3	---	---	---	---	2.0E+00	---	---	8.0E+01
	Ci	---	---	---	---	1.1E-07	---	---	4.4E-06
Sr-90	m^3	5.4E-02	---	1.4E+03	2.1E+04	5.0E+03	---	8.6E-01	3.2E+04
	Ci	7.3E-04	---	5.4E-02	3.1E-01	4.4E-01	---	6.9E+01	2.8E+02
Tb-157	m^3	---	---	5.6E+00	---	6.9E-01	---	---	2.8E+01
	Ci	---	---	4.5E-08	---	5.6E-09	---	---	2.2E-07

— = None reported for this waste disposal region.

[a] Inventories given by volume (m^3) and activity (Ci).

Table 20 (Continued)
Radionuclide Inventories for the MDA G Performance Assessment by Waste Disposal Region

Radionuclide	Measurement Units [a]	Waste Disposal Region							
		1	2	3	4	5	6	7	8
Tc-97	m^3	---	---	---	4.0E-01	1.1E+00	---	---	5.1E+00
	Ci	---	---	---	7.0E-09	2.4E-06	---	---	1.1E-05
Tc-99	m^3	---	---	1.8E+01	1.9E+02	3.6E+02	---	6.0E-04	1.1E+03
	Ci	---	---	9.9E-03	2.8E-02	3.0E-01	---	1.2E-08	1.4E+00
Th-228	m^3	---	---	1.2E+01	3.0E+01	1.9E+02	---	1.1E+00	6.7E+02
	Ci	---	---	4.9E-04	4.5E-05	1.6E-03	---	3.0E-05	4.2E-03
Th-229	m^3	---	---	9.3E+00	7.5E+00	2.9E+01	---	3.8E-03	1.4E+02
	Ci	---	---	6.9E-05	4.8E-07	3.5E-04	---	5.4E-08	1.7E-03
Th-230	m^3	---	---	3.4E+00	2.5E+01	1.3E+02	---	6.0E-04	5.0E+02
	Ci	---	---	2.2E-08	5.2E-07	1.2E-03	---	6.0E-09	3.1E-03
Th-232	m^3	3.8E-03	---	1.7E+02	1.2E+02	1.6E+03	5.7E-02	4.0E+00	3.5E+03
	Ci	2.2E-06	---	1.6E-02	1.4E-03	3.2E-02	4.0E-04	2.0E-01	9.7E-01
TH88	m^3	---	---	---	1.9E+00	3.7E-02	---	---	---
	Ci	---	---	---	3.7E-02	2.0E-09	---	---	---
Ti-44	m^3	---	---	8.5E+00	---	6.0E+01	---	---	2.8E+02
	Ci	---	---	3.8E-04	---	4.0E-04	---	--	3.5E-03
U10	m^3	---	---	---	---	---	---	---	---
	Ci	---	---	---	---	---	---	---	---
U11	m^3	---	---	---	---	3.1E+00	---	---	---
	Ci	---	---	---	---	8.7E-06	---	---	---

--- = None reported for this waste disposal region.

[a] Inventories given by volume (m^3) and activity (Ci).

Table 20 (Continued)
Radionuclide Inventories for the MDA G Performance Assessment by Waste Disposal Region

Radionuclide	Measurement Units [a]	Waste Disposal Region							
		1	2	3	4	5	6	7	8
U12	m^3	---	---	---	---	---	---	---	---
	Ci	---	---	---	---	---	---	---	---
U-232	m^3	---	---	3.0E+00	6.4E+00	6.1E+00	---	---	6.6E+01
	Ci	---	---	1.8E-08	5.2E-04	3.6E-04	---	---	2.9E-03
U-233	m^3	---	---	1.1E+01	1.8E+01	3.5E+01	---	2.2E-02	2.0E+02
	Ci	---	---	7.5E-03	5.4E-04	5.0E-03	---	6.5E-04	5.1E-02
U-234	m^3	---	---	1.4E+03	1.3E+04	4.4E+03	---	2.4E+00	1.0E+04
	Ci	---	---	2.9E-02	2.9E-01	9.2E-01	---	1.2E-01	1.1E+01
U-235	m^3	1.1E-02	---	2.2E+03	1.4E+04	7.1E+03	1.9E-02	3.3E+01	2.3E+04
	Ci	5.2E-05	---	1.0E-02	5.3E-01	3.3E-01	1.0E-05	5.8E-03	5.7E-01
U-236	m^3	---	---	5.6E+01	2.6E+00	1.8E+02	---	3.5E-04	1.0E+03
	Ci	---	---	3.2E-05	1.3E-07	3.5E-04	---	4.3E-06	5.8E-04
U-238	m^3	7.6E-03	---	2.0E+03	1.3E+04	5.9E+03	1.1E-01	1.8E+01	2.0E+04
	Ci	5.0E-07	---	5.4E+00	4.3E+00	2.7E+00	1.0E-09	6.7E-01	2.6E+01
U35	m^3	---	---	---	---	---	---	---	---
	Ci	---	---	---	---	---	---	---	---
U36	m^3	---	---	---	---	---	---	---	---
	Ci	---	---	---	---	---	---	---	---
U38	m^3	---	---	---	2.8E-02	2.6E+00	---	---	---
	Ci	---	---	---	3.0E-02	2.0E-02	---	---	---

--- = None reported for this waste disposal region.

[a] Inventories given by volume (m^3) and activity (Ci).

Table 20 (Continued)
Radionuclide Inventories for the MDA G Performance Assessment by Waste Disposal Region

Radionuclide	Measurement Units [a]	Waste Disposal Region							
		1	2	3	4	5	6	7	8
U39	m^3	---	---	---	---	2.3E+01	---	---	---
	Ci	---	---	---	---	3.1E-03	---	---	---
U81	m^3	---	---	---	1.1E+01	3.2E-02	---	---	---
	Ci	---	---	---	3.5E-06	5.7E-04	---	---	---
U(NAT)	m^3	---	---	---	---	---	---	6.2E-01	---
	Ci	---	---	---	---	---	---	1.8E-01	---
Zr-93	m^3	---	---	1.1E-01	---	1.4E-02	---	---	5.7E-01
	Ci	---	---	2.0E-08	---	2.5E-09	---	---	1.0E-07

--- = None reported for this waste disposal region.

[a] Inventories given by volume (m^3) and activity (Ci).

Table 21
Radionuclide Inventories for the MDA G Composite Analysis by Waste Disposal Region

Radionuclide	Measurement Unit [a]	Waste Disposal Region							
		1	2	3	4	5	6	7	8
Ac-227	m^3	9.1E-01	—	4.2E-01	—	5.8E-02	—	6.0E-04	1.5E-01
	Ci	8.6E-01	—	7.0E-02	—	4.0E-06	—	5.9E-07	1.2E-05
Ag-108m	m^3	—	—	1.0E+01	9.4E+00	1.8E+01	—	1.7E+00	1.7E+02
	Ci	—	—	1.1E-04	4.9E-05	2.0E-05	—	5.0E+00	2.2E+01
Al-26	m^3	—	—	—	—	3.9E-02	—	—	4.7E-02
	Ci	—	—	—	—	2.9E-04	—	—	1.3E-03
Am-241	m^3	3.0E+03	1.9E+00	3.3E+03	1.9E+04	1.0E+04	1.4E+00	4.0E+01	4.2E+04
	Ci	2.4E+03	1.3E-01	1.7E+00	1.8E+01	1.1E+01	1.4E-03	7.3E-02	3.0E+01
Am-243	m^3	2.9E-02	—	2.5E+01	5.0E+01	2.1E+02	—	6.6E-02	8.9E+02
	Ci	2.0E-02	—	1.3E-05	1.3E-06	8.9E-03	—	1.1E-09	3.9E-02
Ba-133	m^3	2.6E-02	—	1.3E+01	6.7E+00	6.9E+01	—	4.4E-03	3.9E+02
	Ci	2.5E-04	—	6.2E-06	1.6E-06	9.0E-03	—	1.4E-03	4.1E-02
Be-10	m^3	—	—	—	—	1.8E+01	—	—	8.0E+01
	Ci	—	—	—	—	5.1E-03	—	—	2.3E-02
Bi-207	m^3	—	—	—	3.8E-03	4.1E+00	—	1.3E-01	1.6E+01
	Ci	—	—	—	7.4E-05	7.1E-03	—	6.0E-05	3.2E-02
Bk-247	m^3	—	—	—	—	3.3E+01	—	—	6.7E+01
	Ci	—	—	—	—	3.1E-07	—	—	1.1E-06
C-14	m^3	3.5E-01	—	1.2E+01	4.9E+01	1.8E+02	6.3E-01	2.0E+01	7.4E+02
	Ci	1.0E-02	—	3.4E-06	2.1E-01	3.7E+00	1.1E+00	1.8E+01	9.6E+01

— = None reported for this waste disposal region.

[a] Inventories given by volume (m^3) and activity (Ci).

Table 21 (Continued)
Radionuclide Inventories for the MDA G Composite Analysis by Waste Disposal Region

Radionuclide	Measurement Unit [a]	Waste Disposal Region							
		1	2	3	4	5	6	7	8
Ca-41	m^3	---	---	---	---	1.8E+01	---	---	8.1E+01
	Ci	---	---	---	---	3.1E-01	---	---	1.4E+00
Cf-249	m^3	1.3E+00	---	3.3E+00	---	3.2E+00	---	---	2.6E+01
	Ci	2.4E-03	---	4.1E-04	---	3.8E-07	---	---	3.6E-06
Cf-251	m^3	1.5E-01	---	8.5E-02	---	0.0E+00	---	---	---
	Ci	2.7E-03	---	1.6E-03	---	0.0E+00	---	---	---
Cf-252	m^3	7.0E-01	2.8E-01	2.8E-02	---	1.4E-01	2.8E-02	4.8E-03	4.7E-03
	Ci	6.3E+01	8.6E-03	8.0E-06	---	1.4E-05	5.6E-04	7.6E-08	1.4E-07
Cl-36	m^3	---	---	---	---	1.8E+01	---	6.0E-04	8.1E+01
	Ci	---	---	---	---	2.0E-02	---	1.1E-08	8.8E-02
Cm-243	m^3	---	---	5.4E+00	---	2.0E+01	---	---	1.0E+02
	Ci	---	---	7.2E-07	---	4.6E-05	---	---	2.1E-04
Cm-244	m^3	7.4E-01	---	---	---	3.4E-01	5.7E-03	2.1E-02	1.6E+00
	Ci	1.9E-01	---	---	---	1.1E-04	5.0E-05	4.5E-09	5.0E-04
Cm-245	m^3	---	---	---	---	2.5E+01	---	---	1.1E+02
	Ci	---	---	---	---	5.2E-05	---	---	2.3E-04
Co-60	m^3	8.0E-01	6.8E-01	1.8E+03	1.8E+04	4.0E+03	6.1E+00	1.0E+02	2.2E+04
	Ci	1.0E+03	2.0E-03	1.1E+03	1.3E+02	3.8E+01	1.6E+03	3.5E+03	1.2E+04
Cs-135	m^3	---	---	1.8E+00	3.8E+01	9.0E+01	---	2.7E+00	2.1E+02
	Ci	---	---	5.9E-07	1.0E-04	3.7E-01	---	4.5E-06	5.6E-04

--- = None reported for this waste disposal region.

[a] Inventories given by volume (m^3) and activity (Ci).

Table 21 (Continued)
Radionuclide Inventories for the MDA G Composite Analysis by Waste Disposal Region

Radionuclide	Measurement Unit [a]	Waste Disposal Region							
		1	2	3	4	5	6	7	8
Cs-137	m^3	1.9E+00	7.6E-01	2.1E+03	1.9E+04	6.1E+03	9.4E-01	6.1E+00	2.7E+04
	Ci	4.3E+01	1.5E-01	1.0E+00	1.1E+03	3.4E+00	1.5E+01	6.8E+01	1.4E+01
D38	m^3	---	---	1.1E+02	3.5E+02	5.8E+02	---	6.7E+00	---
	Ci	---	---	4.1E-01	2.0E-01	2.5E+00	---	2.4E+00	---
Eu-152	m^3	9.3E-02	---	1.1E+01	5.3E+03	7.7E+02	1.1E-01	1.4E+00	1.5E+04
	Ci	1.2E-01	---	2.7E-03	1.2E-02	3.5E-01	1.9E-03	4.1E-04	6.3E-01
Eu-154	m^3	---	---	2.8E+00	3.9E+01	2.1E+02	3.4E-01	4.4E-03	6.5E+02
	Ci	---	---	2.1E-06	1.2E-04	4.6E-02	9.7E-02	1.4E-06	8.6E-02
Gd-148	m^3	---	---	---	5.7E-02	7.1E-03	---	6.0E-04	2.9E-01
	Ci	---	---	---	1.0E-05	1.2E-06	---	8.6E-09	5.0E-05
H-3	m^3	3.4E+01	1.1E+01	3.8E+02	6.4E+03	3.4E+03	2.4E+01	1.6E+02	2.3E+04
	Ci	6.1E+04	5.0E-01	6.2E+03	1.4E+03	5.5E+02	4.1E+04	2.5E+06	9.8E+05
Ho-163	m^3	---	---	---	---	2.6E+01	---	2.0E+00	6.9E+01
	Ci	---	---	---	---	1.0E+00	---	7.8E-02	4.9E+00
Ho-166m	m^3	---	---	2.5E+00	---	3.2E+00	---	---	2.5E+01
	Ci	---	---	6.2E-06	---	1.4E-06	---	---	3.4E-05
I-129	m^3	---	---	2.3E-01	3.6E+01	3.2E+01	---	---	3.0E+02
	Ci	---	---	1.0E-06	1.1E-06	2.9E-05	---	---	1.4E-04
K-40	m^3	---	---	9.3E+01	2.1E+02	2.4E+02	---	1.2E+00	1.4E+03
	Ci	---	---	3.3E-04	1.8E-03	3.0E-03	---	4.8E-07	1.1E-02

--- = None reported for this waste disposal region.

[a] Inventories given by volume (m^3) and activity (Ci).

Table 21 (Continued)
Radionuclide Inventories for the MDA G Composite Analysis by Waste Disposal Region

Radionuclide	Measurement Unit [a]	Waste Disposal Region							
		1	2	3	4	5	6	7	8
Kr-85	m^3	9.8E-02	---	2.6E-01	1.5E+00	1.5E+01	2.3E+00	---	1.4E+02
	Ci	2.7E-03	---	1.0E-03	4.3E-02	5.0E-03	4.5E-04	---	5.9E-02
Lu-176	m^3	---	---	---	---	2.3E-01	---	---	1.0E+00
	Ci	---	---	---	---	1.9E-06	---	---	8.5E-06
MAP	m^3	1.1E+02	1.1E+02	1.5E+02	2.6E+03	2.5E+03	7.0E+01	2.2E+02	---
	Ci	4.7E+02	8.9E-01	7.6E+02	3.2E+02	1.3E+02	1.1E+04	8.0E+03	---
MFP	m^3	1.0E+02	1.7E+01	7.2E+01	8.5E+02	1.1E+03	6.6E+00	1.0E+00	---
	Ci	7.8E+03	4.7E-02	6.0E+02	3.6E+01	2.5E+01	3.3E+03	7.0E+01	---
Mo-93	m^3	---	---	---	---	1.9E-01	---	3.0E+01	1.3E+02
	Ci	---	---	---	---	2.3E-05	---	1.5E-02	6.5E-02
Nb-91	m^3	---	---	---	---	6.4E-02	---	---	2.8E-01
	Ci	---	---	---	---	5.6E-07	---	---	2.5E-06
Nb-92	m^3	---	---	---	---	6.4E-02	1.1E-01	---	2.8E-01
	Ci	---	---	---	---	3.4E-06	4.0E-03	---	1.5E-05
Nb-93m	m^3	---	---	---	---	3.1E+00	---	---	3.9E+00
	Ci	---	---	---	---	2.5E-05	---	---	1.1E-04
Nb-94	m^3	---	---	8.5E-01	1.1E-01	9.6E+00	---	---	2.2E+01
	Ci	---	---	1.7E-05	1.0E-05	4.2E-02	---	---	7.5E-02
Nd-144	m^3	---	---	---	5.7E-02	7.1E-03	---	---	2.8E-01
	Ci	---	---	---	1.0E-08	1.2E-09	---	---	5.0E-08

--- = None reported for this waste disposal region.

[a] Inventories given by volume (m^3) and activity (Ci).

Table 21 (Continued)
Radionuclide Inventories for the MDA G Composite Analysis by Waste Disposal Region

Radionuclide	Measurement Unit [a]	Waste Disposal Region							
		1	2	3	4	5	6	7	8
Ni-59	m^3	—	—	2.3E-01	5.3E+01	5.1E+01	—	3.7E+00	3.8E+02
	Ci	—	—	6.1E-06	2.4E-03	4.0E-03	—	2.8E+00	1.3E+01
Ni-63	m^3	3.8E-03	—	3.1E+00	3.7E+01	2.4E+02	3.8E+00	4.8E+01	9.1E+02
	Ci	3.0E-05	—	5.5E-04	5.2E-04	2.1E+00	3.2E-04	1.3E+03	5.7E+03
Np-237	m^3	6.3E-01	—	1.1E+02	8.8E+01	2.0E+02	—	1.2E+00	1.6E+03
	Ci	4.2E-03	—	1.1E-04	6.3E-04	2.7E-03	—	3.4E-08	1.2E-02
Os-194	m^3	—	—	—	—	4.5E-01	—	—	2.0E+00
	Ci	—	—	—	—	1.5E-07	—	—	6.5E-07
Pa-231	m^3	—	—	2.3E-01	8.3E+00	6.4E+00	—	1.2E+00	4.1E+01
	Ci	—	—	1.0E-09	1.8E-05	6.2E-05	—	5.7E-08	3.1E-04
Pb-210	m^3	1.9E-02	—	1.4E+03	1.2E+04	1.2E+03	—	1.2E+00	4.5E+02
	Ci	2.3E-09	—	1.6E-01	9.3E-02	3.7E-02	—	2.9E-08	9.5E-01
Pm-145	m^3	—	—	—	—	3.1E+01	—	—	6.0E+01
	Ci	—	—	—	—	1.2E-01	—	—	5.5E-01
Pu-236	m^3	—	—	—	—	6.4E-02	—	—	2.8E-01
	Ci	—	—	—	—	1.1E-09	—	—	5.0E-09
Pu-238	m^3	3.4E+03	1.0E+03	3.6E+03	2.2E+04	8.1E+03	3.7E+01	3.3E+01	4.9E+04
	Ci	4.0E+03	2.0E+02	2.4E+01	6.3E+00	1.1E+01	1.7E-03	2.6E-01	4.3E+01
Pu-239	m^3	5.7E+03	8.8E+02	5.0E+03	2.9E+04	1.2E+04	3.4E+01	4.0E+01	6.4E+04
	Ci	2.7E+02	4.2E+00	8.1E+00	6.0E+00	2.0E+01	6.5E-02	7.1E-02	4.9E+01

— = None reported for this waste disposal region.

[a] Inventories given by volume (m^3) and activity (Ci).

Table 21 (Continued)
Radionuclide Inventories for the MDA G Composite Analysis by Waste Disposal Region

Radionuclide	Measurement Unit [a]	Waste Disposal Region							
		1	2	3	4	5	6	7	8
Pu-240	m^3	3.1E+02	---	1.8E+03	1.3E+04	3.1E+03	---	1.3E+00	1.0E+04
	Ci	4.0E+00	---	6.9E-02	2.7E-01	1.6E-01	---	1.1E-03	1.5E+00
Pu-241	m^3	1.2E-01	---	4.5E+02	3.8E+02	9.9E+02	---	1.3E+00	6.8E+03
	Ci	7.4E-01	---	1.2E+00	6.7E-01	9.8E-01	---	4.2E-02	1.1E+01
Pu-242	m^3	6.6E-03	---	3.6E+02	3.7E+02	8.2E+02	---	2.1E-03	6.1E+03
	Ci	1.2E-04	---	5.1E-04	7.5E-06	2.0E-03	---	1.1E-09	1.0E-02
Pu-244	m^3	---	---	---	---	7.0E+00	---	---	3.1E+01
	Ci	---	---	---	---	3.9E-06	---	---	1.8E-05
PU51	m^3	1.1E+00	---	---	---	---	---	---	---
	Ci	1.6E+00	---	---	---	---	---	---	---
PU52	m^3	1.1E+03	1.4E+02	6.5E+02	1.1E+03	1.4E+03	4.2E-01	6.2E-01	---
	Ci	7.7E+03	2.4E-03	9.1E-02	1.7E+00	5.6E+00	7.3E+00	5.7E-02	---
PU53	m^3	6.1E+00	---	---	1.2E+00	---	---	---	---
	Ci	2.5E+02	---	---	3.7E-04	---	---	---	---
PU54	m^3	1.9E+01	---	---	6.5E+01	7.3E+00	5.7E-01	---	---
	Ci	1.1E+03	---	---	1.3E-01	2.0E-02	2.0E-08	---	---
PU55	m^3	1.4E+00	---	---	---	---	---	---	---
	Ci	6.8E+01	---	---	---	---	---	---	---
PU56	m^3	2.1E+01	---	---	---	---	---	---	---
	Ci	1.2E+03	---	---	---	---	---	---	---

--- = None reported for this waste disposal region.

[a] Inventories given by volume (m^3) and activity (Ci).

Table 21 (Continued)
Radionuclide Inventories for the MDA G Composite Analysis by Waste Disposal Region

Radionuclide	Measurement Unit [a]	Waste Disposal Region							
		1	2	3	4	5	6	7	8
PU57	m^3	1.4E+00	—	—	—	—	—	—	—
	Ci	7.1E+01	—	—	—	—	—	—	—
PU83	m^3	1.3E+02	—	3.8E+02	3.8E+02	2.7E+02	—	—	—
	Ci	5.0E+02	—	9.5E-03	4.2E-03	1.4E-03	—	—	—
Ra-226	m^3	8.5E-02	—	8.9E+01	1.7E+02	1.6E+02	1.3E+00	1.7E+00	1.1E+03
	Ci	1.0E-01	—	1.0E-01	1.0E-01	3.5E-02	2.5E+00	8.6E-01	3.9E+00
Ra-228	m^3	—	—	1.3E+03	1.2E+04	1.2E+03	—	—	1.1E+02
	Ci	—	—	2.4E-03	1.9E-02	2.2E-01	—	—	3.8E-04
Si-32	m^3	—	—	4.0E-01	1.1E-01	2.3E-01	—	—	3.0E+00
	Ci	—	—	1.2E-05	1.1E-07	2.0E-06	—	—	6.1E-05
Sm-151	m^3	—	—	—	7.4E-01	2.2E+01	—	—	1.7E+02
	Ci	—	—	—	9.0E-10	6.1E-09	—	—	1.8E-07
Sn-121m	m^3	—	—	—	—	2.0E+00	—	—	8.0E+01
	Ci	—	—	—	—	4.5E-07	—	—	1.8E-05
Sn-126	m^3	—	—	—	—	2.0E+00	—	—	8.0E+01
	Ci	—	—	—	—	1.1E-07	—	—	4.4E-06
Sr-90	m^3	1.4E+00	7.6E-01	1.8E+03	2.3E+04	5.0E+03	1.3E+00	8.6E-01	3.2E+04
	Ci	1.4E+00	1.7E-01	1.3E+00	1.4E+03	5.6E-01	9.5E-02	6.9E+01	2.8E+02
Tb-157	m^3	—	—	5.6E+00	—	6.9E-01	—	—	2.8E+01
	Ci	—	—	4.5E-08	—	5.6E-09	—	—	2.2E-07

— = None reported for this waste disposal region.

[a] Inventories given by volume (m^3) and activity (Ci).

Table 21 (Continued)
Radionuclide Inventories for the MDA G Composite Analysis by Waste Disposal Region

Radionuclide	Measurement Unit [a]	Waste Disposal Region							
		1	2	3	4	5	6	7	8
Tc-97	m^3	---	---	---	4.0E-01	1.1E+00	---	---	5.1E+00
	Ci	---	---	---	7.0E-09	2.4E-06	---	---	1.1E-05
Tc-99	m^3	---	---	1.8E+01	1.9E+02	3.6E+02	---	6.0E-04	1.1E+03
	Ci	---	---	9.9E-03	2.8E-02	3.0E-01	---	1.2E-08	1.4E+00
Th-228	m^3	---	---	1.2E+01	3.0E+01	1.9E+02	---	1.1E+00	6.7E+02
	Ci	---	---	4.9E-04	4.5E-05	1.6E-03	---	3.0E-05	4.2E-03
Th-229	m^3	---	---	9.3E+00	7.5E+00	2.9E+01	---	3.8E-03	1.4E+02
	Ci	---	---	6.9E-05	4.8E-07	3.5E-04	---	5.4E-08	1.7E-03
Th-230	m^3	1.9E-02	1.1E-02	3.4E+00	2.5E+01	1.3E+02	---	6.0E-04	5.0E+02
	Ci	1.6E+01	9.5E+00	2.2E-08	5.2E-07	1.2E-03	---	6.0E-09	3.1E-03
Th-232	m^3	1.8E-01	---	1.7E+02	1.2E+02	1.6E+03	2.5E+00	4.0E+00	3.5E+03
	Ci	3.1E+00	---	1.7E-02	1.5E-03	3.2E-02	5.0E-03	2.0E-01	9.7E-01
TH88	m^3	5.5E+00	5.9E-02	3.1E+00	2.4E+00	6.0E-02	6.2E+00	---	---
	Ci	5.2E-03	4.4E-04	6.9E-04	6.0E-02	2.6E-03	7.7E-04	---	---
Ti-44	m^3	---	---	8.5E+00	---	6.0E+01	---	---	2.8E+02
	Ci	---	---	3.8E-04	---	4.0E-04	---	---	3.5E-03
U10	m^3	6.2E+00	2.3E-01	3.3E+00	---	---	---	---	---
	Ci	8.8E-01	5.0E-09	5.1E-01	---	---	---	---	---
U11	m^3	---	---	---	4.5E-01	3.3E+00	---	---	---
	Ci	---	---	---	1.3E-01	2.4E-02	---	---	---

— = None reported for this waste disposal region.

[a] Inventories given by volume (m^3) and activity (Ci).

Table 21 (Continued)
Radionuclide Inventories for the MDA G Composite Analysis by Waste Disposal Region

Radionuclide	Measurement Unit [a]	Waste Disposal Region							
		1	2	3	4	5	6	7	8
U12	m^3	4.3E+01	1.6E+01	1.0E+01	4.2E-02	5.7E-03	1.7E+01	---	---
	Ci	8.1E+00	3.2E+00	2.3E+00	2.7E-01	2.4E-03	1.5E+00	---	---
U-232	m^3	3.8E-03	---	3.0E+00	6.4E+00	6.1E+00	---	---	6.6E+01
	Ci	2.1E-01	---	1.8E-08	5.2E-04	3.6E-04	---	---	2.9E-03
U-233	m^3	2.5E+03	---	1.2E+01	1.9E+01	3.5E+01	---	2.2E-02	2.0E+02
	Ci	1.2E+01	---	7.5E-03	1.9E-02	5.0E-03	---	6.5E-04	5.1E-02
U-234	m^3	3.6E-01	---	1.4E+03	1.3E+04	4.4E+03	---	2.4E+00	1.0E+04
	Ci	2.3E-01	---	2.9E-02	2.9E-01	9.2E-01	---	1.2E-01	1.1E+01
U-235	m^3	4.7E+02	6.0E+01	2.5E+03	1.4E+04	7.4E+03	1.2E+01	3.3E+01	2.3E+04
	Ci	4.0E-01	3.5E-03	2.4E-01	9.5E-01	3.9E-01	9.7E-01	5.8E-03	5.7E-01
U-236	m^3	1.2E-01	---	5.6E+01	2.6E+00	1.8E+02	---	3.5E-04	1.0E+03
	Ci	2.5E-05	---	3.2E-05	1.3E-07	3.5E-04	---	4.3E-06	5.8E-04
U-238	m^3	2.1E+02	1.4E+00	2.2E+03	1.4E+04	6.4E+03	7.1E+01	1.8E+01	2.0E+04
	Ci	8.9E+00	1.1E-01	1.1E+01	7.7E+00	4.0E+00	5.0E+00	6.7E-01	2.6E+01
U35	m^3	---	---	---	1.1E+00	0.0E+00	---	---	---
	Ci	---	---	---	4.9E-04	0.0E+00	---	---	---
U36	m^3	---	---	---	1.1E+00	0.0E+00	---	---	---
	Ci	---	---	---	2.2E-05	0.0E+00	---	---	---
U38	m^3	1.1E+01	2.2E+00	6.1E+00	2.7E+01	1.1E+01	---	---	---
	Ci	6.7E-02	7.5E-04	1.4E-02	4.2E-02	3.7E-02	---	---	---

--- = None reported for this waste disposal region.

[a] Inventories given by volume (m^3) and activity (Ci).

Table 21 (Continued)
Radionuclide Inventories for the MDA G Composite Analysis by Waste Disposal Region

Radionuclide	Measurement Unit [a]	Waste Disposal Region							
		1	2	3	4	5	6	7	8
U39	m^3	---	---	---	---	2.3E+01	---	---	---
	Ci	---	---	---	---	3.1E-03	---	---	---
U81	m^3	1.5E+00	---	2.8E-03	1.1E+01	3.2E-02	1.9E+00	---	---
	Ci	1.8E-02	---	2.8E-03	3.5E-06	5.7E-04	4.5E-03	---	---
U(NAT)	m^3	---	---	---	---	---	---	6.2E-01	---
	Ci	---	---	---	---	---	---	1.8E-01	---
Zr-93	m^3	---	---	1.1E-01	---	1.4E-02	---	---	5.7E-01
	Ci	---	---	2.0E-08	---	2.5E-09	---	---	1.0E-07

--- = None reported for this waste disposal region.

[a] Inventories given by volume (m^3) and activity (Ci).

Significant quantities of waste disposed of at MDA G contain activation and fission product waste. Prior to the mid-1990s, the radionuclides in these wastes were often listed in terms of total activities of mixed activation products (MAP) and mixed fission products (MFP). Similarly, the radionuclides in waste containing mixtures of plutonium, thorium, or uranium isotopes were often recorded using a series of material types. The volumes and activities associated with the MAP, MFP, and material type waste were allocated among specific radionuclides in Shuman (2005). The inventories shown in Tables 20 and 21, however, list MAP, MFP, and the various material types and do not assign the associated volumes and activities to specific radionuclides. The data are presented in this manner so the uncertainties associated with the inventory projections may be evaluated.

The activities listed in Tables 19 through 21 represent as-disposed activities. Several radionuclides found in the waste have very short half-lives and, as a result, pose little or no risk to human health and safety and the environment. These radionuclides were eliminated from the MDA G inventory and are not included in Tables 20 and 21. The basis for eliminating radionuclides on the basis of their decay characteristics is discussed in Shuman (2005).

The inventories used in the intruder dose assessment do not correlate directly with the waste disposal region inventories listed in Table 20, in part because the units comprising the 1988–2004 pits and shafts are located in two or more waste disposal regions. While the inventories listed in Table 20 for disposal region 8 represent the sum of the inventories in the 2005–2044 pits and shafts, the intruder analysis evaluated the impacts of these sets of units individually. The inventories used in the intruder assessment are provided in Tables 22 and 23.

Table 22
Inventories Included in the Intruder Dose Assessment

Disposal Units	Volume (m3)	Activity (Ci)
1988-2004 Pits	7.6E+04	1.1E+03
2005-2044 Pits	1.1E+05	2.6E+03
1988-2004 Shafts	4.7E+02	1.8E+06
2005-2044 Shafts	1.2E+03	1.1E+06

The radionuclide inventories listed in Table 23 for the 1988–2004 pits, 2005-2044 pits, and 2005–2044 shafts represent the total inventory for each set of units. In contrast, the inventories provided for the 1988–2004 shafts are listed in terms of the quantities of waste disposed of in the upper 1.5 m of the units and the material disposed of at depths greater than 1.5 m. The manner in which these layer-specific inventories were developed is described in *Attachment II.*

Table 23
Radionuclide Inventories for the Intruder Dose Assessment

Radionuclide	1988–2004 Pits		2005–2044 Pits		1988-2004 Shafts				2005–2044 Shafts	
					Waste in Upper 1.5 m		Waste Deeper than 1.5 m			
	Volume (m3)	Activity (Ci)	Volume (m3)	Activity (Ci)	Volume (m3)	Activity (Ci)	Volume (m3)	Activity (Ci)	Volume (m3)	Activity (Ci)
Ac-227	5.8E-02	4.0E-06	1.4E-01	9.8E-06	5.8E-06	5.7E-09	6.0E-04	5.8E-07	2.7E-03	2.6E-06
Ag-108m	3.7E+01	1.8E-04	1.6E+02	7.9E-04	1.6E-02	4.8E-02	1.7E+00	4.9E+00	7.5E+00	2.2E+01
Al-26	3.9E-02	2.9E-04	4.7E-02	1.3E-03	---	---	---	---	---	---
Am-241	3.0E+04	7.7E+00	4.2E+04	3.0E+01	4.3E+00	6.1E-03	3.5E+01	6.7E-02	4.3E+01	1.2E-02
Am-243	2.8E+02	8.9E-03	8.9E+02	3.9E-02	6.3E-04	1.1E-11	6.5E-02	1.1E-09	2.9E-01	5.0E-09
Ba-133	8.9E+01	9.0E-03	3.9E+02	3.5E-02	2.6E-03	3.5E-05	2.8E-02	1.7E-03	2.8E-03	6.4E-03
Be-10	1.8E+01	5.1E-03	8.0E+01	2.3E-02	---	---	---	---	---	---
Bi-207	4.1E+00	7.2E-03	1.5E+01	3.1E-02	1.5E-03	8.8E-07	1.3E-01	5.9E-05	5.7E-01	2.5E-04
Bk-247	3.3E+01	3.1E-07	6.7E+01	1.1E-06	---	---	---	---	---	---
C-14	2.3E+02	3.7E+00	6.6E+02	1.6E+01	7.4E+00	2.6E-01	1.2E+01	1.8E+01	8.7E+01	8.0E+01
Ca-41	1.8E+01	3.1E-01	8.1E+01	1.4E+00	---	---	---	---	---	---
Cf-249	5.9E+00	8.2E-07	2.6E+01	3.6E-06	---	---	---	---	---	---
Cf-252	1.4E-01	1.4E-05	---	---	3.4E-04	4.2E-09	4.5E-03	7.2E-08	4.7E-03	1.4E-07
Cl-36	1.8E+01	2.0E-02	8.1E+01	8.8E-02	5.8E-06	1.1E-10	6.0E-04	1.1E-08	2.7E-03	5.0E-08
Cm-243	2.6E+01	4.7E-05	1.0E+02	2.1E-04	---	---	---	---	---	---
Cm-244	3.4E-01	1.1E-04	1.5E+00	5.0E-04	2.0E-04	4.3E-11	2.1E-02	4.5E-09	9.5E-02	2.0E-08
Cm-245	2.5E+01	5.2E-05	1.1E+02	2.3E-04	---	---	---	---	---	---

--- = None reported for this waste disposal region.

Table 23 (Continued)
Radionuclide Inventories for the Intruder Dose Assessment

Radionuclide	1988–2004 Pits		2005–2044 Pits		1988-2004 Shafts				2005–2044 Shafts	
					Waste in Upper 1.5 m		Waste Deeper than 1.5 m			
	Volume (m3)	Activity (Ci)	Volume (m3)	Activity (Ci)	Volume (m3)	Activity (Ci)	Volume (m3)	Activity (Ci)	Volume (m3)	Activity (Ci)
Co-60	2.4E+04	4.7E+01	2.2E+04	1.5E+02	2.3E+01	2.8E+02	8.0E+01	3.0E+03	3.0E+02	1.2E+04
Cs-135	1.3E+02	3.7E-01	2.1E+02	5.6E-04	2.3E-01	3.9E-07	2.5E+00	4.1E-06	---	---
Cs-137	2.5E+04	5.1E+00	2.7E+04	1.1E+01	3.3E-01	7.1E+00	6.2E+00	7.5E+01	8.2E+00	2.5E+00
D38	1.0E+03	3.1E+00	---	---	2.3E+00	2.6E-01	4.4E+00	2.1E+00	---	---
Eu-152	6.1E+03	3.7E-01	1.5E+04	6.3E-01	2.4E-02	1.9E-04	1.5E+00	2.1E-03	6.2E+00	3.2E-04
Eu-154	2.5E+02	4.7E-02	6.5E+02	8.6E-02	3.0E-02	8.3E-03	3.2E-01	8.8E-02	2.7E-03	6.0E-06
Gd-148	6.4E-02	1.1E-05	2.8E-01	5.0E-05	5.8E-06	8.3E-11	6.0E-04	8.5E-09	2.7E-03	3.8E-08
H-3	9.6E+03	6.7E+02	2.2E+04	1.6E+03	1.4E+01	1.1E+05	9.8E+01	1.6E+06	6.7E+02	9.8E+05
Ho-163	2.6E+01	1.0E+00	6.0E+01	4.5E+00	1.8E-01	6.7E-03	1.9E+00	7.2E-02	9.1E+00	3.5E-01
Ho-166m	5.7E+00	7.6E-06	2.5E+01	3.4E-05	---	---	---	---	---	---
I-129	6.8E+01	3.1E-05	3.0E+02	1.4E-04	---	---	---	---	---	---
K-40	5.4E+02	5.1E-03	1.4E+03	1.1E-02	1.1E-02	4.6E-09	1.2E+00	4.8E-07	5.2E+00	2.1E-06
Kr-85	1.6E+01	4.8E-02	1.4E+02	5.9E-02	9.8E-05	8.6E-05	1.0E-03	9.1E-04	---	---
Lu-176	2.3E-01	1.9E-06	1.0E+00	8.5E-06	---	---	---	---	---	---
MAP	3.1E+03	1.3E+01	---	---	4.9E+00	4.8E+02	5.2E+01	5.1E+03	---	---
MFP	1.6E+03	1.8E+01	---	---	2.2E-02	1.9E-01	8.0E-01	6.0E+01	---	---
Mo-93	1.9E-01	2.3E-05	8.5E-01	1.0E-04	7.5E+00	1.3E-03	2.2E+01	1.3E-02	1.3E+02	6.5E-02

--- = None reported for this waste disposal region.

Table 23 (Continued)
Radionuclide Inventories for the Intruder Dose Assessment

Radionuclide	1988–2004 Pits		2005–2044 Pits		1988-2004 Shafts				2005–2044 Shafts	
					Waste in Upper 1.5 m		Waste Deeper than 1.5 m			
	Volume (m3)	Activity (Ci)	Volume (m3)	Activity (Ci)	Volume (m3)	Activity (Ci)	Volume (m3)	Activity (Ci)	Volume (m3)	Activity (Ci)
Nb-91	6.4E-02	5.6E-07	2.8E-01	2.5E-06	---	---	---	---	---	---
Nb-92	6.4E-02	3.4E-06	2.8E-01	1.5E-05	9.8E-03	3.4E-04	1.0E-01	3.7E-03	---	---
Nb-93m	3.1E+00	2.5E-05	3.9E+00	1.1E-04	---	---	---	---	---	---
Nb-94	1.0E+01	4.2E-02	2.2E+01	7.5E-02	---	---	---	---	---	---
Nd-144	6.4E-02	1.1E-08	2.8E-01	5.0E-08	---	---	---	---	---	---
Ni-59	1.0E+02	6.4E-03	3.6E+02	6.5E-03	3.5E-02	2.7E-02	3.6E+00	2.8E+00	1.6E+01	1.3E+01
Ni-63	2.8E+02	2.1E+00	7.0E+02	9.2E+00	1.8E+01	1.3E+02	3.0E+01	1.1E+03	2.1E+02	5.7E+03
Np-237	4.0E+02	3.4E-03	1.6E+03	1.2E-02	1.2E-02	3.3E-10	1.2E+00	3.4E-08	5.5E+00	1.5E-07
Os-194	4.5E-01	1.5E-07	2.0E+00	6.5E-07	---	---	---	---	---	---
Pa-231	1.5E+01	8.0E-05	3.5E+01	3.1E-04	1.1E-02	5.4E-10	1.2E+00	5.6E-08	5.2E+00	2.5E-07
Pb-210	1.4E+04	2.9E-01	4.5E+02	9.5E-01	1.3E-02	4.8E-10	1.2E+00	3.1E-08	5.2E+00	1.3E-07
Pm-145	3.1E+01	1.2E-01	6.0E+01	5.5E-01	---	---	---	---	---	---
Pu-236	6.4E-02	1.1E-09	2.8E-01	5.0E-09	---	---	---	---	---	---
Pu-238	3.2E+04	1.4E+01	4.9E+04	4.3E+01	2.9E+00	2.1E-02	3.3E+01	2.4E-01	1.4E+01	1.1E-01
Pu-239	4.0E+04	1.5E+01	6.4E+04	4.9E+01	2.8E+00	5.9E-03	3.6E+01	6.5E-02	3.8E+01	2.6E-02
Pu-240	1.7E+04	5.0E-01	1.0E+04	1.5E+00	1.7E-02	1.3E-05	1.7E+00	1.3E-03	7.8E+00	6.0E-03
Pu-241	1.8E+03	2.8E+00	6.8E+03	1.1E+01	1.2E-02	4.0E-04	1.3E+00	4.1E-02	5.7E+00	1.9E-01

--- = None reported for this waste disposal region.

Table 23 (Continued)
Radionuclide Inventories for the Intruder Dose Assessment

Radionuclide	1988–2004 Pits		2005–2044 Pits		1988-2004 Shafts				2005–2044 Shafts	
					Waste in Upper 1.5 m		Waste Deeper than 1.5 m			
	Volume (m3)	Activity (Ci)	Volume (m3)	Activity (Ci)	Volume (m3)	Activity (Ci)	Volume (m3)	Activity (Ci)	Volume (m3)	Activity (Ci)
Pu-242	1.6E+03	2.5E-03	6.1E+03	1.0E-02	2.0E-05	1.1E-11	2.1E-03	1.1E-09	9.5E-03	5.0E-09
Pu-244	7.0E+00	3.9E-06	3.1E+01	1.8E-05	---	---	---	---	---	---
PU52	1.4E+03	5.1E+00	---	---	3.6E-02	5.0E-03	3.8E-01	5.2E-02	---	---
Ra-226	4.2E+02	3.9E-02	1.1E+03	5.8E-02	2.3E-02	5.6E-02	1.7E+00	8.1E-01	7.3E+00	3.8E+00
Ra-228	1.4E+04	2.4E-02	1.1E+02	3.8E-04	---	---	---	---	---	---
Si-32	7.4E-01	1.4E-05	3.0E+00	6.1E-05	---	---	---	---	---	---
Sm-151	2.3E+01	7.0E-09	1.7E+02	1.8E-07	---	---	---	---	---	---
Sn-121m	2.0E+00	4.5E-07	8.0E+01	1.8E-05	---	---	---	---	---	---
Sn-126	2.0E+00	1.1E-07	8.0E+01	4.4E-06	---	---	---	---	---	---
Sr-90	2.8E+04	8.0E-01	3.2E+04	1.5E+00	2.5E-02	1.1E+00	8.9E-01	6.8E+01	3.2E+00	2.8E+02
Tb-157	6.2E+00	5.0E-08	2.8E+01	2.2E-07	---	---	---	---	---	---
Tc-97	1.5E+00	2.4E-06	5.1E+00	1.1E-05	---	---	---	---	---	---
Tc-99	5.7E+02	3.4E-01	1.1E+03	1.4E+00	5.8E-06	1.1E-10	6.0E-04	1.2E-08	2.7E-03	5.2E-08
Th-228	2.3E+02	2.2E-03	6.7E+02	4.1E-03	7.6E-02	2.5E-06	1.0E+00	2.8E-05	4.9E+00	1.3E-04
Th-229	4.5E+01	4.2E-04	1.4E+02	1.7E-03	3.3E-04	4.7E-09	3.5E-03	4.9E-08		
Th-230	1.6E+02	1.2E-03	5.0E+02	3.1E-03	5.8E-06	5.7E-11	6.0E-04	5.9E-09	2.7E-03	2.6E-08
Th-232	1.9E+03	4.9E-02	3.4E+03	7.6E-02	2.5E-01	1.2E-02	3.9E+00	1.9E-01	1.8E+01	8.9E-01

--- = None reported for this waste disposal region.

Table 23 (Continued)
Radionuclide Inventories for the Intruder Dose Assessment

Radionuclide	1988–2004 Pits		2005–2044 Pits		1988-2004 Shafts				2005–2044 Shafts	
					Waste in Upper 1.5 m		Waste Deeper than 1.5 m			
	Volume (m3)	Activity (Ci)	Volume (m3)	Activity (Ci)	Volume (m3)	Activity (Ci)	Volume (m3)	Activity (Ci)	Volume (m3)	Activity (Ci)
TH88	1.9E+00	3.7E-02	---	---	---	---	---	---	---	---
Ti-44	6.8E+01	7.8E-04	2.8E+02	3.5E-03	---	---	---	---	---	---
U(NAT)	---	---	---	---	6.2E-01	1.8E-01	---	---	---	---
U11	3.1E+00	8.7E-06	---	---	---	---	---	---	---	---
U-232	1.6E+01	8.8E-04	6.6E+01	2.9E-03	---	---	---	---	---	---
U-233	6.5E+01	1.3E-02	2.0E+02	4.8E-02	2.1E-04	6.3E-06	2.2E-02	6.5E-04	9.7E-02	2.9E-03
U-234	1.9E+04	1.2E+00	9.9E+03	6.8E+00	9.0E-02	8.6E-03	2.3E+00	1.1E-01	4.2E+01	4.0E+00
U-235	2.3E+04	8.7E-01	2.3E+04	3.9E-01	3.3E+00	4.9E-04	3.0E+01	5.4E-03	4.7E+01	1.8E-01
U-236	2.4E+02	3.8E-04	1.0E+03	5.6E-04	3.4E-06	4.1E-08	3.5E-04	4.2E-06	1.6E-03	1.9E-05
U-238	2.1E+04	1.2E+01	2.0E+04	1.6E+01	2.2E+00	3.2E-02	1.6E+01	6.4E-01	6.4E+01	9.8E+00
U38	2.7E+00	5.0E-02	---	---	---	---	---	---	---	---
U81	3.5E+01	3.6E-03	---	---	---	---	---	---	---	---
Zr-93	1.3E-01	2.2E-08	5.7E-01	1.0E-07	---	---	---	---	---	---

--- = None reported for this waste disposal region.

Shuman (2005) identified several sources of uncertainty that are associated with the estimated inventories. One source of uncertainty shared by all waste that has been, or will be, disposed of at MDA G is introduced by the measurement and estimation techniques used to characterize the waste. The accuracy of the activity measurements and estimation techniques is influenced by the radionuclides under consideration and the disposal period. The radionuclides under consideration affect characterization efforts because the types and energies of radiation they emit make measurement more or less difficult. Furthermore, some radionuclides have strict accountability requirements, which dictate that greater effort be expended to measure or estimate the activities associated with packages of waste. The time at which the waste was characterized and disposed of is also important as both detection equipment and efforts to more accurately characterize the material placed in the disposal facility have improved over the years.

Although the errors associated with the activities that are listed in LLW and TRU waste databases cannot be determined with a high degree of accuracy, some generalities can be drawn about the source of uncertainty. The information summarized below is based on discussions with LANL personnel experienced in radiation characterization procedures and measurement techniques (Myers, 2004). For this discussion, the radionuclides included in the MDA G inventory have been divided into a number of classes or groups. These classes include pure beta emitters such as C-14, Ni-63, Sr-90 and Tc-99; strong gamma emitters such as Co-60 and Cs-137; and alpha emitters such as isotopes of americium, plutonium, and uranium; and tritium.

The greatest uncertainties are expected to be associated with the measurement of the activities of the pure beta emitters. The low energy and penetrating power of beta radiation are such that detailed separation techniques must be performed before accurate assessments of the waste activity can be conducted; these techniques were seldom, if ever, performed at the Laboratory. As a result, the activities associated with these radionuclides are expected to be accurate to within an order of magnitude. Although the higher energy emissions associated with many gamma emitters should make accurate characterization an easier task, the level of accuracy for estimated activities of gamma waste disposed of prior to the 1990s is expected to be similar to that of the beta emitters. The magnitude of the errors associated with the gamma emitters decreased during the 1990s to the extent that errors currently range from ±25 to ±100 percent, depending upon the size and composition of the waste package. Small packages, low-density waste matrices, and relatively large amounts of nuclear material all contribute to low errors.

In general, greater effort has been expended on the characterization of waste contaminated with uranium and transuranics because of accountability issues. However, the concentrations of americium, plutonium, and uranium in the waste have a significant impact on the accuracy of the measured activities. Activities of these radionuclides have probably been overestimated in LLW because concentrations in this waste are low and the measurement techniques used did not have very low detection limits. For drums and boxes with detectable quantities of plutonium (i.e.,

about 0.5 g [0.02 oz] or more per package), errors of 20 to 30 percent are expected to apply to measurements conducted in the 1970s and 1980s. For measurements conducted in more recent years, errors of 10 to 20 percent are typical.

The ability to accurately measure quantities of uranium isotopes depends, in part, on the isotopic quantities in the waste package. Although U-235 may go undetected in drums when it is present in small quantities, generators are generally aware of drums that contain greater quantities of U-235 (e.g., 10 g [0.4 oz] or more) and measure the packages directly to determine the waste activity. Measurements of waste containing depleted uranium usually have errors of ±25 to ±100 percent, depending upon the size and composition of the package.

The error ranges discussed above for uranium and transuranics are generally applicable; however, exceptions do exist. For example, in some cases generators measured drums of TRU waste with neutron counters and used scaling factors to estimate isotopic distributions. These scaling factors were inappropriately applied to the waste in some situations, resulting in overestimates of the activities of some isotopes and underestimates of others. Am-241 activities have been underestimated by an order of magnitude or more in a small proportion of TRU waste drums because of the misapplication of scaling factors. As mentioned earlier, U-235 in drums containing small amounts of uranium may go undetected in a small proportion of the packages.

Tritium is pure beta emitter, but it is considered separately from the other beta emitters because of its generation pattern at the Laboratory. While the low-activity tritium waste is expected to have characterization uncertainties similar to those discussed for the pure beta emitters, the high-activity tritium waste receives greater scrutiny. Estimates of the activities associated with the high-activity waste disposed of prior to the 1990s are generally expected to fall within a factor of two of the actual inventories. Improvements since that time have reduced these errors such that activity estimates are expected to be accurate to within ±25 percent.

The information summarized above was used to develop inventory distributions that address the uncertainties introduced by the characterization procedures used to estimate waste activities. The listed inventories for beta emitters were assumed to have triangular distributions with minimum and maximum values that are 0.1 and 10 times the most likely values, where the most likely values are equal to the deterministic inventory estimates. This same distribution was assigned to gamma emitters in waste buried in pits and shafts that were active prior to 1990; a triangular distribution with minimum and maximum values that are 0.5 and 2 times the most likely values was used for gamma emitters disposed of in units that started receiving waste after 1989.

Triangular distributions also were used to describe the characterization uncertainties associated with the uranium and transuranic inventories. For uranium, minimum and maximum values that are 0.25 and 2 times the most likely values were adopted. Separate distributions were developed

for isotopes of americium and plutonium disposed of in units that received waste prior to 1990 and in those that became active after 1989. The minimum and maximum values of the distributions for waste placed in units active prior to this date were assigned values that are 70 and 130 percent of the most likely values. Waste disposed of in pits and shafts that became active after 1989 was assigned distributions with minimum and most likely values that are 80 and 120 percent of the most likely values. The most likely values of all of the distributions were set equal to the deterministic inventory estimates.

A triangular distribution was assigned to tritium waste disposed of in pits and shafts that were active prior to 1990; a separate distribution was adopted for tritiated waste placed in units that started receiving waste after 1989. The minimum and maximum values are 0.5 and 2 times the most likely values for the earlier waste. Minimum and maximum values that are 0.75 and 1.25 times the most likely values, respectively, were adopted for the later waste. These distributions were assigned to all tritium waste; no distinction was made between low- and high-activity waste. Although this approach ignores the higher uncertainty associated with the low-activity waste, more than 99 percent of the tritium activity included in the MDA G inventory is associated with the high-activity material. The most likely values of the tritium waste distributions were set equal to the deterministic inventory estimates.

The information required to develop distributions that describe the uncertainties associated with waste characterization was unavailable for several radionuclides, primarily alpha-emitting isotopes. All of these radionuclides were assigned triangular distributions with minimum and maximum values that are 0.1 and 10 times the most likely values. The most likely values for these radionuclides are the deterministic inventory estimates developed for the performance assessment and composite analysis (Shuman, 2005).

Table 24 summarizes the information that was used to describe the uncertainties in the radionuclide inventories arising from measurement or estimation errors. The factors by which the deterministic inventories were multiplied to estimate the minimum and maximum values of the triangular distributions are listed for each radionuclide included in the MDA G inventory. Separate factors are provided for waste placed in pits and shafts that were active prior to 1990 and for material placed in disposal units that began receiving waste after 1989. As discussed earlier, the most likely values of these distributions were set equal to the deterministic inventory estimates reported in Shuman (2005).

Another source of uncertainty associated with the inventory estimates is introduced by the extrapolation process that was used to estimate the pre-1971 pit inventories and the pit and shaft inventories for waste projected to require disposal from 2004 through 2044. An extrapolation approach was used for the pre-1971 pit inventories because there were insufficient data to directly estimate these values. The pre-1971 inventory was developed, in part, by extrapolating

Table 24
Measurement Uncertainty Factors Associated with MDA G Radionuclide-Specific Inventories

Radionuclide	Uncertainty Factor [a]	
	Waste Disposed of before 1990	Waste Disposed of after 1989
Ac-227	1.0E-01, 1.0E+01	1.0E-01, 1.0E+01
Ag-108m	1.0E-01, 1.0E+01	5.0E-01, 2.0E+00
Al-26	1.0E-01, 1.0E+01	5.0E-01, 2.0E+00
Am-241	7.0E-01, 1.3E+00	8.0E-01, 1.2E+00
Am-243	7.0E-01, 1.3E+00	8.0E-01, 1.2E+00
Ba-133	1.0E-01, 1.0E+01	5.0E-01, 2.0E+00
Be-10	1.0E-01, 1.0E+01	1.0E-01, 1.0E+01
Bi-207	1.0E-01, 1.0E+01	5.0E-01, 2.0E+00
Bk-247	1.0E-01, 1.0E+01	1.0E-01, 1.0E+01
C-14	1.0E-01, 1.0E+01	1.0E-01, 1.0E+01
Ca-41	1.0E-01, 1.0E+01	1.0E-01, 1.0E+01
Cf-249	1.0E-01, 1.0E+01	1.0E-01, 1.0E+01
Cf-251	1.0E-01, 1.0E+01	1.0E-01, 1.0E+01
Cf-252	1.0E-01, 1.0E+01	1.0E-01, 1.0E+01
Cl-36	1.0E-01, 1.0E+01	1.0E-01, 1.0E+01
Cm-243	1.0E-01, 1.0E+01	1.0E-01, 1.0E+01
Cm-244	1.0E-01, 1.0E+01	1.0E-01, 1.0E+01
Cm-245	1.0E-01, 1.0E+01	1.0E-01, 1.0E+01
Co-60	1.0E-01, 1.0E+01	5.0E-01, 2.0E+00
Cs-135	1.0E-01, 1.0E+01	1.0E-01, 1.0E+01
Cs-137	1.0E-01, 1.0E+01	5.0E-01, 2.0E+00
Eu-152	1.0E-01, 1.0E+01	5.0E-01, 2.0E+00
Eu-154	1.0E-01, 1.0E+01	5.0E-01, 2.0E+00
Gd-148	1.0E-01, 1.0E+01	1.0E-01, 1.0E+01
H-3	5.0E-01, 2.0E+00	7.5E-01, 1.3E+00
Ho-163	1.0E-01, 1.0E+01	1.0E-01, 1.0E+01
Ho-166m	1.0E-01, 1.0E+01	5.0E-01, 2.0E+00

[a] *The listed factors were multiplied by the deterministic estimates of the radionuclide-specific inventories to estimate minimum and maximum values of the triangular distributions used to describe the variability in the inventory estimates resulting from measurement errors.*

Table 24 (Continued)
Measurement Uncertainty Factors Associated with MDA G Radionuclide-Specific Inventories

Radionuclide	Uncertainty Factor [a]	
	Waste Disposed of before 1990	Waste Disposed of after 1989
I-129	1.0E-01, 1.0E+01	1.0E-01, 1.0E+01
K-40	1.0E-01, 1.0E+01	1.0E-01, 1.0E+01
Kr-85	1.0E-01, 1.0E+01	1.0E-01, 1.0E+01
Lu-176	1.0E-01, 1.0E+01	1.0E-01, 1.0E+01
Mo-93	1.0E-01, 1.0E+01	1.0E-01, 1.0E+01
Nb-91	1.0E-01, 1.0E+01	1.0E-01, 1.0E+01
Nb-92	1.0E-01, 1.0E+01	5.0E-01, 2.0E+00
Nb-93m	1.0E-01, 1.0E+01	1.0E-01, 1.0E+01
Nb-94	1.0E-01, 1.0E+01	5.0E-01, 2.0E+00
Ni-59	1.0E-01, 1.0E+01	1.0E-01, 1.0E+01
Ni-63	1.0E-01, 1.0E+01	1.0E-01, 1.0E+01
Np-237	1.0E-01, 1.0E+01	1.0E-01, 1.0E+01
Np-239	1.0E-01, 1.0E+01	1.0E-01, 1.0E+01
Os-194	1.0E-01, 1.0E+01	1.0E-01, 1.0E+01
Pa-231	1.0E-01, 1.0E+01	1.0E-01, 1.0E+01
Pb-210	1.0E-01, 1.0E+01	1.0E-01, 1.0E+01
Pm-145	1.0E-01, 1.0E+01	1.0E-01, 1.0E+01
Pu-236	7.0E-01, 1.3E+00	8.0E-01, 1.2E+00
Pu-238	7.0E-01, 1.3E+00	8.0E-01, 1.2E+00
Pu-239	7.0E-01, 1.3E+00	8.0E-01, 1.2E+00
Pu-240	7.0E-01, 1.3E+00	8.0E-01, 1.2E+00
Pu-241	1.0E-01, 1.0E+01	1.0E-01, 1.0E+01
Pu-242	7.0E-01, 1.3E+00	8.0E-01, 1.2E+00
Pu-244	7.0E-01, 1.3E+00	8.0E-01, 1.2E+00
Ra-226	1.0E-01, 1.0E+01	1.0E-01, 1.0E+01
Ra-228	1.0E-01, 1.0E+01	1.0E-01, 1.0E+01
Si-32	1.0E-01, 1.0E+01	1.0E-01, 1.0E+01
Sm-151	1.0E-01, 1.0E+01	1.0E-01, 1.0E+01

[a] *The listed factors were multiplied by the deterministic estimates of the radionuclide-specific inventories to estimate minimum and maximum values of the triangular distributions used to describe the variability in the inventory estimates resulting from measurement errors.*

Table 24 (Continued)
Measurement Uncertainty Factors Associated with MDA G Radionuclide-Specific Inventories

Radionuclide	Uncertainty Factor [a]	
	Waste Disposed of before 1990	Waste Disposed of after 1989
Sn-121m	1.0E-01, 1.0E+01	1.0E-01, 1.0E+01
Sn-126	1.0E-01, 1.0E+01	1.0E-01, 1.0E+01
Sr-90	1.0E-01, 1.0E+01	1.0E-01, 1.0E+01
Tb-157	1.0E-01, 1.0E+01	1.0E-01, 1.0E+01
Tc-97	1.0E-01, 1.0E+01	1.0E-01, 1.0E+01
Tc-99	1.0E-01, 1.0E+01	1.0E-01, 1.0E+01
Th-227	1.0E-01, 1.0E+01	1.0E-01, 1.0E+01
Th-228	1.0E-01, 1.0E+01	1.0E-01, 1.0E+01
Th-229	1.0E-01, 1.0E+01	1.0E-01, 1.0E+01
Th-230	1.0E-01, 1.0E+01	1.0E-01, 1.0E+01
Th-232	1.0E-01, 1.0E+01	1.0E-01, 1.0E+01
Ti-44	1.0E-01, 1.0E+01	1.0E-01, 1.0E+01
U-232	2.5E-01, 2.0E+00	2.5E-01, 2.0E+00
U-233	2.5E-01, 2.0E+00	2.5E-01, 2.0E+00
U-234	2.5E-01, 2.0E+00	2.5E-01, 2.0E+00
U-235	2.5E-01, 2.0E+00	2.5E-01, 2.0E+00
U-236	2.5E-01, 2.0E+00	2.5E-01, 2.0E+00
U-238	2.5E-01, 2.0E+00	2.5E-01, 2.0E+00
Zr-93	1.0E-01, 1.0E+01	1.0E-01, 1.0E+01

[a] *The listed factors were multiplied by the deterministic estimates of the radionuclide-specific inventories to estimate minimum and maximum values of the triangular distributions used to describe the variability in the inventory estimates resulting from measurement errors.*

waste data from 1971 through 1977 back to the earlier period. For the future inventory, extrapolation was the only viable option. The future inventory was estimated on the basis of waste disposal data for 1996 through 2003.

The use of the extrapolation approach implicitly assumes that the composition of pre-1971 and future waste is similar to that of the waste disposed of during the periods from which the extrapolation datasets were drawn. In fact, the waste disposed of during these different time periods is expected to differ in ways that introduce errors into the inventory estimates. Pollard and Shuman (1999) found that the extrapolation approach used to establish the pre-1971 pit inventory yielded values for some radionuclides and waste streams similar to those estimated using available historic data, but projected other inventory values that were much greater than those estimated using the historic disposal data. In terms of future waste, several sources of uncertainty could compromise the estimated pit and shaft inventories.

No attempt was made to quantify the uncertainties introduced by the extrapolation approach. Although the extrapolated quantities of pre-1971 waste are significantly greater than those indicated by the available disposal data, it is unclear if the disposal data address all of the waste that was placed at MDA G during this period. Therefore, the assignment of any distributions to describe this uncertainty would be arbitrary at best. Only time will tell if it is appropriate to use the extrapolation process to estimate future inventories; differences between projected and actual inventories will be monitored through the disposal receipt reviews that are conducted annually under the MDA G Performance Assessment and Composite Analysis Maintenance Program (Shuman et al., 2003).

Significant quantities of waste disposed of at MDA G contain activation and fission product waste. As mentioned, prior to the mid-1990s, the radionuclides in these packages were often listed in terms of total activities of MAP and MFP. One step of the inventory development effort was to allocate these activities to specific radionuclides so they could be considered in the performance assessment and composite analysis modeling.

The MFP waste was allocated to specific radionuclides using fission yield data published by England and Rider (1994). The estimated activities are subject to several sources of uncertainty, the most important of which include the nature of the fission reactions that generated the fission products and the age of the MFP waste at the time of disposal. In terms of the reactions responsible for the waste, it is evident that Pu-239 and U-235 fission are the primary reactions that led to the generation of the MFP waste. However, it is unclear what proportion of the waste was generated by Pu-239 fission as opposed to reactions involving U-235, and what proportion of the waste was the result of interactions with thermal (versus fast) neutrons.

Historical reviews of LANL reactor operations (e.g., Bunker, 1983; Widner et al., 2004) indicate that most reactors in operation prior to the 1990s were fueled by enriched uranium. This supports the conclusion that most fission products were the result of neutron interactions with U-235. Nevertheless, the presence of plutonium fission products is also expected. During the time MFP waste was accepted at MDA G, one reactor in operation used molten plutonium as a fuel. Furthermore, plutonium fission products will occur in the waste from the uranium-based reactors as a result of interactions between fast neutrons and U-238. These plutonium fissions may represent a significant proportion of the total fission events; in commercial reactors they may account for one-third or more of the total fission events during the latter stages of operation.

It is not possible to provide a definitive assessment of the proportion of the MFP waste that was generated as a result of Pu-239 and U-235 fission events without more information. For the deterministic analysis, it was assumed that 15 percent of the waste was generated by Pu-239 fissions, with the remainder from U-235 fissions. All fission events were assumed to result from interactions with thermal neutrons. While some fission products will result from interactions with fast neutrons, the majority of the waste will be generated by thermal fission. The proportion of waste generated by plutonium fission events was assigned a triangular distribution with minimum, most likely, and maximum values equal to 0, 0.15, and 0.30, respectively.

The majority of the radionuclides generated by the fission process are very short-lived, with half-lives ranging from a few minutes to a few days. As a result, the radionuclides present in the MFP waste at the time of disposal will be significantly influenced by the amount of elapsed time between the fission events that generated the waste and the disposal of the waste at MDA G. Although the age of the waste at the time of disposal is expected to vary, the information needed to quantify this parameter for the material placed at MDA G is unavailable. It was assumed for the deterministic modeling that all MFP waste was 2 years old at the time of disposal. For the probabilistic modeling, the waste assumed integer ages of 1 to 10 years with a most likely age of 2 years; a triangular distribution was used to represent this variability.

The fission yield data used to allocate the 1- to 10-year-old MFP waste to specific radionuclides are summarized in Tables 25 and 26. The activity fractions shown in these tables represent the proportions of the total MFP waste activity attributable to the listed radionuclides following thermal fission of U-235 and Pu-239. These fractions were calculated by multiplying the fission yields found in England and Rider (1994) by the radionuclide decay constants, and normalizing these activities by the total MFP activity. Only those radionuclides with activity fractions of 1.0×10^{-6} or more are included in these tables.

Table 25
Radionuclide Activity Fractions for 1- to 5-Year-Old Mixed Fission Product Waste Generated by Thermal Fission of U-235 and Pu-239

	Waste Age = 1 yr		Waste Age = 2 yr		Waste Age = 3 yr		Waste Age = 4 yr		Waste Age = 5 yr	
Radionuclide	U-235	Pu-239	U-235	Pu-239	U-235	Pu-239	U-235	Pu-239	U-235	Pu-239
Cd-115m	3.9E-06	---	---	---	---	---	---	---	---	---
Ce-141	---	4.0E-06	---	---	---	---	---	---	---	---
Ce-144	4.5E-01	2.3E-01	5.3E-01	1.9E-01	3.3E-01	1.4E-01	1.7E-01	9.0E-02	8.3E-02	5.2E-02
Cs-137	4.9E-02	7.3E-02	1.3E-01	1.4E-01	2.0E-01	2.5E-01	2.5E-01	3.8E-01	2.8E-01	5.2E-01
Eu-154	---	1.1E-05	1.3E-06	2.1E-05	1.9E-06	3.4E-05	2.3E-06	5.0E-05	2.4E-06	6.4E-05
Eu-155	1.2E-05	1.3E-04	2.9E-05	2.3E-04	3.8E-05	3.5E-04	4.3E-05	4.8E-04	4.2E-05	5.8E-04
Kr-85	5.6E-02	3.3E-03	1.5E-01	6.2E-03	2.1E-01	1.0E-02	2.5E-01	1.5E-02	2.7E-01	2.0E-02
Nb-95	2.0E-05	1.6E-05	---	---	---	---	---	---	---	---
Pm-147	---	---	---	1.1E-06		1.5E-06	---	1.8E-06	---	2.0E-06
Ru-103	8.7E-06	7.0E-05	---	---	---	---	---	---	---	---
Ru-106	1.1E-05	6.1E-01	1.6E-05	6.2E-01	1.2E-05	5.6E-01	8.1E-06	4.4E-01	4.7E-06	3.1E-01
Sb-124	1.7E-05	1.7E-05	---	---	---	---	---	---	---	---
Sb-125	1.9E-04	7.0E-04	4.2E-04	1.1E-03	5.0E-04	1.5E-03	5.0E-04	1.8E-03	4.5E-04	2.0E-03
Sm-151	---	1.6E-06	---	3.2E-06	---	5.6E-06	---	8.8E-06	---	1.2E-05
Sn-119m	1.5E-06	7.3E-06	1.8E-06	6.2E-06	1.1E-06	4.6E-06	---	3.1E-06	---	1.8E-06
Sn-121m	1.6E-05	4.6E-05	4.3E-05	9.1E-05	6.5E-05	1.6E-04	8.2E-05	2.4E-04	9.3E-05	3.4E-04
Sn-123	8.0E-03	1.6E-02	3.2E-03	4.5E-03	6.9E-04	1.1E-03	1.2E-04	2.5E-04	2.0E-05	4.9E-05
Sn-126	4.8E-06	2.8E-06	1.4E-05	5.6E-06	2.1E-05	9.9E-06	2.7E-05	1.6E-05	3.1E-05	2.2E-05
Sr-89	2.1E-02	2.8E-03	4.0E-04	3.7E-05	4.1E-06	---	---	---	---	---

— = None

Table 25 (Continued)
Radionuclide Activity Fractions for 1- to 5-Year-Old Mixed Fission Product Waste Generated by Thermal Fission of U-235 and Pu-239

Radionuclide	Waste Age = 1 yr		Waste Age = 2 yr		Waste Age = 3 yr		Waste Age = 4 yr		Waste Age = 5 yr	
	U-235	Pu-239	U-235	Pu-239	U-235	Pu-239	U-235	Pu-239	U-235	Pu-239
Sr-90	6.3E-02	1.2E-02	1.7E-01	2.5E-02	2.6E-01	4.2E-02	3.2E-01	6.5E-02	3.6E-01	8.8E-02
Tb-160	---	3.6E-06	---	---	---	---	---	---	---	---
Te-127m	---	2.2E-06	---	---	---	---	---	---	---	---
Te-129m	2.0E-06	1.1E-05	---	---	---	---	---	---	---	---
Y-91	6.8E-04	7.7E-04	2.5E-05	2.1E-05	---	---	---	---	---	---
Zr-95	3.5E-01	5.2E-02	1.9E-02	2.0E-03	5.5E-04	6.8E-05	1.4E-05	2.1E-06	---	---

— = None

Table 26
Radionuclide Activity Fractions for 6- to 10-Year-Old Mixed Fission Product Waste Generated by Thermal Fission of U-235 and Pu-239

	Waste Age = 6 yr		Waste Age = 7 yr		Waste Age = 8 yr		Waste Age = 9 yr		Waste Age = 10 yr	
Radionuclide	U-235	Pu-239	U-235	Pu-239	U-235	Pu-239	U-235	Pu-239	U-235	Pu-239
Ce-144	3.7E-02	2.7E-02	1.6E-02	1.3E-02	6.9E-03	5.7E-03	3.0E-03	2.5E-03	5.4E-04	4.5E-04
Cs-137	3.0E-01	6.4E-01	3.1E-01	7.2E-01	3.2E-01	7.7E-01	3.2E-01	8.0E-01	3.3E-01	8.3E-01
Eu-154	2.4E-06	7.4E-05	2.4E-06	7.9E-05	2.3E-06	8.0E-05	2.2E-06	7.8E-05	2.0E-06	7.2E-05
Eu-155	4.0E-05	6.3E-04	3.7E-05	6.2E-04	3.3E-05	5.9E-04	3.0E-05	5.4E-04	2.4E-05	4.4E-04
Kr-85	2.8E-01	2.3E-02	2.8E-01	2.5E-02	2.7E-01	2.6E-02	2.6E-01	2.6E-02	2.5E-01	2.5E-02
Pm-147	---	1.9E-06	---	1.7E-06	---	1.4E-06	---	1.1E-06	---	---
Ru-106	2.6E-06	2.0E-01	1.4E-06	1.2E-01	---	6.5E-02	---	3.5E-02	0.0E+00	9.6E-03
Sb-125	3.8E-04	2.0E-03	3.1E-04	1.8E-03	2.5E-04	1.5E-03	2.1E-04	1.2E-03	1.3E-04	8.1E-04
Sm-151	---	1.5E-05	---	1.7E-05	---	1.9E-05	---	2.0E-05	1.0E-06	2.1E-05
Sn-121m	1.0E-04	4.1E-04	1.0E-04	4.7E-04	1.1E-04	5.1E-04	1.1E-04	5.3E-04	1.1E-04	5.5E-04
Sn-123	3.1E-06	8.6E-06	---	1.4E-06	---	---	---	---	---	---
Sn-126	3.3E-05	2.7E-05	3.5E-05	3.1E-05	3.7E-05	3.4E-05	3.8E-05	3.6E-05	4.1E-05	3.9E-05
Sr-90	3.8E-01	1.1E-01	4.0E-01	1.2E-01	4.0E-01	1.3E-01	4.1E-01	1.3E-01	4.2E-01	1.4E-01

— = None

— = None

Fission product waste may contain several hundred different radionuclides at the time of generation. Although most of these isotopes have very short half-lives and decay to negligible levels within a few days or weeks, some may give rise to daughter products that are longer-lived than their parents. These daughter products may contribute to estimated MFP waste activities well beyond the time of generation. The contributions of any such daughter products were ignored during the development of the MDA G inventory and were not evaluated quantitatively. Ignoring these radionuclides will underestimate the activities of any long-lived daughters that result from decay and will overestimate the activities of the radionuclides that were included in the final fission product allocations.

The MAP waste was allocated to specific radionuclides using information provided by a major generator of the waste. The Los Alamos Neutron Science Center (formerly the Los Alamos Meson Physics Facility) generates three major waste streams of activated waste including trash, beam-line inserts, and targets; the activity allocation factors adopted for the inventory update are based on a characterization of the trash from this facility. Although similar activated materials may occur in all three waste streams, it is unclear if the allocation factors developed for the trash accurately represent the targets and beam-line inserts.

Many of the radionuclides in the MAP waste are short-lived and will undergo significant decay between the time of generation and disposal. As with the MFP waste, the decay dynamics of the MAP waste will have a significant impact on the fractional abundances of radionuclides in the waste. Unfortunately, the ages of the waste at the time the allocation factors were developed and at the time it was disposed of at MDA G are unknown. Lacking this information, it was assumed these ages were the same. If this is not the case, the relative activities of the radionuclides found in the waste will be different. Without additional information, it is not possible to provide a quantitative evaluation of the uncertainties associated with the MAP waste inventory.

Several plutonium and uranium material types have been used in the past to describe the waste that has been disposed of at the Laboratory; these material types refer to specific radionuclide mixtures of plutonium and uranium isotopes. The MDA G inventory includes approximately 11,000 Ci of activity reported using these material types. More than 98 percent of this activity is represented by material types PU52, PU53, PU54, PU56, and PU83, which represent various mixtures of plutonium isotopes. Material types U10, U12, and D38 are important contributors to uranium isotopic inventories. Waste was assigned to these material types based on the mass fractional contents of Pu-238, Pu-240, and U-235; the ranges in mass fractional contents upon which assignments were made are shown in Table 27. The LANL LLW and TRU waste databases used to project the MDA G inventory have adopted point estimates of the mass fractional contents of these radionuclides and additional isotopes of plutonium and uranium for each material type. These mass fraction contents are listed in Table 28, along with the corresponding activity-based allocation factors.

Table 27
Material Type Mass Allocation Fractions for the Predominant Material Types Disposed of at MDA G

Material Type Code	Type	Description
PU52	Pu-239	4.0 to < 7.0 % Pu-240
PU53	Pu-239	7.0 to < 10.0 % Pu-240
PU54	Pu-239	10.0 to < 13.0 % Pu-240
PU56	Pu-239	16.0 to < 20.0 % Pu-240
PU83	Pu-238	Total
U10	U – depleted in U-235	Total U-238
U12	U – depleted in U-235	0.21 to 0.24 % U-235
U15[a]	U – depleted in U-235	0.28 to < 0.31 % U-235

[a] *Material types U-15 and D-38 have been used interchangeably in terms of radionuclide allocation fractions.*

Table 28
Point Estimates of the Mass and Activity Allocation Factors for the Predominant Material Types Disposed of at MDA G

Material Type	Radionuclides	Fractional Abundance	
		Mass Basis	Activity Basis
PU52	Pu-238	1.0E-04	6.1E-03
	Pu-239	9.4E-01	2.1E-01
	Pu-240	6.0E-02	4.9E-02
	Pu-241	2.0E-03	7.4E-01
	Pu-242	2.0E-04	2.8E-06
PU53	Pu-238	3.0E-04	1.1E-02
	Pu-239	9.1E-01	1.2E-01
	Pu-240	8.5E-02	4.2E-02
	Pu-241	3.7E-03	8.2E-01
	Pu-242	7.1E-04	6.1E-06
PU54	Pu-238	4.6E-04	8.5E-03
	Pu-239	8.7E-01	5.9E-02
	Pu-240	1.2E-01	2.8E-02
	Pu-241	8.1E-03	9.0E-01
	Pu-242	2.2E-03	9.4E-06
PU56	Pu-238	6.1E-04	8.0E-03
	Pu-239	8.2E-01	3.9E-02
	Pu-240	1.6E-01	2.9E-02
	Pu-241	1.2E-02	9.3E-01
	Pu-242	3.5E-03	1.1E-05
PU83	Pu-238	8.7E-01	9.9E-01
	Pu-239	1.2E-01	5.0E-04
	Pu-240	1.3E-02	1.9E-04
	Pu-241	1.7E-03	1.2E-02
	Pu-242	5.3E-04	1.4E-07
U10	U-238	1.0E+00	1.0E+00
U12	U-234	2.0E-05	2.7E-01
	U-235	2.3E-03	1.0E-02
	U-238	1.0E+00	7.2E-01
D38	U-234	2.3E-05	2.9E-01
	U-235	3.0E-03	1.3E-02
	U-238	1.0E+00	6.9E-01

Using the allocation factors listed in Table 28 ignores the fact that each material type may have a range of associated radionuclide contents and, therefore, introduces uncertainty into the inventory estimates. The potential errors that may result from the use of the allocation factors were evaluated for material types PU52, PU53, PU54, PU56, PU83, U12, and D38, all of which made important contributions to the inventories projected for plutonium and uranium isotopes. Uncertainty in the radionuclide allocations was not evaluated for material type U10 because all of the activity listed for this waste is assigned to a single radionuclide.

The data needed to definitively evaluate the radionuclide abundances for all of the major material types were unavailable. Consequently, a variety of approaches was used to estimate the variability inherent in the radionuclide allocation factors. Distributions of the radionuclide-specific mass contents of material type PU52 were estimated using spectral data collected with a high-purity germanium detector; material type PU52 accounts for about 70 percent of the total activity assigned to material types. For the remaining material types, information found in Taggart (1992), Wachter (1993a and 1993b), and an unattributed source was used to represent the uncertainty in the allocation factors.

The data used to characterize material type PU52 waste are summarized in Table 29. This table lists the mass fraction for the five plutonium isotopes comprising material type PU52 for 32 different waste packages. Using these data, triangular distributions were developed for the mass fractions of the isotopes comprising PU52; the minimum and maximum mass fractions were used to define the end points of these distributions and the median mass fractions were adopted as the most likely values. Pearson correlation coefficients were calculated and used to correlate the isotope-specific distributions to one another.

Two of the waste packages included in Table 29 have fractional contents of Pu-240 above the upper limit of approximately 7 percent that is used to define material type PU52. These results suggest that the generator(s) misidentified these waste packages. Nevertheless, the data for these waste packages were included in the characterization of the uncertainty associated with the material type definitions. This approach was adopted because it is reasonable to expect that similar errors have been made in the past, especially given the frequency with which PU52 was shipped to MDA G for disposal.

Spectroscopy data were unavailable for waste packages containing the other predominant plutonium material types. However, several estimates of the radionuclide-specific mass fractional contents were found for each material type. These estimates were used to develop linear regression equations that were subsequently employed to estimate the ranges of the mass-fractional contents for the plutonium isotopes in the waste. Regression equations were developed for material types PU53, PU54, and PU56 to estimate the mass fractional contents of Pu-238, Pu-241, and Pu-242 on the basis of the Pu-240 contents in the waste. These equations were used to estimate the mass fractions of Pu-238, Pu-241, and Pu-242 that correspond to the range of

Table 29
Spectroscopy Data for Material Type PU52

Waste Package Number	Mass Fraction				
	Pu-238	Pu-239	Pu-240	Pu-241	Pu-242
52555	1.4E-04	9.1E-01	8.4E-02	1.9E-03	6.0E-04
52884	1.4E-04	9.4E-01	5.7E-02	1.4E-03	3.9E-04
53237	1.6E-04	9.3E-01	6.3E-02	1.7E-03	5.2E-04
53907	1.8E-04	9.3E-01	6.4E-02	1.6E-03	5.4E-04
54370	1.1E-04	9.4E-01	5.6E-02	1.6E-03	3.4E-04
54481	9.5E-05	9.3E-01	6.5E-02	1.5E-03	4.9E-04
54518	4.5E-04	9.3E-01	6.2E-02	2.0E-03	8.2E-04
54658	2.1E-04	9.3E-01	6.4E-02	1.5E-03	5.6E-04
54689	1.2E-04	9.4E-01	5.9E-02	1.6E-03	4.1E-04
54690	1.4E-04	9.4E-01	5.8E-02	1.6E-03	4.0E-04
54694	1.4E-04	9.4E-01	5.8E-02	1.6E-03	4.9E-04
54697	1.6E-04	9.4E-01	6.2E-02	1.6E-03	4.7E-04
54722	1.9E-04	9.4E-01	6.0E-02	1.9E-03	4.9E-04
55226	4.2E-04	9.2E-01	7.9E-02	1.6E-03	1.1E-03
55267	1.9E-04	9.4E-01	5.4E-02	1.6E-03	4.6E-04
55624	1.4E-04	9.4E-01	6.3E-02	1.6E-03	4.7E-04
56118	3.5E-04	9.4E-01	6.0E-02	1.6E-03	6.8E-04
56137	1.4E-03	9.4E-01	5.7E-02	1.7E-03	1.5E-03
56138	2.8E-04	9.3E-01	6.2E-02	1.5E-03	8.2E-04
57936	1.8E-04	9.3E-01	6.9E-02	1.5E-03	6.1E-04
57958	3.0E-04	9.4E-01	6.1E-02	1.6E-03	6.5E-04
57964	1.5E-04	9.4E-01	5.8E-02	1.4E-03	4.3E-03
57966	3.3E-04	9.4E-01	5.3E-02	1.7E-03	5.7E-04
57975	1.7E-04	9.4E-01	5.7E-02	1.6E-03	4.8E-04
57976	1.6E-04	9.4E-01	6.0E-02	1.6E-03	3.8E-04
58076	9.6E-05	9.4E-01	5.7E-02	1.5E-03	3.7E-04
58143	1.3E-04	9.4E-01	5.8E-02	1.6E-03	3.8E-04
58159	1.2E-04	9.4E-01	6.2E-02	1.6E-03	4.4E-04
58175	1.5E-04	9.4E-01	5.5E-02	1.9E-03	3.9E-04
60668	1.3E-04	9.4E-01	5.8E-02	1.1E-03	4.1E-04
60694	1.2E-04	9.4E-01	5.9E-02	1.7E-03	3.9E-04
61770	1.6E-04	9.5E-01	4.7E-02	1.0E-03	3.4E-04

Pu-240 contents postulated to occur in the waste (shown in Table 27). The predicted values were adopted as the minimum and maximum values of triangular distributions for the three plutonium isotopes; the most likely value was set equal to the mass fraction used in the disposal databases (shown in Table 28). The distribution for Pu-240 was defined using the end points and point estimate provided in Tables 27 and 28. Mass-fraction distributions were not explicitly defined for Pu-239; the material type content of this radionuclide was calculated by subtracting the sampled mass fractions of Pu-238, Pu-240, Pu-241, and Pu-242 from 1.0.

The radionuclide abundances for PU83 were estimated by the approach outlined above, using Pu-238 mass contents to predict the abundances of Pu-240, Pu-241, and Pu-242. Pu-238 mass fractions ranging from 80 to 90 percent were assumed for these calculations, consistent with the two enrichments listed by Wachter (1993a) and other estimates of mass content. The mass-fraction distribution for Pu-239 was estimated by taking the difference between 1.0 and the sum of the mass fractions for the other isotopes.

There were no direct measurements of radionuclide abundances in waste identified as U12 and D38. An attempt was made to establish distributions of U-234 and U-238 using the regression approach described for the plutonium material types. The results of this evaluation were ambiguous and, consequently, the distributions of the U-234 mass fractions for these material types were estimated visually. The end points of the triangular distributions were set to the approximate end points indicated by the available data; the midpoints of these distributions were set to the point estimates adopted for the LANL waste databases. The end points of the distributions of mass contents of U-235 in material types U12 and D38 were defined using the ranges provided in Table 29, with the most likely values being assigned the point estimates that were adopted for the databases. Mass-fraction distributions were not explicitly defined for U-238; the material type content of this radionuclide was calculated by subtracting the sampled mass fractions of U-234 and U-235 from 1.0.

Table 30 summarizes the distributions that were constructed to evaluate the impacts of the uncertainty associated with the material type allocation factors. Given the relative lack of data available to develop this information, these distributions must be considered approximate at best. To significantly improve upon these distributions, data similar to those compiled for the PU52 waste packages would need to be collected. This may be necessary if the errors introduced by uncertainties associated with material type definitions prove to have significant impacts on the exposures projected for the performance assessment and composite analysis.

Definitions were unavailable for several material types: these include material types GAMMA, GRALPH, GRBETA, PU41, U71, and TRU. As a result, waste assigned these material types was excluded from the inventory characterization. This is not expected to introduce significant error into the final inventory projections because the total activity associated with all of these material types is small, approximately 1.5 Ci.

Table 30
Distributions of Radionuclide Mass Allocation Factors for the Predominant Material Types Disposed of at MDA G

Material Type	Radionuclide [a]	Distribution [b]		
		Minimum	Most Likely	Maximum
PU52	Pu-238	9.5E-05	1.6E-04	1.4E-03
	Pu-240	4.7E-02	6.0E-02	8.4E-02
	Pu-241	1.0E-03	1.6E-03	2.0E-03
	Pu-242	3.4E-04	4.8E-04	4.3E-03
PU53	Pu-238	2.3E-04	3.0E-04	4.1E-04
	Pu-240	7.0E-02	8.5E-02	1.0E-01
	Pu-241	1.9E-01	3.7E-01	7.7E-01
	Pu-242	0.0E+00	7.1E-02	2.5E-01
PU54	Pu-238	1.5E-04	4.6E-04	8.9E-04
	Pu-240	1.0E-01	1.2E-01	1.3E-01
	Pu-241	4.1E-03	8.1E-03	1.7E-02
	Pu-242	0.0E+00	2.2E-03	7.1E-03
PU56	Pu-238	0.0E+00	6.1E-04	1.2E-03
	Pu-240	1.6E-01	1.7E-01	2.0E-01
	Pu-241	0.0E+00	1.0E-02	2.2E-02
	Pu-242	0.0E+00	3.5E-03	6.4E-03
PU83	Pu-238	8.0E-01	8.7E-01	9.0E-01
	Pu-240	7.7E-03	1.3E-02	2.3E-02
	Pu-241	7.5E-04	1.7E-03	3.8E-03
	Pu-242	4.7E-04	5.3E-04	7.1E-04
U12	U-234	1.0E-05	2.0E-05	2.0E-05
	U-235	2.1E-03	2.3E-03	2.4E-03
D38	U-234	2.0E-05	3.0E-05	4.0E-05
	U-235	2.8E-03	3.0E-03	3.1E-03

[a] The mass allocation factors for Pu-239 and U-238 were estimated as the difference between 1.0 and the sum of the mass allocation factors of the other radionuclides comprising the material type.

[b] Distribution designations are triangular with minimum, most likely, and maximum values.

The intruder analysis was conducted to estimate exposures associated with waste disposed of since September 27, 1988 and to establish radionuclide concentration limits for waste that will be disposed of in the Zone 4 expansion area. The modeling conducted to estimate intruder exposures evaluated the uncertainties associated with the waste inventories using the approach described above. The WAC were estimated using unit inventories for all radionuclides that were disposed of at MDA G in the past, except for those that were eliminated on the basis of half-life considerations. No uncertainty was assumed to be associated with these unit inventories.

5.5 Atmospheric Transport Parameters

Atmospheric transport parameters are used to estimate concentrations of airborne radionuclides at the various off-site exposure locations and above the inadvertent intruder's lot. The distributions assigned to these parameters are included in Table 14. The information used to develop these distributions is discussed below.

5.5.1 Dust Loading and Soil Disturbance Factor

Dust loading is a measure of the particulate concentration in air, and is used to estimate airborne radionuclide concentrations above the receptor locations for the atmospheric, all pathways, and intruder scenarios. Information from the literature was used to estimate a distribution for this parameter. Baes et al. (1984) cite values for dust loading at U.S. locations that range from 3.2 to 52.4 $\mu g/m^3$ (2.0×10^{-10} to 3.3×10^{-9} lb/ft^3); the data are lognormally distributed. A default value of 15.5 $\mu g/m^3$ (9.7×10^{-10}) was adopted by Baes et al. as the geometric mean for food-chain transport modeling analyses. The National Council on Radiation Protection and Measurements (NCRP, 1984) cites dust-loading values for various suburban locations in the U.S. that range from 9 to 79 $\mu g/m^3$ (5.6×10^{-10} to 4.9×10^{-9} lb/ft^3).

Other studies provide additional insight into the appropriate magnitude of dust loading. Measurements conducted at the Idaho National Engineering and Environmental Laboratory (INEEL, 1994) from 1983 through 1990 indicated an average dust loading of 25.4 $\mu g/m^3$ (1.58×10^{-9} lb/ft^3). A decision analysis performed for a contaminated site at the DOE Nevada Test Site (NTS, 1995) adopted a dust loading of 30 $\mu g/m^3$ (1.87×10^{-9} lb/ft^3), with a geometric standard deviation of 1.6. This distribution was considered to be representative for nonurban areas of the U.S. Higher rates of resuspension may result following disturbance of the site, such as that caused by people walking over the contaminated soils. The NTS study cites data that suggest air concentrations may be 1.1 to 2.6 times greater for disturbed sites than for those in areas unaffected by humans. For screening purposes, the NCRP adopted a dust loading of 80 $\mu g/m^3$ (5.0×10^{-9} lb/ft^3) for a residential scenario that includes small-scale gardening and a value of 150 $\mu g/m^3$ (9.36×10^{-9} lb/ft^3) for a construction scenario (NCRP, 1999). Finally,

Anspaugh et al. (1975) recommend a default of 100 $\mu g/m^3$ (6.24×10^{-9} lb/ft^3) in the absence of site-specific data.

A lognormal distribution was used to represent the variability of dust loading for the off-site and residential intruder exposure scenarios; this distribution was defined using a geometric mean and geometric standard deviation of 30 $\mu g/m^3$ (1.87×10^{-9} lb/ft^3) and 1.6; the geometric mean of this distribution was adopted as the point estimate. This distribution is identical to that adopted for the NTS decision analysis (NTS, 1995), and generally agrees with the other data cited. The soil disturbance factor was assigned a triangular distribution with minimum, most likely, and maximum values of 1.1, 2.0, and 3.0, also consistent with the NTS study. Deterministic modeling was conducted using the most likely value of this distribution.

A higher dust loading was adopted for the intruder that builds a house at MDA G to account for greater rates of resuspension that may occur during construction activities. Lacking specific information, it was assumed that the mean dust loading is 1.5 times that for the members of the public and residential intruders, or 45 $\mu g/m^3$ (2.81×10^{-9} lb/ft^3). The geometric standard deviation and distribution of soil disturbance factors were the same as those adopted for the residential intruder.

5.5.2 *Vertical Flux*

The vertical flux, which specifies the rate at which particulates are suspended from the surface of the disposal site, is used to define the source term for the All Pathways – Atmospheric Scenario. The vertical flux decreases with height above the site because heavier soil particles fall back to the surface due to gravity. Vertical fluxes measured 1 to 3 m (3.3 to 9.8 ft) above the surface are typically used to estimate fluxes for the smaller particulates that are susceptible to long-distance transport with the prevailing winds.

A vertical flux of 0.05 $kg/m^2/yr$ (0.01 $lb/ft^2/yr$) was adopted for the 1997 MDA G performance assessment and composite analysis; this value was based on work performed by Radian (1995), which assumed that particulates are dislodged and made available for resuspension as a result of site disturbance. Specifically, it was assumed that a vehicle would be driven over the entire site once a year, on average. The estimated resuspension rate assumed that 50 percent of the site was covered by nonerodible surfaces including plants, uncontaminated roads, and buildings. Further reflection on the Radian study concluded that the assumptions upon which this vertical flux is based are not valid for the postclosure configuration of MDA G, leading to possibly inaccurate estimates of the resuspension potential.

Following closure of MDA G, the disposal site is expected to transition from a grassland ecosystem to a piñon-juniper woodland ecosystem. Rates of particulate resuspension at the site

will vary during this transitional period. To estimate rates of resuspension during the time when the site will be primarily grassland, several sources of information were consulted. The first was a study conducted under the MDA G Performance Assessment and Composite Analysis Maintenance Program in which vertical fluxes were estimated at MDA J (Whicker and Breshears, 2005). This facility, which is located about 2 km (1.2 mi) to the west of MDA G on Mesita del Buey, was used for the disposal of classified material. In 2002, a final cover was applied over MDA J and the area was seeded with a mixture of native grasses. The MDA J cover is expected to resemble the conditions at MDA G shortly after final closure of the facility.

Whicker and Breshears (2005) placed total suspended particulate samplers at heights of 1 and 3 m (3.3 and 9.8 ft) above MDA J. Sampling conducted over a period of 5½ months was used, in conjunction with wind and friction velocity measurements, to estimate vertical fluxes of particulates. The vertical flux approximately 2 m (6.6 ft) above the ground surface averaged 0.0017 $kg/m^2/yr$ (3.4×10^{-4} $lb/ft^2/yr$) over the 5½-month sampling period. Fluxes ranged from -0.013 to 0.015 $kg/m^2/yr$ (-0.0027 $lb/ft^2/yr$ to 0.0031 $lb/ft^2/yr$), where negative values indicate a net downward deposition (i.e., into the sampling area). The median flux of 0 $kg/m^2/yr$ indicates little, if any, net loss of soil from the area.

The vertical fluxes estimated by Whicker and Breshears (2005) may be compared to other measurements conducted in semiarid locations in the western U.S. Breshears et al. (2003) conducted vertical flux measurements over 6-to-8-month periods at several locations: a grassland adjacent to the Rocky Flats Environmental Technology site near Denver, Colorado; a shrubland near Carlsbad, New Mexico; and a forest dominated by ponderosa pine along the western edge of the Laboratory. The median vertical fluxes approximately 2 m (6.6 ft) above the ground were 0.0083, 0.015, and 0.0091 $kg/m^2/yr$ (0.0017, 0.0031, and 0.0019 $lb/ft^2/yr$) for the grassland, shrubland, and forest sites, respectively. Fluxes ranged from -0.0059 to 0.038 $kg/m^2/yr$ (-0.0012 to 7.8×10^{-4} $lb/ft^2/yr$) at the grassland site, -0.08 to 0.16 $kg/m^2/yr$ (-1.6×10^{-4} to 0.033 $lb/ft^2/yr$) within the shrubland, and -0.015 to 0.055 $kg/m^2/yr$ (-0.0031 to 0.011 $lb/ft^2/yr$) at the forest site (Whicker, 2005). The fluxes listed for the forested site were based on samplers located approximately 100 m (330 ft) from the forest canopy; vertical fluxes within the canopy would likely be smaller.

The vertical flux measurements summarized above represent the net movement of soil at the sample locations, taking into account material that is deposited on-site and soil particles that are removed from the site due to resuspension. Consequently, this information is not entirely appropriate for defining the rates at which contaminated particulates are resuspended from the surface of MDA G. To more accurately quantify contaminant resuspension rates it would be necessary to track the movement of soil from portions of the disposal facility that are

uncontaminated and to track the movements of contaminated particulates originating over the pits and shafts.

The detailed information needed to definitively quantify the rates at which contaminated particulates are suspended from the surface of MDA G is unavailable. In its absence, the data collected by Whicker and Breshears (2005) were used to estimate these resuspension rates in a manner that is expected to be reasonably conservative. Specifically, the resuspension rate was defined on the basis of the non-negative fluxes measured by the investigators, under the assumption that these fluxes represent the net removal of contaminated soils from the surface of the site. This subset of the Whicker and Breshears data indicates fluxes ranging from 0.0021 to 0.023 $kg/m^2/yr$ (4.3×10^{-4} to 0.0047 $lb/ft^2/yr$). A truncated normal distribution with a mean of 0.013 $kg/m^2/yr$ (0.0026 $lb/ft^2/yr$) and a standard deviation of 0.0084 $kg/m^2/yr$ (0.0017 $lb/ft^2/yr$) was adopted for the performance assessment and composite analysis; the mean of this distribution was used in the deterministic modeling.

The vertical flux distribution adopted for the performance assessment and composite analysis modeling represents the particulate flux at a height of 2 m (6.6 ft) above the ground surface. In contrast, the atmospheric transport modeling used a default ground-level flux. Because of uncertainties about the errors that might be introduced by applying the modeling results to the 2 m (6.6 ft) fluxes, the effects of release height on downwind concentrations were investigated. Using the CALPUFF air dispersion model (Scire et al., 2000a, 2000b), simulations were conducted in which unit fluxes (1 $g/m^2/s$ [0.024 $lb/ft^2/s$]) were assumed to occur at 2 m (6.6 ft) and ground level; simulations were conducted for releases from atmospheric source area 1 using 3 years of meteorological data (Jacobson, 2005). Dispersion factors were estimated for all cells of the atmospheric modeling domain; ratios of the factors estimated for the 2 m (6.6 ft) release height to those projected for the ground-level release results were calculated and used to compare the effects of release height on projected downwind impacts.

The release height ratios described above varied among cell locations within the atmospheric transport modeling domain and among the 3 years of meteorological data. For cells not located within the MDA G boundary and atmospheric source areas, which represent about 93 percent of the total cells, the ratios ranged from 0.38 to 1.1. An average of the ratios for each cell over the 3 years yielded values that ranged from 0.38 to 0.97. Excluding several cells located just outside the boundary narrowed the range of average ratios to 0.69 to 0.97; more than 99 percent of these cells had average ratios of 0.84 and above. The calculated ratios for cells within the MDA G boundary or atmospheric source areas were more variable, ranging from 0.18 to 0.99 across all locations; the flux ratios ranged from 0.42 to 0.92 when averaged over the 3 years of meteorological data.

The results summarized above indicate that treating a 2 m (6.6 ft) vertical flux as if it was a ground-level release will typically result in an overestimation of downwind air concentrations by 3 to 16 percent. Greater differences are noted at cells within or next to the fence line, probably because these are points of release (or are immediately adjacent to such) and deposition. Even at these locations, however, treating the 2 m (6.6 ft) vertical flux as a ground-level release will result in higher-than-expected downwind air concentrations. This, in combination with the fact that differences in air concentrations due to variations in release height are small for most of the receptor locations, led to the decision to treat the 2 m (6.6 ft) vertical fluxes as ground-level fluxes without any further adjustment to the flux data.

5.5.3 Enhancement Factor

The vertical flux measurements discussed above apply to the suspendable fraction of the soil, which generally includes particles with a median diameter of about 10 μm (3.9×10^{-4} in.) or less. In contrast, soil concentrations estimated using the GoldSim models are based on the total soil, including the suspendable fraction and much larger particle sizes. Because soil radionuclide concentrations are often a function of particle size, it is necessary to modify the vertical fluxes before they are used in the GoldSim models. This is done by multiplying the vertical fluxes by the enhancement factor, or enrichment ratio, which is the ratio of radionuclide concentrations in the suspendable fraction to the concentrations in the total soil.

The enhancement factor is a complex function of many parameters, including the degree of soil disturbance, the soil texture, the site vegetation, and the radionuclides under consideration. In their plutonium resuspension studies at the Marshall Islands, Shinn et al. (1997) observed enhancement factors ranging from 0.41 in a coconut grove to 3.1 for a disturbed, bare soil. Factors less than 1 were normal for undisturbed soils, while an enhancement factor of 2.5 was estimated for a road with traffic. Shinn (1992) reported enhancement factors of 0.87 and 1.04 for Pu-239 at two NTS sites that were characterized by desert pavement and 5 to 20 percent plant cover. In the same publication, factors ranging from 0.21 to 0.79 were reported for bare cultivated fields in South Carolina and California. Disturbances such as traffic, bulldozer blading, wildfire, and freeze-thaw cycling caused enhancement factors to increase by a factor of 2.2 to 6.5. At Palomares in Spain, Shinn (2002) estimated an enhancement factor of 0.3 for undisturbed soils that had been contaminated by plutonium following a mid-air collision of U.S. military aircraft in 1966. The median aerodynamic diameters of the particles considered in these studies generally ranged from 2 to 6 μm (7.9×10^{-5} to 2.4×10^{-4} in.).

Cooper et al. (1994) reported enhancement factors for americium and plutonium as part of an investigation conducted at a former nuclear weapons testing site in Maralinga, Australia. Particle size and activity distribution data were used to estimate enhancement factors for the soil fraction that was less than 45 μm (0.0018 in.) and for the inhalable fraction, which was defined as the

portion of the soil with aerodynamic diameters of 7 μm (0.0028 in.) or less. Enhancement factors ranged from 3.4 to 22.2 for the less-than-45 μm (0.0018 in.) fraction, and from 1.1 to 10.8 for the inhalable fraction. The same investigators also estimated enhancement factors for the inhalable soil fraction on the basis of artificial resuspension studies. The factors from these studies ranged from 0.3 to 32.5. Cooper et al. recommended an enhancement factor of 6 for the inhalable fraction of the soil based on the results of the field measurements and other resuspension studies.

Van Pelt and Zobeck (2005) sampled and analyzed soils, sediments in transport over eroding fields, and attic dust from a small area in the southern high plains of Texas. The results of this effort were used to estimate enrichment ratios for 13 plant nutrients and approximately 30 other trace elements. In general, enrichment ratios were less than 1 within an area characterized by 0.3 m (1 ft) high ridges that were designed to trap sediments moving as a result of creep or saltation; ratios generally ranged from 1 to 4 within a windbreak of Arizona cypress that was surrounded by a stable mowed grass surface. The investigators estimated enrichment factors for different particle-size classes of soil and for suspended sediments collected at heights of up to 1 m (3.3 ft) above the ground surface. Average enrichment ratios ranged from about 0.5 for soil particle diameters greater than 250 μm (0.0098 in.) to about 3.5 for particles with diameters less than 53 μm (0.0021 in.). The average enrichment factors for suspended sediments ranged from slightly more than 1 for collection heights of 0.2 m (0.7 ft) or less to approximately 2 for a collection height of 1 m (3.3 ft). Finally, enrichment ratios for different particle-size classes of attic dust ranged from about 2 for particle diameters greater than 53 μm (0.0021 in.) to slightly more than 6 for particles with diameters of 10 μm or less (3.9×10^{-4} in.).

It is evident from the work conducted by Cooper et al. (1994) and Van Pelt and Zobeck (2005) that the enhancement factor (or enrichment ratio) is strongly dependent upon the particle-size class under consideration. As discussed earlier, the median diameter of the suspendable soil fraction is generally expected to be on the order of 10 μm (3.9×10^{-4} in.) or less. The data reported by Cooper et al. and by Van Pelt and Zobeck for attic dust suggest average enhancement factors on the order of 6 for the smaller particles within this size fraction. Enhancement factors for slightly larger particles would appear to range from 3 to 4 based on the soil and attic dust data collected by Van Pelt and Zobeck.

The enhancement factors reported by Cooper et al. (1994) and Van Pelt and Zobeck (2005) are significantly higher than the values reported by Shinn (1992 and 2002) and Shinn et al. (1997). In most cases, the values reported by Shinn and Shinn et al. are less than 1; only the enhancement factors reported for disturbed conditions approach the Cooper et al. and Van Pelt and Zobeck values. On the basis of these variations in reported values, a triangular distribution with minimum, most likely, and maximum values of 1, 3, and 6 was used to represent the enhancement factor. All radionuclides were assigned the same enhancement factor. This

distribution is consistent with the data presented by Van Pelt and Zobeck for soils and for the majority of the trace elements in smaller particle size classes of attic dust. It generally overestimates the factors reported by Shinn and Shinn et al. for undisturbed conditions, but does not capture some of the more extreme values reported by the others. The most likely value of the distribution was used for the deterministic modeling.

5.5.4 Dispersion Factor and Deposition Rate

The dispersion factor is defined here as the ratio of the radionuclide concentration in air at a specified location to the rate of contaminant release from the disposal site. It is used in the performance assessment and composite analysis to estimate atmospheric radionuclide concentrations downwind of MDA G. The deposition rate specifies the rate at which airborne radionuclides are deposited at locations downwind of the disposal site; it is used to estimate radionuclide concentrations in plants and soil at the receptor locations. Both parameters are a function of meteorological conditions and features of the landscape.

Complex terrain atmospheric transport modeling was conducted using the CALPUFF modeling system to estimate the dispersion factors and deposition rates that were used in the performance assessment and composite analysis (Jacobson, 2005). To conduct this modeling, a 7.4 km^2 (2.8 mi^2) modeling domain was established that included the disposal site and surrounding lands. This domain was divided into 8,100 30-m^2 (320-ft^2) cells. Releases of radionuclides to the air above the site were modeled for three atmospheric source areas; these areas are shown in Figure 6 and discussed in Section 2.2. The modeling projected air concentrations and rates of deposition as a function of time for contaminants originating in each source area, at all cells or exposure locations within the domain. A complete description of the modeling effort is provided in Jacobson (2005).

The dispersion factors and deposition rates adopted for the performance assessment and composite analysis are those associated with the points of maximum exposure outside of the DOE-controlled boundary. During the 100-year active institutional control period, this is assumed to be the Laboratory boundary; however, once the passive institutional control period begins, this boundary is assumed to coincide with the MDA G fence line. The locations where maximum exposures occur outside of these boundaries will depend upon the rates at which radionuclides become airborne across the disposal facility, the dispersion patterns to which these releases are subject, and the contaminant-specific risks represented by the various isotopes.

The points of maximum exposure were identified using a screening process. A location screening value was calculated for each cell of the modeling domain as follows:

$$LSV_x = \sum_{i=1}^{3}\left[\frac{\chi}{Q_{i,x}} \times DSF_i\right] \qquad 75$$

Where

LSV_x = location screening value for grid location x

$\frac{\chi}{Q_{i,x}}$ = air dispersion factor for source area i at grid location x (s/m^3)

DSF_i = dose screening factor for source area i (mrem-m^3/yr)

In this equation, three dispersion factors for a given cell (one factor for each of the three source areas) are multiplied by the corresponding dose screening factors and the results are summed to yield an overall screening value for the cell under consideration. The dose screening factor is given by the following expression:

$$DSF_i = \sum_{j=1}^{n}\left[DCF_{inh,j} \times A_{j,i}\right] \qquad 76$$

Where

$DCF_{inh,j}$ = inhalation dose conversion factor for radionuclide j (mrem/yr per Ci/m^3)

$A_{j,i}$ = inventory of radionuclide j in source area i (Ci)

In the screening approach outlined above, effects of dispersion on exposure are accounted for using the air dispersion factor. The dispersion factors used in the screening were average values based on CALPUFF model runs using 10 years of meteorological data. The dose screening factor accounts for differences in radionuclide inventories among the three source areas and the inhalation risk posed by each contaminant. The use of this factor implicitly assumes that releases of radionuclides to the air above the site are not isotope-specific.

Location screening values were calculated using Equations 75 and 76 for all grid or exposure locations outside the Laboratory boundary and locations outside the MDA G fence line. Separate calculations were conducted for the two land uses considered in the atmospheric modeling; rangeland was used to represent the grassland-dominated site while forest was used to represent piñon-juniper woodland. For each land use, the location with the greatest screening value represents the point of maximum exposure. The dispersion factors and deposition rates for the identified points of maximum exposure were used to estimate doses for the Atmospheric Scenario.

Figure 18 shows the points of maximum exposure at or outside of the Laboratory boundary and the MDA fence line. Maximum exposure locations for particulate releases differ between the performance assessment and composite analysis, but these locations coincide for both analyses for the vapor- and gas-phase releases. For particulate releases, the points of maximum exposure outside of the LANL boundary lie to the north (performance assessment) and northeast (composite analysis) of the active portion of the disposal facility. The points of maximum exposure adjacent to the MDA G fence line occur north of the Zone 4 expansion area and slightly east of the active portion of the facility for the performance assessment and composite analysis, respectively. The location outside of the LANL boundary that yields the highest exposures to vapor- and gas-phase releases lies to the north of the active portion of the disposal facility; the location along the MDA G fence line is south of the facility boundary. The dispersion factors and deposition rates corresponding to the points of maximum exposure are included in Table 14; separate factors and rates are provided for the two land uses. The distributions shown are based on simulations conducted using 10 years of meteorological data.

As indicated above, Jacobson (2005) conducted two sets of CALPUFF simulations to examine the impacts of vegetation characteristics on atmospheric transport. The first of these assumed the disposal site and surrounding lands consisted of rangeland (grassland); the second assumed the region was forested (piñon-juniper woodland). The data for these two simulation sets were used as "end members" to estimate changes in atmospheric transport conditions as MDA G transitions from grassland to woodland, based on the simplifying assumption that this transition is linear. For example, dispersion factors and deposition rates halfway between those listed in Table 14 were assumed to apply when the site had achieved 50 percent of the transition from grassland to woodland.

5.6 Groundwater Transport Parameters

Groundwater transport parameters include the data used to model the release and transport of radionuclides to the regional aquifer. The results of the groundwater modeling are used to determine groundwater pathway doses and to estimate rates of contaminant depletion from surface soils due to leaching. The distributions assigned to these parameters are included in Table 14, the bases of these distributions are provided below.

5.6.1 MDA G Infiltration Rate

The rates at which radionuclides are leached from the waste and transported to the regional aquifer are a function of the mesa-top infiltration rate. Annual infiltration rates through the disposal site have been estimated through a variety of techniques. Newman et al. (2005) used chloride profiles to develop flux estimates through paved and unpaved portions of the disposal site. Newman and Schofield (2005) conducted numerous simulations of the near-surface water balance at MDA G, using the results to estimate rates of infiltration for the final cover proposed for the facility.

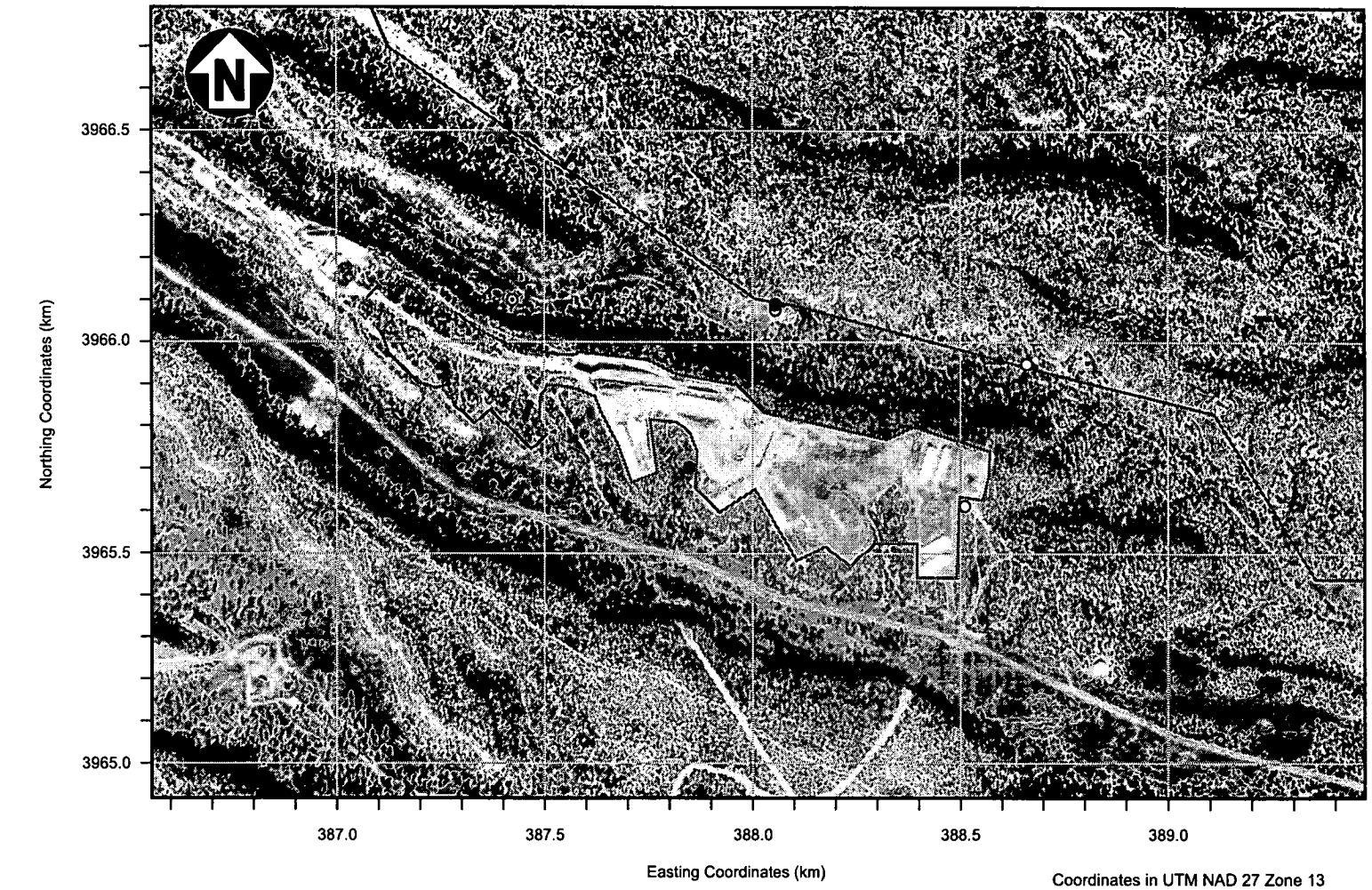

Figure 18
Points of Maximum Exposure for Releases from MDA G

Data developed by Newman et al. (2005) and Newman and Schofield (2005) were used to define the annual mesa-top infiltration rate distribution for the performance assessment and composite analysis modeling. The data upon which the distribution is based are summarized in Figure 13 of Newman and Schofield (2005) and reproduced below in Table 31. A lognormal distribution was defined using a geometric mean of 0.26 mm/yr (0.01 in./yr) and a geometric standard deviation of 4.

Table 31
Measured and Projected Flux Rates for MDA G

Data Source	Flux (cm/yr)	Notes
Chloride Profiles	0.001	Borehole P3
	0.01	Borehole IC2
	0.01	Borehole J2
	0.01	Borehole P1
	0.01	Borehole J3
	0.01	Borehole G1
	0.01	Borehole IC3
	0.02	Borehole G3
	0.02	Borehole IC1
	0.02	Borehole 17B
	0.02	Borehole J1
	0.03	Borehole IC4
	0.04	Borehole P2
	0.06	Borehole Pit2
	0.2	Borehole Pit17
	0.3	Borehole Pit24
	0.3	Borehole 7B
HYDRUS Simulations	0.003	1000 yr simulation; 1 m cover; 2 m profile thickness; -10 m initial pressure head; K_{sat} = 0.039 mm/hr
	0.0047	1000 yr simulation; 5 m cover; 6 m profile thickness; -10 m initial pressure head; K_{sat} = 0.039 mm/hr
	0.008	1000 yr simulation; 1 m cover; 2 m profile thickness; -10 m initial pressure head; root uptake assigned 50% of total evapotranspiration; K_{sat} = 0.028 mm/hr
	0.009	1000 yr simulation; 1 m cover; 6 m profile thickness; -10 m initial pressure head; K_{sat} = 0.039 mm/hr

Table 31 (Continued)
Measured and Projected Flux Rates for MDA G

Data Source	Flux (cm/yr)	Notes
HYDRUS Simulations (Continued)	0.012	1000 yr simulation; 1 m cover; 2 m profile thickness; -1 m initial pressure head; K_{sat} = 0.028 mm/hr
	0.012	1000 yr simulation; 1 m cover; 2 m profile thickness; -1 m initial pressure head; K_{sat} = 0.039 mm/hr
	0.018	1000 yr simulation; 5 m cover; 6 m profile thickness; -1 m initial pressure head; K_{sat} = 0.039 mm/hr
	0.05	9 yr simulation; 1 m cover; 2 m profile thickness; -10 m initial pressure head; K_{sat} = 0.039 mm/hr
	0.07	5 yr simulation; 1 m cover; 2 m profile thickness; -10 m initial pressure head; root uptake assigned 50% of total evapotranspiration; K_{sat} = 0.028 mm/hr
	0.07	5 yr simulation; 1 m cover; 2 m profile thickness; -10 m initial pressure head; K_{sat} = 0.028 mm/hr
	0.07	1000 yr simulation; 1 m cover; 6 m profile thickness; -10 m initial pressure head; K_{sat} = 0.039 mm/hr
	0.1	9 yr simulation; 1 m cover; 3 m profile thickness; -10 m initial pressure head; K_{sat} = 0.039 mm/hr
	0.13	1000 yr simulation; 1 m cover; 2 m profile thickness; -10 m initial pressure head; entire cover constructed of crushed tuff; K_{sat} = 0.028 mm/hr
	0.16	9 yr simulation; 1 m cover; 6 m profile thickness; -10 m initial pressure head; K_{sat} = 0.039 mm/hr
	0.19	5 yr simulation; 5 m cover; 15 m profile thickness; -10 m initial pressure head; K_{sat} = 0.039 mm/hr

Source: Newman et al. (2005); Newman and Schofield (2005).

The distribution discussed above represents the annual infiltration rate for MDA G; however, the groundwater flow and transport modeling conducted in support of the performance assessment and composite analysis requires the average annual infiltration rate over the simulation period. The annual infiltration rate distribution was sampled, with replacement, for each year in the simulation period and the mean of these values was calculated. This process was repeated 500 times to generate a distribution of infiltration rates that represents the mean annual infiltration rate over the simulation period; the resulting distribution was used in the probabilistic modeling. This evaluation yielded a normal distribution with a mean and standard deviation of 0.69 and 0.053 mm/yr, respectively.

5.6.2 Contaminant Capture Fraction

The contaminant capture fraction represents the portion of the contaminant plume intercepted by a hypothetical domestic well located downgradient of MDA G. Effectively, it determines the fraction of the groundwater contamination that contributes to the exposures projected for the receptors in the Groundwater Resource Protection and All Pathways – Groundwater Scenarios.

The contaminant capture fraction is dependent on the area over which radionuclides are discharged to the aquifer, the dispersion characteristics of the aquifer, and the pumping characteristics of the well. Capture fractions were estimated for waste disposal regions 1 through 5 and 8 for a range of transverse dispersivities and well pumping rates. A complete description of this modeling is provided in Stauffer et al. (2005).

The contaminant capture fractions for the different disposal regions, transverse dispersivities, and well pumping rates are summarized in Table 32. The listed values represent the fraction of the contaminant plume that is captured by the receptor's well for the specified pumping rate. The pumping rates generally encompass the range of water usage rates expected for the receptors included in the performance assessment and composite analysis modeling.

Capture fractions were not explicitly modeled for the disposal shafts in waste disposal regions 6 and 7. The former region includes shafts located near the east end of pit 6, which is located in disposal region 2; on this basis the capture fractions for regions 2 and 6 were assumed to be the same. The shafts in disposal region 7 are located among the pits over much of region 3. Therefore, the capture fractions for these shafts were assumed to be the same as those for the pits in disposal region 3.

The contaminant capture fractions are generally proportional to the north-south dimension of the disposal region. For example, the capture fractions for waste disposal region 2, the region with the smallest north-south dimension, tend to be greater than the fractions for the other regions. Within a disposal region, capture fractions tend to be inversely proportional to the transverse dispersivity, and proportional to the well pumping rate.

Contaminant capture fractions were estimated on a disposal-region-specific basis using the results summarized in Table 32. Because there were no data available to characterize the transverse dispersivity within the aquifer, it was decided to use the results for the no-dispersion case, which yields the highest capture fractions. For most of the disposal regions, the no-dispersion fractions are the same for all four pumping rates. The capture fraction for disposal region 8 increases by a factor of three as the pumping rate increases from 50 to 2,500 m^3/yr (1.3×10^4 to 6.6×10^5 gal/yr). Based on these results, the capture fractions corresponding to a well pumping rate of 2,500 m^3/yr (6.6×10^5 gal/yr) were adopted for the modeling; the variability inherent in these capture fractions was not considered in the probabilistic modeling.

Table 32
Contaminant Capture Fractions for the MDA G Waste Disposal Regions

Waste Disposal Region	Transverse Dispersivity (m)	Well Pumping Rate (m^3/yr)			
		50	600	1,200	2,500
1	0	4.1E-02	4.1E-02	4.1E-02	4.1E-02
	1	1.7E-03	9.9E-03	1.9E-02	3.1E-02
	2	1.5E-03	9.2E-03	1.5E-02	2.6E-02
	5	2.0E-03	5.3E-03	1.3E-02	2.0E-02
2	0	1.1E-01	1.1E-01	1.1E-01	1.1E-01
	1	6.7E-03	2.3E-02	3.9E-02	7.1E-02
	2	5.3E-03	8.6E-03	2.2E-02	4.7E-02
	5	7.3E-04	6.7E-03	1.2E-02	2.7E-02
3	0	3.6E-02	3.6E-02	3.6E-02	3.6E-02
	1	1.2E-03	5.4E-03	9.7E-03	2.4E-02
	2	3.1E-03	2.8E-03	6.8E-03	1.4E-02
	5	3.0E-04	4.1E-03	4.2E-03	7.7E-03
4	0	3.6E-02	3.6E-02	3.6E-02	3.6E-02
	1	5.6E-04	5.0E-03	5.9E-03	1.7E-02
	2	1.0E-08	1.6E-03	5.5E-03	1.1E-02
	5	2.6E-04	2.1E-03	2.7E-03	4.8E-03
5	0	5.8E-02	5.8E-02	5.8E-02	5.8E-02
	1	1.5E-03	9.2E-03	9.3E-03	1.9E-02
	2	5.8E-04	2.0E-03	5.5E-03	1.3E-02
	5	2.8E-04	2.2E-03	1.4E-03	3.9E-03
6	0	1.1E-01	1.1E-01	1.1E-01	1.1E-01
	1	6.7E-03	2.3E-02	3.9E-02	7.1E-02
	2	5.3E-03	8.6E-03	2.2E-02	4.7E-02
	5	7.3E-04	6.7E-03	1.2E-02	2.7E-02
7	0	3.6E-02	3.6E-02	3.6E-02	3.6E-02
	1	1.2E-03	5.4E-03	9.7E-03	2.4E-02
	2	3.1E-03	2.8E-03	6.8E-03	1.4E-02
	5	3.0E-04	4.1E-03	4.2E-03	7.7E-03
8	0	2.7E-02	2.7E-02	3.2E-02	8.1E-02
	1	1.7E-03	7.3E-03	8.0E-03	2.1E-02
	2	1.0E-08	4.1E-03	4.9E-03	1.2E-02
	5	2.6E-04	1.3E-03	3.9E-03	5.1E-03

5.6.3 Exposure Location Infiltration Rates

Radionuclides deposited in surface soils at the receptor locations for the atmospheric, canyon, and groundwater pathway scenarios will be depleted over time as water percolating through the exposure locations carries the contamination downward. The rate of depletion is proportional to the infiltration rate at a given location; the infiltration may represent naturally infiltrating water and irrigation water. Consequently, to model the effects of depletion, the infiltration rates at the various off-site receptor locations must be determined.

In general, infiltration rates to the east of MDA G and in adjacent canyons are poorly understood. Estimates of annual infiltration in Pajarito Canyon have been made using chloride mass-balance flux data collected from regional characterization wells R-20 and R-32 (Newman et al., 2005); these data suggest rates of about 1.6 to 2.0 mm/yr (0.063 to 0.079 in./yr). Water fluxes ranging from about 35 to 60 cm/yr (14 to 24 in./yr) have been estimated at regional characterization well R-32 based on nitrate flux data and the assumption that the nitrate is anthropogenic (Newman, 2005). Nylander et al. (2003) assigned net infiltration indices to canyons at the Laboratory, taking into account the proximity of the headwaters, the existence of anthropogenic sources of water, the persistence of surface water, and observations of alluvial water. Based on the index assigned to the portion of Pajarito Canyon that lies adjacent to MDA G, an infiltration rate of 300 mm/yr (12 in./yr) was estimated. More recently, Kwicklis et al. (2005) developed an infiltration map for the Los Alamos region; rates of infiltration ranging from about 20 to 50 cm/yr (7.9 to 20 in./yr) are estimated for the canyon based on this map.

Conditions in Cañada del Buey are considerably drier than those in Pajarito Canyon; this is substantiated by the available estimates of annual infiltration rates. An infiltration rate of 1.3 mm/yr (0.050 in/yr) was estimated on the basis of chloride mass-flux data from regional characterization well R-21, while unpublished data for monitoring hole CDBM-1 indicate an upward flux of 1.8 mm/yr (0.071 in/yr) at a depth of 7.6 to 13 m (25 to 45 ft) and a downward flux of 4.4 mm/yr (0.17 in/yr) at depths between 26 and 58 m (85 and 190 ft) (Newman, 2005). Nylander et al. (2003) estimated a net infiltration rate of 1 mm/yr (0.039 in/yr) for Cañada del Buey. The infiltration map developed by Kwicklis et al. (2005) for the Pajarito Plateau indicates an infiltration rate of about 0 to 2 mm/yr (0 to 0.08 in/yr) for Cañada del Buey.

Even less information is available to characterize rates of infiltration at locations immediately east of the MDA G fence line. Nylander et al. (2003) assigned an infiltration rate of 1 mm/yr (0.04 in/yr) for mesa-top locations at the Laboratory. Examination of the infiltration map of Kwicklis et al. (2005) suggests infiltration rates on the order of 0 to 10 mm/yr (0 to 0.4 in/yr).

Lacking more definitive information, annual infiltration rates in Pajarito Canyon adjacent to MDA G were assumed to range between 20 and 60 mm (0.79 to 2 in.), consistent with the nitrate data and the infiltration map developed by Kwicklis et al. (2005). Water is present in this portion of the canyon,

suggesting the chloride mass-balance flux data have underestimated actual infiltration rates. The infiltration rate in Cañada del Buey, which is one of the driest canyons at the Laboratory, was assumed to range from 0 to 4.4 mm/yr (0 to 0.17 in/yr), consistent with the data summarized above. Finally, infiltration rates at exposure locations immediately east of MDA G were assumed to range from 0 to 10 mm/yr (0 to 0.4 in/yr). In all cases, these ranges were assumed to represent the end points of triangular distributions; the most likely values were set equal to the midpoints of these intervals.

The modeling conducted in support performance assessment and composite analysis requires the average annual infiltration rate over the simulation period for each of the exposure locations. To determine this rate for a given location, sampling of the annual infiltration rate distribution was conducted, with replacement, for each year in the simulation period and the mean of these values was calculated. This process was repeated 200 times to generate a distribution of infiltration rates that represents the mean annual infiltration rate over the simulation period; the resulting distribution was used in the probabilistic modeling. This analysis yielded the distributions listed in Table 14.

The contributions of irrigation water to the depletion of contaminants in the surface soils at the exposure locations were not taken into account in the GoldSim models. The assumption was made that most of this water would be taken up by the receptor's crops and would not contribute significantly to the downward migration of radionuclides. Thus, the infiltration rates discussed above were not modified to include the effects of irrigation.

5.7 Sediment Transport Parameters

The sediment transport parameters address the movement of sediment from the mesa top to Cañada del Buey and Pajarito Canyon and within the canyons themselves. The parameters used to characterize sediment transport are described below.

5.7.1 Sediment Allocation Fractions

Sediment generated on top of Mesita del Buey may be transported with surface runoff to Cañada del Buey to the north of MDA G or Pajarito Canyon to the south. The sediment allocation fractions are used to model the movement of sediment to these canyons, including specific catchment areas within each (Figure 15). The general patterns of sediment transport projected to occur at the site have been presented and discussed in Section 3.2.

The sediment allocation fractions shown in Table 33 are average values, taking into account sediment behavior projected for the three erosion scenarios at times ranging from 100 to 10,000 years postclosure. Additional insight into the projected patterns of sediment transport at MDA G is provided by the data summarized in Tables 34 and 35. Table 34 shows the allocation fractions for the waste disposal regions averaged over erosion scenarios at various times; Table 35 provides fractions averaged over time for each scenario. Together, these tables suggest that, with some exceptions, the patterns of sediment allocation are relatively constant with time and severity of erosion.

Table 33
Sediment Allocation Factors for the Catchment Areas in Cañada del Buey and Pajarito Canyon

Waste Disposal Region	Sediment Allocation Fraction by Canyon Catchment Area								
	CdB1	CdB2	PC0	PC1	PC2	PC3	PC4	PC5	PC6
1	3.1E-01	9.9E-02	—	—	—	—	—	3.4E-01	2.5E-01
2	5.3E-01	—	—	—	—	—	—	4.7E-01	—
3	2.0E-01	—	—	—	—	1.1E-01	5.7E-01	1.3E-01	—
4	4.5E-01	—	—	—	2.6E-01	1.5E-01	1.3E-01	—	—
5	4.8E-01	—	—	2.3E-01	2.9E-01	—	—	—	—
6	9.9E-01	—	—	—	—	—	—	7.5E-03	—
7	2.0E-01	—	—	—	—	1.1E-01	5.7E-01	1.3E-01	—
8	6.6E-01	—	2.4E-01	1.0E-01	—	—	—	—	—

— = The sediment allocation factor is zero.

Table 34
Sediment Allocation Fractions Averaged over Erosion Scenarios at Various Times after Facility Closure

Waste Disposal Region	Time (yr postclosure)	Sediment Allocation Fraction by Canyon Catchment Area (mean ± std deviation)								
		CdB1	CdB2	PC0	PC1	PC2	PC3	PC4	PC5	PC6
1	100	2.4E-01 ±8.5E-02	1.2E-01 ±4.5E-02	---	---	---	---	---	3.6E-01 ±1.3E-01	2.7E-01 ±4.9E-02
	200	2.2E-01 ±1.0E-01	9.9E-02 ±3.0E-02	---	---	---	---	---	4.5E-01 ±1.4E-01	2.3E-01 ±5.5E-02
	500	3.4E-01 ±8.8E-02	9.6E-02 ±1.1E-01	---	---	---	---	---	2.8E-01 ±1.1E-01	2.9E-01 ±9.5E-02
	1,000	3.9E-01 ±7.1E-02	5.4E-02 ±1.6E-02	---	---	---	---	---	3.4E-01 ±8.2E-02	2.1E-01 ±8.1E-02
	5,000	3.5E-01 ±1.5E-01	1.4E-01 ±2.5E-02	---	---	---	---	---	2.9E-01 ±5.6E-02	2.2E-01 ±8.8E-02
	10,000	3.2E-01 ±4.1E-01	8.3E-02 ±8.3E-02	---	---	---	---	---	2.9E-01 ±1.8E-01	3.1E-01 ±1.5E-01
2	100	5.1E-01 ±4.4E-02	---	---	---	---	---	---	4.9E-01 ±4.4E-02	---
	200	5.2E-01 ±3.9E-02	---	---	---	---	---	---	4.8E-01 ±3.9E-02	---
	500	5.4E-01 ±5.0E-02	---	---	---	---	---	---	4.6E-01 ±5.0E-02	---
	1,000	5.5E-01 ±6.1E-02	---	---	---	---	---	---	4.5E-01 ±6.1E-02	---
	5,000	5.4E-01 ±9.7E-02	---	---	---	---	---	---	4.6E-01 ±9.7E-02	---
	10,000	5.1E-01 ±1.6E-01	---	---	---	---	---	---	4.9E-01 ±1.6E-01	---
3	100	1.9E-01 ±3.2E-02	---	---	---	---	---	6.0E-01 ±3.6E-02	2.2E-01 ±4.7E-02	---
	200	1.9E-01 ±3.5E-02	---	---	---	---	6.7E-02 ±1.2E-01	5.6E-01 ±1.2E-01	1.8E-01 ±2.7E-02	---

--- = The sediment allocation fraction is zero.

Table 34 (Continued)
Sediment Allocation Fractions Averaged over Erosion Scenarios at Various Times after Facility Closure

Waste Disposal Region	Time (yr postclosure)	Sediment Allocation Fraction by Canyon Catchment Area (mean ± std deviation)								
		CdB1	CdB2	PC0	PC1	PC2	PC3	PC4	PC5	PC6
3 (Cont.)	500	1.8E-01 ±3.0E-02	—	—	—	—	2.0E-01 ±1.8E-01	4.5E-01 ±1.2E-01	1.7E-01 ±8.0E-02	—
	1,000	1.8E-01 ±8.3E-03	—	—	—	—	1.2E-01 ±2.0E-01	6.3E-01 ±2.3E-01	7.8E-02 ±6.3E-02	—
	5,000	1.9E-01 ±1.8E-02	—	—	—	—	—	7.1E-01 ±1.3E-01	1.0E-01 ±1.1E-01	—
	10,000	2.5E-01 ±4.2E-02	—	—	—	—	2.6E-01 ±2.3E-01	4.5E-01 ±2.1E-01	4.6E-02 ±6.8E-03	—
4	100	5.0E-01 ±7.8E-02	—	—	—	1.9E-01 ±5.1E-02	2.0E-01 ±2.9E-02	1.2E-01 ±4.3E-03	—	—
	200	5.0E-01 ±7.5E-02	—	—	—	2.1E-01 ±4.3E-02	2.1E-01 ±9.4E-02	8.3E-02 ±7.2E-02	—	—
	500	4.8E-01 ±5.0E-02	—	—	—	2.7E-01 ±3.1E-02	2.1E-01 ±6.8E-02	3.9E-02 ±6.8E-02	—	—
	1,000	4.7E-01 ±6.1E-02	—	—	—	2.8E-01 ±1.4E-02	1.5E-01 ±1.5E-01	9.6E-02 ±8.6E-02	—	—
	5,000	3.7E-01 ±9.0E-02	—	—	—	3.1E-01 ±1.5E-01	7.1E-03 ±8.3E-03	3.0E-01 ±2.3E-01	—	—
	10,000	4.0E-01 ±6.2E-02	—	—	—	3.1E-01 ±1.1E-01	1.3E-01 ±1.1E-01	1.6E-01 ±2.8E-01	—	—
5	100	5.4E-01 ±3.6E-02	—	—	2.1E-01 ±1.9E-02	2.5E-01 ±5.5E-02	—	—	—	—
	200	5.0E-01 ±5.4E-02	—	—	2.4E-01 ±1.5E-02	2.6E-01 ±5.8E-02	—	—	—	—
	500	4.7E-01 ±7.3E-02	—	—	2.4E-01 ±9.6E-03	2.8E-01 ±6.5E-02	—	—	—	—
	1,000	4.4E-01 ±5.3E-02	—	—	2.7E-01 ±3.6E-02	2.9E-01 ±5.1E-02	—	—	—	—

— = The sediment allocation fraction is zero.

Table 34 (Continued)
Sediment Allocation Fractions Averaged over Erosion Scenarios at Various Times after Facility Closure

Waste Disposal Region	Time (yr postclosure)	Sediment Allocation Fraction by Canyon Catchment Area (mean ± std deviation)								
		CdB1	CdB2	PC0	PC1	PC2	PC3	PC4	PC5	PC6
5 (Cont.)	5,000	4.6E-01 ±9.2E-02	---	---	2.3E-01 ±6.9E-02	3.1E-01 ±2.4E-02	---	---	---	---
	10,000	4.8E-01 ±4.5E-02	---	---	2.0E-01 ±3.3E-02	3.3E-01 ±1.7E-02	---	---	---	---
6	100	1.0E ±00 ±0.0E ±00	---	---	---	---	---	---	---	---
	200	1.0E ±00 ±0.0E ±00	---	---	---	---	---	---	---	---
	500	1.0E ±00 ±0.0E ±00	---	---	---	---	---	---	---	---
	1,000	1.0E ±00 ±0.0E ±00	---	---	---	---	---	---	---	---
	5,000	9.8E-01 ±2.3E-02	---	---	---	---	---	---	1.6E-02 ±2.3E-02	---
	10,000	9.7E-01 ±3.8E-02	---	---	---	---	---	---	2.9E-02 ±3.8E-02	---
8	100	6.2E-01 ±3.0E-02	---	2.9E-01 ±3.7E-02	9.3E-02 ±1.7E-02	---	---	---	---	---
	200	6.3E-01 ±5.4E-02	---	2.9E-01 ±5.1E-02	8.4E-02 ±2.6E-03	---	---	---	---	---
	500	6.6E-01 ±1.4E-01	---	2.3E-01 ±1.4E-01	1.1E-01 ±1.0E-01	---	---	---	---	---
	1,000	6.9E-01 ±6.8E-02	---	2.0E-01 ±7.9E-02	1.1E-01 ±1.4E-01	---	---	---	---	---
	5,000	6.9E-01 ±5.2E-02	---	1.9E-01 ±8.4E-02	1.3E-01 ±8.5E-02	---	---	---	---	---
	10,000	6.9E-01 ±6.8E-02	---	2.4E-01 ±2.0E-02	7.3E-02 ±5.2E-02	---	---	---	---	---

--- = The sediment allocation fraction is zero.

Table 35
Sediment Allocation Fractions Averaged over Time after Facility Closure

Waste Disposal Region	Erosion Scenario	Sediment Allocation Fraction by Canyon Catchment Area (mean ± std deviation)								
		CdB1	CdB2	PC0	PC1	PC2	PC3	PC4	PC5	PC6
1	Low	3.7E-01 ±2.5E-01	9.5E-02 ±7.4E-02	—	—	—	—	3.4E-01 ±2.1E-01	1.9E-01 ±9.8E-02	—
	Moderate	2.7E-01 ±1.6E-01	1.2E-01 ±5.5E-02	—	—	—	—	3.3E-01 ±7.2E-02	2.8E-01 ±8.2E-02	—
	High	2.9E-01 ±5.7E-02	7.8E-02 ±3.8E-02	—	—	—	—	3.4E-01 ±1.5E-02	2.9E-01 ±4.4E-02	—
2	Low	5.4E-01 ±7.6E-02	—	—	—	—	—	4.6E-01 ±7.6E-02	—	—
	Moderate	5.5E-01 ±5.6E-02	—	—	—	—	—	4.5E-01 ±5.6E-02	—	—
	High	4.9E-01 ±8.2E-02	—	—	—	—	—	5.1E-01 ±8.2E-02	—	—
3	Low	1.9E-01 ±4.6E-02	—	—	—	9.0E-02 ±1.5E-01	5.9E-01 ±2.0E-01	1.3E-01 ±1.3E-01	—	—
	Moderate	1.8E-01 ±1.3E-02	—	—	—	1.8E-01 ±2.1E-01	5.2E-01 ±1.7E-01	1.2E-01 ±5.8E-02	—	—
	High	2.2E-01 ±2.7E-02	—	—	—	4.7E-02 ±1.2E-01	5.9E-01 ±1.2E-01	1.4E-01 ±6.1E-02	—	—
4	Low	4.3E-01 ±2.2E-02	—	—	3.0E-01 ±7.7E-02	1.8E-01 ±9.6E-02	9.0E-02 ±7.4E-02	—	—	—
	Moderate	4.5E-01 ±1.8E-02	—	—	2.8E-01 ±7.6E-02	2.0E-01 ±1.1E-01	6.5E-02 ±7.3E-02	—	—	—
	High	4.8E-01 ±1.4E-01	—	—	2.0E-01 ±7.7E-02	7.7E-02 ±8.2E-02	2.5E-01 ±2.3E-01	—	—	—

— = The sediment allocation fraction is zero.

Table 35 (Continued)
Sediment Allocation Fractions Averaged over Time after Facility Closure

Waste Disposal Region	Erosion Scenario	Sediment Allocation Fraction by Canyon Catchment Area (mean ± std deviation)								
		CdB1	CdB2	PC0	PC1	PC2	PC3	PC4	PC5	PC6
5	Low	4.9E-01 ±8.2E-02	---	2.5E-01 ±3.1E-02	2.6E-01 ±6.0E-02	---	---	---	---	---
	Moderate	4.8E-01 ±5.3E-02	---	2.4E-01 ±4.1E-02	2.8E-01 ±4.6E-02	---	---	---	---	---
	High	4.7E-01 ±5.7E-02	---	2.1E-01 ±3.6E-02	3.2E-01 ±2.2E-02	---	---	---	---	---
6	Low	1.0E ±00 ±1.1E-03	---	---	---	---	---	4.6E-04 ±1.1E-03	---	---
	Moderate	1.0E ±00 ±4.5E-03	---	---	---	---	---	2.8E-03 ±4.5E-03	---	---
	High	9.8E-01 ±3.1E-02	---	---	---	---	---	1.9E-02 ±3.1E-02	---	---
8	Low	6.6E-01 ±7.0E-02	2.5E-01 ±9.5E-02	8.8E-02 ±7.2E-02	---	---	---	---	---	---
	Moderate	6.9E-01 ±9.4E-02	2.4E-01 ±7.1E-02	6.1E-02 ±2.4E-02	---	---	---	---	---	---
	High	6.3E-01 ±2.6E-02	2.1E-01 ±7.2E-02	1.5E-01 ±8.0E-02	---	---	---	---	---	---

--- = The sediment allocation fraction is zero.

The sediment allocation fractions listed in Table 33 were used to model exposures for persons residing in Cañada del Buey and Pajarito Canyon. Although these fractions are subject to uncertainty, as indicated by the results in Tables 34 and 35, they were specified deterministically for the modeling. This approach was adopted because the model projections are not sufficiently detailed to establish the true variability inherent in the fractions or the correlations between the sediment allocations within a given waste disposal region.

The allocation fractions used in the modeling take into account model projections for times as great as 10,000 years postclosure. Data for times greater than 1,000 years were used to estimate the fractions because they provide insight into facility performance at times moderately greater than the compliance period. In general, allocation fractions for times up to 1,000 years postclosure fall within 20 percent of those estimated on the basis of 10,000 years.

5.7.2 Sediment Dispersal Fraction

The exposures projected for persons residing in Cañada del Buey and Pajarito Canyon ultimately depend upon the concentrations of radionuclides in the canyon floor soils. These concentrations, in turn, depend upon the manner in which the sediments are dispersed as they are transported to the receptor locations. Patterns of sediment dispersal are expected to be complex, affected by the spatial and temporal patterns of runoff from the disposal facility and numerous characteristics of the side slopes of the mesa and the canyon floors.

Although the SIBERIA model provided estimates of the sediment transported from the mesa top, the version of the program available at the time the modeling was conducted was incapable of modeling sediment particle paths from the mesa to the floors of Cañada del Buey and Pajarito Canyon. Consequently, the sediment dispersal fraction was estimated and applied to the modeling; the product of this factor and the catchment area (Table 36) yields the area over which contaminated sediment was assumed to spread within that catchment.

All sediment is assumed to be deposited on the canyon floor in the same year in which it is transported from the mesa top. The area over which the contaminated sediment is deposited within a given catchment could range from a small portion of the canyon to the entire canyon floor. Lacking the information to define the area over which the sediments actually disperse, it was assumed that the material transported from the mesa top would cover 10 to 50 percent of each catchment. On this basis, the sediment dispersal fraction was assigned a triangular distribution with minimum and maximum values of 0.1 and 0.5, respectively. The midpoint of this range was adopted as the most likely value for the distribution and was used for the deterministic modeling.

While further analysis is required to estimate suitable sediment dispersal factors, those selected for the modeling are expected to be reasonable. A portion of the sediment transported from the mesa will disperse along the slopes of the mesa, and will not reach the canyon floor until some years after it

leaves the mesa top. This increase in the area of dispersal, which was not accounted for in the development of the dispersal factors, will further reduce radionuclide concentrations in the canyon soils. Also, it is considered likely that any sediment reaching the canyon floor will generally disperse over more than 10 percent of the catchment area, the lower bound of the adopted distribution.

Table 36
Size of Catchments in Cañada del Buey and Pajarito Canyon

Catchment	Surface Area (m^2)
Cañada del Buey	
CdB1	1.8E+05
CdB2	7.3E+04
Pajarito Canyon	
PC0	1.4E+05
PC1	4.8E+04
PC2	2.8E+04
PC3	3.4E+04
PC4	3.1E+04
PC5	2.6E+04
PC6	3.4E+04

5.7.3 Canyon Sediment Transport Rates

Sediments deposited in Cañada del Buey and Pajarito Canyon will be transported down the canyons over time. Rates of sediment transport within the canyons will depend upon various characteristics of the canyons, the frequency of flooding within the canyons, and the patterns of sediment deposition. Although a detailed evaluation of sediment transport rates within the canyons adjacent to MDA G has not been undertaken, information provided by Malmon et al. (2005) provides insight into this phenomenon.

Malmon et al. (2005) modeled rates of Cs-137–contaminated sediment transport in Upper Los Alamos Canyon, between its confluence with DP Canyon and the LANL boundary and compared the projected rates of transport to measured Cs-137 loadings in the modeled region. The modeling projected rates of transport of coarse sediments within the stream channel and fine sediments located in the floodplains adjacent to the streambed. Residence times of the coarse sediments within the stream channel were relatively short, with flushing times for the entire 5-km (3.1-mi.) reach projected to be about 20 to 25 years. In contrast, the residence time of fine sediments in the floodplains was about 60 years.

The sediment residence times projected by Malmon et al. (2005) for Upper Los Alamos Canyon are not necessarily applicable to Cañada del Buey and Pajarito Canyon, each of which is expected to be unique in terms of sediment transport. Based on field observations, it is expected that Pajarito Canyon will effectively trap sediments for long periods of time (Reneau, 2005). This is because much of the bottom of the canyon consists of large inactive borrow pits that function as wetlands. Water spreads out into these small depressions at times of flooding, losing much of its energy and depositing sediments into heavy grasses. As a result, rates of erosion along the channel margins are expected to be small.

Sediment transport behavior in Cañada del Buey is expected to be much different than that observed in Upper Los Alamos Canyon (Malmon et al., 2005) or Pajarito Canyon (Reneau, 2005). Flow and, therefore, flooding within the canyon are infrequent. Higher sediment transmission losses are expected and the large sediment supply is expected to encourage deposition when water is flowing down the canyon. Thus, it is likely that sediment residence times within Cañada del Buey will be no shorter than those observed in Upper Los Alamos Canyon, and perhaps significantly longer.

It is reasonable to expect that contaminated sediments within Cañada del Buey and Pajarito Canyon will eventually be transported down the canyons as a result of flooding. The hypothetical canyon receptors would most likely come into contact with contamination deposited along the floodplains in these canyons. Therefore, the behavior of floodplain sediments is of most interest from the perspective of the performance assessment and composite analysis modeling. Malmon et al. (2005) found particle residence times of about 60 years over a 5 km (3.1 mi) stretch of Upper Los Alamos Canyon; this translates into flushing rate of about 0.015/yr for that segment of the canyon. As indicated above, the corresponding rates for the canyons adjacent to MDA G are probably no more than this and may be much less.

The available information is not adequate for developing definitive estimates of sediment transport rates within Cañada del Buey and Pajarito Canyon. Lacking additional information, it was assumed that the mean particle residence time in the canyons adjacent to MDA G is about 200 years. This is substantially longer than the residence times estimated for Upper Los Alamos Canyon, especially considering that the canyon stretch investigated in that canyon (5 km [3.1 mi]) is about five times the lengths of the canyon reaches along MDA G. Based on this assumption, a sediment transport rate of 0.005/yr was selected as the mean of a normal distribution; the coefficient of variation of this distribution was assumed to be 0.2.

5.8 Food-Chain Transport Parameters

Food-chain transport parameters were used to estimate radionuclide concentrations in crops and animals raised by a receptor as food sources. The point estimates and distributions used to describe these parameters and the information on which these data were based, are discussed below.

5.8.1 Crop Uptake Factor

The plant uptake factors for vegetable crops are used to model root uptake of radionuclides from contaminated soils. Compilations of uptake factors have been published by Baes et al. (1984), the International Atomic Energy Agency (IAEA, 1994), the NCRP (1999), Napier et al. (2004), and the NRC (1992), among others. The uptake factors for many elements included in these syntheses come from the same original sources.

The plant uptake factors compiled by Napier et al. (2004) were adopted for the performance assessment and composite analysis; these factors are listed in Table 37. This source was selected because it addresses a comprehensive list of elements and draws on more recent data than some of the other compilations. Napier et al. (2004) provide uptake factors for leafy vegetables, root vegetables, and grain. The factors provided for leafy vegetables and grain were used to estimate contaminant concentrations in those crops, while the factors for root vegetables were used to model plant uptake in all other produce.

Baes et al. (1984) conducted an extensive literature review of uptake factors and found that these parameters were generally lognormally distributed. Geometric means and standard deviations were estimated for the elements with sufficient data, and the geometric means of the distributions were generally adopted as the best estimates of plant uptake. Based on this work, the values taken from Napier et al. (2004) were assumed to represent geometric means of the lognormal distributions used in the uncertainty analyses. Sufficient data to define element-specific geometric standard deviations for these distributions were not found; consequently, a standard deviation of 3.5 was assumed for all plant uptake distributions except tritium (see below). This value is the approximate average of the standard deviations reported by Baes et al. for those elements whose distributions could be estimated.

The geometric standard deviation of 3.5 adopted for the plant uptake distributions is also consistent with other information in the literature. The NCRP (1999) adopted geometric standard deviations ranging from 2.5 to 3.0 to estimate soil-screening criteria. Sheppard and Evenden (1997) list appropriate geometric standard deviations for stochastic evaluations of plant uptake ranging from 1.5 to 5.7, depending upon available site and crop information. A geometric standard deviation of 3.3 is considered appropriate when information exists about the crop type but not about the site or soil characteristics. Finally, a geometric standard deviation of 3.5 is equal to the value cited by the NCRP (1984) for cesium in food and forage crops, but less than the cited NCRP value of 4.1 for strontium.

Napier et al. (2004) did not provide plant uptake factors for some of the elements in the performance assessment and composite analysis, including aluminum, berkelium, lutetium, titanium, and hydrogen. Plant uptake factors for four of these elements were assigned values common to other elements in the same groups. The factors for aluminum were set equal to the

Table 37
Parameter Values and Distributional Information for Plant Uptake Factors

Element	Leafy Vegetables and Pasture Grass (dry weight)		Produce (dry weight)		Grain (dry weight)	
	Geometric Mean	Geometric Standard Deviation	Geometric Mean	Geometric Standard Deviation	Geometric Mean	Geometric Standard Deviation
Ac	4.7E-04	3.5E+00	3.5E-04	3.5E+00	2.2E-05	3.5E+00
Ag	2.7E-04	3.5E+00	1.3E-03	3.5E+00	2.5E-01	3.5E+00
Al [a]	4.0E-03	3.5E+00	4.0E-04	3.5E+00	4.0E-04	3.5E+00
Am	4.7E-04	3.5E+00	3.5E-04	3.5E+00	2.2E-05	3.5E+00
Ba	1.5E-01	3.5E+00	1.5E-02	3.5E+00	1.5E-02	3.5E+00
Be	1.0E-02	3.5E+00	1.5E-03	3.5E+00	2.0E-03	3.5E+00
Bi	5.0E-01	3.5E+00	5.0E-01	3.5E+00	5.0E-01	3.5E+00
Bk [b]	4.7E-04	3.5E+00	3.5E-04	3.5E+00	2.2E-05	3.5E+00
C	7.0E-01	3.5E+00	7.0E-01	3.5E+00	7.0E-01	3.5E+00
Ca	3.5E+00	3.5E+00	3.5E-01	3.5E+00	3.5E-01	3.5E+00
Cf	4.7E-04	3.5E+00	3.5E-04	3.5E+00	2.2E-05	3.5E+00
Cl	7.0E+01	3.5E+00	7.0E+01	3.5E+00	7.0E+01	3.5E+00
Cm	7.7E-04	3.5E+00	4.3E-04	3.5E+00	2.1E-05	3.5E+00
Co	2.3E-01	3.5E+00	6.7E-02	3.5E+00	3.7E-03	3.5E+00
Cs	4.6E-01	3.5E+00	1.3E-01	3.5E+00	2.6E-02	3.5E+00
Eu	2.0E-02	3.5E+00	2.0E-02	3.5E+00	2.0E-02	3.5E+00
Gd	2.0E-02	3.5E+00	2.0E-02	3.5E+00	2.0E-02	3.5E+00

Source: Napier et al. (2004) unless otherwise indicated

[a] Uptake factors for Al were set equal to the corresponding factors for Ga, In, and Tl.

[b] Uptake factors for Bk were set equal to the values for Am.

[c] Plant uptake factors for tritium were estimated using specific activity models. See discussion in text.

[d] Uptake factors for Lu were set equal to the corresponding factors for Eu, Gd, and Ti.

[e] Uptake factors for Ti were set equal to the corresponding factors for Hf and Zr.

— = Element exists solely as a gas and was ignored in terms of food-chain transport

Table 37 (Continued)
Parameter Values and Distributional Information for Plant Uptake Factors

Element	Leafy Vegetables and Pasture Grass (dry weight)		Produce (dry weight)		Grain (dry weight)	
	Geometric Mean	Geometric Standard Deviation	Geometric Mean	Geometric Standard Deviation	Geometric Mean	Geometric Standard Deviation
H [c]	---	---	---	---	---	---
Ho	2.0E-02	3.5E+00	2.0E-02	3.5E+00	2.0E-02	3.5E+00
I	4.0E-02	3.5E+00	4.0E-02	3.5E+00	4.0E-02	3.5E+00
K	1.0E+00	3.5E+00	5.5E-01	3.5E+00	5.5E-01	3.5E+00
Kr	---	---	---	---	---	---
Lu [d]	2.0E-02	3.5E+00	2.0E-02	3.5E+00	2.0E-02	3.5E+00
Mo	8.0E-01	3.5E+00	8.0E-01	3.5E+00	8.0E-01	3.5E+00
Nb	2.5E-02	3.5E+00	2.5E-02	3.5E+00	2.5E-02	3.5E+00
Nd	2.0E-02	3.5E+00	2.0E-02	3.5E+00	2.0E-02	3.5E+00
Ni	2.8E-01	3.5E+00	6.0E-02	3.5E+00	3.0E-02	3.5E+00
Np	3.2E-02	3.5E+00	1.3E-02	3.5E+00	2.7E-03	3.5E+00
Os	1.5E-02	3.5E+00	3.5E-03	3.5E+00	3.5E-03	3.5E+00
Pa	4.7E-04	3.5E+00	3.5E-04	3.5E+00	2.2E-05	3.5E+00
Pb	1.0E-02	3.5E+00	6.0E-03	3.5E+00	4.7E-03	3.5E+00
Pm	2.0E-02	3.5E+00	2.0E-02	3.5E+00	2.0E-02	3.5E+00
Pu	6.0E-05	3.5E+00	1.1E-03	3.5E+00	8.6E-06	3.5E+00
Ra	4.9E-02	3.5E+00	2.0E-03	3.5E+00	1.2E-03	3.5E+00

Source: Napier et al. (2004) unless otherwise indicated

[a] Uptake factors for Al were set equal to the corresponding factors for Ga, In, and Tl.

[b] Uptake factors for Bk were set equal to the values for Am.

[c] Plant uptake factors for tritium were estimated using specific activity models. See discussion in text.

[d] Uptake factors for Lu were set equal to the corresponding factors for Eu, Gd, and Ti.

[e] Uptake factors for Ti were set equal to the corresponding factors for Hf and Zr.

--- = Element exists solely as a gas and was ignored in terms of food-chain transport

Table 37 (Continued)
Parameter Values and Distributional Information for Plant Uptake Factors

Element	Leafy Vegetables and Pasture Grass (dry weight)		Produce (dry weight)		Grain (dry weight)	
	Geometric Mean	Geometric Standard Deviation	Geometric Mean	Geometric Standard Deviation	Geometric Mean	Geometric Standard Deviation
Si	3.5E-01	3.5E+00	7.0E-02	3.5E+00	7.0E-02	3.5E+00
Sm	2.0E-02	3.5E+00	2.0E-02	3.5E+00	2.0E-02	3.5E+00
Sn	3.0E-02	3.5E+00	6.0E-03	3.5E+00	6.0E-03	3.5E+00
Sr	3.0E+00	3.5E+00	5.0E-01	3.5E+00	2.1E-01	3.5E+00
Tb	2.0E-02	3.5E+00	2.0E-02	3.5E+00	2.0E-02	3.5E+00
Tc	2.1E+02	3.5E+00	2.4E-01	3.5E+00	7.3E-01	3.5E+00
Th	1.8E-03	3.5E+00	3.3E-04	3.5E+00	3.4E-05	3.5E+00
Ti [e]	1.0E-03	3.5E+00	1.0E-03	3.5E+00	1.0E-03	3.5E+00
U	8.3E-03	3.5E+00	1.2E-02	3.5E+00	1.3E-03	3.5E+00
Zr	1.0E-03	3.5E+00	1.0E-03	3.5E+00	1.0E-03	3.5E+00

Source: Napier et al. (2004) unless otherwise indicated

[a] Uptake factors for Al were set equal to the corresponding factors for Ga, In, and Tl.

[b] Uptake factors for Bk were set equal to the values for Am.

[c] Plant uptake factors for tritium were estimated using specific activity models. See discussion in text.

[d] Uptake factors for Lu were set equal to the corresponding factors for Eu, Gd, and Ti.

[e] Uptake factors for Ti were set equal to the corresponding factors for Hf and Zr.

— = Element exists solely as a gas and was ignored in terms of food-chain transport

values for gallium, indium, and thallium, while uptake factors for berkelium were set equal to those for americium. The uptake factors for lutetium were set equal to the values provided for europium, gadolinium, and terbium. Finally, the plant uptake factors for titanium were set equal to the factors given for hafnium and zirconium.

Plant concentrations of hydrogen as tritium were estimated using the specific activity model described in Section 3.6.3.3. Implementation of this model required information about the fraction of water in the vegetation and the fraction of hydrogen in plants. The water fraction was estimated using the dry-to-wet-weight fractions discussed below. The fraction of hydrogen in plants was assumed to be 0.062 (dry-weight basis) for all crops (Napier et al., 1988).

5.8.2 Dry-to-Wet-Weight Fraction

Dry-to-wet-weight fractions are used to convert plant uptake factors and forage intake rates from a dry-to-wet-weight basis. Point estimates and distributions were defined for these fractions using moisture content data from Baes et al. (1984) and the EPA (1997) for various species of leafy vegetables, produce, and grain; these data are summarized in Table 38. Crop-specific data were used to define the distributions shown in Table 14 for the various crop categories or types.

Peterson (1983) provides fresh-to-dry-weight ratios for forage of 4.44, 5.0, 5.5, and 4.2 for alfalfa, clover, grass, and silage, respectively. These data indicate dry-to-wet-weight fractions ranging from 0.18 to 0.24. Data cited in IAEA Technical Report 364 (1994) include dry-to-wet-weight fractions of 0.19 and 0.1 for alfalfa and grass, respectively. Because no additional information was available, a value of 0.2 was adopted as the most likely value of a triangular distribution for the forage eaten by cows and cattle. Minimum and maximum values were assumed to be 0.15 and 0.25, respectively. The point estimate and distribution for the dry-to-wet-weight fraction for grain (Table 14) were used to define the dry-to-wet-weight fraction for the feed consumed by chickens.

5.8.3 Translocation Factor

Translocation factors describe the portion of the contamination deposited on the exterior of the crops that passes into the plant tissues and becomes assimilated. Limited data exist to develop distributions of the crop-specific factors. The NCRP (1984) cites default values of 1.0 and 0.1 for leafy vegetables and other produce, respectively. Ng et al. (1978) list translocation factors for various crops and radionuclides. The maximum translocation factor listed for produce (excluding fruit) and grain is 0.36; data provided for leafy vegetables are limited to cabbage, which has a translocation factor as high as 0.12, depending upon the radionuclide under consideration. The factors for cabbage are significantly lower than the default value of 1.0 recommended for leafy vegetables by the NCRP (1984). Ng et al. (1978) assigned a translocation factor of 1.0 to all radionuclides for hay and other types of animal forage and feed. Hinton (1994), cited by the Oak Ridge National Laboratory guidance (ORNL, 1999), provided translocation factors for cesium,

Table 38
Dry-to-Wet-Weight Fractions for Crops

Crop	Dry-to-Wet-Weight Fraction	Crop	Dry-to-Wet-Weight Fraction
Leafy Vegetables			
Alfalfa Sprouts	8.9E-02	Green onions	1.2E-01
Beets – Greens	7.9E-02	Kale	1.6E-01
Broccoli	9.7E-02 [a]	Leeks	1.7E-01
Brussel Sprouts	1.5E-01 [a]	Lettuce	4.8E-02 [a]
Cabbage	8.4E-02 [a]	Mung bean sprouts	9.6E-02
Cauliflower	8.0E-02 [a]	Mustard greens	9.2E-02
Celery	5.8E-02 [a]	Parsley	1.2E-01
Collards	6.1E-02	Rhubarb	6.4E-02
Cress	1.1E-01 [a]	Spinach	7.9E-02 [a]
Dandelion Greens	1.4E-01	Swiss chard	7.3E-02
Endive	6.2E-02	Turnips – tops	8.9E-02
Escarole	1.3E-01		
Produce			
Asparagus	7.4E-02 [a]	Parsnips	2.0E-01
Beans - Lima	3.0E-01	Peas	2.6E-01
Beans – Snap, Italian, Green, Yellow	1.0E-01 [a]	Peppers - sweet	7.2E-02
Beets	1.3E-01	Potatoes	1.9E-01 [a]
Carrots	1.2E-01 [a]	Pumpkin	8.4E-02
Chili Peppers	1.2E-01	Radishes - roots	5.2E-02
Corn - Sweet	2.5E-01 [a]	Rutabaga	1.0E-01
Cucumbers	3.9E-02 [a]	Shallots	2.0E-01
Eggplant	7.7E-02 [a]	Soybeans	3.1E-01
Garlic	4.1E-01	Squash	8.6E-02 [a]
Kohlrabi	9.0E-02	Sugar beet	1.6E-01
Lentils - Whole	3.3E-01	Sweet potato	2.9E-01 [a]
Mushrooms	8.2E-02	Tomatoes	6.0E-02 [a]
Okra	1.0E-01	Turnips - roots	8.1E-02
Onions	1.1E-01 [a]		
Grain			
Barley	8.9E-01 [a]	Rye	8.9E-01 [a]
Corn – Grain, Bran	9.2E-01 [a]	Sorghum (incl. milo)	9.1E-01
Millet	9.1E-01	Soybean	9.3E-01
Oats	9.2E-01 [a]	Wheat	8.9E-01 [a]

Sources: Baes et al., (1984) and EPA (1997)

[a] *Listed values represent mean values for the crop.*

strontium, iodine, and plutonium in winter barley and wheat, root vegetables, other vegetables, and fruits. With the exception of potatoes, which had a translocation factor of 0.5, all crops had factors less than or equal to 0.02.

On the basis of the data provided above, the translocation factor for leafy vegetables was assigned a point estimate of 1.0 for use in the deterministic modeling. The parameter was assigned a triangular distribution with minimum, most likely, and maximum values of 0.8, 0.9, and 1.0. This distribution ignores the very low translocation factor estimated for cabbage by Ng et al. (1978), but considers reduced rates of assimilation by the plants. The same deterministic value and distribution were assumed to apply to pasture grass grown for animal consumption. The translocation factors for produce and grain were also assumed to have a triangular distribution with minimum, most likely, and maximum values of 0.01, 0.1, and 0.4, respectively. The end points of the distribution roughly coincide with the data discussed above; the most likely value was used for the deterministic modeling.

5.8.4 Agricultural Productivity

Crop productivities are used to model radionuclide concentrations in vegetable and forage crops due to atmospheric deposition. Baes et al. (1984) provide maps of the U.S. showing ranges of productivities for various crops in northern New Mexico. The fresh weight productivities range from 0.5 to 1.5 kg/m^2 (0.1 to 0.3 lb/ft^2) for leafy vegetables and protected produce, 0.1 to 1.5 kg/m^2 (0.02 to 0.3 lb/ft^2) for exposed produce, and 0.1 to 0.2 kg/m^2 (0.02 to 0.04 lb/ft^2) for grain. NCRP Report 76 (1984) cites default values of 2 kg/m^2 (0.4 lb/ft^2) for produce and leafy vegetables and 0.6 kg/m^2 (0.1 lb/ft^2) for other aboveground vegetables; all productivities are given in terms of fresh weight. Ng et al. (1982) provide yields for various crops in Georgia and South Carolina. The average yields by vegetation class are 1.35 (one observation), 0.64, and 0.17 kg/m^2 (0.3, 0.1, and 0.03 lb/ft^2) (fresh weight) for leafy vegetables, produce, and grain, respectively. The RESRAD computer code (ANL, 2001) uses default values of 1.5 kg/m^2 (0.3 lb/ft^2) (fresh weight) for leafy vegetables, and 0.7 kg/m^2 (0.14 lb/ft^2) (fresh weight) for fruit, other vegetables, and grain. Oak Ridge National Laboratory guidance on risk assessment (ORNL, 1999) adopts fresh weight productivities of 2.0 kg/m^2 (0.4 lb/ft^2) for leafy vegetables (taken from NCRP, 1984), 0.62 kg/m^2 (0.13 lb/ft^2) for nonleafy vegetables, and 0.67 kg/m^2 (0.14 lb/ft^2) for root vegetables for DOE sites in Portsmouth, Ohio and Paducah, Kentucky. The ORNL report cites a range of 0.112 to 1.12 kg/m^2 (0.02 to 0.2 lb/ft^2) for leafy vegetables and 0.224 to 1.12 kg/m^2 (0.04 to 0.2 lb/ft^2) for root vegetables in the Paducah area.

NCRP Report 76 (1984) cites crop yields of 0.7 kg/m^2 (0.14 lb/ft^2) (fresh weight) and 0.3 kg/m^2 (0.06 lb/ft^2) (dry weight) for pasture vegetation, while Ng et al. (1978) provide a yield for hay of 0.5 kg/m^2 (0.1 lb/ft^2) (dry weight). ORNL risk assessment guidance (1999) provides dry weight yields for pasture grass, citing a range of 0.112 to 0.225 kg/m^2 (0.023 to 0.046 lb/ft^2) for the

Paducah, Kentucky and Portsmouth, Ohio areas. Baes et al. (1984) provide estimates of yield for hay in northern New Mexico ranging from 0.3 to 0.6 $kg/m^2/yr$ (0.06 to 0.12 lb/ft^2) (dry weight). The U.S. Department of Agriculture (USDA, 2004a) provides commercial yields for alfalfa, alfalfa mixtures, and other types of hay. The annual yield of alfalfa and alfalfa mixtures in New Mexico averaged about 1.1 kg/m^2 (0.22 lb/ft^2) (dry weight) between 2001 and 2003, while the annual yield of all other types of hay was about 0.5 kg/m^2 (0.1 lb/ft^2) (dry weight).

Triangular distributions were used to describe crop productivities for the performance assessment and composite analysis. The distributions use minimum, most likely, and maximum values of 1.0, 1.5, and 2.0 kg/m^2 (0.2, 0.3. and 0.4 lb/ft^2) for leafy vegetables; 0.5, 1.0, and 1.5 kg/m^2 (0.1, 0.2, and 0.3 lb/ft^2) for produce; and 0.2, 0.5, and 0.75 kg/m^2 (0.04, 0.1, 0.15 lb/ft^2) for grain. These values, all of which are given in terms of fresh weight, generally encompass the observations discussed above. The distribution for pasture grass productivity was defined using the data cited above for pasture grass and hay; minimum, most likely, and maximum values of 0.1, 0.5, and 0.7 kg/m^2 (0.02, 0.1, and 0.14 lb/ft^2) (dry weight) were assumed. The most likely values in all of these distributions were used as the best estimates in the deterministic modeling.

5.8.5 Growing Season

Radionuclides deposited on plant surfaces will be depleted throughout the growing season as a result of weathering. The length of the growing season will vary with the crop under consideration and the conditions under which the crops are grown. Ng et al. (1978) adopted a 3-month (2,190-hour) growing season to model food-chain transport at the DOE Savannah River Site. Regulatory Guide 1.109 (NRC, 1977) suggests a growing season of 1,440 hours for vegetables, produce, and grain, and 720 hours for forage. The value for forage is based on the average time between successive grazing episodes by cattle. The RESRAD computer code (ANL, 2001) adopts a default growing season of 1,490 hours for fruits, vegetables, and grain, and 2,190 hours for leafy vegetables. Baes et al. (1984) indicate that the average time between successive hay harvests is 1,440 hours.

Time-to-maturity data for vegetables provide additional information about the periods of time crops may be exposed to contaminant releases. Table 39 summarizes representative maturity times for a variety of leafy vegetables, produce, and grain. On the basis of these data, maturity times for leafy vegetables range from 40 to 120 days; the median of the midpoints of the ranges listed in the table is about 60 days. The maturity times for produce range from 46 to 150 days, while a limited amount of information for grain indicates a time to maturity ranging from 70 to 120 days. Median growing seasons for produce and grain, calculated using the midpoints of the listed ranges, are 80 and 110 days, respectively.

Table 39
Time-to-Maturity Data for Representative Vegetables

Crop Type/Crop	Time to Harvest or Maturity (d)	Source
Leafy Vegetables		
Beet greens	50	Lerner and Dana, 2001
Cabbage	62–120 [a]	LSU, 2003; CUCES, 1999; TAMU, 2001; Smith, 1995
Collards	60–85	Lerner and Dana, 2001; LSU, 2003; TAMU, 2001; CUCES, 1999
Endive	85–100	Lerner and Dana, 2001; TAMU, 2001
Kale	50–60	Lerner and Dana, 2001; TAMU, 2001; CUCES, 1999
Lettuce	40–80	LSU, 2003; CUCES, 1999
Lettuce, leaf	40–50	Lerner and Dana, 2001; TAMU, 2001; Smith, 1995
Lettuce, other [b]	30–85	TAMU, 2001; CUCES, 1999; Smith, 1995
Mustard	35–60	Lerner and Dana, 2001; LSU, 2003; TAMU, 2001; CUCES, 1999; Smith, 1995
Spinach	35–75	Lerner and Dana, 2001; LSU, 2003; TAMU, 2001; CUCES, 1999; Smith, 1995
Swiss chard	45–60	Lerner and Dana, 2001; LSU, 2003; TAMU, 2001
Turnip greens	40	Lerner and Dana, 2001
Produce		
Beans [c]	46–90	CUCES, 1999; LSU, 2003; TAMU, 2001; Smith, 1995
Beets	50–80	CUCES, 1999; LSU, 2003; TAMU, 2001; Smith, 1995
Carrots	50–95	CUCES, 1999; LSU, 2003; TAMU, 2001; Smith, 1995
Corn	64–100	CUCES, 1999; LSU, 2003; TAMU, 2001; Smith, 1995
Cucumbers	48–72	CUCES, 1999; LSU, 2003; TAMU, 2001; Smith, 1995
Eggplant	60–85 [a]	CUCES, 1999; LSU, 2003; TAMU, 2001; Smith, 1995
Onions, bulb	85–150	CUCES, 1999; LSU, 2003; TAMU, 2001; Smith, 1995
Peas	58–85	CUCES, 1999; LSU, 2003; TAMU, 2001; Smith, 1995
Peppers, hot and sweet	60–80 [a]	CUCES, 1999; LSU, 2003; TAMU, 2001; Smith, 1995
Potatoes	90–120 [a]	CUCES, 1999; LSU, 2003; TAMU, 2001; Smith, 1995
Potatoes, Irish	90–120	CUCES, 1999; LSU, 2003
Pumpkins	90–120	LSU, 2003; TAMU, 2001; Smith, 1995
Squash, summer	40–120	CUCES, 1999; LSU, 2003; TAMU, 2001; Smith, 1995
Squash, winter	50–120	CUCES, 1999; TAMU, 2001; Smith, 1995
Tomatoes	70–100 [a]	CUCES, 1999; LSU, 2003; TAMU, 2001; Smith, 1995
Turnips	40–75	CUCES, 1999; LSU, 2003; TAMU, 2001; Smith, 1995
Grain		
Millet	70–90	Croissant and Echols, 1998
Oats	100–120	Croissant and Echols, 1998
Wheat	110–120	Croissant and Echols, 1998

[a] *Plants may be started from transplants.*

[b] *Types of lettuce include head, butterhead, and cos.*

[c] *Includes snap, pole, half-runner, lima, pole lima, and edible soybeans.*

The time-to-maturity data provided in Table 39 played a key role in the development of distributions of growing seasons for vegetables. A triangular distribution was defined for leafy vegetables using minimum, most likely, and maximum values of 40, 60, and 100 days. The endpoints are reasonable estimates of the ranges listed for individual crops. The most likely value of 60 days is representative of the midpoints of the individual crop ranges and agrees with guidance in Regulatory Guide 1.109 (NRC, 1977). The growing season for produce was assumed to have minimum, most likely, and maximum values of 45, 80, and 120 days, respectively. The midpoint of the triangular distribution defined for the growing season of grain was set equal to 110 days, while the minimum and maximum values were assumed to be 70 and 120 days, respectively. The distributions for produce and grain generally conform to the time to maturity data listed in Table 39, and bracket the 3-month period adopted by Ng et al. (1978). The triangular distribution defined for pasture grass has minimum and maximum values of 30 and 60 days, consistent with data found in NRC (1977) and Baes et al. (1984). The midpoint of this range was adopted as the most likely value. The most likely values for all of these distributions were used as best estimates for the deterministic modeling.

5.8.6 Plant Mass Loading Factor

Plant mass-loading factors are used to estimate rates of radionuclide deposition on plant surfaces due to rainsplash. Estimates of mass-loading factors taken from several investigations are summarized in Table 40. Most of this information comes from Hinton (1992) and Pinder and McLeod (1989); original references for the data are included in the table. These factors are given in terms of concentration, rather than inventory. Pinder and McLeod (1989) discuss the fact that estimating concentration-based factors is complicated by plant biomass and canopy structure. The inventory-based factors are expected to be less variable and, therefore, preferable for use in dose assessment models. However, the data required to estimate the plant-loading factor on an inventory basis for the studies cited in the table are generally unavailable.

Concentration-based mass-loading factors were used for the performance assessment and composite analysis. The distribution for leafy vegetables was based on the information provided in Pinder and McLeod (1989) for lettuce. A normal distribution with a mean and standard error of 260 and 100 mg soil/g plant (0.24 and 0.09 lb soil/lb plant) (dry weight), respectively, was adopted for the uncertainty analysis; the distribution was truncated to prevent the occurrence of negative values of the parameter. The mass-loading factors range from about 1 to 210 mg soil/g plant (9×10^{-4} to 0.19 lb soil/lb plant) (dry weight) for the nonleafy vegetables included in Table 40. The factors for all crops except squash are 60 mg soil/g plant (0.06 lb soil/lb plant) (dry weight) or less. The higher mass loading observed for squash pertains only to the lower portions of the plant; factors based on the entire plant will be significantly smaller. Based on this information, a point estimate of 30 mg soil/g plant (0.03 lb soil/lb plant) (dry weight) was adopted for the performance assessment and composite analysis. A triangular distribution was assumed to apply, and was defined using minimum, most likely, and maximum values of 1, 30, and 100 mg soil/g plant (9×10^{-4}, 0.03, and 0.09 lb soil/lb plant) (dry weight).

Table 40
Summary of Plant Mass Loading

Crop	Location	Mass-Loading Factor (mg soil/g dry vegetation)	Reference [a]
Bush Beans	New Mexico	3.0E+01 – 6.0E+01	White et al., 1981
Broccoli	South Carolina	1.0E+01 ± 8.1E+00 [b]	McLeod et al., 1984a
Cabbage	South Carolina	1.1E+00 ± 1.1E+00	McLeod et al., 1984a
Corn	South Carolina	1.7E+00; 1.4E+00 [c]	Pinder and McLeod, 1989
Lettuce	South Carolina	2.6E+02 ± 1.0E+02 [b]	McLeod et al., 1984a
Soybean	South Carolina	8.4E+00; 2.1E+00 [b]	Pinder and McLeod, 1989
Squash	New Mexico	1.4E+02 – 2.1E+02 [d]	White et al., 1981
		3.0E+01 – 4.0E+01 [e]	White et al., 1981
Sunflower	South Carolina	2.6E+00 ± 9.0E-01 [b]	Pinder and McLeod, 1989
Tobacco	South Carolina	2.1E+00 ± 6.0E-01 [b]	McLeod et al., 1984b
Tomatoes	New Mexico	1.7E+01 [f]	Dreicer et al., 1984
		3.0E+01 [g]	Dreicer et al., 1984
Turnips	South Carolina	3.2E+01 ± 1.1E+01 [b]	McLeod et al., 1984a
Wheat	South Carolina	4.3E+00; 4.8E+00 [c]	Pinder and McLeod, 1989
Pasture	Sellafield, UK	7.0E+01	Green and Dodd, 1988
Pasture	Sellafield, UK	1.8E+02	Beresford and Howard, 1991
		3.0E+01 [h]	
		3.0E+02 [i]	
Pasture	Norway	<1.0E+00 [h]	Oughton, 1990
	Byelorussia	3.0E+02 – 5.0E+02	
Pasture	Colorado	1.8E+01 ± 4.8E+01 [j]	Arthur and Alldredge, 1982
Pasture	Sellafield, UK	5.0E+01 – 2.0E+02	Summerling et al., 1984
Pasture	South Carolina	9.0E+00 ± 1.7E+00 [b]	Pinder et al., 1991
Pasture	Kloten, Switzerland	7.0E+00 ± 1.1E+00 [b]	Hinton et al., 1995
Sagebrush	Wyoming	2.4E+01	Skinner, 1982

[a] Many of the cited data were taken from Hinton (1992) and Pinder and McLeod (1989). The references listed in the table are the original references for each investigation.

[b] Measurement represents mean ± standard error.

[c] First value represents the mean mass loading factor across all sampling times; second value represents the mean at the time of harvest.

[d] Mass loading factor pertains to plant heights of 0.2 m or less.

[e] Mass loading factor pertains to plant heights greater than 0.2 m.

[f] Mass loading factor pertains to particle sizes less than 0.53 µm.

[g] Mass loading factor pertains to particle sizes less than 100 µm.

[h] Measurements were taken in summer.

[i] Measurements were taken in winter.

[j] Measurement represents mean ± standard deviation.

The mass-loading factors listed for pasture grass in Table 40 range from less than 1 to 500 mg soil/g plant (9×10^{-4} to 0.47 lb soil/lb plant) (dry weight). However, the distribution adopted for the nonleafy vegetables was applied to animal forage as well. This distribution is a conservative representation of data presented in Hinton et al. (1995) and Pinder et al. (1991) and omits from consideration data that pertain to conditions that are not expected to exist at MDA G or the receptor locations. For example, the mass-loading factors developed by Beresford and Howard (1991) and Oughton (1990) are considered to be indicative of extreme conditions (Hinton, 1992). Also ignored is the mass loading of almost 250 mg soil/g plant (0.23 lb soil/lb plant) (dry weight) that was estimated by Arthur and Alldredge (1982); this value pertained to a single sample, mass loadings for 25 other samples were several times smaller. Finally, some of the higher mass loadings listed in Table 40 for pasture grass were estimated using techniques that will tend to overestimate mass loadings for the suspendable portion of the soil (Pinder et al., 1991).

5.8.7 Rainsplash Enhancement Factor

The plant mass-loading factors discussed above are defined in terms of the suspendable fraction of the soil. In contrast, the soil concentrations estimated using the GoldSim models are based on the total soil; concentrations are not calculated as a function of soil particle size. Given this difference, it is necessary to modify the mass-loading factors discussed above before they are applied in the GoldSim models. This is done by multiplying the mass-loading factors by the rainsplash enhancement factor (the ratio of radionuclide concentrations in the suspendable fraction to the concentrations in the total soil).

In terms of mass loading on plants, the suspendable fraction is typically defined as particles less than or equal to 125 μm (0.0049 in.) in diameter; soil particles of this size may be readily suspended by wind and rainsplash and appear to be preferentially retained on plant surfaces (Dreicer et al., 1984 and Wallwork-Barber and Hakonson, 1981, as cited in Pinder and McLeod, 1989). Because radionuclide concentrations in soil tend to increase with decreasing soil particle size (Livens and Baxter, 1988), the enhancement factor for the suspendable fraction tends to be greater than 1.0. Pinder and McLeod (1989) found Pu-238 concentrations in the suspendable soil fraction to be 1.5 times the concentrations in the total soil. Similarly, Pu-238 concentrations in soil particles less than or equal to 100 μm in diameter were found by White et al. (1981) to be 1.7 times the concentrations in the total soil.

Livens and Baxter (1988) examined radionuclide concentrations in four West Cumbrian (England) soils as a function of particle size; the radionuclides evaluated included Am-241, Cs-137, Ru-106, Pu-238, and Pu-239/240. The results of this investigation were used to estimate the enhancement factor for soil particles less than 125 μm (0.0049 in.) in diameter. The factors for a sandy soil were greatest, ranging from 4.5 to 6.7 across the radionuclides evaluated. Factors for a gley soil (which develop in areas of poor drainage) ranged from 0.74 to 2.1; the factors for

woodland and pasture soils ranged from 1.7 to 1.9 and 1.3 to 1.4, respectively. The higher factors for the sand were thought to be due to the very small fraction of fine material (i.e., < 32 μm [0.001 in.] in diameter) and the low radionuclide uptake capacity of the predominant quartz fraction.

Nyhan et al. (1976a, 1976b) provide additional insight into the distribution of radionuclides as a function of soil particle size. In one study, alluvial soils from three liquid effluent discharge areas at LANL were sampled and used to determine Pu-238 and Pu-239/240 concentrations as a function of particle size (Nyhan et al., 1976a). Radionuclide concentrations in soil particles less than 53 μm (0.021 in.) in diameter were approximately 10 times the concentrations in the 2 to 23 μm (7.9×10^{-5} to 9.0×10^{-5} in.) diameter fraction; a similar relationship was evident for 53 to 105 μm (0.021 to 0.041 in.) diameter soil particles relative to the 2 to 23 μm (7.9×10^{-5} to 9.0×10^{-5} in.) diameter fraction. Nyhan et al. (1976b) examined the distribution of Pu-239/240 as a function of particle size in soils collected downwind of the Trinity site in New Mexico. In several instances the concentrations on particle sizes of 105 μm (0.041 in.) or less were greater than those in larger size classes, although exceptions were observed. In both of these studies, however, contaminant concentrations in the suspendable fractions were less than those in the total soil, yielding enhancement factors less than 1.0.

The data summarized above present a mixed picture with respect to the magnitude of the enhancement factor. Lacking definitive information it was decided to assign this parameter a triangular distribution with minimum, most likely, and maximum values of 1.0, 1.5, and 2.0, respectively. This distribution generally encompasses the data discussed by Pinder and McLeod (1989), White et al. (1981), and Livens and Baxter (1988), but ignores the possibility raised by Nyhan et al. (1976a, 1976b) that enhancement factors may be less than 1.0 under some conditions. An enhancement factor of 1.5 was adopted for the deterministic modeling.

5.8.8 Plant Interception Fraction and Coefficient

The plant interception fraction specifies the fraction of particulates deposited on plant surfaces that is initially retained by the crops. The NCRP (1984) cites default values of 0.20 and 0.25 for the interception fraction for vegetable crops and pasture grass, respectively, while the RESRAD code (ANL, 2001) uses 0.25 as a default value for all vegetation types. Miller (1980) reviewed a number of studies and found interception fractions for pasture grass ranging from 0.02 to 0.82 for wet and dry deposition. Interception fractions following the dry deposition of particulates ranged from 0.06 to 1.2 for peanut, squash, soybean, and sorghum plants; the majority of the values were 0.49 or less. The values greater than 1 were attributed to the bush-like form of the plants in combination with the experimental methods used to estimate interception fraction.

The GoldSim models estimate the plant interception fraction as a function of agricultural productivity using Equation 57 (Section 3.6.3.3). This equation was taken from Ng et al. (1978),

who adopted a value of 3.0 m^2/kg for the interception coefficient, μ. Using this coefficient, the ranges of agricultural productivities discussed above, and the best estimates of dry-to-wet-weight fractions provided earlier yields plant interception factors of about 0.2 to 0.4 for leafy vegetables and produce, 0.4 to 0.9 for grain, and 0.3 to 0.9 for pasture grass.

Peterson (1983) provides interception fractions for four grasses exposed to simulated fallout particles; these fractions range from 0.69 to 0.82 for vegetative productivities of 0.4 to 0.8 kg/m^2 (0.08 to 0.16 lb/ft^2) (dry weight). Peterson also cites work performed by Chamberlain (1970) who relates the interception fraction to the dry forage density using an equation similar in form to that developed by Ng et al. (1978). Values for the interception coefficient were found to range from 2.3 to 3.3 m^2/kg (11.2 to 16.1 ft^2/lb) for various forage crops. Other investigations cited in Peterson had values of μ ranging from 1.3 to 18.2 m^2/kg (6.4 to 89 ft^2/lb) for common varieties of leafy vegetables, produce, and grass. Pinder et al. (1988) estimated the interception coefficient for grass canopies using data collected by other investigators. A value of 2.9 m^2/kg (14.2 ft^2/lb) was estimated when the data from several studies were combined; estimates of the interception coefficient for the individual studies ranged from 2.3 to 3.3 m^2/kg (11.2 to 16.1 ft^2/lb).

Baes et al. (1984) used models to estimate interception fractions as a function of vegetation coverage and productivity. One model estimates interception fractions for leafy vegetables on the basis of the ground surface area covered by vegetation. This model was used to predict time-weighted average and maximum interception fractions of 0.15 and 0.39, respectively. These values account for the change in plant coverage with growth, and are weighted to address a range of leafy vegetables. When the same general approach was applied to exposed produce (i.e., three types of fruit grown on trees, snap beans, and tomatoes), an interception fraction of 0.052 was estimated. Baes et al. (1984) also developed equations similar in form to Equation 57 and used data collected by Hoffman and Baes (1979) to estimate an interception coefficient of 2.88 m^2/kg (14.1 ft^2/lb) for pasture grass on a dry-weight basis. Interception coefficients of 0.085 and 0.032 m^2/kg (0.4 to 0.16 ft^2/lb) (wet-weight basis) were estimated for leafy vegetables and exposed produce, respectively, based on alternate sources of data. When these coefficients are applied to the ranges of agricultural productivities discussed in Section 5.8.4, the resulting interception fractions range from about 0.1 to 0.2 for leafy vegetables and 0.05 or less for exposed produce.

Interception coefficients are provided in IAEA (1994) for grass, wheat, and corn, taking into account several particle types and sizes. Mean coefficients range from 0.24 to 3.6 m^2/kg (1.2 to 17.6 ft^2/lb) for productivities expressed on a dry-weight basis, and from 0.46 to 9.6 m^2/kg (2.2 to 47 ft^2/lb) for use with wet-weight productivities.

The data cited above indicate a wide range of interception fractions and coefficients for pasture grass and food crops, both within and between studies. An interception coefficient of 3.0 m^2/kg

(14.7 ft^2/lb) was selected for use with productivities stated in terms of dry weight. This value was assumed to be the most likely value in a triangular distribution ranging from 2.0 to 4.0 m^2/kg (9.8 to 19.6 ft^2/lb), which is generally consistent with the information cited above.

5.8.9 Weathering Half-Life

The weathering half-life is the time needed to remove 50 percent of the contamination deposited on plant surfaces due to processes such as wind removal and washoff. Regulatory Guide 1.109 (NRC, 1977) assumes a weathering half-life of 14 days, a value that is frequently used as a default for radiological risk assessments. Miller and Hoffman (1982; cited in NCRP, 1984) indicate that weathering half-lives range from 4.5 to 34 days, depending upon the radionuclide and vegetation under consideration. Data provided for particulates on herbaceous vegetation indicate a median and mean of 17 and 19 days, respectively, and a geometric standard deviation of 1.6. Peterson (1983) discusses weathering half-lives due to wind that range from 1 to 23 days and half-lives due to washoff that range from 6 to 56 days, depending upon rainfall. Measured effective half-lives ranged from 2.7 to more than 30 days on various plant types.

The data reported by Miller and Hoffman (1982) for particulates were used to define the weathering half-life for the performance assessment and composite analysis. A best estimate of 17 days was adopted. This value was set equal to the geometric mean of a lognormal distribution having a geometric standard deviation of 1.6.

5.8.10 Animal Product Transfer Factor

Transfer factors for beef, milk, chicken, and eggs represent the fraction of the daily elemental intake in food that is transferred to a volume or mass of the food product. These factors were used in the performance assessment and composite analysis to estimate radionuclide concentrations in animal products resulting from the ingestion of contaminated forage or feed, water, and soil or grit. Several compilations of transfer factors exist in the literature, including those found in Baes et al. (1984), IAEA (1994), Napier et al. (2004), NCRP Report 129 (1999), and the NRC's Regulatory Guide 1.109 (1977). Many of the factors included in these compilations come from the same original sources; the authors have made various assumptions to estimate transfer factors for elements for which data are unavailable.

The transfer factors for beef and milk found in Napier et al. (2004) were adopted as point estimates of these parameters for the performance assessment and composite analysis. This source addresses a comprehensive list of elements and draws on more recent data than some of the other compilations. While NCRP Report 129 (1999) is of a similar vintage, the transfer factors included in that reference were selected in a more conservative manner to serve as screening values. In fact, the majority of the transfer factors listed in that report are greater than those found in two or more of the other compilations.

The beef and milk transfer factors adopted from Napier et al. (2004) were used to represent the geometric means of lognormal distributions (Table 41). Geometric standard deviations of 3.0 and 2.5 were adopted for the beef and milk transfer factors, respectively. These values are consistent with the maximum standard deviations adopted by the NCRP (1999) and other sources of data. The NCRP used geometric standard deviations ranging from 1.2 to 2.8 for beef and from 1.6 to 2.5 for milk. NCRP Report 76 (1984) noted that, in general, the variability of beef transfer factors derived from stable element concentrations in unassociated meat and vegetation is characterized by geometric standard deviations ranging from 1.3 to 3.8. The NCRP report cites a study by Little (1979) who found transfer factors for cesium in beef to be lognormally distributed, with a geometric standard deviation of 2.3. Hoffman (1979), also cited in the NCRP report, found that milk transfer factors for strontium, iodine, and cesium were lognormally distributed, and had geometric standard deviations of 1.6 to 1.8.

There is considerably less information available to characterize transfer factors for chicken and eggs. Perhaps the most complete compilation is found in Napier et al. (2004); this reference was used to define transfer factors for most elements. The point estimates found in this report were adopted for the deterministic modeling, and adopted as the geometric means of lognormal distributions. The geometric standard deviations of these distributions were estimated based on the assumption that the first and ninety-ninth percentiles were 0.1 and 10 times the mean values. The implied ranges are generally consistent with, or greater than, those indicated for selected elements in the IAEA report (1994). The chicken and egg transfer factors used in the performance assessment and composite analysis are summarized in Table 42.

Animal product transfer factors were not included in Napier et al. (2004) for seven elements included in the performance assessment and composite analysis. These elements were aluminum, berkelium, krypton, lutetium, titanium, hydrogen, and carbon. Transfer factors for aluminum were set equal to the maximum factors for other elements in the same group, including gallium, indium, and thallium; the transfer factors for berkelium were set equal to those for americium. Krypton exists solely as a gas and was ignored in terms of food-chain transport. The animal-product transfer factors for lutetium were set equal to those for gadolinium, europium, and terbium, while the factors for titanium were assumed to be equal to the maximum of the factors listed for hafnium and zirconium.

Transfer factors for hydrogen, as H-3, and carbon, as C-14, were estimated using specific activity models. The animal product information needed to estimate the tritium transfer factors were taken from Napier et al. (1988). The water fractions of beef, milk, chicken, and eggs were set equal to 0.6, 0.88, 0.7, and 0.75, respectively. The fractional contents of hydrogen and carbon in several substances were needed to implement the specific activity models. The hydrogen fraction of water was set to 0.11 while the carbon fraction of all crops, including the pasture grass consumed by cows and cattle and the grain consumed by chickens, is 0.45 (dry-weight basis) The carbon fraction of soil was set to 0.03 and that of water was set to $2.0 \times 10\text{-}5$. The fractions of beef, milk, chicken, and eggs that are carbon are 0.6, 0.58, 0.67, and 0.6 (dry-weight basis), respectively.

Table 41
Parameter Values and Distributional Information for Beef and Milk Transfer Factors

Element	Forage-to-Beef Transfer Factor (d/kg)		Forage-to-Milk Transfer Factor (d/kg)	
	Geometric Mean	Geometric Standard Deviation	Geometric Mean	Geometric Standard Deviation
Ac	4.0E-04	3.0E+00	2.0E-05	2.5E+00
Ag	3.0E-03	3.0E+00	5.0E-05	2.5E+00
Al [a]	4.0E-02	3.0E+00	2.0E-03	2.5E+00
Am	4.0E-05	3.0E+00	1.5E-06	2.5E+00
Ba	2.0E-04	3.0E+00	4.8E-04	2.5E+00
Be	1.0E-03	3.0E+00	9.0E-07	2.5E+00
Bi	4.0E-04	3.0E+00	5.0E-04	2.5E+00
Bk [b]	4.0E-05	3.0E+00	1.5E-06	2.5E+00
C [c]	---	---	---	---
Ca	2.0E-03	3.0E+00	3.0E-03	2.5E+00
Cf	4.0E-05	3.0E+00	1.5E-06	2.5E+00
Cl	2.0E-02	3.0E+00	1.7E-02	2.5E+00
Cm	4.0E-05	3.0E+00	2.0E-05	2.5E+00
Co	1.0E-02	3.0E+00	3.0E-04	2.5E+00
Cs	5.0E-02	3.0E+00	7.9E-03	2.5E+00
Eu	2.0E-05	3.0E+00	3.0E-05	2.5E+00
Gd	2.0E-05	3.0E+00	3.0E-05	2.5E+00
H [c]	---	---	---	---
Ho	2.0E-05	3.0E+00	3.0E-05	2.5E+00
I	4.0E-02	3.0E+00	9.0E-03	2.5E+00
K	2.0E-02	3.0E+00	7.2E-03	2.5E+00
Kr	NA	NA	NA	NA
Lu [d]	2.0E-05	3.0E+00	3.0E-05	2.5E+00
Mo	1.0E-03	3.0E+00	1.7E-03	2.5E+00
Nb	3.0E-07	3.0E+00	4.1E-07	2.5E+00

Source: Napier et al. (2004)

NA = Not applicable; element exists solely as a gas and was ignored in terms of food-chain transport.

[a] Transfer factors for Al were set equal to the maximum of the factors for Ga, In, and Tl.

[b] Transfer factors for Bk were set equal to the factors for Am.

[c] Transfer factors for C and H were estimated using specific activity models; see discussion in text.

[d] Transfer factors for Lu were set equal to the corresponding factors for Gd, Eu, and Tb.

[e] Transfer factors for Ti were set equal to the maximum of the factors for Hf and Zr.

Table 41 (Continued)
Parameter Values and Distributional Information for Beef and Milk Transfer Factors

Element	Forage-to-Beef Transfer Factor (d/kg)		Forage-to-Milk Transfer Factor (d/kg)	
	Geometric Mean	Geometric Standard Deviation	Geometric Mean	Geometric Standard Deviation
Nd	2.0E-05	3.0E+00	3.0E-05	2.5E+00
Ni	5.0E-03	3.0E+00	1.6E-02	2.5E+00
Np	1.0E-03	3.0E+00	5.0E-06	2.5E+00
Os	4.0E-01	3.0E+00	5.0E-03	2.5E+00
Pa	4.0E-05	3.0E+00	5.0E-06	2.5E+00
Pb	4.0E-04	3.0E+00	2.6E-04	2.5E+00
Pm	2.0E-05	3.0E+00	3.0E-05	2.5E+00
Pu	1.0E-05	3.0E+00	1.1E-06	2.5E+00
Ra	9.0E-04	3.0E+00	1.3E-03	2.5E+00
Si	4.0E-05	3.0E+00	2.0E-05	2.5E+00
Sm	2.0E-05	3.0E+00	3.0E-05	2.5E+00
Sn	8.0E-02	3.0E+00	1.0E-03	2.5E+00
Sr	8.0E-03	3.0E+00	2.8E-03	2.5E+00
Tb	2.0E-05	3.0E+00	3.0E-05	2.5E+00
Tc	1.0E-04	3.0E+00	1.4E-04	2.5E+00
Th	4.0E-05	3.0E+00	5.0E-06	2.5E+00
Ti [e]	1.0E-03	3.0E+00	5.5E-07	2.5E+00
U	3.0E-04	3.0E+00	4.0E-04	2.5E+00
Zr	1.0E-06	3.0E+00	5.5E-07	2.5E+00

Source: Napier et al. (2004)

NA = Not applicable; element exists solely as a gas and was ignored in terms of food-chain transport.

[a] Transfer factors for Al were set equal to the maximum of the factors for Ga, In, and Tl.

[b] Transfer factors for Bk were set equal to the factors for Am.

[c] Transfer factors for C and H were estimated using specific activity models; see discussion in text.

[d] Transfer factors for Lu were set equal to the corresponding factors for Gd, Eu, and Tb.

[e] Transfer factors for Ti were set equal to the maximum of the factors for Hf and Zr.

Table 42
Parameter Values and Distributions for Chicken and Egg Transfer Factors

Element	Forage-to-Chicken Transfer Factor (d/kg)		Forage-to-Egg Transfer Factor (d/kg)	
	Deterministic Value	Distribution [a]	Deterministic Value	Distribution [a]
Ac	6.0E-03	6.0E-04, 6.0E-03, 6.0E-02	4.0E-03	4.0E-04, 4.0E-03, 4.0E-02
Ag	2.0E+00	2.0E-01, 2.0E+00, 2.0E+01	5.0E-01	5.0E-02, 5.0E-01, 5.0E+00
Al [b]	8.0E-01	8.0E-02, 8.0E-01, 8.0E+00	1.0E+00	1.0E-01, 1.0E+00, 1.0E+01
Am	6.0E-03	6.0E-04, 6.0E-03, 6.0E-02	4.0E-03	4.0E-04, 4.0E-03, 4.0E-02
Ba	9.0E-03	9.0E-04, 9.0E-03, 9.0E-02	9.0E-01	9.0E-02, 9.0E-01, 9.0E+00
Be	4.0E-01	4.0E-02, 4.0E-01, 4.0E+00	2.0E-02	2.0E-03, 2.0E-02, 2.0E-01
Bi	9.8E-02	9.8E-03, 9.8E-02, 9.8E-01	2.6E-01	2.6E-02, 2.6E-01, 2.6E+00
Bk [c]	6.0E-03	6.0E-04, 6.0E-03, 6.0E-02	4.0E-03	4.0E-04, 4.0E-03, 4.0E-02
C [d]	---	---	---	---
Ca	4.0E-02	4.0E-03, 4.0E-02, 4.0E-01	4.0E-01	4.0E-02, 4.0E-01, 4.0E+00
Cf	6.0E-03	6.0E-04, 6.0E-03, 6.0E-02	4.0E-03	4.0E-04, 4.0E-03, 4.0E-02
Cl	3.0E-02	3.0E-03, 3.0E-02, 3.0E-01	2.7E+00	2.7E-01, 2.7E+00, 2.5E+01
Cm	6.0E-03	6.0E-04, 6.0E-03, 6.0E-02	4.0E-03	4.0E-04, 4.0E-03, 4.0E-02
Co	2.0E+00	2.0E-01, 2.0E+00, 2.0E+01	1.0E-01	1.0E-02, 1.0E-01, 1.0E+00
Cs	3.0E+00	3.0E-01, 3.0E+00, 3.0E+01	4.0E-01	4.0E-02, 4.0E-01, 4.0E+00
Eu	2.0E-03	2.0E-04, 2.0E-03, 2.0E-02	4.0E-05	4.0E-06, 4.0E-05, 4.0E-04

Source: Napier et al. (2004)

NA = Not applicable; element exists solely as a gas and was ignored in terms of food-chain transport.

[a] Distribution designations are triangular; values represent minimum, most likely, maximum.

[b] Transfer factors for Al were set equal to the maximum of the factors for Ga, In, and Tl.

[c] Transfer factors for Bk were set equal to the factors for Am.

[d] Transfer factors for C and H were estimated using specific activity models, see discussion in text.

[e] Transfer factors for Lu were set equal to the corresponding factors for Gd, Eu, and Tb.

[f] Transfer factors for Ti were set equal to the maximum of the factors for Hf and Zr.

Table 42 (Continued)
Parameter Values and Distributions for Chicken and Egg Transfer Factors

Element	Forage-to-Chicken Transfer Factor (d/kg)		Forage-to-Egg Transfer Factor (d/kg)	
	Deterministic Value	Distribution [a]	Deterministic Value	Distribution [a]
Gd	2.0E-03	2.0E-04, 2.0E-03, 2.0E-02	4.0E-05	4.0E-06, 4.0E-05, 4.0E-04
H [d]	---	---	---	---
Ho	2.0E-03	2.0E-04, 2.0E-03, 2.0E-02	4.0E-05	4.0E-06, 4.0E-05, 4.0E-04
I	5.0E-02	5.0E-03, 5.0E-02, 5.0E-01	3.0E+00	3.0E+00, 3.0E+00, 2.5E+01
K	4.0E-01	4.0E-02, 4.0E-01, 4.0E+00	1.0E+00	1.0E-01, 1.0E+00, 1.0E+01
Kr	NA	NA	NA	NA
Lu [e]	2.0E-03	2.0E-04, 2.0E-03, 2.0E-02	4.0E-05	4.0E-06, 4.0E-05, 4.0E-04
Mo	1.8E-01	1.8E-02, 1.8E-01, 1.8E+00	9.0E-01	9.0E-02, 9.0E-01, 9.0E+00
Nb	3.0E-04	3.0E-05, 3.0E-04, 3.0E-03	1.0E-03	1.0E-04, 1.0E-03, 1.0E-02
Nd	2.0E-03	2.0E-04, 2.0E-03, 2.0E-02	4.0E-05	4.0E-06, 4.0E-05, 4.0E-04
Ni	1.0E-03	1.0E-04, 1.0E-03, 1.0E-02	1.0E-01	1.0E-02, 1.0E-01, 1.0E+00
Np	6.0E-03	6.0E-04, 6.0E-03, 6.0E-02	4.0E-03	4.0E-04, 4.0E-03, 4.0E-02
Os	8.4E-02	8.4E-03, 8.4E-02, 8.4E-01	7.1E-02	7.1E-03, 7.1E-02, 7.1E-01
Pa	6.0E-03	6.0E-04, 6.0E-03, 6.0E-02	4.0E-03	4.0E-04, 4.0E-03, 4.0E-02
Pb	8.0E-01	8.0E-02, 8.0E-01, 8.0E+00	1.0E+00	1.0E-01, 1.0E+00, 1.0E+01
Pm	2.0E-03	2.0E-04, 2.0E-03, 2.0E-02	2.0E-02	2.0E-03, 2.0E-02, 2.0E-01

Source: Napier et al. (2004)

NA = Not applicable; element exists solely as a gas and was ignored in terms of food-chain transport.

[a] *Distribution designations are triangular; values represent minimum, most likely, maximum.*

[b] *Transfer factors for Al were set equal to the maximum of the factors for Ga, In, and Tl.*

[c] *Transfer factors for Bk were set equal to the factors for Am.*

[d] *Transfer factors for C and H were estimated using specific activity models, see discussion in text.*

[e] *Transfer factors for Lu were set equal to the corresponding factors for Gd, Eu, and Tb.*

[f] *Transfer factors for Ti were set equal to the maximum of the factors for Hf and Zr.*

Table 42 (Continued)
Parameter Values and Distributions for Chicken and Egg Transfer Factors

Element	Forage-to-Chicken Transfer Factor (d/kg)		Forage-to-Egg Transfer Factor (d/kg)	
	Deterministic Value	Distribution [a]	Deterministic Value	Distribution [a]
Pu	3.0E-03	3.0E-04, 3.0E-03, 3.0E-02	5.0E-04	5.0E-05, 5.0E-04, 5.0E-03
Ra	3.0E-02	3.0E-03, 3.0E-02, 3.0E-01	3.1E-01	3.1E-02, 3.1E-01, 3.1E+00
Si	8.0E-01	8.0E-02, 8.0E-01, 8.0E+00	1.0E+00	1.0E-01, 1.0E+00, 1.0E+01
Sm	2.0E-03	2.0E-04, 2.0E-03, 2.0E-02	4.0E-05	4.0E-06, 4.0E-05, 4.0E-04
Sn	8.0E-01	8.0E-02, 8.0E-01, 8.0E+00	1.0E+00	1.0E-01, 1.0E+00, 1.0E+01
Sr	8.0E-02	8.0E-03, 8.0E-02, 8.0E-01	2.0E-01	2.0E-02, 2.0E-01, 2.0E+00
Tb	2.0E-03	2.0E-04, 2.0E-03, 2.0E-02	4.0E-05	4.0E-06, 4.0E-05, 4.0E-04
Tc	3.0E-02	3.0E-03, 3.0E-02, 3.0E-01	3.0E+00	3.0E-01, 3.0E+00, 2.5E+01
Th	6.0E-03	6.0E-04, 6.0E-03, 6.0E-02	4.0E-03	4.0E-04, 4.0E-03, 4.0E-02
Ti [f]	6.0E-05	6.0E-06, 6.0E-05, 6.0E-04	2.0E-04	2.0E-05, 2.0E-04, 2.0E-03
U	1.0E+00	1.0E-01, 1.0E+00, 1.0E+01	1.0E+00	1.0E-01, 1.0E+00, 1.0E+01
Zr	6.0E-05	6.0E-06, 6.0E-05, 6.0E-04	2.0E-04	2.0E-05, 2.0E-04, 2.0E-03

Source: Napier et al. (2004)

NA = Not applicable; element exists solely as a gas and was ignored in terms of food-chain transport.

[a] Distribution designations are triangular; values represent minimum, most likely, maximum.

[b] Transfer factors for Al were set equal to the maximum of the factors for Ga, In, and Tl.

[c] Transfer factors for Bk were set equal to the factors for Am.

[d] Transfer factors for C and H were estimated using specific activity models, see discussion in text.

[e] Transfer factors for Lu were set equal to the corresponding factors for Gd, Eu, and Tb.

[f] Transfer factors for Ti were set equal to the maximum of the factors for Hf and Zr.

5.8.11 Animal Food, Water, and Soil Ingestion Rates

Radionuclide concentrations in meat, milk, chicken, and eggs are proportional to the amount of contaminated material ingested by the respective animals. Cows and cattle were assumed to ingest forage crops (e.g., pasture grass) grown in contaminated soils, water drawn from the regional aquifer, and soil; chickens were assumed to eat contaminated feed, water, and grit. In terms of cow and cattle food consumption rates, Regulatory Guide 1.109 (NRC, 1977) lists a value of 50 kg/d (110 lb/d) (fresh weight), while the RESRAD code (ANL, 2001) uses default values of 55 and 68 kg/d (120 and 150 lb/d) for cows and cattle, respectively. NCRP Report 76 (1984) lists estimates of 16 and 12 kg/d (35 and 26 lb/d) (dry weight) for cows and cattle, respectively. Values tabulated by the IAEA (1994) include a default ingestion rate of 16.1 kg/d (35 lb/d) (dry weight) for cows, with a range of 10 to 25 kg/d (22 to 55 lb/d). A default value of 7.2 kg/d (16 lb/d) (dry weight) is given by the IAEA for 500 kg (1,100 lb) cattle, with a range of 5 to 10 kg/d (11 to 22 lb/d). A daily intake rate (dry weight) of 2.5 to 3 percent of the animal's live weight is commonly used to estimate range requirements for cows and cattle (e.g., Lyons et al., 1999; Pratt and Rasmussen, 2001). Assuming an average animal weight of 600 kg (1,300 lb), these percentages yield intake rates ranging from 15 to 18 kg/d (33 to 40 lb/d) (dry weight).

The forage intake rates provided by the IAEA (1994) for cows were adopted for the performance assessment and composite analysis. The value of 16 kg/d (35 lb/d) (dry weight) was used in the deterministic modeling, while the range was used to define the end points of a triangular distribution. The intake rates listed in IAEA (1994) for cattle appear to be low in comparison to the other sources cited above. Consequently, the value of 12 kg/d (26 lb/d) (dry weight) reported by the NCRP (1984) was adopted for the deterministic modeling. A triangular distribution with minimum and maximum values of 7.5 and 18 kg/d (16 and 40 lb/d) (dry weight) was assumed for this parameter; this range is generally consistent with the information cited above.

Regulatory Guide 1.109 (NRC, 1977) estimates rates of water intake for cows and cattle at 60 and 50 L/d (15 and 13 gal/d), respectively. The RESRAD computer code (ANL, 2001) uses the NRC value for cattle as a default, but assumes 160 L/d (40 gal/d) for cows. This value for cows includes a base consumption rate of 50 L/d (13 gal/d) and water required to produce approximately 40 L (10 gal) of milk per day. Ng et al. (1978) adopt water consumption rates of 60 and 38 L/d (15 and 10 gal/d) for cows and cattle, respectively. Oak Ridge National Laboratory risk assessment guidance (ORNL, 1999) cites default values of 75 L/d (20 gal/d) for cows and 50 L/d (13 gal/d) for cattle, while the IAEA (1994) lists ranges of 50 to 100 L/d (13 to 26 gal/d) for cows and 20 to 60 L/d (5 to 15 gal/d) for beef cattle. Based on this information, triangular distributions were adopted to define water intake rates. The water consumption rate for cows was defined using minimum and maximum values of 50 and 100 L/d (13 and 26 gal/d), while corresponding values of 20 and 60 L/d (5 and 15 gal/d) were adopted for cattle. These values approximate the ranges of the data listed above, but exclude the additional intake used by

the RESRAD code to account for milk production. The midpoints of these ranges were used to define the most likely values of the distributions, and were used as best estimates for the deterministic modeling.

Oak Ridge National Laboratory risk assessment guidance (ORNL, 1999) cites a number of studies concerned with rates of soil ingestion by cows and cattle. Smith (1977) estimates an ingestion rate of 0.25 to 0.5 kg/d (0.55 to 1.1 lb/d) for cattle; McKone and Ryan (1989) summarize six studies and report mean ingestion rates of 0.39 and 0.41 kg/d (0.86 to 0.90 lb/d) for cattle and cows, respectively. Zach and Mayoh (1984) suggest that soil ingestion rates may range from 0.1 to 2.2 kg/d (0.2 to 5 lb/d), while Mayland et al. (1977) report rates of 0.73 and 0.99 kg/d (1.6 to 2.2 lb/d) in June and August, respectively. The ORNL guidance notes that soil ingestion rates for cows and cattle are generally assigned default values of 1 kg/d (2.2 lb/d), while the RESRAD code (ANL, 2001) uses a default soil ingestion rate of 0.5 kg/d (1.1 lb/d). Studies cited in IAEA (1994) add to this information. Healy (1968) quoted soil intake equivalent to 4 to 8 percent of herbage intake, while Beresford and Howard (1991) gave intake rates ranging from 2 to 4 percent. Based on work conducted by Zach and Mayoh (1984) and Green and Dodd (1988), the IAEA report suggests a soil intake rate equal to 6 percent of forage intake (dry weight) for grazing cattle. Using the point estimates adopted above for food intake (i.e., 16.1 and 12 kg/d [35 and 25 lb/d] [dry weight] for cows and cattle, respectively), a soil intake rate of 6 percent represents soil ingestion rates of about 1 and 0.7 kg/d (2.2 and 1.5 lb/d).

A single distribution based on the data cited above was used to describe soil ingestion for cows and cattle. The distribution was assumed to be triangular with minimum, most likely, and maximum values of 0.4, 1.0, and 2.2 kg/d (0.9, 2.2, and 5 lb/d). The most likely value of 1.0 kg/d (2.2 lb/d) was used for the deterministic modeling.

Limited information exists with respect to food, water, and soil ingestion rates for chickens. The IAEA report (1994) lists an expected food intake rate of 0.1 kg/d (0.2 lb/d) (dry weight) for laying hens, with a range of 0.07 to 0.15 kg/d (0.15 to.33 lb/d) (dry weight). Food intake rates for chickens include an expected value of 0.07 kg/d (0.15 lb/d) (dry weight) and a range of 0.05 to 0.15 kg/d (0.11 to 0.33 lb/d) (dry weight). These data were used to define a triangular distribution with minimum, most likely, and maximum values of 0.05, 0.07, and 0.15 kg/d (0.11, 0.15, and 0.33 lb/d) (dry weight). Water intake rates ranging from 0.1 to 0.3 L/d (0.03 to 0.08 gal/d) for laying hens and chickens are listed in IAEA (1994). These values were used to define the end points of a triangular distribution; the most likely value of this distribution was set to 0.2 L/d (0.05 gal/d). In a study cited by the ORNL guidance report (1999), 2 percent grit by weight in the diet is thought to be optimum for digestion in chickens (NRC, 1994). Therefore, grit intake was estimated by multiplying the food intake by 0.02.

5.9 Biotic Intrusion Model Parameters

The biotic intrusion modeling conducted in support of the performance assessment and composite analysis considers the potential for plants and animals to intrude into the disposed waste and, subsequently, to transport radioactive contamination to the surface of the disposal facility. A variety of parameters are required to simulate rates of intrusion into the waste by the plant and animal communities inhabiting the closed site. The sources of information used to develop point estimates and distributions for these parameters are discussed below.

5.9.1 Time to Climax

The potential impacts of biotic intrusion depend upon the plant and animal communities present at the site. These communities are expected to change over time as the site transitions from a landscape dominated by grasses and forbs at the time of closure to piñon-juniper woodland that is characteristic of the undisturbed portions of MDA G. The time required for the site to transition to a fully functioning piñon-juniper woodland community is referred to here as the time to climax.

The length of time required for the site to pass from the early stages of succession to a climax condition depends upon conditions at the disposal site, many of which are difficult to predict with certainty. However, information gathered by Arnold et al. (1964) provides some insight into the temporal aspects of succession in these communities. These investigators compared transect measurements from burned areas to measurements taken in adjacent unburned piñon-juniper stands at three locations in northern Arizona. Measurements were taken in 1954, approximately 70 to 90 years after the fires had occurred. At a site that had been burned about 80 years prior, tree canopy intercept was about 0.1 percent of that in the adjacent unburned areas; intercepts of mid-grasses and shrub cover were 2.8 and 5.8 times greater in the burned area than in the adjacent mature woodland. Tree cover in 70- and 90-year-old burns was 12 and 15 percent of the cover measured in adjacent unburned communities, while grasses and shrubs were still much more abundant in the burned areas.

Based on the data from Arnold et al. (1964), it appears that considerably more than 100 years will be required to establish mature piñon-juniper woodland at MDA G. This conclusion is supported by published studies and informal analyses specific to MDA G. Tress and Klopatek (1987) estimated the rate of succession in piñon-juniper woodlands in north-central Arizona based on several postfire communities. Based on crown cover estimates, it was estimated that slightly more than 200 years would be required for the community to return to pre-burn conditions. Longer periods of time for recovery were indicated by other measures of community structure. Ludwig et al. (1977, cited in Schott and Pieper, 1987) evaluated rates of recovery for northern New Mexico piñon-juniper communities that had been bulldozed and estimated that full recovery of the tree canopy would require at least 100 years.

Koniak (1985) examined vegetation recovery in burned piñon-juniper woodlands located in Nevada and California. Trees began to recolonize the sites 20 to 30 years after the fires, but cover was still minimal after 60 years. Work cited by Koniak suggests that trees will rapidly increase in density and cover from this point onward, and will dominate the sites within 100 to 150 years after burning. Barney and Frischknecht (1974) examined postfire vegetation changes in the piñon-juniper type of west-central Utah. They found tree density (numbers) was greater in 86-year-old burn areas than in areas that had been undisturbed for more than 100 years. However, crown cover and basal area in the 86-year-old burns were about 50 and 25 percent, respectively, of the corresponding quantities in the 100-year-old-plus communities. Miller and Tausch (2001) cite information indicating tree densities in northern Arizona piñon-juniper woodlands have increased significantly in the past 100 to 200 years, even in stands with trees in excess of 300 years old. These results suggest the transition to climax woodland requires from 100 to several hundred years to complete. Consistent with these observations, Grier et al. (1992) observed tree canopy cover in a 350-year-old piñon juniper woodland in northern Arizona that was about twice the cover estimated for a 90-year-old woodland. Finally, Gallegos (1999) simulated the passage of MDA G to piñon-juniper woodland for a preliminary assessment of surface erosion rates at the site. The initial appearance of trees at the site varied for different parts of the site. Trees were projected to appear in areas adjacent to the disposal pits first, showing up 30 to 40 years after closure. The appearance of trees over closed pits was projected to require 40 to 50 years. Much longer periods of time will be required for trees to fully populate the site.

Based on the information summarized above, it appears the time at which climax will likely be attained may be in the range of 100 to several hundred years. On this basis, a triangular distribution was developed to define the time to climax. Minimum, most likely, and maximum values of 100, 200, and 300 years were adopted, values which are in general agreement with the cited studies. The most likely value was used for the deterministic modeling.

5.9.2 Shape Factors

The functions used to define the distributions of root mass and burrows with depth are series of curves defined using beta distributions (see Section 3.1.2). The shape of these functions is determined by the shape factors. For both sets of curves, the alpha-shape factor is assigned a constant value of zero while the beta-shape factor is assigned a discrete distribution wherein values of 1.5, 2, 3, 4, 5, 6, 7, and 9 have equal probabilities of being sampled.

5.9.3 Maximum Rooting Depth

Plant root distributions estimate the mass of plant roots as a function of depth below the ground surface. These distributions are used to estimate the portions of the plant root systems that penetrate into the disposed waste; the amount of contamination deposited on the surface of

disposal site due to litterfall is ultimately determined by the fraction of the root system contacting the waste. Maximum rooting depths are used in conjunction with root distribution functions to model the root distributions for grasses, forbs, shrubs, and trees.

Foxx et al. (1984) reviewed the rooting characteristics of native and crop plants within the U.S., focusing their efforts on 53 species of plants found on LLW disposal sites at the Laboratory. Based on this review, they constructed a database of plant rooting depths, and used this information to estimate rooting depth distributions for individual plant species. Table 43 summarizes the rooting depths estimated by Foxx et al. for a variety of grasses, forbs, shrubs, and trees. Measurements of plant rooting depths taken at the Laboratory are provided in Tierney and Foxx (1987); these data are summarized in Table 44 along with other literature-based rooting depths given in Tierney and Foxx. More recently, Canadell et al. (1996) and Jackson et al. (1999) conducted literature reviews and measured maximum rooting depths. With few exceptions, the maximum rooting depths reported by these investigators for the plant species that inhabit LANL disposal sites are within the rooting depth ranges developed by Foxx et al. (1984).

The rooting data reported by Foxx et al. (1984) and Tierney and Foxx (1987) were used to develop distributions of maximum rooting depths for grasses, forbs, and shrubs. In general, minimum and maximum values of triangular distributions were defined using the rooting depth ranges reported for each growth form; the medians of the datasets were used to define the most likely values. For the distribution of maximum rooting depth in grasses, this approach yields minimum, most likely, and maximum values of 0.76, 1.7, and 4.0 m (2.5, 5.6, and 13 ft), respectively. The corresponding values for forbs are 0.3, 2.4, and 9.1 m (1.0, 7.9, and 30 ft) and those for shrubs are 1.4, 2.9, and 9.1 m (4.6, 9.5, and 30 ft). The rooting depth data for alfalfa were modified prior to defining the distribution for forbs. Specifically, the two highest rooting depths reported for this species (i.e., 19 and 39 m (62 and 130 ft) were eliminated, leaving a maximum rooting depth of 9.1 m (30 ft) for the species. The eliminated data were from plants associated with mine shafts, which represent conditions that are not relevant to MDA G.

Relatively few data exist to define the distribution of maximum rooting depths for trees. Information provided by Foxx et al. (1984) and Tierney and Foxx (1987) suggest maximum depths are generally about 6 m (20 ft) for piñon pine and one-seed juniper. Although Foxx et al. (1984) found a rooting depth of 61 m (200 ft) for juniper, Tierney and Foxx (1987) estimated rooting depths of 1.1 to 1.7 m (3.6 to 5.6 ft) for three species of pine and juniper trees. For modeling purposes, a triangular distribution was defined using minimum, most likely, and maximum values of 2, 6, and 10 m (6.6, 20, and 33 ft), respectively. The range of the distribution generally coincides with the cited data and with estimates of maximum rooting depths for *Pinus* spp. (e.g., Canadell et al., 1996), but omits the extreme rooting depth noted by Foxx et al. (1984). The most likely value is approximately equal to the rooting depths of 5.8 and 6.4 m (19 and 21 ft) cited in Foxx et al. (1984) for the one-seed juniper and the 6.4 m (21 ft) rooting depth cited by the same authors for piñon pine.

Table 43
Literature-Based Rooting Depths for Grasses, Forbs, Shrubs, and Trees Growing at Los Alamos National Laboratory

Growth Form and Common Name	Scientific Name	Rooting Depth (cm)	
		Average	Range
Grasses			
Blue Grama	*Bouteloua gracilis*	1.2E+02	3.8E+01 – 4.0E+02
Bluegrass	*Poa* spp.	8.8E+01	3.5E+01 – 2.1E+02
Brome Grass	*Bromus inermis*	2.0E+02	1.7E+02 – 2.3E+02
Buffalo Grass	*Buchloe dactyloides*	1.6E+02	4.6E+01 – 2.1E+02
Downy Chess	*Bromus tectorum*	7.0E+01	3.0E+01 – 1.1E+02
Fescue	*Festuca* spp.	7.8E+01	5.0E+00 – 1.5E+02
Indian Rice Grass	*Oryzopsis hymenoides*	8.4E+01	4.5E+01 – 1.2E+02
June Grass	*Koeleria cristata*	5.8E+01	3.0E+01 – 7.6E+01
Little Bluestem	*Andropogon scoparius*	1.7E+02	7.1E+01 – 2.7E+02
Mountain Muhly	*Muhlenbergia montana*	9.1E+01	2.0E+01 – 1.4E+02
Needle-and-Thread	*Stipa comata*	1.1E+02	6.3E+01 – 1.7E+02
Sand Dropseed	*Sporobolus crypandrus*	9.9E+01	9.1E+01 – 1.2E+02
Sideoats Grama	*Bouteloua curtipendula*	2.2E+02	7.6E+01 – 4.0E+02
Three-Awn	*Aristida* spp.	1.1E+02	7.6E+01 – 1.5E+02
Western Wheatgrass	*Agropyron smithii*	1.5E+02	6.8E+01 – 3.1E+02
Forbs			
Alfalfa	*Medicago sativa*	6.9E+02	3.8E+01 – 3.9E+03
Aster	*Aster* spp.	1.5E+02	1.5E+01 – 3.4E+02
Blazing Star	*Mentzelia* spp.	5.8E+01	1.1E+01 – 1.5E+02
Buckwheat	*Erigonum* spp.	1.7E+02	6.4E+01 – 3.1E+02
Cinquefoil	*Potentilla* spp.	1.1E+02	5.3E+01 – 2.3E+02
Estafiata	*Artemisia frigida*	1.0E+02	4.6E+01 – 2.4E+02
Evening Primrose	*Oenothera* spp.	2.1E+02	5.3E+01 – 3.1E+02
False Tarragon	*Artemisia dracunculus*	2.1E+02	—
Gayfeather	*Liatris punctata*	3.1E+02	1.2E+02 – 4.8E+02
Globe Mallow	*Spheralcea* spp.	2.6E+02	8.0E+01 – 4.0E+02
Goldenaster	*Chrysopsis villosa*	2.8E+02	1.3E+02 – 4.0E+02
Goldenrod	*Solidago* spp.	2.6E+02	1.1E+02 – 3.4E+02
Goldenweed	*Haplopappus* spp.	2.9E+02	1.1E+02 – 5.2E+02

Source: Foxx et al., 1984

— = Only one rooting depth was provided; as a result no range is specified.

Table 43 (Continued)
Literature-Based Rooting Depths for Grasses, Forbs, Shrubs, and Trees Growing at Los Alamos National Laboratory

Growth Form and Common Name	Scientific Name	Rooting Depth (cm)	
		Average	Range
Groundsel	*Senecio* spp.	1.1E+02	3.0E+01 – 1.5E+02
Indian Paintbrush	*Castilleja* spp.	2.8E+01	2.5E+01 – 3.0E+01
Lamb's Quarter	*Chenopodium album*	1.2E+02	—
Penstemon	*Penstemon* spp.	1.3E+02	3.6E+01 – 3.1E+02
Pigweed	*Amaranthus* spp.	1.0E+02	1.0E+01 – 2.4E+02
Pingue	*Hymenoxys richardsonii*	9.0E+01	—
Prairie Clover	*Petalostemon* spp.	1.7E+02	8.5E+01 – 2.1E+02
Puccoon	*Lithospermum* spp.	2.2E+02	1.8E+02 – 3.1E+02
Russian Thistle	*Salsola kali var tenuifolia*	6.7E+01	—
Summer Cypress	*Kochia scoparia*	2.0E+02	—
Sweetclover	*Melilotus* spp.	1.3E+02	8.5E+01 – 1.5E+02
Vetch	*Vicia* spp.	8.0E+01	2.0E+01 – 1.4E+02
Yucca	*Yucca* spp.	1.1E+02	3.0E+01 – 2.1E+02
Shrubs and Subshrubs			
Apache Plum	*Fallugia paradoxa*	1.2E+02	6.0E+01 – 1.4E+02
Big Sagebrush	*Artemisia tridentate*	2.5E+02	1.1E+02 – 9.1E+02
Chamisa	*Chrysothamnus nauseosus*	2.9E+02	1.0E+02 – 4.6E+02
Four-Wing Saltbush	*Atriplex canescens*	3.9E+02	1.1E+02 – 7.6E+02
Gambel's Oak	*Quercus gambelli*	2.4E+02	8.0E+01 – 4.0E+02
Mountain Mahogany	*Cercocarpus montanus*	1.1E+02	4.0E+01 – 1.5E+02
Snakeweed	*Gutierrezia* spp.	1.2E+02	5.1E+01 – 2.4E+02
Wild rose	*Rosa* spp.	3.9E+02	9.1E+01 – 6.4E+02
Trees			
Elm	*Ulmus pumila*	1.3E+02	—
One-Seed Juniper	*Juniperus monosperma*	2.4E+03	5.8E+02 – 6.1E+03
Piñon Pine	*Pinus edulis*	6.4E+02	—
Ponderosa Pine	*Pinus ponderosa*	4.5E+02	1.0E+01 – 2.4E+03

Source: Foxx et al., 1984

— = Only one rooting depth was provided; as a result no range is specified.

Table 44
Measured, Estimated, and Literature-Based Plant Rooting Depths for Plants at Los Alamos National Laboratory

Growth Form and Common Name	Scientific Name	Rooting Depth Ranges(cm)		
		Measured	Estimated [a]	Literature-Based
Grasses				
Blue Grama	*Bouteloua gracilis*	5.3E+01 – 5.8E+01	---	3.8E+01 – 4.0E+02
Forbs				
Mullein	*Verbascum thapsus*	2.8E+01 – 4.2E+01	---	NA
Narrowleaf Yucca	*Yucca angustissima*	2.0E+01	---	4.0E+01 – 1.5E+02
Prickly pear	*Opuntia polyacantha*	8.0E+00 – 2.8E+01	---	2.0E+00 – 3.7E+02
Sunflower	*Helianthus petiolaris*	4.0E+01 – 4.5E+01	---	NA
Shrubs and Subshrubs				
Apache Plum	*Fallugia paradoxa*	6.0E+01 – 1.3E+02	1.7E+02 – 2.9E+02	NA
Big Sagebrush	*Artemisia tridentata*	1.0E+01 – 1.5E+02	1.3E+02 – 1.8E+02	1.1E+02 – 9.1E+02
Chamisa	*Chrysothamnus nauseosus*	1.0E+02 – 1.8E+02	1.4E+02 – 2.1E+02	1.0E+02 – 4.6E+02
Four-Wing Saltbush	*Atriplex canescens*	6.0E+01 – 1.1E+02	1.9E+02 – 2.2E+02	8.0E+01 – 7.6E+02
Mountain Mahogany	*Cercocarpus montanus*	4.0E+01 [b]	5.0E+01 [b]	4.0E+01 – 1.5E+02
New Mexico Locust	*Robinia neomexicana*	1.0E+02 – 1.4E+02	---	NA
Oak	*Quercus* spp.	4.5E+01 – 1.0E+02	1.5E+02 – 3.2E+02	8.0E+01 – 4.0E+02
Snakeweed	*Gutierrezia sarothrae*	6.0E+01 – 1.3E+02	1.7E+02 – 2.9E+02	5.1E+01 – 2.4E+02
Squawberry	*Rhus trilobata*	1.5E+02 – 1.7E+02	2.1E+02 – 2.3E+02	NA
Wax Currant	*Ribes cereum*	7.0E+01 – 1.5E+02	8.0E+01 – 2.9E+02	NA
Trees				
One-Seed Juniper	*Juniperus monosperma*	1.5E+02 [b]	1.7E+02 [b]	5.8E+02 – 6.1E+03
Piñon Pine	*Pinus edulis*	3.0E+01 – 6.0E+01	1.1E+02 – 1.3E+02	NA
Ponderosa Pine	*Pinus ponderosa*	1.3E+02 – 1.5E+02	1.5E+02 – 1.6E+02	1.0E+01 – 2.4E+03

Source: Tierney and Foxx (1987)

--- = Indicates no root depths were estimated for the species.

NA = Not applicable; no range in rooting depths was reported.

[a] Estimated root lengths are provided for roots that broke during excavation and roots that could not be completely excavated due to safety considerations and/or the soil profile.

[b] No range is provided either because all root length measurements were the same length or because only a single measurement of root length was collected.

5.9.4 Aboveground Biomass Density

Litter generated by leaf fall and plant death contributes to soil formation as the organic matter decays; radionuclides that are assimilated by the plants will also enter into the soil. The rate at which organic material is added to surface soils is a function of the aboveground biomass of the plant and the fraction of this biomass that becomes litter. Estimates of aboveground biomass were developed using growth-form-specific information in the literature; these estimates addressed the site during early succession and after the piñon-juniper climax condition was attained. The studies upon which these estimates are based are discussed below.

Estimates of understory biomass for the early successional stages at MDA G were based on information from several different sites. These sites included piñon-juniper woodlands that had been disturbed by fire or physical means, piñon-juniper grasslands, and areas adjacent to mature woodlands. Although the conditions at MDA G are not expected to exactly coincide with the conditions at any one of these sites, understory production data obtained from these communities are expected to provide reasonable estimates of conditions at the disposal site.

Direct measurements of aboveground production of grasses, forbs, and shrubs were found for a number of sites in the western U.S.; those used to develop biotic intrusion modeling data are summarized in Table 45. Clary (1989) evaluated the production of grasses, forbs, and shrubs on areas that had been disturbed by chaining and cabling 2 to 30 years prior. The treated areas were reseeded with a mix of grass and forb species after chaining or cabling; seeding would also be undertaken at MDA G after the final cover was constructed. Average yields across the four sites and the 4 years in which measurements were conducted were 570 kg/ha (510 lb/ac) for grasses, 33 kg/ha (30 lb/ac) for forbs, and 76 kg/ha (70 lb/ac) for shrubs. Clary (1971) evaluated understory production prior to and following the cabling of piñon-juniper woodland located in northern Arizona. Yields of grasses, forbs, and shrubs averaged 250, 480, and 380 kg/ha (220, 425, and 340 lb/ac), respectively, 4 to 11 years after cabling and seeding had occurred.

Dwyer and Pieper (1967) measured production of grasses and forbs in burned and unburned areas on piñon-juniper rangeland in south-central New Mexico. The unburned area was largely free of trees and, as such, was considered to be a reasonable approximation of MDA G in its early successional stages. The data for the site, collected over a 3-year period, indicated an average production of about 890 kg/ha (800 lb/ac) for grasses and 140 kg/ha (125 lb/ac) for forbs.

Additional work conducted by Pieper (1968) in south-central New Mexico examined the effects of grazing on herbage production in piñon-juniper grasslands. Aboveground production ranged from 680 to 730 kg/ha (600 to 650 lb/ac) on two open grassland areas that were protected from grazing; grass production on two grazed areas ranged from 330 to 620 kg/ha (290 to 550 lb/ac). The basal cover was 9.4 to 12 percent at the two ungrazed sites, and 9.6 to 14 percent at the sites that had been grazed. Grasses accounted for 81 to 98 percent of the total plant cover. O'Rourke and Ogden (1969) evaluated

Table 45
Summary of Cover and Production Studies Used to Estimate Aboveground Biomass (early successional stages at MDA G)

Community Characteristics	Reference	Cover (%)			Aboveground Production (kg/ha)		
		Grasses	Forbs	Shrubs	Grasses	Forbs	Shrubs
Piñon-Juniper Woodland in Central Utah (4 sites)	Clary, 1989	—	—	—	2.9E+02 – 7.7E+02	0 – 1.0E+02	7.9E+00 – 1.8E+02
Piñon-Juniper Woodland in Northern Arizona (4 plots, 4 – 11 years after cabling and seeding)	Clary, 1971	—	—	—	2.5E+02 (avg.)	4.8E+02 (avg.)	3.8E+02 (avg.)
Piñon-Juniper Woodland in Arizona (22 plots)	Clary and Jameson, 1981	—	—	—	1.1E+03 (avg.)	2.8E+02 (avg.)	1.1E+02 (avg.)
Piñon-Juniper Rangeland in South-central New Mexico (3 transects)	Dwyer and Pieper, 1967	1.3E+01 – 2.7E+01	1.7E-01– 8.7E-01	NA	8.1E+02 – 1.0E+03	7.1E+02 – 2.4E+03	NA
Piñon-Juniper Rangeland in Southcentral New Mexico (2 ungrazed sites)	Pieper, 1968	7.6E+00 – 1.1E+01, (basal cover)	3.0E-01 – 1.8E+00	NA	6.8E+02 and 7.3E+02 (total herbage)		
(2 grazed sites)		9.2E+00 – 1.4E+01 (basal cover)			3.3E+02 and 6.2E+03 (total herbage)		
Piñon-Juniper Woodland in Northern Arizona	O'Rourke and Ogden, 1969	1.4E+01 – 2.4E+01 (perennial basal cover) 1.0E+00 – 1.4E+01 (annual basal cover)	1.2E+00 – 5.6E+00	Statistically similar to cover for woodland (3.0E-01 – 2.1E+00)	2.8E+01 – 3.9E+03 (perennial grasses)	NA	NA
Grasslands Surrounding Piñon-Juniper Woodlands in Arizona (sites without trees)	Arnold et al., 1964	3.7E+00 (mean basal cover)	5.0E-01 (mean basal cover)	3.9E+00 (mean canopy cover)	7.0E+02		
Piñon-juniper rangeland in south-central New Mexico	Pieper, 1990	—	—	—	9.0E+02 – 1.1E+03 (areas with 10% tree cover; three species of grass accounted for 7.0E+02 – 8.5E+02 kg/ha of this amount)		
Piñon-Juniper Woodland Sites Converted to Grassland (5 sites)	Aro, 1971	—	—	—	5.6E+02 – 1.5E+03	NA	NA

— = Measurements were not performed.

NA = Not applicable; growth form was not considered in the study.

the effects of piñon-juniper control on herbage (i.e., grasses and forbs) production at four woodland sites in north-central Arizona. The 2-year study included measurements of mean basal cover of grass, forbs, and shrubs in areas that had been cleared of trees 4 to 5 years prior and grazed for a total of 4 months over a 2-year period; perennial grass production was also measured. Perennial grass cover ranged from 14 to 24 percent, cover for annual grasses ranged from 1 to 14 percent over the four sites. The mean basal cover for forbs ranged from 1.2 to 5.6 percent while the cover for shrubs ranged from 0.3 to 2.1 percent. Total production of perennial grasses ranged from 28 to 390 kg/ha (25 to 350 lb/ac).

Aro (1971) evaluated the effectiveness of converting piñon-juniper woodland to grassland using a variety of techniques, including chaining, chaining followed by windrowing, and fire. Approximately 50 sites that had undergone tree removal prior to 1963 were examined; among the data collected at these sites were yields of grasses. A yield of 560 kg/ha (500 lb/ac) was observed at one site in Colorado following chaining, while yields at sites that had been windrowed ranged from 560 to over 1,100 kg/ha (500 to over 980 lb/ac). Yields at three sites that had been burned ranged from 560 to over 1,450 kg/ha (500 to over 1,300 lb/ac).

Arnold et al. (1964) developed estimates of total herbage yields for piñon-juniper woodlands as a function of tree canopy intercept. Yields were about 700 kg/ha (625 lb/ac) of air-dry vegetation in areas that were free of trees, but dropped to about 400 kg/ha (350 lb/ac) for areas with 10 percent tree canopy cover. Pieper (1990) conducted an analysis similar to that of Arnold et al. for piñon-juniper woodland in south-central New Mexico. A yield of about 1,060 kg/ha (945 lb/ac) of grasses and forbs was predicted for areas without trees; production was estimated to decrease to 900 kg/ha (800 lb/ac) for areas with tree cover of 10 percent. Three species of grass accounted for 80 percent of the total production, with other grasses and forbs accounting for the remainder. Clary and Jameson (1981) measured production in piñon-juniper woodland, before and after overstory removal, on 22 plots at 11 sites. Production of grasses, forbs, and shrubs was measured 4, 6, and 8 years after vegetation was killed by girdling and sawing the trees and through herbicide use. Production of grasses averaged 1,050 kg/ha (935 lb/ac) over the 3 years of measurements, while forbs and shrub production averaged 275 and 114 kg/ha (250 and 100 lb/ac), respectively.

The studies summarized above were used to develop distributions of aboveground biomass for grasses, forbs, and shrubs for MDA G while it is in the early stages of succession; Table 46 lists the data adopted from these investigations. Pieper's 1968 production estimates were divided between grasses and forbs based on percent cover of each growth form, while his 1990 estimate for "other grasses and forbs" was assumed to represent forbs. The median of each growth form's production data was used to define the most likely values of the triangular distributions, while the minimum and maximum values were defined using the ranges. The most likely values were used for the deterministic modeling. The distributions of aboveground biomass are summarized in Table 14. The sum of the median grass and forbs production data is less than the overall production estimates of 700 and 1,060 kg/ha (625 and 945 lb/ac) reported by Arnold et al. (1964) and Pieper (1990), respectively.

Table 46
Aboveground Production of Grasses, Forbs, and Shrubs
(early successional stages of piñon-juniper cover types)

Study	Aboveground Production (kg/ha, dry weight)		
	Grasses	Forbs	Shrubs
Clary, 1989			
Church Hills Site – 1982	3.9E+02	9.5E+01	1.8E+02
Church Hills Site – 1985	4.3E+02	1.0E+02	8.5E+01
Clay Springs Site – 1980	2.9E+02	3.7E+01	7.5E+01
Clay Springs – 1985	4.9E+02	2.0E+01	2.0E+01
Eight Mile Site No. 1 – 1980			
Side Slope	7.7E+02	3.4E+00	1.3E+01
Ridge Crest	4.1E+02	1.5E+01	8.6E+01
Eight Mile Site No. 1 – 1982			
Side Slope	5.6E+02	1.1E+00	2.4E+01
Ridge Crest	4.1E+02	3.8E+01	1.1E+02
Eight Mile Site No. 1 – 1985			
Side Slope	7.1E+02	0.0E+00	7.9E+00
Ridge Crest	5.5E+02	1.5E+01	5.8E+01
Eight Mile Site No. 2 – 1980			
Side Slope	6.3E+02	1.7E+01	4.5E+01
Ridge Crest	5.7E+02	1.6E+01	4.2E+01
Eight Mile Site No. 1 – 1981			
Side Slope	6.9E+02	4.7E+01	1.2E+02
Ridge Crest	7.7E+02	1.9E+01	1.2E+02
Eight Mile Site No. 1 – 1985			
Side Slope	7.6E+02	8.6E+01	1.5E+02
Ridge Crest	6.7E+02	2.2E+01	8.1E+01
Clary, 1971	2.5E+02	4.8E+02	3.8E+02
Dwyer and Pieper, 1967			
Unburned Site – 1964	8.1E+02	7.1E+01	---
Unburned Site – 1965	1.0E+03	2.4E+02	---

--- = Indicates no estimate of production was available for growth form.

[a] Production was presented in the report as total herbage (i.e., grass and forbs) production. These yields were divided between grasses and forbs based on percent cover.

Table 46 (Continued)
Aboveground Production of Grasses, Forbs, and Shrubs
(early successional stages of piñon-juniper cover types)

Study	Aboveground Production (kg/ha, dry weight)		
	Grasses	Forbs	Shrubs
Unburned Site – 1966	8.5E+02	1.1E+02	—
Pieper, 1968			
Loamy Bottomland – Ungrazed	6.2E+02[a]	6.0E+01 [a]	—
Loamy Upland - Ungrazed	5.9E+02[a]	1.4E+02 [a]	—
O'Rourke and Ogden, 1969			
Boundary Site – 1961	2.0E+02	—	—
Boundary Site – 1962	1.8E+02	—	—
Ryan Site – 1961	2.8E+01	—	—
Ryan Site – 1962	1.3E+02	—	—
Second Site – 1961	2.0E+02	—	—
Second Site – 1962	2.2E+02	—	—
Chevelon Site – 1961	3.9E+02	—	—
Chevelon Site – 1962	3.9E+02	—	—
Pieper, 1990	8.5E+02	2.1E+02	—
Clary and Jameson, 1981	1.1E+03	2.8E+02	1.1E+02
Aro, 1971			
Colorado Site	5.6E+02	—	—
Windrowed Site No. 1	5.6E+02	—	—
Windrowed Site No. 2	1.1E+03	—	—
Fire Site No. 1	5.6E+02	—	—
Fire Site No. 2	6.7E+02	—	—
Fire Site No. 3	1.5E+03	—	—

— = Indicates no estimate of production was available for growth form.

[a] Production was presented in the report as total herbage (i.e., grass and forbs) production. These yields were divided between grasses and forbs based on percent cover.

Biomass estimates for grasses, forbs, and shrubs in the mature piñon-juniper woodland were developed in a manner similar to that described above for the disturbed site. The data used to generate these estimates are summarized in Table 47, which includes a description of the sites that were investigated and a summary of the production and cover information that was taken from the reports. Some of these studies provide direct estimates of understory production in the mature woodland. Clary (1971) studied the effects of tree removal on herbage yields in piñon-juniper woodlands in northern Arizona. Herbage yields of grasses, forbs, and shrubs averaged 71, 77, and 100 kg/ha/yr (63, 68, and 90 lb/ac), respectively, in areas where no trees were removed. In other work, Clary (1989) reported yields ranging from 20 to 140 kg/ha (20 to 125 lb/ac) for grasses, 10 to 45 kg/ha (9 to 40 lb/ac) for forbs, and 30 to 130 kg/ha (26 to 115 lb/ac) for shrubs in mature piñon-juniper woodlands in central Utah. Clary and Jameson (1981) measured production in piñon-juniper woodland on 22 plots at 11 sites, piñon-juniper crown cover ranged from 0 to 43 percent with a median value of about 17 percent. Production of grasses, forbs, and shrubs averaged 100, 46, and 216 kg/ha (90, 40, and 190 lb/ac), respectively, at these locations.

Pieper (1968) estimated total herbage production and cover in piñon-juniper rangeland located in south-central New Mexico. Aboveground production was 630 kg/ha (560 lb/ac) at an ungrazed piñon-juniper community with grass understory, while production on a grazed site was 530 kg/ha 470 lb/ac). Grasses accounted for about 98 percent of the total vegetation at both sites. O'Rourke and Ogden (1969) measured the basal cover of grass, forbs, and shrubs at four undisturbed woodland sites in north-central Arizona; the canopy cover of trees and perennial grass production were also evaluated. Perennial grass cover ranged from 8 to 21 percent over the 2-year study, while the cover for annual grasses ranged from 0 to 0.3 percent. The mean basal cover for shrubs ranged from 0.3 to 2.1 percent and the canopy cover for trees ranged from 13 to 44 percent. Total production of perennial grasses ranged from about 60 to 230 kg/ha (53 to 200 lb/ac).

Aro (1971) measured grass yields of about 110 kg/ha (100 lb/ac) at two sites prior to their conversion from woodland to grassland, and approximately 30 and 220 kg/ha (26 and 195 lb/ac) at two other pretreatment sites. As discussed earlier, Arnold et al. (1964) developed a relationship between total herbage yield and tree canopy intercept (shown in Figure 19a). Clary (1971) developed a similar relationship between tree cover and total understory production (i.e., grasses, forbs, and shrubs) in his work in northern Arizona (Figure 19b); Pieper (1990) related canopy cover to total herbage production for woodlands in New Mexico (Figure 19c).

Table 47
Summary of Cover and Production Studies Used to Estimate Understory Biomass (MDA G climax condition)

Community Characteristics	Reference	Cover (%)				Aboveground Production (kg/ha)		
		Grasses	Forbs	Shrubs	Trees	Grasses	Forbs	Shrubs
Piñon-Juniper Woodland in Northern Arizona (4 plots)	Clary, 1971	---	---	---	1.0E+01 – 4.5E+01 (crown cover)	7.1E+01 (4-year avg.)	7.7E+01 (4-year avg)	1.0E+02 (4-year avg.)
Piñon-Juniper Woodland in Central Utah (2 sites)	Clary, 1989	---	---	---	---	2.0E+01 – 1.4E+02	1.0E+01 – 4.5E+01	3.0E+01 – 1.3E+02
Piñon-Juniper Woodland in Arizona (22 plots)	Clary and Jameson, 1981	---	---	---	0E+00 – 4.3E+01 (crown cover)	1.0E+02 (avg)	4.6E+01 (avg)	7.0E+01 (avg)
Piñon-Juniper Rangeland in South-Central New Mexico (grazed and ungrazed sites)	Pieper, 1968	1.2E+01 – 1.8E+01 (basal cover)	1.3E+00 – 1.7E+00 (basal cover for forbs and other vegetation)			5.3E+02 (total herbage, grazed site) 6.3E+02 (total herbage, ungrazed site)		
Piñon-Juniper Woodland in North-Central Arizona (4 sites)	O'Rourke and Ogden, 1969	8.0E+00 – 2.2E+01 (perennial basal cover) 1E+00 – 2E+00 (annual basal cover)	0E+00 – 0.3E+00 (mean basal cover)	0.3E+00 – 2.1E+00 (mean basal cover)	1.3E+01 – 4.4E+01 (mean crown cover)	6.0E+01 – 2.3E+02 (perennial grasses)	NA	NA
Piñon-Juniper Woodland Sites, Western U.S. (4 sites)	Aro, 1971	---	---	---	---	3.0E+01 – 2.2E+02	NA	NA
Piñon-Juniper Woodland Communities in Northern Arizona	Arnold et al., 1964	---	---	---	---	Estimates of total herbage production as a function of tree canopy cover		

--- = Cover measurements were not performed.

NA = Not applicable; growth-form was not considered in the study.

Figure 19
Relationship between Canopy Cover and Herbage Yields

The production data of Clary (1971, 1989), Clary and Jameson (1981), Pieper (1968), O'Rourke and Ogden (1969), and Aro (1971) were used to generate distributions for aboveground production for grasses, forbs, and shrubs in mature piñon-juniper woodland. Table 48 lists the data estimated on the basis of these studies. Pieper's production estimates for ungrazed sites were divided between grasses and forbs based on the percent cover measurements provided in that study. Perennial grass production data provided by O'Rourke and Ogden were adjusted upward to account for the contributions from annual grasses. The most likely values of the triangular distributions were defined using the medians of the growth-form production data; minimum and maximum values were defined on the basis of the ranges. The medians of the distributions were used for the deterministic modeling. The biomass distributions are summarized in Table 14. The median productivities suggest a woodland community with crown cover of approximately 30 to 45 percent based on the relationships developed by Arnold et al. (1964) and Clary (1971) (Figure 19a and 19b). This is consistent with work by Padien and Lajtha (1992) that suggests the total canopy cover at MDA G may be about 37 to 50 percent after the site has transitioned to a piñon-juniper community. In contrast, the median productivities suggest a woodland canopy cover of approximately 85 percent based on the relationship developed by Pieper (1990) (Figure 19c).

Limited information exists with respect to the aboveground biomass of trees in piñon-juniper woodlands. Grier et al. (1992) estimated aboveground biomass and aboveground net productivity for 90- and 350-year-old piñon-juniper communities in northern Arizona. Tree biomass was estimated using regression equations developed from destructive analysis of the two tree species, taking into account the full diameter range of trees found at the study sites. Net productivity was estimated as the sum of the annual biomass increment and litterfall.

The estimates developed by Grier et al. (1992) are summarized in Table 49. Total tree biomass of the 350-year-old woodland was 2.3 times greater than that estimated for the 90-year-old stand. These biomass estimates fall at the low end of the range reported for piñon-juniper woodlands in other regions. Meeuwig (1979), cited in Grier et al., reported aboveground biomass for Great Basin woodlands consisting of singleleaf piñon (*Pinus monophylla*) and Utah juniper (*Juniperus osteosperma*) ranging from 60 to 121 Mg/ha (27 to 54 T/ac). The oldest trees in these stands were about 320 and 260 years old, respectively. Grier et al. observed that the productivities measured in the northern Arizona piñon-juniper communities are also low compared to most other forests and woodlands in North America. Though limited in nature, the information provided in Grier et al. was used to develop the distribution for aboveground biomass in trees. A triangular distribution was assumed and assigned minimum and maximum values of 2.3×10^4 and 1.2×10^5 kg/ha (2.0×10^4 and 1.1×10^5 lb/ac), respectively. These values represent the tree biomass estimated by Grier et al. for the young piñon-juniper stand and the maximum biomass reported by Meeuwig. The biomass estimate developed by Grier et al. for the mature woodland, 5.3×10^4 kg/ha (4.7×10^4 lb/ac), was adopted for the most likely value and used in the deterministic modeling.

Table 48
Aboveground Production of Grasses, Forbs, and Shrubs in Mature Piñon-Juniper Woodlands

Study	Aboveground Production (kg/ha, dry weight)		
	Grasses	Forbs	Shrubs
Clary, 1971	7.1E+01	7.7E+01	1.0E+02
Clary, 1989			
Church Hills Site – 1980	4.7E+01	4.5E+01	5.7E+01
Church Hills Site – 1982	1.4E+02	1.6E+01	1.3E+02
Church Hills Site – 1985	7.7E+01	3.5E+01	7.2E+01
Clay Springs Site – 1980	2.0E+01	1.0E+01	3.0E+01
Clary and Jameson, 1981	1.0E+02	4.6E+01	7.0E+01
Pieper, 1968	6.2E+02	1.1E+01	---
O'Rourke and Ogden, 1969			
Boundary Site – 1961	2.5E+02	---	---
Boundary Site – 1962	1.7E+02	---	---
Ryan Site – 1961	9.8E+01	---	---
Ryan Site – 1962	2.1E+02	---	---
Second Site – 1961	1.0E+02	---	---
Second Site – 1962	6.7E+01	---	---
Chevelon Site – 1961	1.6E+02	---	---
Chevelon Site – 1962	9.4E+01	---	---
Aro, 1971			
Colorado Site	2.8E+01	---	---
Fire Site No. 1	1.1E+02	---	---
Fire Site No. 2	1.1E+02	---	---
Fire Site No. 3	2.2E+02	---	---

--- = No production measurements were conducted for the indicated growth form.

Table 49
Aboveground Biomass and Net Primary Productivity Estimates for Trees in Piñon-Juniper Woodlands

Component	90-Year-Old Stand			350-Year-Old Stand		
	Piñon Pine	Juniper	Total	Piñon Pine	Juniper	Total
Biomass (Mg/ha, dry weight)						
Canopy						
Foliage	2.7E+00	1.7E+00	4.4E+00	2.4E+00	3.3E+00	5.7E+00
Foliage-Bearing Twigs	1.6E+00	1.6E-01	1.7E+00	1.0E+00	4.1E-01	1.4E+00
Living Branches (incl. bark)	6.5E+00	4.2E+00	1.1E+01	1.3E+01	1.5E+01	2.9E+01
Dead Branches	6.9E-01	2.7E-01	9.6E-01	2.2E+00	1.4E+00	3.5E+00
Stem (wood and bark)	3.4E+00	1.5E+00	4.9E+00	7.2E+00	6.5E+00	1.4E+01
Total	1.5E+01	7.9E+00	2.3E+01	2.6E+01	2.7E+01	5.3E+01
Productivity (Mg/ha/yr, dry weight)						
Biomass Increment						
Living Wood	2.0E-01	5.0E-02	2.5E-01	3.2E-01	1.1E-01	4.3E-01
Attached Dead Material	2.0E-02	Trace	2.0E-02	7.0E-02	1.0E-02	8.0E-02
Bark	4.0E-02	1.0E-02	5.0E-02	6.0E-02	2.0E-02	8.0E-02
Foliage Production	7.0E-01	4.5E-01	1.2E+00	9.0E-01	8.2E-01	1.7E+00
Total			1.5E+00			2.3E+00
Litterfall			3.0E-02			5.0E-02

Source: Grier et al. (1992)

5.9.5 Litter Production Rate

The litter production rate is defined as the fraction of the aboveground biomass that dies and falls to the ground surface on an annual basis. Insight into the litter production rates of grasses and forbs may be gained by using the biomass distribution data collected by Grier et al. (1992) and Cox (1984). Grier et al. measured biomass distribution in young and mature stands of piñon-juniper in north-central Arizona. Those investigators found that standing dead material accounted for approximately 40 percent of the interspace (i.e., between trees) vegetation biomass during the growing season; the dominant species growing in these areas was blue grama (*Bouteloua gracilis*), a perennial grass. Cox (1984) found that standing dead matter accounted for at least 26 to 72 percent of the biomass in a perennial grassland community in southeast Arizona. Sims and Singh (1978) evaluated mass transfers among various biotic compartments for 10 North American grasslands; one such transfer was the passage, during the growing season, of live material to standing dead material. The results of the study indicated that 2 to 100 percent of the live matter was incorporated into the standing dead compartment.

Scurlock et al. (2003) summarized biomass data collected from 31 grassland sites located around the world. Eight of the sites are in the U.S. and include a high mountain meadow, dry and humid temperate steppes, and a subtropical semidesert steppe. The data collected for all but the high mountain meadow were used to estimate the fraction of the aboveground biomass consisting of dead material. Fractions for these seven sites ranged from 0.0 to 1.0, with a median fraction of about 0.5; similar results were observed for the dry temperate steppes, which are expected to have vegetation most like that at MDA G shortly after closure.

The data for standing dead matter cited above may be used to estimate rates of litter production for grasses and forbs if it is assumed that the subject woodland and grassland communities have been under steady-state conditions and that all aboveground biomass has died each year. Under these conditions, the litter production rate may be estimated as the complement of the fraction of the aboveground biomass that is standing dead matter. Using this approach, litter production rates of 0.28/yr to 0.74/yr are estimated using the data of Cox (1984), while a rate of 0.6/yr is calculated using the data from Grier et al. (1992). The data of Scurlock et al. (2003) yield litter production rates that range from 0/yr to 1.0/yr, with a median production rate of 0.5/yr. Sims and Singh (1978) indicate litter production rates of 0/yr to 0.98/yr.

Other estimates of litter production rates may be developed using biomass accumulation ratios. This ratio is the dry-weight biomass divided by the annual net primary productivity. Whittaker (1975) provides ranges of the accumulation ratio (for aboveground parts of plants) for different terrestrial communities; normal ranges are from 2 to 10 in the desert, 1 to 3 in grasslands, 3 to 12 in shrublands, 10 to 30 in woodlands, and 20 to 50 in mature forests. Assuming the plant community is under steady-state conditions, the inverse of these ratios estimates the fraction of

the aboveground biomass that goes into annual litter production. Using this approach and the data provided by Whittaker for grasslands, it is estimated that 33 to 100 percent of the aboveground biomass of grasses and forbs will enter into annual litter production. Separately, Rodin and Bazilevich (1967, cited in Strojan et al., 1979) note that 45 to 60 percent of the above- and belowground biomass in grasslands becomes litter each year.

The litter production rate for grasses and forbs was assigned a triangular distribution using the data summarized above. The minimum and maximum values of the distribution were set to 0.3/yr and 1.0/yr, and the most likely value was set to 0.6/yr. The range of this distribution is consistent with the rates estimated using the data from Cox (1984) and the biomass accumulation ratios published by Whittaker (1975), but it does not capture the low end of the distribution indicated using the data published by Scurlock et al. (2003) and Sims and Singh (1978). The most likely value of 0.6/yr is consistent with the findings of Grier et al. (1992) and Rodin and Bazilevich (1967). The same distribution was assumed to apply to grasses and forbs in the grassland and piñon-juniper woodland communities.

Litter production in shrubs has been investigated on a number of occasions. Strojan et al. (1979) collected litter from six shrub species in the northern Mojave Desert. Their results indicate that 7 to 83 percent of live aboveground biomass was shed annually as litter; the fraction of aboveground biomass going to litter was typically less than 60 percent. These investigators cite results from Charley and Cowling (1968) who estimated that approximately 46 percent of the aboveground biomass of bladder saltbush was converted to litter. West (1985) examined litter production in three species of shrubs found in northwestern Utah, the Great Basin sagebrush, shadscale, and white sage. Litterfall was found to average 10, 38, and 63 percent of the midsummer aboveground biomass.

Parmenter et al. (1987) cite studies conducted by West and Gunn (1974) and Mack (1977) that indicate 5.8 to 13.4 percent of the aboveground biomass of sagebrush in the Great Basin desert is converted to litter annually. Biomass accumulation ratios for shrublands may be used in the manner described above for grasslands to arrive at additional estimates of litter production rates. Using the data published by Whittaker (1975) suggests that 8 to 33 percent of the aboveground biomass of shrubs will enter into annual litter production.

The data cited above were used to construct a triangular distribution for the shrub litter production rate. The minimum and maximum values of the distribution were set to 0.06/yr and 0.60/yr; this range generally agrees with the data summarized above. The most likely value was set to 0.13/yr, which is equivalent to the litter production fraction observed by Mack (1977) and is the inverse of the midpoint of the bioaccumulation ratios cited by Whittaker (1975).

As discussed earlier, Grier et al. (1992) estimated aboveground biomass, net productivity, and litterfall for young and mature stands of piñon-juniper. The litter production rates estimated by Grier et al. are approximately 0.1 percent of the aboveground biomass estimates for the two woodland communities (see Table 49). This relative rate of production cannot be compared to data for other piñon-juniper woodlands because no such data were found. Nevertheless, it appears this production rate is significantly smaller than rates indicated for other forest communities. This conclusion is based on several lines of evidence.

Hinesley et al. (1991) measured litter production in four stands of oak-hickory-pine forests in northern Mississippi. Annual litter production ranged from 3 to 6.5 percent of the tree biomass, and was highest in the stands that were predominantly pine. Rodin and Bazilevich (1967, cited in Strojan et al., 1979) note that 1 to 4 percent of forest biomass is shed as litter. Whittaker (1975) reported that litter production in a young mixed deciduous forest in the northeastern U.S. was approximately 3.7 percent of the aboveground biomass. Whittaker also reported a range of biomass accumulation ratios of 10 to 30 for aboveground parts of plants in woodlands. These ratios are largely determined by the presence of trees in the communities. If it is assumed that these ratios remain relatively constant over time, taking the inverse of the ratios yields estimates of the portion of the biomass that goes into litter production each year. This calculation yields annual litter generation rates that are 3 to 10 percent of the aboveground biomass.

An indirect method of estimating the litter production fraction for trees considers the relative contributions of foliage to aboveground biomass and litter. Ricklefs (1979) reported that leaves comprise between 1 and 10 percent of the aboveground biomass of forests; evergreen forests tended to occupy the high end of this range. Grier et al. (1992) found that leaves were 11 and 19 percent of the total aboveground tree biomass in the two piñon-juniper woodlands they studied. In terms of litter, Williams and Gray (1974) indicate that leaf material accounts for approximately 70 percent of forest litter in gymnosperms.

Using an assumed lifetime for leaf material, the data cited above can be used to estimate litter production fractions. For example, using a life span of 3 years for the leaf material and the data from Grier et al. (1992), it is estimated that 3.7 to 6.3 percent of the aboveground tree biomass falls as leaf litter in a given year. However, if this litter comprises only 70 percent of the annual litterfall, as indicated by Williams and Gray (1974), the total annual litter production factor is around 5 to 9 percent. Annual litter production fractions ranging from 8 to 14 percent are estimated for a leaf material life span of 2 years, while fractions ranging from 4 to 7 percent are estimated using a leaf life span of 4 years.

The information provided above suggests annual litter production in coniferous forests may be about 1 to 14 percent of the aboveground biomass, much higher than the litter production fractions estimated by Grier et al. (1992). In the absence of data needed to confirm the results of

Grier et al. (1992), the 1 to 14 percent range was used to define the distribution for the parameter. A triangular distribution was defined with minimum and maximum values of 0.01/yr and 0.14/yr. The most likely value was set to 0.075/yr, the midpoint of this range, and was used for the deterministic modeling.

5.9.6 Litter Decomposition Half-Life

The rate at which litter decays to form soil will depend upon the climatic conditions under which decomposition occurs and the nature of the plant material. In general, rates of decomposition typically rise with increased temperature and moisture. For example, rates of decomposition tend to be greater in warm, moist tropical forests than in a more temperate, arid environment such as that found at LANL. In terms of plant characteristics, wood is more resistant to decay than leaves, while evergreen leaves generally decompose more slowly than deciduous leaves. Based on these generalizations, it is reasonable to expect that litter from grasses and forbs will tend to decompose relatively quickly, while litter produced from shrubs and trees will take longer to decay.

Whittaker (1975) discusses litter decay in terms of the decomposition half-life, or the time needed for half of the original dry mass of litter to decompose. Half-lives for litter in grasslands, boreal conifer forests, and temperate deciduous forests were estimated at 2.8, 7.0, and 1.0 years, respectively. Koukoura et al. (2003) evaluated rates of litter decomposition in semiarid grassland in northern Greece. Rates of decay were characterized for three perennial grasses and an annual legume; separate estimates were developed for leaves and stems. The rate constants estimated for leaves indicated litter half-lives ranging from 1.0 to 1.8 years, while the data collected for the stems yielded half-lives ranging from 2.2 to 2.8 years. Shariff et al. (1994) reported average annual litter decomposition rates of 12 to 22 percent for ungrazed arid grassland in North Dakota, yielding decomposition half-lives of around 3 to 6 years. Millar (1974) cites work by others in which 10 or more years were required for *Pinus* needles to reach the humus layer of the soil.

Murphy et al. (1998) examined rates of litter decomposition at five sites along an elevational gradient in northern Arizona. These sites include Great Basin Desert scrub, piñon-juniper woodland, ponderosa pine forest, and transition zones between these communities. Litter decomposition rates were measured for leaf litter collected from ponderosa pine, piñon pine, one-seed juniper, and blue grama grass; and for leaves and stems from snakeweed. Based on these measurements, the investigators calculated annual decomposition rate constants for each species. Separate constants were estimated for the first and second years of the 2-year study.

The litter decomposition constants estimated by Murphy et al. (1998) for the five study sites are summarized in Table 50. Decomposition was greatest in the first year, as litter with the most favorable decay characteristics was consumed. Decay of more recalcitrant litter components proceeded at slower rates. If the rate of decay is assumed to remain constant over time, the rate constants for the first year of the study infer a litter half-life of 1.7 years for snakeweed, 2 years

for blue grama, and 3.3 years for piñon and juniper trees (averaged over the two species). Similarly, if the rate constants for the second year were assumed to be constant, litter half-lives for the shrub, grass, and tree species are 2.8, 5.4, and 4.7 years, respectively. Even longer half-lives may be anticipated for the more substantial woody litter from mature shrubs and trees.

Table 50
Litter Decomposition Rate Constants

Plant Species	Decomposition Rate Constant (/yr)	
	First Year	Second Year
Snakeweed	-4.2E-01	-2.5E-01
Blue Grama	-3.4E-01	-1.3E-01
One-Seed Juniper	-2.2E-01	-1.5E-01
Piñon Pine	-2.0E-01	-1.5E-01
Ponderosa Pine	-2.2E-01	-1.3E-01

Source: Murphy et al. (1998)

The data cited above suggest that litter generated from grasses, forbs, and the leaves of shrubs may require a minimum of 5 to 10 years to fully decompose, while the leaf material from piñon pine and juniper may require 15 years or more to fully decay. The time required for the woody litter from shrubs and trees may require longer still. A single, triangular distribution was adopted to describe the litter half-life for all growth forms. This distribution was assigned minimum and maximum values of 1 and 6 years, respectively; the most likely value of 2 years was used for the deterministic modeling.

5.9.7 Native Vegetation Plant Uptake Factor

The radionuclide plant uptake factors characterize the extent to which contaminants in the waste are taken up by the roots of native vegetation growing at MDA G. Authors such as Baes et al. (1984) suggest applying plant uptake factors for leafy vegetables to fresh forage such as grass; however, other information indicates that plant uptake factors for native plants may be greater than those observed for agricultural crops. Sheppard and Evenden (1997) have shown that native plants have higher cesium uptake factors than agricultural crops. Wirth (1999) compared uptake factors for plants growing in arid and semiarid climates to those for agricultural crops and found native species had mean uptake factors that were one to two times greater than those for crops.

There are relatively few data available to characterize plant uptake for native species. Given this, the plant uptake factors provided in NCRP Report 129 (1999) for grass and fodder were adopted for the biotic intrusion modeling. Uptake factors for leafy vegetables were taken from Napier et al. (2004) for elements that were not included in the NCRP report; the factor for tritium was estimated using the specific activity model described earlier. In adopting this approach, it was assumed that patterns of

plant uptake in grasses will more nearly approximate those in native vegetation, relative to agricultural crops. In fact, these factors are typically larger than those adopted for agricultural crops and generally agree with the plant uptake factors reported by Wirth (1999) for selected elements. These values, shown in Table 51, were assumed to represent the geometric means of lognormal distributions. A geometric standard deviation of 3.5 was assumed for all elements, consistent with the geometric standard deviation selected for the lognormal distributions of uptake factors for crops.

5.9.8 Maximum Burrow Depth

Maximum burrowing depths for harvester ants, various species of mice, pocket gophers, chipmunks, and ground squirrels are used to model burrow distributions with depth for these species. Limited information exists on the burrowing habits of animals; several studies relevant to the performance assessment and composite analysis are summarized below.

McKenzie et al. (1982) provide burrow distributions with depth for several species of burrowing animals. These data suggest a maximum burrowing depth of more than 2 m (6.6 ft) for harvester ants. Jensen and Hooten (2000) summarized burrowing depths of ant species inhabiting the transition desert and piñon-juniper communities at the Nevada Test Site. Those investigators noted that colonies of *Pogonomyrmex rugosa* have been observed to extend 3 to 4 m (9.8 to 13 ft) bgs (Wheeler and Wheeler, 1986), while colonies of *P. occidentalis* and *P. salinus* have been found to a depth of 2.7 m (8.8 ft) (Lavigne, 1969; Fitzner et al., 1979). All three of these species of ants occur in New Mexico.

Many species of mice use burrows abandoned by other species; others excavate new burrows. For example, silky pocket mice have been observed to use the abandoned burrows of kangaroo rats and pocket gophers (Best and Skupsi, 1994). Other species, such as the western harvest mouse, commonly build nests on the ground surface as well as nesting in burrows (Webster and Jones, 1982). Brush, deer, and piñon mice build their nests in a variety of locations including abandoned burrows, hollow branches, logs, rock crevices, and at the base of shrubs.

Mouse burrows generally extend to moderate depths. Best and Skupsi (1994) provide data suggesting the nests of the silky pocket mouse are generally 40 cm (16 in.) or less from the ground surface. MacMahon (1985) indicates that the burrows of this species are generally not more than 10 cm (3.9 in.) deep. A burrow excavated by a hispid pocket mouse (*Chaetodipus hispidus)* in Texas extended to a depth of about 40 cm (16 in.) (Davis and Schmidley, 1997); this species occurs in southern New Mexico. Reynolds and Laundre (1988) characterized the distribution of deer mouse burrows, finding that none of the 43 burrows examined extended deeper than 50 cm (20 in.). Winter burrows of the Great Basin pocket mouse have been noted to extend up to 1.8 m (2.6 ft) (Whitaker, 1980); Suter et al. (1993) and Cline et al. (1982, cited in Hakonson, 2002) list maximum depths of 1.4 and 1.9 m (4.6 and 6.2 ft), respectively, for this species. McKenzie et al. (1982) list a maximum burrowing depth of 2 m (6.6 ft) for pocket mice and kangaroo rats. Cline et al. (1982, cited in Hakonson, 2002) list a burrowing depth of 52 to 62 cm (20 to 24 in.) for the little pocket mouse (*Perognathus longmembris*).

Table 51
Parameter Values and Distributional Information for Native Plant Uptake Factors

Element	Geometric Mean [a]	Geometric Standard Deviation
Ac	4.0E-03	3.5E+00
Ag	1.0E-01	3.5E+00
Al	2.0E-02	3.5E+00
Am	4.0E-03	3.5E+00
Ba	1.0E-01	3.5E+00
Be	2.0E-02	3.5E+00
Bi	5.0E-01	3.5E+00
Bk	4.0E-03	3.5E+00
C	7.0E-01 [b]	3.5E+00
Ca	5.0E+00	3.5E+00
Cf	4.0E-03	3.5E+00
Cl	1.0E+02	3.5E+00
Cm	4.0E-03	3.5E+00
Co	2.0E+00	3.5E+00
Cs	2.0E-01	3.5E+00
Eu	5.0E-02	3.5E+00
Gd	5.0E-02	3.5E+00
H [c]	---	---
Ho	5.0E-02	3.5E+00
I	1.0E-01	3.5E+00
K	3.0E+00	3.5E+00
Kr [d]	---	---
Lu	1.5E-02	3.5E+00
Mo	4.0E-01	3.5E+00
Nb	1.0E-01	3.5E+00
Nd	5.0E-02	3.5E+00
Ni	1.0E+00	3.5E+00
Np	1.0E-01	3.5E+00
Os	2.0E-01	3.5E+00
Pa	5.0E-02	3.5E+00
Pb	9.0E-02	3.5E+00
Pm	5.0E-02	3.5E+00
Pu	1.0E-03	3.5E+00

[a] *Source: NCRP (1999) except as noted.*

[b] *Source: Napier et al. (2004).*

[c] *Plant uptake factors for tritium were estimated using a specific activity models; see discussion in text.*

[d] *Element exists solely as a gas and was ignored in terms of food-chain transport.*

Table 51
Parameter Values and Distributional Information for Native Plant Uptake Factors

Element	Geometric Mean [a]	Geometric Standard Deviation
Ra	2.0E-01	3.5E+00
Se	5.0E-01	3.5E+00
Si	1.0E-01	3.5E+00
Sm	5.0E-02	3.5E+00
Sn	1.0E+00	3.5E+00
Sr	4.0E+00	3.5E+00
Tb	5.0E-02	3.5E+00
Tc	4.0E+01	3.5E+00
Th	1.0E-03	3.5E+00
Ti	5.0E-03	3.5E+00
U	1.0E-01	3.5E+00
Zr	5.0E-03	3.5E+00

[a] *Source: NCRP (1999) except as noted.*

[b] *Source: Napier et al. (2004).*

[c] *Plant uptake factors for tritium were estimated using a specific activity models; see discussion in text.*

[d] *Element exists solely as a gas and was ignored in terms of food-chain transport.*

Information cited by Gonzales et al. (2000) indicates that the deeper portions of pocket gopher burrow systems typically occur at 0.5 to 1.5 m (1.6 to 4.9 ft) bgs. Some observations exist on the depth of burrowing in pocket gophers that are specific to LANL. Tierney and Foxx (1987) observed gopher burrows at depths of 95 to 110 cm (37 to 43 in.) during the excavation of plant roots. Gonzales et al. (1995) evaluated the impacts of pocket gopher burrowing on erosion using simulated waste covers. Pocket gopher activity extended to a depth of 1.5 m (4.9 ft) in that study. Results from a study conducted by Hakonson et al. (1982) indicate that gophers had not penetrated into waste below a 1.25-m (4.1-ft) cover over a 4-year period. McKenzie et al. (1982) list a maximum burrowing depth of 1 m (3.3 ft) for pocket gophers; Cline et al. (1982, cited in Hakonson, 2002) list burrowing depths ranging from 5 to 35 cm (2 to 14 in.) for valley and northern pocket gophers (*Thomomys bottae* and *T. talpoides*, respectively). In a summary of maximum reported burrow depths, Suter et al. (1993) list a burrowing depth in excess of 1 m (3.3 ft) for the northern pocket gopher, while Miller (1957, cited in Hakonson, 2002) reported a burrowing depth of 2 m (6.6 ft) for the valley gopher. Anderson (1980) noted that the nesting galleries of the northern pocket gopher may range from 1 to 3 m (3.3 to 9.8 ft) deep.

Kawamichi (1989) examined the burrow structure of Siberian chipmunks (*Eutamias sibiricus*) as a function of season. The deepest burrows were excavated when the animals were preparing to hibernate. These burrows averaged 79 to 83 cm (31 to 33 in.) in depth, and extended as deep as 107 cm (3.5 ft). Sources cited in Gano and States (1982) indicate that the burrows of the eastern chipmunk (*Tamias striatus*) and western species of chipmunks (*Eutamias* spp.) generally extend to depths of 30 to 40 cm (12 to 16 in.). Suter et al. (1993) list a maximum burrowing depth of 1 m (3.3 ft) for the eastern chipmunk.

The nesting burrows of thirteen-lined ground squirrels extended to an average depth of 24 cm (9.5 in.) in Oklahoma (Hoffmeister, 1986, cited in SLTERP, 2003); in Texas, burrows extended to depths of 10 to 115 cm (3.9 to 45 in.) (Davis, 1974, cited in SLTERP, 2003). Oaks et al. (1987) cite studies that found rock squirrel burrowing depths ranging from 0.3 to 1 m (1 to 3.3 ft). The white-tailed antelope squirrel often uses abandoned burrows, and animals have been observed using burrows with depths ranging from 25 to 66 cm (9.8 to 26 in.) (Belk and Smith, 1991). Golden-mantled ground squirrels often dig their own burrows; Bartels and Thompson (1993) cite studies in which burrow depths ranged up to 90 cm (2.9 ft). Reynolds and Laundre (1988) reported a maximum burrowing depth of approximately 1.3 m (4.3 ft) for the Townsend's ground squirrel (*Spermophilus townsendii*) in southeastern Idaho. McKenzie et al. (1982) report a maximum burrowing depth of 2 m (6.6 ft) for ground squirrels, based on data for the Mohave (*Citellus mohavensis*), Townsend's, thirteen-lined, Columbian (*Citellus columbianus*), Franklin (*Citellus franklini*), and Californian (*Citellus beecheyi*) ground squirrels.

Although the burrowing depth data are admittedly sparse, the studies summarized above were used to estimate parameter distributions for the performance assessment and composite analysis. Triangular distributions were assumed in all cases. Minimum, most likely, and maximum values of 2, 3, and 4 m (6.6, 9.8, and 13 ft) were adopted to describe the maximum burrowing depth of harvester ants. The range of these data approximately bounds the observations summarized in Jensen and Hooten (2000) for *Pogonomyrmex* spp.; the midpoint of this range was assumed to be the most likely value and was adopted for the deterministic modeling.

The use of the deer mouse as a surrogate for all mouse species that may inhabit the closed disposal site complicates the development of distributions for burrowing depth. The information cited above suggests the species present during the early successional stages will likely burrow to depths of about 50 cm (20 in.) or less. Although some species of pocket mice may burrow to depths as great as 1.5 to 2 m (4.9 to 6.6 ft), these species are not expected to occur in great numbers at MDA G. On the basis of available data, a distribution with minimum, most likely, and maximum values of 0.5, 1, and 2 m (1.6, 3.3, and 6.6 ft) was assumed for the performance assessment and composite analysis. This distribution was assumed to apply to all mouse species inhabiting the site, from the early successional stages to the piñon-juniper climax condition.

Minimum, most likely, and maximum values of the burrowing depth of pocket gophers are 0.5, 1.25, and 2 m (1.6, 4.1, and 6.6 ft), respectively. The minimum value is generally consistent with the observations of Gonzales et al. (2000) and Cline et al. (1982, as cited in Hakonson (2002); the maximum value bounds all but one of the observations discussed above. The most likely value — the midpoint of this range — is generally consistent with observed gopher burrowing depths at LANL.

The distribution of maximum burrowing depth for chipmunks and ground squirrels was described using minimum, most likely, and maximum values of 0.5, 1, and 2 m (1.6, 4.1, and 6.6 ft), respectively. These values generally coincide with the range of burrow depths discussed above, although many of the species of ground squirrels discussed are not expected to occur at the closed disposal site. The most likely value of the distribution was adopted for the deterministic modeling.

5.9.9 Burrow Density

Burrow densities are used in conjunction with estimates of the amount of soil excavated per burrow and with burrow renewal fractions to calculate the annual mass of soil excavated by ants, mice, chipmunks, and ground squirrels. The burrow density for harvester ants was set equal to colony density. Numerous estimates of colony density are found in the literature for harvester ants of the genus Pogonomyrmex; Table 52 summarizes several of these. These data were used to construct a normal distribution with a mean and standard deviation of 28.3 and 20.2 colonies/ha (11.5 and 8.2 colonies/ac), respectively; the mean was adopted as the point estimate for the deterministic modeling. Harvester ants are assumed to be present at the disposal site during early succession and after the site transitions to piñon-juniper woodland. The same distribution of colony density was used throughout the simulation period.

Data describing burrow densities for mice, chipmunks, and ground squirrels are generally lacking. In lieu of this information, it was assumed that the burrow densities of these species were equivalent to animal densities. This approach may be quite conservative, depending upon when estimates of animal densities are collected. For example, densities of many species will be greatest during the breeding season, while the young of the year still reside with or near their parents. Assuming that burrow density is equal to the animal density during these times may result in significant overestimation of the actual number of burrows present. Nevertheless, few alternatives to this approach exist.

Estimates of mouse densities at MDA G took into account the trapping data of Biggs et al. (1995 and 1997) and Bennett et al. (1997, 1998, and 2002), as well as density estimates from the literature. Biggs et al. and Bennett et al. trapped small mammals at two waste disposal sites within MDA G and in undisturbed piñon-juniper woodlands from 1994 through 1998. Estimates of total animal densities at these sites are summarized in Table 53.

Table 52
Summary of Harvester Ant (*Pogonomyrmex* spp.) Colony Densities

Colony Density (ha^{-1})	Species, Habitat, and Comments	Reference
7.2E+01	*P. occidentalis*; shortgrass prairie; average over 15-yr study	Keeler, 1993
2.3E+01 ± 9.0E+00	*P. occidentalis*; shortgrass prairie; ungrazed; mean ± std dev.	Rogers and Lavigne, 1974
2.8E+01 ± 1.6E+01	*P. occidentalis*; shortgrass prairie; light grazing; mean ± std dev.	Rogers and Lavigne, 1974
3.1E+01 ± 9.0E+00	*P. occidentalis*; shortgrass prairie; moderate grazing; mean ± std dev.	Rogers and Lavigne, 1974
3.0E+00 ± 4.0E+00	*P. occidentalis*; shortgrass prairie; heavy grazing; mean ± std dev.	Rogers and Lavigne, 1974
3.0E+01 – 4.3E+01	*P. occidentalis*; sagebrush/wheatgrass dominant; lightly grazed, recent burns; range	Clark and Comanor, 1975 [a]
2.5E+01	*P. occidentalis*; grassland; moderate grazing	Coffin and Lauenroth, 1988 [a]
3.1E+01	*P. occidentalis*; grassland; light grazing	Coffin and Lauenroth, 1990 [a]
1.7E+01	*P. occidentalis*; piñon-juniper woodland	Carlson and Whitford, 1991
1.4E+01	*P. occidentalis*; ponderosa pine community	Carlson and Whitford, 1991
4.0E+01	*P. occidentalis*, grass-shrub community	Mandel and Sorenson, 1982 [b]
4.5E+01	*P. occidentalis*, shrubland	Cole et al., 2001
3.1E+00; 4.5E+00	*P. rugosus*, *P. babatus*, *P. occidentalis*; shortgrass prairie; w/ and w/o prairie dogs	Kretzer and Cully, 2001
1.6E+01; 1.0E+00 – 3.6E+01	*P. occidentalis*; pasture; light grazing; mean and range	Crist and Wiens, 1996 [c]
9.0E+00; 0.0E+00 – 5.0E+01	*P. occidentalis*; pasture; moderate grazing; mean and range	Crist and Wiens, 1996 [c]
5.8E+00; 0.0E+00 – 1.3E+01	*P. occidentalis*; pasture; heavy grazing; mean and range	Crist and Wiens, 1996 [c]
1.8E+01	*P.* spp.	Scott, 1951 [d]
2.8E+01	*P. owyheei*; sagebrush steppe	Soule and Knapp, 1996
4.0E+01	*P. owyheei*; saltbush and halogeton dominant; "misused/depleted"	Sharp and Barr, 1960 [a]
9.0E+00	*P. owyheei*; saltbush dominant; "vigorous stand"	Sharp and Barr, 1960 [a]
1.2E+01	*P. owyheei*; shadscale dominant	Sharp and Barr, 1960 [a]
4.9E+01 – 7.4E+01	*P. owyheei*, cheatgrass dominant; range	Willard and Crowell, 1965 [a]
4.0E+01	*P. owyheei*; mixed sagebrush/greasewood association; mean density	Porter and Jorgensen, 1988
3.2E+01	*P. owyheei*; shrubland/grassland	Johnson et al., 1938 [e]
8.0E+01, 5.7E+01	*P. owyheei*; shrubland/grassland; 1962 and 1974 measurements	Sneva, 1979
6.0E+00 – 2.1E+01	*P. rugosus*; Chihuahuan desert; range	Whitford and DiMarco, 1995 [f]
2.2E+01	*P. rugosus*; shrubland community	Lei, 2000
0.0E+00 – 1.6E+02 [g]	*P. salinus*; range over seven vegetation communities	Blom et al., 1991

[a] Cited in Soule and Knapp, 1996
[b] Cited in Carlson and Whitford, 1991
[c] Cited in Peters et al., 2002
[d] Cited in MAFES, 1999
[e] Cited in Sneva, 1979
[f] Cited in Lobry de Bruyn, 1999
[g] Colony densities for all but one sample plot ranged from 0.0E+00 to 6.9E+01 colonies/ha.

Table 53
Small Mammal Densities at MDA G and Background/Control Areas

Site Name	Site Number[a]	Animal Density (individuals /ha)					Mean Density (individuals/ha)
		1994	1995	1996	1997	1998	
Waste Burial Site	5	2.4E+01	3.2E+01	2.3E+01	1.0E+01	1.7E+01	2.1E+01
Waste Burial Site	7	2.1E+01	1.4E+01	1.1E+01	2.0E+01	ND	1.6E+01
Control Site	8	3.3E+00	---	1.5E+00	7.7E+00	3.1E+01	1.1E+01
Background Site	9	ND	8.7E+00	ND	4.9E+00	8.5E+01	3.3E+01

Source: Biggs et al. (1995, 1997) and Bennett et al. (1997, 1998, and 2002).
ND = No data
--- = No animals were captured at the site.
[a] Site number, as assigned for the 1997 trapping effort. The characteristics of these sites are provided in the text.

The vast majority of the animals trapped at the two waste sites were deer mice; the densities observed at these sites generally coincide with deer mouse densities noted in the literature. For example, Burt and Grossenheider (1976) note that summertime densities of 25 to 37 animals/ha (10 to 15 animals/ac) are high. Data summarized in EPA (1993b) include summertime and winter densities ranging from 12.8 to 22.4 and 3.4 to 8.4 animals/ha (5.2 to 9 and 1.4 to 3.4 animals/ac), respectively, in a subalpine meadow in Utah (Cranford, 1984). Additional citations in EPA (1993b) indicate densities ranging from 12.7 to 45.5 animals/ha (5.1 to 18.4 animals/ac) in burnt slash in British Columbia, a range of 3.9 to 28 animals/ha (1.6 to 11.3 animals/ac) was observed in understory along a river in Montana. Smith and Urness (1984) observed mean deer mouse densities ranging from 6.7 to 24.2 animals/ha (2.7 to 9.8 animals/ac) in sagebrush and crested wheatgrass communities in Utah; a range of 7.2 to 28 animals/ha (2.9 to 11.3 animals/ac) was found in the transitional zone between these communities. Banfield (1974; cited in Nowak, 2003) reported that the densities of deer mice generally range from about 1 to 25 animals/ha (0.4 to 10 animals/ac). Densities of this species in Kansas ranged from 4 animals/ha (1.6 animals/ac) in weedy areas during the spring and summer to about 19 animals/ha (7.7 animals/ac) in a bluestem grass community during the fall (Hansen and Fleharty, 1974). Finally, Verner and Boss (1980) reported densities of up to 10 to 25 animals/ha (4 to 10 animals/ac) in the Sierra Nevada of California.

The majority of the small mammals trapped by Biggs et al. (1995 and 1997) and Bennett et al. (1997, 1998, and 2002) at the piñon-juniper woodland sites were piñon mice, although deer mice, harvester mice, brush mice, and silky pocket mice were also caught. The mean animal densities estimated for these sites ranged from 1.5 to 85 animals/ha (0.6 to 34 animals/ac), respectively. The densities observed in 1998, the last year for which trapping data are available, were 4 to 10 times greater than densities measured at the two control sites between 1994 and

1997. The reason for this rise was attributed to increases in moisture that, in turn, led to greater food supplies and increased cover availability (Bennett et al., 2002).

Estimates of mouse species other than deer mice are also available in the literature. Brant (1962, cited in CDFG, 2003) and Meserve (1977, cited in CDFG, 2003) found densities of the western harvest mouse ranging from 2.5 to 123 animals/ha (1 to 50 animals/ac) in California coastal scrub communities. Gray (1943; cited in Webster and Jones, 1982) observed a western harvest mouse density of 11.9 animals/ha (4.8 animals/ac) in a sagebrush community in Washington. Whitford (1976, cited in Webster and Jones, 1982) found densities of 4 to 60 animals/ha (1.6 to 24 animals/ac) for this species in New Mexico; the latter density was observed when ground vegetation became dense following September rains. Merritt (1974, cited in Verner and Boss, 1980) reported densities of piñon mice ranging from 2.5 animals/ha (1 animals/ac) in oak-bay woodland to 86 animals/ha (35 animals/ac) in chaparral. Storer et al. (1944, cited in CDFG, 2003) observed densities ranging from 2 to 17.3 animals/ha (1 to 7 animals/ac) for resident brush mice in the Sierra Nevada of California. Best and Skupsi (1994) summarized information regarding silky pocket mouse densities. While most densities were less than 8 animals/ha (3 animals/ac), Whitford (1976, cited in Webster and Jones, 1982) reported a density of 13 animals/ha (5 animals/ac) and Britt (1972) observed densities ranging from 20.8 to 53 animals/ha (8.4 to 21 animals/ac) at sites in New Mexico.

The density estimates for mouse species summarized above are in general agreement with those estimated by Biggs et al. (1995 and 1997) and Bennett et al. (1997, 1998, and 2002) Consequently, the data from these investigators' trapping studies were used to develop point estimates and distributions for the performance assessment and composite analysis. Densities estimated for the disposal units were used to represent the site during early succession, while densities reported for piñon-juniper woodland were used to represent the climax condition. Mouse densities within each community were assumed to be normally distributed with mean densities equal to the overall average densities. The standard deviations of these distributions were defined using a coefficient of variation of 0.25, which is generally consistent with the variability observed in the density estimates.

Chipmunks and ground squirrels are assumed to be present only in piñon-juniper woodland; these species have not been trapped at or near the disposal units at MDA G, but are common inhabitants of mature woodlands. Limited information is available regarding the densities of chipmunks. Burt and Grossenheider (1976) cite densities of 5 to 10 animals/ha (2 to 4 animals/ac) for the eastern chipmunk (*Tamias striatus*). Rosenberg and Anthony (1993) found densities of the Townsend's chipmunk (*Eutamis townsendii*) ranged from 1.9 to 7.7 animals/ha (0.8 to 3.1 animals/ac) during the autumn and spring in second- and old-growth forests in western Oregon. Goodwin and Hungerford (1979, cited in CDFG, 2003) estimated densities of golden-mantled ground squirrels at 0.6 animals/ha (0.2 animals/ac) in dense stands of ponderosa

pine in Arizona, and about 0.1 animals/ha (0.04 animals/ac) in open stands. Verner and Boss (1980) provide density estimates of 1 to 3 animals/ha (0.4 to 1.2 animals/ac) for this species. Johnson (1981, cited in Oaks et al., 1987) reported a springtime density of 13 animals/ha (5.3 animals/ac) for the rock squirrel in Texas; Juelson (1970, cited in Oaks et al., 1987) reported densities of 2 and 5.7 animals/ha (0.8 and 2 animals/ac) for marginal and good habitat, respectively. McKenzie et al. (1982) summarized the work of several investigators, and reported a mean density of 25 animals/ha (10 animals/ac) for several species of ground squirrels; densities ranged from 5.7 to 74 animals/ha (2.3 to 30 animals/ac). Only one of the four species upon which these estimates are based, the thirteen-lined ground squirrel, occurs in New Mexico. Streubel and Fitzgerald (1978) provided several density estimates for the thirteen-lined ground squirrel. These include values of 2.5 to 5.0 animals/ha (1 to 2 animals/ac) in the spring and 24.6 animals/ha (10 animals/ac) following the emergence of young (Rongstad, 1965); 18 animals/ha (7 animals/ac) on grazed prairie in Colorado (Mitchell, 1972); and 4.5 animals/ha (1.8 animals/ac) on ungrazed prairie in Colorado (Grant, 1972).

The point estimate and distribution of chipmunk/ground squirrel density were determined using the information summarized above. Density estimates for species that may be found at MDA G appear to be less than the mean and maximum densities listed in McKenzie et al. (1982). Taking this into account, a triangular distribution was defined using minimum, most likely, and maximum values of 5, 15, and 25 animals/ha (2, 6, and 10 animals/ac), respectively. The most likely value was adopted for the deterministic modeling.

5.9.10 Harvester Ant Burrow Mass

Limited information exists on the mass of soil excavated by harvester ant colonies. Rogers and Lavigne (1974) estimated that an average of 2.8 kg (6.2 lb) of soil was excavated by harvester ant colonies in northeastern Colorado. Using this mass and the maximum colony density observed by the investigators, the total amount of soil excavated is approximately 87 kg/ha (77 lb/ac). Carlson and Whitford (1991) estimated that the average mass of ant mounds in piñon-juniper woodlands near Los Alamos was 38 ± 4.8 kg (84 ± 4.38 lb), while the mass of mounds in a ponderosa pine community averaged 48 ± 5.5 kg (105 ± 12.1 lb); information regarding the range of mound sizes was not provided. The total amount of soil removed in the two communities was about 650 kg/ha (580 lb/ac). Cole (1994) used measurements of harvester ant mounds in Colorado shrubland to estimate the volume of soil brought to the surface. The mean volume of 53 mounds was estimated to be 0.039 m^3 (1.4 ft^3). Assuming a bulk density of 1300 kg/m^3 (80 lb/ft^3), this volume represents about 50 kg (110 lb) of soil per mound. Mandel and Sorenson (1982) reported an average mound volume of 0.32 m^3 (11.3 ft^3) for work conducted in Colorado, this volume represents a mass of about 42 kg (92 lb) if the bulk density of the material is 1,300 kg/m^3 (80 lb/ft^3).

Given the limited amount of information on harvester ant burrow mass, the work conducted by Carlson and Whitford (1991) was relied upon to estimate a distribution for the parameter. Minimum and maximum values of a triangular distribution were defined using the approximate lower bound of the mound mass at the piñon-juniper study site (i.e., 23 kg [50 lb]) and the approximate upper bound of the mound mass at the ponderosa pine study site (i.e., 65 kg [143 lb]). The mean mound mass of 38 kg (84 lb) observed for the piñon-juniper study site was adopted as the most likely value and the point estimate for the deterministic modeling.

5.9.11 Harvester Ant Colony Life Span

The proportion of burrows established by harvester ants each year will depend upon the life span of the individual colonies and whether the number of colonies at MDA G is increasing, decreasing, or remaining constant. Information from the literature indicates life spans for harvester ant colonies range from 5 to 58 years under a variety of conditions. These data, summarized in Table 54, were used to construct a triangular distribution for colony life span, using the range of lifetimes noted above to define the minimum and maximum values. The most likely value of the distribution was set to 21 years, the median of the data listed in the table.

Table 54
Summary of Harvester Ant Colony Lifetimes

Species	Colony Lifetime (yr)	Reference
Unknown	5.0E+00 – 3.0E+01	Various [a]
Pogonomyrmex owyheei	1.4E+01, 1.5E+01	Porter and Jorgensen, 1988
P. owyheei	1.4E+01, 2.8E+01, 3.0E+01	Sharp and Barr, 1960[a]
P. occidentalis	2.9E+01 – 5.8E+01	Coffin and Lauenroth, 1990[b]
P. occidentalis	2.1E+01 – 4.4E+01	Keeler, 1993
P. barbatus	1.5E+01 – 2.0E+01	Gordon, 1991[c]

[a] *Cited in Porter and Jorgensen, 1988.*
[b] *Cited in Keeler, 1993.*
[c] *Cited in Barton et al., 2002.*

5.9.12 Pocket Gopher Soil Removal Rate

Hakonson (2002) and McKenzie et al. (1982) cite several references in which estimates of the soil removal rate of pocket gophers are found. Hakonson (2002) cites the work of Mielke (1977) and Spencer et al. (1985), stating that the amount soil brought to the surface by gophers ranges from 16 to 103 T/ha/yr (7.2 to 46 t/ac/yr). Hakonson et al. (1982) examined soil excavation rates by pocket gophers on a LLW disposal site at LANL. Over the 401-day study, the animals excavated soil at a rate of about 11 T/ha/yr (5 t/ac/yr), or about 8.3 m^3/ha/yr (120 ft^3/ac/yr) of

material. McKenzie et al. (1982) estimate that the volume of soil excavated annually by pocket gophers ranges from 0.51 to almost 82 m^3/ha (7.3 to almost 1,200 ft^3/ac), based on numerous references in the literature. They list a mean soil volume of 8.3 m^3/ha (120 ft^3/ac), which was the volume of soil brought to the surface in the study conducted by Hakonson et al. (1982).

A triangular distribution was developed for the pocket gopher soil removal rate based on the information provided in McKenzie et al. (1982). The minimum, most likely, and maximum values were assigned values of 0.51, 8.3, and 82 m^3/ha/yr (7.3, 120, and 1,170 ft^3/ac/yr), respectively. The most likely value of this distribution was adopted as the point estimate for this parameter.

Pocket gophers are expected to reside at MDA G as long as the site is in a relatively disturbed condition. Visual observations at the site indicate the species prefers disturbed areas; the animals are generally less common in piñon-juniper woodland. Where pocket gophers do occur in the woodland habitat, they tend to occur either in very limited areas or in disturbed areas such as those that occur along the sides of roads. Based on these observations and general information about habitat preference, the pocket gopher was not assumed to be present at MDA G after it undergoes succession to piñon-juniper woodland. Consistent with this assumption, the soil removal rate for the species at the climax site was set to zero.

5.9.13 Mouse, Chipmunk, and Ground Squirrel Burrow Volume

McKenzie et al. (1982) summarize information about the burrow volumes of selected small mammal species. Minimum, mean, and maximum volumes of 0.003, 0.014, and 0.001 m^3 (0.1, 0.5, and 0.04 ft^3) are listed for pocket mice and kangaroo rats; these values were used to define a triangular distribution that was applied to all mouse species. The minimum, mean, and maximum burrow volumes listed for ground squirrels (i.e., 0.008, 0.02, and 0.0772 m^3 [0.3, 0.7, and 2.7 ft^3]) were used to define the distribution for chipmunks and ground squirrels. The most likely values of these distributions were used for the deterministic modeling.

5.9.14 Burrow Renewal Fraction

The burrow renewal fraction is the ratio of new burrows constructed each year to the number of burrows constructed by animals in their first year at the closed site. This fraction is used to adjust the annual soil removal rates for pocket gophers, mice, and chipmunks. Distributions for the renewal fractions for these species were defined using data taken from McKenzie et al. (1982), who found renewal fractions ranging from 0.5 to 1.0 for ground squirrels, 0.75 to 1.0 for pocket mice and kangaroo rates, and 0.75 to 1.0 for pocket gophers. These ranges were used to define the minimum and maximum values of triangular distributions; the midpoints of these ranges were adopted as the most likely values. The distribution for ground squirrels was adopted for chipmunks, while the distribution for pocket mice and kangaroo rats was assumed to apply to all species of mice inhabiting MDA G.

5.10 Erosion Model Parameters

Erosion model parameters are used to estimate rates of surface erosion across the disposal site. The effect of surface erosion on facility performance is twofold. First, the rate at which the cover erodes will influence the degree to which plant roots and animal burrows extend into the waste, and will determine the amount of waste excavated during inadvertent human intrusion. Second, contamination deposited on the surface of MDA G by the plants and animals that penetrate into the waste will be transported into the adjacent canyons by surface runoff. The parameters used to characterize the impacts of surface erosion are discussed below.

5.10.1 Shape Factors

The normalized cover loss functions used in the surface erosion modeling consisted of a series of curves defined using beta distributions (see Section 3.2.1). The shape of these functions is determined by the shape factors. The alpha shape factor is assigned a constant value of zero for the cover loss functions adopted for the performance assessment and composite analysis modeling. The beta shape factor is assigned a discrete distribution wherein values of 1, 1.5, 2, 2.5, 3, 3.5, and 4 have equal probabilities of being sampled. The same beta shape factor is assumed to apply to all waste disposal regions and erosion zones for a given realization.

5.10.2 Erosion Zone Interval Data

As discussed in Section 3.2, the spatial effects of erosion at MDA G are modeled using a series of 10 erosion zones. These erosion zones are defined in terms of the amount of cover remaining over a given portion of the site. The cover depth intervals associated with each zone are presented in Table 5.

The cover loss functions described in Section 3.2.1 are structured to ensure that the appropriate amount of cover, as defined in Table 5, remains over each erosion zone within a disposal region. Because each erosion zone is associated with a span of remaining cover depths, however, the cover erosion rates for a given zone will vary. To illustrate, consider soil loss in erosion zone 5, which includes cells with 1 to 1.25 m (6.6 to 7.4 ft) of cover remaining at the end of the simulation. Based on an initial cover depth of 3.5 m (11 ft), 2.25 to 2.5 m (7.4 to 8.2 ft) of cover material will be lost during the simulation period. Assuming a linear rate of soil loss, this translates to erosion rates of 2.3×10^{-4} to 2.5×10^{-4} m/yr (7.4×10^{-4} to 8.2×10^{-4} ft/yr).

The normalized erosion rates are multiplied by the total amount of cover that is eroded during the simulation to determine erosion rates for a given erosion zone. The total cover depth eroded is simply the initial cover depth minus the final cover depth remaining at the end of the simulation. This quantity is calculated using distributions of the final depths remaining, consistent with the depth intervals that are used to define the different erosion zones. For example, the final cover depth for erosion zone 5 is described using a triangular distribution with minimum, most likely,

and maximum values of 1.0, 1.125, and 1.25 m (3.3, 3.7, and 4.1 ft). The distributions of final cover depths for erosion zones 1 through 9 were developed using this approach; the final cover depth for portions of the site assigned to erosion zone 10 was assumed to be 2.5 m (8.2 ft) in all realizations.

5.11 Exposure Pathway Parameters

Exposure pathway parameters define the receptor activities and intakes necessary to estimate doses for the exposure scenarios included in the performance assessment and composite analysis. The data used to describe these parameters are included in Table 14; the information upon which the selected data are based is discussed below.

5.11.1 Indoor and Outdoor Time Allotments

The indoor and outdoor time allotments define the time spent by the receptor indoors and outdoors at the receptor location. The time allotments sum to 24 hr/d or less; if less, it is assumed that any additional time is spent at uncontaminated locations. The NRC (1986) and NCRP (1999) adopted nominal values of 12 hr/d for the time spent indoors by a resident at a contaminated site; a period of 4.9 hr/d is adopted by the NRC (1986) for the time spent outdoors while the NCRP (1999) adopted a value that is almost twice that for their screening assessment. The RESRAD code (ANL, 2001) uses default average indoor and outdoor exposure times of 12 and 6 hr/d, respectively, while values of 13.2 and 4.7 hr/d were used for a residential scenario in a decommissioning study (NRC, 1992). The Exposure Factors Handbook (EPA, 1997) provides distributions of time spent inside and outside of a residence for various segments of the population.

A total exposure period of 500 hours was adopted for the Intruder-Construction Scenario (NRC, 1986); it was assumed that all of this time was spent outdoors. Information in the Exposure Factors Handbook (EPA, 1997) was used to define distributions of occupancy times for the residential intruder and off-site exposure scenarios; these distributions were based on occupancy times averaged over all segments of the population. The distribution for indoor occupancy time was truncated at the fifth percentile value to ensure a nominal amount of time was spent inside at the point of exposure. Outdoor exposure times were adjusted as necessary to assure that the sum of the indoor and outdoor exposure times did not exceed 24 hr/d.

5.11.2 Excavation Occupancy Fraction

The severity of the external exposures projected for the Intruder-Construction Scenario will depend upon the location of the receptor relative to the waste. In many cases, rates of exposure will be greatest during the time spent in the basement excavation because the amount of shielding between the receptor and the waste will be at a minimum at this location. Given this, the NRC (1986) assumed that the entire exposure period was spent in the excavation. It is more

realistic to expect that a person will spend considerably less than the total construction time at the bottom of the basement excavation. Consistent with this expectation, the excavation occupancy factor was assigned a triangular distribution with minimum, most likely, and maximum values of 0, 0.1, and 0.2, respectively.

5.11.3 Soil Mixing Depth

As its name implies, this parameter specifies the depth to which surface soils are mixed at the receptor locations. The soil mixing depth was set to 15 cm (6 in.) for all off-site receptor locations, for both the deterministic and probabilistic modeling. This value was selected based on the assumption that soils will be plowed or otherwise mixed to this depth during construction of the residence and the establishment of a garden. The same mixing depth was applied to the Intruder – Post-Drilling Scenario. The soil mixing depth for the Intruder-Construction and Intruder-Agriculture Scenarios was set equal to the volume of soil excavated during house construction divided by the net area of the intruder's lot.

5.11.4 Direct Radiation Shielding Factor

The direct radiation shielding factor is used to describe the attenuation of direct radiation during the time spent inside; it represents the fraction of the radiation that passes through the structure in which the receptor resides. The RESRAD code (ANL, 2001) uses a default shielding factor of 0.7 for time spent indoors. The NRC's Regulatory Guide 1.109 (1977) suggests using this value for the maximally exposed individual and a value of 0.5 for the general population for the entire time spent at the site. NCRP Report 129 (1999) compiles shielding factors for the time spent inside a variety of buildings. Shielding factors cited in the NCRP report include 0.02 to 0.5 for prefabricated housing; 0.25 for a single family, two-story house; 0.40 for light construction; 0.23 to 0.43 for wood-frame, one-story houses; 0.07 ± 0.06 for brick houses; 0.13 ± 0.06 for wood houses; and most likely values ranging from 0.02 to 0.4 for residential structures. The magnitude of the shielding factor will partially depend upon the energies of the photons emitted by the radionuclides of interest. The NCRP (1999) used a shielding factor for radionuclides with the highest energy photons that ranged from about 0.2 to 0.6 for the development of soil screening criteria; shielding factors for radionuclides with the lowest emission energies ranged from 0.004 to 0.16. NCRP Report 76 (1984) suggests the shielding factors are uniformly distributed.

The direct shielding factor was assigned a uniform distribution ranging from 0.2 to 0.6. This distribution is consistent with the range adopted by the NCRP (1999) for high-energy photons and generally coincides with the building-specific data summarized above; the shape of the distribution is consistent with NCRP Report 76 (1984). The midpoint of the range was adopted for the deterministic modeling.

5.11.5 Inhalation Rate

The inhalation rate is used to estimate the intake of contamination from breathing airborne radioactivity. Recommended mean inhalation rates for adults have typically been about 20 m^3/d (700 ft^3/d). The International Commission on Radiation Protection adopted values of 21 and 23 m^3/d (740 and 810 ft^3/d) for women and men, respectively (ICRP, 1975, cited in NCRP, 1984); the average of these values was used in Regulatory Guide 1.109 (NRC, 1977) and the Part 61 Impacts Analysis (NRC, 1986). NCRP Report 129 (1999) reports a value of 22 m^3/d (775 ft^3/d) adopted by the United Nations Scientific Committee on the Effects of Atomic Radiation (UNSCEAR, 1993) and a range of 16 to 20 m^3/d (565 to 700 ft^3/d) cited in ICRP Publication 66 (1994). The EPA (1997) recommended lower average inhalation rates of 11.3 and 15.2 m^3/d (400 and 540 ft^3/d) for women and men, respectively.

The data provided by the EPA (1997) suggest that inhalation rates of about 20 m^3/d (700 ft^3/d) will overstate actual air intake rates for the average individual. Consequently, the performance assessment and composite analysis modeling adopted inhalation rates that are expected to more realistically represent long-term average inhalation rates. The deterministic evaluation used an inhalation rate of 15.2 m^3/d (540 ft^3/d), which is the average inhalation rate cited by the EPA (1997) for adult men. The range of average inhalation rates for adult men is from 13 to 17 m^3/d (460 to 600 ft^3/day), depending upon the age class of the individual. A triangular distribution was defined for the average inhalation rate using these values; this distribution has minimum, most likely, and maximum values of 13, 15.2, and 17 m^3/d (460, 540, 600 ft^3/d), respectively.

It is reasonable to expect that the intruder homebuilder will achieve a higher level of activity than members of the public and residential intruders addressed by the other exposure scenarios. For the Intruder-Construction Scenario, then, an hourly inhalation rate of 1.5 m^3/hr (53 ft^3/hr) was adopted; this value is the mean inhalation rate cited for outdoor workers by the EPA (1997) for moderate activity levels. Inhalation data cited by the EPA for various classes of workers had coefficients of variation of approximately 0.4. This coefficient was applied to the inhalation rate adopted for the intruder analysis to arrive at a standard deviation of 0.6 m^3/hr (21 ft^3/hr). The distribution was truncated at 0.5 m^3/hr (18 ft^3/hr), which is the approximate mean inhalation rate cited in the Exposure Factors Handbook (EPA, 1997) for adults at rest.

5.11.6 Average Wind Speed

The average wind speed is used to model inadvertent intruder exposures to vapor- and gas-phase radionuclides diffusing from MDA G. Meteorological monitoring is conducted across the Laboratory; one of the monitoring towers used to collect these measurements is located at TA-54, to the east of MDA G. Average daily wind speed data for this tower (Rishel et al., 2003) were used to define the distribution for this parameter. Data collected from January 1992 through April 2005 at a height of 12 m (39 ft) above the ground are lognormally distributed and exhibit a geometric mean and standard deviation of 2.7 m/s (8.7 ft/s) and 1.4, respectively.

5.11.7 Atmospheric Mixing Height

Atmospheric mixing height refers to the height at which airborne radionuclides are mixed above the disposal site. It is used in the intruder diffusion model to define a dilution volume for vapor- and gas-phase radionuclides that are inhaled by the receptor. A mixing height of 2 m (6.6 ft) was used in the intruder modeling, consistent with the value used in RESRAD (Yu et al., 1993).

5.11.8 Irrigation Rate and Fraction

The irrigation rate and fraction of the year crops are irrigated are used to estimate radionuclide concentrations in plants due to wet deposition. The rate of irrigation will depend on the crops being grown, the nature of the soil in which the crops are grown, and site meteorological conditions. The 1997 performance assessment and composite analysis assumed an irrigation rate of 5 to 18 cm/wk (2 to 7 in./wk) for all but the last 2 weeks of the growing season. Using the point estimates of the growing seasons discussed earlier and an application rate of 12 cm/wk (5 in./wk) over the periods indicated yields irrigation rates ranging from about 80 to 160 cm/yr (30 to 60 in./yr).

A reevaluation of irrigation rates indicates that the annual rates estimated above may overestimate actual watering rates. Baes et al. (1984) estimated annual irrigation rates of 40 to 70 cm/yr (16 to 27 in./yr) in the general vicinity of Los Alamos, based on data taken from the 1974 Census of Agriculture. The 1998 and 2003 Farm and Ranch Irrigation Surveys (USDA, 1999 and 2004b) provide total irrigated acres and quantities of water applied to such on a state-by-state basis. The data for New Mexico indicate an annual irrigation rate of about 72 cm/yr (28 in./yr), which falls at the high end of the range cited by Baes et al. (1984).

Data from the 2003 Farm and Ranch Irrigation Survey (USDA, 2004b) attest to the crop-specific nature of irrigation needs. Annual irrigation rates for lettuce and beans are about 12 and 60 cm (5 and 24 in.), respectively, while rates for various grains range from about 40 to 60 cm per season (16 to 24 in. per season); 70 to 100 cm (27 to 40 in.) of water is applied through irrigation for various varieties of corn. An average of 85 cm (34 in.) is applied to alfalfa and alfalfa mixtures, while pasture and all other hay receive about 60 cm (24 in.) of water through irrigation.

Additional insight into irrigation needs may be gained through an examination of the water needs of various crops. Table 55 summarizes estimates of these needs for several crops. The irrigation application rates are a function of the crop's water needs and the efficiency of the irrigation system, defined here as the ability of the irrigation system to apply water equally across the area under cultivation. Although large-scale sprinkler-based irrigation systems may have efficiencies ranging from about 50 to 90 percent (e.g., Martin, 2000), the efficiency of concern is the homeowner's system of watering crops. For modeling purposes, it was assumed that this efficiency was 75 percent. On this basis, the water needs listed in Table 55 may be multiplied by 1.3 to estimate the corresponding irrigation water application rates; these rates assume that natural precipitation makes no significant contribution to the water needs of the plants.

Table 55
Water Needs of Crops

Crop	Seasonal Water Needs (cm)				
	Eastern Colorado [a]	Western Colorado [a]	Generic Estimates [b]	Eastern Oregon [c]	Southwestern U.S. [d]
Alfalfa and Alfalfa Mixtures	7.6E+01 – 9.9E+01	3.3E+01 – 9.2E+01	8.0E+01 – 1.6E+02	1.1E+02	2.0E+02
All Other Hay	---	---	---	---	---
Barley/Oats/Wheat	---	---	4.5E+01 – 6.5E+01	---	---
Beans	---	---	3.0E+01 – 5.0E+01	6.1E+01	---
Beans – Dry, Edible	4.0E+01 – 4.9E+01	5.1E+01	---	---	---
Broccoli	---	---	---	---	5.0E+01
Cabbage	---	---	3.5E+01 – 5.0E+01	---	---
Cauliflower	---	---	---	---	4.7E+01
Corn – Grain, Seed	5.2E+01 – 7.0E+01	6.4E+01	---	---	---
Corn – Silage	4.6E+01 – 6.2E+01	4.1E+01 – 5.8E+01	---	---	---
Corn – Sweet	5.2E+01 – 5.8E+01	---	---	---	5.0E+01
Corn – Field	---	---	---	7.6E+01	---
Grain – Small (oats, rye)	---	---	---	---	---
Grain – Spring (barley, wheat)	2.7E+01 – 3.9E+01	2.9E+01 – 5.0E+01	---	---	---
Lettuce and Romaine	---	---	---	---	2.2E+01
Onions	---	---	3.5E+01 – 5.5E+01	8.1E+01	5.9E+01
Pastureland, All Types	6.6E+01 – 8.7E+01	3.5E+01 – 8.5E+01	---	9.1E+01	---

--- = Crop was not addressed by source

[a] *Broner and Schneekloth, 2003*

[b] *Brouwer and Heibloem, 1986*

[c] *Jensen and Shock, 2001*

[d] *Erie, et al., 1982*

Table 55 (Continued)
Water Needs of Crops

Crop	Seasonal Water Needs (cm)				
	Eastern Colorado [a]	Western Colorado [a]	Generic Estimates [b]	Eastern Oregon [c]	Southwestern U.S. [d]
Peas	---	---	3.5E+01 – 5.0E+01	---	---
Peppers	---	---	6.0E+01 – 9.0E+01	---	---
Potatoes	7.1E+01	4.2E+01	5.0E+01 – 7.0E+01	7.6E+01	---
Sorghum, Grain	4.1E+01 – 5.8E+01	---	---	---	---
Sorghum/Millet	---	---	4.5E+01 – 6.5E+01	---	---
Soybean	---	---	4.5E+01 – 7.0E+01	---	---
Tomatoes	---	---	4.0E+01 – 8.0E+01	---	---
Vegetables – Small	4.5E+01 – 5.6E+01	1.7E+01 – 4.6E+01	---	---	---
Wheat – Grain, Seed, Winter, Spring	3.6E+01 – 4.9E+01	4.7E+01 – 5.1E+01	---	6.6E+01	6.6E+01

--- = Crop was not addressed by source

[a] *Broner and Schneekloth, 2003*

[b] *Brouwer and Heibloem, 1986*

[c] *Jensen and Shock, 2001*

[d] *Erie et al., 1982*

The irrigation data discussed above were used to estimate distributions for the performance assessment and composite analysis modeling. Irrigation data were grouped by crop type (i.e., leafy vegetables, produce, grain, and pasture grass) and used to define triangular distributions of water application rates; these distributions are summarized in Table 14. The most likely values were estimated as the average of the listed seasonal water application rates; in cases where ranges of application rates were given, the midpoints were used in these calculations. The minimum and maximum values were defined on the basis of the ranges of application rates.

5.11.9 Inadvertent Soil Ingestion Rate

The soil ingestion rate is used to estimate doses for receptors who inadvertently ingest small quantities of contaminated soil. The Exposure Factors Handbook (EPA, 1997) cites several studies that examined rates of inadvertent soil ingestion. Hawley (1985) suggests adult soil ingestion rates of 480 mg/d (0.017 oz/d) during outdoor activities, 0.56 to 110 mg/d (2×10^{-5} to 0.004 oz/d) of house dust during indoor activities, and an annual average of 60.5 mg/d (0.002 oz/d). Krablin (1989) indicates a soil ingestion rate of 10 mg/d (3.5×10^{-4} oz/d) for adults, while Calabrese et al. (1990) estimated a range of 30 to 100 mg/d (0.001 to 0.0035 oz/d) for adults. The EPA (1997) recommends a central estimate of 50 mg/d (0.0017 oz/d) for adults, but gives this value a low confidence rating. Work performed by the Risk Assessment Corporation (RAC, 1999) at Rocky Flats in Colorado adopted a median soil ingestion rate of 200 mg/d (0.007 oz/d) for both children and adults. A lognormal distribution was defined using this value and a geometric standard deviation of 2.2. Simon (1998) conducted an exhaustive review of soil ingestion data for humans and estimated distributions for a variety of conditions. A geometric mean of 100 mg/d (0.0035 oz/d) was assigned for adults in rural residential lifestyles in heavily vegetated (i.e., forests and fields) areas and for occupations at construction sites; a geometric mean of 200 mg/d (0.007 oz/d) was estimated for a rural residential lifestyle in a sparsely vegetated area. A geometric standard deviation of 3.2 was adopted for all three scenarios. The NCRP (1999) adopted inadvertent soil ingestion rates of 50 and 100 mg/d (0.0017 to 0.0035 oz/d) for receptors in rural settings with heavy and sparse vegetation, respectively, while a value of 100 mg/d (0.0035 oz/d) was used for a construction scenario. The NCRP report noted the need to "have wide uncertainty distributions that allow for high values to occur with finite probability." Towards this end, a geometric standard deviation of 3.2 was adopted for the purpose of developing soil screening limits.

A soil ingestion rate of 100 mg/d (0.0035 oz/d) was used to conduct the deterministic modeling for all exposure scenarios. This value is consistent with estimates for construction site exposures cited above and equals or exceeds the ingestion rates provided for rural lifestyles in areas with heavy vegetation. A lognormal distribution was used to describe soil ingestion rates, and was defined using a geometric mean and standard deviation of 100 mg/d (0.0035 oz/d) and 3.2, respectively. The standard deviation is the same as that applied by Simon (1998) and the NCRP (1999).

5.11.10 Drinking Water Ingestion Rate

The drinking water rate is used to estimates doses for the Groundwater Resource Protection and All Pathways – Groundwater Scenarios. The Exposure Factors Handbook (EPA, 1997) discusses rates of tap-water consumption at length, and suggests distributional informational. New Mexico drinking water regulations adopt the majority of 40 CFR Part 141 (EPA, 2000); this regulation prescribes the use of a drinking water ingestion rate of 2 L/d (0.5 gal/d) to demonstrate compliance with the CFR requirements. Consequently, this ingestion rate was used to model exposures for the Groundwater Resource Protection Scenario and no distribution of this rate was considered in the probabilistic modeling. Information for adults aged 20 through 64 was used to define the distribution of ingestion rates for the All Pathways – Groundwater Scenario; this distribution is included in Table 14. The median of this distribution was adopted as the point estimate.

5.11.11 Indoor Water Usage Rate

The indoor water usage rate specifies the amount of water used by the groundwater pathway receptors for personal needs such as food preparation, clothes washing, and bathing. This quantity is used in conjunction with other information to estimate the well pumping rate for the Groundwater Resource Protection and All Pathways – Groundwater Scenarios.

The EPA (2002) has summarized several studies that monitored water usage in suburban households in the U.S. These studies, which lasted as long as three months, found average daily usage rates ranged from 0.2 to 0.3 m^3 (50 to 70 gal) per person. Data collected by Mayer et al. (1999) from 1,188 households in 12 cities across the country showed daily per capita indoor water use was lognormally distributed with a median usage rate of about 0.23 m^3 (60 gal). Using these data, a distribution of indoor water usage rates was estimated, with the geometric mean set to the median reported by Mayer et al. The geometric standard deviation was set to 1.49 to yield a distribution that generally resembled that reported by the investigators.

5.11.12 Types of Animals Raised

The receptors for all but the Groundwater Resource Protection and the Intruder-Construction Scenarios are exposed to radiation through the intake of contaminated vegetables and animal products. In terms of animal product intake, it was assumed that the receptors raise cattle and cows to supply a portion of their beef and milk intake, or chickens to supply meat and eggs. The probabilities of raising cattle and cows or of raising chickens were assumed to be equal; deterministic modeling was based on the assumption that cattle and cows were raised by the receptors.

5.11.13 Fraction of Diet Raised at Receptor Location

Most of the receptors included in the performance assessment and composite analysis are assumed to raise a portion of their diet at the exposure location. The Exposure Factors Handbook

(EPA, 1997) provides estimates of the fraction of the vegetable diet grown by households that garden and those that farm. In terms of gardening households, the report cites a range of 0.106 to 0.233 for exposed, protected, and root vegetables, and a fraction of 0.173 averaged over all crops. A range of 0.173 to 0.42 for exposed, protected, and root vegetables was found for households that farm; averaging over all vegetables yielded a fraction of 0.308. The range and mean for households that farm were adopted for the modeling; these data were used to construct a triangular distribution. A value of 0.308 was used for the deterministic modeling.

The EPA (1997) also provides data for the fraction of animal product intake that is home-produced. For households that raise animals, the fractions given for beef, total dairy, chicken, and eggs are 0.48, 0.21, 0.15, and 0.21, respectively; the corresponding fractions for households that farm are 0.49, 0.25, 0.16, and 0.15. These data were used to develop triangular distributions for each animal product. It was assumed that the receptors raised enough animals to provide 50 and 25 percent of the beef and milk they consumed, respectively. Similarly, the individuals were assumed to raise enough chickens to provide 15 and 20 percent of the chicken and eggs they consumed. Triangular distributions were defined for all four parameters based on the assumption that the fractions varied over a range of ± 20 percent.

The diet fractions sampled from the distributions described above were adjusted downward if the areas required to raise the crops or animals exceeded the available area at the receptor location. The portion of the receptor's lot that was available for the production of food was first allocated to vegetable crops; any remaining area was assumed to be available for raising animals.

5.11.14 Crop Ingestion Rates

The doses received from the consumption of contaminated crops are directly proportional to the ingestion rates of those foods. The RESRAD code (ANL, 2001) uses default ingestion rates of 14 kg/yr (30 lb/yr) for leafy vegetables and 160 kg/yr (350 lb/yr) for fruit, other vegetables, and grain. Data provided in the NRC's Regulatory Guide 1.109 (NRC, 1977) indicate a consumption rate for the average adult of 190 kg/yr (420 lb/yr) for fruit, vegetables, and grain; 520 kg/yr (1,150 lb/yr) is listed for the maximally exposed individual. The NRC (1992) adopted an average consumption rate of 177 kg/yr (390 lb/yr) for fruit, vegetables, and grain to estimate doses from residual contamination following facility decommissioning; essentially the same rate is provided by Yang and Nelson (1986). Data adapted from Rupp (1980) indicate a best estimate of 170 kg/yr (375 lb/yr) for the consumption of fruit, vegetables, and grain by persons older than 18.

The Exposure Factors Handbook (EPA, 1997) includes a large amount of information on vegetable consumption rates; data contained in this report for adults aged 20 to 75 were used to develop the distributions shown in Table 14. The data used to estimate consumption rates were provided in terms of grain and total vegetables. It was assumed that 85 percent of the listed consumption rates for vegetables other than grain consisted of produce, while the remaining 15

percent consisted of leafy vegetables. This allocation is consistent with the per capita intake data provided in the Exposure Factors Handbook for different food classes. All consumption rates were given in terms of daily intake per unit body mass; these rates were converted to total daily intakes by multiplying them by an adult body mass of 71.8 kg (160 lb) (EPA, 1997). The medians of the consumption rate distributions were adopted for the deterministic modeling.

5.11.15 Animal Product Ingestion Rates

Ingestion rates for beef, milk, chicken, and eggs are used to estimate doses for the off-site receptors and two of the intruder scenarios. For the average adult, Regulatory Guide 1.109 (NRC, 1977) lists ingestion rates of 95 kg/yr (210 (lb/yr) for meat and poultry, and 110 L/yr (30 gal/yr) for milk; the maximum exposed adult is assumed to consume 110 kg/yr (240 lb/yr) of meat and poultry and 310 L/yr (80 gal/yr) of milk. RESRAD (ANL, 2001) uses a meat and poultry consumption rate of 63 kg/yr (140 lb/yr), and a value of 92 L/yr (25 gal/yr) for milk. Rupp (1980) lists average adult consumption rates of 31 kg/yr, 9.5 kg/yr, 95 L/yr, and 15 kg/yr (68 lb/yr, 21 lb/yr, 25 gal/yr, and 33 lb/yr) for beef, poultry, milk, and eggs, respectively. Yang and Nelson (1986) list rates of 32 kg/yr, 11 kg/yr, 92 L/yr, and 9.8 kg/yr (70 lb/yr, 24 lb/yr, 24 gal/yr, and 22 lb/yr) for beef, poultry, milk, and eggs, respectively, while the NRC (1992) adopted values of 59 kg/yr, 9 kg/yr, 100 L/yr, and 10 kg/yr (130 lb/yr, 20 lb/yr, 26 gal/yr, and 22 lb/yr) for these same food products.

The EPA's Exposure Factors Handbook (EPA, 1997) contains consumption data for beef, poultry, eggs, and dairy products for various age groups. Using this information, distributions of consumption rates were calculated for persons 20 years and older; these distributions were adopted for the performance assessment and composite analysis modeling. The calculations used an adult body mass of 71.8 kg (160 lb), assumed that the consumption rates listed for poultry represented chicken, and assumed that 80 percent of the dairy intake consisted of milk. The means of these distributions were used for the deterministic modeling.

5.11.16 Animal Numbers

The fraction of a receptor's diet that comes from home-raised animals will be influenced by the number of animals that are required to supply the food. Simply put, as the numbers of animals required to provide the receptor's food increases, the likelihood that the receptor will have the necessary land to raise the cattle, cows, or chickens decreases. Estimates of the number of animals needed to supply the specified food requirements depend on various animal production parameters.

The numbers of cattle and chickens required to supply the specified quantities of beef and chicken depend upon the live weights of the animals at the time they are killed and the fractions of the live weights represented by edible meat. The live weights of the animals (cattle) at the time of slaughter were assumed to average 500 kg (1,100 lb); this weight is consistent with the animal forage consumption rate selected for the modeling and generally agrees with average live

weights reported in USDA (2005a). A standard deviation of 25 kg (55 lb) was adopted based on an assumed coefficient of variation of 5 percent. The fraction of the animal's live weight that consists of meat was estimated as the product of the carcass-to-live-weight ratio, or dressing percentage, and the cutability index, which represents the fraction of the carcass with saleable retail meat. The dressing percentage was assumed to be normally distributed with a mean and standard deviation of 0.64 and 0.02, based on data provided by the University of Nebraska Cooperative Extension (UNCE, 2001) and Harris et al. (1997). The cutability index was assumed to be normally distributed with a mean and standard deviation of 0.5 and 0.024, based on information provided by UNCE and May et al. (2000).

The number of chickens necessary to provide the specified food requirements of the receptor is estimated using data for various meat-type chickens. The USDA (2004a) reported an average live weight of 2.4 kg (5.2 lb) for young chickens at the time of slaughter. This is approximately the midpoint of the average live weights provided by Skinner and Sunde (1983) for Cornish game hens (0.8 kg [1.8 lb]), broilers/fryers (1.8 kg [4 lb]), and roasters (3.6 kg [8 lb]). Using this information, the live weights of the birds at the time of slaughter were assumed to be normally distributed with a mean and standard deviation of 2.3 and 0.45 kg (5.0 and 1.0 lb), respectively. The standard deviation was selected so the distribution ranged approximately from 0.9 to 3.6 kg (2 to 8 lb).

The ratio of the ready-to-cook and live-weight production data provided in USDA (2004a) was used to estimate a ready-to-cook weight fraction for chickens. Based on monthly data for 2000 through 2002, a mean and standard deviation of 0.74 and 0.0045 were calculated. Lacking specific information on the fraction of the ready-to-cook carcass that is meat, a fraction of 0.5 was assumed.

The number of milk cows required to supply the specified milk intakes is directly dependent upon the milk production rate of the animals. This rate was assumed to be normally distributed with a mean of 8,600 kg/yr (1.9×10^4 lb/yr), consistent with data found in USDA (2005b). Information needed to describe the variability associated with this value was not found; in its absence a standard deviation of 150 kg/yr (330 lb/yr) was selected which yields production rates that generally span the range of those projected using the minimum and maximum mean monthly milk production rates.

An egg production rate of 260 eggs/yr (USDA, 2005c) was used to estimate the number of layers required to meet the specified intake. Lacking information needed to characterize the variability of egg production, a coefficient of variation of 5 percent was assumed. This assumption results in a distribution that approximately spans the average rates given for 42 states. The USDA (1995) provides data for weight classes of shell eggs; the minimum egg mass for medium, large, extra large, and jumbo eggs ranges from approximately 0.05 to 0.07 kg (0.11 to 0.16 lb). Using these data, a normal distribution of egg mass was developed with a mean and standard deviation of

0.06 and 0.0035 kg (0.13 and 0.0078 lb). The mean of the distribution was estimated as the midpoint of the minimum mass for large and extra large eggs and the standard deviation was selected so that the distribution generally ranged over the minimum egg masses provided above. The shell of the egg was assumed to contribute 10 percent of the total mass.

5.11.17 Receptor's Lot, House, and Well Dimensions

All of the off-site receptors are assumed to take up residence downwind or downgradient of the disposal facility. The 200 m^2 (2,200 ft^2) house is assumed to sit on a 2,300 m^2 (2.5×10^4 ft^2) lot, leaving as much as 2,100 m^2 (2.3×10^4 ft^2) for raising crops and animals; the same house and lot dimensions are used for the intruder analysis. The well drilled through the disposal site under the Intruder – Post-Drilling Scenario is assumed to be 25 cm (10 in.) in diameter.

5.11.18 House Ventilation Rate

The ventilation rate of the intruder's house specifies the frequency with which air inside the dwelling is replaced with fresh air. The parameter is used to estimate doses received by the receptor from the inhalation of vapor- and gas-phase radionuclides during the time spent indoors. The EPA (1997) cites several studies that address air exchange rates in domestic dwellings. Nazaroff et al. (1988) evaluated the data collected by other investigators. Air exchange rates in low-income houses with a median age of 45 years had a geometric mean and standard deviation of 0.90 ± 2.13 air exchanges per hour (ACH). Measurements taken during the heating season in 312 houses with a median age of 10 years indicated a geometric mean and standard deviation of 0.53 ± 1.71 ACH.

Versar (1990) provides distributional information for air exchange rates in houses in several states; air exchange measurements were generally taken during the cooler months at most locations, although some summertime data are included. In general, the mean air exchange rate ranged from 0.22 to 0.9; the means for three locations exceeded 1.0 and measurements at two of these locations were conducted in midsummer when windows would most likely be open. Koontz and Rector (1995) evaluated data from numerous studies and estimated air exchange rates for different segments of the U.S. (i.e., west, north-central, northeast, and south). Data from each state were weighted to compensate for imbalances in locations where measurements were taken. For the west region, the air exchange rate had a geometric mean and standard deviation of 0.47 ± 2.11 ACH.

Using essentially the same data as Koontz and Rector, but without the compensating weights, Murray and Burmaster (1995) developed estimates of air exchange rates for different climate regions (i.e., coldest, colder, warmer, and warmest) and seasons. The regions were defined on the basis of heating degree days; seasons were defined as 3-month intervals, beginning with December, January, and February for winter. Using a base temperature of 18°C (65°F), the

annual heating degree days for Los Alamos is approximately 6,400 (WRCC, 2005), qualifying the site for inclusion in the colder climate region. Mean air exchange rates for this region range from 0.35 in the fall to 1.3 in the summer.

The ventilation rate adopted for the performance assessment and composite analysis was based on the results for the western region cited by Koontz and Rector (1995). This distribution generally agrees with the seasonal data provided by Murray and Burmaster (1995) and is consistent with the data for newer houses found in Nazaroff et al. (1988).

Information needed to characterize air exchange rates during the time spent by the construction worker within the basement excavation was not found. Lacking the necessary data, the air exchange rate for the excavation was assumed to be the same as that described above for the intruder's house.

5.12 Miscellaneous Parameters

Table 56 presents the radionuclide half-lives and dose conversion factors used in the GoldSim modeling. The radionuclides found in the table include all isotopes for which radionuclide inventories were developed or that were explicitly included in decay and ingrowth calculations. In general, daughter products with half-lives of less than 1 year were assumed to be in secular equilibrium with their parents. The half-lives included in Table 56 were taken from KAPL (2002).

The dose conversion factors used in the performance assessment and composite analysis were taken from federal guidance reports 11 and 12 (EPA, 1988, 1993a). The factors listed in Table 56 represent those of the parent radionuclides and any daughters assumed to be in secular equilibrium with those isotopes.

Table 56
Radionuclide Half-Lives and Dose Conversion Factors

Radionuclide	Half-Life (yr)	Ingestion (mrem/pCi)	Inhalation (mrem/pCi)	Direct Radiation (mrem-m³/yr-pCi)		
				15 cm Depth	Infinite Depth	Air Immersion
Ac-227	2.2E+01	1.5E-02	6.7E+00	1.2E-06	1.3E-06	2.2E-03
Ag-108m	4.2E+02	7.6E-06	2.8E-04	5.4E-06	6.1E-06	9.2E-03
Al-26	7.1E+05	1.5E-05	8.0E-05	9.0E-06	1.1E-05	1.6E-02
Am-241	4.3E+02	3.6E-03	4.4E-01	2.7E-08	2.7E-08	9.6E-05
Am-243	7.4E+03	3.6E-03	4.4E-01	5.4E-07	5.6E-07	1.2E-03
Ba-133	1.1E+01	3.4E-06	7.8E-06	1.2E-06	1.2E-06	2.1E-03
Be-10	1.5E+06	4.7E-06	3.5E-04	6.6E-10	6.7E-10	1.3E-06
Bi-207	3.2E+01	5.5E-06	2.0E-05	5.1E-06	5.9E-06	8.8E-03
Bk-247	1.4E+03	4.7E-03	5.7E-01	2.6E-07	2.7E-07	5.5E-04
C-14	5.7E+03	2.1E-06	2.1E-06	8.4E-12	8.4E-12	2.6E-08
Ca-41	1.0E+05	1.3E-06	1.3E-06	0.0E+00	0.0E+00	0.0E+00
Cd-113m	1.4E+01	1.6E-04	1.5E-03	4.0E-10	4.1E-10	8.1E-07
Cf-249	3.5E+02	4.7E-03	5.8E-01	1.1E-06	1.2E-06	1.8E-03
Cf-251	9.0E+02	4.8E-03	5.9E-01	3.2E-07	3.3E-07	6.5E-04
Cf-252	2.6E+00	1.1E-03	1.6E-01	1.1E-10	1.1E-10	5.9E-07
Cl-36	3.0E+05	3.0E-06	2.2E-05	1.4E-09	1.5E-09	2.6E-06
Cm-243	2.9E+01	2.5E-03	3.1E-01	3.5E-07	3.6E-07	6.9E-04
Cm-244	1.8E+01	2.0E-03	2.5E-01	7.9E-11	7.9E-11	5.7E-07
Cm-245	8.5E+03	3.7E-03	4.6E-01	2.1E-07	2.1E-07	4.6E-04
Cm-247	1.6E+07	3.4E-03	4.1E-01	1.1E-06	1.2E-06	1.9E-03
Cm-248	3.5E+05	1.4E-02	1.7E+00	5.5E-11	5.5E-11	4.0E-07
Co-60	5.3E+00	2.7E-05	2.2E-04	8.5E-06	1.0E-05	1.5E-02
Cs-135	2.3E+06	7.1E-06	4.6E-06	2.4E-11	2.4E-11	6.6E-08
Cs-137	3.0E+01	5.0E-05	3.2E-05	1.9E-06	2.1E-06	3.2E-03
Dy-154	3.0E+06	0.0E+00	0.0E+00	0.0E+00	0.0E+00	0.0E+00
Eu-152	1.4E+01	6.5E-06	2.2E-04	3.8E-06	4.4E-06	6.6E-03
Eu-154	8.6E+00	9.5E-06	2.9E-04	4.1E-06	4.8E-06	7.2E-03
Gd-148	7.5E+01	2.2E-04	3.3E-01	0.0E+00	0.0E+00	0.0E+00
Gd-150	1.8E+06	0.0E+00	0.0E+00	0.0E+00	0.0E+00	0.0E+00

Table 56 (Continued)
Radionuclide Half-Lives and Dose Conversion Factors

Radionuclide	Half-Life (yr)	Ingestion (mrem/pCi)	Inhalation (mrem/pCi)	Direct Radiation (mrem-m³/yr-pCi)		
				15 cm Depth	Infinite Depth	Air Immersion
H-3	1.2E+01	6.4E-08	6.4E-08	0.0E+00	0.0E+00	0.0E+00
Hf-182	9.0E+06	2.2E-05	3.4E-03	5.0E-06	5.7E-06	8.8E-03
Ho-163	4.6E+03	0.0E+00	0.0E+00	0.0E+00	0.0E+00	0.0E+00
Ho-166m	1.2E+03	8.1E-06	7.7E-04	5.7E-06	6.4E-06	9.9E-03
I-129	1.6E+07	2.8E-04	1.7E-04	8.1E-09	8.1E-09	4.4E-05
K-40	1.3E+09	1.9E-05	1.2E-05	5.3E-07	6.5E-07	9.4E-04
Kr-81	2.3E+05	0.0E+00	0.0E+00	1.8E-08	1.9E-08	3.1E-05
Kr-85	1.1E+01	0.0E+00	0.0E+00	8.1E-09	8.9E-09	1.4E-05
La-137	6.0E+04	4.6E-07	8.8E-05	8.8E-09	8.8E-09	4.7E-05
Lu-176	3.8E+10	7.3E-06	6.6E-04	1.5E-06	1.6E-06	2.7E-03
Mo-93	3.5E+03	1.3E-06	2.8E-05	3.7E-10	3.7E-10	2.9E-06
Nb-91	7.0E+02	0.0E+00	0.0E+00	0.0E+00	0.0E+00	0.0E+00
Nb-92	3.5E+07	0.0E+00	0.0E+00	0.0E+00	0.0E+00	0.0E+00
Nb-93m	1.6E+01	5.2E-07	2.9E-05	6.5E-11	6.5E-11	5.2E-07
Nb-94	2.0E+04	7.1E-06	4.1E-04	5.3E-06	6.1E-06	9.0E-03
Nd144	2.4E+15	0.0E+00	0.0E+00	0.0E+00	0.0E+00	0.0E+00
Ni-59	7.6E+04	2.1E-07	1.3E-06	0.0E+00	0.0E+00	0.0E+00
Ni-63	1.0E+02	5.8E-07	3.1E-06	0.0E+00	0.0E+00	0.0E+00
Np-237	2.1E+06	4.4E-03	5.4E-01	6.5E-07	6.9E-07	1.2E-03
Os-194	6.0E+00	1.6E-05	6.7E-04	3.1E-07	3.4E-07	5.3E-04
Pa-231	3.3E+04	1.1E-02	1.3E+00	1.1E-07	1.2E-07	2.0E-04
Pb-210	2.2E+01	7.3E-03	2.3E-02	3.7E-09	3.8E-09	1.0E-05
Pd-107	6.5E+06	1.5E-07	1.3E-05	0.0E+00	0.0E+00	0.0E+00
Pm-145	1.8E+01	4.7E-07	3.0E-05	1.8E-08	1.8E-08	8.3E-05
Pu-236	2.9E+00	1.2E-03	1.4E-01	1.4E-10	1.4E-10	7.4E-07
Pu-238	8.8E+01	3.2E-03	3.9E-01	9.4E-11	9.5E-11	5.7E-07
Pu-239	2.4E+04	3.5E-03	4.3E-01	1.8E-10	1.8E-10	5.0E-07
Pu-240	6.6E+03	3.5E-03	4.3E-01	9.2E-11	9.2E-11	5.5E-07
Pu-241	1.4E+01	6.8E-05	8.3E-03	3.7E-12	3.7E-12	8.5E-09

Table 56 (Continued)
Radionuclide Half-Lives and Dose Conversion Factors

Radionuclide	Half-Life (yr)	Ingestion (mrem/pCi)	Inhalation (mrem/pCi)	Direct Radiation (mrem-m³/yr-pCi)		
				15 cm Depth	Infinite Depth	Air Immersion
Pu-242	3.8E+05	3.4E-03	4.1E-01	8.0E-11	8.0E-11	4.7E-07
Pu-244	8.0E+07	3.3E-03	4.0E-01	1.1E-06	1.3E-06	1.9E-03
Ra-226	1.6E+03	1.3E-03	8.6E-03	5.9E-06	7.0E-06	1.0E-02
Ra-228	5.8E+00	1.4E-03	5.1E-03	3.2E-06	3.7E-06	5.6E-03
Se-79	2.9E+05	8.7E-06	9.8E-06	1.2E-11	1.2E-11	3.5E-08
Si-32	1.6E+02	1.1E-05	1.0E-03	7.0E-09	7.4E-09	1.2E-05
Sm-146	1.0E+08	2.0E-04	8.3E-02	0.0E+00	0.0E+00	0.0E+00
Sm-147	1.1E+11	1.9E-04	7.5E-02	0.0E+00	0.0E+00	0.0E+00
Sm-151	9.0E+01	3.9E-07	3.0E-05	6.2E-13	6.2E-13	4.2E-09
Sn-121m	4.4E+01	1.6E-06	1.2E-05	1.2E-09	1.2E-09	7.0E-06
Sn-126	2.3E+05	1.9E-05	1.0E-04	9.2E-08	9.2E-08	2.5E-04
Sr-90	2.9E+01	1.5E-04	1.3E-03	1.4E-08	1.5E-08	2.3E-05
Tb-157	7.0E+01	1.2E-07	9.2E-06	1.8E-09	1.8E-09	7.9E-06
Tb-158	1.8E+02	4.4E-06	2.6E-04	2.6E-06	3.0E-06	4.5E-03
Tc-97	4.2E+06	1.7E-07	9.9E-07	5.1E-10	5.1E-10	3.9E-06
Tc-99	2.1E+05	1.5E-06	8.3E-06	7.8E-11	7.8E-11	1.9E-07
Th-228	1.9E+00	8.1E-04	3.4E-01	5.1E-06	6.4E-06	9.4E-03
Th-229	7.3E+03	4.0E-03	2.2E+00	9.2E-07	1.0E-06	1.7E-03
Th-230	7.5E+04	5.5E-04	3.3E-01	7.5E-10	7.6E-10	2.0E-06
Th-232	1.4E+10	2.7E-03	1.6E+00	3.2E-10	3.3E-10	1.0E-06
Ti-44	6.0E+01	2.5E-05	1.0E-03	7.4E-06	8.5E-06	1.3E-02
U-232	7.0E+01	1.3E-03	6.6E-01	5.6E-10	5.6E-10	1.7E-06
U-233	1.6E+05	2.9E-04	1.4E-01	8.5E-10	8.7E-10	1.9E-06
U-234	2.5E+05	2.8E-04	1.3E-01	2.5E-10	2.5E-10	8.9E-07
U-235	7.0E+08	2.7E-04	1.2E-01	4.6E-07	4.7E-07	9.0E-04
U-236	2.3E+07	2.7E-04	1.3E-01	1.3E-10	1.3E-10	5.9E-07
U-238	4.5E+09	2.7E-04	1.2E-01	7.4E-08	8.3E-08	1.4E-04
Zr-93	1.5E+06	1.7E-06	3.2E-04	0.0E+00	0.0E+00	0.0E+00

6.0 References

Abeele, W.V., 1984, *Geotechnical Aspects of Hackroy Sandy Loam and Crushed Tuff*, Los Alamos National Laboratory Report LA-9916-MS.

Abeele, W.V., 1986, *Determination of Hydraulic Conductivity in Crushed Bandelier Tuff*, Los Alamos Scientific Laboratory Report LA-8147-MS.

Abeele, W.V. and M.L. Wheeler, 1981, *Geohydrology of Bandelier Tuff*, Los Alamos National Laboratory Report LA-8962-MS.

Allen, E.J., 1996, "Harvester Ants: Specialists in Plant Seeds," *New Mexico Wildlife*, Vol. 41, No. 1, pp. 22–23.

Anderson, G.G., 1980, *Rodent Control on Agricultural Land in British Columbia*, Province of British Columbia, Ministry of Agriculture, Victoria.

ANL, 2001, *User's Manual for RESRAD Version 6*, Argonne National Laboratory Report ANL/EAD-4, July.

Anspaugh, L.R., J.H. Shinn, P.L. Phelps, and N.C. Kennedy, 1975, "Resuspension and Redistribution of Plutonium in Soils," *Health Physics*, Vol. 29, pp. 571–582.

Arnold, J. F., D.A. Jameson, and E.H. Reid, 1964, *The Piñon-Juniper Type of Arizona: Effects of Grazing, Fire, and Tree Control*, U.S. Department of Agriculture, Forest Service, Production Research Report No. 84, September.

Aro, R.S., 1971, "Evaluation of Piñon-Juniper Conversion to Grassland," *J. Range Manage.*, Vol. 24, 188–197.

Arthur, W.J., III and A.W. Alldredge, 1982, "Importance of Plutonium Contamination on Vegetation Surfaces at Rocky Flats, CO," *Environ. Exp. Botany*, Vol. 22, pp. 33–38.

ATSDR, 2001, *Landfill Gas Primer — An Overview for Environmental Health Professionals*, Department of Human Health and Services, Agency for Toxic Substances and Disease Registry, November.

Baes, C.F. III, R.D. Sharp, A.L. Sjoreen, and R.W. Shor, 1984, *A Review and Analysis of Parameters for Assessing Transport of Environmentally Released Radionuclides through Agriculture*, Oak Ridge National Laboratory, ORNL-5786, September.

Banfield, A.W.F., 1974, *The Mammals of Canada*," University of Toronto Press, Toronto.

Barney, M.A. and N.C. Frischknecht, 1974, "Vegetation Changes Following Fire in the Piñon-Juniper Type of West-Central Utah," *J. of Range Manage.*, Vol. 27, No. 2, pp. 91–96.

Bartels, M.A. and D.P. Thompson, 1993, "Mammalian Species — *Spermophilus lateralis*," *The Society of Mammalogists*, No. 440, April.

Barton, K.E., N.J. Sanders, and D.M. Gordon, 2002, "The Effects of Proximity and Colony Age on Interspecific Interference Competition between the Desert Ants *Pogonomyrmex barbatus* and *Aphaenogaster cockerelli*," *American Midland Naturalist,* Vol. 148, pp. 376–382.

Bechtel/SAIC, 2004, *Radionuclide Transport Models under Ambient Conditions*, prepared for U.S. Department of Energy, Office of Civilian Radioactive Waste Management, by Bechtel SAIC Company, DOC.20041101.0002, October.

Belk, M.C. and H.D. Smith, 1991, "Mammalian Species — *Ammospermophilus luecurus*," *The Society of Mammalogists* No. 368, April.

Bennett, K., J. Biggs, and P. Fresquez, 1997, *Radionuclide Contaminant Analysis of Small Mammals at Area G, TA-54, Los Alamos National Laboratory, 1995*, Los Alamos National Laboratory Report LA-13242-MS, January.

Bennett, K., J. Biggs, and P. Fresquez, 1998, *Radionuclide Contaminant Analysis of Small Mammals at Area G, Technical Area 54, G 1997 (with cumulative summary 1994–1997)*, Los Alamos National Laboratory Report LA-13517-MS, December.

Bennett, K.D., R.J. Robinson, and P.R. Fresquez, 2002, *Radionuclide Contaminant Analysis of Small Mammals at Area G, Technical Area 54, 1998 (with cumulative summary 1994–1998)*, Los Alamos National Laboratory Report LA-13874-MS, January.

Beresford, N.A. and B.J. Howard, 1991, "The Importance of Soil Adhered to Vegetation as a Source of Radionuclides Ingested by Grazing Animals," *Sci. Total Environ.,*Vol. 107, pp. 237–254.

Best, T.L. and M.P. Skupsi, 1994, "Mammalian Species — *Perognathus flavus*," *The Society of Mammalogists,* No. 471, December.

Biggs, J.R., K.D. Bennett, and P.R. Fresquez, 1995, *Radionuclide Contaminant Analysis of Small Mammals at Area G, TA-54, 1994*," Los Alamos National Laboratory Report LA-13015-MS, September.

Biggs, J.R., K.D. Bennett, and P.R. Fresquez, 1997, *Radionuclide Contaminant Analysis of Small Mammals at Area G, Technical Area 54, 1996 (with cumulative summary for 1994-1995)*, Los Alamos National Laboratory Report LA-13345-MS, July.

Blom, P.E., W.H. Clark, and J.B. Johnson, 1991, "Colony Densities of the Seed Harvesting Ant *Pogonomyrmex salinus* in Seven Plant Communities on the Idaho National Engineering Laboratory," *Journal of the Idaho Academy of Science*, Vol. 27, No. 1, pp. 28–36.

Brant, D.H., 1962, "Measures of the Movements and Population Densities of Small Rodents," *Univ. Calif. Publ. Zool.* Vol. 62, pp. 105–184.

Breshears, D.D., J.J. Whicker, M.P. Johansen, and J.E. Pinder, 2003, "Wind and Water Erosion and Transport in Semi-Arid Shrubland, Grassland, and Forest Ecosystems: Quantifying Dominance of Horizontal Wind-Driven Transport," *Earth Surface Processes and Landforms*, Vol. 28, pp. 1,189–1,209.

Britt, L.G., 1972, "Some Aspects of the Ecology of *Perognathus flavus*, *Dipodomys ordi*, and *Dipodomys merriami*," Ph.D. dissertation, University of New Mexico, Albuquerque.

Broner, I. and J. Schneekloth, 2003, *Seasonal Water Needs and Opportunities for Limited Irrigation for Colorado Crops*, Colorado State University Cooperative Extension Crop Series Irrigation No. 4.718, Colorado State University, Fort Collins, CO. <http://www.ext.colostate.edu /pubs/crops/04718.html>.

Brookins, D.G., 1984, *Geochemical Aspects of Radioactive Waste Disposal*, Springer-Verlag, New York.

Brouwer, C. and M. Heibloem, 1986, *Irrigation Water Needs, Training Manual No. 3*, Land and Water Development Division, Food and Agriculture Organization of the United Nations, Rome, Italy.

Bunker, M.E., 1983, "Early Reactors," *Los Alamos Science*, Vol. Winter/Spring.

Burt, W.H. and R.P. Grossenheider, 1976, *Mammals*, Houghton Mifflin, New York.

Calabrese, E.J., E.J. Stanek, C.E. Gilbert, and R.M. Barnes, 1990, "Preliminary Adult Soil Ingestion Estimates; Results of a Pilot Study," *Regul. Toxicol. Pharmacol.*, Vol. 12, pp. 88–95.

Canadell, J., R.B. Jackson, J.B. Ehleringer, H.A. Mooney, O.E. Sala, and E.D. Schulze, 1996, "Maximum Rooting Depth of Vegetation Types at the Global Scale," *Oecologia,* Vol. 108, pp. 583–595.

Carlson, S.R. and W.G. Whitford, 1991, "Ant Mound Influence on Vegetation and Soil in a Semiarid Mountain Ecosystem," *American Midland Naturalist,* Vol. 126, No. 1, pp. 125–139.

Carroll, L.E. and H.H. Genoways, 1980, "Mammalian Species — *Lagurus curtatus*," *The American Society of Mammalogists* No. 124, April.

CDFG, 2003, *California Wildlife Habitat Relationships System*, California Department of Fish and Game, Wildlife and Habitat Data Analysis Branch, <http://www.dfg.ca.gov/ whdab/html/cwhr.html>.

Chamberlain, A.C., 1970, "Interception and Retention of Radioactive Aerosols by Vegetation," *Atmospheric Environment,* Vol. 4, pp. 57–63.

Chapman, J.A., 1975, "Mammalian Species — *Sylvilagus nuttalli*," *American Society of Mammalogists,* No. 56, November.

Charley, J.L. and S.W. Cowling, 1968, "Changes in Soil Nutrient Status Resulting from Overgrazing and their Consequences in Plant Communities of Semiarid Areas," *Proceedings of the Ecological Society of Australia*, Vol. 3, pp. 28–38.

Clark, W.H. and P.L. Comanor, 1975, "Removal of Annual Plants from the Desert Ecosystem by Western Harvester Ants, *Pogonomyrmex occidentalis*," *Env. Entomol.*, Vol. 4, pp. 52–56.

Clary, W.P., 1971, "Effects of Utah Juniper Removal on Herbage Yields from Springerville Soils," *J. Range Manage.*, Vol. 24, pp. 373–378.

Clary, W.P., 1989, *Test of RPA Production Coefficients and Local Assumptions for the Piñon-Juniper Ecosystem in Central Utah*, U.S. Forest Service, Intermountain Research Station, Research Paper INT-403, May.

Clary, W.P. and D.A. Jameson, 1981, "Herbage Production Following Tree and Shrub Removal in the Piñon-Juniper Type of Arizona," *J. Range Manage.*, Vol. 34, No. 2, pp. 109–113.

Cline J.F., D.A. Cataldo, W.E. Skiens, and K.A. Gado, 1982, *Long Term Biobarriers to Plant and Animal Intrusion of Uranium Tailings*, Pacific Northwest Laboratory Report PNL-4340, September.

Coffin, D.P., and W.K. Lauenroth, 1988, "The Effects of Disturbance Size and Frequency on a Shortgrass Plant Community," *Ecology*, Vol. 69, pp. 1609–1617.

Coffin, D.P. and W.K. Lauenroth, 1990, "Vegetation Associated with Nest Sites of Western Harvester Ants (*Pogonomyrmex occidentalis Cresson*) in a Semiarid Grassland," *American Midland Naturalist,* Vol. 123, pp. 226–235.

Cole, B.J., 1994, "Nest Architecture in the Western Harvester Ant, *Pogonomyrmex occidentalis* (Cresson)," *Ins. Soc.*, Vol. 41, pp. 401–410.

Cole, B.J., K. Haight, and D.C. Wiernasz, 2001, "Distribution of *Myrmecocystus mexicanus* (Hymenoptera: Formicidae): Association with *Pogonomyrmex occidentalis* (Hymenoptera: Formicidae)," *Ann. Entomol. Soc. Am.*, Vol. 94, No. 1, pp. 59–63.

Cooper, M.B., P.A. Burn, B.L. Tracy, M.J. Wilks, and G.A. Williams., 1994, "Characterization of Plutonium Contamination at the Former Nuclear Weapons Testing Range at Maralinga in South Australia," *J. Radioanalytical and Nuclear Chemistry,* Vol. 177, No. 1, pp. 161–184.

Cox, J.R., 1984, "Shoot Production and Biomass Transfer of Big Sacaton [*Sporobolus wrightii*]," *J. Range Manage.*, Vol. 34, No. 7, pp. 377–380.

Cranford, J. A., 1984, "Population Ecology and Home Range Utilizations of Two Subalpine Meadow Rodents (*Microtus longicaudus* and *Peromyscus maniculatus*)," in *Winter Ecology of Small Mammals:* v. 10, J.F. Merrit, ed., Spec. Publ. Carnegie Mus. Nat. Hist.

CRC, 1999, *CRC Handbook of Chemistry and Physics*, 79th Edition, CRC Press.

Crist, T. O. and J. A. Wiens, 1996, "The Distribution of Ant Colonies in a Semiarid Landscape: Implications for Community and Ecosystem Processes." *Oikos,* Vol. 76, pp. 301–311.

Croissant, R.L. and J.W. Echols, 1998, *Planting Guide for Field Crops*, Colorado State University Cooperative Extension Report No. 103.

CUCES, 1999, *Planning a Garden*, Clemson University Cooperative Extension Service, Home & Garden Information Center Report HGIC 1256.

Davis, W.B., 1974, *The Mammals of Texas*, Texas Parks and Wildlife Department, Bulletin 41, pp. 146–148.

Davis, W.B. and D.J. Schmidly, 1997, "Mammals of Texas — Online Edition," <www.nsrl.ttu.edu/tmot1/Default.htm> (2002).

Day, M.S., C.K. Anderson, and C.D. Pedersen, 2005, *Conceptual Design of the Earthen Cover for at Los Alamos National Laboratory Technical Area 54, Material Disposal Area G,* URS Corporation Report to LANL, Los Alamos National Laboratory Report LA-UR-05-7394, September.

DOE, 1979, *Final Environmental Impact Statement, Los Alamos National Laboratory Site, Los Alamos, New Mexico*, U.S. Department of Energy Report DOE/EIS-0018, December 1979.

DOE, 1988, *Radioactive Waste Management*, U.S. Department of Energy Order 5820.2A, September 26.

DOE, 2001a, *Radioactive Waste Management*, U.S. Department of Energy Order DOE O 435.1 (change 1 to document issued July 9, 1999), August 28.

DOE, 2001b, *Radioactive Waste Management Manual*, U.S. Department of Energy Report DOE M 435.1-1 (change 1 to document approved on July 9, 1999), June 19.

Dreicer, M., T.E. Hakonson, G.C. White, and F.W. Whicker, 1984, "Rainsplash as a Mechanism for Soil Contamination of Plant Surfaces," *Health Phys.,* Vol. 46, pp. 177–187.

Dwyer, D.D. and R.D. Pieper, 1967, "Fire Effects on Blue Grama-Piñon-Juniper Rangeland in New Mexico," *J. Range Manage.,* Vol. 20, pp. 359–362.

England, T.R. and B.F. Rider, 1994, *Evaluation and Compilation of Fission Product Yields 1993*, Los Alamos National Laboratory Report LA-UR-94-3106, October.

Environment Canada, 2003, *Landfill Gas Capture and Combustion Quantification Protocol*, Environment Canada, <http://www.ec.gc.ca/pdb/ghg/lfg_protocol_e.cfm>.

EPA, 1988, *Limiting Values of Radionuclide Intake and Air Concentration and Dose Conversion Factors for Inhalation, Submersion, and Ingestion,*" U.S. Environmental Protection Agency, Federal Guidance Report 11.

EPA, 1993a, *External Exposure to Radionuclides in Air, Water, and Soil*, U.S. Environmental Protection Agency Federal Guidance Report 12, EPA 402-R-93-081, September.

EPA, 1993b, *Wildlife Exposure Factors Handbook, Appendix: Literature Review Database Volume II of II*, U.S. Environmental Protection Agency Report EPA/600/R93-187, December.

EPA, 1997, *Exposure Factors Handbook*, U.S. Environmental Protection Agency, EPA/600/P-95/002Fa, August.

EPA, 2000, "Part II, Environmental Protection Agency, 40 CFR Parts 9, 141, and 142, National Primary Drinking Water Regulations; Radionuclides; Final Rule," Federal Register, Vol. 65, No. 236, pp. 76708–76753, December 7, <http://www.epa.gov/fedrgstr/EPA-GENERAL/2000/December/Day-07/g30421.pdf>.

EPA, 2002, *Onsite Wastewater Treatment Systems Manual*, U.S. Environmental Protection Agency, EPA/625/R-00/008, February.

EPA, 2005, *Landfill Gas Emissions (LandGEM) Version 3.02 User's Guide*, U.S. Environmental Protection Agency, EPA-600/R-05/47, May.

Erie, L.J., O.F. French, D.A. Bucks, and K. Harris, 1982, *Consumptive Use of Water by Major Crops in the Southwestern United States*, U.S. Department of Agriculture, Agricultural Research Service, Conservation Research Report Number 29, 40 p.

Fitzner, R.E., K.A. Gano, W.H. Rickard and L.E. Rogers, 1979, *Characterization of the Hanford 300 Area Burial Grounds, Task IV — Biological Transport*, Pacific Northwest Laboratory Report PNL-2774.

Foxx, T.S., G.D. Tierney, and J.M. Williams, 1984, *Rooting Depths of Plants on Low-Level Waste Disposal Sites*, Los Alamos National Laboratory Report LA-10253-MS, November.

Gallegos, A.F., 1999, *Surface Erosion Study of Several TRU Mixed Waste Pits at MDA G at LANL*, Los Alamos National Laboratory.

Gano, K.A., and J.B. States, 1982, *Habitat Requirements and Burrowing Depths of Rodents in Relation to Shallow Waste Burial Sites*," Pacific Northwest Laboratory Report PNL-4140, May.

GoldSim, 2005a, *User's Guide — GoldSim Probabilistic Simulation Environment, Version 8.02.3*, GoldSim Technology Group, January.

GoldSim, 2005b, *User's Guide — GoldSim Contaminant Transport Module, Version 2.22.2*, GoldSim Technology Group, January.

Gonzales, G.J., M.T. Saladen, T.E. Hakonson, 1995, "Effects of Pocket Gopher Burrowing on Cesium-133 Distribution on Engineered Test Plots," *J. of Env. Qual.*, Vol. 24, pp. 1,056–1,062.

Gonzales, G.J., R.L. Budd, P.R. Fresquez, and R.J. Wechsler, 2000, *Source Document: The Relationship Between Pocket Gophers (Thomomys bottae) and the Distribution of Buried*

Radioactive Waste at the Los Alamos National Laboratory, Los Alamos National Laboratory Report LA-13719-MS, July.

Goodwin, J.G., Jr., and C.R. Hungerford, 1979, *Rodent Population Densities and Food Habits in Arizona Ponderosa Pine Forests*, USDA, For. Serv., Rocky Mtn. For. and Range Exp. Sta. Res. Pap. RM-214.

Gordon, D.M., 1991, "Behavioral Flexibility and the Foraging Ecology of Seed-Eating Ants," *Am. Nat.*, Vol. 138, pp. 379–411.

Grant, W.E., 1972, *Small Mammal Studies on the Pawnee Site During the 1971 Field Season*, U.S. IBP Grassland Biome Tech. Rep., Colorado State Univ., Fort Collins.

Gray, J.A., Jr., 1943, "Rodent Populations in the Sagebrush Desert of the Yakima Valley, Washington," *J. Mamm.*, Vol. 24, pp. 191–193.

Green, N. and N.J. Dodd, 1988, "The Uptake of Radionuclides from Inadvertent Consumption of Soil by Grazing Animals," *Sci. Total Environ.*, Vol. 69, pp. 367–377.

Grier, C.C., K.J. Elliott, and D.G. McCullough, 1992, "Biomass Distribution and Productivity of *Pinus edulis–Juniperus monosperma* Woodlands of North-Central Arizona," *Forest Ecology and Management*, Vol. 50, pp. 331–350.

Grove Engineering, 1996, *MICROSHIELD Version 5 User's Manual*, October 1996.

Haagenstad, M.P., 2002, "Stochastic Groundwater Flow and Transport Models Using GoldSim; A Thesis," New Mexico Highlands University Research Publication, Las Vegas, New Mexico.

Hakonson, T.E., 2002, *Review of Sandia National Laboratories/New Mexico Evapotranspiration Cap Closure Plans for the Mixed Waste Landfill*, Environmental Evaluation Services, February.

Hakonson, T.E., J.L. Martinez, and G.C. White, 1982, "Disturbance of a Low-Level Waste Burial Site Cover by Pocket Gophers," *Health Physics*, Vol. 42, No. 6, pp. 871–873.

Hall, E.R., 1928, "Notes of the Life History of the Sagebrush Meadow Mouse (*Lagurus*)," *J. Mammal.*, Vol. 9, pp. 201–204.

Hall, E.R., 1946, *Mammals of Nevada*, Univ. California Press, Berkeley.

Hansen, C.M. and E. D. Fleharty, 1974, "Structural Ecological Parameters of a Population of *Peromyscus maniculatus* in West-Central Kansas," *Southwestern Natur.*, Vol. 19, pp. 293–303.

Harris, J.J., D.K. Lunt, S.B. Smith, W.L. Mies, D.S. Hale, M. Koohmaraie, and J.W. Savell, 1997, "Live Animal Performance, Carcass Traits, and Meat Palatability of Calf- and Yearling-Fed Cloned Steers," *J. Anim. Sci.*, Vol. 75, pp. 986–992.

Haufler, J.B., and J.G. Nagy, 1984, "Summer Food Habits of a Small Mammal Community in the Piñon-Juniper Ecosystem," *Great Basin Naturalist*, Vol. 44, No. 1, pp. 145–150.

Hawley, J.K., 1985, "Assessment of Health Risk from Exposure to Contaminated Soil," *Risk Analysis*, Vol. 5, pp. 289–302.

Healy, W.B., 1968, "Ingestion of Soil by Dairy Cows," *N. Z. J. Agric. Res.*, Vol. 11, pp. 487–499.

Hinesley, L.E., L.E. Nelson, and G.L. Switzer, 1991, "Weight and Nutrient Content of Litter During Secondary Succession on Well-Drained Uplands of the East Gulf Coastal Plain in Mississippi," *Can. J. For. Res.*, Vol. 21, pp. 848–857.

Hinton, T.G., 1992, "Contamination of Plants by Resuspension: A Review, with Critique of Measurement Methods," *The Science of the Total Environment*, Vol. 121, pp. 177–193.

Hinton, T.G., 1994, "Sensitivity Analysis of ECOSYS-87: An Emphasis on the Ingestion Pathway as a Function of Radionuclide and Type of Deposition," *Health Physics*, Vol. 66, No. 5, pp. 513–531.

Hinton, T.G., J.M. Stoll, and L. Tobler, 1995, "Soil Contamination of Plant Surfaces from Grazing and Rainfall Interactions," *J. Environ. Radioactivity*, Vol. 29, No. 1, pp. 11–26.

Hoffman, F.O., 1979, "The Coefficient for the Transfer of Radionuclides from Animal Intake to Milk, F_M," in *A Statistical Analysis of Selected Parameters for Prediction of Food Chain Transport and Internal Dose of Radionuclides*, F.O. Hoffman and C.F. Baes, eds., NUREG/CR-1004.

Hoffman, F. O. and C. F. Baes, III (eds.), 1979, *A Statistical Analysis of Selected Parameters for Predicting Food Chain Transport and Internal Dose of Radionuclides, Final Report*, Oak Ridge National Laboratory Report ORNL/NUREG/TM-282.

Hoffmeister, D.F., 1986, *Mammals of Arizona*, University of Arizona Press, Tucson.

Hollis, D., E. Vold, R. Shuman, K. Birdsell, K. Bower, W. Hansen, D. Krier, P. Longmire, B. Newman, D. Rogers, E. Springer, 1997, *Performance Assessment and Composite Analysis for the Los Alamos National Laboratory Disposal Area G*, Los Alamos National Laboratory Report LA-UR-97-85, Report-54G-013, March.

IAEA, 1994, *Handbook of Parameter Values for the Prediction of Radionuclide Transfer in Temperate Environments*, International Atomic Energy Agency, Technical Report Series No. 364, Vienna, Austria.

ICRP, 1975, *Report of the Task Group on Reference Man*, International Commission on Radiation Protection Publication 23.

ICRP, 1994, *Human Respiratory Tract Model for Radiological Protection*, International Commission on Radiation Protection Publication 66.

INEEL, 1994, *Radioactive Waste Management Complex Low-Level Waste Radiological Performance Assessment*, Idaho National Engineering and Environmental Laboratory Report EGG-WM-8773, May.

Ingles, L.D., 1941, "Natural History of the Audubon Cottontail," *J. Mammal.*, Vol. 22, No. 3, pp. 227–250.

Jackson, R.B., J. Canadell, J.R. Ehleringer, H.A. Mooney, O.E. Sala, and E.D. Schulze, 1996, "A Global Analysis of Root Distributions for Terrestrial Biomes," *Oecologia*, Vol. 108, pp. 389–411.

Jackson, R.B., L.A. Moore, W.A. Hoffmann, W.T. Pockman, and C.R. Linder, 1999, "Ecosystem Rooting Depth Determined with Caves and DNA," *Proc. Nat. Acad. Sci.*, Vol. 96, pp. 11,387–11,392.

Jacobson, K.W., 2005, *Air Dispersion Analysis for Los Alamos National Laboratory Technical Area 54, Material Disposal Area G*, Los Alamos National Laboratory Report LA-UR-05-7232, September.

James, W.B. and E.S. Booth, 1952, "Biology and Life History of the Sagebrush Vole," Walla Walla College Publ., *Dept. Biol. Sci.*, Vol. 1, pp. 23–43.

Jensen, L. and C.C. Shock, 2001 Strategies for Reducing Irrigation Water Use, Oregon State University Extension, Corvallis OR, EM8783 <http://eesc.orst.edu/agcomwebfile/EdMat /html /EM/EM8783/em8783.html>.

Jensen, P. and M.M. Hooten, 2000, *Burrowing Depths of Ant Species of the Transition Desert and Piñon-Juniper Plant Communities of the Nevada Test Site*, Neptune and Co., Inc. Document No. 05100-02.

Johnson, K., 1981, "Social Organization in a Colony of Rock Squirrels (*Spermophilus variegatus*, Sciuridae)," *Southwestern Nat.*, Vol. 26, pp. 237–242.

Johnson, et al., 1938, "The Influence of the Harvester Ant *(Pogomyrmex occidentalis* Cress), upon Range Vegetation," Unpub. Rep. Squaw Butte Oregon Agr. Exp. Sta.

Juelson, T.C., 1970, "A Study of the Ecology and Ethology of the Rock Squirrel *Spemophilus variegatus* (Erxleben) in Northern Utah," unpublished Ph.D. dissertation, Univ. Utah, Salt Lake City.

KAPL, 2002, *Nuclides and Isotopes, Chart of the Nuclides, 16th Edition*, Knolls Atomic Power Laboratory, Baum, E.M., H.D. Knox, and T.R. Miller, eds.

Kawamichi, 1989, "Nest Structure Dynamics and Seasonal Use of Nests by Siberian Chipmunks (*Eutamias sibiricus*)," *J. Mammal.*, Vol. 70, No. 1, pp. 44–57.

Keeler, K.H., 1993, "Fifteen Years of Colony Dynamics in *Pogonomyrmex Occidentialis*: The Western Harvester Ant, in Western Nebraska," *The Southwestern Naturalist*, Vol. 38, No. 3, pp. 286–289.

Koniak, S., 1985, "Succession in Piñon-Juniper Woodlands Following Wildfire in the Great Basin," *Great Basin Naturalist*, Vol. 45, No. 3, pp. 556–566.

Koontz, M.D., and H.E. Rector, 1995, *Estimation of Distributions for Residential Air Exchange Rates*, U.S. Environmental Protection Agency Contract No. 68-D9-0166, Work Assignment No. 3-19, U.S. Environmental Protection Agency, Office of Pollution Prevention and Toxics, Washington, D.C.

Koopman, 1965, Memorandum from F.C. Koopman, US Dept of the Interior Geological Survey, to Salvatore E. Russo, Engineering 3, LASL, June 30.

Kopp, B., 1991, Personal communication between B. Kopp, Los Alamos National Laboratory, and R. Shuman, Rogers and Associates Engineering Corporation.

Koukoura, Z., A.P. Mamolos, and K.L. Kalburtji, 2003, "Decomposition of Dominant Plant Species Litter in a Semiarid Grassland," *Applied Soil Ecology*, Vol. 23, pp. 13–23.

Krablin, R., 1989, Personal communication with Jonathan Z. Cannon concerning soil ingestion rates, Denver, CO, Arco Coal Co, October 13.

Kretzer, J.E. and J.F. Cully, Jr., 2001, "Prairie Dog Effects on Harvester Ant Species Diversity and Density," *J. Range Manage.*, Vol. 54, pp. 11–14.

Krier, D., P.A. Longmire, R.H. Gilkeson, and H.J. Turin, 1997, *Geologic, Geohydrologic, and Geochemical Data Summary of Material Disposal Area G, Technical Area 54, Los Alamos National Laboratory*, Los Alamos National Laboratory Report LA-UR-95-2696, February.

Kwicklis, E., M. Witkowski, K. Birdsell, B. Newman, and D. Walther, 2005, "Development of an Infiltration Map for the Los Alamos Area, New Mexico," *Vadose Zone Journal,* Vol. 4, pp. 672–693).

LANL, 1975, Memorandum "Solid Radioactive Waste Disposal Guidelines" from L.J. Johnson, H8-WM-461 at LASL, to Distribution. April 24.

LANL, 1998, *Material Disposal Unit Design, Construction, Use, and Closure*, Los Alamos National Laboratory Report, Draft DOP-54G-013, Rev. 1, August.

LANL, 2006, *Performance Assessment and Composite Analysis for Los Alamos National Laboratory Technical Area 54, Material Disposal Area G, Revision 3.0,* Los Alamos National Laboratory Report LA-UR-06-4525.

Lavigne, R.J, 1969, "Bionomics and Nest Structure of *Pogonomyrmex occidentalis* (Hymenoptera: Formicidae)," *Ann. Ent. Soc. Am.*, Vol. 62, pp. 1,166–1,175.

Lei, S.A., 2000, "Ecological Impacts of Seed Harvester Ants on Soil Attributes in a *Larrea*-Dominated Shrubland," *Western North Am. Nat.,* Vol. 60, No. 4, pp. 439–444.

Lerner, B.R. and M.N. Dana, 2001, *Leafy Greens for the Home Garden*, Purdue University Cooperative Extension Service, HO-29-W, April.

Little, C.A., 1979, "The Coefficient for the Transfer of Radionuclides from Animal Intake to Meat, F_f," In *A Statistical Analysis of Selected Parameters for Predicting Food Chain Transport and Internal Dose of Radionuclides*, Hoffman, F.O. and C.F. Baes, III, eds., Oak Ridge National Laboratory Report ORNL/NUREG/TM-282.

Livens, F.R. and M.S. Baxter, 1988, "Particle Size and Radionuclide Levels in Some West Cumbrian Soils," *Sci. Tot. Environ.*, Vol. 70, pp. 1–17.

Loaiza, D. and E. Vold, 1995, *Moisture Profiles Measured in Subsurface Monitor Holes at the Los Alamos LLRW Disposal Site*, Los Alamos National Laboratory Report LA-UR-95-1922.

Lobry de Bruyn, L.A., 1999, "Ants as Bioindicators of Soil Function in Rural Environments," *Agriculture, Ecosystems and Environment*, Vol. 74, pp. 425–441.

Longmire, P., C.R. Cotter, I.R. Triay, J.J. Kitten, C. Hall, J. Bentley, D. Hollis, and A.I. Adams, 1996, *Batch Sorption Results for Americium, Neptunium, Plutonium, Technetium, and Uranium Transport through the Bandelier Tuff, Los Alamos, New Mexico,* Los Alamos National Laboratory Report LA-UR-96-4716.

LSU, 2003, *Louisiana Vegetable Planting Guide*, Louisiana State University Agricultural Center, Publication 1980, April.

Ludwig, J.L., W.G. Whitford, A.B. Rodney, and R.E. Grieve, 1977, "An Evaluation of Transmission Line Construction on Piñon-Juniper Wood-Land and Grassland Communities in New Mexico," *J. Environ. Manage.*, Vol. 5, pp. 127–137.

Lyons, R.K., R. Machen, and T.D.A. Forbes, 1999, *Understanding Forage Intake in Range Animals*, Texas Agricultural Extension Service publication L-5152, January 1999.

Mack, R.N., 1977, "Mineral Return via the Litter of *Artemisia tridentata*," *American Midland Naturalist*, Vol. 97, pp. 189–197.

MacMahon, J.A., 1985, *The Audubon Society Nature Guides: Deserts*, Alfred A. Knopf, New York.

MAFES, 1999, *Impact of Imported Fire Ants on Mississippi*, Mississippi Agricultural and Forestry Experiment Station, Technical Bulletin 223, May.

Malmon, D.V., S.L. Reneau, T. Dunne, D. Katzman, and P.G. Drakos, 2005, "Influence of Sediment Storage on Downstream Delivery of Contaminated Sediment," *Water Resour. Res.*, Vol. 41, W05008.

Mandel, R.D. and C.J. Sorenson, 1982, "The Role of the Western Harvester Ant (*Pogonomyrmex occidentalis*) in Soil Formation," *Soil Sci. Soc. Am. J.*, Vol. 46, pp. 785–788.

Marrero, T.R. and E.A. Mason, 1972,"Gaseous Diffusion Coefficients," *J. Phys. Chem. Ref. Data*, Vol. 1, pp. 3–118.

Martin, E.C., 2000, *Determining the Amount of Irrigation Water Applied to a Field*, Univ of Arizona, Cooperative Extension, Arizona Water Series, No. 29, AZ1157.

Maser, C., E.W. Hammer, C. Brown, R.E. Lewis, R.L. Rausch, and M.L. Johnson., 1974, "The Sage Vole, *Lagurus curtatus* (Cope, 1868)," In Crooked River National Grassland, Jefferson County, Oregon: A Contribution to its Life History and Ecology, *Saugetierk. Mitt.*, Vol. 22, pp. 193–222.

May, S.G., W.L. Mies, J.W. Edwards, J.J. Harris, J.B. Morgan, R.P. Garrett, F.L. Williams, J.W. Wise, H.R. Cross, and J.W. Savell, 2000, "Using Live Estimates and Ultrasound Measurements to Predict Beef Carcass Cutability," *J. Anim. Sci.*, Vol. 78, pp. 1,255–1,261.

Mayer, P.W., W.B. DeOreo, E.M. Opitz, J.C. Kiefer, W.Y. Davis, B. Dziegielewski, and J.O. Nelson., 1999, *Residential End Uses of Water*, Report to AWWA Research Foundation and American Water Works Association (AWWA), Denver, CO.

Mayland, H.F., G.E. Shewmaker, and R.C. Bull, 1977, "Soil Ingestion by Cattle Grazing Crested Wheatgrass," *J. of Range Manage.*, Vol. 30, pp. 264–265.

McKenzie, D.H., L.L. Cadwell, L.E. Eberhardt, W.E. Kennedy, Jr., R.A. Peloquin, and M.A. Simmons, M.A., 1982, *Relevance of Biotic Pathways to the Long-Term Regulation of Nuclear Waste Disposal*, prepared by Pacific Northwest Laboratory for the U.S. Nuclear Regulatory Commission, NUREG/CR-2675, Volume 2, October.

McKone, T.E. and P.B. Ryan, 1989, "Human Exposures to Chemicals through Food Chains: An Uncertainty Analysis," *Environ. Sci. Technol.*, Vol. 23, pp. 1,154–1,163.

McLeod, K.W., J.J. Alberts, D.C. Adriano, and J.E. Pinder III, 1984a, "Plutonium Contents of Broadleaf Vegetable Crops Grown Near a Nuclear Fuel Chemical Separations Facility," *Health Phys.*, Vol. 46, pp. 261–267.

McLeod, K.W., J.E. Pinder III, and J.R. Watts, Jr., 1984b, "Contribution of a Nuclear Fuel Chemical Separations Facility to the Plutonium Content of a Tobacco Crop," *Health Phys.*, Vol. 46, pp. 1,205–1,211.

Meeuwig, R.O., 1979, *Growth Characteristics of Piñon-Juniper Stands in the Western Great Basin*, U.S. Dept. Agriculture Forest Service Paper INT-238.

Merritt, J.F., 1974, "Factors Influencing the Local Distribution of *Peromyscus californicus* in Northern California," *J. Mammal.*, Vol. 55, pp. 102–114.

Meserve, P.L., 1977, "Three-Dimensional Home Ranges of Cricetid Rodents," *J. Mammal.*, Vol. 58, pp. 549–558.

Mielke, H.W., 1977, "Mound Building by Pocket Gophers (Geomyidae): Their Impact on Soils and Vegetation in North America," *J. of Biogeography*, Vol. 4, pp. 171–180.

Millar, C.S., 1974, "Decomposition of Coniferous Leaf Litter," In *Biology of Plant Litter Decomposition, Volume II*, Dickinson, C.H. and G.J.F. Pugh, eds., Academic Press, London.

Miller, C.W., 1980, "An Analysis of Measured Values for the Fraction of a Radioactive Aerosol Intercepted by Vegetation," *Health Physics*, Vol. 38, pp. 705–712.

Miller, C.W. and F.O. Hoffman, 1982, "An Analysis of Reported Values of the Environmental Half-Times for Radionuclides Deposited on the Surfaces of Vegetation," in *Environmental Migration of Long-Lived Radionuclides*, International Atomic Energy Agency, IAEA-STI/PUB/597.

Miller, M.A. 1957, "Burrows of the Sacramento Valley Pocket Gopher in Flood-Irrigated Alfalfa Fields," *Hilgardia*, Vol. 26, pp. 431–452.

Miller, R.F. and R.J. Tausch, 2001, *The Role of Fire in Juniper and Piñon Woodlands: A Descriptive Analysis*, Tall Timbers Research Station Miscellaneous Publication No. 11, pp. 15–30.

Millington, R.J., 1959, "Gas Diffusion in Porous Media," *Science,* Vol. 130, pp.100–102.

Mitchell, R.S., 1972, *Small Rodents of the Flood Plain of the South Platte River at the Proposed Narrows Reservoir Site*, M.A. thesis, Univ. Northern Colorado, Greeley.

Murphy, K.L., J.M. Klopatek, and C.C. Klopatek, 1998, "The Effects of Litter Quality and Climate on Decomposition along an Elevational Gradient," *Ecological Applications*, Vol. 8, No. 4, pp. 1,061–1,071.

Murray, D.M. and D.E. Burmaster, 1995, "Residential Air Exchange Rates in the United States: Empirical and Estimated Parametric Distribution by Season and Climatic Region," *Risk Analysis,* Vol. 15, No. 4, pp. 459–465.

Myers, S., 2004, E-mail from Steve Myers, LANL Nuclear Waste and Infrastructure Services — Solid Waste Operations, to Rob Shuman, URS Corporation, regarding measurement errors, June 15.

Napier, B.A., R.A. Peloquin, D. L. Strenge, and J. V. Ramsdell, 1988, *GENII — The Hanford Environmental Radiation Dosimetry Software System*, Pacific Northwest Laboratory Report PNL-6584.

Napier, B.A., D.L. Strenge, J.V. Ramsdell, Jr., P.W. Eslinger, and C.J. Fosmire, 2004, GENII Version 2 Software Design Document, PNNL-14584, Pacific Northwest National Laboratory.

Nazaroff, W.W., B.A. Moed, and R.G. Sextro, 1988, "Radon Entry via Potable Water," In *Radon and Its Decay Products in Indoor Air*, Nazaroff, W.W. and A.V. Nero, eds., John Wiley and Sons, NY. pp. 131–157.

NCRP, 1984, *Radiological Assessment: Predicting the Transport, Bioaccumulation, and Uptake by Man of Radionuclides Released to the Environment*, National Council on Radiation Protection and Measurements, Report No. 76, March.

NCRP, 1999, *Recommended Screening Limits for Contaminated Surface Soil and Review of Factors Relevant to Site-Specific Studies*, National Council on Radiation Protection and Measurements, Report No. 129.

Newman, B.D., 2005, Personal communication from B. Newman, Los Alamos National Laboratory, to R. Shuman, URS Corporation, May, 6.

Newman, B.D., M. Gard, D. Counce, E. Kluk, L. Martinez, D. Newell, J. Salazar, 2005, *Spatial Variation in Near-Surface Hydrologic Behavior at Los Alamos National Laboratory Technical Area 54, Material Disposal Area G*, Los Alamos National Laboratory Report LA-UR-05-6898, September.

Newman, B.D and T.G. Schofield, 2005, *Modeling of an Evapotranspiration Cover for the Groundwater Pathway at Los Alamos National Laboratory Technical Area 54, Material Disposal Area G*, Los Alamos National Laboratory Report LA-UR-05-7094, September.

Ng, Y.C., W.D. Phillips, Y.E. Ricker, and R.K. Tandy, 1978, *Methodology for Assessing Dose Commitment to Individuals and to the Population from Ingestion of Terrestrial Foods Contaminated by Emissions from a Nuclear Fuel Reprocessing Plant at the Savannah River Plant*, Lawrence Livermore Laboratory, UCID-17743, March.

Ng, Y.C., C. Colsher, and S.E. Thompson, 1982, *Transfer Coefficients for Assessing Dose from Radionuclides in Meat and Eggs*, U.S. Nuclear Regulatory Commission, NUREG/CR-2976.

Nielson, K.K., V.C. Rogers, R.B. Holt, T.D. Pugh, W.A. Grondzik, and R.J. de Meijer, 1997, "Radon Penetration of Concrete Slab Cracks, Joints, Pipe Penetrations, and Sealants," *Health Physics*, Vol. 73, pp. 668–678.

Nowak, R.M., 2003, *Walker's Mammals of the World Online*, Johns Hopkins University Press, Baltimore.

NRC, 1977, *Regulatory Guide 1.109, Calculation of Annual Doses to Man from Routine Release of Effluents for the Purpose of Evaluating Compliance with 10 CRR Part 50, Appendix I*, U.S. Nuclear Regulatory Commission, Revision 1, October.

NRC, 1986, *Update of Part 61 Impacts Analysis Methodology, Methodology Report*, U.S. Nuclear Regulatory Commission, NUREG/CR-4370, Vol. 1, January.

NRC, 1989, *Regulatory Guide 3.64, Calculation of Radon Flux Attenuation by Earthen Uranium Mill Tailings Covers*, U.S. Nuclear Regulatory Commission, June.

NRC, 1992, *Residual Radioactive Contamination from Decommissioning – Technical Basis for Translating Contamination Levels to Annual Total Effective Dose Equivalent: Final Report*, prepared by Pacific Northwest Laboratory for the U.S. Nuclear Regulatory Commission, NUREG/CR-5512, October.

NRC, 1994, *Nutrient Requirements of Poultry*, Eighth Revised Edition, National Research Council, National Academy Press, Washington, D.C.

NTS, 1995, *Cost/Risk/Benefit Analysis of Alternative Cleanup Requirements for Plutonium-Contaminated Soils on and near the Nevada Test Site*, DOE/NV-399, May.

Nyhan, J.W., F.R. Miera, and R.J. Peters, R. J 1976a, "Distribution of Plutonium in Soil Particle Size Fractions of Liquid Effluent-Receiving Areas at Los Alamos," *J. Environ. Qual.*, Vol. 5, No. 1, pp. 50–56.

Nyhan, J.W., F.R. Micra, Jr., and R.E. Neher., 1976b, "Distribution of Plutonium in Trinity Soils after 28 Years," *J. Environ. Qual.*, Vol. 5, No. 1, pp. 431–437.

Nylander, C.L, K.A. Bitner, G. Cole, E.H. Keating, S. Kinkead, P. Longmire, B. Robinson, D.B. Rogers, and D. Vaniman, 2003, *Groundwater Annual Status Report for Fiscal Year 2002*, Los Alamos National Laboratory Report LA-UR-03-0244.

O'Rourke, J.T. and P.R. Ogden, 1969, "Vegetative Response Following Piñon-Juniper Control in Arizona," *J. Range Manage.*, Vol. 22, No. 6, pp. 416–418.

Oaks, E.C., P.J. Young, and G.L. Kirkland, Jr., 1987, "Mammalian Species – *Spermophilus variegatus*," *The Society of Mammalogists* No. 272, February.

Opseth, D.A., 1998, *Landfill Gas Generation at a Semi-Arid Landfill*, Thesis, University of Regina, Regina, Saskatchewan, Canada, December.

ORNL, 1999, *Guidance for Conducting Risk Assessments and Related Risk Activities for the DOE-ORO Environmental Management Program*, Oak Ridge National Laboratory, BJC/OR-271, April.

Orr, R.T., 1940, "The Rabbits of California," *Occas. Papers California Acad. Sci.*, Vol. 17, pp. 1–227.

Oughton, D.H., 1990, "Radiocesium Association with Soil Components: The Application of a Sequential Extraction Technique," In *International Union of Radioecologists VIIth Report of the Working Group Soil-to-Plant Transfer Factors*, M.J. Frissel ed., Uppsala, Sweden, September.

Padien, D.J. and K. Lajtha, 1992, "Plant Spatial Pattern and Nutrient Distribution in Piñon-Juniper Woodlands along an Elevational Gradient in Northern New Mexico," *Int. J. Plant Sci.*, Vol. 153, No. 3, pp. 425–433.

Parmenter, R.R., M.R. Mesch, and J.A. Macmahon, 1987, "Shrub Litter Production in a Sagebrush-Steppe Ecosystem: Rodent Population Cycles as a Regulating Factor," *J. Range Manage.*, Vol. 40, No. 1, pp. 50–54.

Peters, D.P.C., W.K. Lauenroth, and I.C. Burke, 2002, "The Role of Disturbances in Shortgrass Steppe Community and Ecosystem Dynamics," In *Ecology of the Shortgrass Steppe: Perspectives from Long-Term Research*, Lauenroth, W.K. and I.C. Burke, eds., Oxford Press, in press.

Peterson, J.T., Jr., 1983, "Terrestrial and Aquatic Food Chain Pathways," in *Radiological Risk Assessment, A Textbook on Environmental Dose Analysis*, Till, J.E. and H.R. Meyer, eds., NUREG/CR-3332.

Philip, J.R. and D.A. DeVries, 1957, "Moisture Movement in Porous Materials under Temperature Gradients," Trans., *Amer. Geophys. Union*, Vol. 38, No. 2, pp. 222–232.

Pieper, R.D., 1968, "Comparison of Vegetation on Grazed and Ungrazed Piñon-Juniper Grassland Sites in Southcentral New Mexico," *J. Range Manage.*, Vol. 21, pp.51–53.

Pieper, R.D., 1990, "Overstory-Understory Relations in Piñon-Juniper Woodlands in New Mexico," *J. Range Manage.*, Vol. 43, No. 5, pp. 413–415.

Pinder, J.E., III, T.G. Ciravolo, and J.W. Bowling, 1988, "The Interrelationships Among Plant Biomass, Plant Surface Area and the Interception of Particulate Deposition by Grasses," *Health Physics*, Vol. 55, No. 1, pp. 51–58.

Pinder, J.E., and K.W. McLeod, 1989, Mass Loading of Soil Particles on Plant Surfaces," *Health Physics*, Vol. 57, No. 6, pp. 935–942.

Pinder, J.E., III, K.W. McLeod, R.F. Lide, and K.C. Sherrod, 1991, "Mass Loading of Soil Particles on a Pasture Grass," *J. Environ. Radioactivity*, Vol. 13, pp. 341–354.

Pollard, C.G. and R. Shuman, 1999, *Evaluation of Pre-1971 Radioactive Waste Disposal Data for TA-54 MDA G*, Rogers and Associates Engineering Corporation Report RAE-9629/3005-3, December.

Polzer, W.L., et al., 1985, *Equilibrium Sorption of Cobalt, Cesium, and Strontium on Bandelier Tuff: Analysis of Alternative Mathematical Modeling*, Los Alamos National Laboratory Report LA-UR-85-785.

Porter, S.D. and C.D. Jorgensen, 1988, "Longevity of Harvester Ant Colonies in Southern Idaho," *J. Range Manage.*, Vol. 41, No. 2, pp. 104–107.

Pratt, M. and G.A. Rasmussen, 2001, *Determining Your Stocking Rate*, Utah State University Extension Range Management Fact Sheet NR/RM/04, May.

RAC, 1999, *Final Report, Task 3: Inputs and Assumptions, Radionuclide Soil Action Level Oversight Panel*, Risk Assessment Corporation, RAC Report No. 15-RSALOP-RFSAL-1999-FINAL, October.

Radian, 1995, *Air Quality Impacts Analysis for Area G*, Final Report 4/4 from Radian to CST-14, Los Alamos National Laboratory under DOE subcontract 6345L0013-31.

RAE, 1998, *User's Guide for PRESTO-EPA-CLNCPG/CLNPOP Operation System*, Rogers and Associates Engineering Croporation report RAE-9535/14-1, September.

Reneau, S., 2005, Personal communication (e-mail) from Steven Reneau, Los Alamos National Laboratory, to Rob Shuman, URS Corporation, September 16.

Reynolds, T.D. and J.W. Laundre, 1988, "Vertical Distribution of Soil Removed by Four Species of Burrowing Rodents in Disturbed and Undisturbed Soils," *Health Physics*, Vol. 54, No. 4, pp. 445–450.

Ricklefs, R.E., 1979, *Ecology*, Second Edition, Chiron Press, New York.

Rishel, J., S.D. Johnson, H.D. Holt, and W.A. Olsen, 2003, *Meteorological Monitoring at Los Alamos*, Los Alamos National Laboratory Report LA-UR-03-8097.

Rodin, L.E. and N.I. Bazilevich, 1967, *Production and Mineral Cycling in Terrestrial Vegetation*, English Translation, G.E. Fogg, ed., Oliver and Boyd, Edinburgh, Scotland and London, England.,

Rogers, D.B. and B.M. Gallaher, 1995, *The Unsaturated Hydraulic Characteristics of the Bandelier Tuff*, Los Alamos National Laboratory Report LA-12968-MS, September.

Rogers, L.E. and R.J. Lavigne, 1974, "Environmental Effects of Western Harvester Ants on the Shortgrass Plains Ecosystem," *Environmental Entomology*, Vol. 3, No. 6, pp. 994–997.

Rogers, V.C., K.K. Nielson, and D.R. Kalkwarf, 1984, *Radon Attenuation Handbook for Uranium Mill Tailings Cover Design*, U.R. Nuclear Regulatory Commission Report NUREG/CR-3533, April.

Rogers, V.C. and K.K. Nielson, 1991, Correlations for Predicting Air Permeabilities and 222Rn Diffusion Coefficients of Soils, *Health Physics*, Vol. 61, No. 2, pp. 225–230.

Rogers, V.C., K.K. Nielson, R.B. Holt, and R. Snoddy., 1994, "Radon Diffusion Coefficients for Residential Concretes," *Health Physics*, Vol. 67, No. 3, pp. 261–265.

Rogers, V.C., K.K. Nielson, and R.B. Holt, 1995, "Radon Diffusion Coefficients for Aged Residential Concretes," *Health Physics*, Vol. 68, No. 6, pp. 832–834.

Rongstad, O.J., 1965, "A Life History Study of Thirteen-Lined Ground Squirrels in Southern Wisconsin," *J. Mamm.*, Vol. 46, pp. 76–87.

Rosenberg, D.K. and R.G. Anthony, 1993, "Differences in Townsend's Chipmunk Populations Between Second- and Old-Growth Forest in Western Oregon," *J. Wildlife Manage.*, Vol. 57, No. 2, pp. 365–373.

Rupp, E.M., 1980, "Age Dependent Values of Dietary Intake for Assessing Human Exposures to Environmental Pollutants," *Health Physics,* Vol. 39, pp. 151.

Sander, R., 1999, "Compilation of Henry's Law Constants for Inorganic and Organic Species of Potential Importance in Environmental Chemistry," Air Chemistry Department Max-Planck Institute of Chemistry, Version 3 <http://www.mpch-mainz.mpg.de/~sander/res/henry.html> (April 8, 1999).

Schack-Kirchner, H., T.V. Gaertig, K. Wilpert, and E.E. Hildebrand, 2001, "A Modified McIntyre and Phillip Approach to Measure Top Soil Gas Diffusivity in International Telecommunication Union," *J. Plant Nutr. Soil Sci.*, Vol. 164, pp. 253–258.

Schott, M.R. and R.D. Pieper, 1987, "Succession of Piñon-Juniper Communities after Mechanical Disturbance in Southcentral New Mexico," *J. Range Manage.*, Vol. 40, No. 1, pp. 88–94.

Scire, J.S., D. G. Stimanitis., and R.J. Yamartino, 2000a, *A Users Guide for the CALPUFF Dispersion Mode (Version 5)*, Earth Tech. Inc., Concord, Massachusetts, January.

Scire, J.S., F.R. Robe, M.E. Fernau and R.J. Yamartino, 2000b, *A User's Guide for the CALMET Meteorological Model (Version 5)*, Earth Tech, Inc., Concord, Massachusetts.

Scott, H.W., 1951, "The Geological Work of the Mound-Building Ants in Western United States," *J. Geol.*, Vol. 59, pp. 173–175.

Scurlock, J.M.O., K.R. Johnson, and R.J. Olson, 2003, *NPP Grassland: NPP Estimates from Biomass Dynamics for 31 Sites, 1948-1994*, Dataset available on-line [http://www.daac.ornl.gov] from Oak Ridge National Laboratory Distributed Active Archive Center, Oak Ridge, TN.

Severson, K.E., 1986, "Small Mammals in Modified Piñon-Juniper Woodlands, New Mexico," *J. Range Manage.*, Vol. 39, No. 1, pp. 31–34.

Shan, C. and D. Stephens, 1995, "An Analytical Solution for Vertical Transport of Volatile Chemicals in the Vadose Zone," *J. Contaminant Hydrology*, Vol. 18, pp. 259–277.

Shariff, A.R., M.E. Biondini, and C.E. Grygiel, 1994, "Grazing Intensity Effects on Litter Decomposition and Soil Nitrogen Mineralization," *J. Range Manage.,* Vol. 47, No. 6, pp. 444–449.

Sharp, L.E., and W.F. Barr, 1960, "Preliminary Investigations of Harvester Ants on Southern Idaho Rangelands," *J. Range Manage.*, Vol. 13, pp. 131–134.

Sheppard, S.C. and W.G. Evenden, 1997, "Variation in Transfer Factors for Stochastic Models: Soil-to-Plant Transfer," *Health Physics*, Vol. 72, No. 5, pp. 727–733.

Shinn, J.H., 1992, "Enhancement Factors for Resuspended Aerosol Radioactivity: Effects of Topsoil Disturbance," In *Precipitation Scavenging and Atmosphere-Surface Exchange, Volume 3*, Schwartz, S.E. and W.G.N. Slinn, eds., Hemisphere Publishing Corp., Washington, Philadelphia, and London.

Shinn, J.H., 2002, *Complementary Pu Resuspension Study at Palomares, Spain*, Lawrence Livermore National Laboratory Report UCRL-ID-150980.

Shinn, J.H., D.N. Homan, and W.L. Robison, 1997, "Resuspension Studies in the Marshall Islands," *Health Physics*, Vol. 73, pp. 248–257.

Shuman, R., 1999, *An Evaluation of the Potential Impacts of Plant and Animal Intrusion into Disposed Waste at TA-54, MDA G*, Rogers and Associates Engineering Corporation, RAE-9629/3005-1, April.

Shuman, R., 2005, *Radioactive Waste Inventory for Los Alamos National Laboratory Technical Area 54, Material Disposal Area G*, Los Alamos National Laboratory Report LA-UR-05-6996, September.

Shuman, R., S. French, and C. Pollard, 2003, *Performance Assessment and Composite Analysis Maintenance Program Plan for MDA G — 2003*, Los Alamos National Laboratory Report LA-UR-03-3472.

Simon, S.L., 1998, "Soil Ingestion by Humans: A Review of History, Data, and Etiology with Application to Risk Assessment of Radioactively Contaminated Soil," *Health Physics*, Vol. 74, No. 6, pp. 647–672.

Sims, P.L. and J.S. Singh, 1978, "The Structure and Function of Ten Western North American Grasslands; IV Compartmental Transfers and Energy Flow Within the Ecosystem," *Journal of Ecology*, Vol. 66, pp. 983–1,009.

Skinner, D.J., 1982, *^{226}Ra Contamination of Soil and Foliage as a Function of Distance Downwind from Uranium Mill Tailings*, M.S. Thesis, Colorado State Univ., Fort Collins.

Skinner, J.L. and M.L. Sunde, 1983, *Raising Meat-Type Chickens*, University of Wisconsin Cooperative Extension Service publication A3225.

SLTERP, 2003, *Sevilleta Long-Term Ecological Research Program*, University of New Mexico, <http://sevilleta.unm.edu/data/species/>.

Smith, C.B. and P.J. Urness, 1984, "Small Mammal Abundance on Native and Improved Foothill Ranges, Utah," *J. Range Manage.*, Vol. 37, No. 4, pp. 353–357.

Smith, D.D., 1977, "Grazing Studies on a Contaminated Range of the Nevada Test Site," Iin *Environmental Plutonium on the Nevada Test Site and Environs*, ERDA Report NVO-171, Nevada Operations Office, NTIS.

Smith, R.C., 1995, *Vegetable Maturity Dates, Yields and Storage*, North Dakota State University Extension Service publication H-912, April.

Sneva, F.A., 1979, "The Western Harvester Ants: Their Density and Hill Size in Relation to Herbaceous Productivity and Big Sagebrush Cover," *J. Range Manage.*, Vol. 32, No. 1, pp. 46–47.

Soule, P.T. and P.A. Knapp, 1996, "The Influence of Vegetation Removal of by Western Harvester Ants (*Pogonomyrmex owyheei*) in a Relict Area of Sagebrush-Steppe in Central Oregon," *American Midland Naturalist*, Vol. 136, No. 2, pp. 336–345.

Spencer, S.R., G.N. Cameron, B.D. Eshelman, L.C. Cooper, and L.R. Williams, 1985, "Influence of Pocket Gopher Mounds on a Texas Coastal Prairie," *Oecologia*, Vol. 66, pp.111–115.

Springer, E.P., 2004, *Statistical Exploration of Matrix Hydrologic Properties for the Bandelier Tuff, Los Alamos, New Mexico*, Los Alamos National Laboratory Report LA-UR-04-2830.

Stauffer, P.H., H.S. Viswanathan, B.A. Robinson, C.W. Gable, G.L. Cole, D.E. Broxton, E.P. Springer, T.G. Schofield, 2005, *Groundwater Pathway Model for the Los Alamos National Laboratory Technical Area 54, Material Disposal Area G*, Los Alamos National Laboratory Report LA-UR-05-7393, September.

Storer, T.I., F.C. Evans, and F.G. Palmer, 1944, "Some Rodent Populations in the Sierra Nevada of California," *Ecol. Monogr.*, Vol. 14, pp. 166–192.

Streubel, D.P. and J.P. Fitzgerald, 1978, "Mammalian Species — *Spermophilus tridecemlineatus*," *The Society of Mammalogists* No. 103, September.

Strojan, C.L., F.B. Turner, and R. Castetter, 1979, "Litter Fall from Shrubs in the Northern Mojave Desert," *Ecology*, Vol. 60, No. 5, pp. 891–900.

Summerling, T.J., N.J. Dodd, and N. Green, 1984, "The Transfer of ^{90}Sr and ^{137}Cs to Milk in a Dairy Herd Grazing Near a Major Nuclear Installation," *Sci. Total. Environ.*, Vol. 34, pp. 57–72.

Suter, G.W., R.J. Luxmoore, and E.D. Smith, 1993, "Compacted Soil Barriers at Abandoned Landfill Sites are Likely to Fail in the Long Term," *J. Environ. Qual.*, Vol. 22, pp. 217–226.

Taggart, D., 1992, "Final Documentation for Radwaste Oracle Database's List of Acceptable Radioisotopes, Specific Activities, Categories and Regulatory Limits," memorandum from D. Taggart, Los Alamos National Laboratory, to J. Harper, Los Alamos National Laboratory, EM-7D-92-71, February 3

TAMU, 2001, *Vegetable Grower's Handbook*, Web Edition, Texas A&M University, Texas Agricultural Extension Service, January, <http://aggie-horticulture.tamu.edu/extension/veghandbook/index.html>.

Thibault, D.H., M.I. Sheppard, and P.A. Smith, 1990, *A Critical Compilation and Review of Default Soil Solid/Liquid Partition Coefficients, K_d, for use in Environmental Assessments*, Atomic Energy of Canada Limited Report AECL-10125, March.

Tierney, G.D., and T.S. Foxx, 1987, *Root Lengths of Plants on Los Alamos National Laboratory Lands*," Los Alamos National Laboratory Report LA-10865-MS, January.

Tress, J.A. Jr. and J.M. Klopatek, 1987, "Successional Changes in Community Structure of Piñon-Juniper Woodlands on North-Central Arizona," in *Proceedings – Piñon-Juniper Conference*, U.S. Dept. Agriculture Forest Service, Intermountain Research Station, General Technical Report INT-215, January.

UNCE, 2001, *Understanding Beef Carcass Contest Information*, University of Nebraska Cooperative Extension, G01-1431-A.

UNSCEAR, 1993, *Sources and Effects of Ionizing Radiation*, United Nations Scientific Committee of the Effects of Atomic Radiation, report to the General Assembly, Publication E.94.IX.2.

USDA, 1995, *United States Standards, Grades, and Weight Classes for Shell Eggs*, U.S. Agriculture Department, Agricultural Marketing Service AMS-56, April.

USDA, 1999, *Farm and Ranch Irrigation Survey (1998), Volume 3*, 1997 Census of Agriculture, U.S. Department of Agriculture.

USDA, 2004a, *Agricultural Statistics 2004*, National Agricultural Statistics Service, U.S. Department of Agriculture.

USDA, 2004b, *Farm and Ranch Irrigation Survey (2003), Volume 3*, Special Studies, Part 1, 2002 Census of Agriculture, U.S. Department of Agriculture, November.

USDA, 2005a, *Livestock Slaughter*, National Agricultural Statistics Service, U.S. Department of Agriculture, May.

USDA, 2005b, *Milk Production*, National Agricultural Statistics Service, U.S. Department of Agriculture, May.

USDA, 2005c, *Chickens and Eggs — 2004 Summary, February 2005*, National Agricultural Statistics Service, U.S. Department of Agriculture, Pou 2-4 (05).

Van Pelt, R.S. and T.M. Zobeck, 2005, "Chemical Constituents of Fugitive Dust," In review, *Environmental Management and Assessment.*

Verner, J. and A.S. Boss, 1980, *California Wildlife and Their Habitats: Western Sierra Nevada*, Pacific Southwest Forest and Range Experimental Station, General Technical Report PSW-37, Berkeley.

Versar, 1990, *Database of Perfluorocarbon Tracer (PFT) Ventilation Measurements: Description and User's Manual*, U.S. Environmental Protection Agency Contract No. 68-02-4254, Task No. 39. Washington, D.C., U.S. Environmental Protection Agency, Office of Toxic Substances.

Wachter, J.R., 1993a, "Revised Plutonium Average Isotopic Values," memorandum from J.R. Wachter, Los Alamos National Laboratory, to T.L. Cremers, Los Alamos National Laboratory, NMT-04-93-517, November 10.

Wachter, J.R., 1993b, "Correction to Memorandum," memorandum from J.R. Wachter, Los Alamos National Laboratory, to T.L. Cremers, Los Alamos National Laboratory, NMT-04-93-536, November 23.

Wallwork-Barber, M.K. and T.E. Hakonson, 1981, *Accumulation and Retention of Soil Particles on Plants in Environmental Surveillance at Los Alamos During 1980*, Los Alamos National Laboratory Report LA-8810-ENV.

Webster, W.D. and J.K. Jones Jr., 1982, "Mammalian Species — *Reithrodontomys megalotis*," *The Society of Mammalogists* No. 167, May.

West, N.E., 1985, "Aboveground Litter Production of Three Temperate Semidesert Shrubs," *American Midland Naturalist,* Vol. 113, No. 1, pp. 158–169.

West, N.E. and C. Gunn, 1974, *Phenology, Productivity and Nutrient Dynamics of Some Cool Desert Shrubs*, U.S./ IBP Desert Biome Res. Memo. 74-7.

Wheeler, G.C. and J.N. Wheeler, 1986, *The Ants of Nevada*, Natural History Museum of Los Angeles County, Los Angeles, California.

Whicker, J.J., 2005, Personal Communication from J. Whicker, Los Alamos National Laboratory, to R. Shuman, URS Corporation, January 3.

Whicker, J.J. and D.D. Breshears, 2005, *Assessing Wind Erosion as a Contaminant Transport Mechanism for Los Alamos National Laboratory Technical Area 54, Material Disposal Area G*, Los Alamos National Laboratory Report LA-UR-05-5371, September.

Whitaker, J.O., Jr., 1980, *National Audubon Society Field Guide to North American Mammals*, Alfred A. Knopf, Inc., New York.

White, G.C., T.E. Hakonson, and A.J. Ahlquist, 1981, "Factors Affecting Radionuclide Availability to Vegetables Grown at Los Alamos," *Journal of Environmental Quality*, Vol. 10, pp. 294–299.

Whitford, W.G., 1976, "Temporal Fluctuations in Density and Diversity of Desert Rodent Populations," *J. Mamm.*, Vol. 57, pp. 351–369.

Whitford, W.G. and DiMarco, R., 1995, "Variability in Soils and Vegetation Associated with Harvester Ant (*Pogonomyrmex rugosus*) Nests in Chihuahuan Desert Watershed," *Biol. Fertility of Soils,* Vol. 20, pp.169–173.

Whittaker, R.H., 1975, *Communities and Ecosystems*, MacMillan Publishing Co., New York.

Widner, T., J. Shonka, S. Flack, J. O'Brien, R. Burns, J. Buddenbaum, D. Shonka, et al., 2004, *Draft Interim Report of the Los Alamos Historical Document Retrieval and Assessment (LAHDRA) Project*, prepared by individuals from ENSR Corporation, Shonka Research Associates, Inc., and ChemRisk, Inc. for the Centers for Disease Control and Prevention, March.

Willard, J.R. and H.H. Crowell, 1965, "Biological Activities of the Harvester Ant, *Pogonomyrmex owyheei*, in Central Oregon," *J. Econ. Entomol,* Vol. 58, pp. 484–489.

Willgoose, G.R. and S. Riley, 1998, "The Long Term Stability of Engineered Landforms of the Ranger Uranium Mine, Northern Territory, Australia: Application of a Catchment Evolution Model," *Earth Surf. Process. Landf.*, Vol. 23, No. 3, pp. 237–259.

Williams, S.T. and T.R.G. Gray, 1974, "Decomposition of Litter on the Soil Surface," In *Biology of Plant Litter Decomposition, Volume II*, Dickinson, C.H. and G.J.F. Pugh, eds., Academic Press, London.

Wilson, J.C.J., K.J. Crowell, and L.J. Lane, 2005, *Surface Erosion Modeling for the Repository Waste Cover at Los Alamos National Laboratory Technical Area 54, Material Disposal Area G*, Los Alamos National Laboratory Report LA-UR-05-7771, September.

Wirth, S., 1999, *Modeling the Potential Biological Effects on the Performance of TRU Waste Buried in GCD Boreholes at the Nevada Test Site*, IT Corporation Report, February.

Wolfsberg, K., 1980, "Sorptive Properties of Tuff and Nuclide Transport and Retardation," pp. 39–48 In *Evaluation of Tuff as a Medium for a Nuclear Waste Repository: Interim Status Report on the Properties of Tuff*, Sandia National Laboratory Report SAND80-1464, July.

Wood, M.I., R. Khaleel, P.D. Rittman, A.H. Lu, S.H. Finfrock, R.J. Serne, K.J. Cantrell, and T.H. DeLorenzo., 1994, *Performance Assessment for the Disposal of Low-Level Waste in the 200 West Area Burial Grounds*, Westinghouse Hanford Company, WHC-EP-0645, November.

WRCC, 2005, Western Regional Climate Center, Reno, NV, <www.wrcc.dri.edu>.

Yang, Y. and C.B. Nelson, 1986, "An Estimation of Daily Food Usage Factors for Assessing Radionuclide Intakes in the U.S. Population," *Health Physics*, Vol. 50, No. 2, pp. 245–257.

Yu, C., C. Loureiro, J.-J. Cheng, L.G. Jones, Y.Y. Wang, Y.P. Chia, and E. Faillace, 1993, *Data Collection Handbook to Support Modeling Impacts of Radioactive Material in Soil*, Environmental Assessment and Information Sciences Division Argonne National Laboratory, Argonne, Illinois, April.

Zach, R. and K.R. Mayoh, 1984, "Soil Ingestion by Cattle: A Neglected Pathway," *Health Physics,* Vol. 46, No. 2, pp. 426–431.

Zarn, M., 1977, *Ecological Characteristics of Piñon-Juniper Woodlands on the Colorado Plateau, A Literature Survey*, U.S. Department of the Interior — Bureau of Land Management, Technical Note, December.